

The Texas Medical Center Library

DigitalCommons@TMC

The University of Texas MD Anderson Cancer
Center UTHealth Graduate School of
Biomedical Sciences Dissertations and Theses
(Open Access)

The University of Texas MD Anderson Cancer
Center UTHealth Graduate School of
Biomedical Sciences

5-2022

Modeling of CNS Cancer with a Focus on the Immune Component

Daniel Zamler

Follow this and additional works at: https://digitalcommons.library.tmc.edu/utgsbs_dissertations



Part of the [Biological Phenomena, Cell Phenomena, and Immunity Commons](#), [Computer Sciences Commons](#), [Data Science Commons](#), [Nervous System Diseases Commons](#), [Neurology Commons](#), [Oncology Commons](#), and the [Statistics and Probability Commons](#)

Recommended Citation

Zamler, Daniel, "Modeling of CNS Cancer with a Focus on the Immune Component" (2022). *The University of Texas MD Anderson Cancer Center UTHealth Graduate School of Biomedical Sciences Dissertations and Theses (Open Access)*. 1159.

https://digitalcommons.library.tmc.edu/utgsbs_dissertations/1159

This Dissertation (PhD) is brought to you for free and open access by the The University of Texas MD Anderson Cancer Center UTHealth Graduate School of Biomedical Sciences at DigitalCommons@TMC. It has been accepted for inclusion in The University of Texas MD Anderson Cancer Center UTHealth Graduate School of Biomedical Sciences Dissertations and Theses (Open Access) by an authorized administrator of DigitalCommons@TMC. For more information, please contact digitalcommons@library.tmc.edu.

The
TMC LIBRARY
Health Sciences Resource Center

Modeling of CNS Cancer with a Focus on the Immune Component

by

Daniel Bernard Zamler B.Sc.

APPROVED:

Giulio F. Draetta, M.D./Ph.D.

Advisory Professor

Jian Hu, Ph.D.

Co-Advisor

Ronald A. DePinho, M.D.

Paul Scheet, Ph.D.

Jason Huse, M.D./Ph.D.

APPROVED:

Dean, The University of Texas

MD Anderson Cancer Center UTHealth Graduate School of Biomedical Sciences

Modeling of CNS Cancer with a Focus on the Immune Component

A

Dissertation

Presented to the Faculty of

The University of Texas

MD Anderson Cancer Center UTHealth

in Partial Fulfillment

of the Requirements

for the Degree of

Doctor of Philosophy

by

Daniel Bernard Zamler B.Sc.

Houston, Texas

May, 2022

Modeling of CNS Cancer with a Focus on the Immune Component

Daniel Bernard Zamler B.Sc.

Advisory Professor: Giulio Draetta, M.D./Ph.D.

Co-advisory Professor: Jian Hu Ph. D.

The knowledge surrounding cancers of the central nervous system remains poorly developed, in particular with regard to the immune component. The works contained in this thesis look at craniopharyngioma, glioblastoma, and several forms of brain metastasis. While some attention is given to the tumor cells themselves, as well as the patient setting which these studies model, the immune component of disease progression and treatment plays a strong role in each and is the primary focus of the works contained.

Craniopharyngioma is a relatively rare tumor in adults. Although histologically benign, it can be locally aggressive and may require additional therapeutic modalities to surgical resection. In the first set of experiments contained within, multiplatform analyses including next generation sequencing, chromogenic and *in situ* hybridization, immunohistochemistry, and gene amplification were used to profile craniopharyngiomas (n=6) to identify frequent therapeutic targets. Sixty-seven percent of patients had the *BRAF V600E* missense mutation, frequent in the papillary craniopharyngioma subtype. One patient had a missense mutation in the WNT pathway, specifically a mutation in *CTNNB1* associated with the adamantinomatous subtype. Craniopharyngiomas lacked microsatellite instability, had relatively low tumor mutational burden, but did express PD-L1 protein, indicating potential use therapeutic use for immune checkpoint inhibition. We identified mutations not previously described, including an *E318K* missense mutation in the *MITF* gene, an *R1407* frameshift in the *SETD2* gene of the

PIK3CA pathway, *R462H* in the *NF2* gene, and a *I463V* mutation in *TSC2*. Two patients testing positive for epidermal growth factor receptor (EGFR) expression were negative for the EGFRvIII variant. Herein, we identified several alterations such as those in *BRAF V600E* and PD-L1, which may be considered as targets for combination therapy of residual craniopharyngiomas. We hope that these insights may lead to better treatment of patients with this disease in the future.

Novel therapeutic strategies, including immunotherapeutics, targeting glioblastoma (GBM) often fail in the clinic, at least partly because available preclinical models do not recapitulate the human disease. To address this challenge in our second set of experiments, we took advantage of our previously developed spontaneous *Qk/trp53/Pten* (QPP) triple-knockout model of human GBM and compared its immune microenvironment components with those of patient-derived tumors in effort to determine whether this model might provide an opportunity for gaining insights into tumor physiopathology as well as for preclinical evaluation of therapeutic agents. Immune profiling analyses and single-cell sequencing of implanted and spontaneous tumors from QPP mice as well as from GBM patients revealed intratumoral immune components that were predominantly myeloid cells (e.g., monocytes, macrophages, and microglia) with minor populations of T, B, and NK cells. When comparing spontaneous and implanted mouse samples, we found that there were more neutrophils, T and NK cells in the implanted model. Neutrophils, T and NK cells were increased in abundance in samples derived from human high-grade glioma (HGG) compared to those derived from low grade glioma (LGG). Overall, our data demonstrate that our implanted and spontaneous QPP models recapitulate the immunosuppressive myeloid dominant nature of the tumor microenvironment of human gliomas. Our model provides a suitable tool for investigating the complex immune compartment of gliomas and it may contribute to a better understanding of the resistance of human glioblastoma to currently available immunotherapeutics. Given that we established the QPP model as viable for immune

studies we next sought to pursue a therapeutic target in the form of Arginase-1 using this system.

An average GBM has roughly 30% infiltration of myeloid cells, the highest reported case at 70% infiltration, with some variation dependent on subtype. When we consider this fact in combination with the advent and success of immunotherapies in similar cancer types, the logical next step follows that myeloid cells, which are of the immune lineage, have the potential to clear this aberrant growth. Known for their incredible phagocytic capacity, myeloid cells are among the first responders to an injury to control pathogens and clear apoptotic cells from the site of an insult. Myeloid cells, through poorly understood mechanisms, undergo a switch after 3-5 days from attacking pathogens and clearing dead cells to secretion of growth cytokines to promote wound healing. We posit these myeloid cells may be tricked into erroneously supporting the tumor cells in an attempt to “heal the wound” instead of mounting an immune response. The enzyme responsible for this switch from pathogen response to wound healing is called Arginase-1 (Arg1). When Arg1 is upregulated, it has a two-pronged effect, the first is creation of peroxynitrite which is actively immunosuppressive to both myeloid and T-cells. The second is an increase in ornithine when Arg1 cleaves arginine into ornithine and urea, which can be used to create the building blocks for cellular growth as well as to create collagen, which is necessary for wound repair and found in high levels in brain tumors. Our hypothesis is that through manipulation of the Arg1 axis in myeloid cells we will increase anti-tumor response. We show the groundwork for evaluating whether or not this is a viable therapeutic target in GBM as well as assess currently available compounds for inhibition of Arg1 in the CNS.

It is a truism in cancer medicine that 90% of deaths are caused by cancer metastasis. While unfortunately difficult to collect information on, there are datasets that suggest the trend in increased metastatic cancer deaths has outpaced primary cancer deaths in recent decades.

Metastasis to the brain is a large cause of mortality and roughly 300,000 cases are diagnosed annually. In an effort to address this urgent patient need we aimed to build a library of metastatic tumor models that were representative of the patient population and determine whether the models could be used for preclinical utility. We first assessed the growth patterns, latency and penetrance of our models and found that in general models tended to grow or not with little impact on survival from starting cell number. We came across several modeling problems including lack of engraftment and extracranial growth of tumors that presented challenges for modeling certain types of metastases to the CNS. We next chose to put several of our models through a battery of therapeutic regimens including Csfr1 inhibition, checkpoint blockade in the forms of anti-Pd-1 and anti-Lag-3 monoclonal antibodies, as well as radiotherapy. We used these single agent studies to inform upon potentially synergistic combinations that would then inform upon clinical trials.

Table of Contents

Approval Page..... i

Title Page	ii
Abstract	iii
Table of Contents	vi
List of Figures	ix
List of Tables	xi
Introduction	1
Chapter 1 – Craniopharyngioma	9
Results	9
Demographics.....	9
Craniopharyngiomas are genomically stable but express PD-L1	10
Craniopharyngiomas express a variety of mutations with known pathogenic effects	14
Craniopharyngiomas overexpress EGFR.....	15
Discussion	15
Chapter 2 – Immune Profiling of QPP Models and Human Glioma	20
Results	20
Comparison of the QPP models to Glioblastoma.....	20
Comparison of the immune infiltrates of QPP models to Glioma.....	24
Comparison of the diversity of immune species in QPP and human disease	282
Discussion	293
Chapter 3 – Arginase as a target in GBM	298
Results	298
Investigate the Cellular Role of Arg1 on Immune Cell Function in Normal Brain and GBM	298
Determine the Impact of Arginine Metabolism in Glioma Progression.....	301
Discussion	311
Chapter 4 – Modeling Brain Metastasis	314
Results	314
Implantation of Cell Line Library	314
Radiotherapy	322
Immune Modulation	323
Discussion	326
Discussion	329
References	332
Material and Methods	352
Study population.....	352
Mouse Models	352
Cell Lines.....	352

Patient Data	352
Genetic analysis	352
Gene amplification and expression	353
Materials Availability	354
Data and Code Availability.....	354
KEY RESOURCES TABLE	355
Cell lines.....	356
Murine glioma models.	356
Immunohistochemistry.	357
Single-cell sequencing.	358
Gene Ontology Analysis.	361
Phenoptics	361
<i>Vita</i>.....	362

List of Figures

Figure Number	Page Number
Figure 1 – Representative IHC Craniopharyngioma.	15
Figure 2 - Histopathological staining of representative QPP gliomas arising spontaneously or implanted in mice, displaying the hallmark features of glioblastoma.	22
Figure 3 - Survival and tumor mutational burden (TMB) of QPP Models.	25
Figure 4 - Immune profiling of spontaneous and implanted QPP tumors and human glioblastoma.	35
Figure 5 - Comparison of freshly isolated naïve mouse brains and previously frozen naïve mouse brains.	38
Figure 6 - Quality control metrics for the spontaneous QPP dataset.	40
Figure 7 - Clustering identifies major immune constituents.	42
Figure 8 - Immune constituents of spontaneous QPP tumors.	44
Figure 9 - Quality control metrics for the implanted QPP dataset.	72
Figure 10 - Immune constituents of implanted QPP tumors.	74
Figure 11 - QPP7 Tumors Show Macroscopic Heterogeneity.	118
Figure 12 - Quality control metrics for the combined QPP dataset.	120
Figure 13 - Comparison of QPP Immune Constituents.	122
Figure 14 - Heterogeneity between QPP mice and glioblastoma (GBM) patients.	165
Figure 15 - Quality control metrics for the glioblastoma (GBM) patient dataset.	167
Figure 16 - Comparison of human GBM and human low-grade glioma (LGG) immune constituents.	187
Figure 17 - Clustering to reveal subtypes.	189
Figure 18 - Lymphoid cell subtypes of human GBM are identified in the QPP model.	362
Figure 19 - Myeloid cell subtypes of human GBM are identified in the QPP model.	364
Figure 20 - Arginine Metabolism in Myeloid Cells.	390
Figure 21 - IHC for Immune Markers in the Naïve Mouse Brain.	390
Figure 22 - Genotyping of Founders of Inducible Arg1 Knock-out Colony.	391
Figure 23 - Dietary L-Arginine Hydrochloride Survival Curve.	392
Figure 24 - mTmG Tracer experiments with Cx3Cr1-Cre ^{ERT2} mice.	393
Figure 25 - Survival of QPP7 cells injected into ACM Mice with Tamoxifen Injection every 2 weeks.	394

Figure 26 - Survival of QPP7 cells injected into ACM Mice with Tamoxifen Injection every week.	395
Figure 27 - Arginase Expression in Control and Tamoxifen Injected Mice.	396
Figure 28 - Inducible Nitric Oxide Synthase Expression in Control and Tamoxifen Injected Mice.	397
Figure 29 - Survival of QPP7 cells injected into ACM Mice with Tamoxifen Slow Release Pellets.	398
Figure 30 - IACS-009102 is a Reversible, Selective, Potent Inhibitor of Arg1 in a Cell-free Setting.	399
Figure 31 - IACS-009102 is a Reversible, Selective, Potent Inhibitor of Arg1 in-vitro.	399
Figure 32 - Distribution of IACS-070400 in Naïve Mice.	401
Figure 33 - Distribution of IACS-070400 in sQPP Bearing Mice.	402
Figure 34 - MRI of Kidney Cancer Models.	411
Figure 35 - MRI of Lung Cancer Models.	412
Figure 36 - Post-mortem Photographs of Skin Cancer Models.	412
Figure 37 - Response of BP and YUMM3.1 Models to 20gY Spatially Fractionated Radiotherapy.	413
Figure 38 - Response of BP and YUMM3.1 Models to Various Immunomodulatory Therapies.	414
Figure 39 - Quantification of Immune Infiltrates of BP Model.	415
Figure 40 - Quantification of Immune Infiltrates of YUMM3.1 Model.	416
Figure 41 - Response of BP and YUMM3.1 Models to anti-Lag-3 Monoclonal Antibody.	417

List of Tables

Table Number	Page Number
Table 1 – Study Demographics.	9
Table 2 – Patient Mutational Profiles.	11
Table 3 – Patient Mutational Profiles GBM.	27
Table 4 – Antibody RRID's.	33
Table 5 - Mouse Spontaneous 0.1 Resolution.	46
Table 6 - Mouse Implanted 0.1 Resolution.	76
Table 7 - Mouse Aggregated 0.1 Resolution.	124
Table 8 - Human Aggregated 0.1 Resolution.	169
Table 9 - Mouse Aggregated 0.65 Resolution.	191
Table 10 - Human Aggregated 0.65 Resolution.	284
Table 11 - Cell Number that Pass QC.	364
Table 12 – Shannon Heterogeneity.	364
Table 13 – Conserved Gene Ontology (GO) pathways from immune isolates of QPP- derived tumors and human GBM.	368
Table 14 – Metastatic Model Library.	406
Table 15 – Survival Statistics for Metastatic Models.	410

Introduction

Cancers of the Central Nervous System (CNS) are a poorly understood subtype of cancer, at least in part due to the fact that there is a relatively poor comprehension of the host organ. Despite this, they affect a large portion of patients and, with rare exception, have poor prognosis. Even more poorly understood is the immune component of CNS cancers. Indeed, as recently as twenty years ago the brain was thought to be strictly an immune privileged organ that was exempt from most forms of immune surveillance. The works contained in this thesis investigate the current state of study of several CNS tumors including craniopharyngioma and glioma with a particular focus on the immune component.

Craniopharyngioma is a rare, benign but heterogeneous tumor of the pituitary stalk, comprising 1-3% of all brain tumors. (Garrè and Cama, 2007) It is the most common childhood supratentorial tumor; however, it has a bimodal age distribution and may be observed in adults between age 50 and the late 70s (Jane and Laws, 2006), who are the focus of these experiments. Two theories have been debated regarding the etiology of craniopharyngioma. The first proposes that craniopharyngioma develop from the transformation of oral ectodermal embryologic remnants of the Rathke pouch, whereas the other hypothesis argues that this tumor originates from metaplasia of the primordial adenohypophysis cells. These tumors are typically treated with surgery; however, residual tumor and recurrence can pose a treatment quandary because little is known about the genetic landscape of these tumors beyond two defining mutations: *BRAF V600E* and *CTNNB1*.

Papillary craniopharyngioma, primarily seen in adults, is associated with *BRAF V600E* mutation (Brastianos et al., 2014) whereas the adamantinomatous type, which is more common in children, is linked to mutations in the β -catenin gene or a mediator of the Wnt pathway *CTNNB1* (Buslei et al., 2005); however, both subtypes have been described in

adults. Craniopharyngiomas are not histologically malignant, but they often are locally aggressive and can thus cause debilitating visual, endocrine, and neurologic symptoms and a decrease in survival. There are two treatment options available, either attempting an aggressive complete resection, or performing a more conservative resection in preparation for adjuvant radiation therapy. Both options have potential complications, including cerebrovascular injury (Lo et al., 2014; Olsson et al., 2015) neurocognitive decline (Fjalldal et al., 2013), and metabolic alterations (Ahmet et al., 2006) including frequent panhypopituitarism (Lo et al., 2014). Furthermore, the partial resection and radiation therapy combination leaves residual tumor, which can lead to recurrence and repetitive surgical risks (Gutin et al., 1980). Consequently, genetic profiling may provide insight into new therapeutic strategies and a better understanding of the etiology, development and progression of these tumors. As such, we hypothesized that sequencing for cancer hotspot mutations may reveal novel therapeutic targets that could be considered in scenarios where patients have subtotally resected or unresectable craniopharyngioma. In the first set of experiments contained herein we performed cancer hot-spot sequencing of six craniopharyngiomas, provide descriptive demographics as well as the results of the mutational profiling and discuss potential therapeutic avenues of the future.

The second set of experiments looks into a newly developed model of glioblastoma and how the model compares to what is observed in the patients. While this paper confirms and expands previous observations about the tumor cells themselves, the body of the work investigates the immune response to the mouse model and how it compares to the immune response of the human disease. Efforts to advance novel drugs to treat another type of primary brain tumor, glioblastoma (GBM), have yet to substantially impact disease outcome despite it being the most common brain tumor. GBM thus remains the deadliest primary brain tumor, with a dismal median survival of only 15 months. Immunotherapies have

substantially improved clinical outcomes in some indications, and patients with certain cancers previously recalcitrant to treatment have experienced disease remission or cure (Gubin et al., 2018). Unfortunately, current immunotherapeutic strategies have not provided clinical benefit for most patients with GBM, probably owing to several factors, including T cell exhaustion and sequestration in the bone marrow, significant inter- and intra-patient heterogeneity, lack of synergy with standard-of-care treatment, low tumor mutational burden (2.7/megabase [MB] average), and presence of an overwhelming intratumoral immune-suppressive myeloid cell population (Chongsathidkiet et al., 2018; Woroniecka et al., 2018) (Chalmers et al., 2017)(De Groot et al., 2018). In GBM, tumor-associated myeloid cells (TAMs), which likely originate from both tissue-resident microglia and monocytes recruited from the peripheral circulation, are heterogeneous and can act in either an immunostimulatory or immunosuppressive capacity. The functions of the various TAM subpopulations remain unclear, and this issue is further confused by the lack of standardized nomenclature to describe TAM subpopulations. Notably, the TAM infiltrate of GBM remains understudied relative to infiltrating T cells in GBM, likely attributable to the success achieved by targeting T cells in other solid tumor types.

Currently, the most used preclinical model of GBM is the GL261 mouse glioma system. While tumors from GL261 mice can grow in syngeneic animals, compared to human GBM, these allograft tumors have low clonotypic diversity, are more highly antigenic, and have a higher tumor mutational burden (TMB; ~4978 mutations per MB) (Johanns et al., 2016). High TMB is associated with improved anti-tumoral efficacy of immune checkpoint blockade (ICB), and the high TMB in GL261 allografts might contribute to the anti-tumor efficacy of ICB that has been observed using drugs which have then gone on to fail in human clinical trials (Genoud et al., 2018).

To address the need for a preclinical model of GBM that more closely recapitulates the human tumor immune microenvironment, we characterized our immunocompetent murine spontaneous GBM model, (Shingu et al., 2017) which harbors deletion of three common tumor suppressor genes in human gliomas: Quaking (*Qk* in mouse and *QKI* in human) (Verhaak et al., 2010), *trp53* (Cerami et al., 2012a), and *Pten* (Cerami et al., 2012a). Termed QPP mice, this model uses an inducible cre-lox recombination system to delete the aforementioned genes under a *nestin* promoter that is expressed in neural stem cells, and QPP mice develop tumors with histopathological features of human GBM. The histopathological and transcriptomic heterogeneity observed among spontaneously arising tumors in QPP mice can manifest as any one of the four TCGA-described human GBM subtypes: proneural, classical, mesenchymal or neural [Shingu et al., 2017]. This model and the original description of the histopathological features and heterogeneity of the tumor are originally described in Shingu et al., 2017, and the model may be obtained by contacting Dr. Jian Hu.

Originally identified as an RNA-binding protein (Ebersole et al., 1996), *QKI* also binds directly to DNA (Shin et al., 2021; Zhou et al., 2021), and its RNA/DNA binding activity promotes the transcription of genes involved in lipid metabolism in oligodendrocytes, lens epithelial cells, and microglia (Ren et al., 2021; Shin et al., 2021; Zhou et al., 2021, 2020). *QKI* is mutated or deleted in approximately 34% of human glioblastomas (30% hemizygous deletions, 2% homozygous deletions, 2% mutations) (Brennan et al., 2013). In addition, *QKI* downregulation by methylation of the *QKI* promoter was reported in 50 (20%) of 250 GBM samples (Chen et al., 2012). The significance of *QKI* deregulation in brain tumors is further highlighted by the observation that 90% of angiocentric gliomas, a type of low-grade pediatric glioma, contain *MYB-QKI* fusions, which transform cells by concomitantly activating *MYB* and suppressing *QKI* (Bandopadhyay et al., 2016; Qaddoumi et al., 2016).

Here, we characterize the immune microenvironments of spontaneous and allograft QPP tumors, as well as patient-derived tumors. Immunohistochemistry (IHC) and single-cell sequencing (scSeq) analyses of immune infiltrates determined that both spontaneous and allograft QPP tumors broadly recapitulated the intratumoral heterogeneity and inter-patient variability of human gliomas. Overall, mouse and human tumors were infiltrated by similar immune cell populations, both regarding the type and proportion of immune cells present. Our findings indicate that QPP tumors are infiltrated by immune cells that broadly recapitulate the immune microenvironment of human GBM, and that the QPP mice represent an important preclinical model to investigate the factors that influence the response of GBM to immunotherapeutics.

Once we established that the QPP models were suitable for performing immune studies in GBM we aimed to look at a therapeutic target using this system. The third set of experiments in this thesis are describing a potential therapeutic target for glioblastoma nestled in the immunotherapeutic category. Specifically, these experiments focus on an enzyme Arginase-1 that is expressed in the myeloid arm of the immune system and is one of the canonical markers for Tumor Associated Myeloid cells (TAMs). These experiments are ongoing and may hopefully lead to a targeted therapy. Recent advancements in immunotherapies have been paradigm shifting for cancer treatment, even for diseases with immunosuppressive tumor microenvironments (e.g. melanoma). However, clinical trials testing anti-PD-1/PD-L1 and anti-CTLA-4 drugs in GBM have been cut short due to lack of efficacy. One possible reason for failure is that T cell infiltration is relatively poor in GBM compared to tumor types where immunotherapy has been effective. Further, GBM tumors are unique because the “immune privileged” microenvironment of the brain is different than that of any other organ in the body (i.e. CSF vs. blood). Thus, there persists an urgent clinical need

to develop mechanism-based immunotherapeutic strategies against glioma and, in particular, the need for approaches that address the unique immune compartment of GBM. To these ends, factors regulating immune system-tumor crosstalk in the GBM microenvironment must be identified.

Studies have conservatively estimated 30% myeloid cell infiltration in GBM, with some estimates as high as 70%. (Geraldo et al., 2019) Arginase-1 (Arg1) is a canonical marker for tumor-associated myeloid cells (TAMs). In normal physiology, Arg1 is the final enzyme of the urea cycle, where it converts L-arginine to urea and L-ornithine to feed essential bioenergetics pathways and detoxify nitrogen from protein degradation. (Caldwell et al., 2018) The function of arginine metabolism is appreciated in several physiological contexts, including pathogen response in myeloid cells, and there is some limited research to suggest that targeting this pathway in glioblastoma may prove useful. (Miska et al., 2021; Pilanc et al., 2021)

During pathogen response, myeloid cells and neutrophils are amongst the first responders and quickly initiate production of reactive oxygen species (ROS) and reactive nitrogen species (RNS) to clear pathogens and dead cells. After 3-5 days, macrophages begin to upregulate Arg1 and transition to an alternatively activated state to promote wound healing. This upregulation of Arg1 has a two-pronged effect: 1) increasing L-ornithine, which is shunted into polyamine and collagen synthesis pathways and supports a growth-conducive microenvironment for tumors; and 2) over-competition with inducible nitric oxide synthase (iNOS) for the shared substrate arginine, which yields uncoupling of iNOS, producing superoxide molecules and peroxynitrite that are immunosuppressive to both myeloid and T cells. (Caldwell et al., 2018) Overall, these findings suggest that upregulation of Arg1 may play a role in promoting oncogenic microenvironments.

Given the prevalence of TAMs in the GBM tumor microenvironment and their upregulation of Arg1, I hypothesized that manipulation of arginine metabolism will impact

TAM function and can influence GBM growth. I further hypothesized that altered arginine metabolism in TAMs will affect T cell function in GBM through production of peroxynitrite and deprivation of extracellular arginine. This research holds high translational potential, as it represents a novel approach to identify a biological mechanism that may harness the brain immune microenvironment to attack GBM cells. Although these experiments have not had the originally predicted impact we hope that, with careful systems biology considerations of the system, we will have an effective therapy by the end of this work.

The final set of experiments contained in this thesis focus on modeling of tumors that metastasize to the brain. It is an upsetting truism in cancer that 90% of deaths are caused by metastasis. It is difficult to find data on this phrase but there is one dataset from Norway that indicates primary cancer deaths remained stagnant over the period of 2005-2016 and metastatic cancer deaths nearly tripled. (Dillekås et al., 2019) Brain cancer metastasis occurs in a large patient population with a, almost universally, poor prognosis. While there have been some advances, namely targeted therapies and checkpoint blockade, unfortunately more failures exist. In these experiments we aimed to first establish a landscape of potential models for CNS metastasis, expose them to various therapeutic modalities with real world clinical implications, and then determine how they performed in these studies and potentially in further ones.

For this set of experiments we chose to focus on four primary tumor types that metastasize to the brain, namely lung cancer, melanoma, kidney cancer, and breast cancer. (Internò et al., 2021; Shen et al., 2022) We began by acquiring a library of cancer cell lines from each of these indications including 3 melanoma lines, (Cooper et al., 2014; Meeth et al., 2016) 2 NSCLC lines, (Gibbons et al., 2009) 2 MDST Breast cancer lines, (Federico et al., 2017) and 2 internally developed RCC Kidney cancer lines. We implanted all these lines heterotopically into the striatum of immunocompetent mice of the same genetic background

in varying numbers and found that penetrance and latency move by small amounts but altering the number of cells implants but for the most part they engraft or not with a similar latency and penetrance. The ultimate aim of this project, through partnership with the brain metastasis clinic, is to first establish models that reasonably recapitulate what is observed in the patient setting, second to test therapeutics first as monotherapies and then as informed combinations to achieve the final aim of launching a clinical trial. The therapeutics tested include radiation, a small molecule to inhibit Colony Stimulating Factor 1 Receptor (Csf1r) on myeloid cells, and two forms of checkpoint blockade targeting Programmed Death 1 (Pd-1) and Lymphocyte activation gene 3 (Lag-3) with monoclonal antibodies. We found that one of our melanoma models was completely sensitive to radiotherapy while the other was completely resistant. That Csf1r inhibition was not effective in either model, and one of our models was sensitive to checkpoint blockade while the other was resistant. After testing these therapeutics, we hope to test combinations based on informed research and are poised to achieve the goal of launching a clinical trial.

The experiments contained in this thesis have made significant contributions the knowledge surrounding CNS cancers. In primary tumor cells available the mutational profile of craniopharyngiomas has been expanded, a mouse model of GBM has been confirmed as similar to the patient setting and expounded upon from previous observations as well as a therapeutic target identified, and several mouse models of cancer metastasis to the brain were characterized. The immune compartment in all these settings has had a particular focus with immunotherapeutic potential discussed in craniopharyngioma, profiling and targeting in the GBM setting, and immunotherapeutics tested in the metastatic setting.

Chapter 1 – Craniopharyngioma

The text in the chapter is based on “Kassab, C., Zamler, D., Kamiya-Matsuoka, C., Gatalica, Z., Xiu, J., Spetzler, D., Heimberger, A.B., 2019. Genetic and immune profiling for potential therapeutic targets in adult human craniopharyngioma. Clin. Oncol. Res. 2, 2–8. <https://doi.org/10.31487/j.COR.2019.03.05>” reprinted with permission from the journal

Results

Demographics

The study cohort included six adult patients who were diagnosed with craniopharyngioma. The patients’ ages ranged from 33 to 78 years, with the median age being 54.5 years. Four patients presented with a newly diagnosed craniopharyngioma, and the disease was metastatic in one patient. The mass was in the suprasellar location in one patient, in the suprasellar region in two, parasellar in one, in the Rathke pouch in one, in the frontal lobe (recurrent) in one, and in an unspecified location in another. Based on histology, 50% of the tumors were papillary, 17% adamantinomatous, and 33% were undefined (**Table 1**).

Table 1: Study demographics

Number of patients (<i>n</i>)	6
Age	
Median, years (range)	54.5 (33-78)
Sex	

Male, <i>n</i> (%)	3 (50%)
Female, <i>n</i> (%)	3 (50%)
Primary, <i>n</i> (%)	4 (66.6%)
Recurrent, <i>n</i> (%)	1 (16.7%)
NOS, <i>n</i> (%)	1 (16.7%)
Type	
• Papillary, <i>n</i> (%)	3 (50%)
• Adamantinomatous, <i>n</i> (%)	1 (16.7%)
• Undefined, <i>n</i> (%)	2 (33.3%)
Location	
• Parasellar, <i>n</i> (%)	1 (16.7%)
• Suprasellar, <i>n</i> (%)	2 (33.3%)
• Rathke pouch, <i>n</i> (%)	1 (16.7%)
• Frontal lobe, <i>n</i> (%)	1 (16.7%)
• NOS, <i>n</i> (%)	1 (16.7%)

NOS: not otherwise specified

Craniopharyngiomas are genomically stable but express PD-L1

To clarify whether craniopharyngiomas expressed biomarkers associated with a potential response to immune checkpoint inhibitors, the tumors were assessed for both MSI and TMB. Of the patients tested (n=4), none showed MSI and all showed a relatively low TMB (**Table 2**).

Table 2: Patient Mutational Profiles

	Patient 1	Patient 2	Patient 3	Patient 4	Patient 5	Patient 6
Microsatellite Instability	NS	NS	Stable	Stable	Stable	Stable
Tumor Mutational Burden	NS	NS	7 per Mb	8 per Mb	6 per Mb	4 per Mb
Mutations of Known Significance						
BRAF		V600E	V600E	V600E		V600E
CTNNB1					G34E	
MITF			E318K			
PIK3CA	Mutated					
SETD2					R140fs	
Commonly Mutated Oncogenes						
ALK	NS	NS	WT	WT	WT	WT
BCL2	NS	NS	WT	WT	WT	WT
BRAF	NS	V600E	V600E	V600E	WT	V600E
KIT	NS	NS	WT	WT	WT	WT

MYCN	NS	NS	WT	WT	WT	WT
HER2	NS	NS	WT	WT	WT	WT
JAK2	NS	NS	WT	WT	WT	WT
KRAS	NS	NS	WT	WT	WT	WT
HRAS	NS	Ind	WT	WT	WT	WT
N-ras	NS	NS	WT	WT	WT	WT
Commonly Mutate Tumor Suppressors						
APC	NS	NS	WT	WT	WT	WT
BRCA1	NS	NS	WT	WT	WT	WT
BRCA2	NS	NS	WT	WT	WT	WT
CDKN2A	NS	NS	WT	WT	WT	WT
SMAD4	NS	NS	WT	WT	WT	WT
Men1	NS	NS	WT	WT	WT	WT
NF1	NS	NS	WT	WT	WT	WT
NF2	NS	NS	WT	WT	R462H	WT
Pten	NS	NS	WT	WT	WT	WT
Rb	NS	NS	WT	WT	WT	WT
TP53	NS	NS	WT	WT	WT	WT
TSC1	NS	NS	WT	WT	WT	WT

TSC2	NS	NS	WT	I463V	WT	WT
Targeted Therapy Status						
EGFR	Positive	Positive	NS	NS	NS	NS
PD-L1	NS	Positive	Positive	Negative	Positive	Positive

NS = Not Studied, Ind = Indeterminate due to low coverage

Tumors in four of the five patients profiled were positive for PD-L1 expression, as assayed by IHC at a cut point of 2+ staining intensity of at least 5% cells (**Figure 1**). All tumors demonstrated some PD-L1 staining.

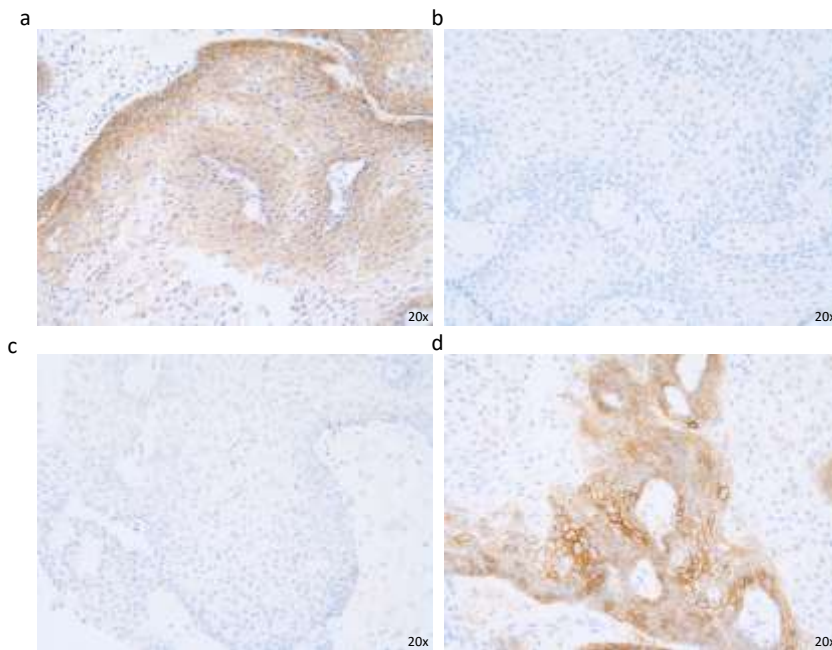


Figure 1: Representative immunohistochemical analysis of (a) the epidermal growth factor receptor (EGFR), (b) Her2, (c) ALK, (d) PD-L1 in tumor cells from patient #2. Staining was positive for expression of both the EGFR and PD-L1, but not for Her2 or ALK. (Magnification = 20X in a through d.)

Craniopharyngiomas express a variety of mutations with known pathogenic effects

Pathogenic mutations known for craniopharyngiomas are summarized in **Table 2**. Sixty-seven percent of patients had mutations in *BRAF*, specifically the *V600E* missense mutation known to be expressed in the papillary subtype of craniopharyngioma. One patient had a mutation in the WNT pathway, specifically a missense mutation in *CTNNB1* typically associated with adamantinomatous craniopharyngiomas. The same patient with mutation in *CTNNB1* also had a mutation in the *NF2* gene—specifically an *R462H* mutation of unknown significance that

may act as a driver. Novel mutations not previously described included an *E318K* missense mutation in the *MITF* gene and an *R1407* frameshift in the *SETD2* gene. One patient had a kinase domain mutation in exon 20 (H1047R) in *PIK3CA* gene that's been reported to activate the PI3K/Akt/mTOR pathway.

Craniopharyngiomas overexpress EGFR

Using fluorescent and chromogenic *in situ* hybridization, we evaluated for amplifications of cMET (n=2) and Her2 (n=3) and no amplification were seen. ALK FISH was tested on one tumor and no gene fusion was detected. RNA sequencing was done on another two tumors and no gene fusion was detected of the 52 genes interrogated. Gene copy number alteration was also evaluated on 442 of the 592 genes sequenced on the four tumors and no amplification event was seen. Immunohistochemistry on EGFR was done in two tumors and showed overexpression on both (2/2).

Discussion

To date, there has not been comprehensive sequencing information or extensive immune profiling reported on craniopharyngiomas. Previous craniopharyngioma sequencing studies have only focused on either codon hotspot mutations in *BRAF* and *CTNNB1* (Brastianos et al., 2014; Hara et al., 2019; Marucci et al., 2015) or evaluations that were limited to 23- or 46-gene panels (Ballester et al., 2017; Goschzik et al., 2017). Immune profiling is limited to one previous study (Coy et al., 2018). As such, we performed genetic sequencing of 592 genes, gene amplification assessments, and immune profiling analysis on craniopharyngiomas to study the TMB, MSI, and genetic alterations that could be further explored as therapeutic targets. Consistent with prior reports, our study found that the *BRAF*

V600E mutation was the most common mutation in craniopharyngiomas, and we also identified another tumor with a *CTNNB1* mutation with a *G34E* substitution (Hara et al., 2019). These two unique mutations have been previously described to occur exclusively in the papillary (*BRAF V600E*) and adamantinomatous (*CTNNB1*) subtypes, respectively, and were proposed to be driver mutations of their correspondent subtypes (Brastianos et al., 2014); however, their single driver oncogenic potential has been questioned (Larkin et al., 2014). Despite the relatively low mutational burden seen in craniopharyngiomas, we found several unique mutations, including one in the melanocyte-inducing transcription factor (*MITF*) gene (*E318K*) and another in the *SET* Domain Containing 2 gene (*SETD2*) (*R1407* frameshift). These two mutations have not been previously described in craniopharyngiomas but are associated with other types of tumors. *MITF* (*E318K*) mutation has been associated with neural crest-derived tumors (Castro-Vega et al., 2016), melanomas (Bertolotto et al., 2011), and renal cell carcinomas, (Bertolotto et al., 2011) whereas the *SETD2* frameshift mutation was previously described in gastrointestinal tumors (Choi et al., 2014). Histone deacetylase (HDAC)-inhibitor drugs could be considered for treatment in the clinical scenario of upregulated *MITF* (Alonso et al., 2008) and *SETD2* inhibitors are currently being investigated in the treatment of leukemia (Chen et al., 2017; Zheng et al., 2012).

The higher the tumor mutational burden is, the more the immune system recognizes the cell as non-self and attacks it. In our study, the levels of TMB and MSI (a condition known as genetic hypermutation) were low, but we observed expression of the PD-L1 immune checkpoint in most samples regardless of the tumor subtype. The utility of a given biomarker such as TMB, MSI, or PD-L1 to correlate with therapeutic response to immune checkpoint inhibitors is lineage dependent and it is unknown if these types of agents would be efficacious for craniopharyngiomas. PD-L1 expression in the stromal fibrovascular core in the papillary subtypes of craniopharyngiomas and on the cystic lining in the adamantinomatous subtypes has been previously described (Coy et al., 2018). In an attempt to find treatment strategies,

Coy et al., specifically looked at overlap between PD-L1 expression and genetic alterations such as *BRAF* papillary and *CTNNB1* mutations. With such substantial overlap between *BRAF* mutations and PD-L1 expression, our combined findings would support consideration of a clinical trial using BRAF/MEK inhibitors in combination with immune checkpoint inhibitors in patients with refractory craniopharyngiomas. This regimen may be used as neoadjuvant for radiation therapy for newly diagnosed or for the treatment of refractory disease. This combination is currently being evaluated for safety and efficacy in melanoma patients (NCT02130466).

Craniopharyngiomas could result from a loss-of-function mutation in a tumor suppressor gene or a gain of function in an oncogene. For loss-of-function mutations, both alleles of a tumor suppressor gene must be lost in order to induce a tumor, unlike the case in oncogenes in which only one allele needs to be mutated. In the current study, we found losses of the neurofibromatosis (*NF*) type 2 (*R462H*) gene and the tuberous sclerosis type 2 (*I463V*) gene, which have not been previously described. *NF2* alterations have been previously shown to be associated with schwannoma, ependymoma, and meningioma (Slattery, 2015), and tuberous sclerosis with ependymoma (MACCARTY and RUSSELL, 1958). It is unclear what role these two genes may play in the underlying development of craniopharyngioma, including in the rare instance of familial craniopharyngioma (G et al., 1984; Green et al., 2002), but this is an area for future investigation. Our molecular profiling also showed that the phosphoinositide-3-kinase, catalytic, alpha polypeptide (*PIK3CA*) gene, which is involved in cellular proliferation and inhibition of apoptosis, was mutated in one case. Somatic mutations of *PIK3CA* are common in a variety of primary tumors such as those of the colon, breast, and stomach. Phosphatidylinositol 3-kinase (*PIK3*) is known to regulate the tuberous sclerosis (*TSC*) tumor suppressor gene (Dan et al., 2002). Both the *PIK3CA* and the *TSC2* mutations were observed in two patients in our study, suggesting that the roles of *PIK3CA* and *TSC2* merit further investigation as to their contributions to the etiology of craniopharyngioma. The

only FDA-approved pan-PIK3 inhibitor is Copanlisib, but it is nonspecific and may have unacceptable toxicity due to off-target effect (Markham, 2017). Specific PIK3 inhibitors are being employed in clinical trials of advanced stage cancers (Janku et al., 2011), and the positive overall response rates and progression-free survival rates being observed for *PIK3CA*-mutant tumors (Juric et al., 2018) may make this a useful therapeutic strategy for a subset of craniopharyngiomas.

The epidermal growth factor receptor (EGFR), but not the EGFRvIII variant, is expressed in craniopharyngiomas, and EGFR upregulation is implicated in cell differentiation, proliferation, apoptosis, and migration of these tumors (Hölsken et al., 2011). Furthermore, EGFR phosphorylation has been shown to enhance adamantinomatous craniopharyngioma cell migration (Hölsken et al., 2010) and has been proposed as an escape mechanism for radiation therapy (Stache et al., 2016). EGFR inhibitors such gefitinib, erlotinib, and lapatinib are now routine treatments in non-small cell lung cancer and breast cancer and could be considered for off-label use in craniopharyngiomas. The response to BRAF inhibitors in papillary craniopharyngioma has shown promise, but the tumor recurs shortly after treatment interruption in most cases (Aylwin et al., 2016). Subsequently, BRAF inhibition combined with the MEK inhibitor trametinib has shown a decrease in proliferation of tumor cells *in vitro* and in preclinical xenograft models (Apps et al., 2018) and produced a dramatic response in a refractory papillary craniopharyngioma case (Brastianos and Santagata, 2016). This is not entirely surprising because this is an established combination strategy for the treatment of melanoma (Flaherty et al., 2012). However, it is unclear whether the genetic variability that underlies each subtype would uniformly demonstrate clinical benefit, but based on the aforementioned data, a clinical trial of this combination would be justified in the adult craniopharyngioma patient population.

We would have liked to profile many more of these cases, as further exploration of several mutations in a larger population is warranted. This is likely to require multicenter efforts

and commitment to increase the sample size and increase the power of such extensive sequencing. Another limitation of the current study is that the sequencing was done from FFPE blocks, resulting in low coverage for some of the genes in the panel sequenced, and thereby their exclusion. We also are unable to associate the genetic findings with prognosis nor to conclude whether their roles are as driver mutations. Moreover, we note that many studies currently focus on the adamantinomatous subtype, taking for granted the high frequency of the *BRAF V600E* mutation and the availability of BRAF and MEK inhibitors, which have demonstrated marked antitumor activity within the CNS (Davies et al., 2017). As such, the current study provides additional justification for the triple combination of BRAF and MEK inhibitors plus immune checkpoint inhibitors.

Chapter 2 – Immune Profiling of QPP Models and Human Glioma

Results

Comparison of the QPP models to Glioblastoma

We characterized immune infiltrates in spontaneous QPP tumors arising in GEMMs as well as in QPP-derived tumors implanted into syngeneic host animals. For the latter, we prioritized our most widely distributed QPP tumor cell line model, QPP7 (**Fig. 2a**), which we confirmed generates tumors with near complete penetrance upon orthotopic implantation into the striatum of C57BL/6J mice (**Fig. 2e**). Both spontaneous and implanted QPP tumors displayed key histopathological features of human GBM, including necrotic areas (**Fig. 2b, f**), invasive leading edges (**Fig. 2c, g**), and a high proliferative index as assessed by Ki67 staining (**Fig. 2d, h**).

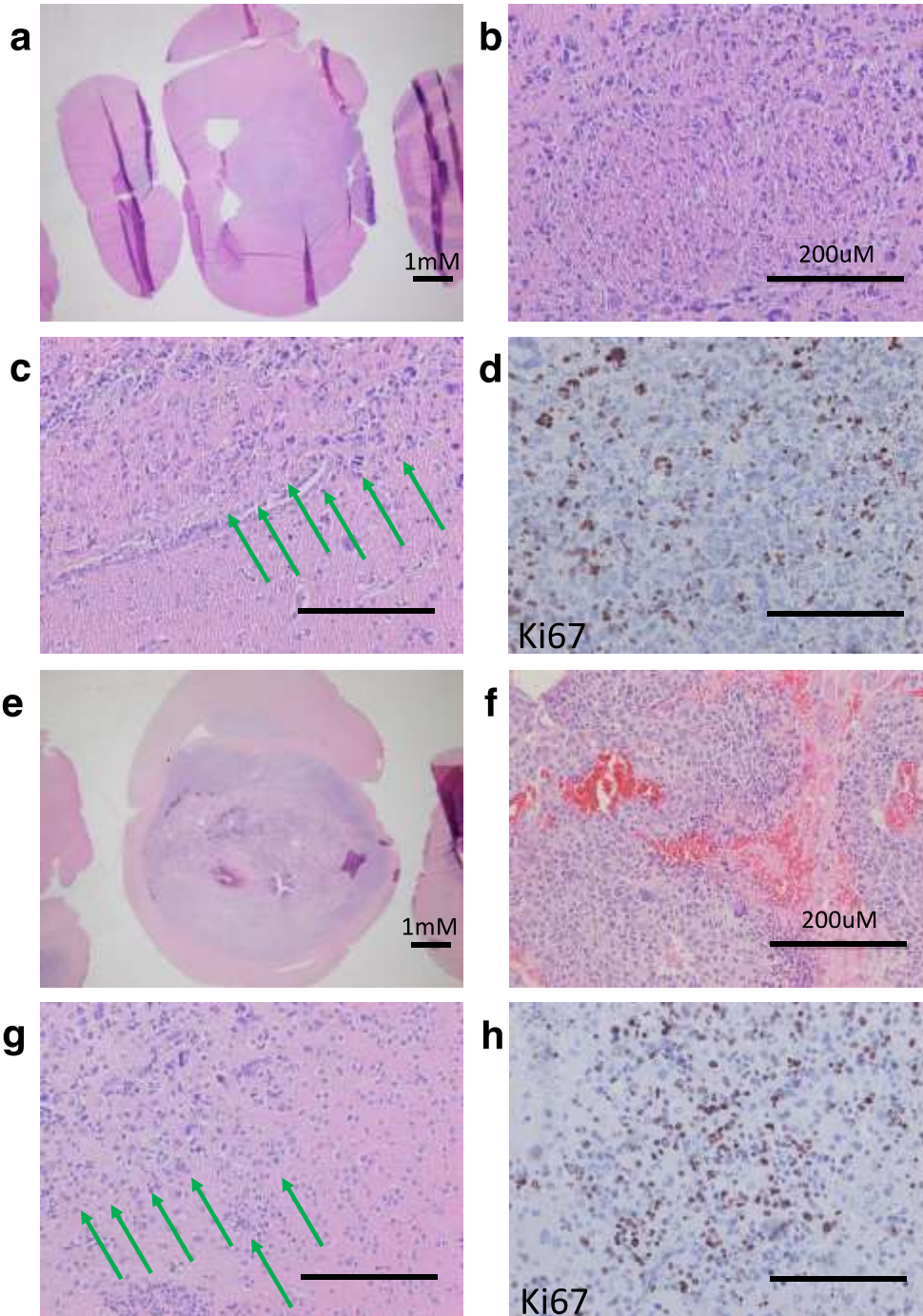


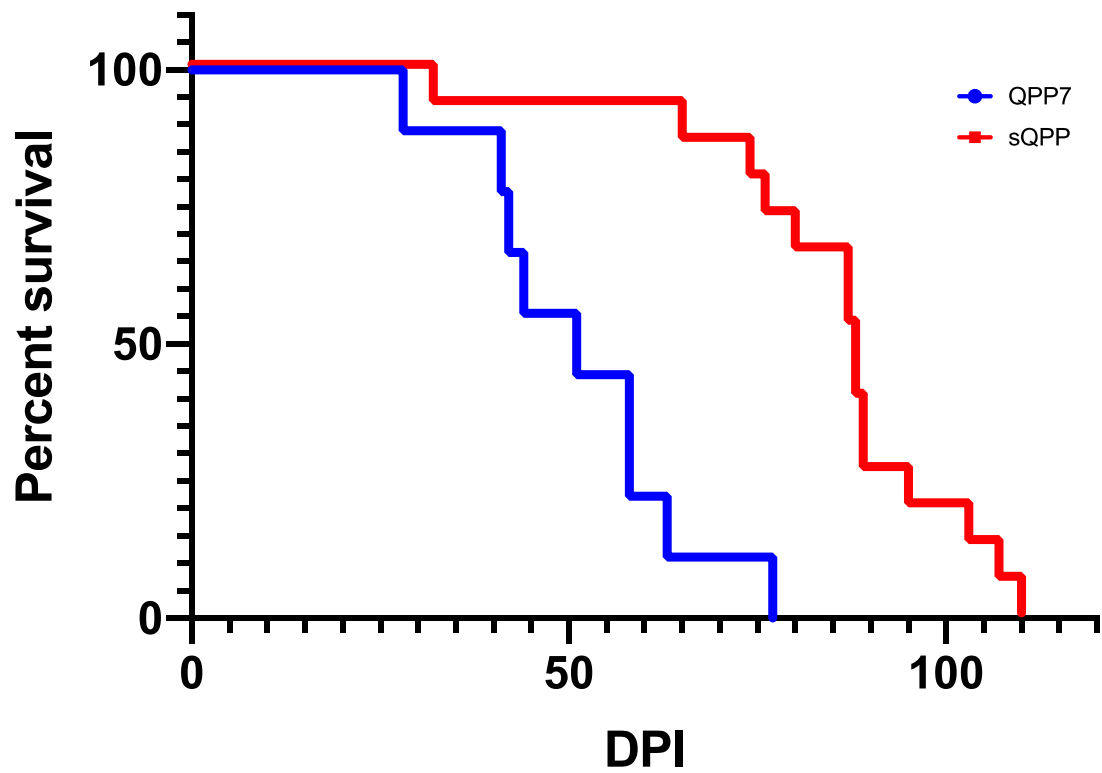
Figure 2: Histopathological staining of representative QPP gliomas arising spontaneously or implanted in mice, displaying the hallmark features of glioblastoma.

a. Representative hematoxylin and eosin (H & E)-stained whole-mount coronal section of brain with spontaneous QPP tumor at 1x magnification. **b.** Necrosis of the spontaneous tumor. **c.** Invasive infiltrating edge of the spontaneous tumor marked by green arrows. **d.** Ki67 staining within the spontaneous QPP glioma demonstrating the high number of active proliferating cells. **e.** Representative H & E-stained whole-mount coronal section of brain with implanted QPP tumor at 1x magnification **f.** Necrosis of the QPP implanted tumor. **g.** Invasive infiltrating edge of the implanted QPP tumor. **h.** Ki67 staining within the implanted QPP border to determine location of proliferating cells. (scale bar = 200 μ M).

GEMM QPP mice developed GBM with 100% penetrance and had a median survival time of approximately 90 days, consistent with previous findings (Shingu et al., 2017). By comparison, mice with QPP7-derived allograft tumors had a median survival time of approximately 45 days which is more aggressive (**Figure 3a**).

To assess the TMB of the two models, we collected matched tumor and tail tissue from five QPP GEMM mice, and we also analyzed tissue derived directly from the spontaneous tumor from which the QPP7 cell line was generated. All tumors used in this analysis harbored the wild type *Idh1* allele. Isolated DNA was multiplexed and sequenced, and we used the standard gatk pipeline to call variants according to the MuTect filters (Auwera et al., 2013; Cibulskis et al., 2013; DePristo et al., 2011; McKenna et al., 2010). TMB values varied among the spontaneous tumors (22.225, 49.225, 8.375, 386.9, and 4.875 mutations/MB), and in the QPP7 tumors, the TMB was 2.775 (**Figure 3b**). By comparison, the reported TMB for GL261 allografts is 4,978 mutations/MB, which is order of magnitude higher than the average human GBM TMB of 2.7 mutations/MB.

a Comparison of Survival of QPP Models



b Tumor Mutational Burden of QPP Models

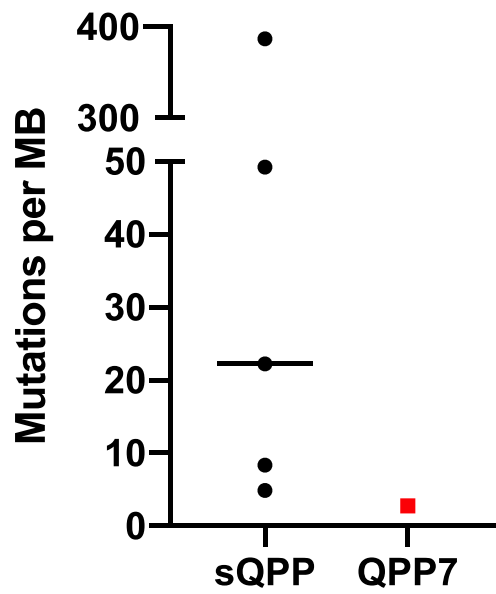


Figure 3: Survival and tumor mutational burden (TMB) of QPP Models.

a. Survival of n=15 QPP mixed background mice injected with 20uL subcutaneous tamoxifen on P7 and P8. Survival of n=9 C57Bl6/j mice implanted with 50,000 QPP7 cells into their striatum. **b.** Tumor mutational burden of n=5 Spontaneous QPP mice and the QPP7 cell line.

Comparison of the immune infiltrates of QPP models to Glioma

Next, immunohistochemistry (IHC) analysis was performed on QPP spontaneous and QPP7 allograft tumors (n = 5 tumors each), and on patient-derived tumor samples (n = 5 samples) using antibodies against major immune constituents. Characteristics of the mouse and human samples are provided in **Table 3**, and the antibodies used are listed in **Table 4**).

Table 3

Current status 12/15/2021	Gender	Diagnosis	Primary or Recurrent	Location	IDH status	Molecular Characterization
Alive	M	Oligodendroglioma grade II	Primary	Right frontal	Mutant	1p19q deletion, 1 and 19 monosomy
Deceased 11/28/2019	M	GBM	N/A	Right temporal	WT	P53 negative, ATRX retained
Deceased 12/19/2019	M	GBM	N/A	Right temporal	WT	BRAFv600e negative, P53 focally positive, ATRX +
Deceased 4/8/2021	M	GBM	N/A	Right frontal	WT	BRAFv600e negative, P53 focally positive, ATRX +
Deceased 10/21/2019	M	GBM	N/A	Right basal ganglia	WT	MGMT methylation negative, Mutation of : TP53, TERT, MBM4, KRAS
Deceased 9/12/2019	F	GBM	Primary	Right temporo-occipital	WT	BRAF negative, P53 5% positive, ATRX retained

Alive	F	DIFFUSE ASTROCYTO MA WHO grade II	Primary	Left frontal	Muta nt	Positive for MGMT promoter methylation, IDH1 protein status (IHC): POSITIVE for mutant IDH1 p.R132H, 1p/19q status (FISH): NEGATIVE for codeletion (isolated 1p deletion; 19q intact) ATRX protein status (IHC): LOSS of expression in tumor cell population p53 protein status (IHC): POSITIVE for nuclear expression (strong, diffuse)
Deceased 10/29/20 20	M	GBM	N/A	Left temporal	WT	No loss ATRX (IHC), TERT 124 promotor mutation, EGFRvIII, +MGMT, MIB=70%
Alive	M	DIFFUSE ASTROCYTO MA WHO grade II	Primary	Left parietal	Muta nt	Negative for MGMT promoter methylation, positive for IDH1 R132H and p53 and negative for ATRX (loss of nuclear

						staining). MIB-1 (Ki67) immunostaining reveals a low proliferation index peaking at 4.2%
Deceased 2/25/2020	M	GBM	N/A	Left parieto-occipital	WT	IDH1 protein status (IHC): NEGATIVE for IDH1 p.R132H expression ATRX protein status (IHC): Retained nuclear expression MGMT status (methylation specific PCR): Negative for promoter methylation
Alive	M	Anaplastic Oligodendroglioma Grade 3	Primary	Frontal	Mutant	IDH1 protein status (IHC): POSITIVE for p.R132H expression ATRX protein status (IHC): RETAINED wildtype nuclear expression p53 protein status (IHC): Nuclear staining in a minor subset (30%) 1p/19q status (FISH):

						POSITIVE for codeletion
Alive	M	Oligodendroglioma grade II	Primary	Frontotemporal	Mutant	IDH1 protein status (IHC): POSITIVE for IDH1 p.R132H expression ATRX protein status (IHC): RETAINED nuclear expression p53 protein status (IHC): NEGATIVE 1p/19q status (FISH): POSITIVE for codeletion
Alive	M	Astrocytoma Grade 4	Primary	Frontal	Mutant	IDH1 protein status (IHC): POSITIVE for p.R132H expression ATRX protein status (IHC): LOSS of nuclear expression p53 protein status (IHC): POSITIVE for nuclear expression (strong, diffuse; 90% of glioma cell population)
Alive	F	Astrocytoma Grade 2	Primary	Frontal	Mutant	IDH1 protein status (IHC):

						<p>POSITIVE for p.R132H expression in glioma cells</p> <p>ATRX protein status (IHC): LOSS of nuclear expression in glioma cells</p> <p>p53 protein status (IHC): Nuclear staining in a major subset of glioma cells (string, diffuse; 80%)</p>
Alive	F	Diffuse ASTROCYTOMA WHO grade II	Primary	Frontoparietal	Mutant	<p>IDH1 protein status (IHC): POSITIVE for p.R132H expression in glioma cells</p> <p>ATRX protein status (IHC): RETAINED wildtype nuclear expression in glioma cells</p> <p>p53 protein status (IHC): Nuclear staining in a minor subset (5%) of glioma cells</p> <p>1p/19q status (FISH): NEGATIVE for codeletion (positive for loss of 1p and</p>

						monosomy 19)
--	--	--	--	--	--	-----------------

Table 4

	Target	Dilution	Catalogue #	Company	RRID
1	CD3	1:200	A045229-2	Agilent	AB_2335677
2	CD4	1:200	ab183685	Abcam	AB_2686917
3	CD8	1:200	98941S	Cell Signaling Technology	AB_2756376
4	Arginase-1	1:250	ab91279	Abcam	AB_10674215
5	LAMP-1	1:100	1D4B	DHSB	AB_2134500
6	NCR1	1:250	ab214468	Abcam	AB_2814876

The immune infiltrate was similar between both spontaneous and implanted QPP tumors as well as between both mouse models and the human tumor samples. Specifically, myeloid and lymphoid infiltrates, including T and NK cells, were detected in all three datasets (antibodies listed in **Table 4**), and the pervasiveness and intensity of myeloid cell markers, including Cd11b and arginase 1, were much higher compared to lymphoid markers in all three tumor models (**Figure 2** and **Figure 4a, b**).

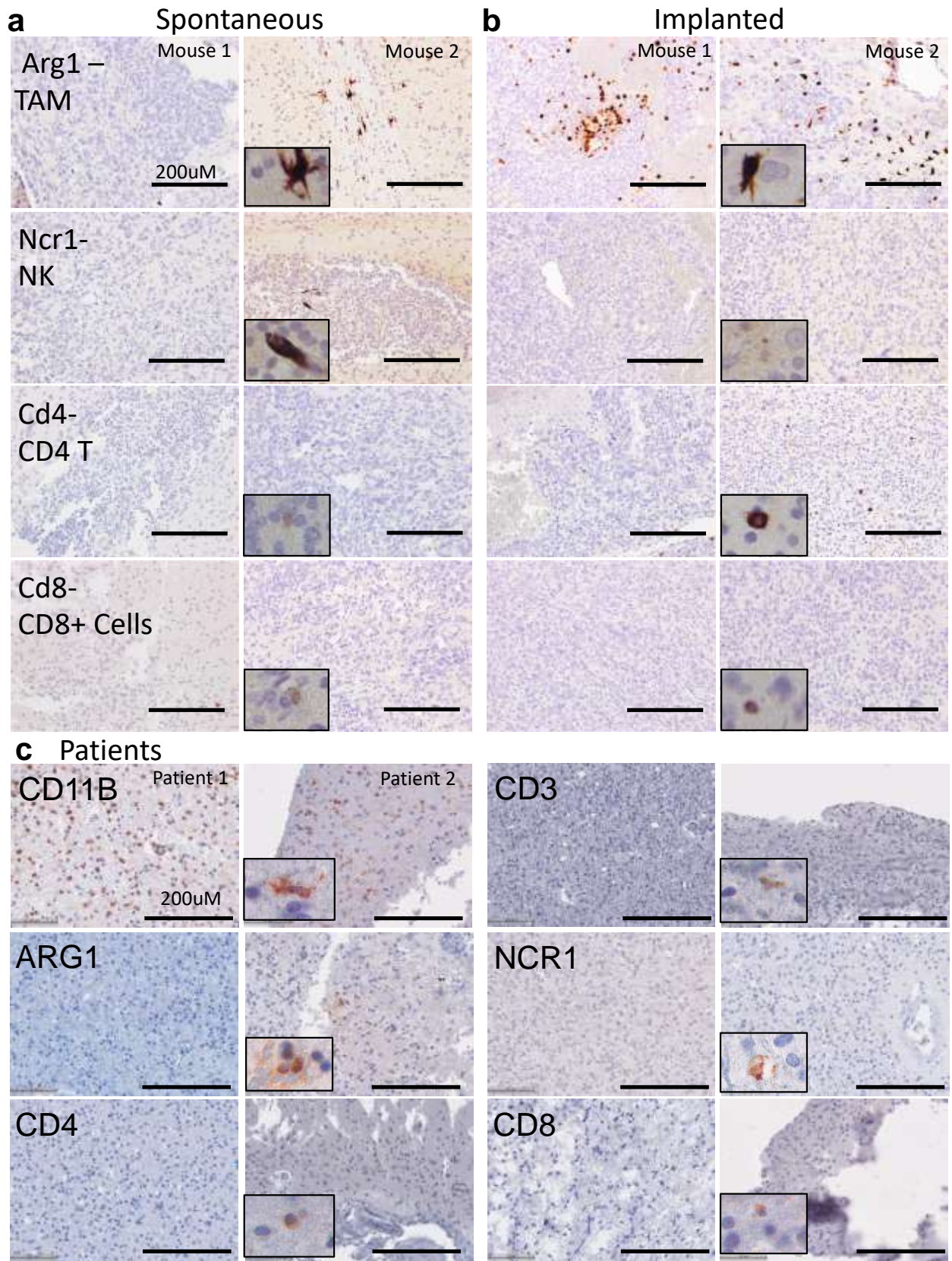


Figure 4: Immune profiling of spontaneous and implanted QPP tumors and human glioblastoma. a-c. Representative images of immunohistochemistry (IHC) analysis of tumors from (a) spontaneous and (b) implanted QPP models as well as from (c) glioma patients.

Only Cd11b, which is expressed on tissue-resident microglia, was detected in non-tumor-bearing control brain tissues isolated from C57BL/6J mice (n = 5 samples; **data not shown**), confirming that these immune cell populations are restricted to the pathogenic brain. These findings align with previous characterizations of GBM tumors (De Groot et al., 2018; Hussain et al., 2006). Quantification of the stains showed that, in both the spontaneous and implanted QPP models, there were significantly more myeloid cells than T cells. In addition, both myeloid and T cell infiltrates were more abundant in the implanted versus spontaneous tumors, and the immune infiltrates were similar to those from the human tumor tissue (**Figure 4c**).

Approaches like IHC use single markers or limited marker profiles to define cell populations, but these techniques may be unable to account for all differences that may exist in the immune cell populations from diverse species. (Mestas and Hughes, 2004) (Shay et al., 2013) (Yue et al., 2014) We then used scSEQ to delineate and compare the specific immune cell populations in spontaneous QPP, QPP7 allograft, and human tumor tissues. Freshly isolated or previously frozen samples from mouse or human GBM tissue was processed using the 10x Genomics (6230 Stoneridge Mall Road, Pleasanton, CA 94588) scSEQ platform. Batch-corrected cohorts of CD45⁺-enriched immune cells from spontaneous (n=3) and implanted (n=3) QPP tumors, as well as from the same cohort of human tumors (n=15) were analyzed. Although small compared to other GBM datasets (Cerami et al., 2012b), our analyses were conducted on purified immune cells, whereas

previous studies have conducted ancillary analyses of immune cells in a mixed population with tumor cells. Our analysis showed that the myeloid and lymphoid constituents were similar between batch-corrected CD45⁺ cells isolated from fresh compared to frozen tumor-free mouse brains (**Figure 5**), indicating that there was no effect of storage on these cell populations.

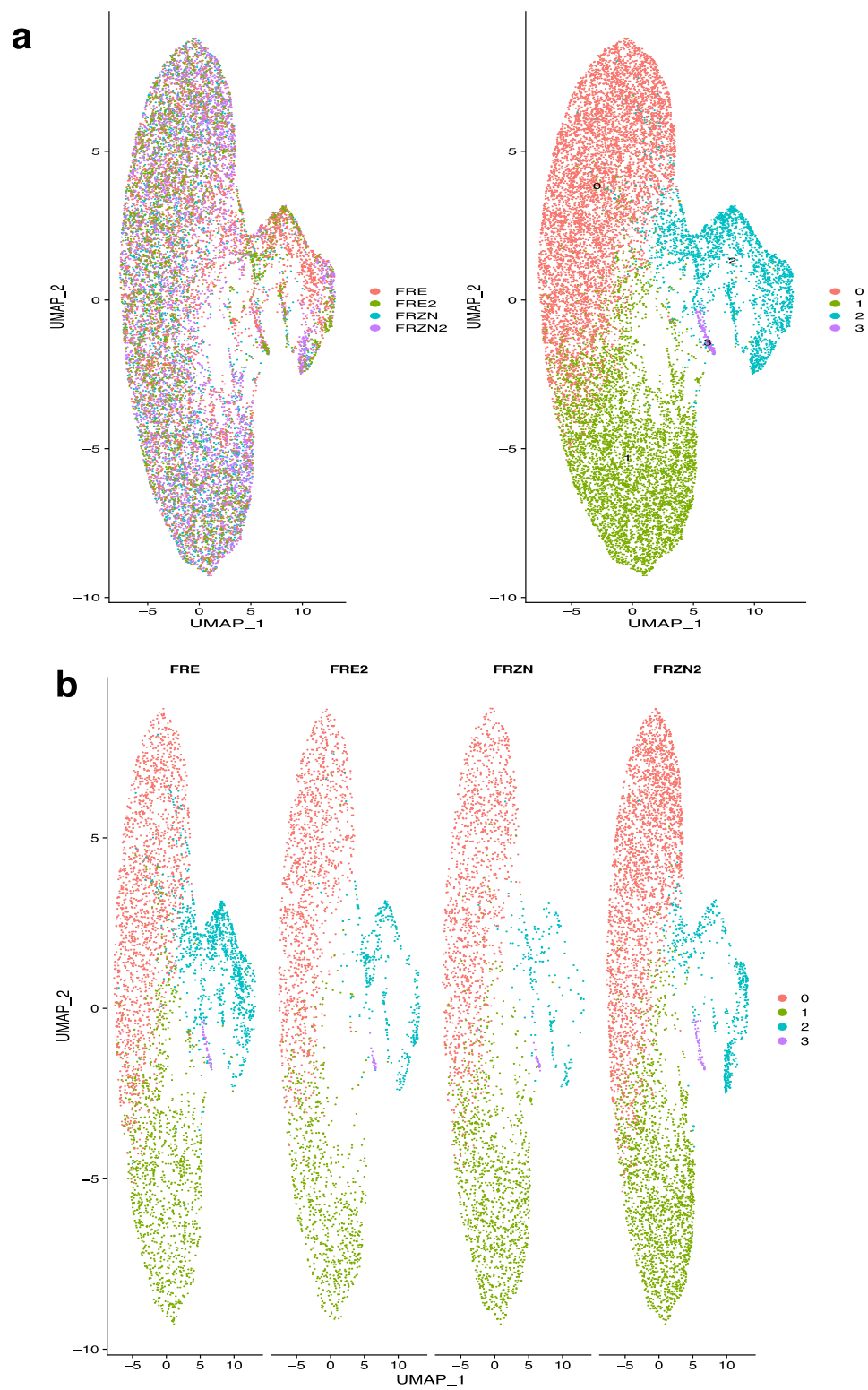


Figure 5: Comparison of freshly isolated naïve mouse brains and previously frozen naïve mouse brains. a. UMAP shows aggregated clustering of CD45+ cells of n=2 freshly isolated naïve mouse brains and n=2 previously frozen mouse brains. **b.** Demonstrates the contributions of individual mice to **a**.

scSeq analysis of spontaneous QPP tumors demonstrated that the majority of intratumoral immune cells were myeloid (**Figure 6**), and four subtypes were identified (**Fig. 7a**): macrophages, microglia (**Fig. 8b**), neutrophils (**Fig. 8c**), and myeloid antigen-presenting-like cells (APCs; **Fig. 8d**). T, B and NK cells were also detected in these samples, but their levels were insufficient for subtype cluster analysis (**Fig. 8e, f, g**). All clusters were defined on the basis of the three representative markers shown in **Figure 8** as well as using a variety of other markers selected from the top differentially expressed genes for that cluster. The full list of genes upregulated for each cluster is presented in **Table 5**.

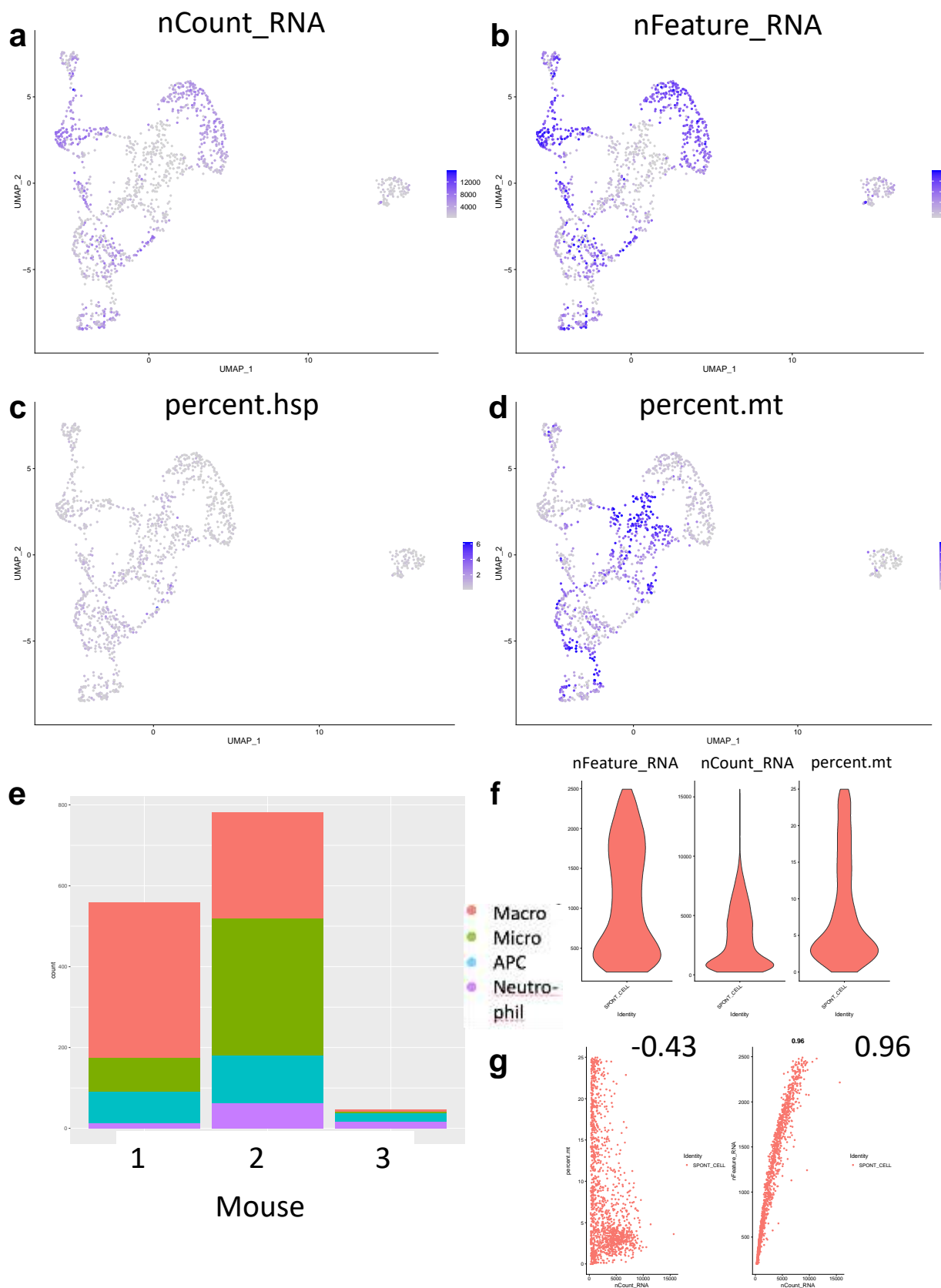


Figure 6: Quality control metrics for the spontaneous QPP dataset. **a.** Featureplot showing the counts of RNA molecules detected per cell. **b.** Featureplot showing the number of unique genes expressed in each cell. **c.** Featureplot showing the percent of heat shock proteins expressed in each cell. **d.** Featureplot showing the percent of mitochondrial RNA molecules for each cell. **e.** Barplot showing the number of cells for each cluster for individual mice. **f.** Violin plot showing the distribution of (left) unique gene counts, (center) RNA molecule counts, and (right) mitochondrial RNA percentage for the dataset. **g.** Scatter plots showing the correlation of (left) mitochondrial percentage to total RNA counts and (right) unique genes to total RNA counts after normalization.

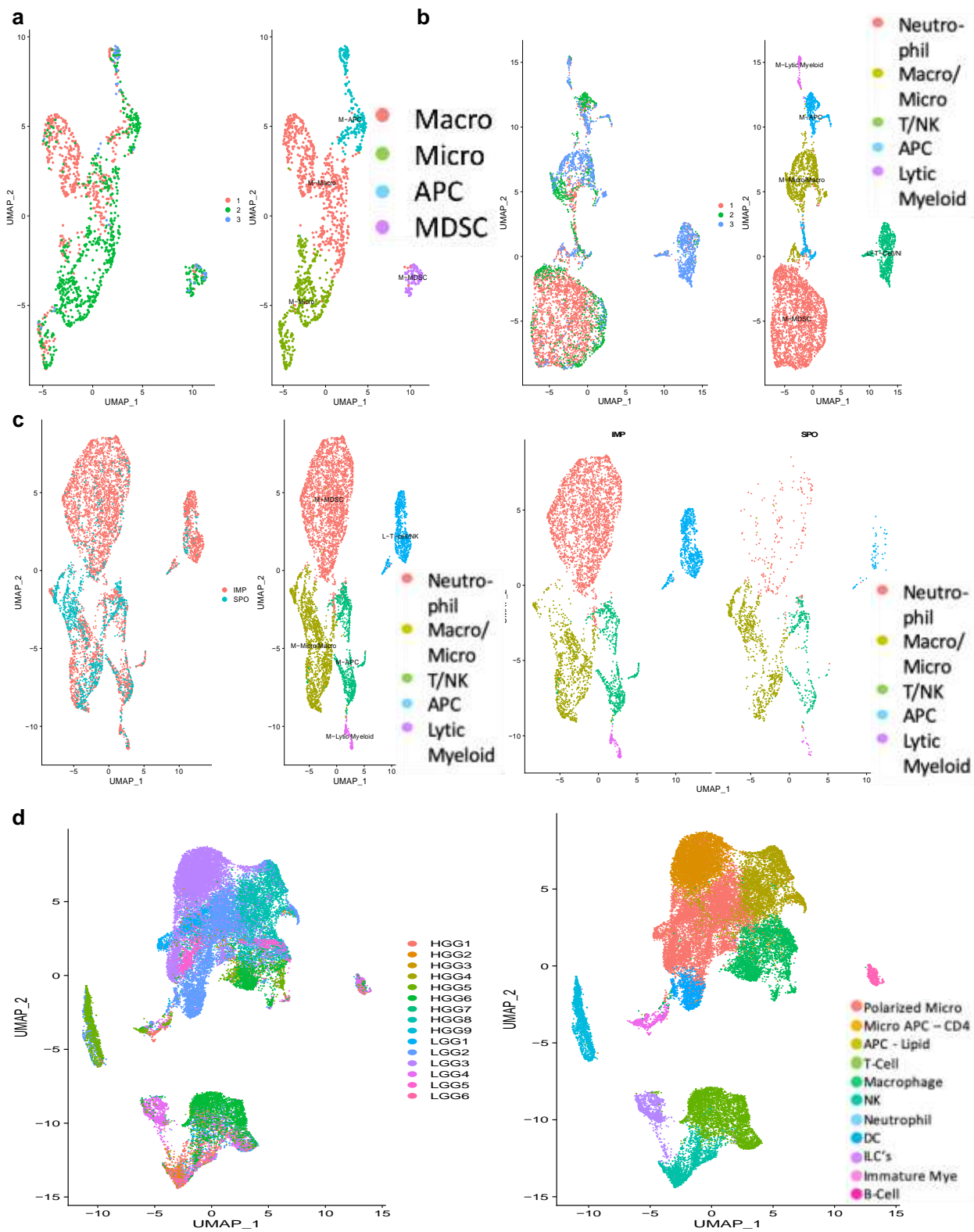


Figure 7: Clustering identifies major immune constituents. Resolution (0.1) **a.** UMAPs of immune constituents from n=3 spontaneous QPP mice are macrophages, microglia, antigen-presenting-like cells (APCs), and neutrophils with 9 PC's determined by elbowplot **b.** UMAPs of immune constituents from n=3 implanted QPP7 mice are neutrophils, microglia/macrophages, T cells/NKs, APCs, lytic myeloid with 9 PC's determined by elbowplot **c.** Comparison of the implanted and spontaneous QPP tumor clusters shows neutrophils, microglia/macrophages, T cells/NKs, APCs, lytic myeloid with 9 PC's determined by elbowplot **d.** UMAPs of immune constituents from n=15 glioma patients are with 20 PC's determined by elbowplot showing clusters of polarized microglia, APC microglia, APCs, T-cells, Macrophages, NK-cells, Neutrophils, DC's, ILCs, Immature myeloid cells, and B-cells.

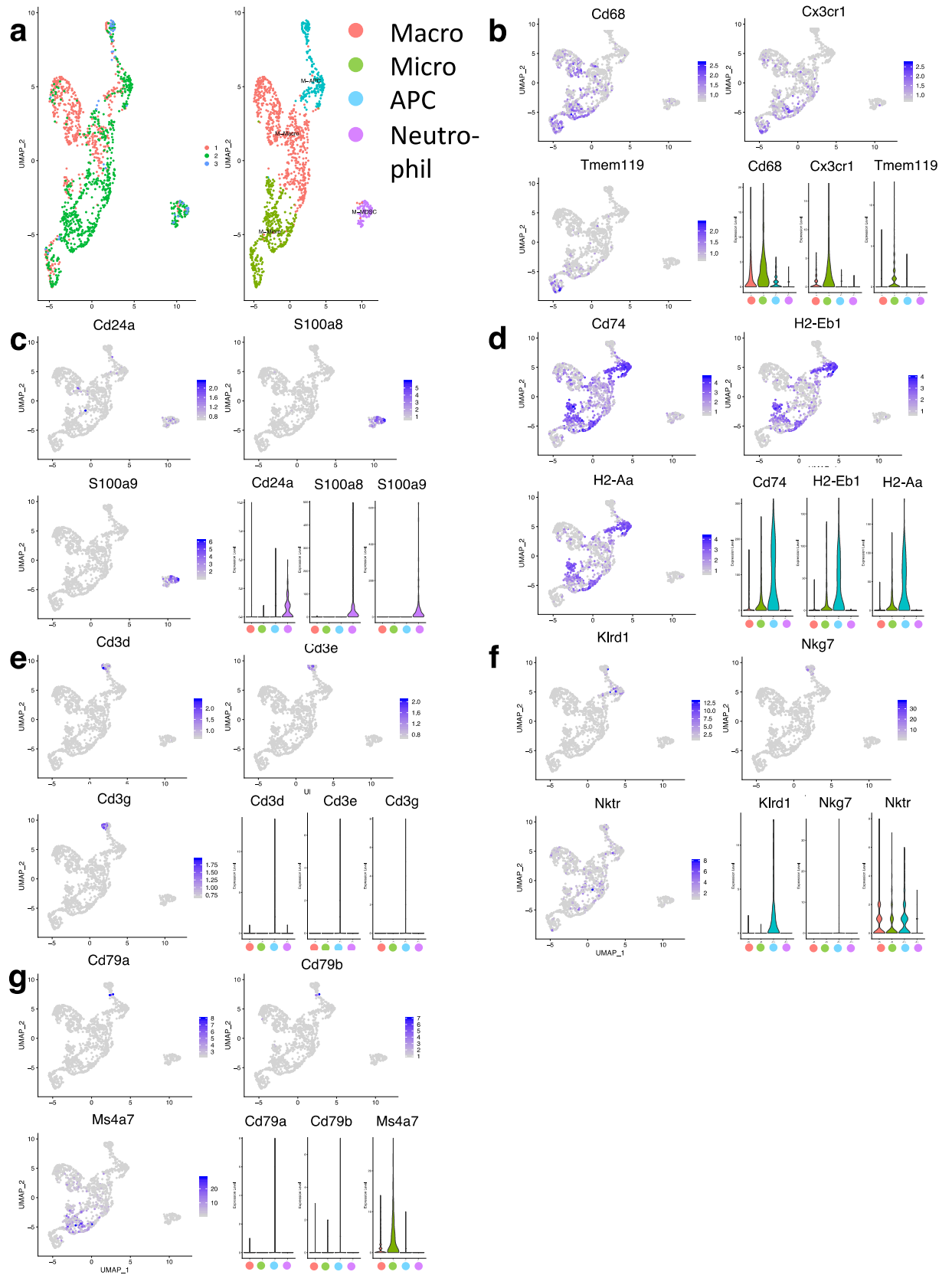


Figure 8: Immune constituents of spontaneous QPP tumors. **a.** UMAPS showing aggregate of CD45+ immune infiltrates from n=3 spontaneous QPP tumors at moribund timepoint. **b.-g.** UMAPS show (b) microglia and macrophage clusters identified by Cd68, Cx3cr1, and Tmem119 markers; (c) neutrophil clusters identified by Cd24a, S100a8, and S100a9 markers; (d) APC clusters identified by Cd74, H2-Eb1, and H2-Aa markers; (e) T-cell clusters identified by Cd3d, Cd3e, and Cd3g markers; (f) natural killer cell clusters identified by Klrd1, Nkg7, and Nktr markers; and (g) UMAPS show B-cell clusters identified by Cd79a, Cd79b, and Ms4a7 markers. All violin plots show the specificity of given markers for macrophages (red), microglia (green), APC (blue), and neutrophils (purple).

Table 5

	Mouse Spontaneous 0.1 Resolution					cluster	gene
	p_val	avg_logFC	pct.1	pct.2	p_val_adj		
Chil3	9.74E-66	1.85619467	0.447	0.063	1.11E-61	0	Chil3
Ly6c2	5.68E-44	1.0671112	0.363	0.061	6.45E-40	0	Ly6c2
Zeb2	4.88E-71	0.97674403	0.813	0.444	5.54E-67	0	Zeb2
Tgfbf	1.80E-61	0.85762002	0.847	0.481	2.04E-57	0	Tgfbf
S100a4	7.77E-42	0.83714382	0.568	0.23	8.83E-38	0	S100a4
Ifitm3	4.78E-44	0.80062064	0.936	0.62	5.42E-40	0	Ifitm3
Plac8	4.50E-49	0.79077007	0.678	0.298	5.11E-45	0	Plac8
Vim	9.71E-31	0.74042636	0.698	0.411	1.10E-26	0	Vim
Fn1	8.86E-44	0.68099725	0.406	0.093	1.01E-39	0	Fn1
S100a6	1.40E-39	0.66011224	0.795	0.452	1.59E-35	0	S100a6
Irf7	1.95E-23	0.63778664	0.398	0.176	2.22E-19	0	Irf7
Mafb	1.97E-44	0.61358085	0.755	0.439	2.24E-40	0	Mafb
Ifi27l2a	3.57E-27	0.61086416	0.851	0.583	4.05E-23	0	Ifi27l2a
H3f3b	5.91E-50	0.59930901	0.995	0.866	6.71E-46	0	H3f3b
Ccr2	5.77E-34	0.59128515	0.511	0.232	6.55E-30	0	Ccr2
Slfn4	2.44E-31	0.57614597	0.259	0.04	2.77E-27	0	Slfn4
Lgals3	1.88E-39	0.54640416	0.85	0.549	2.14E-35	0	Lgals3
Ifi204	4.16E-35	0.52891169	0.395	0.121	4.73E-31	0	Ifi204
Xist	6.23E-27	0.52884297	0.426	0.159	7.07E-23	0	Xist
Ms4a4c	4.18E-22	0.5286296	0.38	0.17	4.75E-18	0	Ms4a4c
Isg15	2.76E-14	0.52045996	0.374	0.199	3.13E-10	0	Isg15
Cebpb	2.69E-45	0.52011754	0.651	0.3	3.06E-41	0	Cebpb
Pid1	2.54E-36	0.51935518	0.412	0.129	2.89E-32	0	Pid1
Tgm2	2.82E-14	0.51764987	0.288	0.138	3.20E-10	0	Tgm2
Prdx5	6.19E-25	0.50557061	0.844	0.65	7.03E-21	0	Prdx5
Jun	9.32E-38	0.49856335	0.786	0.477	1.06E-33	0	Jun
Gm42418	1.11E-20	0.49477643	1	0.999	1.26E-16	0	Gm42418
Lyz2	3.90E-26	0.48627171	0.988	0.714	4.43E-22	0	Lyz2
Malat1	1.33E-27	0.4792525	0.997	0.888	1.51E-23	0	Malat1
F10	2.43E-48	0.46523859	0.274	0.007	2.76E-44	0	F10
S100a10	9.12E-18	0.45039497	0.331	0.14	1.04E-13	0	S100a10
Ifi203	1.26E-24	0.44756536	0.392	0.161	1.43E-20	0	Ifi203
Fos	4.88E-21	0.44661578	0.582	0.364	5.54E-17	0	Fos
Ahnak	7.90E-29	0.44306382	0.337	0.097	8.97E-25	0	Ahnak
Slfn5	2.89E-24	0.43491932	0.386	0.155	3.28E-20	0	Slfn5
Capg	3.02E-26	0.43024941	0.378	0.144	3.42E-22	0	Capg

Son	3.23E-22	0.42849429	0.764	0.58	3.67E-18	0	Son
Parp14	2.41E-31	0.42701132	0.391	0.128	2.73E-27	0	Parp14
Rrbp1	7.00E-20	0.41778735	0.87	0.718	7.95E-16	0	Rrbp1
Crip1	9.87E-17	0.4176421	0.669	0.452	1.12E-12	0	Crip1
Prkcd	3.96E-22	0.40388057	0.459	0.234	4.50E-18	0	Prkcd
Fyb	2.34E-25	0.39611064	0.815	0.584	2.66E-21	0	Fyb
Sat1	2.74E-17	0.39240742	0.873	0.696	3.11E-13	0	Sat1
Samhd1	1.40E-20	0.3862907	0.453	0.243	1.59E-16	0	Samhd1
Neat1	1.72E-15	0.38294213	0.489	0.293	1.96E-11	0	Neat1
Ifi209	5.67E-23	0.36293494	0.302	0.098	6.44E-19	0	Ifi209
Rsrp1	2.57E-16	0.35836407	0.613	0.439	2.92E-12	0	Rsrp1
Ly6e	3.39E-15	0.35569035	0.93	0.772	3.85E-11	0	Ly6e
Mndal	2.27E-14	0.35379472	0.368	0.198	2.58E-10	0	Mndal
Oasl2	2.87E-21	0.34713015	0.335	0.128	3.26E-17	0	Oasl2
Cstb	1.23E-05	0.34457658	0.4	0.316	0.14008343	0	Cstb
Apobec1	1.63E-22	0.33786551	0.384	0.165	1.85E-18	0	Apobec1
Mef2a	4.36E-21	0.32768478	0.407	0.189	4.95E-17	0	Mef2a
Hk2	7.73E-11	0.32386146	0.366	0.226	8.78E-07	0	Hk2
Tmsb10	5.38E-17	0.3185416	0.908	0.688	6.11E-13	0	Tmsb10
Camk2d	3.08E-18	0.31692176	0.366	0.172	3.50E-14	0	Camk2d
Nktr	1.33E-10	0.31681177	0.378	0.245	1.51E-06	0	Nktr
Ifi211	5.69E-26	0.31311426	0.282	0.069	6.46E-22	0	Ifi211
Cwc22	9.19E-09	0.31277301	0.424	0.311	0.00010433	0	Cwc22
Rbm25	1.49E-10	0.30900963	0.444	0.313	1.70E-06	0	Rbm25
Atp2b1	1.81E-10	0.3069918	0.453	0.302	2.05E-06	0	Atp2b1
mt-Co1	4.92E-13	0.30520931	0.998	0.992	5.58E-09	0	mt-Co1
Adap2	1.70E-17	0.30369062	0.296	0.12	1.93E-13	0	Adap2
Lrp1	5.98E-14	0.30367964	0.436	0.257	6.79E-10	0	Lrp1
Cybb	3.20E-16	0.30131744	0.677	0.485	3.64E-12	0	Cybb
Zbp1	4.73E-21	0.30040354	0.305	0.105	5.37E-17	0	Zbp1
Luc7l2	3.35E-08	0.29847434	0.389	0.285	0.00038013	0	Luc7l2
Anxa2	4.36E-08	0.29348975	0.366	0.251	0.00049542	0	Anxa2
Tspo	2.01E-11	0.29214667	0.766	0.625	2.28E-07	0	Tspo
Ifitm6	1.81E-17	0.29087565	0.253	0.083	2.06E-13	0	Ifitm6
Ccnl1	3.63E-13	0.28755742	0.368	0.204	4.12E-09	0	Ccnl1
mt-Nd4	4.35E-06	0.28714767	0.962	0.941	0.04941936	0	mt-Nd4
Emp3	4.53E-08	0.28711137	0.395	0.296	0.00051491	0	Emp3
Pnp	1.47E-07	0.27386887	0.357	0.259	0.00166758	0	Pnp
9930111J21Rik2	3.11E-12	0.26994363	0.383	0.228	3.54E-08	0	9930111J21Rik2
Tgfb1	2.57E-07	0.26953505	0.484	0.402	0.00292354	0	Tgfb1

Emilin2	6.81E-18	0.26932131	0.311	0.124	7.73E-14	0	Emilin2
Msrbl	1.25E-28	0.26606165	0.72	0.429	1.42E-24	0	Msrbl
Ifi207	4.25E-15	0.26414875	0.326	0.157	4.83E-11	0	Ifi207
Ms4a6c	1.37E-18	0.26278783	0.832	0.624	1.56E-14	0	Ms4a6c
Slfn1	1.82E-20	0.26024236	0.334	0.12	2.06E-16	0	Slfn1
Irf2bp2	5.88E-11	0.2573977	0.381	0.237	6.67E-07	0	Irf2bp2
Zufsp	9.78E-15	0.25659434	0.3	0.14	1.11E-10	0	Zufsp
Nisch	4.65E-10	0.25586622	0.331	0.202	5.28E-06	0	Nisch
Rgs2	2.11E-11	0.25541261	0.646	0.481	2.39E-07	0	Rgs2
Tagln2	2.25E-05	0.25519612	0.342	0.257	0.25563939	0	Tagln2
Epb41l2	2.55E-07	0.25443944	0.358	0.257	0.00290072	0	Epb41l2
Klf13	9.26E-12	0.25405396	0.381	0.233	1.05E-07	0	Klf13
Rnh1	3.34E-05	0.25288754	0.343	0.267	0.37963648	0	Rnh1
Sirpb1c	8.79E-23	0.25259776	0.279	0.079	9.98E-19	0	Sirpb1c
Stat1	2.54E-10	0.25109504	0.338	0.198	2.88E-06	0	Stat1
Inpp5d	5.52E-09	0.25011407	0.407	0.283	6.27E-05	0	Inpp5d
Iqgap1	1.16E-07	0.25008037	0.492	0.386	0.00131809	0	Iqgap1
C1qa	1.11E-164	2.26906002	0.955	0.479	1.27E-160	1	C1qa
Apoe	9.19E-147	2.13228283	1	0.734	1.04E-142	1	Apoe
C1qb	4.33E-164	1.99076831	0.962	0.501	4.91E-160	1	C1qb
C1qc	6.63E-171	1.94569463	0.962	0.438	7.53E-167	1	C1qc
Ctsd	1.18E-71	1.57337809	0.901	0.7	1.34E-67	1	Ctsd
Cd81	3.37E-154	1.4733007	0.756	0.079	3.83E-150	1	Cd81
Cd63	2.16E-130	1.41275811	0.854	0.257	2.45E-126	1	Cd63
Hexb	7.01E-104	1.38373635	0.901	0.516	7.96E-100	1	Hexb
Fcrls	2.50E-138	1.29572355	0.667	0.049	2.84E-134	1	Fcrls
Trem2	4.29E-117	1.10250166	0.709	0.122	4.87E-113	1	Trem2
Spp1	6.86E-44	1.06232948	0.394	0.087	7.79E-40	1	Spp1
Selenop	1.02E-116	1.04576583	0.739	0.149	1.15E-112	1	Selenop
Lgmn	8.30E-103	1.02189091	0.951	0.601	9.43E-99	1	Lgmn
Olfml3	3.92E-121	1.00169291	0.66	0.078	4.45E-117	1	Olfml3
Cst3	4.41E-67	0.98034909	0.981	0.931	5.01E-63	1	Cst3
Ctsz	1.13E-82	0.95729459	0.972	0.784	1.28E-78	1	Ctsz
Ctsl	1.06E-65	0.95378039	0.54	0.128	1.20E-61	1	Ctsl
Ctsb	4.71E-73	0.9328628	0.962	0.789	5.35E-69	1	Ctsb
Ctss	2.15E-86	0.93234602	0.991	0.919	2.44E-82	1	Ctss
Tmem176b	2.38E-80	0.79602415	0.69	0.188	2.70E-76	1	Tmem176b
Ctsc	2.48E-47	0.79565698	0.873	0.644	2.82E-43	1	Ctsc
Ms4a7	5.49E-45	0.7708773	0.61	0.246	6.23E-41	1	Ms4a7
Tmem176a	1.17E-74	0.76354583	0.608	0.143	1.33E-70	1	Tmem176a

Lpl	2.01E-72	0.7629371	0.491	0.072	2.28E-68	1	Lpl
Csf1r	3.40E-61	0.72698041	0.878	0.569	3.86E-57	1	Csf1r
Itm2b	2.18E-52	0.72693542	0.974	0.909	2.48E-48	1	Itm2b
Calr	1.22E-58	0.71544582	0.901	0.661	1.39E-54	1	Calr
Hexa	3.46E-81	0.71273036	0.739	0.249	3.93E-77	1	Hexa
Grn	6.03E-46	0.70699664	0.89	0.706	6.85E-42	1	Grn
Trf	8.32E-70	0.6986149	0.636	0.186	9.45E-66	1	Trf
Cx3cr1	1.91E-54	0.67704946	0.613	0.21	2.16E-50	1	Cx3cr1
Cd9	2.75E-35	0.66350131	0.486	0.181	3.13E-31	1	Cd9
Timp2	3.84E-71	0.66016876	0.484	0.078	4.36E-67	1	Timp2
Vcam1	5.74E-60	0.64648098	0.392	0.049	6.51E-56	1	Vcam1
Mt1	5.64E-52	0.62329199	0.477	0.113	6.40E-48	1	Mt1
Pf4	1.12E-63	0.62253272	0.34	0.023	1.27E-59	1	Pf4
Gatm	9.18E-50	0.62134353	0.589	0.206	1.04E-45	1	Gatm
Ctsa	2.52E-50	0.59627965	0.878	0.6	2.86E-46	1	Ctsa
Ftl1	2.91E-37	0.59356918	0.995	0.981	3.31E-33	1	Ftl1
Hsp90b1	1.67E-43	0.59137965	0.838	0.589	1.89E-39	1	Hsp90b1
Itgb5	2.78E-54	0.58828106	0.667	0.237	3.15E-50	1	Itgb5
Ptgs1	3.20E-74	0.58590455	0.467	0.056	3.63E-70	1	Ptgs1
Pdia3	1.93E-48	0.5819207	0.657	0.287	2.20E-44	1	Pdia3
Creg1	2.22E-49	0.57836732	0.585	0.22	2.52E-45	1	Creg1
Aif1	5.11E-45	0.57714628	0.772	0.454	5.80E-41	1	Aif1
Tmem119	8.54E-72	0.57557643	0.408	0.036	9.70E-68	1	Tmem119
Bsg	3.42E-45	0.57414328	0.601	0.243	3.88E-41	1	Bsg
Abhd12	4.83E-58	0.55402387	0.5	0.119	5.48E-54	1	Abhd12
H2-Aa	1.57E-12	0.54850178	0.716	0.644	1.78E-08	1	H2-Aa
Cd74	5.15E-11	0.53355291	0.803	0.764	5.85E-07	1	Cd74
Rplp1	4.82E-38	0.52928563	0.988	0.988	5.48E-34	1	Rplp1
Acp5	8.51E-35	0.52918078	0.418	0.132	9.66E-31	1	Acp5
Pmepa1	4.77E-42	0.52608954	0.573	0.208	5.41E-38	1	Pmepa1
Cd68	1.68E-47	0.52500704	0.876	0.584	1.91E-43	1	Cd68
Pdia6	1.07E-39	0.52123404	0.554	0.222	1.21E-35	1	Pdia6
Psap	1.08E-29	0.51746187	0.984	0.896	1.22E-25	1	Psap
Gusb	2.70E-46	0.50691092	0.523	0.164	3.06E-42	1	Gusb
H2-Ab1	1.53E-11	0.50258825	0.725	0.665	1.74E-07	1	H2-Ab1
Hspa5	1.09E-19	0.49517815	0.824	0.72	1.24E-15	1	Hspa5
Mpeg1	4.72E-32	0.48599447	0.871	0.665	5.36E-28	1	Mpeg1
Syng1	8.36E-51	0.47900835	0.345	0.047	9.49E-47	1	Syng1
Fcgr3	2.79E-43	0.47870186	0.725	0.326	3.17E-39	1	Fcgr3
Mif	3.16E-24	0.47124886	0.509	0.256	3.59E-20	1	Mif

Lamp1	3.57E-35	0.46875858	0.8	0.543	4.05E-31	1	Lamp1
Fth1	7.12E-31	0.46131044	0.995	0.988	8.08E-27	1	Fth1
H2-Eb1	7.86E-11	0.4527198	0.683	0.601	8.93E-07	1	H2-Eb1
Serinc3	1.34E-31	0.45007468	0.556	0.262	1.52E-27	1	Serinc3
Cd72	3.72E-44	0.43620309	0.397	0.083	4.22E-40	1	Cd72
Ly86	1.08E-34	0.43004206	0.674	0.327	1.23E-30	1	Ly86
Fabp5	5.25E-17	0.42757758	0.303	0.118	5.96E-13	1	Fabp5
Itm2c	7.97E-32	0.42302275	0.488	0.203	9.05E-28	1	Itm2c
Rps2	1.43E-22	0.42177819	0.958	0.96	1.63E-18	1	Rps2
Tubb5	1.01E-25	0.4158886	0.481	0.221	1.15E-21	1	Tubb5
Plxdc2	2.32E-50	0.41567455	0.362	0.052	2.63E-46	1	Plxdc2
Rgs10	2.68E-30	0.40883477	0.531	0.233	3.04E-26	1	Rgs10
Rps12	6.83E-25	0.4070861	0.955	0.975	7.76E-21	1	Rps12
Gapdh	7.12E-12	0.40200853	0.908	0.916	8.08E-08	1	Gapdh
Ssr4	1.33E-31	0.39844013	0.678	0.389	1.51E-27	1	Ssr4
Lpcat2	2.18E-35	0.39183722	0.453	0.146	2.48E-31	1	Lpcat2
Adgre1	4.72E-50	0.38977383	0.397	0.073	5.35E-46	1	Adgre1
Tuba1b	3.64E-18	0.37799861	0.413	0.202	4.14E-14	1	Tuba1b
Cxcl16	2.20E-35	0.37463661	0.566	0.214	2.50E-31	1	Cxcl16
Rpl10a	2.44E-18	0.37210824	0.93	0.913	2.77E-14	1	Rpl10a
Bcl2a1b	9.75E-40	0.36796433	0.467	0.135	1.11E-35	1	Bcl2a1b
Tyrobp	1.53E-27	0.362234	0.998	0.931	1.74E-23	1	Tyrobp
Rpl32	6.04E-20	0.36045279	0.962	0.973	6.86E-16	1	Rpl32
Prdx1	5.27E-18	0.36041203	0.646	0.438	5.98E-14	1	Prdx1
Ucp2	7.74E-16	0.36040595	0.831	0.787	8.78E-12	1	Ucp2
Erp29	8.67E-23	0.35939158	0.751	0.533	9.85E-19	1	Erp29
Pld3	1.34E-29	0.35925621	0.324	0.091	1.52E-25	1	Pld3
Cadm1	9.81E-44	0.35827103	0.369	0.067	1.11E-39	1	Cadm1
Ctsh	1.77E-24	0.35787207	0.871	0.696	2.02E-20	1	Ctsh
Rnase4	9.49E-45	0.35707566	0.385	0.079	1.08E-40	1	Rnase4
Glmp	6.34E-33	0.35612782	0.432	0.147	7.20E-29	1	Glmp
Arl6ip1	3.21E-21	0.355457	0.488	0.249	3.65E-17	1	Arl6ip1
Sdf2l1	6.18E-35	0.35481505	0.418	0.127	7.02E-31	1	Sdf2l1
Rpl12	6.53E-24	0.34731482	0.908	0.855	7.42E-20	1	Rpl12
Gpr34	5.41E-53	0.34393868	0.284	0.018	6.14E-49	1	Gpr34
Lipa	2.75E-24	0.33661099	0.366	0.137	3.12E-20	1	Lipa
H2-DMa	2.04E-21	0.33518373	0.634	0.362	2.32E-17	1	H2-DMa
Npm1	9.59E-17	0.33315898	0.669	0.482	1.09E-12	1	Npm1
mt-Nd3	1.48E-15	0.33294209	0.817	0.676	1.68E-11	1	mt-Nd3
Blvrb	5.74E-26	0.33285357	0.354	0.121	6.52E-22	1	Blvrb

Clec4n	1.33E-25	0.33240746	0.345	0.111	1.51E-21	1	Clec4n
Eef1a1	5.04E-15	0.33122888	0.977	0.982	5.72E-11	1	Eef1a1
mt-Nd1	5.78E-15	0.32805983	0.915	0.841	6.57E-11	1	mt-Nd1
Asah1	2.56E-28	0.32748644	0.415	0.152	2.90E-24	1	Asah1
mt-Co3	1.26E-11	0.32712112	0.995	0.997	1.43E-07	1	mt-Co3
Abca1	2.67E-29	0.32121778	0.352	0.099	3.04E-25	1	Abca1
Canx	2.10E-25	0.32062967	0.5	0.231	2.38E-21	1	Canx
Axl	6.96E-30	0.31846981	0.493	0.183	7.91E-26	1	Axl
Slamf9	2.97E-44	0.31764695	0.362	0.067	3.37E-40	1	Slamf9
Lyz21	6.49E-18	0.31674929	0.934	0.802	7.37E-14	1	Lyz2
Rps29	1.98E-17	0.31670375	0.969	0.99	2.25E-13	1	Rps29
P4hb	2.03E-26	0.31559206	0.467	0.195	2.31E-22	1	P4hb
Igf1	5.74E-48	0.31530908	0.272	0.02	6.52E-44	1	Igf1
Rpl23	2.83E-13	0.31530803	0.979	0.985	3.21E-09	1	Rpl23
Cxcl14	8.28E-43	0.31131307	0.261	0.024	9.40E-39	1	Cxcl14
Gnas	9.62E-11	0.31009335	0.723	0.631	1.09E-06	1	Gnas
Hspe1	1.34E-17	0.30812284	0.479	0.263	1.52E-13	1	Hspe1
Tmem86a	1.22E-24	0.30763747	0.465	0.197	1.39E-20	1	Tmem86a
Tcn2	3.63E-23	0.30714404	0.359	0.135	4.12E-19	1	Tcn2
Atpif1	1.07E-17	0.30245916	0.477	0.259	1.21E-13	1	Atpif1
Ppib	5.51E-19	0.30094888	0.627	0.389	6.25E-15	1	Ppib
Hebp1	3.52E-44	0.2987763	0.305	0.04	3.99E-40	1	Hebp1
Cyba	2.81E-15	0.29763532	0.967	0.905	3.19E-11	1	Cyba
Fcer1g	7.01E-21	0.29759434	1	0.906	7.97E-17	1	Fcer1g
Unc93b1	9.75E-17	0.29757623	0.735	0.549	1.11E-12	1	Unc93b1
Rps26	5.10E-12	0.29720544	0.915	0.935	5.79E-08	1	Rps26
Lgals3bp	2.05E-17	0.29712215	0.444	0.216	2.33E-13	1	Lgals3bp
Manf	3.57E-15	0.29612614	0.413	0.219	4.06E-11	1	Manf
Sirpa	1.90E-18	0.29582811	0.493	0.258	2.16E-14	1	Sirpa
Atp5g2	2.29E-18	0.29556737	0.566	0.343	2.60E-14	1	Atp5g2
C3ar1	2.44E-30	0.29350339	0.408	0.127	2.77E-26	1	C3ar1
Anxa3	7.93E-27	0.29215311	0.42	0.153	9.00E-23	1	Anxa3
Npc2	5.83E-25	0.29019583	0.969	0.837	6.62E-21	1	Npc2
Tmsb4x	9.12E-10	0.28967886	0.993	0.991	1.04E-05	1	Tmsb4x
Rpl3	6.81E-17	0.28790219	0.92	0.912	7.73E-13	1	Rpl3
H2-DMb1	1.98E-10	0.28591318	0.418	0.249	2.25E-06	1	H2-DMb1
Pla2g7	4.57E-17	0.28386435	0.42	0.2	5.18E-13	1	Pla2g7
Itgax	1.36E-19	0.28336648	0.437	0.2	1.55E-15	1	Itgax
Spcs2	1.12E-17	0.28298291	0.469	0.248	1.28E-13	1	Spcs2
Basp1	3.02E-22	0.27974392	0.502	0.225	3.43E-18	1	Basp1

Cd300c2	1.70E-19	0.27917356	0.547	0.289	1.93E-15	1	Cd300c2
Ppp1r14b	6.40E-23	0.27708633	0.366	0.14	7.27E-19	1	Ppp1r14b
Tmem37	9.87E-30	0.27707918	0.319	0.081	1.12E-25	1	Tmem37
Cpd	9.39E-32	0.27440263	0.298	0.065	1.07E-27	1	Cpd
Gpr65	3.53E-28	0.27301765	0.369	0.114	4.01E-24	1	Gpr65
Ntpcr	4.20E-24	0.27106701	0.352	0.123	4.77E-20	1	Ntpcr
mt-Cytb	1.75E-12	0.27058167	0.986	0.974	1.99E-08	1	mt-Cytb
Ptms	1.69E-16	0.26999464	0.495	0.261	1.92E-12	1	Ptms
Rpl27a	6.98E-11	0.26631558	0.979	0.979	7.93E-07	1	Rpl27a
Laptm5	1.45E-14	0.26537066	0.93	0.906	1.65E-10	1	Laptm5
Tmed9	2.70E-18	0.26509258	0.439	0.225	3.07E-14	1	Tmed9
Ltc4s	3.11E-30	0.26431143	0.27	0.052	3.54E-26	1	Ltc4s
B2m	3.54E-11	0.26278382	0.953	0.932	4.02E-07	1	B2m
Lap3	2.29E-38	0.26110019	0.279	0.041	2.61E-34	1	Lap3
Rps17	5.07E-10	0.26030581	0.728	0.651	5.76E-06	1	Rps17
Ybx1	7.65E-10	0.26023295	0.793	0.722	8.68E-06	1	Ybx1
Snx5	1.78E-19	0.25928564	0.406	0.183	2.02E-15	1	Snx5
Ndufc2	3.11E-17	0.25625697	0.385	0.186	3.54E-13	1	Ndufc2
Tpp1	7.69E-20	0.25347434	0.338	0.132	8.73E-16	1	Tpp1
mt-Atp6	4.50E-09	0.2530921	0.993	0.991	5.11E-05	1	mt-Atp6
Rpl22l1	2.82E-10	0.25140513	0.547	0.394	3.20E-06	1	Rpl22l1
Lrpap1	1.95E-18	0.25013771	0.338	0.139	2.22E-14	1	Lrpap1
Rps8	9.95E-13	0.25002829	0.965	0.98	1.13E-08	1	Rps8
Ifitm1	2.99E-25	1.17374563	0.361	0.104	3.40E-21	2	Ifitm1
H2-Eb11	2.78E-18	1.14317126	0.708	0.611	3.15E-14	2	H2-Eb1
Ly6a	4.62E-40	1.05096092	0.426	0.091	5.25E-36	2	Ly6a
H2-Ab11	4.52E-17	1.02647223	0.722	0.676	5.13E-13	2	H2-Ab1
H2-Aa1	6.91E-18	1.0244608	0.727	0.655	7.84E-14	2	H2-Aa
Cd741	6.58E-16	0.94192167	0.787	0.774	7.47E-12	2	Cd74
Lsp1	1.19E-48	0.73570176	0.718	0.243	1.35E-44	2	Lsp1
Id2	1.96E-33	0.70594571	0.588	0.217	2.23E-29	2	Id2
Klrd1	1.25E-123	0.66037707	0.481	0.006	1.42E-119	2	Klrd1
Napsa	2.77E-31	0.62100471	0.579	0.226	3.15E-27	2	Napsa
Tmsb101	1.99E-27	0.61400375	0.931	0.766	2.26E-23	2	Tmsb10
Rpl121	6.38E-37	0.61006219	0.958	0.856	7.24E-33	2	Rpl12
Rpsa	2.71E-45	0.59942045	0.981	0.965	3.08E-41	2	Rpsa
Syng2	1.46E-25	0.57445519	0.593	0.288	1.66E-21	2	Syng2
Rps11	4.77E-41	0.57232184	0.977	0.978	5.42E-37	2	Rps11
H2-Oa	5.20E-84	0.55951649	0.407	0.02	5.91E-80	2	H2-Oa
Rps15a	4.01E-34	0.55779035	0.986	0.955	4.55E-30	2	Rps15a

Crip11	2.02E-21	0.55295812	0.782	0.512	2.30E-17	2	Crip1
Ltb	2.75E-51	0.54971326	0.356	0.039	3.12E-47	2	Ltb
Rps24	9.65E-39	0.54358189	0.981	0.972	1.10E-34	2	Rps24
Rps7	1.22E-37	0.53991155	0.972	0.925	1.39E-33	2	Rps7
H2-Q7	2.75E-23	0.53216814	0.352	0.106	3.12E-19	2	H2-Q7
Cbfa2t3	3.52E-62	0.53162553	0.5	0.075	3.99E-58	2	Cbfa2t3
Sub1	2.55E-38	0.5257647	0.694	0.281	2.90E-34	2	Sub1
Rpl17	3.92E-32	0.51941666	0.977	0.947	4.45E-28	2	Rpl17
Cd7	8.79E-69	0.51931682	0.269	0.003	9.99E-65	2	Cd7
Rpl13	1.48E-41	0.51787494	0.991	0.979	1.68E-37	2	Rpl13
Rps27	1.21E-31	0.51742724	0.986	0.944	1.38E-27	2	Rps27
Ccnd2	4.12E-45	0.504974	0.472	0.095	4.68E-41	2	Ccnd2
Rps4x	6.17E-36	0.50377401	0.986	0.941	7.00E-32	2	Rps4x
AW112010	0.00036493	0.49965398	0.296	0.213	1	2	AW112010
Rnase6	6.88E-42	0.49727419	0.389	0.07	7.81E-38	2	Rnase6
H2-DMb11	2.66E-23	0.49593993	0.569	0.251	3.02E-19	2	H2-DMb1
Rpl30	6.08E-29	0.49285267	0.968	0.956	6.90E-25	2	Rpl30
Rpl18a	1.53E-35	0.48366309	0.986	0.979	1.74E-31	2	Rpl18a
Rpl27	1.87E-32	0.4833316	0.843	0.505	2.12E-28	2	Rpl27
H2afy	7.48E-27	0.46819485	0.681	0.334	8.49E-23	2	H2afy
Ccnd1	2.03E-23	0.46641501	0.37	0.115	2.31E-19	2	Ccnd1
Rps6	3.35E-29	0.46481679	0.949	0.868	3.80E-25	2	Rps6
Rps18	2.87E-33	0.46441321	0.981	0.942	3.25E-29	2	Rps18
Rpl39	8.66E-30	0.46433254	0.972	0.957	9.83E-26	2	Rpl39
Rps16	1.95E-31	0.46294188	0.991	0.977	2.22E-27	2	Rps16
Ptprcap	5.40E-73	0.45867872	0.273	0.001	6.13E-69	2	Ptprcap
H2-DMb2	2.21E-48	0.45842737	0.306	0.029	2.51E-44	2	H2-DMb2
Eef1b2	4.47E-25	0.45763439	0.88	0.693	5.08E-21	2	Eef1b2
Ciita	4.54E-30	0.45703206	0.481	0.147	5.15E-26	2	Ciita
Rps19	1.97E-32	0.45175462	0.977	0.966	2.23E-28	2	Rps19
Rps10	1.54E-29	0.45171338	0.986	0.959	1.75E-25	2	Rps10
Mdh2	3.68E-22	0.44842431	0.523	0.227	4.18E-18	2	Mdh2
Rpl9	1.57E-28	0.44683799	0.968	0.942	1.78E-24	2	Rpl9
Rpl14	1.01E-26	0.44156047	0.954	0.855	1.15E-22	2	Rpl14
Rpl8	2.17E-30	0.4393928	0.981	0.936	2.46E-26	2	Rpl8
Ms4a4b	2.58E-17	0.43448794	0.255	0.073	2.93E-13	2	Ms4a4b
Rplp0	7.21E-30	0.42799464	0.972	0.952	8.19E-26	2	Rplp0
Cnn2	1.32E-31	0.42790316	0.481	0.149	1.49E-27	2	Cnn2
Itgb7	6.64E-39	0.42658689	0.477	0.114	7.54E-35	2	Itgb7
Rpl4	2.13E-28	0.42550226	0.917	0.762	2.41E-24	2	Rpl4

Rpl5	3.69E-24	0.42297319	0.884	0.768	4.19E-20	2	Rpl5
Rps3a1	1.82E-27	0.42235128	0.991	0.95	2.07E-23	2	Rps3a1
Rpl18	4.27E-33	0.42127935	0.977	0.959	4.84E-29	2	Rpl18
Rpl38	1.08E-23	0.41785288	0.986	0.939	1.23E-19	2	Rpl38
Rps3	1.50E-30	0.41620716	0.986	0.945	1.70E-26	2	Rps3
Rpl13a	5.00E-29	0.41095632	0.593	0.226	5.68E-25	2	Rpl13a
Rpl34	1.54E-27	0.40911878	0.972	0.96	1.75E-23	2	Rpl34
Rps13	8.42E-25	0.40634093	0.972	0.952	9.57E-21	2	Rps13
Rps5	4.26E-28	0.40551005	0.977	0.95	4.84E-24	2	Rps5
Eef1a11	5.49E-27	0.40485771	0.995	0.978	6.23E-23	2	Eef1a1
Klrk1	2.79E-59	0.40404455	0.31	0.018	3.16E-55	2	Klrk1
Rps20	2.27E-22	0.39936491	0.981	0.97	2.58E-18	2	Rps20
Rps14	4.19E-27	0.39661063	0.968	0.967	4.76E-23	2	Rps14
Psmb8	2.94E-23	0.39636172	0.824	0.552	3.34E-19	2	Psmb8
Plbd1	2.44E-16	0.39448458	0.505	0.251	2.77E-12	2	Plbd1
Ckb	2.37E-18	0.39219758	0.398	0.157	2.69E-14	2	Ckb
Rpl321	2.80E-23	0.38748327	0.972	0.969	3.18E-19	2	Rpl32
Rpl21	8.64E-26	0.3867106	0.986	0.964	9.81E-22	2	Rpl21
Rpl36	2.44E-24	0.38570656	0.981	0.948	2.77E-20	2	Rpl36
Rps21	4.54E-25	0.38555563	0.986	0.968	5.15E-21	2	Rps21
Fyn	3.61E-50	0.38296785	0.38	0.05	4.10E-46	2	Fyn
Rps23	1.14E-23	0.38281058	0.972	0.956	1.30E-19	2	Rps23
Nsa2	1.64E-26	0.37798732	0.676	0.307	1.86E-22	2	Nsa2
Rps15	8.87E-23	0.37530518	0.963	0.859	1.01E-18	2	Rps15
Rpl37	1.09E-23	0.3749568	0.977	0.962	1.24E-19	2	Rpl37
Rack1	9.49E-25	0.37208038	0.963	0.896	1.08E-20	2	Rack1
Rplp11	1.75E-24	0.37152544	0.995	0.986	1.99E-20	2	Rplp1
Ccnd3	2.26E-23	0.37036324	0.417	0.141	2.57E-19	2	Ccnd3
Tpt1	2.99E-21	0.3674923	1	0.986	3.39E-17	2	Tpt1
Rpl19	2.83E-24	0.367168	0.986	0.969	3.22E-20	2	Rpl19
Rpl36a	1.29E-17	0.36552257	0.884	0.765	1.46E-13	2	Rpl36a
Gm2a	6.31E-08	0.3643412	0.708	0.653	0.00071647	2	Gm2a
Aes	8.05E-25	0.36372108	0.537	0.218	9.14E-21	2	Aes
Actb	1.46E-13	0.36284179	1	0.994	1.66E-09	2	Actb
Cd47	1.03E-21	0.36101288	0.653	0.304	1.17E-17	2	Cd47
Rps9	3.59E-23	0.36034809	0.986	0.979	4.08E-19	2	Rps9
Kmo	4.73E-69	0.35999357	0.338	0.015	5.37E-65	2	Kmo
Dnajc7	1.63E-18	0.35787177	0.352	0.123	1.85E-14	2	Dnajc7
Eif3f	2.90E-21	0.35505096	0.792	0.513	3.29E-17	2	Eif3f
Rpl23a	1.93E-20	0.35308906	0.898	0.757	2.19E-16	2	Rpl23a

Limd2	2.97E-22	0.35242152	0.495	0.196	3.38E-18	2	Limd2
Rpl15	1.64E-21	0.34841184	0.949	0.922	1.87E-17	2	Rpl15
Rpl24	1.11E-21	0.34626191	0.963	0.911	1.27E-17	2	Rpl24
Cox7a2l	1.75E-21	0.3455606	0.569	0.252	1.98E-17	2	Cox7a2l
Jaml	8.53E-55	0.34431449	0.37	0.038	9.68E-51	2	Jaml
Traf1	1.20E-47	0.34431449	0.333	0.037	1.37E-43	2	Traf1
Rac2	2.56E-13	0.34383951	0.611	0.364	2.91E-09	2	Rac2
Pdcd4	2.16E-30	0.34375987	0.273	0.045	2.46E-26	2	Pdcd4
Rpl7	7.44E-25	0.34294421	0.986	0.897	8.45E-21	2	Rpl7
Rpl27a1	1.27E-21	0.33843112	0.977	0.98	1.44E-17	2	Rpl27a
Rps121	1.93E-24	0.33356009	0.986	0.966	2.19E-20	2	Rps12
Rpl33	2.09E-19	0.33176903	0.954	0.907	2.38E-15	2	Rpl3
Eef1g	1.01E-18	0.32725483	0.546	0.259	1.15E-14	2	Eef1g
Mbnl1	1.49E-17	0.32670588	0.639	0.32	1.69E-13	2	Mbnl1
Rpl6	2.19E-21	0.32629211	0.977	0.944	2.48E-17	2	Rpl6
Rps28	7.53E-18	0.32302125	0.986	0.934	8.55E-14	2	Rps28
Rpl231	2.35E-22	0.32254489	0.995	0.981	2.67E-18	2	Rpl23
Ptma	2.31E-15	0.32119215	0.944	0.905	2.62E-11	2	Ptma
Rpl22	2.79E-19	0.31900628	0.94	0.869	3.17E-15	2	Rpl22
Pak1	2.63E-23	0.31849501	0.338	0.095	2.99E-19	2	Pak1
Rplp2	3.53E-18	0.31735637	0.977	0.962	4.01E-14	2	Rplp2
Bcl11a	2.77E-47	0.31719868	0.273	0.02	3.14E-43	2	Bcl11a
Rpl28	3.36E-21	0.31686561	0.977	0.956	3.81E-17	2	Rpl28
H2-DMa1	1.93E-10	0.31110111	0.593	0.418	2.19E-06	2	H2-DMa
S100a101	6.21E-12	0.31100926	0.417	0.196	7.05E-08	2	S100a10
Rps81	6.25E-19	0.30978879	0.977	0.975	7.10E-15	2	Rps8
Rpl35	7.60E-18	0.3092754	0.912	0.827	8.63E-14	2	Rpl35
Naca	2.91E-16	0.3079882	0.875	0.768	3.30E-12	2	Naca
Ndufa6	5.50E-18	0.30767917	0.574	0.281	6.25E-14	2	Ndufa6
Eif3h	2.13E-21	0.30521776	0.639	0.303	2.42E-17	2	Eif3h
Ywhah	2.39E-16	0.30404059	0.5	0.232	2.71E-12	2	Ywhah
Rpl26	2.15E-21	0.30156652	0.977	0.96	2.44E-17	2	Rpl26
Cnp	3.45E-23	0.30088103	0.301	0.074	3.92E-19	2	Cnp
Set	3.33E-21	0.30044993	0.593	0.257	3.78E-17	2	Set
Rpl37a	7.32E-15	0.30027464	0.991	0.978	8.31E-11	2	Rpl37a
H2afz	8.78E-11	0.30004857	0.773	0.599	9.97E-07	2	H2afz
Rps261	5.45E-19	0.29835006	0.954	0.925	6.19E-15	2	Rps26
Rinl	1.29E-33	0.29347569	0.296	0.047	1.46E-29	2	Rinl
Sh3bgrl3	1.06E-11	0.29229664	0.907	0.873	1.20E-07	2	Sh3bgrl3
Psmb9	2.10E-13	0.29161807	0.394	0.184	2.39E-09	2	Psmb9

Slamf7	1.65E-21	0.28961909	0.315	0.085	1.87E-17	2	Slamf7
Tmsb4x1	8.09E-08	0.28680391	0.986	0.992	0.00091872	2	Tmsb4x
Sumo2	3.84E-16	0.28629615	0.537	0.266	4.36E-12	2	Sumo2
Marcksl1	1.48E-05	0.2806325	0.259	0.146	0.16790703	2	Marcksl1
Rpl11	1.33E-19	0.27969157	0.981	0.956	1.51E-15	2	Rpl11
Rps27a	4.61E-16	0.27818722	0.981	0.971	5.23E-12	2	Rps27a
Uba52	1.52E-14	0.27729309	0.343	0.136	1.73E-10	2	Uba52
Dpp4	4.93E-47	0.27627272	0.278	0.021	5.60E-43	2	Dpp4
Tagln21	6.79E-10	0.27607399	0.481	0.263	7.71E-06	2	Tagln2
Dbnl	5.91E-15	0.27484664	0.398	0.176	6.71E-11	2	Dbnl
Rpl41	3.18E-18	0.27416275	0.991	0.982	3.61E-14	2	Rpl41
Eif3e	2.30E-15	0.27361731	0.412	0.181	2.61E-11	2	Eif3e
Eef2	3.11E-13	0.27133489	0.884	0.818	3.54E-09	2	Eef2
Il2rg	6.75E-24	0.27089691	0.37	0.106	7.66E-20	2	Il2rg
Rpl35a	6.06E-15	0.26912053	0.968	0.972	6.88E-11	2	Rpl35a
Selplg	5.74E-16	0.26858864	0.63	0.329	6.51E-12	2	Selplg
Flt3	5.61E-62	0.26858509	0.259	0.005	6.37E-58	2	Flt3
Rpl31	5.17E-12	0.26784741	0.801	0.588	5.87E-08	2	Rpl31
Olfm1	2.92E-28	0.26362272	0.269	0.047	3.32E-24	2	Olfm1
Atp5d	5.83E-17	0.26360703	0.62	0.303	6.61E-13	2	Atp5d
Wdfy4	2.65E-17	0.2633464	0.301	0.096	3.01E-13	2	Wdfy4
H2-K1	0.00676592	0.26329597	0.843	0.864	1	2	H2-K1
Pfdn5	5.31E-11	0.26306477	0.722	0.535	6.03E-07	2	Pfdn5
Nfkb1	4.76E-09	0.2585357	0.421	0.236	5.41E-05	2	Nfkb1
Uqcrh	1.68E-13	0.25853324	0.731	0.494	1.90E-09	2	Uqcrh
Cytip	1.19E-22	0.25762027	0.435	0.142	1.35E-18	2	Cytip
Park7	3.55E-16	0.25758608	0.449	0.198	4.03E-12	2	Park7
Hmgb1	6.09E-11	0.25710461	0.565	0.327	6.92E-07	2	Hmgb1
Siglecg	5.15E-54	0.25592135	0.255	0.009	5.85E-50	2	Siglecg
Rpl10a1	7.89E-18	0.2556175	0.977	0.907	8.96E-14	2	Rpl10a
Stap1	2.79E-25	0.25494126	0.324	0.077	3.17E-21	2	Stap1
6-Sep	1.41E-47	0.25191431	0.282	0.022	1.60E-43	2	6
Tbc1d10c	2.26E-54	0.25137413	0.278	0.015	2.57E-50	2	Tbc1d10c
S100a9	3.68E-262	4.00697504	0.891	0.002	4.17E-258	3	S100a9
S100a8	2.72E-224	3.73626372	0.891	0.013	3.09E-220	3	S100a8
Retnlg	9.03E-99	2.1509506	0.348	0.001	1.03E-94	3	Retnlg
Il1b	2.11E-77	2.03054854	0.924	0.193	2.39E-73	3	Il1b
Srgn	1.93E-39	1.67931232	0.978	0.785	2.19E-35	3	Srgn
Dusp1	2.14E-56	1.56038758	0.783	0.176	2.43E-52	3	Dusp1
Stfa2l1	9.90E-125	1.4621477	0.424	0	1.12E-120	3	Stfa2l1

Cxcr2	1.09E-230	1.39441349	0.772	0	1.24E-226	3	Cxcr2
Lrg1	2.23E-114	1.39400888	0.457	0.005	2.53E-110	3	Lrg1
Txnip	4.16E-46	1.31630941	0.761	0.219	4.72E-42	3	Txnip
Msrp11	1.58E-37	1.30797928	0.946	0.539	1.80E-33	3	Msrp11
S100a11	6.68E-33	1.29728576	0.87	0.432	7.59E-29	3	S100a11
Csf3r	4.81E-84	1.28443126	0.837	0.127	5.46E-80	3	Csf3r
Gm5483	7.52E-80	1.27730408	0.272	0	8.53E-76	3	Gm5483
Slpi	1.46E-44	1.2015469	0.543	0.085	1.66E-40	3	Slpi
Eif1	6.86E-41	1.19358659	1	0.879	7.79E-37	3	Eif1
Cdk2ap2	8.09E-29	1.18237178	0.674	0.244	9.18E-25	3	Cdk2ap2
Btg1	1.86E-34	1.17162205	0.935	0.614	2.12E-30	3	Btg1
Cxcl2	1.12E-66	1.11442451	0.391	0.018	1.27E-62	3	Cxcl2
Hdc	2.75E-102	1.10251375	0.511	0.016	3.12E-98	3	Hdc
Cebpb1	2.85E-21	1.08509029	0.793	0.442	3.23E-17	3	Cebpb1
Mcl1	2.16E-29	1.04552593	0.848	0.578	2.45E-25	3	Mcl1
Ifitm2	1.17E-31	1.04008925	0.946	0.582	1.33E-27	3	Ifitm2
Txn1	4.24E-19	1.02869601	0.685	0.358	4.81E-15	3	Txn1
Mmp9	4.17E-127	1.02036174	0.5	0.005	4.74E-123	3	Mmp9
Rnf149	9.37E-27	1.01999431	0.739	0.334	1.06E-22	3	Rnf149
Junb	1.06E-26	0.99629372	0.891	0.572	1.20E-22	3	Junb
Ifitm11	1.33E-33	0.9687901	0.565	0.114	1.51E-29	3	Ifitm11
Cebpd	4.36E-38	0.94139569	0.576	0.124	4.95E-34	3	Cebpd
Lcn2	3.88E-28	0.93123119	0.261	0.026	4.41E-24	3	Lcn2
Neat11	5.66E-25	0.92475186	0.793	0.356	6.43E-21	3	Neat11
Il1r2	4.16E-65	0.92009541	0.467	0.032	4.73E-61	3	Il1r2
Tyrobp1	1.00E-31	0.9094037	1	0.948	1.14E-27	3	Tyrobp1
Mxd1	2.63E-41	0.90782646	0.511	0.08	2.98E-37	3	Mxd1
Pim1	2.19E-19	0.90704749	0.62	0.259	2.48E-15	3	Pim1
Sorl1	2.49E-44	0.90413391	0.717	0.181	2.82E-40	3	Sorl1
Tnfaip2	2.07E-28	0.8867388	0.609	0.18	2.36E-24	3	Tnfaip2
Gsr	6.22E-36	0.88234973	0.62	0.149	7.07E-32	3	Gsr
Klf2	6.99E-29	0.87302652	0.457	0.093	7.94E-25	3	Klf2
Cxcr4	3.00E-42	0.86469412	0.598	0.114	3.41E-38	3	Cxcr4
Btg2	5.63E-18	0.86133581	0.804	0.517	6.39E-14	3	Btg2
Rac21	4.04E-20	0.85549957	0.707	0.381	4.59E-16	3	Rac21
Lcp1	2.80E-25	0.84719	0.848	0.609	3.18E-21	3	Lcp1
Hp	1.74E-15	0.83562349	0.37	0.107	1.97E-11	3	Hp
Ier5	9.39E-35	0.82949247	0.772	0.276	1.07E-30	3	Ier5
Pilra	1.02E-36	0.81941416	0.63	0.154	1.16E-32	3	Pilra
Tpd52	6.76E-22	0.80115266	0.728	0.351	7.67E-18	3	Tpd52

Ccr1	4.70E-19	0.79775904	0.609	0.266	5.34E-15	3	Ccr1
Vasp	2.00E-21	0.78380116	0.652	0.297	2.27E-17	3	Vasp
Grina	4.38E-22	0.77948569	0.609	0.241	4.97E-18	3	Grina
Gcnt2	1.08E-41	0.77468393	0.609	0.124	1.22E-37	3	Gcnt2
Fos1	1.08E-11	0.76919234	0.685	0.451	1.23E-07	3	Fos
Jund	2.71E-20	0.76233387	0.707	0.336	3.07E-16	3	Jund
Fcer1g1	5.87E-22	0.73730635	1	0.931	6.66E-18	3	Fcer1g
Gabarap	3.54E-26	0.72729568	0.946	0.715	4.02E-22	3	Gabarap
Ier3	6.47E-16	0.71742999	0.424	0.134	7.35E-12	3	Ier3
Fxyd5	5.68E-18	0.70438275	0.967	0.798	6.45E-14	3	Fxyd5
Map1lc3b	2.05E-21	0.7030947	0.63	0.277	2.33E-17	3	Map1lc3b
Marcks	1.65E-21	0.70187577	0.793	0.405	1.87E-17	3	Marcks
Lyst	5.23E-27	0.68252412	0.5	0.122	5.94E-23	3	Lyst
Pfn1	1.22E-17	0.66785813	1	0.902	1.39E-13	3	Pfn1
Cd91	1.02E-13	0.66736278	0.565	0.254	1.16E-09	3	Cd9
Selplg1	1.23E-13	0.66705747	0.641	0.357	1.39E-09	3	Selplg
Gda	3.29E-17	0.66448079	0.38	0.105	3.73E-13	3	Gda
Fgl2	3.29E-21	0.66169671	0.478	0.144	3.73E-17	3	Fgl2
Fth11	2.54E-13	0.65397991	1	0.989	2.88E-09	3	Fth1
Trim30b	1.47E-46	0.65204723	0.478	0.058	1.67E-42	3	Trim30b
Clec4e	7.44E-14	0.65159729	0.315	0.083	8.45E-10	3	Clec4e
Cd52	9.23E-21	0.64916609	0.989	0.953	1.05E-16	3	Cd52
Igfbp6	1.51E-30	0.64647214	0.38	0.059	1.72E-26	3	Igfbp6
Zfp36	1.82E-13	0.645371	0.609	0.315	2.07E-09	3	Zfp36
Egr1	3.33E-20	0.64522127	0.467	0.133	3.79E-16	3	Egr1
Adipor1	1.93E-19	0.64209259	0.478	0.156	2.19E-15	3	Adipor1
H3f3a	5.70E-20	0.64201423	0.989	0.863	6.47E-16	3	H3f3a
Ubb	1.24E-20	0.63956657	1	0.904	1.41E-16	3	Ubb
Pnrc1	4.30E-14	0.63836098	0.457	0.182	4.89E-10	3	Pnrc1
Ier2	9.28E-14	0.63521273	0.543	0.262	1.05E-09	3	Ier2
Gmfg	1.87E-16	0.62957438	0.641	0.342	2.12E-12	3	Gmfg
Nfkb1a	1.16E-06	0.61887909	0.435	0.259	0.01322289	3	Nfkb1a
Lst1	3.95E-12	0.61699094	0.707	0.482	4.49E-08	3	Lst1
Alox5ap	2.20E-14	0.61663168	0.75	0.478	2.50E-10	3	Alox5ap
Stk17b	8.26E-20	0.60550735	0.511	0.167	9.38E-16	3	Stk17b
Arpc1b	1.55E-20	0.59678455	1	0.887	1.76E-16	3	Arpc1b
Socs3	3.06E-15	0.59598244	0.402	0.128	3.47E-11	3	Socs3
Clec4d	2.43E-24	0.59512315	0.435	0.096	2.76E-20	3	Clec4d
Cd24a	3.11E-39	0.59375937	0.424	0.054	3.53E-35	3	Cd24a
Cd300lf	1.01E-24	0.58999259	0.587	0.18	1.14E-20	3	Cd300lf

Ccrl2	5.17E-12	0.58982512	0.337	0.11	5.88E-08	3	Ccrl2
Ptprc	1.68E-16	0.57988128	0.935	0.744	1.91E-12	3	Ptprc
Rgs21	1.01E-08	0.57737963	0.717	0.547	0.0001148	3	Rgs2
Ncf2	3.19E-10	0.57696808	0.598	0.382	3.63E-06	3	Ncf2
G0s2	2.25E-70	0.57653464	0.261	0.002	2.55E-66	3	G0s2
Samsn1	2.81E-15	0.57646455	0.413	0.134	3.19E-11	3	Samsn1
Spi1	6.80E-13	0.57591888	0.804	0.653	7.73E-09	3	Spi1
Pglyrp1	1.51E-26	0.57127072	0.391	0.071	1.71E-22	3	Pglyrp1
Taldo1	2.16E-09	0.56968952	0.739	0.652	2.45E-05	3	Taldo1
Atp6v1g1	9.00E-10	0.56686904	0.62	0.432	1.02E-05	3	Atp6v1g1
Iqgap11	5.58E-13	0.56543787	0.685	0.418	6.34E-09	3	Iqgap1
Marcksl11	1.15E-06	0.56445463	0.326	0.152	0.01303804	3	Marcksl1
Nfam1	2.84E-17	0.56442028	0.511	0.191	3.23E-13	3	Nfam1
Neurl3	3.00E-12	0.55479436	0.587	0.295	3.41E-08	3	Neurl3
Adgre5	3.66E-12	0.54850655	0.467	0.201	4.16E-08	3	Adgre5
Anxa21	1.67E-08	0.54632707	0.522	0.29	0.00018934	3	Anxa2
Msn	1.40E-13	0.54454178	0.793	0.575	1.59E-09	3	Msn
Cyp4f18	1.56E-14	0.54318335	0.533	0.229	1.77E-10	3	Cyp4f18
Gng5	2.89E-20	0.53659792	0.967	0.808	3.28E-16	3	Gng5
Calm2	1.19E-12	0.53400073	0.587	0.311	1.35E-08	3	Calm2
Ddx5	9.15E-12	0.52975765	0.859	0.732	1.04E-07	3	Ddx5
Osgin1	3.10E-37	0.52866821	0.326	0.031	3.52E-33	3	Osgin1
Atp11b	6.63E-17	0.5260337	0.38	0.104	7.53E-13	3	Atp11b
Il1f9	8.94E-83	0.52575351	0.293	0.001	1.02E-78	3	Il1f9
Pkm	8.41E-10	0.51922632	0.891	0.756	9.55E-06	3	Pkm
F630028O10Rik	6.23E-18	0.51851584	0.326	0.074	7.08E-14	3	F630028O10Rik
Rabac1	3.63E-11	0.51717983	0.489	0.245	4.12E-07	3	Rabac1
Gpsm3	3.71E-09	0.5160232	0.5	0.286	4.21E-05	3	Gpsm3
Atp6v0e	4.18E-08	0.51096863	0.576	0.413	0.00047427	3	Atp6v0e
Slfn11	3.41E-08	0.50794145	0.424	0.206	0.00038709	3	Slfn1
Slfn2	6.22E-06	0.50747168	0.576	0.446	0.07061883	3	Slfn2
Ncf1	4.56E-11	0.50627616	0.543	0.286	5.18E-07	3	Ncf1
Ptafr	3.84E-20	0.50185695	0.489	0.146	4.36E-16	3	Ptafr
Plek	2.99E-06	0.50038245	0.402	0.239	0.03392662	3	Plek
Ninj1	4.63E-08	0.49544256	0.457	0.247	0.00052566	3	Ninj1
Myl12b	1.05E-09	0.49137072	0.609	0.384	1.19E-05	3	Myl12b
Gadd45b	1.16E-11	0.48849578	0.272	0.075	1.32E-07	3	Gadd45b
Ltb1	5.82E-25	0.48788751	0.38	0.068	6.61E-21	3	Ltb1
Ogfrl1	1.17E-17	0.48499315	0.478	0.159	1.33E-13	3	Ogfrl1
Ppp1r2	1.83E-18	0.48340133	0.413	0.117	2.07E-14	3	Ppp1r2

Cd300ld	3.09E-31	0.47762392	0.348	0.046	3.51E-27	3	Cd300ld
Zyx	1.10E-12	0.47661488	0.467	0.198	1.24E-08	3	Zyx
AC110211.1	6.69E-83	0.47465179	0.293	0.001	7.60E-79	3	AC110211.1
Cd33	1.19E-13	0.47362939	0.402	0.137	1.36E-09	3	Cd33
Gsn	1.05E-08	0.47318531	0.467	0.25	0.00011909	3	Gsn
Cd53	2.67E-06	0.47110404	0.5	0.347	0.03033835	3	Cd53
2310001H17Rik	1.11E-18	0.47073309	0.315	0.066	1.26E-14	3	2310001H17
S100a61	2.55E-05	0.46679331	0.772	0.602	0.28962305	3	S100a6
Rhog	4.97E-07	0.46461711	0.478	0.303	0.00564887	3	Rhog
Rps271	6.85E-15	0.46211475	1	0.947	7.78E-11	3	Rps27
Gnai2	9.09E-12	0.46200157	0.967	0.868	1.03E-07	3	Gnai2
Ftl1	1.61E-08	0.46036559	1	0.985	0.00018244	3	Ftl1
Cd37	1.54E-17	0.45898497	0.5	0.165	1.75E-13	3	Cd37
Timm10b	4.21E-08	0.45693675	0.457	0.251	0.00047847	3	Timm10b
H2-Q10	7.44E-56	0.45630266	0.337	0.016	8.45E-52	3	H2-Q10
Ostf1	5.93E-08	0.45496296	0.522	0.318	0.00067303	3	Ostf1
2810474O19Rik	2.66E-10	0.45255787	0.435	0.194	3.02E-06	3	2810474O19
Tsc22d3	1.20E-10	0.44319602	0.326	0.113	1.36E-06	3	Tsc22d3
Pygl	1.07E-16	0.44306871	0.359	0.096	1.22E-12	3	Pygl
Trem1	1.48E-26	0.44201133	0.272	0.032	1.68E-22	3	Trem1
Ypel3	2.91E-08	0.43942718	0.457	0.25	0.00033081	3	Ypel3
Ptpn6	3.24E-10	0.43660633	0.576	0.315	3.68E-06	3	Ptpn6
Ppp1r18	5.33E-08	0.43562478	0.457	0.256	0.00060484	3	Ppp1r18
Fau	7.28E-10	0.43450539	1	0.99	8.27E-06	3	Fau
Cd44	3.76E-09	0.43075274	0.424	0.2	4.26E-05	3	Cd44
Emilin2	2.66E-10	0.42813842	0.446	0.195	3.02E-06	3	Emilin2
Cox17	1.02E-09	0.42731006	0.391	0.177	1.16E-05	3	Cox17
Il17ra	6.68E-09	0.42636754	0.402	0.192	7.58E-05	3	Il17ra
H3f3b1	1.87E-11	0.4217262	1	0.922	2.12E-07	3	H3f3b
Ddx3x	5.36E-08	0.40810888	0.359	0.168	0.00060861	3	Ddx3x
Sdcbp	0.0003136	0.40660862	0.457	0.351	1	3	Sdcbp
Cytip1	7.28E-10	0.40588517	0.402	0.172	8.27E-06	3	Cytip
Zfp36l2	0.00039551	0.40394803	0.489	0.358	1	3	Zfp36l2
Mrpl33	2.67E-06	0.40033831	0.435	0.264	0.03030107	3	Mrpl33
C5ar1	2.91E-08	0.40012693	0.391	0.178	0.00032988	3	C5ar1
Arpc2	7.86E-09	0.3999487	0.935	0.834	8.93E-05	3	Arpc2
Cap1	2.21E-05	0.3979362	0.489	0.354	0.25129146	3	Cap1
Lsp11	1.45E-06	0.39690511	0.511	0.303	0.01647302	3	Lsp1
Actg1	1.02E-05	0.39432218	0.957	0.907	0.11560379	3	Actg1
Ssh2	6.80E-10	0.3931856	0.489	0.245	7.72E-06	3	Ssh2

	1-Jun	1.12E-05	0.38487967	0.739	0.614	0.12744394	3	Jun
Fam104a		7.41E-12	0.38375003	0.424	0.164	8.41E-08	3	Fam104a
Kdm6b		3.02E-11	0.37869015	0.337	0.114	3.43E-07	3	Kdm6b
Retreg1		2.05E-09	0.37863508	0.359	0.146	2.32E-05	3	Retreg1
Pla2g71		1.41E-06	0.37511126	0.446	0.255	0.01595922	3	Pla2g7
Pak2		1.02E-06	0.3750321	0.435	0.259	0.01161292	3	Pak2
Lmnbl		2.83E-08	0.3746602	0.293	0.114	0.00032094	3	Lmnbl
Rac1		5.84E-05	0.37452923	0.522	0.417	0.66340384	3	Rac1
H2-D1		4.23E-05	0.37335217	0.967	0.88	0.4800524	3	H2-D1
Zcchc6		5.67E-06	0.36996633	0.402	0.226	0.06440256	3	Zcchc6
Ubc		3.03E-05	0.36951388	0.739	0.686	0.34429804	3	Ubc
Nudt4		7.36E-21	0.36684904	0.326	0.061	8.35E-17	3	Nudt4
Arpc5		2.19E-05	0.36663017	0.543	0.407	0.24825981	3	Arpc5
Pgd		1.07E-05	0.36546339	0.391	0.237	0.12160014	3	Pgd
Cox8a		1.87E-06	0.36215704	0.88	0.811	0.02122473	3	Cox8a
Rab7		2.77E-06	0.36128823	0.424	0.258	0.03142901	3	Rab7
Supt4a		3.21E-07	0.359201	0.413	0.224	0.00364995	3	Supt4a
Pilrb2		7.78E-10	0.35824144	0.304	0.104	8.83E-06	3	Pilrb2
Itgam		8.25E-05	0.35747704	0.424	0.276	0.93623189	3	Itgam
Litaf	0.00013618	0.35280882	0.359	0.225		1	3	Litaf
Oaz1	2.81E-07	0.35252262	0.924	0.804	0.00319605		3	Oaz1
Ube2b	3.78E-06	0.34896856	0.326	0.166	0.04287988		3	Ube2b
Card19	2.71E-07	0.34812638	0.424	0.224	0.00307795		3	Card19
Klf6	0.00020319	0.34798819	0.37	0.239		1	3	Klf6
Srsf5	7.70E-06	0.34329516	0.543	0.376	0.08744789		3	Srsf5
Siglece	2.98E-11	0.34329188	0.293	0.089	3.38E-07		3	Siglece
D8Ertd738e	0.00117339	0.34295107	0.413	0.317		1	3	D8Ertd738e
Fam32a	9.35E-07	0.34253354	0.337	0.166	0.01061235		3	Fam32a
Grb2	3.30E-06	0.34242436	0.478	0.303	0.03752213		3	Grb2
Fgr	6.62E-07	0.3418923	0.435	0.237	0.00751697		3	Fgr
Coro1a	9.84E-07	0.34114631	0.967	0.844	0.01117668		3	Coro1a
Sbno2	0.00027947	0.33848901	0.348	0.223		1	3	Sbno2
Gm5150	1.26E-09	0.33779114	0.304	0.109	1.44E-05		3	Gm5150
Sell	1.58E-07	0.33726725	0.283	0.11	0.00179346		3	Sell
Max	4.70E-09	0.33453687	0.337	0.136	5.34E-05		3	Max
Scand1	0.00041235	0.33275054	0.446	0.33		1	3	Scand1
Myd88	1.83E-08	0.3304199	0.38	0.171	0.00020791		3	Myd88
Myl6	1.43E-07	0.32836108	0.902	0.809	0.00162729		3	Myl6
Trim30a	0.00094951	0.32571944	0.38	0.259		1	3	Trim30a
Hnrnpf	0.00789737	0.32560062	0.457	0.404		1	3	Hnrnpf

Dazap2	2.91E-05	0.325363	0.413	0.266	0.33006473	3	Dazap2
Celf2	0.00024649	0.3247429	0.402	0.276	1	3	Celf2
Mdh21	0.00137744	0.32033855	0.37	0.266	1	3	Mdh2
Psenen	0.00020141	0.31985129	0.413	0.289	1	3	Psenen
Actn1	1.85E-13	0.3198352	0.293	0.075	2.10E-09	3	Actn1
Cdc42	1.04E-05	0.31929247	0.75	0.717	0.11827611	3	Cdc42
Snx20	1.39E-06	0.31810344	0.391	0.209	0.01580376	3	Snx20
Ptpn1	0.00202945	0.31685623	0.478	0.374	1	3	Ptpn1
Eif5	0.00136366	0.31583873	0.424	0.337	1	3	Eif5
Apbb1ip	0.00053348	0.31285375	0.522	0.401	1	3	Apbb1ip
Serf2	2.80E-07	0.31275571	1	0.918	0.0031814	3	Serf2
Rin3	9.50E-08	0.31246835	0.293	0.117	0.00107906	3	Rin3
Tctex1d2	6.37E-06	0.3123335	0.315	0.157	0.07233027	3	Tctex1d2
Arpp19	0.00507624	0.31136877	0.348	0.273	1	3	Arpp19
Cd300a	1.08E-05	0.3109475	0.424	0.245	0.12227622	3	Cd300a
Gcnt1	1.52E-12	0.30980399	0.304	0.086	1.73E-08	3	Gcnt1
Kctd12	9.39E-05	0.30950328	0.337	0.196	1	3	Kctd12
Atp5l	7.33E-05	0.3080454	0.652	0.584	0.83205943	3	Atp5l
Pxn	6.01E-10	0.30641792	0.348	0.13	6.82E-06	3	Pxn
Pten	9.56E-06	0.30499747	0.315	0.158	0.10857575	3	Pten
Sema4a	9.78E-12	0.30463871	0.293	0.084	1.11E-07	3	Sema4a
Grk2	0.0001059	0.30462091	0.348	0.212	1	3	Grk2
Pbxip1	8.78E-06	0.30081228	0.348	0.186	0.09972012	3	Pbxip1
Rhoa	5.89E-05	0.29965954	0.696	0.634	0.66892843	3	Rhoa
Furin	0.00032121	0.29604592	0.326	0.196	1	3	Furin
Tax1bp1	9.01E-05	0.29567173	0.391	0.253	1	3	Tax1bp1
Prdx5	1.99E-07	0.29498858	0.924	0.728	0.00226287	3	Prdx5
Picalm	0.00062207	0.29412673	0.413	0.291	1	3	Picalm
Ezr	1.02E-05	0.2921174	0.283	0.134	0.11577404	3	Ezr
Rgs3	3.13E-17	0.29093998	0.304	0.063	3.55E-13	3	Rgs3
Hcls1	0.00044203	0.28964974	0.424	0.31	1	3	Hcls1
Atg3	1.64E-05	0.28949617	0.304	0.154	0.18567481	3	Atg3
Snap23	1.68E-09	0.28691017	0.315	0.114	1.91E-05	3	Snap23
1810058l24Rik	0.00059734	0.28685602	0.315	0.197	1	3	1810058l24Rik
Sh3bgrl3	1.91E-05	0.28652671	0.924	0.875	0.21647792	3	Sh3bgrl3
Slc38a2	0.0033367	0.28417849	0.348	0.24	1	3	Slc38a2
Il13ra1	1.08E-05	0.2787134	0.261	0.119	0.12278866	3	Il13ra1
Klf7	3.06E-10	0.27828705	0.272	0.081	3.48E-06	3	Klf7
Acsl1	4.07E-09	0.27828705	0.272	0.088	4.63E-05	3	Acsl1
Csf2rb	0.00253588	0.27810257	0.348	0.243	1	3	Csf2rb

Abr	0.00533064	0.27807659	0.348	0.251	1	3	Abr
Tspan13	0.00542936	0.27794358	0.304	0.208	1	3	Tspan13
Chchd2	1.55E-05	0.27710481	0.739	0.665	0.17611861	3	Chchd2
Ptpre	0.00049064	0.27665178	0.402	0.276	1	3	Ptpre
Rbms1	0.00121394	0.27658721	0.337	0.221	1	3	Rbms1
Ubl5	0.00352936	0.27586679	0.446	0.373	1	3	Ubl5
Il6ra	1.34E-06	0.27567734	0.359	0.173	0.01526258	3	Il6ra
Xbp1	0.00169636	0.27305913	0.37	0.251	1	3	Xbp1
Fcgr31	0.00319771	0.27238232	0.533	0.442	1	3	Fcgr3
7-Mar	0.00029235	0.27234015	0.261	0.137	1	3	7
Myh9	0.00073942	0.26980658	0.478	0.358	1	3	Myh9
Serp1	0.00130517	0.26971091	0.38	0.273	1	3	Serp1
Ptbp3	0.00140764	0.26904324	0.413	0.286	1	3	Ptbp3
Chmp2a	0.00019349	0.26680692	0.424	0.297	1	3	Chmp2a
Themis2	0.00027013	0.26625489	0.261	0.141	1	3	Themis2
1600014C10Rik	0.0001018	0.26505152	0.293	0.152	1	3	1600014C10
Tsc22d4	0.00031163	0.26175522	0.38	0.249	1	3	Tsc22d4
Cfl1	0.00154255	0.26126088	0.967	0.906	1	3	Cfl1
Clic1	0.00452628	0.26102281	0.772	0.745	1	3	Clic1
R3hdm4	0.00029799	0.26097086	0.272	0.149	1	3	R3hdm4
Arid5a	2.62E-07	0.26034697	0.261	0.097	0.00297127	3	Arid5a
Sf3b2	0.00730874	0.26014165	0.348	0.269	1	3	Sf3b2
Jak1	1.95E-05	0.2587774	0.359	0.199	0.22096937	3	Jak1
Rps91	0.0001074	0.25852028	0.989	0.979	1	3	Rps9
Tnfrsf1a	0.00112288	0.25764483	0.348	0.239	1	3	Tnfrsf1a
Gnb2	0.00529766	0.25731141	0.598	0.576	1	3	Gnb2
Atp6v1e1	0.00385179	0.25488093	0.315	0.222	1	3	Atp6v1e1
Rbm39	0.0029969	0.25461688	0.717	0.677	1	3	Rbm39
Lyn	0.00208597	0.25441807	0.489	0.384	1	3	Lyn
Snx18	0.00116837	0.25440485	0.261	0.15	1	3	Snx18
Gm26740	6.16E-08	0.25190482	0.304	0.117	0.0006994	3	Gm26740
Hcst	3.86E-06	0.25120412	0.272	0.114	0.0437897	3	Hcst
Clec5a	0.00011741	0.25117079	0.272	0.139	1	3	Clec5a
Mark2	9.75E-05	0.25048584	0.283	0.153	1	3	Mark2

In the dataset from implanted QPP7 tumors (**Figure 9**), scSEQ analysis identified 5 clusters (**Fig. 7b**): microglia/macrophages (**Fig. 10b**), neutrophils (**Fig. 10c**), APCs (**Fig. 10d**), lytic myeloid cells (**Fig. 10e**), and T, B and NK cells (**Fig. 10f, g, h**). The full list of genes upregulated for each cluster can be found in **Table 6**. These cell populations are consistent with our IHC analysis in both spontaneous and implanted QPP mouse tumors and are also congruent with reported human data (Chen and Hambardzumyan, 2018). The heterogeneity observed in the immune cell compartment among QPP7 allograft tumors is consistent with the macroscopic heterogeneity of the tumors when implanted as well as with the genomic instability described in (Shingu et al., 2017). Representative images of tumor slices from the implanted QPP7 line can be found in **Figure 11**.

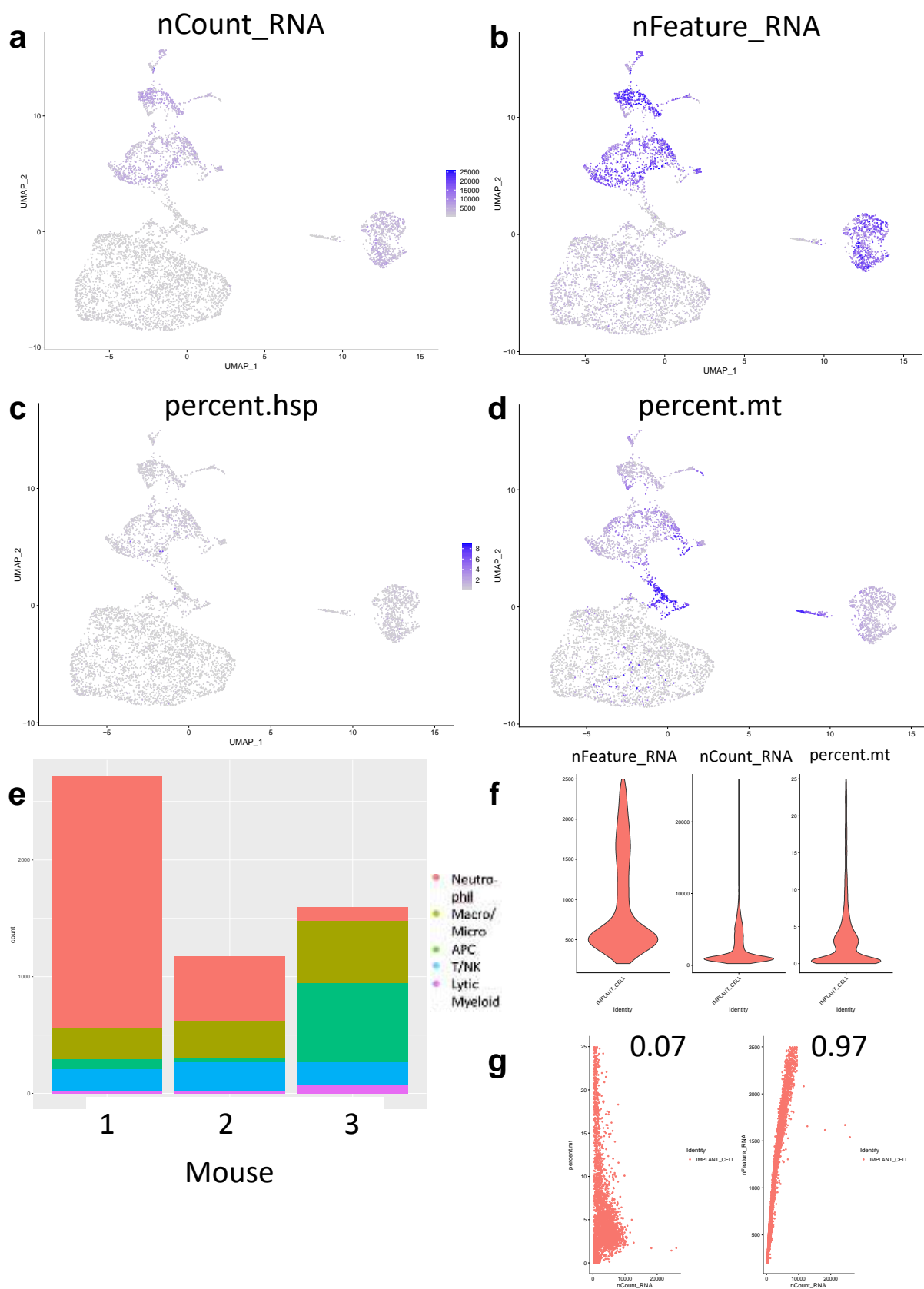


Figure 9: Quality control metrics for the implanted QPP dataset. **a.** Featureplot showing the counts of RNA molecules detected per cell. **b.** Featureplot showing the number of unique genes expressed in each cell. **c.** Featureplot showing the percent of heat shock proteins expressed in each cell. **d.** Featureplot showing the percent of mitochondrial RNA molecules for each cell. **e.** Barplot showing the number of cells per cluster for individual mice. **f.** Violin plot showing the distribution of (left) unique gene counts, (center) RNA molecule counts, and (right) mitochondrial RNA percentage for the dataset. **g.** Scatter plot showing the correlation of (right) mitochondrial percentage to total RNA counts and (left) unique genes to total RNA counts after normalization.

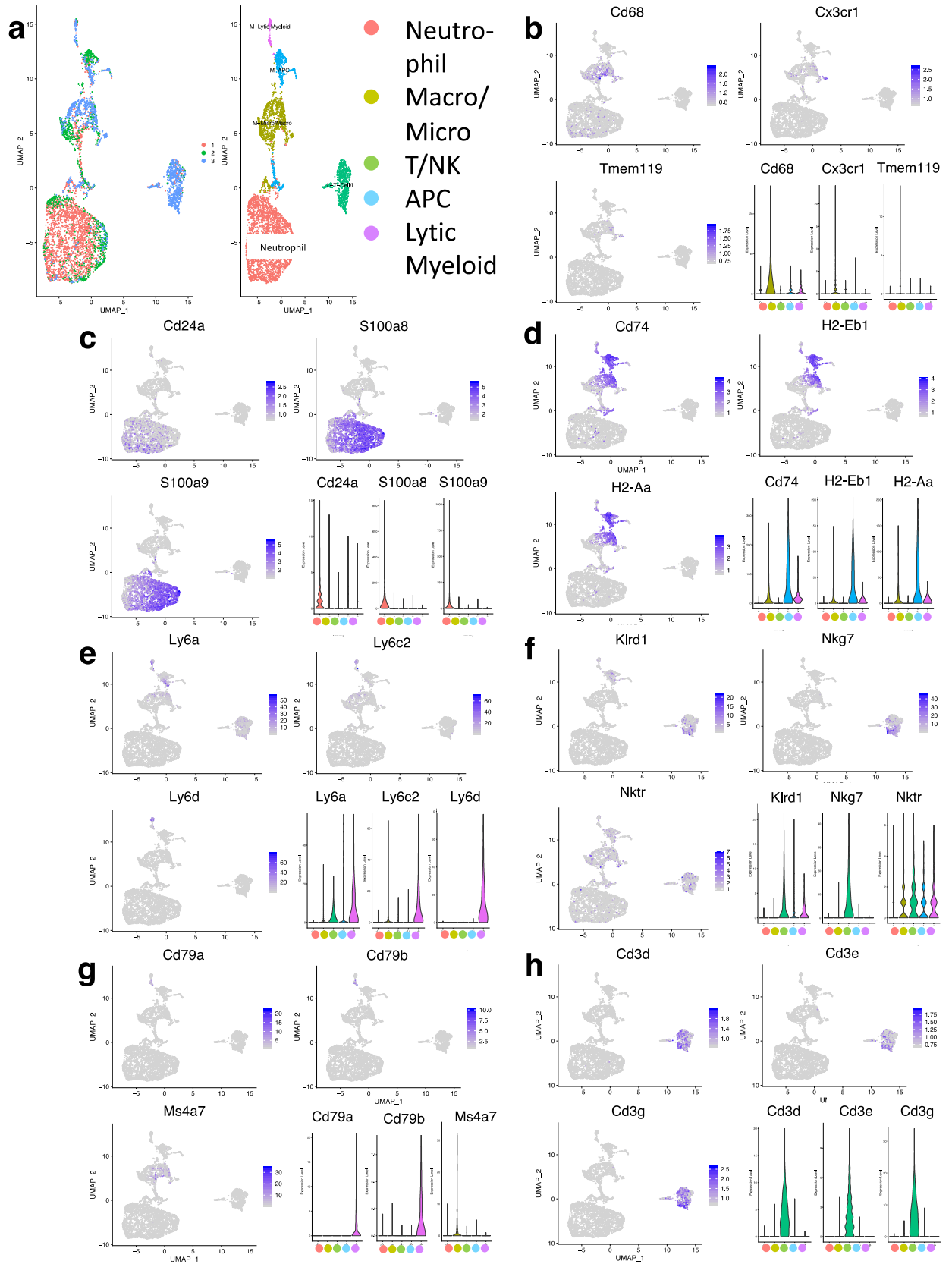


Figure 10: Immune constituents of implanted QPP tumors. a. UMAPs showing aggregate of CD45+ immune infiltrates from n=3 Implanted QPP tumors at moribund timepoint. **b-h.** UMAPs show (b) microglia and macrophage clusters identified by Cd68, Cx3cr1, and Tmem119 markers; (c) neutrophil clusters identified by Cd24a, S100a8, and S100a9 markers; (d) antigen-presenting cell clusters identified by Cd74, H2-Eb1, and H2-Aa markers; (e) lytic myeloid clusters identified by Ly6a, Ly6c2, and Ly6d markers; (f) natural killer (NK) cell clusters identified by Klrd1, Nkg7, and Nktr markers; (g) B-cell clusters identified by Cd79a, Cd79b, and Ms4a7 markers; and (h) T cell clusters identified by Cd3d, Cd3e, and Cd3g markers. All violin plots show the specificity of given markers for neutrophils (red), macrophages/microglia (lime), T and NK cells (green), APCs (blue), and lytic myeloid cells (purple).

Table 6

Mouse Implanted 0.1 Resolution							
	p_val	avg_logFC	pct.1	pct.2	p_val_adj	cluster	gene
S100a8	0	3.28559004	0.961	0.087	0	0	S100a8
S100a9	0	3.08621374	0.933	0.079	0	0	S100a9
Cxcl2	0	1.66183747	0.505	0.035	0	0	Cxcl2
Srgn	0	1.53596864	0.954	0.5	0	0	Srgn
Eif1	0	1.29510285	0.962	0.568	0	0	Eif1
Fth1	0	1.2329241	0.986	0.924	0	0	Fth1
Msrb1	0	1.19413268	0.844	0.217	0	0	Msrb1
Mcl1	0	1.16773939	0.886	0.273	0	0	Mcl1
Cd9	0	1.07795424	0.697	0.138	0	0	Cd9
Cebpb	0	1.04047737	0.845	0.301	0	0	Cebpb
Ier3	0	1.03800715	0.64	0.116	0	0	Ier3
Dusp1	0	1.00653461	0.751	0.168	0	0	Dusp1
Tyrobp	0	1.00230617	0.964	0.587	0	0	Tyrobp
S100a11	0	1.00201589	0.761	0.345	0	0	S100a11
Csf3r	0	0.99060821	0.707	0.055	0	0	Csf3r
Btg1	0	0.96663688	0.906	0.452	0	0	Btg1
Ftl1	0	0.95273185	0.988	0.774	0	0	Ftl1
Fxyd5	0	0.93661463	0.9	0.497	0	0	Fxyd5
Junb	0	0.91735349	0.76	0.296	0	0	Junb
Grina	0	0.89256151	0.71	0.123	0	0	Grina
Cxcr2	0	0.88005146	0.595	0.026	0	0	Cxcr2
Gabarap	0	0.78951515	0.78	0.323	0	0	Gabarap
Fcer1g	0	0.7822392	0.929	0.526	0	0	Fcer1g
Rnf149	0	0.77667131	0.71	0.23	0	0	Rnf149
Pnrc1	0	0.76284879	0.65	0.183	0	0	Pnrc1
Mxd1	0	0.74540241	0.592	0.1	0	0	Mxd1
Cd24a	0	0.73214535	0.562	0.053	0	0	Cd24a
Clec4d	0	0.72512606	0.581	0.094	0	0	Clec4d
Lyst	0	0.71519856	0.585	0.083	0	0	Lyst
AC110211.1	0	0.66324441	0.468	0.014	0	0	AC110211.1
Il1b	3.42E-288	1.14814269	0.616	0.154	4.49E-284	0	Il1b
S100a6	1.62E-278	1.08820233	0.849	0.541	2.13E-274	0	S100a6
Cstb	2.54E-266	0.99719445	0.648	0.221	3.34E-262	0	Cstb

Cd300lf	4.46E-259	0.57603637	0.539	0.112	5.87E-255	0	Cd300lf
Hdc	2.92E-255	0.67337599	0.406	0.021	3.84E-251	0	Hdc
Cd63	2.15E-244	0.76777795	0.599	0.16	2.83E-240	0	Cd63
Ubb	7.30E-241	0.64159968	0.829	0.599	9.60E-237	0	Ubb
H3f3b	1.51E-240	0.65239383	0.917	0.785	1.98E-236	0	H3f3b
Marcks	1.20E-231	0.6570323	0.676	0.275	1.58E-227	0	Marcks
Cd44	1.13E-227	0.59718449	0.579	0.177	1.49E-223	0	Cd44
Pkm	2.52E-226	0.65187379	0.748	0.396	3.32E-222	0	Pkm
Retnlg	3.23E-224	1.02025957	0.345	0.01	4.25E-220	0	Retnlg
Basp1	2.99E-223	0.88708811	0.566	0.18	3.93E-219	0	Basp1
Egr1	2.25E-220	0.61400052	0.508	0.117	2.97E-216	0	Egr1
Hcar2	6.84E-219	0.65709067	0.347	0.014	9.00E-215	0	Hcar2
Cxcr4	5.47E-217	0.52515865	0.492	0.109	7.19E-213	0	Cxcr4
Il1r2	1.13E-204	0.57560025	0.416	0.062	1.49E-200	0	Il1r2
Ubc	4.17E-198	0.57804016	0.694	0.384	5.48E-194	0	Ubc
E230032D23Rik	7.52E-197	0.41462628	0.325	0.017	9.89E-193	0	E230032D23Rik
Adipor1	1.73E-195	0.44676081	0.448	0.096	2.27E-191	0	Adipor1
Neat1	4.64E-193	0.58811719	0.649	0.283	6.11E-189	0	Neat1
Gapdh	1.08E-189	0.6957304	0.773	0.535	1.42E-185	0	Gapdh
Ccr1	1.78E-189	0.53269261	0.575	0.204	2.34E-185	0	Ccr1
Tnfaip2	1.33E-188	0.54556957	0.441	0.096	1.74E-184	0	Tnfaip2
Chd7	8.32E-186	0.49432579	0.492	0.137	1.09E-181	0	Chd7
Lcp1	6.54E-183	0.58545265	0.682	0.392	8.60E-179	0	Lcp1

Btg2	1.04E-179	0.63388737	0.629	0.292	1.36E-175	0	Btg2
Gng5	1.53E-178	0.52074938	0.686	0.407	2.01E-174	0	Gng5
Igf1r	1.55E-174	0.37606778	0.309	0.023	2.04E-170	0	Igf1r
Jun	6.88E-170	0.66088834	0.646	0.334	9.05E-166	0	Jun
Cd14	4.15E-168	0.62653305	0.425	0.098	5.45E-164	0	Cd14
Ifitm2	2.48E-167	0.63615222	0.676	0.34	3.26E-163	0	Ifitm2
H3f3a	5.26E-167	0.50866651	0.791	0.584	6.92E-163	0	H3f3a
Rgs2	2.45E-166	0.54951051	0.568	0.233	3.22E-162	0	Rgs2
Gadd45b	2.65E-166	0.7712839	0.398	0.086	3.49E-162	0	Gadd45b
Map1lc3b	6.56E-164	0.46409205	0.534	0.211	8.63E-160	0	Map1lc3b
Cyp4f18	1.04E-163	0.55037072	0.496	0.168	1.37E-159	0	Cyp4f18
Cd33	7.59E-162	0.3807916	0.376	0.074	9.98E-158	0	Cd33
Gm5483	2.01E-161	0.92899637	0.257	0.006	2.65E-157	0	Gm5483
Stfa2l1	3.68E-159	0.67631934	0.257	0.008	4.84E-155	0	Stfa2l1
Lcn2	1.29E-157	0.57065966	0.278	0.019	1.70E-153	0	Lcn2
Txnip	4.18E-156	0.52861805	0.55	0.236	5.49E-152	0	Txnip
Id1	1.52E-151	0.43023113	0.294	0.031	2.00E-147	0	Id1
Son	4.76E-151	0.4708678	0.663	0.372	6.26E-147	0	Son
Csf1	6.92E-150	0.42931917	0.325	0.049	9.11E-146	0	Csf1
Nudt4	1.54E-149	0.3316961	0.321	0.048	2.02E-145	0	Nudt4
Tpd52	5.91E-149	0.44583725	0.568	0.244	7.78E-145	0	Tpd52
Tnfrsf23	6.20E-149	0.31223981	0.261	0.016	8.16E-145	0	Tnfrsf23
Dmxi2	2.07E-147	0.33457181	0.3	0.037	2.72E-143	0	Dmxi2

Lrg1	4.27E-143	0.46686311	0.261	0.019	5.62E-139	0	Lrg1
lqsec1	7.40E-143	0.31981241	0.309	0.046	9.74E-139	0	lqsec1
Ctsd	8.37E-143	0.35070738	0.677	0.349	1.10E-138	0	Ctsd
Plk3	9.28E-143	0.37122847	0.328	0.057	1.22E-138	0	Plk3
Ninj1	8.95E-142	0.46568102	0.457	0.147	1.18E-137	0	Ninj1
Sorl1	1.87E-141	0.39315181	0.403	0.114	2.46E-137	0	Sorl1
Ccrl2	1.70E-140	0.52273181	0.318	0.054	2.23E-136	0	Ccrl2
Slc7a11	8.86E-138	0.48835323	0.314	0.053	1.17E-133	0	Slc7a11
Mirt1	4.68E-136	0.29398931	0.255	0.021	6.16E-132	0	Mirt1
Fos	4.25E-135	0.57135415	0.587	0.292	5.59E-131	0	Fos
Trib1	5.35E-135	0.38195693	0.381	0.1	7.04E-131	0	Trib1
Alox5ap	3.19E-134	0.51184918	0.619	0.337	4.19E-130	0	Alox5ap
Pygl	1.53E-132	0.31186664	0.292	0.044	2.02E-128	0	Pygl
Ptafr	8.04E-129	0.3698548	0.38	0.105	1.06E-124	0	Ptafr
Slpi	1.20E-127	0.54869056	0.317	0.063	1.57E-123	0	Slpi
Il1rn	1.37E-126	0.50342444	0.315	0.064	1.81E-122	0	Il1rn
Rab7	2.66E-123	0.41814805	0.484	0.21	3.50E-119	0	Rab7
Ccl3	4.97E-117	0.43298049	0.331	0.078	6.54E-113	0	Ccl3
Card19	1.11E-116	0.38737055	0.393	0.126	1.46E-112	0	Card19
Klhdc4	2.98E-114	0.26861333	0.251	0.035	3.92E-110	0	Klhdc4
Retreg1	9.80E-114	0.28661829	0.324	0.08	1.29E-109	0	Retreg1
Ier5	6.31E-113	0.37952509	0.522	0.252	8.30E-109	0	Ier5
Gcnt1	1.94E-111	0.27056265	0.28	0.054	2.55E-107	0	Gcnt1

Txn1	1.52E-109	0.64593787	0.569	0.347	2.00E-105	0	Txn1
1810058l24Rik	5.26E-107	0.35259317	0.4	0.151	6.92E-103	0	1810058l24Rik
Neurl3	8.45E-106	0.40694463	0.486	0.225	1.11E-101	0	Neurl3
Gcnt2	7.72E-104	0.29634116	0.323	0.089	1.02E-99	0	Gcnt2
Smox	1.26E-103	0.31296127	0.284	0.063	1.66E-99	0	Smox
Zfp36	5.65E-103	0.41685503	0.516	0.258	7.44E-99	0	Zfp36
Iqgap1	9.25E-100	0.38017079	0.588	0.355	1.22E-95	0	Iqgap1
Gsr	8.72E-99	0.31732159	0.391	0.143	1.15E-94	0	Gsr
Tmem189	3.17E-97	0.29127737	0.318	0.094	4.18E-93	0	Tmem189
Samsn1	1.15E-93	0.37142921	0.385	0.147	1.51E-89	0	Samsn1
Jund	1.41E-92	0.37948086	0.565	0.325	1.85E-88	0	Jund
Pfn1	2.55E-88	0.39424056	0.687	0.549	3.35E-84	0	Pfn1
Nfkbia	4.95E-88	0.48794113	0.536	0.3	6.51E-84	0	Nfkbia
Ypel3	5.32E-88	0.3182724	0.41	0.182	7.00E-84	0	Ypel3
Prdx5	1.01E-86	0.336788	0.603	0.351	1.33E-82	0	Prdx5
1700017B05Rik	1.40E-86	0.2755159	0.28	0.08	1.84E-82	0	1700017B05Rik
Vasp	1.65E-86	0.33368533	0.477	0.25	2.17E-82	0	Vasp
Tsc22d4	2.53E-84	0.33272605	0.419	0.198	3.32E-80	0	Tsc22d4
Ncf2	1.86E-83	0.32027568	0.437	0.207	2.44E-79	0	Ncf2
Ogfrl1	3.04E-80	0.26068102	0.314	0.109	4.00E-76	0	Ogfrl1
Klf2	4.41E-79	0.29524247	0.296	0.093	5.80E-75	0	Klf2
Lasp1	1.99E-78	0.25144321	0.301	0.103	2.62E-74	0	Lasp1
Snx20	2.09E-78	0.29143279	0.394	0.178	2.75E-74	0	Snx20
Bri3	2.78E-78	0.39155305	0.47	0.258	3.66E-74	0	Bri3
Adam8	9.42E-77	0.25281214	0.314	0.108	1.24E-72	0	Adam8
Eno1	3.17E-74	0.33323897	0.436	0.221	4.17E-70	0	Eno1
Zcchc6	4.87E-71	0.28213826	0.385	0.184	6.40E-67	0	Zcchc6
Ppp1r15a	1.02E-70	0.25762582	0.261	0.083	1.35E-66	0	Ppp1r15a
Cdk2ap2	1.03E-69	0.39910439	0.448	0.249	1.36E-65	0	Cdk2ap2
Litaf	1.40E-67	0.25093676	0.35	0.153	1.84E-63	0	Litaf
Skil	3.74E-67	0.25422275	0.355	0.159	4.92E-63	0	Skil
Atp6v1g1	9.13E-67	0.31177594	0.481	0.291	1.20E-62	0	Atp6v1g1
Aldoa	1.51E-65	0.34416948	0.545	0.357	1.99E-61	0	Aldoa
Arpc1b	6.65E-65	0.33442326	0.652	0.529	8.74E-61	0	Arpc1b
Plek	3.00E-63	0.33295774	0.377	0.19	3.94E-59	0	Plek

Apbb1ip	4.21E-62	0.27687774	0.418	0.229	5.54E-58	0	Apbb1ip
2810474O19Rik	1.45E-57	0.30268783	0.406	0.226	1.91E-53	0	2810474O19Rik
Marcksl1	5.92E-57	0.30773225	0.267	0.103	7.79E-53	0	Marcksl1
Bnip3l	4.91E-56	0.32673298	0.329	0.161	6.46E-52	0	Bnip3l
Selplg	3.71E-51	0.31029593	0.492	0.331	4.89E-47	0	Selplg
Gnai2	9.85E-49	0.30382449	0.614	0.524	1.30E-44	0	Gnai2
AA467197	1.21E-47	0.25289338	0.317	0.15	1.59E-43	0	AA467197
Eif5	1.62E-45	0.27491033	0.42	0.27	2.13E-41	0	Eif5
Laptn5	1.98E-44	0.26790666	0.663	0.578	2.60E-40	0	Laptn5
Cd52	3.07E-42	0.3023024	0.866	0.796	4.04E-38	0	Cd52
Myh9	4.72E-42	0.25465647	0.479	0.333	6.21E-38	0	Myh9
Ddx5	4.79E-42	0.277688	0.603	0.512	6.30E-38	0	Ddx5
Ier2	1.03E-41	0.25174479	0.365	0.217	1.35E-37	0	Ier2
Actg1	4.25E-34	0.29755107	0.786	0.707	5.59E-30	0	Actg1
Msn	6.57E-34	0.25065771	0.531	0.426	8.64E-30	0	Msn
Ldha	1.59E-10	0.25005373	0.419	0.384	2.09E-06	0	Ldha
Apoe	0	2.53198428	0.859	0.135	0	1	Apoe
Lyz2	0	2.18840922	0.868	0.207	0	1	Lyz2
C1qb	0	1.65563219	0.472	0.039	0	1	C1qb
Ctss	0	1.46733512	0.951	0.216	0	1	Ctss
Tgfb1	0	1.26234589	0.798	0.221	0	1	Tgfb1
C1qc	0	1.22048213	0.421	0.025	0	1	C1qc
Lgmn	0	1.17115996	0.702	0.073	0	1	Lgmn
Mafb	0	1.02565622	0.713	0.036	0	1	Mafb
Fn1	0	0.93584593	0.44	0.021	0	1	Fn1
Ms4a6c	0	0.8392184	0.691	0.068	0	1	Ms4a6c
Ctsc	0	0.8017988	0.645	0.054	0	1	Ctsc
Ccr2	0	0.77832418	0.564	0.075	0	1	Ccr2
Npc2	0	0.75929137	0.808	0.262	0	1	Npc2
Aif1	0	0.73711422	0.594	0.065	0	1	Aif1
Ms4a6d	0	0.69913306	0.54	0.03	0	1	Ms4a6d
Cybb	0	0.67308904	0.559	0.061	0	1	Cybb
Csf1r	0	0.64845164	0.652	0.103	0	1	Csf1r
Fcgr2b	0	0.63011785	0.567	0.065	0	1	Fcgr2b
Fcgr1	0	0.55744799	0.486	0.016	0	1	Fcgr1
Lrp1	0	0.53690516	0.512	0.043	0	1	Lrp1
Msr1	0	0.4245546	0.369	0.009	0	1	Msr1
C3ar1	0	0.41709513	0.337	0.007	0	1	C3ar1
C1qa	8.97E-297	1.488722	0.407	0.032	1.18E-292	1	C1qa

Ms4a7	1.52E-295	0.62915526	0.368	0.018	2.00E-291	1	Ms4a7
Itgb5	1.49E-291	0.46802002	0.429	0.038	1.96E-287	1	Itgb5
F13a1	1.28E-279	0.62058792	0.333	0.013	1.68E-275	1	F13a1
Cd68	1.92E-268	0.60036583	0.645	0.154	2.52E-264	1	Cd68
Trem2	1.56E-263	0.49207181	0.309	0.011	2.05E-259	1	Trem2
Mmp14	1.59E-260	0.41455942	0.356	0.024	2.09E-256	1	Mmp14
Ctsa	5.65E-255	0.48360553	0.585	0.123	7.43E-251	1	Ctsa
Chil3	1.07E-250	1.63681058	0.421	0.054	1.40E-246	1	Chil3
Ifi204	9.81E-243	0.49974903	0.419	0.052	1.29E-238	1	Ifi204
Pid1	8.42E-240	0.44127543	0.406	0.047	1.11E-235	1	Pid1
Lair1	4.12E-239	0.40328464	0.419	0.05	5.41E-235	1	Lair1
Ifitm3	2.40E-236	0.98509527	0.707	0.235	3.16E-232	1	Ifitm3
Clec4a3	4.73E-234	0.31909482	0.277	0.01	6.22E-230	1	Clec4a3
Ccl9	1.20E-229	0.49495737	0.303	0.017	1.58E-225	1	Ccl9
Grn	1.33E-226	0.69725806	0.673	0.219	1.74E-222	1	Grn
Cxcl16	1.85E-226	0.51828132	0.431	0.062	2.44E-222	1	Cxcl16
Ctsh	1.00E-223	0.52751503	0.635	0.167	1.32E-219	1	Ctsh
Ctsz	2.03E-222	0.65739373	0.752	0.284	2.67E-218	1	Ctsz
Ms4a4c	5.07E-215	0.52231766	0.401	0.055	6.67E-211	1	Ms4a4c
Pld4	2.78E-208	0.38141539	0.439	0.072	3.66E-204	1	Pld4
Selenop	6.23E-208	0.43083016	0.301	0.023	8.19E-204	1	Selenop
Zeb2	9.87E-203	0.53602178	0.645	0.19	1.30E-198	1	Zeb2
Lgals3	2.92E-201	0.94534933	0.761	0.326	3.85E-197	1	Lgals3

Calr	3.16E-200	0.61154123	0.671	0.243	4.16E-196	1	Calr
Ifi207	1.00E-196	0.3338499	0.348	0.042	1.32E-192	1	Ifi207
Rrbp1	3.27E-196	0.52081778	0.716	0.26	4.31E-192	1	Rrbp1
Psap	2.64E-194	0.56529219	0.928	0.469	3.47E-190	1	Psap
Cx3cr1	2.35E-190	0.46480216	0.318	0.035	3.09E-186	1	Cx3cr1
Hspa8	7.53E-186	0.60045442	0.794	0.359	9.90E-182	1	Hspa8
Mpeg1	1.02E-184	0.48245534	0.721	0.258	1.35E-180	1	Mpeg1
Apobec1	1.18E-184	0.28079626	0.326	0.038	1.55E-180	1	Apobec1
Ccr5	2.74E-180	0.3496131	0.35	0.051	3.60E-176	1	Ccr5
Lamp1	5.54E-177	0.43018541	0.581	0.174	7.29E-173	1	Lamp1
Prdx1	2.59E-175	0.5304786	0.536	0.155	3.41E-171	1	Prdx1
Anxa5	2.81E-173	0.3697606	0.403	0.077	3.70E-169	1	Anxa5
Axl	3.13E-171	0.26331151	0.254	0.02	4.11E-167	1	Axl
S100a4	4.62E-171	0.74683008	0.579	0.182	6.08E-167	1	S100a4
Lgals3bp	1.18E-170	0.38287646	0.333	0.049	1.55E-166	1	Lgals3bp
mt-Co2	5.86E-170	0.57186652	0.968	0.699	7.70E-166	1	mt-Co2
Cndp2	1.94E-168	0.25576286	0.283	0.03	2.56E-164	1	Cndp2
Hsp90b1	2.08E-168	0.49984819	0.567	0.183	2.73E-164	1	Hsp90b1
H2-DMa	6.85E-168	0.39819516	0.473	0.107	9.00E-164	1	H2-DMa
H2-Ab1	7.08E-168	0.76189313	0.567	0.154	9.32E-164	1	H2-Ab1
Emp3	1.41E-167	0.54447663	0.573	0.195	1.86E-163	1	Emp3
Fcgr4	9.23E-163	0.35083189	0.337	0.053	1.21E-158	1	Fcgr4
Akr1a1	1.69E-162	0.41000177	0.577	0.19	2.22E-158	1	Akr1a1

mt-Co3	1.67E-159	0.61906001	0.968	0.718	2.20E-155	1	mt-Co3
Cd74	2.35E-158	0.7317123	0.621	0.203	3.09E-154	1	Cd74
Dbi	3.70E-158	0.35107887	0.406	0.089	4.87E-154	1	Dbi
Ecm1	1.82E-156	0.42549705	0.276	0.033	2.39E-152	1	Ecm1
Pnp	3.65E-156	0.40304585	0.428	0.1	4.79E-152	1	Pnp
Pdia6	1.18E-152	0.33659243	0.376	0.077	1.55E-148	1	Pdia6
H2-Aa	5.86E-150	0.73438224	0.535	0.155	7.70E-146	1	H2-Aa
Plekho1	4.91E-149	0.29501044	0.382	0.078	6.46E-145	1	Plekho1
Hck	1.52E-146	0.30117786	0.379	0.079	2.00E-142	1	Hck
AY036118	2.97E-146	0.6310786	0.403	0.101	3.91E-142	1	AY036118
Plac8	3.71E-146	0.72015547	0.458	0.123	4.88E-142	1	Plac8
Camk2d	5.00E-145	0.28268799	0.34	0.062	6.57E-141	1	Camk2d
Ly86	2.76E-144	0.50091441	0.374	0.081	3.63E-140	1	Ly86
mt-Atp6	5.85E-144	0.58557297	0.968	0.701	7.69E-140	1	mt-Atp6
Unc93b1	7.78E-144	0.35294794	0.49	0.142	1.02E-139	1	Unc93b1
mt-Co1	1.06E-142	0.50019099	0.972	0.75	1.39E-138	1	mt-Co1
Capza2	1.71E-142	0.36714199	0.561	0.194	2.25E-138	1	Capza2
H2-DMb1	2.44E-142	0.36312226	0.393	0.086	3.20E-138	1	H2-DMb1
Wfdc17	5.12E-139	0.46639796	0.521	0.159	6.74E-135	1	Wfdc17
Bst2	6.32E-134	0.28802915	0.391	0.092	8.31E-130	1	Bst2
Sirpa	1.31E-129	0.33431421	0.465	0.14	1.73E-125	1	Sirpa
Ctsb	1.79E-128	0.68950302	0.794	0.408	2.36E-124	1	Ctsb
Snx5	5.64E-128	0.27004102	0.336	0.07	7.42E-124	1	Snx5

Ly6e	2.46E-126	0.50016906	0.736	0.372	3.24E-122	1	Ly6e
Ms4a6b	2.33E-125	0.3406802	0.452	0.134	3.06E-121	1	Ms4a6b
Ctsl	2.25E-123	0.5095875	0.311	0.063	2.96E-119	1	Ctsl
Irf7	1.04E-119	0.36901674	0.331	0.074	1.37E-115	1	Irf7
Ifi27l2a	9.57E-119	0.46625656	0.543	0.195	1.26E-114	1	Ifi27l2a
H2-Eb1	2.79E-115	0.63411588	0.484	0.155	3.67E-111	1	H2-Eb1
Zbp1	4.16E-115	0.29434569	0.311	0.067	5.47E-111	1	Zbp1
Ahnak	1.51E-114	0.37509176	0.404	0.118	1.99E-110	1	Ahnak
Tgfb1	1.57E-114	0.34385297	0.45	0.147	2.06E-110	1	Tgfb1
Slfn5	3.11E-113	0.37188127	0.355	0.091	4.09E-109	1	Slfn5
Ly6c2	8.04E-113	0.50958344	0.322	0.075	1.06E-108	1	Ly6c2
Cst3	1.25E-110	0.55359706	0.817	0.424	1.65E-106	1	Cst3
Lst1	2.60E-109	0.35842898	0.609	0.256	3.42E-105	1	Lst1
Lgals1	3.17E-109	0.46313928	0.514	0.184	4.17E-105	1	Lgals1
Atp1a1	4.16E-109	0.25912742	0.358	0.095	5.47E-105	1	Atp1a1
Crip1	5.43E-109	0.51858571	0.517	0.197	7.15E-105	1	Crip1
Eif4a1	6.43E-107	0.3718185	0.608	0.287	8.46E-103	1	Eif4a1
Ucp2	2.32E-104	0.38035531	0.648	0.315	3.06E-100	1	Ucp2
Gpx1	6.35E-103	0.47620731	0.644	0.314	8.35E-99	1	Gpx1
Pdia3	9.81E-102	0.29513865	0.427	0.145	1.29E-97	1	Pdia3
Tkt	3.83E-101	0.27060672	0.39	0.122	5.04E-97	1	Tkt
Epb41l2	4.01E-101	0.2541774	0.315	0.079	5.27E-97	1	Epb41l2
mt-Nd1	3.33E-98	0.39162211	0.79	0.457	4.37E-94	1	mt-Nd1
Mt1	7.21E-96	0.50060292	0.272	0.062	9.48E-92	1	Mt1

Cd300c2	8.71E-95	0.31465514	0.534	0.22	1.15E-90	1	Cd300c2
Pycard	1.19E-94	0.26680373	0.374	0.117	1.57E-90	1	Pycard
Gm2a	3.52E-93	0.29481968	0.547	0.223	4.63E-89	1	Gm2a
Slc25a5	4.90E-93	0.28435938	0.477	0.188	6.45E-89	1	Slc25a5
F10	4.95E-93	0.27051426	0.27	0.06	6.52E-89	1	F10
Fyb	7.06E-93	0.3404731	0.646	0.317	9.28E-89	1	Fyb
Psmb10	4.86E-92	0.25464259	0.357	0.109	6.39E-88	1	Psmb10
Manf	7.88E-92	0.27096441	0.334	0.098	1.04E-87	1	Manf
Vim	3.08E-90	0.78294012	0.603	0.337	4.05E-86	1	Vim
Itm2b	6.14E-89	0.47795924	0.751	0.465	8.07E-85	1	Itm2b
C3	4.19E-87	0.26224712	0.274	0.068	5.52E-83	1	C3
Ssr4	1.98E-85	0.26261973	0.467	0.188	2.61E-81	1	Ssr4
mt-Nd2	2.59E-85	0.34154365	0.777	0.45	3.41E-81	1	mt-Nd2
Ppib	4.97E-85	0.27010012	0.525	0.227	6.54E-81	1	Ppib
Erp29	2.57E-84	0.26051563	0.445	0.173	3.38E-80	1	Erp29
Rpl7a	2.79E-84	0.28194438	0.741	0.369	3.67E-80	1	Rpl7a
Arhgdia	6.46E-81	0.25421436	0.535	0.243	8.50E-77	1	Arhgdia
mt-Nd4	2.26E-78	0.31923271	0.843	0.548	2.98E-74	1	mt-Nd4
Tspo	4.62E-77	0.34823724	0.577	0.3	6.08E-73	1	Tspo
Pla2g7	1.93E-76	0.25796157	0.45	0.183	2.53E-72	1	Pla2g7
mt-Nd3	1.95E-76	0.31135706	0.609	0.3	2.56E-72	1	mt-Nd3
lsg15	4.85E-74	0.54174257	0.316	0.105	6.38E-70	1	lsg15
Sec61g	3.76E-73	0.30249835	0.53	0.262	4.95E-69	1	Sec61g
Aprt	6.01E-73	0.2816793	0.434	0.183	7.90E-69	1	Aprt
Hexb	9.76E-73	0.61527843	0.341	0.124	1.28E-68	1	Hexb
Samhd1	1.99E-71	0.36690263	0.485	0.23	2.61E-67	1	Samhd1
Rpl36al	9.57E-71	0.25614664	0.478	0.214	1.26E-66	1	Rpl36al
Ybx1	1.07E-69	0.28685265	0.598	0.327	1.41E-65	1	Ybx1
mt-Cytb	2.10E-69	0.32373557	0.862	0.604	2.76E-65	1	mt-Cytb
Rps17	8.86E-68	0.25276821	0.626	0.327	1.17E-63	1	Rps17
Fcgr3	1.21E-65	0.25864759	0.622	0.328	1.59E-61	1	Fcgr3
Tgm2	6.91E-65	0.37517389	0.378	0.157	9.09E-61	1	Tgm2
Tmsb4x	7.54E-62	0.2921015	0.991	0.95	9.91E-58	1	Tmsb4x
S100a10	2.69E-61	0.31882869	0.394	0.163	3.53E-57	1	S100a10
Parp14	3.48E-60	0.25204665	0.279	0.096	4.58E-56	1	Parp14
Hspa5	7.33E-58	0.39248359	0.573	0.35	9.64E-54	1	Hspa5
B2m	1.20E-55	0.4385338	0.766	0.616	1.58E-51	1	B2m
Rap1b	1.75E-54	0.25949978	0.475	0.248	2.30E-50	1	Rap1b
Tmsb10	2.30E-54	0.30331043	0.555	0.294	3.03E-50	1	Tmsb10
Sat1	8.53E-54	0.37476835	0.648	0.398	1.12E-49	1	Sat1

Gngt2	5.89E-50	0.25026082	0.427	0.205	7.75E-46	1	Gngt2
Stat1	2.94E-42	0.27832305	0.348	0.173	3.86E-38	1	Stat1
Prdx51	3.35E-42	0.29562578	0.676	0.432	4.41E-38	1	Prdx5
Gm42418	8.59E-39	0.7785662	0.986	0.958	1.13E-34	1	Gm42418
Ccl6	8.18E-36	0.35603476	0.31	0.152	1.08E-31	1	Ccl6
Hmox1	5.36E-26	0.51741513	0.276	0.148	7.05E-22	1	Hmox1
Ccl5	0	1.93112154	0.537	0.057	0	2	Ccl5
AW112010	0	1.77587172	0.904	0.096	0	2	AW112010
Nkg7	0	1.57804017	0.767	0.002	0	2	Nkg7
Cd3g	0	1.48651371	0.854	0.004	0	2	Cd3g
Rps15a	0	1.46204103	0.97	0.554	0	2	Rps15a
Trbc2	0	1.41567738	0.844	0.004	0	2	Trbc2
Rpl12	0	1.20287419	0.958	0.389	0	2	Rpl12
Cd3d	0	1.13208633	0.822	0.005	0	2	Cd3d
Rps24	0	1.08550735	0.973	0.665	0	2	Rps24
Rps18	0	1.0585258	0.96	0.475	0	2	Rps18
Ms4a4b	0	1.04730477	0.651	0.024	0	2	Ms4a4b
Rpsa	0	1.04303951	0.993	0.549	0	2	Rpsa
Rpl3	0	1.00865644	0.933	0.345	0	2	Rpl3
Trac	0	1.00132729	0.758	0.004	0	2	Trac
Rps4x	0	0.99244851	0.96	0.414	0	2	Rps4x
Rpl5	0	0.91905205	0.928	0.377	0	2	Rpl5
Trbc1	0	0.85351518	0.43	0.003	0	2	Trbc1
H2-Q7	0	0.82893673	0.767	0.088	0	2	H2-Q7
Ptprcap	0	0.82506618	0.74	0.021	0	2	Ptprcap
Cd3e	0	0.82003692	0.716	0.001	0	2	Cd3e
S100a101	0	0.79775059	0.747	0.118	0	2	S100a10
Tnfrsf4	0	0.79740443	0.427	0.009	0	2	Tnfrsf4
Klrd1	0	0.79489282	0.516	0.047	0	2	Klrd1
Cd8a	0	0.76754028	0.412	0.005	0	2	Cd8a
Cxcr6	0	0.76587824	0.506	0.001	0	2	Cxcr6
Ctla2a	0	0.76220564	0.506	0.003	0	2	Ctla2a
Cd8b1	0	0.73101841	0.417	0.009	0	2	Cd8b1
Cd2	0	0.70311157	0.609	0.004	0	2	Cd2
Thy1	0	0.69497717	0.639	0.001	0	2	Thy1
Tnfrsf18	0	0.68810357	0.538	0.01	0	2	Tnfrsf18
Il2rb	0	0.66174085	0.587	0.001	0	2	Il2rb
Lck	0	0.66068422	0.663	0.003	0	2	Lck
Gimap4	0	0.61472692	0.56	0.005	0	2	Gimap4
Ctsw	0	0.56524229	0.486	0.003	0	2	Ctsw

Icos	0	0.55774022	0.391	0.003	0	2	Icos
Gimap1	0	0.5447647	0.548	0.009	0	2	Gimap1
Ets1	0	0.52774707	0.514	0.022	0	2	Ets1
Pdcd1	0	0.52002061	0.468	0.002	0	2	Pdcd1
Gimap3	0	0.50739032	0.504	0.004	0	2	Gimap3
Tnfrsf9	0	0.48079404	0.341	0.003	0	2	Tnfrsf9
Ptpn22	0	0.45471672	0.479	0.026	0	2	Ptpn22
Cd28	0	0.44025237	0.408	0.001	0	2	Cd28
Skap1	0	0.43441924	0.453	0.001	0	2	Skap1
Sh2d2a	0	0.43183221	0.412	0.001	0	2	Sh2d2a
Lat	0	0.43182416	0.427	0.004	0	2	Lat
Gm8369	0	0.40526228	0.396	0.011	0	2	Gm8369
Gimap6	0	0.39776211	0.395	0.008	0	2	Gimap6
Cst7	0	0.39691859	0.408	0.009	0	2	Cst7
Lag3	0	0.39228041	0.374	0.014	0	2	Lag3
	1-Sep	0	0.37581599	0.416	0.017	2	1-Sep
Bcl11b	0	0.36933791	0.387	0.001	0	2	Bcl11b
Inpp4b	0	0.36035452	0.375	0.005	0	2	Inpp4b
Gimap5	0	0.3596703	0.38	0.004	0	2	Gimap5
Ablim1	0	0.33957981	0.352	0.009	0	2	Ablim1
Zap70	0	0.32966344	0.33	0.001	0	2	Zap70
Cd247	0	0.31203839	0.299	0.001	0	2	Cd247
Cish	4.60E-308	0.34435294	0.335	0.007	6.05E-304	2	Cish
Ltb	1.79E-303	0.72155193	0.71	0.141	2.36E-299	2	Ltb
Shisa5	9.88E-294	0.70542235	0.807	0.223	1.30E-289	2	Shisa5
Ctla4	1.66E-293	0.37384895	0.285	0.001	2.19E-289	2	Ctla4
Sh2d1a	1.18E-290	0.29664765	0.276	0.001	1.56E-286	2	Sh2d1a
Rpl27a	8.95E-290	0.86625492	0.983	0.722	1.18E-285	2	Rpl27a
Tox	1.46E-289	0.28006932	0.274	0	1.92E-285	2	Tox
Rpl13	1.97E-289	0.94541149	0.979	0.673	2.59E-285	2	Rpl13
Rps7	2.04E-287	0.90691333	0.945	0.502	2.68E-283	2	Rps7
Klrc1	1.97E-285	0.30331537	0.27	0	2.59E-281	2	Klrc1

Serpina3g	8.87E-282	0.42270494	0.402	0.027	1.17E-277	2	Serpina3g
Odc1	1.06E-279	0.61766763	0.4	0.028	1.39E-275	2	Odc1
Rpl10a	4.30E-279	0.81038712	0.915	0.325	5.65E-275	2	Rpl10a
Rps3a1	3.13E-278	0.86814141	0.966	0.642	4.12E-274	2	Rps3a1
Rplp1	1.91E-277	0.85110652	0.986	0.781	2.52E-273	2	Rplp1
H2-K1	8.76E-277	0.90409955	0.964	0.491	1.15E-272	2	H2-K1
Ikzf2	3.14E-276	0.54088821	0.296	0.006	4.13E-272	2	Ikzf2
Ifng	1.85E-274	0.47284094	0.26	0	2.43E-270	2	Ifng
Rpl22l1	2.81E-274	0.72920525	0.745	0.197	3.69E-270	2	Rpl22l1
Rps23	6.44E-274	0.82066909	0.956	0.631	8.47E-270	2	Rps23
Rpl32	7.25E-274	0.93844787	0.965	0.569	9.53E-270	2	Rpl32
Dusp2	3.94E-273	0.53668047	0.484	0.055	5.18E-269	2	Dusp2
Rack1	9.38E-268	0.81449867	0.909	0.413	1.23E-263	2	Rack1
Rps20	3.48E-267	0.89084534	0.956	0.52	4.57E-263	2	Rps20
Eef1a1	1.14E-265	0.87224195	0.98	0.81	1.49E-261	2	Eef1a1
Rps13	2.33E-262	0.81905088	0.95	0.644	3.06E-258	2	Rps13
Rpl19	3.45E-259	0.77382737	0.969	0.693	4.54E-255	2	Rpl19
Rps5	4.35E-259	0.82232933	0.955	0.51	5.72E-255	2	Rps5
Il18r1	6.16E-259	0.2861107	0.271	0.004	8.10E-255	2	Il18r1
Lgals11	2.96E-258	0.7570003	0.726	0.17	3.89E-254	2	Lgals1
Tmsb101	4.83E-254	0.72050928	0.869	0.257	6.36E-250	2	Tmsb10
Rps14	4.62E-253	0.7427874	0.975	0.758	6.08E-249	2	Rps14
Bcl2	3.16E-251	0.45282443	0.362	0.025	4.16E-247	2	Bcl2

Npm1	2.12E-250	0.64280926	0.742	0.197	2.79E-246	2	Npm1
Cd4	1.92E-248	0.30519828	0.259	0.004	2.53E-244	2	Cd4
Rpl30	8.78E-248	0.77934349	0.956	0.656	1.15E-243	2	Rpl30
Cd27	1.04E-247	0.26245031	0.267	0.005	1.36E-243	2	Cd27
Il7r	1.56E-247	0.56893504	0.423	0.043	2.06E-243	2	Il7r
Rpl11	2.21E-246	0.74554742	0.948	0.558	2.90E-242	2	Rpl11
Rps10	5.25E-245	0.76010705	0.969	0.704	6.90E-241	2	Rps10
Rpl7	1.08E-242	0.74150034	0.915	0.454	1.42E-238	2	Rpl7
Rpl22	2.03E-242	0.71391882	0.905	0.397	2.67E-238	2	Rpl22
Rps15	5.22E-242	0.69733422	0.932	0.476	6.86E-238	2	Rps15
Rpl23	5.42E-241	0.75236864	0.975	0.804	7.13E-237	2	Rpl23
Eef1b2	6.45E-240	0.70963472	0.846	0.313	8.48E-236	2	Eef1b2
Rps6	1.70E-237	0.73142128	0.918	0.438	2.24E-233	2	Rps6
Rps3	7.03E-237	0.69506505	0.968	0.639	9.25E-233	2	Rps3
Rpl36a	7.71E-236	0.70924732	0.819	0.287	1.01E-231	2	Rpl36a
Rabgap1l	1.01E-234	0.31025728	0.334	0.021	1.33E-230	2	Rabgap1l
Eif3e	1.25E-234	0.43359856	0.553	0.097	1.65E-230	2	Eif3e
Rplp0	9.13E-234	0.80923121	0.955	0.557	1.20E-229	2	Rplp0
Rpl4	3.28E-233	0.68786003	0.842	0.303	4.32E-229	2	Rpl4
Rpl39	2.23E-229	0.74622462	0.961	0.668	2.93E-225	2	Rpl39
Rpl9	9.83E-227	0.70024959	0.951	0.653	1.29E-222	2	Rpl9
Rpl15	1.08E-226	0.7210431	0.908	0.432	1.42E-222	2	Rpl15
Pla2g16	1.28E-226	0.33198963	0.389	0.038	1.68E-222	2	Pla2g16

Rpl23a	6.83E-226	0.67357526	0.889	0.398	8.98E-222	2	Rpl23a
Tpt1	5.00E-223	0.71960394	0.99	0.955	6.58E-219	2	Tpt1
Dut	1.58E-222	0.26318563	0.255	0.007	2.08E-218	2	Dut
Rpl17	3.10E-221	0.67523659	0.973	0.754	4.08E-217	2	Rpl17
Rhoh	1.05E-219	0.38576326	0.478	0.071	1.38E-215	2	Rhoh
Rpl24	3.13E-218	0.67040312	0.928	0.516	4.12E-214	2	Rpl24
Ly6a	3.75E-216	0.64553422	0.588	0.117	4.94E-212	2	Ly6a
Rpl18a	1.72E-213	0.67132666	0.985	0.767	2.26E-209	2	Rpl18a
Sdf4	1.86E-213	0.83638335	0.555	0.125	2.44E-209	2	Sdf4
Rps12	9.04E-213	0.69823412	0.97	0.737	1.19E-208	2	Rps12
Rpl14	1.18E-212	0.64453121	0.904	0.41	1.55E-208	2	Rpl14
Rpl26	3.86E-210	0.65226905	0.961	0.628	5.07E-206	2	Rpl26
Rpl27	6.69E-209	0.60159398	0.819	0.323	8.80E-205	2	Rpl27
Ifi27	1.34E-206	0.3146715	0.352	0.034	1.76E-202	2	Ifi27
Naca	9.56E-206	0.62052513	0.851	0.366	1.26E-201	2	Naca
Rpl21	1.65E-205	0.64125276	0.955	0.66	2.17E-201	2	Rpl21
Eif3h	5.12E-205	0.51285398	0.672	0.19	6.74E-201	2	Eif3h
Rpl8	7.14E-205	0.6247361	0.96	0.62	9.39E-201	2	Rpl8
Rps16	3.07E-202	0.64314291	0.975	0.812	4.04E-198	2	Rps16
Rps11	9.58E-201	0.67682098	0.97	0.652	1.26E-196	2	Rps11
Fkbp3	4.69E-199	0.29292848	0.349	0.035	6.17E-195	2	Fkbp3
Anxa6	9.42E-198	0.32555455	0.381	0.046	1.24E-193	2	Anxa6
Rpl29	1.09E-197	0.58323596	0.89	0.404	1.44E-193	2	Rpl29

Rac2	4.19E-196	0.58649976	0.817	0.316	5.51E-192	2	Rac2
Prkch	6.77E-195	0.28748881	0.346	0.036	8.91E-191	2	Prkch
Ifi27l2a1	1.83E-194	0.91717506	0.681	0.194	2.40E-190	2	Ifi27l2a
Rps8	1.01E-193	0.65251373	0.974	0.76	1.33E-189	2	Rps8
Rps19	1.10E-192	0.65870326	0.981	0.59	1.45E-188	2	Rps19
Rpl7a1	1.97E-192	0.5873124	0.874	0.37	2.59E-188	2	Rpl7a
Rps2	4.46E-192	0.67882137	0.922	0.54	5.86E-188	2	Rps2
Hsp90ab1	1.67E-191	0.63909219	0.829	0.322	2.20E-187	2	Hsp90ab1
Rpl34	5.50E-191	0.63413342	0.964	0.705	7.24E-187	2	Rpl34
Rinl	6.95E-190	0.3718734	0.463	0.081	9.14E-186	2	Rinl
Rpl18	1.54E-189	0.61556861	0.946	0.604	2.03E-185	2	Rpl18
Ptpn18	2.47E-182	0.51116067	0.689	0.214	3.25E-178	2	Ptpn18
Slc25a4	3.11E-174	0.2871996	0.357	0.047	4.10E-170	2	Slc25a4
Eef1g	2.72E-173	0.46537087	0.587	0.161	3.58E-169	2	Eef1g
Ppia	1.52E-172	0.59429566	0.874	0.431	2.00E-168	2	Ppia
Mbnl1	1.28E-171	0.50058058	0.661	0.202	1.69E-167	2	Mbnl1
Hcst	2.43E-169	0.4614994	0.573	0.152	3.19E-165	2	Hcst
Rpl36	3.18E-168	0.57176377	0.949	0.528	4.18E-164	2	Rpl36
Rpl6	1.20E-167	0.55338997	0.946	0.559	1.58E-163	2	Rpl6
Eef1d	3.74E-167	0.37798215	0.543	0.135	4.92E-163	2	Eef1d
Cd48	4.96E-163	0.34428613	0.423	0.078	6.53E-159	2	Cd48
Arl6ip1	1.74E-159	0.48721374	0.603	0.182	2.28E-155	2	Arl6ip1
H2-Q6	3.08E-157	0.25221353	0.296	0.033	4.06E-153	2	H2-Q6

Klrk1	3.53E-157	0.42013856	0.354	0.055	4.64E-153	2	Klrk1
Il2rg	1.30E-154	0.28479585	0.361	0.057	1.70E-150	2	Il2rg
Hnrnpa1	1.14E-153	0.39971736	0.489	0.119	1.50E-149	2	Hnrnpa1
Ndfip1	3.00E-149	0.26738538	0.306	0.04	3.95E-145	2	Ndfip1
2010111I01Rik	2.40E-147	0.25345757	0.296	0.037	3.15E-143	2	2010111I01Rik
Rplp2	3.81E-146	0.47276136	0.969	0.754	5.02E-142	2	Rplp2
Ybx3	1.46E-145	0.27672698	0.31	0.043	1.91E-141	2	Ybx3
Sumo2	1.25E-144	0.42324918	0.624	0.212	1.65E-140	2	Sumo2
Eif3f	6.05E-144	0.42791832	0.697	0.254	7.96E-140	2	Eif3f
H2afv	1.05E-142	0.30563539	0.349	0.058	1.38E-138	2	H2afv
Rps26	2.74E-142	0.55827356	0.887	0.528	3.60E-138	2	Rps26
Smc4	5.30E-142	0.27281569	0.303	0.041	6.97E-138	2	Smc4
Mettl23	3.07E-141	0.25219824	0.324	0.049	4.04E-137	2	Mettl23
Atp5g2	4.97E-140	0.4030135	0.621	0.208	6.54E-136	2	Atp5g2
Fkbp1a	2.25E-139	0.28700707	0.361	0.065	2.96E-135	2	Fkbp1a
Eif3m	1.85E-138	0.32209748	0.457	0.11	2.43E-134	2	Eif3m
Uqcrh	7.36E-136	0.47252193	0.727	0.325	9.68E-132	2	Uqcrh
H2-T22	3.59E-134	0.27658618	0.361	0.067	4.72E-130	2	H2-T22
Snrpf	2.08E-133	0.30855794	0.432	0.1	2.73E-129	2	Snrpf
Psmb8	1.58E-129	0.42423451	0.709	0.274	2.08E-125	2	Psmb8
Ms4a6b1	1.80E-129	0.37941636	0.514	0.144	2.37E-125	2	Ms4a6b
S100a13	2.60E-129	0.30610166	0.403	0.09	3.42E-125	2	S100a13
Eef2	9.96E-128	0.47172567	0.77	0.369	1.31E-123	2	Eef2

Btf3	1.65E-127	0.42862947	0.77	0.354	2.17E-123	2	Btf3
Rps21	1.46E-125	0.49165684	0.945	0.677	1.91E-121	2	Rps21
Snrpe	1.29E-124	0.33829228	0.516	0.156	1.70E-120	2	Snrpe
Pdcd4	8.06E-124	0.25157295	0.293	0.046	1.06E-119	2	Pdcd4
Rpl13a	2.42E-123	0.33971725	0.476	0.133	3.18E-119	2	Rpl13a
Rpl37a	1.32E-120	0.45230397	0.975	0.765	1.74E-116	2	Rpl37a
AU020206	2.04E-120	0.30156239	0.387	0.086	2.69E-116	2	AU020206
Mndal	1.33E-119	0.31234519	0.423	0.104	1.75E-115	2	Mndal
Cox7a2l	7.29E-118	0.3562523	0.577	0.202	9.58E-114	2	Cox7a2l
Cdk6	1.06E-116	0.26711074	0.285	0.047	1.40E-112	2	Cdk6
Cd82	1.09E-116	0.36943402	0.423	0.112	1.43E-112	2	Cd82
mt-Atp61	1.44E-116	0.45349404	1	0.713	1.90E-112	2	mt-Atp6
Kmt2a	1.12E-115	0.26774294	0.345	0.071	1.47E-111	2	Kmt2a
Limd2	9.81E-115	0.31858949	0.496	0.15	1.29E-110	2	Limd2
Rps27a	1.17E-112	0.43929045	0.948	0.762	1.54E-108	2	Rps27a
Rbm3	1.56E-112	0.4580651	0.776	0.405	2.06E-108	2	Rbm3
S100a41	2.41E-112	0.51369679	0.606	0.203	3.17E-108	2	S100a4
Ran	5.12E-111	0.31951033	0.435	0.121	6.74E-107	2	Ran
Sub1	1.58E-110	0.42020524	0.64	0.259	2.07E-106	2	Sub1
Akap13	8.77E-109	0.39576503	0.582	0.222	1.15E-104	2	Akap13
Serbp1	4.30E-108	0.36215176	0.609	0.238	5.65E-104	2	Serbp1
Hspe1	5.76E-107	0.31305525	0.426	0.119	7.58E-103	2	Hspe1
Ccnd2	1.25E-103	0.3518513	0.446	0.132	1.64E-99	2	Ccnd2

Eif3i	7.16E-103	0.27165973	0.384	0.1	9.42E-99	2	Eif3i
Rps171	2.10E-102	0.40447034	0.71	0.332	2.76E-98	2	Rps17
Rtraf	2.41E-102	0.25931129	0.38	0.097	3.17E-98	2	Rtraf
Cox6c	4.23E-102	0.3404405	0.629	0.257	5.56E-98	2	Cox6c
Nol7	1.08E-100	0.27206397	0.374	0.097	1.42E-96	2	Nol7
AC149090.1	3.52E-100	0.29250445	0.391	0.105	4.63E-96	2	AC149090.1
Aes	2.48E-98	0.27294759	0.411	0.118	3.27E-94	2	Aes
mt-Co31	5.68E-97	0.35730299	0.998	0.729	7.47E-93	2	mt-Co3
Apobec3	6.94E-97	0.26603473	0.435	0.129	9.13E-93	2	Apobec3
Psmb9	2.09E-95	0.2807609	0.446	0.139	2.74E-91	2	Psmb9
Pfdn5	1.07E-93	0.37208715	0.768	0.407	1.41E-89	2	Pfdn5
Ppib1	1.91E-93	0.32541705	0.582	0.237	2.51E-89	2	Ppib
Psmb1	3.98E-93	0.29378176	0.489	0.173	5.23E-89	2	Psmb1
Tmsb4x1	9.16E-93	0.46242587	0.991	0.953	1.20E-88	2	Tmsb4x
Dad1	2.95E-92	0.28724737	0.502	0.18	3.88E-88	2	Dad1
Ndufa4	7.75E-90	0.29438582	0.457	0.156	1.02E-85	2	Ndufa4
mt-Co11	3.51E-89	0.31506324	0.998	0.761	4.61E-85	2	mt-Co1
Krtcap2	4.77E-89	0.26122311	0.4	0.12	6.27E-85	2	Krtcap2
Abrac1	3.04E-88	0.28333607	0.467	0.163	4.00E-84	2	Abrac1
Rpl35a	6.40E-87	0.36082451	0.96	0.779	8.41E-83	2	Rpl35a
B2m1	1.32E-86	0.34777776	0.927	0.598	1.73E-82	2	B2m
Atp5c1	3.34E-85	0.26779232	0.455	0.158	4.40E-81	2	Atp5c1
Hint1	4.21E-85	0.30518507	0.507	0.193	5.54E-81	2	Hint1
Arhgdib	1.42E-83	0.34899763	0.661	0.325	1.86E-79	2	Arhgdib
Ptma	5.88E-82	0.41983003	0.814	0.456	7.73E-78	2	Ptma
Atp5h	2.67E-80	0.31317663	0.638	0.309	3.51E-76	2	Atp5h
Srsf3	3.89E-80	0.28848444	0.472	0.179	5.12E-76	2	Srsf3
Sri	2.37E-79	0.25359516	0.42	0.142	3.12E-75	2	Sri
Rpl31	2.40E-78	0.30135094	0.644	0.309	3.15E-74	2	Rpl31
Rpl28	1.21E-77	0.35076581	0.902	0.604	1.59E-73	2	Rpl28
Anp32b	2.47E-75	0.27384152	0.468	0.181	3.25E-71	2	Anp32b
Cox7c	3.24E-72	0.29844557	0.621	0.304	4.26E-68	2	Cox7c
Ogt	3.54E-67	0.2516185	0.456	0.181	4.66E-63	2	Ogt
Rps25	4.41E-66	0.29900972	0.877	0.596	5.80E-62	2	Rps25
Maf	2.31E-65	0.40445656	0.295	0.09	3.04E-61	2	Maf
Ndufa13	1.27E-64	0.26556286	0.542	0.254	1.67E-60	2	Ndufa13

Atp5d	5.61E-64	0.2635651	0.486	0.214	7.38E-60	2	Atp5d
Rpl38	1.35E-63	0.33277851	0.889	0.593	1.77E-59	2	Rpl38
Pabpc1	7.19E-62	0.3036698	0.624	0.34	9.46E-58	2	Pabpc1
7-Sep	2.38E-61	0.25322259	0.431	0.179	3.13E-57	2	7-Sep
Slc25a3	3.12E-59	0.26554962	0.539	0.264	4.10E-55	2	Slc25a3
H2-D1	5.97E-57	0.32203053	0.907	0.633	7.85E-53	2	H2-D1
mt-Cytb1	1.22E-53	0.25073563	0.918	0.612	1.61E-49	2	mt-Cytb
Gnas	3.42E-53	0.25354526	0.593	0.317	4.50E-49	2	Gnas
Hif1a	5.63E-52	0.28351075	0.377	0.159	7.40E-48	2	Hif1a
Id2	3.13E-49	0.28815179	0.645	0.351	4.12E-45	2	Id2
H2afz	1.22E-47	0.2951095	0.559	0.294	1.60E-43	2	H2afz
Rps27	2.03E-47	0.27230012	0.968	0.873	2.67E-43	2	Rps27
Rpl35	2.48E-46	0.25230621	0.633	0.351	3.26E-42	2	Rpl35
Ccl4	7.63E-09	0.63727299	0.281	0.195	0.00010042	2	Ccl4
Ciita	0	0.65824219	0.584	0.057	0	3	Ciita
Cbfa2t3	0	0.55857522	0.523	0.026	0	3	Cbfa2t3
H2-Eb11	2.31E-305	1.83278512	0.761	0.153	3.04E-301	3	H2-Eb1
H2-Oa	3.33E-300	0.49071386	0.38	0.016	4.38E-296	3	H2-Oa
Cd741	1.29E-293	1.90003411	0.833	0.219	1.70E-289	3	Cd74
H2-Aa1	2.31E-287	1.768665	0.768	0.164	3.04E-283	3	H2-Aa
H2-Ab11	3.06E-276	1.76646849	0.753	0.173	4.02E-272	3	H2-Ab1
H2-DMb2	4.20E-222	0.32690876	0.274	0.01	5.52E-218	3	H2-DMb2
Syngn2	1.35E-205	0.66623865	0.589	0.12	1.78E-201	3	Syngn2
H2-DMb11	1.61E-184	0.59372338	0.532	0.1	2.11E-180	3	H2-DMb1
H2-DMa1	9.38E-169	0.60820716	0.57	0.132	1.23E-164	3	H2-DMa
Ckb	6.43E-159	0.34949895	0.318	0.034	8.45E-155	3	Ckb
Ifi205	2.98E-157	0.38680755	0.271	0.023	3.91E-153	3	Ifi205
Olfm1	4.50E-154	0.25786104	0.265	0.022	5.92E-150	3	Olfm1
Wdfy4	9.49E-153	0.34761021	0.325	0.039	1.25E-148	3	Wdfy4
mt-Co21	1.04E-140	1.07792575	0.997	0.722	1.37E-136	3	mt-Co2

mt-Co12	1.40E-132	0.9911879	0.997	0.77	1.84E-128	3	mt-Co1
Cst31	2.95E-131	1.3807424	0.805	0.466	3.89E-127	3	Cst3
Crip11	4.21E-131	0.90158487	0.636	0.214	5.54E-127	3	Crip1
mt-Co32	4.23E-126	0.98863784	0.998	0.74	5.57E-122	3	mt-Co3
Slamf7	4.12E-117	0.27554452	0.323	0.052	5.42E-113	3	Slamf7
Napsa	4.88E-117	0.51637111	0.51	0.148	6.42E-113	3	Napsa
H2afy	1.52E-116	0.44491359	0.539	0.165	2.00E-112	3	H2afy
mt-Atp62	2.58E-112	0.92143958	0.998	0.724	3.39E-108	3	mt-Atp6
Ccdc88a	4.26E-108	0.2844755	0.278	0.041	5.60E-104	3	Ccdc88a
Klrk11	4.90E-107	0.2935337	0.351	0.066	6.44E-103	3	Klrk1
Rpsa1	2.43E-100	0.59905405	0.922	0.575	3.19E-96	3	Rpsa
Plekho11	1.24E-98	0.30892564	0.416	0.105	1.63E-94	3	Plekho1
Cd72	1.77E-93	0.27514713	0.252	0.039	2.33E-89	3	Cd72
Atox1	5.02E-93	0.61161349	0.677	0.357	6.60E-89	3	Atox1
Rps191	5.29E-84	0.50742834	0.901	0.615	6.96E-80	3	Rps19
Naaa	1.52E-81	0.36773416	0.269	0.055	1.99E-77	3	Naaa
Cxcl161	1.06E-80	0.3492243	0.388	0.105	1.40E-76	3	Cxcl16
Ctsh1	1.09E-80	0.35655812	0.583	0.221	1.43E-76	3	Ctsh
Lsp1	1.27E-75	0.56949507	0.607	0.294	1.66E-71	3	Lsp1
Dock10	3.06E-72	0.29343793	0.414	0.132	4.03E-68	3	Dock10
Tmsb102	3.23E-72	0.55108172	0.651	0.308	4.24E-68	3	Tmsb10
Gm2a1	8.96E-71	0.48822831	0.555	0.254	1.18E-66	3	Gm2a
Psmb81	1.79E-69	0.48187513	0.614	0.303	2.35E-65	3	Psmb8
Ptms	3.74E-69	0.37935065	0.471	0.182	4.92E-65	3	Ptms
Psme1	4.61E-67	0.46819364	0.536	0.249	6.07E-63	3	Psme1
mt-Nd11	1.27E-63	0.79821513	0.786	0.491	1.67E-59	3	mt-Nd1
Atpif1	3.13E-62	0.32390959	0.42	0.158	4.12E-58	3	Atpif1
Plac81	5.62E-62	0.55570303	0.435	0.16	7.39E-58	3	Plac8
H2afz1	1.76E-61	0.60078029	0.573	0.303	2.31E-57	3	H2afz
Rpl10a1	5.15E-60	0.40928263	0.7	0.375	6.77E-56	3	Rpl10a
Sub11	1.57E-59	0.40817051	0.571	0.283	2.06E-55	3	Sub1
Rps4x1	9.46E-58	0.39517596	0.791	0.457	1.24E-53	3	Rps4x

mt-Cytb2	2.04E-57	0.8015934	0.867	0.63	2.69E-53	3	mt-Cytb
Rps111	1.13E-56	0.47688617	0.852	0.679	1.49E-52	3	Rps11
mt-Nd21	3.23E-54	0.79164775	0.742	0.488	4.25E-50	3	mt-Nd2
Slfn51	1.39E-53	0.32950513	0.349	0.118	1.82E-49	3	Slfn5
Traf1	1.57E-53	0.34937598	0.278	0.083	2.06E-49	3	Traf1
Hsp90ab11	1.42E-52	0.31858016	0.675	0.361	1.87E-48	3	Hsp90ab1
Gdi2	1.13E-51	0.32391222	0.523	0.254	1.49E-47	3	Gdi2
Gpx11	1.05E-50	0.33938177	0.644	0.348	1.38E-46	3	Gpx1
Apobec31	1.53E-50	0.25941212	0.383	0.147	2.01E-46	3	Apobec3
mt-Nd31	5.06E-50	0.45480511	0.609	0.332	6.65E-46	3	mt-Nd3
Irf8	9.61E-50	0.53680845	0.372	0.151	1.26E-45	3	Irf8
Ptma1	6.87E-49	0.34434061	0.758	0.477	9.04E-45	3	Ptma
Ifitm31	1.45E-48	0.64038309	0.56	0.301	1.90E-44	3	Ifitm3
Rps201	3.06E-48	0.36529424	0.808	0.556	4.03E-44	3	Rps20
Pou2f2	1.67E-47	0.29708175	0.347	0.127	2.19E-43	3	Pou2f2
Plbd1	3.30E-47	0.30743682	0.446	0.202	4.34E-43	3	Plbd1
mt-Nd41	1.25E-46	0.77684929	0.794	0.585	1.65E-42	3	mt-Nd4
Id21	1.73E-46	0.4160687	0.633	0.364	2.27E-42	3	Id2
Cnn2	3.56E-45	0.26122908	0.393	0.164	4.68E-41	3	Cnn2
Rpl61	7.71E-45	0.34372166	0.813	0.591	1.01E-40	3	Rpl6
Rpl141	1.05E-44	0.36734869	0.69	0.456	1.38E-40	3	Rpl14
Rpl131	5.78E-44	0.34637728	0.898	0.695	7.61E-40	3	Rpl13
Rpl33	1.29E-43	0.30142013	0.693	0.398	1.70E-39	3	Rpl3
Rpl41	7.00E-43	0.28995388	0.633	0.35	9.21E-39	3	Rpl4
Psme2	1.29E-41	0.38147786	0.44	0.212	1.69E-37	3	Psme2
Nsa2	9.30E-41	0.25192451	0.471	0.229	1.22E-36	3	Nsa2
Psmb91	9.25E-40	0.25293856	0.37	0.16	1.22E-35	3	Psmb9
Rps51	9.27E-40	0.33923998	0.771	0.551	1.22E-35	3	Rps5
Rpl351	1.05E-38	0.3668546	0.584	0.368	1.38E-34	3	Rpl35
Rplp01	1.09E-37	0.31474683	0.81	0.59	1.43E-33	3	Rplp0
Rps181	1.21E-37	0.26645225	0.786	0.515	1.59E-33	3	Rps18
Rpl261	3.76E-37	0.28718294	0.847	0.655	4.94E-33	3	Rpl26
Rpl7a2	1.70E-36	0.27751047	0.672	0.415	2.23E-32	3	Rpl7a
Rpl281	2.28E-36	0.3281127	0.805	0.627	3.00E-32	3	Rpl28
Hspa81	6.78E-36	0.29692612	0.674	0.419	8.92E-32	3	Hspa8
Eef1b21	1.36E-35	0.3938326	0.578	0.367	1.78E-31	3	Eef1b2
Malat1	6.17E-35	0.40871119	0.998	0.996	8.12E-31	3	Malat1
Eef21	3.16E-33	0.2728015	0.635	0.401	4.16E-29	3	Eef2
Rpl36a1	6.00E-32	0.29691302	0.563	0.339	7.89E-28	3	Rpl36a
Rpl151	6.02E-32	0.30548369	0.687	0.479	7.91E-28	3	Rpl15

Rps61	1.39E-30	0.25986049	0.696	0.484	1.82E-26	3	Rps6
Rpl361	2.98E-30	0.28387858	0.76	0.568	3.92E-26	3	Rpl36
Tspo1	3.81E-30	0.3682509	0.536	0.333	5.02E-26	3	Tspo
Rpl321	1.40E-27	0.28289186	0.787	0.607	1.84E-23	3	Rpl32
Tagln2	1.31E-24	0.34196236	0.334	0.171	1.72E-20	3	Tagln2
Rps261	6.15E-24	0.2652837	0.729	0.561	8.09E-20	3	Rps26
S100a42	1.42E-23	0.43531226	0.432	0.241	1.86E-19	3	S100a4
Map4k4	8.14E-23	0.28190464	0.268	0.128	1.07E-18	3	Map4k4
Ifitm1	3.13E-22	0.96890432	0.385	0.242	4.12E-18	3	Ifitm1
Rps271	1.56E-17	0.30644717	0.33	0.194	2.06E-13	3	Rps271
Actb	1.45E-12	0.26574417	0.981	0.989	1.91E-08	3	Actb
Tmsb4x2	7.28E-12	0.48999873	0.953	0.959	9.57E-08	3	Tmsb4x
Ly6a1	1.05E-11	0.34933244	0.278	0.174	1.38E-07	3	Ly6a
Calm1	6.24E-07	0.30307627	0.602	0.504	0.00820287	3	Calm1
Gm424181	5.08E-06	0.75028969	0.976	0.962	0.06686391	3	Gm42418
Igkc	0	4.10414412	0.521	0.006	0	4	Igkc
Ly6d	0	2.04503296	0.835	0.001	0	4	Ly6d
Ccr9	0	0.99525373	0.504	0.004	0	4	Ccr9
Cox6a2	0	0.95062846	0.438	0.002	0	4	Cox6a2
Iglc3	0	0.92723626	0.694	0	0	4	Iglc3
Iglc2	0	0.77941423	0.388	0.001	0	4	Iglc2
Cd79a	0	0.70954099	0.405	0	0	4	Cd79a
Mzb1	0	0.69221686	0.488	0	0	4	Mzb1
Atp1b1	0	0.59504864	0.413	0.002	0	4	Atp1b1
Ebf1	0	0.54505561	0.314	0	0	4	Ebf1
Fcrla	0	0.47712544	0.43	0.004	0	4	Fcrla
Gm21762	0	0.43475978	0.355	0.001	0	4	Gm21762
Cd79b	8.92E-298	0.71776081	0.364	0.004	1.17E-293	4	Cd79b
Siglech	1.44E-294	1.55281601	0.562	0.016	1.90E-290	4	Siglech
Bcl11a	1.98E-293	0.85648011	0.636	0.022	2.60E-289	4	Bcl11a
Smim5	8.02E-287	0.42716776	0.331	0.003	1.05E-282	4	Smim5
Ighm	1.48E-283	1.84515879	0.876	0.054	1.95E-279	4	Ighm
Tcf4	6.71E-187	1.26186241	0.719	0.057	8.83E-183	4	Tcf4
Rnase6	2.36E-182	1.0042349	0.661	0.047	3.11E-178	4	Rnase6

Cd7	1.07E-160	0.72411719	0.438	0.02	1.41E-156	4	Cd7
Mef2c	1.65E-159	0.68627823	0.694	0.059	2.17E-155	4	Mef2c
Dnajc7	2.36E-141	0.98512078	0.752	0.087	3.11E-137	4	Dnajc7
Cnp	1.06E-90	0.3921459	0.446	0.042	1.40E-86	4	Cnp
Sell	1.50E-84	0.54118678	0.537	0.066	1.98E-80	4	Sell
Bst21	8.14E-81	1.53293495	0.694	0.14	1.07E-76	4	Bst2
Rpgrip1	3.43E-78	0.35936007	0.289	0.02	4.52E-74	4	Rpgrip1
Gm5547	8.28E-78	0.29116293	0.281	0.018	1.09E-73	4	Gm5547
Plac82	1.05E-76	1.29133145	0.802	0.177	1.38E-72	4	Plac8
Ly861	1.08E-73	0.50674314	0.711	0.128	1.42E-69	4	Ly86
Irf81	4.34E-73	1.38698753	0.727	0.163	5.71E-69	4	Irf8
Nucb2	5.09E-68	0.4240841	0.372	0.039	6.69E-64	4	Nucb2
P2ry14	2.96E-65	0.29249266	0.306	0.027	3.90E-61	4	P2ry14
Tnfrsf13b	7.62E-65	0.29935069	0.339	0.033	1.00E-60	4	Tnfrsf13b
Pafah1b3	4.02E-63	0.31075602	0.339	0.034	5.29E-59	4	Pafah1b3
Ptprcap1	7.77E-62	0.47658343	0.636	0.114	1.02E-57	4	Ptprcap
Ly6c21	1.70E-61	1.36532035	0.579	0.115	2.24E-57	4	Ly6c2
Abhd17b	2.13E-60	0.25293059	0.289	0.026	2.80E-56	4	Abhd17b
Rps202	1.57E-58	1.06903808	0.975	0.575	2.06E-54	4	Rps20
Tubgcp5	9.21E-57	0.26426595	0.281	0.026	1.21E-52	4	Tubgcp5
Cybb1	1.89E-56	0.59743212	0.686	0.15	2.49E-52	4	Cybb
Pkig	2.42E-56	0.31425321	0.331	0.037	3.18E-52	4	Pkig
St8sia4	1.10E-55	0.50074754	0.446	0.069	1.45E-51	4	St8sia4
Apobec32	1.47E-55	0.54232551	0.686	0.162	1.93E-51	4	Apobec3
Serp1	1.75E-55	0.61676719	0.727	0.193	2.30E-51	4	Serp1
Kmo	8.35E-54	0.26119209	0.273	0.026	1.10E-49	4	Kmo
Rps4x2	1.21E-52	0.89518055	0.983	0.483	1.59E-48	4	Rps4x
Rpl311	2.60E-52	1.01138285	0.851	0.347	3.42E-48	4	Rpl31
Rps241	3.12E-52	1.04672189	1	0.703	4.10E-48	4	Rps24
Snx51	3.28E-52	0.47124043	0.562	0.114	4.32E-48	4	Snx5
Ly6a2	5.48E-52	1.07604248	0.686	0.174	7.20E-48	4	Ly6a
Pgls	2.01E-50	0.55168936	0.62	0.147	2.65E-46	4	Pgls
Ptp4a3	4.36E-49	0.27364274	0.281	0.031	5.73E-45	4	Ptp4a3
Dap	1.64E-45	0.44188588	0.43	0.078	2.15E-41	4	Dap
Rps112	1.72E-45	0.79944696	0.959	0.692	2.26E-41	4	Rps11
Fchsd2	4.79E-45	0.29683572	0.306	0.039	6.30E-41	4	Fchsd2
Rabgap1l1	6.47E-43	0.34958164	0.372	0.06	8.51E-39	4	Rabgap1l
Rpl310	1.78E-41	0.67248056	0.95	0.419	2.34E-37	4	Rpl3

Ctsl1	2.71E-41	0.8108862	0.471	0.105	3.56E-37	4	Ctsl
Rell1	4.70E-41	0.32865192	0.355	0.057	6.19E-37	4	Rell1
Slc44a2	8.88E-41	0.42837106	0.471	0.1	1.17E-36	4	Slc44a2
Rpl121	1.58E-40	0.82283195	0.942	0.461	2.08E-36	4	Rpl12
Ly6e1	2.75E-40	0.71911903	0.934	0.435	3.62E-36	4	Ly6e
Tspan13	1.17E-39	0.50602385	0.512	0.123	1.53E-35	4	Tspan13
Ctsh2	2.93E-39	0.71269776	0.711	0.252	3.85E-35	4	Ctsh
Syng21	4.04E-39	0.64779048	0.579	0.163	5.31E-35	4	Syng2
Rpl191	4.38E-39	0.69008624	0.975	0.728	5.76E-35	4	Rpl19
Runx2	5.26E-39	0.39144693	0.372	0.067	6.92E-35	4	Runx2
Rps182	7.12E-39	0.71580147	0.967	0.536	9.36E-35	4	Rps18
Cd47	2.61E-38	0.60744426	0.785	0.299	3.44E-34	4	Cd47
Rpl10a2	6.01E-38	0.64439626	0.95	0.399	7.90E-34	4	Rpl10a
Lair11	2.63E-37	0.61955704	0.479	0.117	3.46E-33	4	Lair1
Ccnd1	3.53E-37	0.35847679	0.306	0.047	4.65E-33	4	Ccnd1
Rps52	4.46E-37	0.68275353	0.967	0.566	5.86E-33	4	Rps5
Rpl36a2	1.08E-36	0.57184773	0.884	0.353	1.41E-32	4	Rpl36a
Mvb12a	2.04E-36	0.36895406	0.388	0.077	2.68E-32	4	Mvb12a
Cd742	2.09E-36	0.40413508	0.868	0.274	2.75E-32	4	Cd74
Pltp	4.17E-36	0.33730922	0.264	0.037	5.48E-32	4	Pltp
Rps161	1.12E-35	0.62403716	0.975	0.832	1.47E-31	4	Rps16
Rpl71	2.33E-35	0.6131333	0.95	0.512	3.07E-31	4	Rpl7
Foxp1	3.07E-35	0.44829789	0.455	0.105	4.04E-31	4	Foxp1
Tmed3	3.69E-35	0.3421428	0.38	0.075	4.86E-31	4	Tmed3
Eif3f1	2.09E-34	0.51253708	0.785	0.308	2.75E-30	4	Eif3f
H2-T23	2.22E-34	0.50141933	0.628	0.201	2.92E-30	4	H2-T23
Rpl51	5.04E-34	0.61178718	0.909	0.448	6.62E-30	4	Rpl5
Rpl262	6.05E-34	0.59916348	0.975	0.67	7.95E-30	4	Rpl26
Rpl18a1	1.73E-33	0.65201097	0.975	0.795	2.27E-29	4	Rpl18a
Abhd17a	1.84E-33	0.28954245	0.372	0.074	2.42E-29	4	Abhd17a
mt-Co33	2.04E-33	0.6077883	1	0.763	2.68E-29	4	mt-Co3
Rps3a11	3.24E-33	0.63218111	0.95	0.684	4.26E-29	4	Rps3a1
Rpl322	3.48E-33	0.67522753	0.975	0.619	4.57E-29	4	Rpl32
Rpl132	6.44E-33	0.71281122	0.975	0.712	8.47E-29	4	Rpl13
Rpl301	1.44E-32	0.62977249	0.967	0.694	1.89E-28	4	Rpl30
Rpl231	2.80E-32	0.5918526	0.975	0.826	3.69E-28	4	Rpl23
Rack11	3.64E-32	0.55816128	0.934	0.475	4.79E-28	4	Rack1
Rps71	4.66E-32	0.6394194	0.95	0.558	6.13E-28	4	Rps7
mt-Atp63	4.68E-32	0.60418704	1	0.749	6.15E-28	4	mt-Atp6
mt-Nd5	1.02E-31	0.44116328	0.719	0.254	1.34E-27	4	mt-Nd5

Zbtb20	2.14E-31	0.34135763	0.331	0.063	2.82E-27	4	Zbtb20
Pld41	5.82E-31	0.50498264	0.488	0.139	7.65E-27	4	Pld4
Lpgat1	6.15E-31	0.25610157	0.281	0.047	8.09E-27	4	Lpgat1
Npm11	9.14E-31	0.424179	0.744	0.266	1.20E-26	4	Npm1
Rpl211	1.20E-30	0.63358163	0.959	0.697	1.57E-26	4	Rpl21
Mbnl11	5.99E-30	0.53908293	0.678	0.26	7.87E-26	4	Mbnl1
Tagln21	8.43E-30	0.45863086	0.57	0.181	1.11E-25	4	Tagln2
mt-Co13	9.57E-30	0.53647414	1	0.791	1.26E-25	4	mt-Co1
Rplp02	1.29E-29	0.53744128	0.967	0.607	1.69E-25	4	Rplp0
Rpl282	1.71E-29	0.51481003	0.959	0.64	2.25E-25	4	Rpl28
Rps15a1	2.21E-29	0.54585458	0.959	0.607	2.91E-25	4	Rps15a
Rpl42	2.63E-29	0.48472851	0.876	0.371	3.46E-25	4	Rpl4
Rpl111	2.67E-29	0.51284877	0.959	0.608	3.51E-25	4	Rpl11
Rpl391	2.85E-29	0.60021999	0.967	0.705	3.75E-25	4	Rpl39
Rps141	4.03E-29	0.52119989	0.967	0.786	5.30E-25	4	Rps14
Rpl81	5.02E-29	0.57069272	0.967	0.663	6.60E-25	4	Rpl8
Rpl142	8.15E-29	0.52100782	0.917	0.473	1.07E-24	4	Rpl14
mt-Co22	1.06E-28	0.45122543	1	0.748	1.39E-24	4	mt-Co2
Rps62	2.66E-28	0.49276609	0.942	0.498	3.50E-24	4	Rps6
Ech1	3.52E-28	0.27294366	0.372	0.085	4.63E-24	4	Ech1
Rps131	4.01E-28	0.60129544	0.942	0.683	5.28E-24	4	Rps13
Jaml	7.73E-28	0.40957456	0.455	0.125	1.02E-23	4	Jaml
Ptma2	9.62E-28	0.52851461	0.901	0.499	1.27E-23	4	Ptma
Rpl27a1	9.67E-28	0.61674651	0.959	0.756	1.27E-23	4	Rpl27a
Herpud1	1.14E-27	0.3045194	0.339	0.073	1.50E-23	4	Herpud1
Rpl91	1.63E-27	0.51352874	0.967	0.691	2.14E-23	4	Rpl9
Gnas1	2.25E-27	0.51760975	0.744	0.349	2.95E-23	4	Gnas
Rplp11	2.55E-27	0.55864437	0.967	0.807	3.36E-23	4	Rplp1
Rpl152	3.44E-27	0.52724434	0.909	0.493	4.52E-23	4	Rpl15
Rps172	3.78E-27	0.46951708	0.793	0.378	4.97E-23	4	Rps17
Pkib	4.85E-27	0.28372891	0.264	0.047	6.38E-23	4	Pkib
Rps81	5.03E-27	0.50438798	0.983	0.787	6.62E-23	4	Rps8
Cd37	7.82E-27	0.40780456	0.579	0.199	1.03E-22	4	Cd37
Rpl35a1	7.85E-27	0.47860802	0.967	0.802	1.03E-22	4	Rpl35a
Rps9	3.16E-26	0.47165393	0.975	0.877	4.15E-22	4	Rps9
Napsa1	6.27E-26	0.42076825	0.554	0.18	8.24E-22	4	Napsa
Svbp	6.95E-26	0.28023213	0.322	0.071	9.14E-22	4	Svbp
Rps192	8.13E-26	0.7228372	0.959	0.64	1.07E-21	4	Rps19
mt-Nd32	8.20E-26	0.38783674	0.818	0.352	1.08E-21	4	mt-Nd3
Rpl291	8.60E-26	0.49365112	0.901	0.466	1.13E-21	4	Rpl29

Sec11c	6.09E-25	0.39148466	0.463	0.141	8.01E-21	4	Sec11c
Krtcap21	1.45E-24	0.34246699	0.488	0.153	1.90E-20	4	Krtcap2
Ppia1	1.45E-24	0.53800951	0.851	0.488	1.90E-20	4	Ppia
Hnrnpa11	1.75E-24	0.30891438	0.521	0.165	2.30E-20	4	Hnrnpa1
Rps101	1.85E-24	0.57711093	0.967	0.738	2.43E-20	4	Rps10
Rpl22l11	1.99E-24	0.36409309	0.694	0.267	2.61E-20	4	Rpl22l1
Cd8b11	3.01E-24	0.5509856	0.298	0.063	3.96E-20	4	Cd8b1
Rpl352	3.04E-24	0.46556131	0.81	0.383	4.00E-20	4	Rpl35
Fyn	3.63E-24	0.30817129	0.339	0.081	4.77E-20	4	Fyn
H2-DMa2	4.91E-24	0.31376147	0.554	0.173	6.46E-20	4	H2-DMa
Serinc3	8.44E-24	0.35007954	0.702	0.287	1.11E-19	4	Serinc3
Ppp1r14b	1.67E-23	0.28060245	0.355	0.09	2.20E-19	4	Ppp1r14b
mt-Nd42	1.99E-23	0.39747019	0.959	0.6	2.62E-19	4	mt-Nd4
Sec61b	2.13E-23	0.51429487	0.694	0.33	2.81E-19	4	Sec61b
Rpl181	2.26E-23	0.49562929	0.959	0.647	2.97E-19	4	Rpl18
Cd69	4.25E-23	0.30634611	0.264	0.053	5.59E-19	4	Cd69
Rpl221	8.27E-23	0.47888281	0.893	0.462	1.09E-18	4	Rpl22
Rps262	8.90E-23	0.49019874	0.909	0.573	1.17E-18	4	Rps26
Rps251	9.38E-23	0.4405356	0.926	0.631	1.23E-18	4	Rps25
Hsp90b11	1.06E-22	0.44939346	0.628	0.252	1.40E-18	4	Hsp90b1
Sub12	1.99E-22	0.47172002	0.669	0.307	2.62E-18	4	Sub1
Rpsa2	2.70E-22	0.51299305	0.959	0.606	3.55E-18	4	Rpsa
Rps271	4.51E-22	0.54642664	0.975	0.885	5.93E-18	4	Rps27
Rps22	5.02E-22	0.45396969	0.934	0.588	6.61E-18	4	Rps2
Rpl10	5.10E-22	0.48850363	0.917	0.652	6.71E-18	4	Rpl10
Rps31	5.17E-22	0.48252162	0.934	0.681	6.80E-18	4	Rps3
Rpl13a1	5.40E-22	0.3506842	0.512	0.176	7.10E-18	4	Rpl13a
mt-Cytb3	6.31E-22	0.32517939	0.975	0.649	8.30E-18	4	mt-Cytb
Rpl362	8.82E-22	0.46862527	0.926	0.582	1.16E-17	4	Rpl36
Rpl7a3	9.18E-22	0.42843053	0.835	0.435	1.21E-17	4	Rpl7a
Smim14	1.14E-21	0.32088009	0.455	0.147	1.51E-17	4	Smim14
Unc93b11	2.59E-21	0.38462006	0.545	0.205	3.41E-17	4	Unc93b1
Eef22	2.86E-21	0.41868802	0.826	0.418	3.76E-17	4	Eef2
Rpl62	4.95E-21	0.45185477	0.934	0.609	6.51E-17	4	Rpl6
Eef1a11	5.35E-21	0.43102351	0.992	0.832	7.04E-17	4	Eef1a1
mt-Nd12	1.09E-20	0.29519653	0.917	0.515	1.43E-16	4	mt-Nd1
Rpl36a1	1.18E-20	0.36292287	0.62	0.26	1.56E-16	4	Rpl36a1
Cd164	3.65E-20	0.2692449	0.405	0.124	4.81E-16	4	Cd164
Atp5g21	6.11E-20	0.35069552	0.62	0.261	8.04E-16	4	Atp5g2
Rps121	7.13E-20	0.45918496	0.959	0.767	9.37E-16	4	Rps12

Rps231	7.29E-20	0.43954232	0.95	0.672	9.58E-16	4	Rps23
Ssr41	9.36E-20	0.35064126	0.587	0.237	1.23E-15	4	Ssr4
Rpl171	1.04E-19	0.45299141	0.959	0.782	1.36E-15	4	Rpl17
Eef1b22	1.65E-19	0.36620584	0.777	0.382	2.17E-15	4	Eef1b2
mt-Nd22	2.66E-19	0.27802337	0.901	0.508	3.50E-15	4	mt-Nd2
Rpl241	2.76E-19	0.40148827	0.942	0.568	3.64E-15	4	Rpl24
Eef1g1	4.37E-19	0.2976729	0.562	0.215	5.75E-15	4	Eef1g
Psme11	4.77E-19	0.32610583	0.645	0.273	6.28E-15	4	Psme1
Rpl23a1	9.45E-19	0.36446856	0.868	0.461	1.24E-14	4	Rpl23a
Sec61g1	1.02E-18	0.36544088	0.661	0.308	1.35E-14	4	Sec61g
Hsp90ab12	1.39E-18	0.38190132	0.785	0.387	1.82E-14	4	Hsp90ab1
Rps28	1.75E-18	0.47153997	0.909	0.59	2.30E-14	4	Rps28
Naca1	3.11E-18	0.37360653	0.802	0.429	4.09E-14	4	Naca
Uqcrh1	4.28E-18	0.32151157	0.76	0.376	5.62E-14	4	Uqcrh
Rps151	4.85E-18	0.42776663	0.893	0.535	6.37E-14	4	Rps15
Eif3h1	4.95E-18	0.30583183	0.595	0.253	6.51E-14	4	Eif3h
Fgfr1op2	7.79E-18	0.28122058	0.43	0.15	1.03E-13	4	Fgfr1op2
Uvrag	1.01E-17	0.26386763	0.388	0.126	1.33E-13	4	Uvrag
H2-Q71	1.45E-17	0.35945593	0.488	0.18	1.91E-13	4	H2-Q7
Rps211	1.56E-17	0.49514773	0.934	0.712	2.06E-13	4	Rps21
Hspe11	1.93E-17	0.31394717	0.446	0.158	2.54E-13	4	Hspe1
Rpl37a1	4.17E-17	0.40268686	0.975	0.792	5.48E-13	4	Rpl37a
Rpl341	4.72E-17	0.46317142	0.95	0.738	6.21E-13	4	Rpl34
Rps27a1	4.75E-17	0.37838084	0.967	0.786	6.25E-13	4	Rps27a
GltP	8.18E-17	0.29087852	0.364	0.12	1.08E-12	4	GltP
Manf1	1.91E-16	0.29554748	0.397	0.14	2.51E-12	4	Manf
Rap1a	4.55E-16	0.34368963	0.521	0.224	5.99E-12	4	Rap1a
Atp5c11	1.96E-15	0.28731803	0.479	0.195	2.58E-11	4	Atp5c1
Eef1d1	2.88E-15	0.25327415	0.471	0.188	3.78E-11	4	Eef1d
Spcs2	3.24E-15	0.27685784	0.479	0.198	4.26E-11	4	Spcs2
Tpt11	4.54E-15	0.32680011	1	0.959	5.98E-11	4	Tpt1
Rpl271	1.84E-14	0.30781148	0.719	0.389	2.41E-10	4	Rpl27
Psmb82	2.45E-14	0.27673506	0.678	0.33	3.22E-10	4	Psmb8
Nsa21	2.94E-14	0.27032884	0.554	0.25	3.87E-10	4	Nsa2
Eif3k	3.81E-14	0.27309689	0.57	0.267	5.01E-10	4	Eif3k
Lsp11	5.62E-14	0.28704546	0.645	0.322	7.40E-10	4	Lsp1
Cox7a2l1	7.20E-14	0.25128706	0.554	0.25	9.47E-10	4	Cox7a2l
Hmgb1	1.38E-13	0.29925081	0.612	0.326	1.82E-09	4	Hmgb1
H2afy1	1.46E-13	0.26473746	0.471	0.201	1.92E-09	4	H2afy
Xbp1	2.03E-13	0.34258426	0.446	0.197	2.66E-09	4	Xbp1

Reep5	5.68E-13	0.31347194	0.471	0.222	7.47E-09	4	Reep5
Rac21	8.31E-13	0.30786079	0.694	0.383	1.09E-08	4	Rac2
Rbm31	1.24E-12	0.27095409	0.777	0.452	1.63E-08	4	Rbm3
Rplp21	2.19E-12	0.33781552	0.95	0.782	2.88E-08	4	Rplp2
Lgals12	3.36E-12	0.32292538	0.521	0.245	4.42E-08	4	Lgals1
Rps29	9.86E-12	0.32795981	0.959	0.847	1.30E-07	4	Rps29
Fau	1.22E-11	0.2691015	1	0.976	1.60E-07	4	Fau
Rpl381	1.33E-11	0.33005034	0.893	0.63	1.74E-07	4	Rpl38
Btf31	1.03E-10	0.25377843	0.694	0.409	1.35E-06	4	Btf3
Rgs10	3.79E-10	0.2565861	0.355	0.153	4.99E-06	4	Rgs10
H2-K11	4.06E-10	0.26710697	0.851	0.554	5.34E-06	4	H2-K1
Ifi203	4.62E-10	0.30365155	0.331	0.138	6.07E-06	4	Ifi203
Npc21	5.25E-10	0.25890451	0.636	0.366	6.91E-06	4	Npc2
Grn1	1.34E-09	0.34092934	0.529	0.306	1.77E-05	4	Grn
Rpl37	3.70E-09	0.28601532	0.909	0.775	4.87E-05	4	Rpl37
Cox4i1	8.10E-09	0.26173518	0.744	0.489	0.00010656	4	Cox4i1
Rpl411	4.39E-08	0.25525076	0.992	0.866	0.00057692	4	Rpl41

a



b

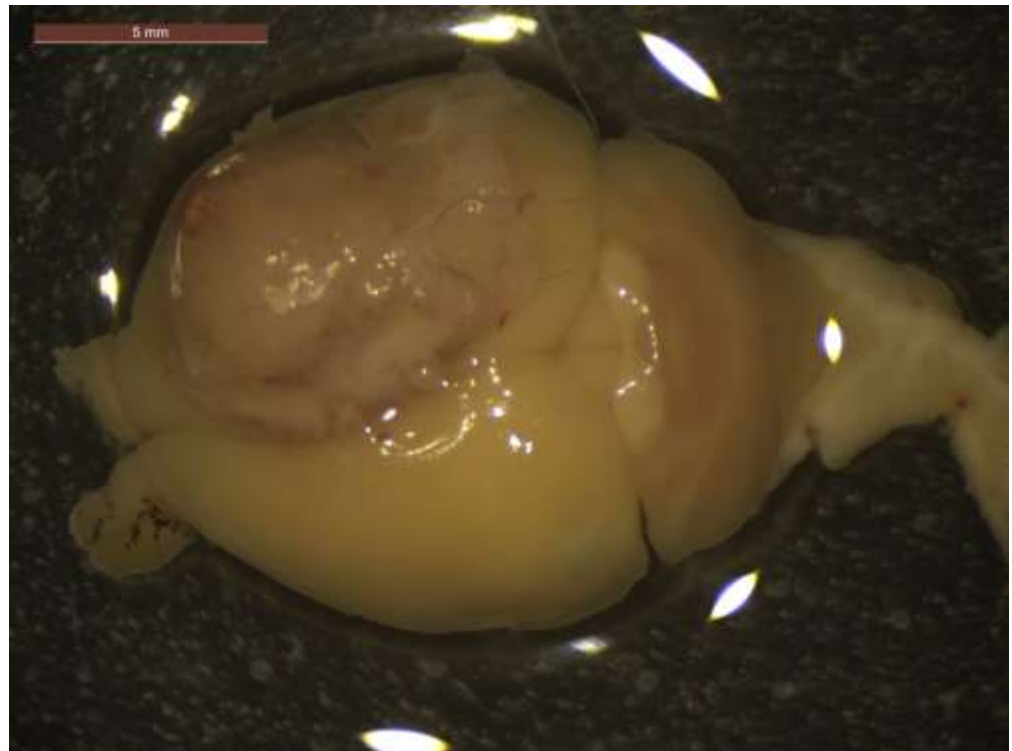


Figure 11: QPP7 Tumors Show Macroscopic Heterogeneity. a-b. QPP7 tumors harvested at the moribund endpoint of a mouse implanted with QPP7 cells. The tumor in panel a has much more hemorrhaging and necrosis compared to that in (b).

We next combined the scSEQ data from the spontaneous and allograft tumors as a single dataset (**Figure 7c, Figure 12**). Five major clusters were identified: neutrophils (**Figure 13b**), microglia/macrophages (**Figure 13c**), myeloid APC-like cells (**Figure 13d**), lytic myeloid cells (**Figure 13e**) and T and NK cells. A population of B cells was also present, although these cells did not cluster (**Figure 13f, g, h**). The full list of genes upregulated for each cluster can be found in **Table 7**.

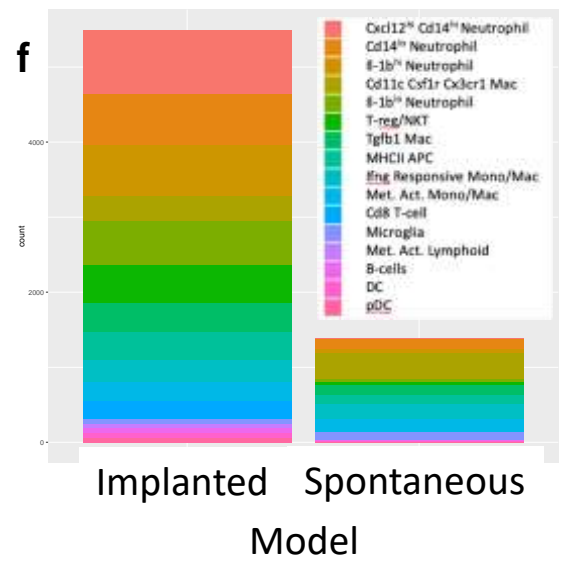
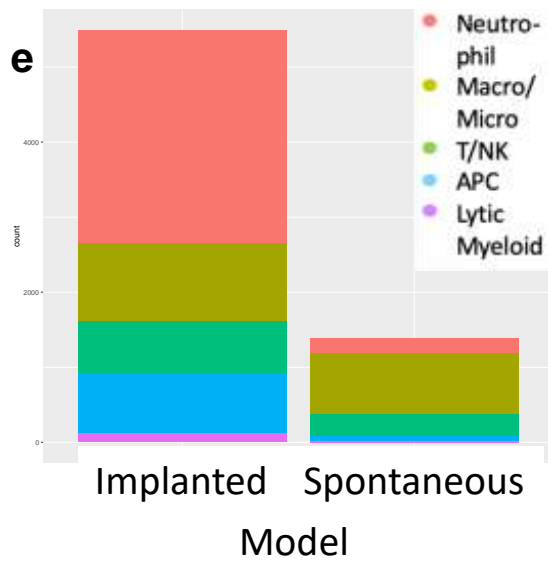
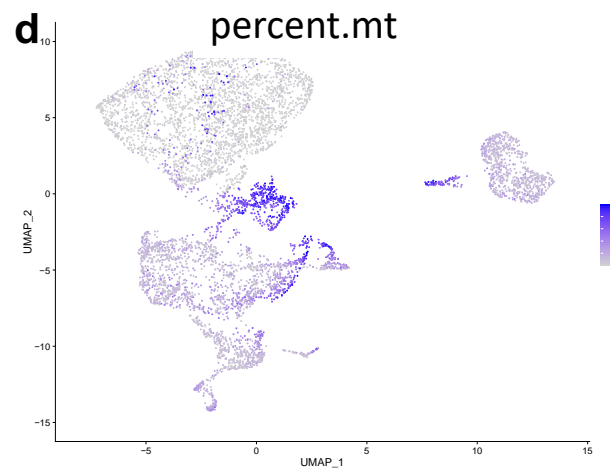
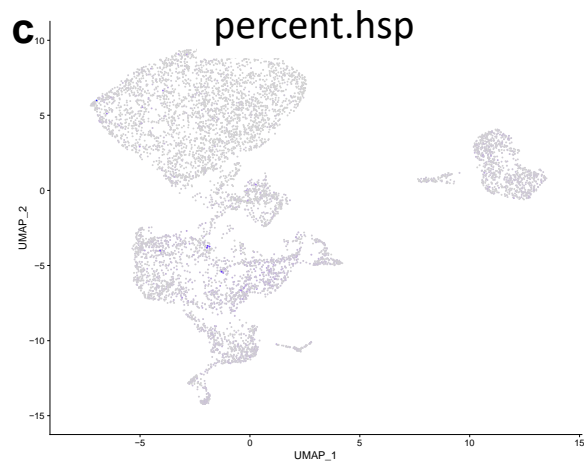
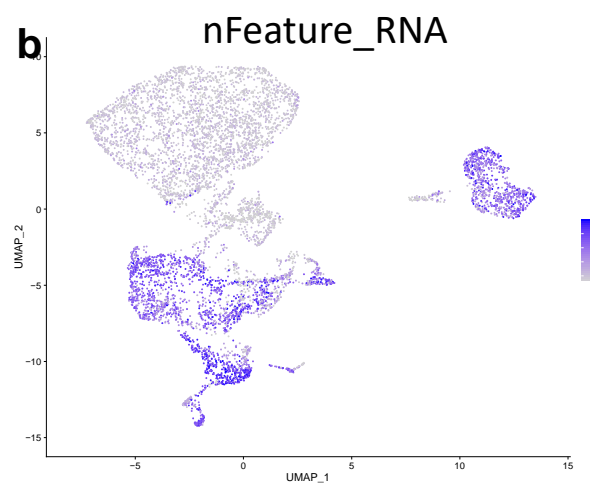
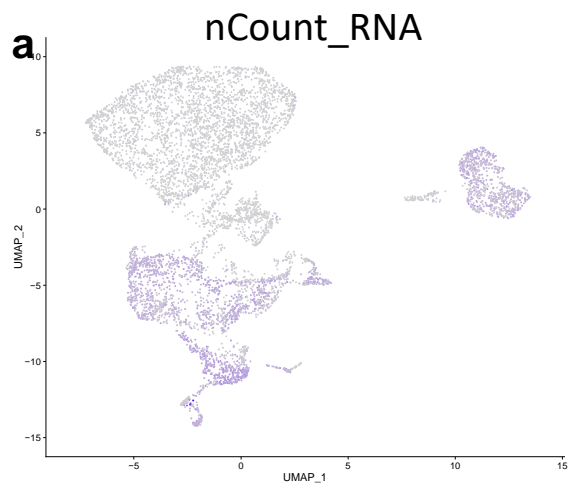


Figure 12: Quality control metrics for the combined QPP dataset. **a.** Featureplot showing the counts of RNA molecules detected per cell. **b.** Featureplot showing the number of unique genes expressed in each cell. **c.** Featureplot showing the percent of heat shock proteins expressed in each cell. **d.** Featureplot showing the percent of mitochondrial RNA molecules for each cell. **e.** Barplot showing the number of cells per cluster for individual mice.

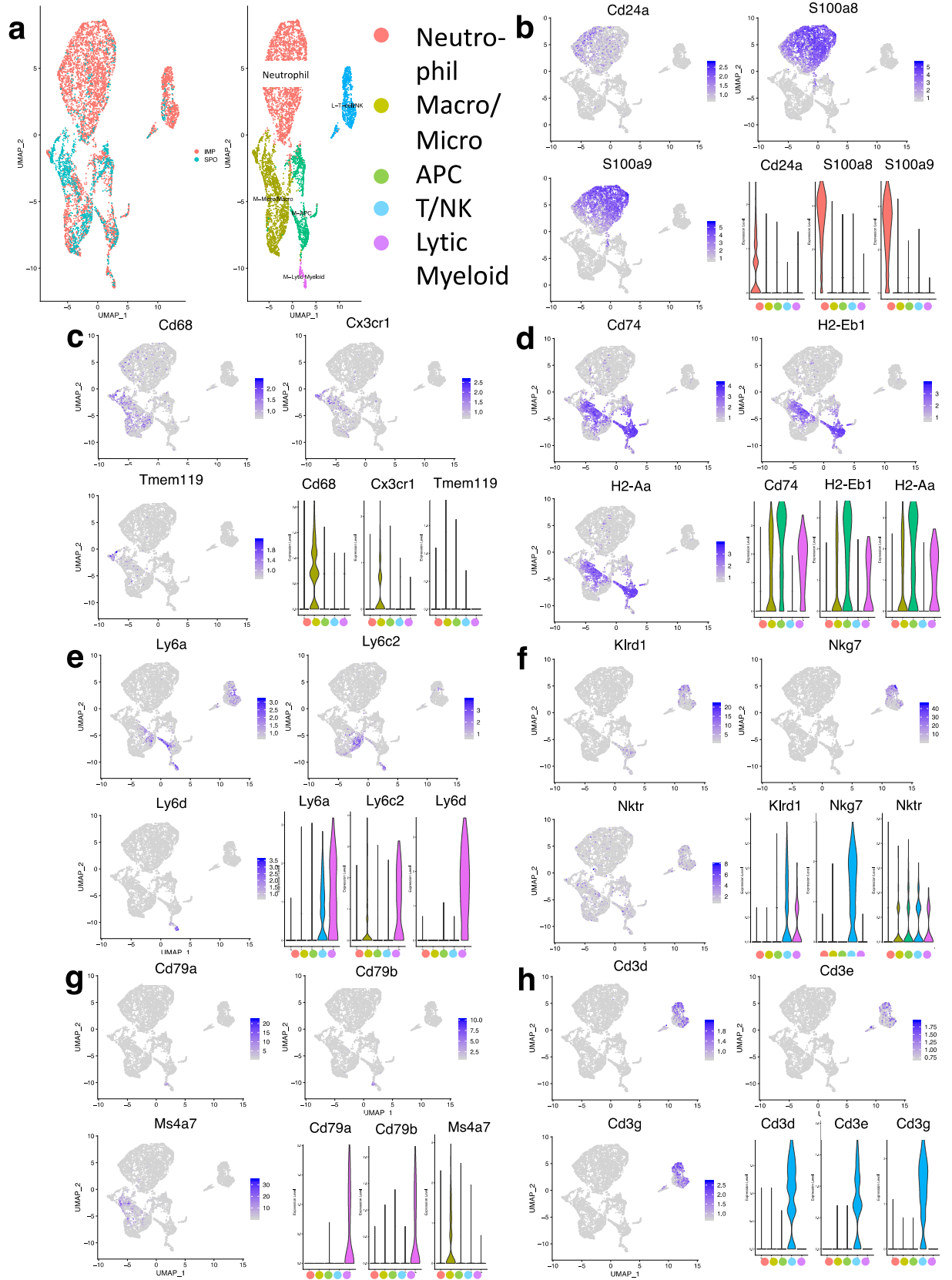


Figure 13: Comparison of QPP Immune Constituents. **a.** UMAPs show aggregate of CD45+ immune infiltrates from n=3 spontaneous QPP tumors and n=3 Implanted QPP tumors at moribund timepoint. **b-h.** UMAPS show (b) neutrophil clusters identified by Cd24a, S100a8, and S100a9 markers; (c) microglia and macrophage clusters identified by Cd68, Cx3cr1, and Tmem119 markers; (d) antigen-presenting cell clusters identified by Cd74, H2-Eb1, and H2-Aa markers; (e) lytic myeloid clusters identified by Ly6a, Ly6c2, and Ly6d markers; (f) natural killer (NK) cell clusters identified by Klrd1, Nkg7, and Nktr markers; (g) B-cell clusters identified by Cd79a, Cd79b, and Ms4a7 markers; and (h) T cell clusters identified by Cd3d, Cd3e, and Cd3g markers. All violin plots show the specificity of given markers for neutrophils (red), macrophages/microglia (lime), T and NK cells (green), APCs (blue), and lytic myeloid cells (purple).

Table 7

Mouse Aggregated 0.1 Resolution							
	p_val	avg_logFC	pct.1	pct.2	p_val_adj	cluster	gene
S100a8	0	3.6775967	0.953	0.112	0	0	S100a8
S100a9	0	3.45439608	0.919	0.086	0	0	S100a9
Cxcl2	0	1.71189627	0.489	0.025	0	0	Cxcl2
Srgn	0	1.70855168	0.955	0.482	0	0	Srgn
Eif1	0	1.33863906	0.961	0.575	0	0	Eif1
Il1b	0	1.22506464	0.616	0.153	0	0	Il1b
Fth1	0	1.18854781	0.987	0.934	0	0	Fth1
Msrb1	0	1.17189575	0.829	0.255	0	0	Msrb1
Mcl1	0	1.15361393	0.874	0.317	0	0	Mcl1
S100a6	0	1.14376056	0.835	0.526	0	0	S100a6
Retnlg	0	1.09606506	0.338	0.003	0	0	Retnlg
Ier3	0	1.07285586	0.619	0.108	0	0	Ier3
Csf3r	0	1.0573152	0.702	0.047	0	0	Csf3r
Dusp1	0	1.04603161	0.736	0.161	0	0	Dusp1
Cd9	0	1.03332827	0.678	0.158	0	0	Cd9
Cebpb	0	1.03242745	0.824	0.31	0	0	Cebpb
Btg1	0	1.01386561	0.901	0.457	0	0	Btg1
S100a11	0	1.00378005	0.747	0.358	0	0	S100a11
Cxcr2	0	0.96386449	0.592	0.008	0	0	Cxcr2
Tyrobp	0	0.94558031	0.967	0.67	0	0	Tyrobp
Fxyd5	0	0.92938611	0.89	0.544	0	0	Fxyd5
Grina	0	0.90801806	0.693	0.132	0	0	Grina
Junb	0	0.90083441	0.752	0.324	0	0	Junb
Ftl1	0	0.88316311	0.989	0.813	0	0	Ftl1
Mxd1	0	0.79709207	0.58	0.078	0	0	Mxd1
Pnrc1	0	0.78826666	0.629	0.166	0	0	Pnrc1
Rnf149	0	0.78606258	0.702	0.241	0	0	Rnf149
Gabarap	0	0.75562441	0.775	0.374	0	0	Gabarap
Cd24a	0	0.74405398	0.546	0.042	0	0	Cd24a
Clec4d	0	0.74225725	0.564	0.083	0	0	Clec4d
Hdc	0	0.7251782	0.404	0.009	0	0	Hdc
Lyst	0	0.72427094	0.569	0.08	0	0	Lyst
AC110211.1	0	0.66982627	0.451	0.005	0	0	AC110211.1
H3f3b	0	0.66444453	0.931	0.77	0	0	H3f3b
Il1r2	0	0.6264641	0.412	0.044	0	0	Il1r2
Cd300lf	0	0.58519667	0.533	0.113	0	0	Cd300lf

Fcer1g	1.10E-305	0.67381872	0.933	0.632	1.49E-301	0	Fcer1g
Cxcr4	1.58E-305	0.5498801	0.484	0.092	2.15E-301	0	Cxcr4
Egr1	2.56E-297	0.63701412	0.499	0.106	3.48E-293	0	Egr1
Cd44	4.94E-293	0.61901517	0.562	0.168	6.71E-289	0	Cd44
Hcar2	6.43E-286	0.65756591	0.334	0.016	8.73E-282	0	Hcar2
Marcks	5.66E-283	0.6758768	0.667	0.291	7.68E-279	0	Marcks
Cstb	1.31E-279	0.94862499	0.621	0.248	1.78E-275	0	Cstb
E230032D23Rik	5.09E-275	0.41562754	0.312	0.01	6.91E-271	0	E230032D23R
Ubb	1.05E-274	0.61543476	0.842	0.651	1.42E-270	0	Ubb
Pkm	1.28E-264	0.64841952	0.745	0.426	1.73E-260	0	Pkm
Ccr1	1.49E-247	0.56869158	0.568	0.204	2.02E-243	0	Ccr1
Adipor1	2.45E-245	0.4509853	0.439	0.1	3.33E-241	0	Adipor1
Neat1	5.90E-245	0.61056992	0.65	0.285	8.02E-241	0	Neat1
Igf1r	2.03E-244	0.38446034	0.299	0.017	2.76E-240	0	Igf1r
Basp1	1.80E-243	0.8551939	0.55	0.205	2.44E-239	0	Basp1
Stfa2l1	3.55E-238	0.71599872	0.257	0.002	4.83E-234	0	Stfa2l1
Lcp1	3.82E-237	0.61374964	0.679	0.391	5.18E-233	0	Lcp1
Gadd45b	3.31E-236	0.78310778	0.386	0.069	4.49E-232	0	Gadd45b
Txnip	8.13E-232	0.60408093	0.547	0.21	1.10E-227	0	Txnip
Lrg1	1.06E-231	0.54172741	0.266	0.008	1.43E-227	0	Lrg1
Tnfaip2	1.93E-231	0.55724392	0.438	0.108	2.62E-227	0	Tnfaip2
Lcn2	5.74E-218	0.58411126	0.271	0.016	7.79E-214	0	Lcn2
Id1	7.74E-218	0.44935582	0.286	0.022	1.05E-213	0	Id1

Cd63	7.91E-218	0.59443902	0.59	0.21	1.07E-213	0	Cd63
Chd7	1.27E-217	0.48699459	0.485	0.151	1.73E-213	0	Chd7
Ubc	2.12E-217	0.5605905	0.685	0.405	2.88E-213	0	Ubc
Map1lc3b	4.27E-213	0.48353707	0.527	0.207	5.80E-209	0	Map1lc3b
Ifitm2	1.43E-211	0.65459018	0.672	0.34	1.94E-207	0	Ifitm2
Nudt4	4.25E-208	0.33880458	0.314	0.041	5.77E-204	0	Nudt4
Cd33	2.13E-205	0.38383234	0.37	0.076	2.89E-201	0	Cd33
Cd14	5.97E-205	0.63246312	0.414	0.105	8.11E-201	0	Cd14
Csf1	3.46E-204	0.43365754	0.315	0.043	4.70E-200	0	Csf1
Tnfrsf23	3.03E-202	0.30848438	0.251	0.013	4.11E-198	0	Tnfrsf23
Btg2	1.06E-199	0.61806	0.622	0.317	1.44E-195	0	Btg2
Dmxl2	1.88E-199	0.34174374	0.293	0.034	2.56E-195	0	Dmxl2
lqsec1	1.27E-195	0.32285134	0.299	0.04	1.73E-191	0	lqsec1
Slc7a11	3.97E-195	0.50163021	0.305	0.043	5.39E-191	0	Slc7a11
Cyp4f18	6.94E-193	0.5458477	0.482	0.174	9.43E-189	0	Cyp4f18
H3f3a	9.99E-193	0.50065437	0.803	0.626	1.36E-188	0	H3f3a
Gng5	5.67E-192	0.48891541	0.692	0.445	7.70E-188	0	Gng5
Tpd52	9.79E-192	0.475531	0.569	0.252	1.33E-187	0	Tpd52
Sorl1	1.25E-185	0.4084354	0.407	0.117	1.69E-181	0	Sorl1
Jun	3.00E-180	0.62228933	0.64	0.365	4.07E-176	0	Jun
Pygl	3.34E-178	0.32107504	0.289	0.044	4.54E-174	0	Pygl
Ccrl2	9.98E-178	0.52371788	0.313	0.058	1.36E-173	0	Ccrl2
Gapdh	2.55E-175	0.60176638	0.788	0.618	3.46E-171	0	Gapdh

Slpi	3.33E-174	0.57486194	0.319	0.062	4.52E-170	0	Slpi
Trib1	6.01E-174	0.39078137	0.369	0.095	8.16E-170	0	Trib1
Plk3	1.84E-170	0.3642921	0.321	0.066	2.50E-166	0	Plk3
Rgs2	1.88E-168	0.52050285	0.566	0.28	2.56E-164	0	Rgs2
Ptafr	6.89E-166	0.37367142	0.374	0.104	9.36E-162	0	Ptafr
Alox5ap	1.10E-164	0.52104774	0.611	0.338	1.49E-160	0	Alox5ap
Rab7	2.55E-164	0.44013852	0.472	0.195	3.46E-160	0	Rab7
Ier5	3.79E-164	0.4206669	0.522	0.235	5.15E-160	0	Ier5
Il1rn	2.83E-160	0.50424507	0.306	0.064	3.85E-156	0	Il1rn
Son	7.93E-160	0.43569034	0.663	0.402	1.08E-155	0	Son
Ninj1	3.89E-159	0.45170102	0.45	0.164	5.28E-155	0	Ninj1
Fos	7.78E-157	0.56023737	0.584	0.303	1.06E-152	0	Fos
Ccl3	1.67E-154	0.49544086	0.318	0.073	2.27E-150	0	Ccl3
Gcnt2	2.66E-153	0.32542402	0.327	0.082	3.61E-149	0	Gcnt2
Gcnt1	2.17E-150	0.27913023	0.277	0.052	2.95E-146	0	Gcnt1
Retreg1	1.85E-144	0.28929792	0.318	0.081	2.51E-140	0	Retreg1
Txn1	1.48E-142	0.66702228	0.562	0.335	2.01E-138	0	Txn1
Gsr	6.45E-138	0.34100806	0.388	0.133	8.75E-134	0	Gsr
Zfp36	6.76E-138	0.45139847	0.516	0.256	9.18E-134	0	Zfp36
1810058l24Rik	1.29E-137	0.35930152	0.388	0.143	1.74E-133	0	1810058l24Rik
Samsn1	9.56E-134	0.39614999	0.378	0.131	1.30E-129	0	Samsn1
Jund	2.80E-131	0.42231124	0.562	0.309	3.80E-127	0	Jund
Card19	1.54E-130	0.37499182	0.386	0.141	2.10E-126	0	Card19

Iqgap1	2.15E-130	0.39857089	0.587	0.35	2.92E-126	0	Iqgap1
Neurl3	4.85E-128	0.40430458	0.48	0.227	6.59E-124	0	Neurl3
Klf2	1.16E-123	0.33679754	0.298	0.079	1.58E-119	0	Klf2
Nfkb1a	1.28E-123	0.52733106	0.523	0.273	1.74E-119	0	Nfkb1a
Vasp	6.74E-120	0.37021101	0.474	0.242	9.15E-116	0	Vasp
Entpd1	5.43E-114	0.26552491	0.284	0.081	7.37E-110	0	Entpd1
Ogfrl1	2.93E-112	0.27904263	0.316	0.105	3.97E-108	0	Ogfrl1
Smox	6.12E-111	0.29619327	0.276	0.078	8.31E-107	0	Smox
Cdk2ap2	5.69E-110	0.46732149	0.449	0.228	7.72E-106	0	Cdk2ap2
Tmem189	1.47E-108	0.27552002	0.306	0.1	1.99E-104	0	Tmem189
Snx20	6.75E-107	0.31330194	0.387	0.168	9.16E-103	0	Snx20
Tsc22d4	5.04E-104	0.33866856	0.41	0.194	6.84E-100	0	Tsc22d4
Ypel3	4.75E-103	0.31380475	0.404	0.187	6.45E-99	0	Ypel3
Adam8	2.33E-102	0.26160047	0.304	0.099	3.16E-98	0	Adam8
1700017B05Rik	3.53E-97	0.26235858	0.27	0.086	4.80E-93	0	1700017B05Rik
Ppp1r15a	2.08E-94	0.26806063	0.251	0.075	2.82E-90	0	Ppp1r15a
Pfn1	1.55E-93	0.36810266	0.708	0.601	2.10E-89	0	Pfn1
Cd52	2.11E-91	0.40595884	0.88	0.805	2.86E-87	0	Cd52
Zcchc6	2.87E-88	0.28740518	0.379	0.181	3.90E-84	0	Zcchc6
Prdx5	3.78E-86	0.31373975	0.597	0.381	5.13E-82	0	Prdx5
2810474O19Rik	8.01E-86	0.33020436	0.4	0.203	1.09E-81	0	2810474O19Rik
AA467197	2.46E-84	0.30420682	0.306	0.116	3.34E-80	0	AA467197
Skil	6.26E-82	0.25306905	0.348	0.158	8.50E-78	0	Skil
Plek	1.30E-80	0.35094293	0.37	0.187	1.76E-76	0	Plek
Bri3	5.89E-78	0.37326698	0.455	0.275	7.99E-74	0	Bri3
Ncf2	1.43E-77	0.30388869	0.435	0.245	1.94E-73	0	Ncf2
Rps27	4.13E-76	0.26889622	0.913	0.845	5.61E-72	0	Rps27
Ccl4	5.74E-75	0.37676379	0.276	0.106	7.80E-71	0	Ccl4
Arpc1b	1.32E-74	0.32412469	0.677	0.571	1.79E-70	0	Arpc1b
Calm2	4.12E-74	0.2883721	0.446	0.265	5.59E-70	0	Calm2

Selplg	2.00E-73	0.35233247	0.489	0.321	2.71E-69	0	Selplg
Atp6v1g1	3.41E-73	0.31418519	0.473	0.304	4.63E-69	0	Atp6v1g1
Aldoa	9.05E-73	0.33874109	0.537	0.367	1.23E-68	0	Aldoa
Marcksl1	1.20E-71	0.31380836	0.266	0.105	1.63E-67	0	Marcksl1
Eno1	3.44E-69	0.31100073	0.431	0.253	4.67E-65	0	Eno1
Bnip3l	4.07E-69	0.32663126	0.32	0.156	5.53E-65	0	Bnip3l
Diaph1	4.83E-68	0.25359841	0.36	0.189	6.56E-64	0	Diaph1
Apbb1ip	2.93E-60	0.2620677	0.421	0.259	3.97E-56	0	Apbb1ip
Eif5	3.45E-60	0.28879635	0.418	0.263	4.69E-56	0	Eif5
Myh9	2.97E-56	0.27464185	0.471	0.322	4.03E-52	0	Myh9
Ddx5	1.24E-55	0.29749796	0.602	0.509	1.68E-51	0	Ddx5
Gnai2	1.88E-55	0.30272429	0.626	0.556	2.56E-51	0	Gnai2
Ier2	1.71E-54	0.26500581	0.365	0.215	2.32E-50	0	Ier2
Spi1	2.38E-53	0.25896669	0.522	0.369	3.23E-49	0	Spi1
Sdcbp	6.48E-52	0.26499915	0.432	0.284	8.80E-48	0	Sdcbp
Ostf1	3.08E-49	0.26481399	0.454	0.319	4.19E-45	0	Ostf1
Msn	1.88E-47	0.28096962	0.53	0.424	2.55E-43	0	Msn
Actg1	1.19E-46	0.31208758	0.796	0.721	1.61E-42	0	Actg1
Myl12b	9.37E-45	0.25584596	0.472	0.357	1.27E-40	0	Myl12b
Zfp36l2	3.13E-44	0.2808978	0.493	0.37	4.25E-40	0	Zfp36l2
Pim1	5.60E-37	0.27454758	0.372	0.253	7.61E-33	0	Pim1
Apoe	0	2.54338017	0.873	0.238	0	1	Apoe
Lyz2	0	2.06964061	0.891	0.261	0	1	Lyz2
C1qa	0	1.82327655	0.486	0.048	0	1	C1qa
C1qb	0	1.7896053	0.538	0.055	0	1	C1qb
C1qc	0	1.47122824	0.501	0.038	0	1	C1qc
Ctss	0	1.42072809	0.958	0.289	0	1	Ctss
Lgmn	0	1.13924553	0.715	0.086	0	1	Lgmn
Tgfb1	0	1.03152493	0.689	0.235	0	1	Tgfb1
Ctsc	0	0.89845096	0.681	0.07	0	1	Ctsc
Mafb	0	0.8745245	0.675	0.063	0	1	Mafb
Ms4a6c	0	0.81688693	0.695	0.089	0	1	Ms4a6c
Npc2	0	0.81402208	0.828	0.256	0	1	Npc2
Ctsz	0	0.79861473	0.783	0.282	0	1	Ctsz
Fn1	0	0.77093336	0.393	0.033	0	1	Fn1
Grn	0	0.75193515	0.689	0.223	0	1	Grn
Aif1	0	0.74348453	0.601	0.078	0	1	Aif1
Csf1r	0	0.73125528	0.679	0.115	0	1	Csf1r
Ms4a7	0	0.71806516	0.412	0.036	0	1	Ms4a7
Ms4a6d	0	0.66804719	0.541	0.039	0	1	Ms4a6d

Cd68	0	0.6509719	0.686	0.151	0	1	Cd68
Psap	0	0.63744463	0.954	0.524	0	1	Psap
Trem2	0	0.62686056	0.379	0.017	0	1	Trem2
Cybb	0	0.62418282	0.574	0.086	0	1	Cybb
Selenop	0	0.58517707	0.391	0.028	0	1	Selenop
Ctsa	0	0.56166807	0.623	0.14	0	1	Ctsa
Fcgr1	0	0.54189186	0.467	0.027	0	1	Fcgr1
Cx3cr1	0	0.5305812	0.389	0.041	0	1	Cx3cr1
Ctsh	0	0.52556578	0.658	0.186	0	1	Ctsh
Itgb5	0	0.50637257	0.471	0.049	0	1	Itgb5
Lrp1	0	0.44907469	0.481	0.059	0	1	Lrp1
Msr1	0	0.37080098	0.332	0.017	0	1	Msr1
C3ar1	0	0.36905605	0.318	0.014	0	1	C3ar1
Lamp1	1.76E-306	0.50048221	0.623	0.171	2.39E-302	1	Lamp1
Fcgr2b	5.12E-305	0.49234166	0.455	0.073	6.95E-301	1	Fcgr2b
Ccr2	1.18E-291	0.62935198	0.493	0.1	1.60E-287	1	Ccr2
Chil3	4.44E-281	1.59471013	0.382	0.053	6.03E-277	1	Chil3
Mpeg1	2.40E-269	0.51768284	0.718	0.256	3.26E-265	1	Mpeg1
Clec4a3	4.34E-262	0.30652838	0.267	0.012	5.89E-258	1	Clec4a3
Cxcl16	5.44E-260	0.45351199	0.424	0.074	7.38E-256	1	Cxcl16
Prdx1	2.57E-257	0.50788583	0.547	0.154	3.49E-253	1	Prdx1
Mmp14	2.60E-256	0.36790837	0.335	0.037	3.53E-252	1	Mmp14
Pld4	6.27E-255	0.37314159	0.449	0.088	8.52E-251	1	Pld4
Ms4a4c	1.15E-254	0.52189841	0.389	0.061	1.56E-250	1	Ms4a4c
Calr	1.98E-253	0.60460883	0.65	0.247	2.69E-249	1	Calr
Hsp90b1	7.18E-245	0.53077554	0.584	0.19	9.75E-241	1	Hsp90b1
Axl	1.76E-242	0.31765102	0.309	0.031	2.39E-238	1	Axl
Lair1	2.53E-240	0.36078921	0.401	0.069	3.44E-236	1	Lair1

Lgals3bp	6.05E-236	0.40225483	0.354	0.054	8.21E-232	1	Lgals3bp
Akr1a1	8.87E-231	0.41494964	0.577	0.19	1.20E-226	1	Akr1a1
Trf	2.61E-230	0.38420018	0.327	0.044	3.54E-226	1	Trf
Unc93b1	1.05E-228	0.4020794	0.54	0.158	1.42E-224	1	Unc93b1
Ly86	4.86E-228	0.48559846	0.432	0.096	6.59E-224	1	Ly86
Ifitm3	7.03E-228	0.96518955	0.622	0.252	9.54E-224	1	Ifitm3
Dbi	1.50E-227	0.37160381	0.42	0.091	2.04E-223	1	Dbi
Ctsb	1.54E-225	0.76198292	0.827	0.435	2.08E-221	1	Ctsb
Bst2	6.74E-224	0.38950422	0.451	0.104	9.15E-220	1	Bst2
Ccl9	3.98E-223	0.39499914	0.266	0.022	5.40E-219	1	Ccl9
Ifi204	1.14E-212	0.41138933	0.362	0.066	1.55E-208	1	Ifi204
Rrbp1	7.56E-209	0.42847127	0.696	0.284	1.03E-204	1	Rrbp1
mt-Co2	1.90E-204	0.40881075	0.99	0.751	2.58E-200	1	mt-Co2
Ifi207	3.17E-204	0.29852009	0.32	0.049	4.31E-200	1	Ifi207
Pdia6	6.20E-203	0.35613484	0.385	0.084	8.42E-199	1	Pdia6
Lgals3	6.85E-202	0.78479589	0.675	0.32	9.30E-198	1	Lgals3
Apobec1	8.40E-202	0.2646107	0.326	0.051	1.14E-197	1	Apobec1
Gatm	5.77E-201	0.36809825	0.289	0.038	7.83E-197	1	Gatm
Hspa8	2.42E-200	0.49475094	0.777	0.4	3.29E-196	1	Hspa8
H2-DMa	2.73E-199	0.36773144	0.471	0.123	3.70E-195	1	H2-DMa
Anxa5	1.05E-197	0.33067452	0.376	0.08	1.43E-193	1	Anxa5
Tmem86a	2.47E-196	0.29944361	0.319	0.053	3.35E-192	1	Tmem86a
Hexb	1.52E-195	0.86538151	0.445	0.131	2.06E-191	1	Hexb

mt-Co3	1.40E-186	0.45492293	0.99	0.765	1.90E-182	1	mt-Co3
Pid1	6.60E-180	0.31820344	0.34	0.068	8.96E-176	1	Pid1
Emp3	7.08E-180	0.4655178	0.514	0.19	9.62E-176	1	Emp3
Pnp	1.24E-179	0.37717902	0.403	0.106	1.69E-175	1	Pnp
Ifi27l2a	1.58E-179	0.69281077	0.544	0.198	2.14E-175	1	Ifi27l2a
Itm2b	7.98E-179	0.56148528	0.798	0.485	1.08E-174	1	Itm2b
Ctsl	1.22E-178	0.53225143	0.328	0.065	1.66E-174	1	Ctsl
Ms4a6b	2.09E-175	0.33833233	0.464	0.14	2.83E-171	1	Ms4a6b
Hexa	6.17E-175	0.35003987	0.419	0.119	8.37E-171	1	Hexa
Stab1	2.35E-174	0.27986308	0.288	0.047	3.19E-170	1	Stab1
Zeb2	4.02E-173	0.37706746	0.588	0.22	5.46E-169	1	Zeb2
Cst3	1.54E-171	0.60303048	0.856	0.484	2.10E-167	1	Cst3
Tmem176b	2.74E-169	0.3654411	0.309	0.059	3.72E-165	1	Tmem176b
Cd81	6.28E-166	0.65887534	0.279	0.051	8.53E-162	1	Cd81
Acp5	1.90E-164	0.36679315	0.265	0.043	2.59E-160	1	Acp5
Ccr5	1.28E-162	0.27879371	0.301	0.059	1.74E-158	1	Ccr5
Plekho1	1.47E-161	0.27006923	0.368	0.093	2.00E-157	1	Plekho1
mt-Atp6	7.94E-160	0.39652001	0.989	0.753	1.08E-155	1	mt-Atp6
Ucp2	2.02E-159	0.40131019	0.659	0.314	2.75E-155	1	Ucp2
Erp29	3.43E-159	0.33273242	0.5	0.182	4.65E-155	1	Erp29
mt-Co1	3.23E-158	0.32191412	0.989	0.795	4.39E-154	1	mt-Co1
Tgfb1	1.17E-157	0.34934739	0.46	0.157	1.59E-153	1	Tgfb1
Capza2	3.23E-154	0.31765012	0.516	0.198	4.38E-150	1	Capza2

H2-Ab1	1.81E-152	0.56502332	0.531	0.19	2.46E-148	1	H2-Ab1
Sirpa	4.16E-152	0.30726401	0.435	0.141	5.64E-148	1	Sirpa
Plac8	4.45E-151	0.69334071	0.418	0.137	6.04E-147	1	Plac8
S100a4	2.04E-147	0.65069294	0.479	0.186	2.78E-143	1	S100a4
Pdia3	8.18E-147	0.33505805	0.439	0.153	1.11E-142	1	Pdia3
Cd74	1.22E-144	0.60264412	0.624	0.295	1.66E-140	1	Cd74
Hck	7.27E-144	0.2570848	0.356	0.097	9.86E-140	1	Hck
Ly6c2	5.00E-143	0.67520839	0.31	0.075	6.78E-139	1	Ly6c2
Lst1	4.77E-140	0.35141131	0.576	0.247	6.48E-136	1	Lst1
Ssr4	2.58E-137	0.28764778	0.486	0.189	3.51E-133	1	Ssr4
H2-DMb1	3.04E-136	0.31949018	0.365	0.104	4.12E-132	1	H2-DMb1
H2-Aa	1.13E-135	0.54869184	0.497	0.186	1.53E-131	1	H2-Aa
Fcgr4	4.69E-135	0.2618242	0.263	0.054	6.37E-131	1	Fcgr4
Lgals1	7.34E-135	0.39739081	0.487	0.183	9.96E-131	1	Lgals1
Irf7	1.52E-133	0.45442747	0.325	0.089	2.07E-129	1	Irf7
Gusb	1.15E-131	0.25071505	0.294	0.072	1.56E-127	1	Gusb
Pycard	1.75E-130	0.2732086	0.375	0.12	2.38E-126	1	Pycard
Ly6e	1.58E-129	0.45721666	0.693	0.396	2.15E-125	1	Ly6e
Eif4a1	1.58E-128	0.32281166	0.585	0.284	2.15E-124	1	Eif4a1
Mt1	2.67E-126	0.43375143	0.277	0.066	3.62E-122	1	Mt1
Gpx1	3.42E-123	0.43452204	0.624	0.323	4.64E-119	1	Gpx1
Creg1	3.15E-122	0.27794874	0.334	0.101	4.28E-118	1	Creg1
Tkt	8.79E-122	0.25746395	0.37	0.125	1.19E-117	1	Tkt

Manf	2.11E-120	0.26363882	0.329	0.099	2.86E-116	1	Manf
Slc25a5	4.97E-116	0.27437753	0.453	0.188	6.75E-112	1	Slc25a5
Zbp1	8.50E-115	0.25801962	0.277	0.072	1.15E-110	1	Zbp1
Wfdc17	8.79E-114	0.28859595	0.431	0.162	1.19E-109	1	Wfdc17
Cd300c2	8.98E-109	0.2750337	0.494	0.217	1.22E-104	1	Cd300c2
Rpl7a	1.91E-108	0.27181749	0.727	0.384	2.59E-104	1	Rpl7a
Crip1	2.41E-108	0.49047568	0.461	0.202	3.27E-104	1	Crip1
Ppib	1.65E-105	0.25555871	0.498	0.226	2.25E-101	1	Ppib
Cyba	2.85E-104	0.28176722	0.844	0.56	3.87E-100	1	Cyba
H2-Eb1	1.39E-103	0.43910514	0.452	0.182	1.89E-99	1	H2-Eb1
Ybx1	2.22E-101	0.28699638	0.604	0.328	3.01E-97	1	Ybx1
Tspo	3.52E-98	0.36198342	0.553	0.298	4.78E-94	1	Tspo
Tmsb4x	5.94E-98	0.3494082	0.987	0.949	8.07E-94	1	Tmsb4x
Slfn5	9.84E-98	0.30072067	0.316	0.107	1.34E-93	1	Slfn5
Pmepa1	1.17E-94	0.28734129	0.279	0.089	1.59E-90	1	Pmepa1
Aprt	4.97E-94	0.26572743	0.409	0.176	6.75E-90	1	Aprt
Fyb	1.13E-92	0.27198262	0.617	0.332	1.54E-88	1	Fyb
Hspa5	1.50E-89	0.39931669	0.593	0.351	2.03E-85	1	Hspa5
Sec61g	3.33E-88	0.25992493	0.504	0.257	4.51E-84	1	Sec61g
mt-Cytb	6.79E-88	0.29936207	0.898	0.681	9.22E-84	1	mt-Cytb
mt-Nd4	2.69E-85	0.26777553	0.867	0.626	3.65E-81	1	mt-Nd4
mt-Nd2	1.55E-84	0.28581798	0.788	0.525	2.10E-80	1	mt-Nd2
mt-Nd1	3.94E-83	0.2988786	0.773	0.528	5.35E-79	1	mt-Nd1
Ahnak	4.79E-83	0.28433902	0.322	0.126	6.51E-79	1	Ahnak
Rpl35	1.64E-82	0.25115088	0.615	0.344	2.23E-78	1	Rpl35
Hsp90ab1	8.68E-81	0.25454652	0.644	0.36	1.18E-76	1	Hsp90ab1
Isg15	1.75E-79	0.50768744	0.306	0.119	2.37E-75	1	Isg15
B2m	2.95E-76	0.37671924	0.825	0.643	4.00E-72	1	B2m
mt-Nd3	1.70E-75	0.2581541	0.581	0.321	2.31E-71	1	mt-Nd3
Tmsb10	3.65E-73	0.36455703	0.544	0.306	4.96E-69	1	Tmsb10
AY036118	7.54E-72	0.41116656	0.274	0.109	1.02E-67	1	AY036118
Vim	6.89E-63	0.65521807	0.501	0.336	9.36E-59	1	Vim

Sat1	5.03E-62	0.29207453	0.638	0.401	6.83E-58	1	Sat1
S100a10	5.73E-59	0.30295864	0.341	0.162	7.77E-55	1	S100a10
Tgm2	1.88E-57	0.33639782	0.319	0.154	2.56E-53	1	Tgm2
Prdx51	4.10E-54	0.27475177	0.643	0.416	5.57E-50	1	Prdx5
Ccl6	6.58E-53	0.28728643	0.306	0.143	8.94E-49	1	Ccl6
Gm42418	2.20E-21	0.43627406	0.991	0.969	2.99E-17	1	Gm42418
Ctsd	5.17E-21	0.67185161	0.592	0.516	7.02E-17	1	Ctsd
Cd741	0	1.57401784	0.85	0.306	0	2	Cd74
H2-Eb11	0	1.56900236	0.708	0.18	0	2	H2-Eb1
Ciita	0	0.62941604	0.531	0.062	0	2	Ciita
Cbfa2t3	0	0.48091301	0.446	0.03	0	2	Cbfa2t3
H2-Oa	6.71E-308	0.43537776	0.324	0.017	9.11E-304	2	H2-Oa
H2-Aa1	1.03E-291	1.4850476	0.714	0.197	1.40E-287	2	H2-Aa
H2-Ab11	2.54E-291	1.50499107	0.715	0.21	3.45E-287	2	H2-Ab1
mt-Co21	9.19E-199	1.06488504	0.998	0.785	1.25E-194	2	mt-Co2
mt-Co11	4.25E-192	1.03215421	0.998	0.822	5.78E-188	2	mt-Co1
mt-Co31	5.77E-187	0.97683633	0.999	0.797	7.83E-183	2	mt-Co3
mt-Atp61	9.10E-170	0.95166141	0.999	0.786	1.24E-165	2	mt-Atp6
Syng2	4.56E-164	0.54785616	0.497	0.148	6.19E-160	2	Syng2
H2-DMb11	1.79E-162	0.49689371	0.475	0.125	2.43E-158	2	H2-DMb1
Wdfy4	1.09E-135	0.28435676	0.271	0.045	1.47E-131	2	Wdfy4
Napsa	6.63E-131	0.47265803	0.476	0.157	9.01E-127	2	Napsa
H2-DMa1	1.32E-130	0.47308431	0.498	0.17	1.80E-126	2	H2-DMa
Ckb	1.36E-118	0.29020847	0.279	0.056	1.85E-114	2	Ckb
H2afy	1.14E-108	0.38168608	0.491	0.191	1.55E-104	2	H2afy
Rpsa	8.74E-105	0.49545875	0.911	0.639	1.19E-100	2	Rpsa
Crip11	9.13E-97	0.634406	0.531	0.229	1.24E-92	2	Crip1
mt-Cytb1	5.28E-94	0.8126602	0.896	0.714	7.16E-90	2	mt-Cytb
mt-Nd11	6.85E-88	0.73061243	0.799	0.56	9.30E-84	2	mt-Nd1

Malat1	1.27E-87	0.47505581	0.995	0.98	1.73E-83	2	Malat1
Cst31	1.28E-81	0.91435813	0.771	0.553	1.74E-77	2	Cst3
mt-Nd41	1.32E-80	0.79112502	0.838	0.667	1.79E-76	2	mt-Nd4
mt-Nd21	3.77E-79	0.76047004	0.77	0.567	5.11E-75	2	mt-Nd2
Dock10	5.65E-79	0.27611709	0.385	0.14	7.67E-75	2	Dock10
Rps19	7.00E-71	0.36633199	0.893	0.686	9.50E-67	2	Rps19
Atox1	4.14E-65	0.43883992	0.587	0.372	5.62E-61	2	Atox1
Gm2a	5.14E-65	0.41529315	0.514	0.286	6.98E-61	2	Gm2a
mt-Nd31	5.64E-63	0.43887371	0.6	0.357	7.66E-59	2	mt-Nd3
Lsp1	1.90E-56	0.42574694	0.506	0.291	2.57E-52	2	Lsp1
Pou2f2	5.31E-53	0.3004948	0.348	0.151	7.21E-49	2	Pou2f2
Ptms	1.42E-50	0.27724911	0.407	0.203	1.92E-46	2	Ptms
Psmb8	3.77E-50	0.34131665	0.534	0.321	5.11E-46	2	Psmb8
Plbd1	2.29E-49	0.26826703	0.409	0.206	3.11E-45	2	Plbd1
Plac81	2.04E-48	0.34344041	0.395	0.182	2.77E-44	2	Plac8
Gdi2	3.31E-48	0.27236439	0.486	0.278	4.49E-44	2	Gdi2
Tmsb101	1.65E-47	0.34782663	0.574	0.336	2.23E-43	2	Tmsb10
Rps4x	1.84E-47	0.26706665	0.783	0.53	2.49E-43	2	Rps4x
Psme1	7.46E-47	0.33039539	0.472	0.277	1.01E-42	2	Psme1
Ptma	8.47E-46	0.26743804	0.747	0.532	1.15E-41	2	Ptma
Slfn51	2.32E-45	0.25358175	0.318	0.138	3.15E-41	2	Slfn5
H2afz	1.14E-42	0.4163673	0.501	0.32	1.55E-38	2	H2afz
Sub1	9.70E-42	0.28536775	0.475	0.282	1.32E-37	2	Sub1
Rps11	6.55E-41	0.33149903	0.856	0.73	8.89E-37	2	Rps11
Id2	2.55E-40	0.34913316	0.534	0.338	3.47E-36	2	Id2
Rrbp11	1.18E-33	0.26550923	0.556	0.369	1.60E-29	2	Rrbp1
Rpl14	1.57E-33	0.26942607	0.645	0.492	2.13E-29	2	Rpl14
Irf8	4.29E-32	0.40444962	0.332	0.188	5.82E-28	2	Irf8
Ifitm31	2.38E-31	0.34150912	0.51	0.326	3.24E-27	2	Ifitm3
mt-Nd5	2.26E-29	0.25910226	0.424	0.263	3.06E-25	2	mt-Nd5
Psme2	1.59E-23	0.25535202	0.371	0.235	2.15E-19	2	Psme2
Gm424181	1.60E-22	0.90380069	0.988	0.973	2.18E-18	2	Gm42418
Eef1b2	1.43E-21	0.26297256	0.51	0.383	1.93E-17	2	Eef1b2
Ifitm1	2.17E-20	0.8172591	0.326	0.217	2.95E-16	2	Ifitm1
Zeb21	7.02E-07	0.3263856	0.356	0.313	0.00952359	2	Zeb2
Ccl5	0	1.96862252	0.544	0.056	0	3	Ccl5
AW112010	0	1.75098099	0.892	0.108	0	3	AW112010
Nkg7	0	1.59265539	0.763	0.001	0	3	Nkg7
Cd3g	0	1.48751977	0.839	0.003	0	3	Cd3g
Trbc2	0	1.43887231	0.838	0.003	0	3	Trbc2

Rps15a	0	1.39016349	0.976	0.627	0	3	Rps15a
Rpl12	0	1.16051827	0.959	0.444	0	3	Rpl12
Cd3d	0	1.13521241	0.808	0.004	0	3	Cd3d
Ms4a4b	0	1.04670742	0.656	0.029	0	3	Ms4a4b
Rps24	0	1.02256463	0.98	0.732	0	3	Rps24
Trac	0	0.99324897	0.743	0.003	0	3	Trac
Rps18	0	0.99138847	0.962	0.559	0	3	Rps18
Rpsa1	0	0.98752452	0.992	0.632	0	3	Rpsa
Rpl3	0	0.91322488	0.937	0.421	0	3	Rpl3
Rps4x1	0	0.91092233	0.963	0.508	0	3	Rps4x
Rpl5	0	0.90225009	0.914	0.404	0	3	Rpl5
H2-Q7	0	0.86666012	0.775	0.088	0	3	H2-Q7
Trbc1	0	0.85623838	0.427	0.002	0	3	Trbc1
Ptpcap	0	0.83052786	0.74	0.018	0	3	Ptpcap
Cd3e	0	0.82752441	0.717	0.001	0	3	Cd3e
Tnfrsf4	0	0.7883967	0.411	0.007	0	3	Tnfrsf4
Klrd1	0	0.77883415	0.501	0.048	0	3	Klrd1
S100a101	0	0.77718683	0.751	0.132	0	3	S100a10
Cxcr6	0	0.77641652	0.506	0	0	3	Cxcr6
Ltb	0	0.76873834	0.713	0.122	0	3	Ltb
Ctla2a	0	0.76697266	0.502	0.005	0	3	Ctla2a
Cd8a	0	0.76242311	0.401	0.004	0	3	Cd8a
Cd8b1	0	0.72707322	0.399	0.008	0	3	Cd8b1
Thy1	0	0.71001543	0.643	0.001	0	3	Thy1
Cd2	0	0.70622733	0.604	0.003	0	3	Cd2
Tnfrsf18	0	0.68976767	0.536	0.01	0	3	Tnfrsf18
Lck	0	0.68826221	0.669	0.002	0	3	Lck
Il2rb	0	0.66140569	0.579	0.001	0	3	Il2rb
Gimap4	0	0.64843944	0.577	0.004	0	3	Gimap4
Ctsw	0	0.60686675	0.507	0.003	0	3	Ctsw
Odc1	0	0.60205871	0.387	0.027	0	3	Odc1
Icos	0	0.57215194	0.397	0.002	0	3	Icos
Gimap1	0	0.55804239	0.56	0.008	0	3	Gimap1
Ets1	0	0.54837711	0.524	0.021	0	3	Ets1
Gimap3	0	0.54703663	0.528	0.004	0	3	Gimap3
Ikzf2	0	0.54604901	0.297	0.006	0	3	Ikzf2
Dusp2	0	0.5377906	0.49	0.052	0	3	Dusp2
Pdcd1	0	0.51180759	0.453	0.005	0	3	Pdcd1
Bcl2	0	0.48852268	0.382	0.029	0	3	Bcl2
Tnfrsf9	0	0.48558911	0.338	0.005	0	3	Tnfrsf9

Ifng	0	0.47230513	0.26	0	0	3	Ifng
Lat	0	0.46887353	0.454	0.004	0	3	Lat
Skap1	0	0.46426397	0.478	0.001	0	3	Skap1
Ptpn22	0	0.46320439	0.487	0.027	0	3	Ptpn22
Sh2d2a	0	0.44600862	0.419	0.001	0	3	Sh2d2a
Cd28	0	0.44386913	0.41	0.001	0	3	Cd28
Gimap6	0	0.42703311	0.415	0.007	0	3	Gimap6
Gm8369	0	0.4207913	0.407	0.011	0	3	Gm8369
1-Sep	0	0.41376587	0.452	0.016	0	3	1-Sep
Bcl11b	0	0.39459896	0.408	0.001	0	3	Bcl11b
Ctla4	0	0.38721057	0.293	0.001	0	3	Ctla4
Inpp4b	0	0.38108726	0.392	0.007	0	3	Inpp4b
Gimap5	0	0.37788063	0.401	0.003	0	3	Gimap5
Cst7	0	0.36385747	0.408	0.022	0	3	Cst7
Ablim1	0	0.36287951	0.369	0.009	0	3	Ablim1
Cish	0	0.36280442	0.353	0.007	0	3	Cish
Zap70	0	0.35406323	0.354	0.001	0	3	Zap70
Cd247	0	0.32986455	0.317	0.001	0	3	Cd247
Klrc1	0	0.31535055	0.274	0	0	3	Klrc1
Sh2d1a	0	0.31114002	0.289	0	0	3	Sh2d1a
Il18r1	0	0.30598114	0.287	0.004	0	3	Il18r1
Tox	0	0.29137361	0.279	0	0	3	Tox
Cd6	0	0.27750857	0.255	0	0	3	Cd6
Gimap7	0	0.27272805	0.256	0.002	0	3	Gimap7
Cd27	0	0.26913272	0.273	0.006	0	3	Cd27
Ikzf3	0	0.26580705	0.262	0.004	0	3	Ikzf3
Itk	0	0.25690213	0.266	0	0	3	Itk
Serpina3g	3.36E-304	0.41140268	0.381	0.029	4.56E-300	3	Serpina3g
Lag3	7.17E-304	0.37350743	0.363	0.024	9.73E-300	3	Lag3
Rpl13	4.60E-302	0.88517901	0.984	0.746	6.25E-298	3	Rpl13
Rpl27a	6.08E-300	0.81409222	0.986	0.774	8.25E-296	3	Rpl27a
Il7r	2.11E-295	0.5718892	0.427	0.044	2.86E-291	3	Il7r
H2-K1	4.44E-294	0.89512278	0.967	0.533	6.02E-290	3	H2-K1
Rps3a1	2.78E-292	0.84217658	0.971	0.695	3.77E-288	3	Rps3a1

Rabgap1l	8.77E-290	0.31808328	0.341	0.022	1.19E-285	3	Rabgap1l
Rps7	4.79E-289	0.860481	0.946	0.566	6.50E-285	3	Rps7
Cd4	2.75E-286	0.30669188	0.255	0.006	3.74E-282	3	Cd4
Rps23	3.16E-285	0.79030936	0.962	0.694	4.29E-281	3	Rps23
Shisa5	3.90E-283	0.6687795	0.795	0.248	5.30E-279	3	Shisa5
Rps13	4.17E-278	0.79813868	0.955	0.693	5.66E-274	3	Rps13
Rplp1	1.57E-276	0.77768049	0.991	0.826	2.13E-272	3	Rplp1
Dut	1.07E-273	0.27420862	0.268	0.01	1.45E-269	3	Dut
Rpl19	1.06E-271	0.73661935	0.978	0.746	1.44E-267	3	Rpl19
Rps14	4.89E-268	0.73144079	0.979	0.784	6.64E-264	3	Rps14
Rpl32	1.30E-264	0.85202156	0.971	0.651	1.77E-260	3	Rpl32
Rpl30	7.28E-264	0.76186378	0.962	0.703	9.89E-260	3	Rpl30
Rack1	9.67E-262	0.75247741	0.914	0.475	1.31E-257	3	Rack1
Eef1a1	1.05E-261	0.77528106	0.985	0.853	1.43E-257	3	Eef1a1
Rps10	5.60E-261	0.74491252	0.974	0.748	7.60E-257	3	Rps10
Rps15	5.56E-258	0.68918686	0.932	0.504	7.55E-254	3	Rps15
Pla2g16	5.74E-253	0.33235564	0.389	0.043	7.80E-249	3	Pla2g16
Rpl22l1	3.22E-252	0.66713558	0.725	0.223	4.37E-248	3	Rpl22l1
Rps5	6.37E-251	0.7536533	0.959	0.59	8.65E-247	3	Rps5
Tbc1d10c	1.89E-250	0.27753885	0.317	0.024	2.57E-246	3	Tbc1d10c
Rps20	2.08E-249	0.80498477	0.957	0.608	2.82E-245	3	Rps20
Ly6a	2.41E-248	0.64335611	0.586	0.116	3.27E-244	3	Ly6a
Rinl	3.90E-248	0.3872667	0.468	0.071	5.30E-244	3	Rinl

Rps3	9.34E-248	0.6805604	0.969	0.69	1.27E-243	3	Rps3
Rps6	8.72E-247	0.71255879	0.919	0.472	1.18E-242	3	Rps6
Rpl9	1.31E-244	0.69672674	0.959	0.695	1.78E-240	3	Rpl9
Rpl7	1.50E-244	0.68980788	0.924	0.51	2.03E-240	3	Rpl7
Lgals11	1.66E-243	0.7298482	0.714	0.2	2.25E-239	3	Lgals1
Rpl11	3.77E-243	0.68394323	0.952	0.628	5.12E-239	3	Rpl11
Rpl17	1.91E-242	0.68893129	0.978	0.773	2.60E-238	3	Rpl17
Rpl23a	2.12E-241	0.67885628	0.882	0.419	2.88E-237	3	Rpl23a
Rpl10a	7.11E-241	0.69336706	0.914	0.411	9.66E-237	3	Rpl10a
Rpl23	9.37E-240	0.6902213	0.979	0.839	1.27E-235	3	Rpl23
Hcst	1.01E-238	0.51624632	0.588	0.133	1.37E-234	3	Hcst
Rpl39	2.79E-238	0.72382711	0.967	0.714	3.78E-234	3	Rpl39
Pkp3	4.55E-238	0.2568669	0.273	0.016	6.17E-234	3	Pkp3
Eif3e	5.99E-237	0.41925318	0.546	0.11	8.13E-233	3	Eif3e
Prkch	8.51E-237	0.29599622	0.35	0.036	1.15E-232	3	Prkch
Eef1b21	1.69E-236	0.67491147	0.833	0.338	2.30E-232	3	Eef1b2
Rpl22	1.80E-236	0.66422	0.903	0.448	2.44E-232	3	Rpl22
Rplp0	3.67E-236	0.75536311	0.963	0.637	4.98E-232	3	Rplp0
Rpl29	3.47E-235	0.6589867	0.866	0.373	4.72E-231	3	Rpl29
Tmsb102	3.85E-233	0.66091736	0.869	0.298	5.23E-229	3	Tmsb10
Tpt1	1.19E-232	0.70333357	0.991	0.943	1.62E-228	3	Tpt1
Rhoh	2.33E-232	0.37584918	0.469	0.077	3.16E-228	3	Rhoh
Rpl27	6.05E-230	0.60949766	0.818	0.329	8.22E-226	3	Rpl27

Rac2	6.65E-228	0.6044368	0.818	0.309	9.02E-224	3	Rac2
Rpl24	3.66E-224	0.64094663	0.929	0.566	4.97E-220	3	Rpl24
Rpl8	1.79E-223	0.62208749	0.97	0.668	2.43E-219	3	Rpl8
Fkbp3	1.44E-221	0.29234957	0.355	0.041	1.95E-217	3	Fkbp3
Rpl4	3.93E-220	0.63699099	0.831	0.343	5.34E-216	3	Rpl4
Rpl18a	4.37E-219	0.64489517	0.987	0.808	5.94E-215	3	Rpl18a
Npm1	1.63E-216	0.56991548	0.725	0.234	2.21E-212	3	Npm1
Rpl36a	2.58E-216	0.6444237	0.81	0.324	3.50E-212	3	Rpl36a
Rpl26	1.85E-215	0.62203982	0.965	0.683	2.52E-211	3	Rpl26
Sdf4	3.49E-215	0.8198258	0.545	0.137	4.74E-211	3	Sdf4
Msi2	1.82E-211	0.25119888	0.27	0.02	2.47E-207	3	Msi2
Rpl15	4.15E-211	0.64104557	0.917	0.499	5.63E-207	3	Rpl15
Rpl21	1.35E-209	0.60847891	0.964	0.718	1.84E-205	3	Rpl21
Rps12	1.08E-207	0.63512569	0.978	0.785	1.47E-203	3	Rps12
Rpl141	1.65E-207	0.60547017	0.9	0.458	2.24E-203	3	Rpl14
Rps16	7.53E-206	0.61182511	0.978	0.841	1.02E-201	3	Rps16
H2-Q6	1.11E-205	0.27959818	0.325	0.036	1.51E-201	3	H2-Q6
Rpl34	1.00E-204	0.62093443	0.969	0.745	1.36E-200	3	Rpl34
Naca	4.49E-203	0.59167294	0.839	0.386	6.09E-199	3	Naca
Rps111	7.59E-203	0.63839998	0.974	0.715	1.03E-198	3	Rps11
Eif3h	1.38E-201	0.48610247	0.664	0.208	1.87E-197	3	Eif3h
Ifi27	3.81E-195	0.29825528	0.342	0.045	5.18E-191	3	Ifi27
Rpl18	5.47E-195	0.59054895	0.954	0.668	7.43E-191	3	Rpl18

Anxa6	1.50E-194	0.31126367	0.384	0.06	2.04E-190	3	Anxa6
Rps8	2.77E-188	0.58920216	0.977	0.811	3.76E-184	3	Rps8
Mbnl1	3.94E-184	0.4959351	0.676	0.22	5.35E-180	3	Mbnl1
Klrk1	2.73E-183	0.42123574	0.343	0.051	3.70E-179	3	Klrk1
Rps191	3.50E-181	0.60439767	0.983	0.677	4.76E-177	3	Rps19
Ptpn18	6.27E-177	0.484388	0.685	0.239	8.52E-173	3	Ptpn18
Ndfip1	7.28E-175	0.26876225	0.308	0.041	9.88E-171	3	Ndfip1
Pdcd4	8.19E-175	0.29515108	0.32	0.045	1.11E-170	3	Pdcd4
Spn	9.64E-175	0.2613446	0.3	0.037	1.31E-170	3	Spn
Rplp2	5.66E-173	0.49530128	0.978	0.776	7.69E-169	3	Rplp2
Eef1g	5.92E-173	0.44671626	0.586	0.178	8.03E-169	3	Eef1g
Rps2	2.17E-172	0.59072675	0.93	0.616	2.95E-168	3	Rps2
Rpl7a1	6.19E-171	0.52556434	0.862	0.421	8.41E-167	3	Rpl7a
Mettl23	5.33E-170	0.25769352	0.325	0.048	7.24E-166	3	Mettl23
Il2rg	8.93E-170	0.28538533	0.37	0.065	1.21E-165	3	Il2rg
Smc4	5.90E-169	0.28393026	0.312	0.044	8.02E-165	3	Smc4
Ppia	1.65E-167	0.55069006	0.884	0.483	2.25E-163	3	Ppia
Eef1d	1.40E-166	0.36732975	0.544	0.153	1.90E-162	3	Eef1d
Rpl36	1.70E-163	0.54011376	0.959	0.599	2.31E-159	3	Rpl36
H2afv	3.57E-162	0.29878377	0.349	0.06	4.84E-158	3	H2afv
Sumo2	3.54E-157	0.42095309	0.62	0.216	4.80E-153	3	Sumo2
Eif3m	2.01E-156	0.32469688	0.46	0.113	2.73E-152	3	Eif3m
Rpl6	7.43E-156	0.49771868	0.95	0.63	1.01E-151	3	Rpl6

Arl6ip1	4.85E-154	0.45780918	0.598	0.2	6.58E-150	3	Arl6ip1
Slc25a4	8.26E-154	0.26388511	0.349	0.063	1.12E-149	3	Slc25a4
Snrpf	1.71E-145	0.30680918	0.437	0.108	2.32E-141	3	Snrpf
Rbm3	3.17E-145	0.51467944	0.774	0.379	4.30E-141	3	Rbm3
Hnrnpa1	1.97E-144	0.37174407	0.483	0.137	2.67E-140	3	Hnrnpa1
Ccnd2	1.81E-143	0.38672865	0.472	0.126	2.46E-139	3	Ccnd2
Hsp90ab11	1.70E-142	0.50122867	0.816	0.382	2.31E-138	3	Hsp90ab11
Rps26	3.00E-141	0.51705045	0.9	0.584	4.08E-137	3	Rps26
Cd82	3.78E-141	0.37275993	0.421	0.105	5.13E-137	3	Cd82
S100a13	1.75E-140	0.30627614	0.406	0.096	2.38E-136	3	S100a13
Uqcrh	2.50E-140	0.45367044	0.719	0.331	3.40E-136	3	Uqcrh
Rps21	5.79E-140	0.49545571	0.955	0.727	7.85E-136	3	Rps21
Ybx3	3.93E-139	0.25934912	0.302	0.052	5.33E-135	3	Ybx3
Cd48	1.96E-133	0.3075257	0.406	0.1	2.67E-129	3	Cd48
Kmt2a	9.41E-133	0.27020368	0.35	0.074	1.28E-128	3	Kmt2a
Cdk6	2.21E-132	0.26689	0.288	0.049	3.00E-128	3	Cdk6
AU020206	2.39E-132	0.30777021	0.397	0.095	3.25E-128	3	AU020206
Eif3f	1.25E-130	0.38694877	0.682	0.278	1.69E-126	3	Eif3f
Btf3	3.81E-129	0.40924281	0.763	0.366	5.17E-125	3	Btf3
Atp5g2	1.42E-128	0.36772814	0.614	0.232	1.92E-124	3	Atp5g2
Rpl13a	4.17E-128	0.34865424	0.49	0.152	5.67E-124	3	Rpl13a
Ifi27l2a1	1.91E-127	0.63562265	0.639	0.241	2.60E-123	3	Ifi27l2a1
Psmb81	2.29E-125	0.40519555	0.702	0.3	3.11E-121	3	Psmb8

Snrpe	4.86E-125	0.32991904	0.516	0.171	6.60E-121	3	Snrpe
H2-T22	5.11E-125	0.25798017	0.351	0.078	6.94E-121	3	H2-T22
Limd2	1.64E-123	0.31849788	0.5	0.158	2.23E-119	3	Limd2
Rps27rt	2.67E-121	0.25215055	0.355	0.083	3.62E-117	3	Rps27rt
Fkbp1a	9.03E-120	0.26088739	0.353	0.083	1.23E-115	3	Fkbp1a
Rpl37a	2.30E-119	0.43396117	0.98	0.802	3.12E-115	3	Rpl37a
Sub11	2.54E-114	0.40890646	0.629	0.264	3.45E-110	3	Sub1
Akap13	6.35E-114	0.38423557	0.585	0.232	8.63E-110	3	Akap13
Eef2	2.21E-112	0.42038961	0.764	0.403	3.00E-108	3	Eef2
Cox7a2l	2.47E-112	0.33375202	0.556	0.21	3.35E-108	3	Cox7a2l
Apobec3	2.93E-112	0.27826548	0.441	0.131	3.98E-108	3	Apobec3
Rps27a	7.65E-111	0.41328527	0.955	0.8	1.04E-106	3	Rps27a
S100a41	1.16E-109	0.4774674	0.599	0.217	1.57E-105	3	S100a4
Pfdn5	1.19E-109	0.39180101	0.763	0.398	1.61E-105	3	Pfdn5
Aes	5.59E-108	0.2842289	0.433	0.134	7.58E-104	3	Aes
Psmb9	6.22E-105	0.28792655	0.448	0.144	8.44E-101	3	Psmb9
Serbp1	1.72E-103	0.33971221	0.609	0.259	2.34E-99	3	Serbp1
Ran	3.72E-103	0.29574326	0.429	0.137	5.06E-99	3	Ran
Eif3i	2.95E-100	0.25423138	0.376	0.109	4.01E-96	3	Eif3i
Rps17	3.29E-100	0.37682252	0.705	0.351	4.46E-96	3	Rps17
Nol7	9.22E-99	0.25570601	0.363	0.103	1.25E-94	3	Nol7
Psmb1	1.70E-98	0.29148857	0.498	0.186	2.30E-94	3	Psmb1
Ms4a6b1	4.93E-97	0.3275663	0.508	0.187	6.69E-93	3	Ms4a6b
Abrac1	7.12E-95	0.28164501	0.472	0.171	9.66E-91	3	Abrac1
Mndal	3.40E-94	0.26084254	0.419	0.133	4.62E-90	3	Mndal
Rpl35a	2.58E-92	0.3591978	0.969	0.81	3.50E-88	3	Rpl35a

Cox6c	2.11E-91	0.30251183	0.622	0.281	2.87E-87	3	Cox6c
Dad1	9.51E-89	0.27174083	0.498	0.195	1.29E-84	3	Dad1
Ogt	1.11E-86	0.27104818	0.468	0.174	1.51E-82	3	Ogt
B2m1	4.82E-85	0.32247491	0.94	0.657	6.55E-81	3	B2m
Srsf3	4.65E-84	0.28401622	0.475	0.188	6.31E-80	3	Srsf3
AC149090.1	8.14E-83	0.25852691	0.393	0.132	1.10E-78	3	AC149090.1
Arhgdib	1.98E-82	0.32812151	0.656	0.334	2.68E-78	3	Arhgdib
Ppib1	2.77E-81	0.28589049	0.57	0.26	3.76E-77	3	Ppib
Ndufa4	4.08E-81	0.27507231	0.464	0.184	5.53E-77	3	Ndufa4
Atp5h	4.92E-79	0.29616556	0.63	0.317	6.68E-75	3	Atp5h
H2-D1	1.33E-78	0.36379937	0.933	0.659	1.80E-74	3	H2-D1
Anp32b	1.56E-77	0.26952433	0.474	0.194	2.11E-73	3	Anp32b
Rps25	1.13E-76	0.31641921	0.88	0.608	1.53E-72	3	Rps25
Tmsb4x1	6.43E-76	0.38441644	0.993	0.954	8.73E-72	3	Tmsb4x
Rpl38	1.18E-75	0.36788218	0.914	0.637	1.61E-71	3	Rpl38
7-Sep	1.87E-74	0.26019721	0.441	0.178	2.54E-70	3	7-Sep
Hint1	2.54E-74	0.27654129	0.51	0.223	3.45E-70	3	Hint1
Id21	1.96E-73	0.35677926	0.653	0.325	2.66E-69	3	Id2
Hspe1	2.43E-73	0.25143482	0.416	0.159	3.30E-69	3	Hspe1
Rpl31	5.41E-72	0.2711998	0.641	0.328	7.35E-68	3	Rpl31
Ptma1	4.97E-68	0.35650288	0.833	0.523	6.75E-64	3	Ptma
Rpl28	1.24E-64	0.29688788	0.919	0.674	1.68E-60	3	Rpl28
Atp5d	1.88E-63	0.25659193	0.488	0.229	2.56E-59	3	Atp5d
Cox7c	2.17E-61	0.25657793	0.611	0.328	2.95E-57	3	Cox7c
Rps271	6.46E-61	0.31128242	0.971	0.861	8.77E-57	3	Rps27
Pabpc1	2.07E-60	0.28387114	0.621	0.351	2.81E-56	3	Pabpc1
Maf	3.86E-56	0.37735533	0.291	0.107	5.24E-52	3	Maf
Hif1a	4.81E-55	0.27671483	0.369	0.157	6.53E-51	3	Hif1a
H2afz1	6.26E-41	0.26179887	0.552	0.316	8.50E-37	3	H2afz
Hmgb2	6.62E-25	0.2701523	0.381	0.224	8.99E-21	3	Hmgb2
Ccl41	9.07E-16	0.6867686	0.278	0.167	1.23E-11	3	Ccl4
Igkc	0	4.2114357	0.496	0.007	0	4	Igkc
Ly6d	0	2.03664996	0.82	0.001	0	4	Ly6d
Ccr9	0	0.99200243	0.518	0.005	0	4	Ccr9
Iglc3	0	0.98918866	0.669	0	0	4	Iglc3
Cox6a2	0	0.98388483	0.432	0.006	0	4	Cox6a2
Iglc2	0	0.90498166	0.381	0.001	0	4	Iglc2
Bcl11a	0	0.89263812	0.655	0.024	0	4	Bcl11a
Mzb1	0	0.8044293	0.504	0	0	4	Mzb1
Cd79a	0	0.69658951	0.374	0	0	4	Cd79a

Atp1b1	0	0.65995069	0.453	0.003	0	4	Atp1b1
Fcrla	0	0.52403163	0.424	0.005	0	4	Fcrla
Ebf1	0	0.50227115	0.288	0	0	4	Ebf1
Gm21762	0	0.42622503	0.338	0.001	0	4	Gm21762
Smim5	4.90E-304	0.4369549	0.324	0.004	6.66E-300	4	Smim5
Cd300c	3.37E-281	0.26239262	0.252	0.002	4.57E-277	4	Cd300c
Siglech	1.81E-274	1.55839173	0.583	0.025	2.46E-270	4	Siglech
Cd79b	1.85E-267	0.7144225	0.353	0.007	2.52E-263	4	Cd79b
Ighm	1.51E-260	1.751128	0.863	0.071	2.05E-256	4	Ighm
Spib	2.08E-247	0.26671815	0.252	0.003	2.82E-243	4	Spib
Lefty1	1.08E-234	0.27690785	0.266	0.004	1.47E-230	4	Lefty1
Rnase6	4.24E-190	1.01901139	0.669	0.056	5.76E-186	4	Rnase6
Cd7	2.00E-176	0.74599541	0.446	0.023	2.72E-172	4	Cd7
Tcf4	8.42E-172	1.2281938	0.727	0.078	1.14E-167	4	Tcf4
Dnajc7	7.81E-155	0.96789596	0.734	0.088	1.06E-150	4	Dnajc7
Mef2c	4.53E-105	0.61366001	0.662	0.096	6.15E-101	4	Mef2c
Rpgrip1	2.32E-100	0.38062096	0.317	0.022	3.15E-96	4	Rpgrip1
Cnp	4.47E-99	0.41392544	0.475	0.051	6.07E-95	4	Cnp
Sell	2.84E-97	0.56265073	0.561	0.073	3.86E-93	4	Sell
Gm5547	3.64E-94	0.31811526	0.295	0.02	4.94E-90	4	Gm5547
Tsc22d1	1.86E-89	0.33498284	0.266	0.017	2.52E-85	4	Tsc22d1
Ptprcap	4.54E-87	0.50787506	0.64	0.098	6.16E-83	4	Ptprcap
Clec10a	2.36E-80	0.28265645	0.252	0.017	3.20E-76	4	Clec10a
Pafah1b3	1.22E-79	0.33070063	0.367	0.037	1.66E-75	4	Pafah1b3
Kmo	8.71E-78	0.29811388	0.324	0.029	1.18E-73	4	Kmo
Dirc2	2.39E-74	0.25801864	0.266	0.02	3.25E-70	4	Dirc2
Plac8	3.97E-74	1.18137084	0.799	0.2	5.38E-70	4	Plac8
Abhd17b	1.88E-73	0.28345665	0.309	0.028	2.56E-69	4	Abhd17b
Bst2	4.95E-73	1.44621961	0.705	0.187	6.73E-69	4	Bst2
Nucb2	7.39E-71	0.44764269	0.403	0.052	1.00E-66	4	Nucb2
Tubgcp5	2.43E-68	0.31159952	0.331	0.035	3.29E-64	4	Tubgcp5

Serp1	3.74E-68	0.62791422	0.763	0.199	5.07E-64	4	Serp1
Irf81	9.32E-68	1.33465202	0.719	0.198	1.26E-63	4	Irf8
Tnfrsf13b	7.99E-67	0.31010916	0.36	0.042	1.08E-62	4	Tnfrsf13b
Ly6a1	4.21E-65	1.12904101	0.691	0.165	5.71E-61	4	Ly6a
P2ry14	3.58E-62	0.29394885	0.295	0.031	4.86E-58	4	P2ry14
Rps201	4.64E-62	1.00423696	0.986	0.645	6.30E-58	4	Rps20
Ly6c21	4.66E-61	1.21618728	0.583	0.13	6.33E-57	4	Ly6c2
St8sia4	5.46E-60	0.50271983	0.446	0.073	7.41E-56	4	St8sia4
Apobec31	1.62E-59	0.52855252	0.662	0.16	2.20E-55	4	Apobec3
Rpl311	2.26E-57	0.9824256	0.842	0.357	3.07E-53	4	Rpl31
Runx2	2.12E-56	0.43440484	0.403	0.064	2.88E-52	4	Runx2
Ptp4a3	1.40E-55	0.29825563	0.317	0.04	1.91E-51	4	Ptp4a3
Pgls	1.07E-54	0.54966379	0.619	0.154	1.46E-50	4	Pgls
Rps4x2	1.30E-54	0.84378501	0.978	0.557	1.76E-50	4	Rps4x
Rabgap11l	2.25E-54	0.35248415	0.374	0.056	3.06E-50	4	Rabgap1l
Dap	2.35E-54	0.44613649	0.446	0.081	3.20E-50	4	Dap
Rps241	2.80E-54	0.97833523	0.993	0.759	3.81E-50	4	Rps24
Pkig	2.16E-53	0.32993025	0.36	0.053	2.94E-49	4	Pkig
Snx5	9.30E-51	0.4391169	0.561	0.129	1.26E-46	4	Snx5
Rps112	1.39E-47	0.75376392	0.942	0.744	1.89E-43	4	Rps11
Rel1	3.34E-47	0.32837402	0.345	0.054	4.54E-43	4	Rel1
Ly861	1.88E-46	0.38925606	0.662	0.177	2.55E-42	4	Ly86
Rpl121	8.46E-44	0.80693106	0.942	0.5	1.15E-39	4	Rpl12
Cybb1	3.35E-43	0.49445456	0.705	0.208	4.54E-39	4	Cybb
Cd47	3.43E-42	0.60135363	0.77	0.296	4.66E-38	4	Cd47
Slc44a2	7.51E-42	0.40420211	0.46	0.104	1.02E-37	4	Slc44a2
Fchsd2	1.87E-41	0.27324985	0.295	0.045	2.53E-37	4	Fchsd2
Lpgat1	2.68E-41	0.28509103	0.317	0.052	3.64E-37	4	Lpgat1
Rps181	4.43E-41	0.68381523	0.971	0.602	6.02E-37	4	Rps18
Cd8b11	7.88E-41	0.61663631	0.317	0.052	1.07E-36	4	Cd8b1
Rpl191	8.83E-41	0.64936858	0.971	0.772	1.20E-36	4	Rpl19
Ccnd1	1.06E-40	0.40254637	0.36	0.067	1.44E-36	4	Ccnd1
Rps3a11	2.32E-40	0.64002114	0.964	0.725	3.15E-36	4	Rps3a1
Rpl33	4.80E-40	0.62422654	0.928	0.477	6.52E-36	4	Rpl3
Syng21	9.76E-40	0.62143738	0.597	0.189	1.33E-35	4	Syng2
Tspan13	4.96E-39	0.48562966	0.496	0.131	6.73E-35	4	Tspan13
Rpl71	1.17E-38	0.58123195	0.964	0.554	1.59E-34	4	Rpl7
Rpl301	2.39E-38	0.64506949	0.957	0.731	3.25E-34	4	Rpl30
Ctsl1	2.44E-38	0.74070439	0.482	0.129	3.31E-34	4	Ctsl
Rps51	2.77E-38	0.63880722	0.964	0.63	3.77E-34	4	Rps5

Ly6e1	3.54E-38	0.61555837	0.928	0.467	4.81E-34	4	Ly6e
Pltp	3.77E-38	0.336318	0.281	0.044	5.12E-34	4	Pltp
Eif3f1	6.57E-38	0.50941032	0.791	0.32	8.92E-34	4	Eif3f
Ech1	7.03E-38	0.30868048	0.396	0.084	9.54E-34	4	Ech1
Foxp1	1.35E-37	0.42985686	0.446	0.107	1.83E-33	4	Foxp1
Rpl10a1	4.60E-37	0.59845923	0.95	0.464	6.25E-33	4	Rpl10a
Rps161	7.54E-37	0.59763588	0.964	0.856	1.02E-32	4	Rps16
Rpl36a1	1.70E-36	0.5285653	0.878	0.375	2.31E-32	4	Rpl36a
Mvb12a	2.67E-36	0.34605688	0.374	0.08	3.63E-32	4	Mvb12a
Rpl51	4.27E-36	0.59874916	0.899	0.46	5.80E-32	4	Rpl5
H2-T23	1.23E-35	0.47866755	0.619	0.206	1.67E-31	4	H2-T23
Tmed3	3.04E-35	0.34329786	0.388	0.087	4.13E-31	4	Tmed3
Herpud1	7.33E-35	0.31195693	0.374	0.08	9.96E-31	4	Herpud1
Rpl131	2.32E-34	0.66230013	0.978	0.772	3.15E-30	4	Rpl13
Rpl18a1	5.97E-34	0.59829927	0.971	0.828	8.11E-30	4	Rpl18a
Jaml	7.80E-34	0.42566435	0.439	0.112	1.06E-29	4	Jaml
Rpl231	7.81E-34	0.56039301	0.978	0.854	1.06E-29	4	Rpl23
Rpl261	8.87E-34	0.56102964	0.971	0.714	1.20E-29	4	Rpl26
Zbtb20	1.13E-33	0.3385998	0.324	0.064	1.54E-29	4	Zbtb20
Rps71	1.18E-33	0.6112216	0.942	0.607	1.60E-29	4	Rps7
Rpl81	1.34E-33	0.56685617	0.971	0.701	1.82E-29	4	Rpl8
Rack11	1.62E-33	0.53311832	0.935	0.522	2.20E-29	4	Rack1
Hmgn1	4.04E-33	0.26341831	0.295	0.055	5.48E-29	4	Hmgn1
Rps15a1	4.05E-33	0.54892937	0.964	0.665	5.50E-29	4	Rps15a
Rpl391	5.27E-33	0.5885133	0.964	0.742	7.16E-29	4	Rpl39
Ctsh1	7.02E-33	0.61658306	0.712	0.305	9.53E-29	4	Ctsh
Rpl321	9.64E-33	0.6098803	0.971	0.686	1.31E-28	4	Rpl32
Abhd17a	1.32E-32	0.27943884	0.36	0.08	1.80E-28	4	Abhd17a
Tagln2	5.26E-32	0.47829424	0.59	0.199	7.14E-28	4	Tagln2
Fyn	9.27E-32	0.33978213	0.353	0.079	1.26E-27	4	Fyn
Rps141	1.27E-31	0.51520981	0.95	0.806	1.72E-27	4	Rps14
Rplp01	1.31E-31	0.5156002	0.964	0.672	1.78E-27	4	Rplp0
Rpl111	2.18E-31	0.48445334	0.964	0.663	2.96E-27	4	Rpl11
Rpl41	4.41E-31	0.45153209	0.885	0.395	5.99E-27	4	Rpl4
Cd37	7.07E-31	0.41587346	0.561	0.188	9.60E-27	4	Cd37
Rpl281	7.84E-31	0.47722528	0.957	0.7	1.06E-26	4	Rpl28
Sub12	7.95E-31	0.48696096	0.712	0.301	1.08E-26	4	Sub1
Rpl91	8.37E-31	0.50974565	0.957	0.723	1.14E-26	4	Rpl9
Mbnl11	1.06E-30	0.49331666	0.676	0.269	1.44E-26	4	Mbnl1
Rpl211	2.67E-30	0.57887621	0.957	0.745	3.62E-26	4	Rpl21

Rps61	3.47E-30	0.48779034	0.935	0.52	4.71E-26	4	Rps6
Rps131	1.15E-29	0.57725649	0.942	0.722	1.56E-25	4	Rps13
Rpl142	4.61E-29	0.49464968	0.906	0.505	6.26E-25	4	Rpl14
Rpl27a1	1.86E-28	0.5781065	0.957	0.797	2.53E-24	4	Rpl27a
Rpl151	3.10E-28	0.498592	0.914	0.544	4.21E-24	4	Rpl15
Gnas	3.91E-28	0.50511897	0.734	0.361	5.31E-24	4	Gnas
Npm11	4.24E-28	0.38122667	0.727	0.287	5.75E-24	4	Npm1
Sec61b	4.67E-28	0.49719966	0.719	0.338	6.34E-24	4	Sec61b
Rpl181	5.94E-28	0.49668335	0.957	0.699	8.06E-24	4	Rpl18
Rps9	8.76E-28	0.45772126	0.964	0.89	1.19E-23	4	Rps9
Rps81	1.74E-27	0.46321272	0.978	0.829	2.36E-23	4	Rps8
Serinc3	2.21E-27	0.35407923	0.712	0.29	3.00E-23	4	Serinc3
Rps251	3.09E-27	0.45824625	0.942	0.636	4.20E-23	4	Rps25
Rpl10	3.82E-27	0.50450595	0.935	0.7	5.19E-23	4	Rpl10
Rplp11	4.69E-27	0.50486947	0.964	0.845	6.37E-23	4	Rplp1
Ptma2	1.00E-26	0.49104037	0.899	0.555	1.36E-22	4	Ptma
Rpl291	1.13E-26	0.52209773	0.82	0.427	1.54E-22	4	Rpl29
Rps101	1.27E-26	0.54937862	0.971	0.772	1.72E-22	4	Rps10
Napsa1	1.42E-26	0.40520283	0.561	0.195	1.93E-22	4	Napsa
Rps171	1.73E-26	0.42517295	0.784	0.388	2.35E-22	4	Rps17
Sec11c	2.73E-26	0.37607162	0.468	0.15	3.70E-22	4	Sec11c
Ppp1r14b	3.26E-26	0.28590782	0.374	0.1	4.42E-22	4	Ppp1r14b
Rpl35a1	3.29E-26	0.43741772	0.971	0.827	4.47E-22	4	Rpl35a
Cd69	6.01E-26	0.29187818	0.266	0.055	8.16E-22	4	Cd69
Rpl13a1	1.06E-25	0.36114959	0.532	0.187	1.44E-21	4	Rpl13a
Pkib	1.12E-25	0.27593661	0.281	0.061	1.52E-21	4	Pkib
Rpl22l11	1.86E-25	0.36207358	0.683	0.278	2.53E-21	4	Rpl22l1
Rps31	2.25E-25	0.4772418	0.95	0.72	3.05E-21	4	Rps3
Rps261	7.13E-25	0.47953496	0.914	0.618	9.69E-21	4	Rps26
Rpl36al	1.14E-24	0.37319411	0.655	0.277	1.55E-20	4	Rpl36al
Rpl61	2.29E-24	0.43884385	0.95	0.665	3.11E-20	4	Rpl6
Ppfia4	2.72E-24	0.26474869	0.324	0.082	3.69E-20	4	Ppfia4
Rpsa2	2.94E-24	0.50491371	0.95	0.672	3.99E-20	4	Rpsa
mt-Co32	4.08E-24	0.34439997	1	0.822	5.54E-20	4	mt-Co3
Lair11	4.58E-24	0.50136069	0.446	0.153	6.22E-20	4	Lair1
Rps192	5.26E-24	0.64406649	0.95	0.71	7.14E-20	4	Rps19
mt-Atp62	8.74E-24	0.36783882	1	0.813	1.19E-19	4	mt-Atp6
Eef1b22	1.16E-23	0.38549149	0.799	0.393	1.58E-19	4	Eef1b2
Hnrnpa11	1.17E-23	0.29455021	0.504	0.174	1.58E-19	4	Hnrnpa1
Rpl351	1.31E-23	0.42896734	0.806	0.409	1.77E-19	4	Rpl35

Cd742	2.95E-23	0.25487685	0.835	0.374	4.01E-19	4	Cd74
Ppia1	4.12E-23	0.48621327	0.842	0.527	5.60E-19	4	Ppia
Krtcap2	4.21E-23	0.32293089	0.482	0.171	5.71E-19	4	Krtcap2
Rps272	4.48E-23	0.54179445	0.971	0.873	6.08E-19	4	Rps27
Rpl221	4.85E-23	0.45710084	0.885	0.498	6.59E-19	4	Rpl22
Eef21	6.25E-23	0.42387285	0.827	0.44	8.49E-19	4	Eef2
mt-Nd51	6.54E-23	0.34639542	0.662	0.278	8.88E-19	4	mt-Nd5
Smim14	1.41E-22	0.30522678	0.424	0.139	1.91E-18	4	Smim14
Rpl241	2.34E-22	0.41575373	0.95	0.605	3.18E-18	4	Rpl24
Atp5g21	2.74E-22	0.34406474	0.633	0.273	3.71E-18	4	Atp5g2
Rpl361	4.50E-22	0.42367395	0.935	0.638	6.11E-18	4	Rpl36
Uvrag	9.37E-22	0.2663336	0.417	0.134	1.27E-17	4	Uvrag
Rpl341	1.02E-21	0.46734567	0.957	0.769	1.39E-17	4	Rpl34
Naca1	1.15E-21	0.39175773	0.82	0.435	1.57E-17	4	Naca
Eif3h1	1.61E-21	0.31173515	0.612	0.258	2.18E-17	4	Eif3h
mt-Co12	1.91E-21	0.26749794	1	0.844	2.60E-17	4	mt-Co1
Cd164	2.07E-21	0.25511464	0.374	0.114	2.80E-17	4	Cd164
Plid41	2.15E-21	0.43168045	0.468	0.179	2.92E-17	4	Plid4
Eef1a11	2.22E-21	0.39552448	0.971	0.868	3.02E-17	4	Eef1a1
Rpl171	5.65E-21	0.44586814	0.95	0.796	7.66E-17	4	Rpl17
H2-DMa2	9.20E-21	0.2973249	0.561	0.21	1.25E-16	4	H2-DMa
Rps231	1.29E-20	0.41412639	0.957	0.723	1.75E-16	4	Rps23
Eef1g1	1.32E-20	0.29716752	0.561	0.223	1.79E-16	4	Eef1g
H2-Q71	7.70E-20	0.3556863	0.468	0.169	1.05E-15	4	H2-Q7
mt-Nd32	9.60E-20	0.27433699	0.799	0.383	1.30E-15	4	mt-Nd3
Rap1a	1.38E-19	0.3499865	0.532	0.222	1.87E-15	4	Rap1a
Rps22	1.55E-19	0.39657673	0.921	0.65	2.10E-15	4	Rps2
Rps121	2.55E-19	0.41306412	0.95	0.806	3.46E-15	4	Rps12
Rpl7a2	3.89E-19	0.36745313	0.82	0.469	5.28E-15	4	Rpl7a
Rps28	4.50E-19	0.44323562	0.906	0.64	6.11E-15	4	Rps28
Sec61g1	7.68E-19	0.32933268	0.655	0.317	1.04E-14	4	Sec61g
Hspe11	9.44E-19	0.3076326	0.482	0.185	1.28E-14	4	Hspe1
Hsp90b11	9.57E-19	0.36196974	0.64	0.289	1.30E-14	4	Hsp90b1
Uqcrh1	9.74E-19	0.30469825	0.741	0.372	1.32E-14	4	Uqcrh
Rpl23a1	1.02E-18	0.34815823	0.842	0.47	1.39E-14	4	Rpl23a
GltP	1.55E-18	0.28515168	0.374	0.128	2.11E-14	4	GltP
Rpl271	2.10E-18	0.32743272	0.734	0.383	2.85E-14	4	Rpl27
Lsp11	4.02E-18	0.35322724	0.655	0.314	5.46E-14	4	Lsp1
Rps211	5.15E-18	0.45028173	0.928	0.753	7.00E-14	4	Rps21
Atp5c1	5.60E-18	0.29042348	0.504	0.209	7.60E-14	4	Atp5c1

Ssr41	7.91E-18	0.31262256	0.583	0.263	1.07E-13	4	Ssr4
Fgfr1op2	1.83E-17	0.26740455	0.41	0.153	2.49E-13	4	Fgfr1op2
Rps27a1	4.57E-17	0.34629005	0.964	0.816	6.21E-13	4	Rps27a
Tpt11	1.47E-16	0.32963614	0.993	0.948	2.00E-12	4	Tpt1
Rpl37a1	1.91E-16	0.36184805	0.978	0.821	2.59E-12	4	Rpl37a
Cox7a2l1	2.05E-16	0.26560837	0.554	0.248	2.79E-12	4	Cox7a2l
Rps151	2.46E-16	0.38519351	0.863	0.552	3.35E-12	4	Rps15
Hsp90ab12	2.78E-16	0.32788428	0.784	0.429	3.78E-12	4	Hsp90ab1
Rac21	8.46E-16	0.30645679	0.698	0.367	1.15E-11	4	Rac2
Hmgb1	1.16E-15	0.28882302	0.619	0.318	1.57E-11	4	Hmgb1
Spcs2	1.29E-15	0.274693	0.482	0.21	1.76E-11	4	Spcs2
Psme11	1.76E-15	0.28289555	0.612	0.298	2.39E-11	4	Psme1
Reep5	1.96E-15	0.31639332	0.496	0.234	2.66E-11	4	Reep5
Psmb82	2.28E-15	0.26665161	0.691	0.344	3.09E-11	4	Psmb8
Mtdh	2.74E-15	0.25918466	0.525	0.236	3.71E-11	4	Mtdh
Rbm31	2.83E-15	0.30750316	0.755	0.422	3.84E-11	4	Rbm3
Manf1	7.64E-15	0.25201461	0.396	0.156	1.04E-10	4	Manf
Eif3k	1.32E-14	0.25540619	0.547	0.261	1.79E-10	4	Eif3k
Lgals12	1.42E-14	0.33568059	0.547	0.259	1.93E-10	4	Lgals1
Nsa2	1.74E-14	0.25260348	0.554	0.261	2.36E-10	4	Nsa2
Xbp1	2.04E-14	0.37159086	0.439	0.199	2.77E-10	4	Xbp1
Unc93b11	4.47E-14	0.29001901	0.532	0.255	6.06E-10	4	Unc93b1
H2afy1	1.17E-13	0.26352623	0.496	0.228	1.59E-09	4	H2afy
Fau	7.46E-13	0.27825592	1	0.964	1.01E-08	4	Fau
Btf31	2.19E-12	0.25200515	0.705	0.41	2.97E-08	4	Btf3
Rplp21	2.28E-12	0.31784276	0.95	0.799	3.09E-08	4	Rplp2
Rpl37	1.03E-11	0.30515566	0.928	0.8	1.39E-07	4	Rpl37
Rpl381	1.45E-10	0.29040101	0.892	0.667	1.98E-06	4	Rpl38
Rps29	1.65E-10	0.27319192	0.957	0.87	2.24E-06	4	Rps29
H2-K11	1.29E-09	0.2616614	0.835	0.583	1.74E-05	4	H2-K1
Ifi203	1.40E-09	0.25808481	0.345	0.157	1.91E-05	4	Ifi203

Notably, our comparison uncovered a higher proportion of neutrophils, T cell, and NK cell infiltrates in QPP7 allograft tumors compared to spontaneous QPP tumors. We also observed slight variations among different mice in both the spontaneous QPP and implanted QPP7 cohorts; specifically, some mice in each cohort had more neutrophils than others (**Fig. 14a, b, c**). This finding is consistent with the heterogeneous nature of the human disease. Importantly, the observed heterogeneity was not caused by technical variations, which were found to be minimal by examining two technical replicates (**data not shown**).

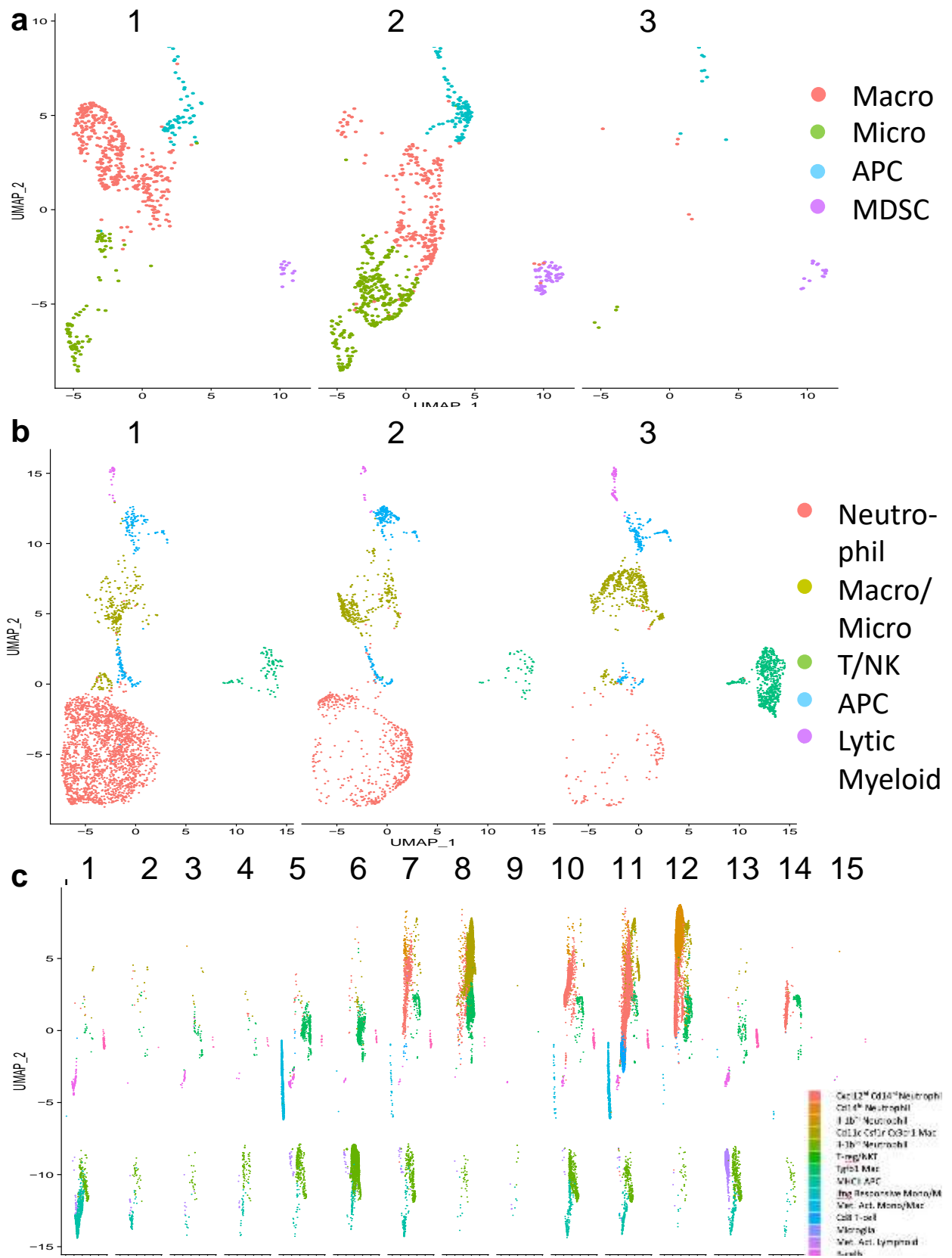


Figure 14: Heterogeneity between QPP mice and glioblastoma (GBM) patients.

a. Demonstrates the contribution of the individual spontaneous QPP mice to the aggregate plot in **Figure 7a**. **b.** Demonstrates the contribution of the individual implanted QPP mice to the aggregate plot in **Figure 7b**. **c.** Demonstrates the contribution of the individual GBM patients to the aggregate plot in **Figure 7d**.

scSEQ analysis of the cohort of human glioma samples (resolution = 0.15; **Figure 15**) identified eleven clusters (**Figure 7d**): polarized microglia (**Fig. 16b**), micro APC – CD4, APC – Lipid **Fig. 16c**), T cells (**Fig. 16d**), macrophages, NK cells (**Fig. 16e**), DCs (**Fig. 16f**), neutrophils (**Fig. 16g**), ILCs, immature myeloid cells, and B cells (**Supplemental Fig. 16h**). The full list of genes upregulated for each cluster is presented in **Table 8**. The intratumoral immune infiltrates were similar across all samples and were largely dominated by myeloid populations with minor lymphoid components (**Fig. 16**). Microglia and macrophages were present across all samples (**Fig. 14c**). Further, the dominant intratumoral immune cell populations identified by scSEQ (**Figure 7**) aligned with our IHC analysis (**Figure 2**), and they were also congruent with those reported by other human GBM studies (Chen and Hambardzumyan, 2018). Taken together, our scSEQ analysis demonstrated that both spontaneous QPP and QPP7 allograft tumors harbor immune cell populations that are similar to the infiltrates observed in human GBM.

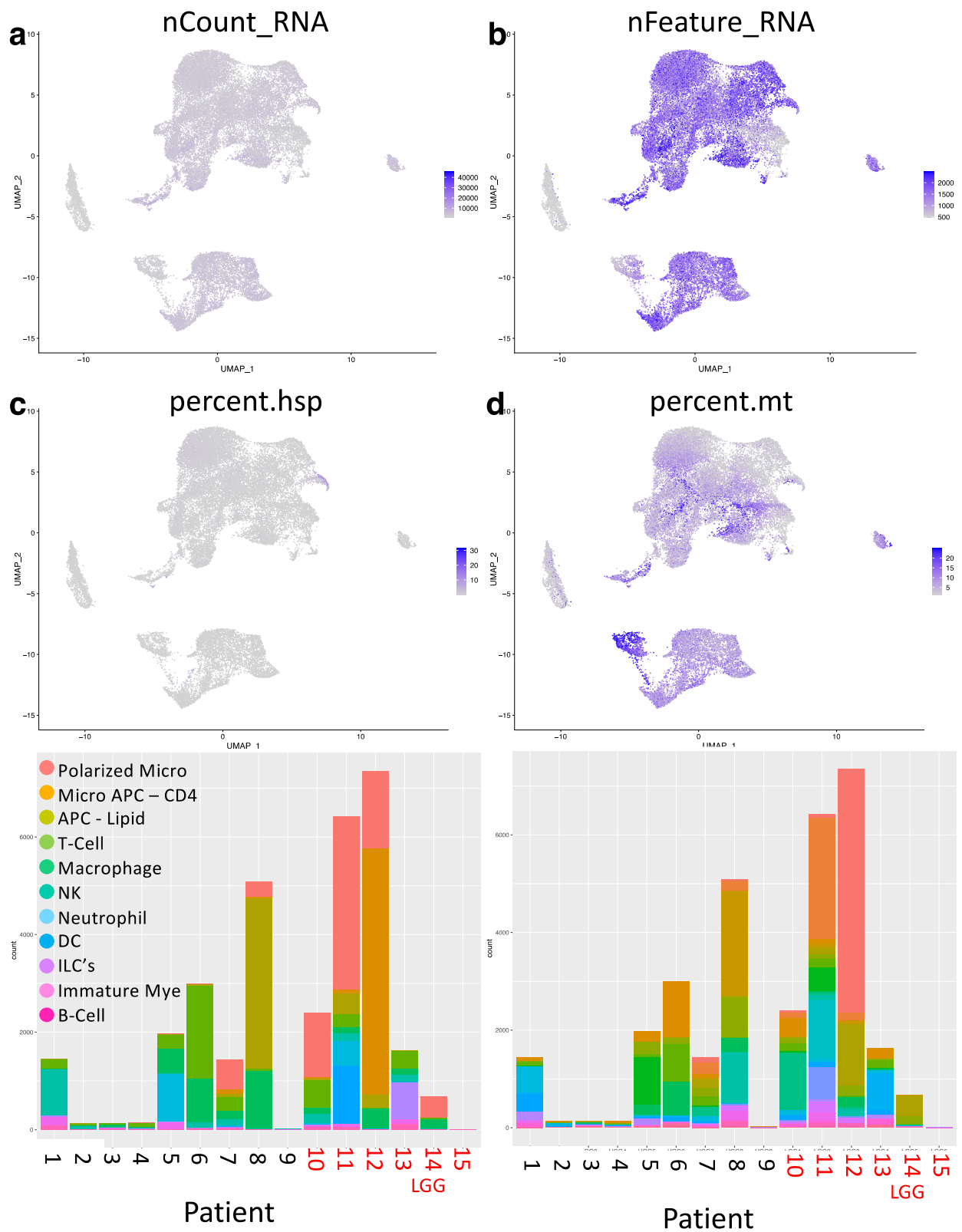


Figure 15: Quality control metrics for the glioblastoma (GBM) patient dataset. a.

Featureplot showing the counts of RNA molecules detected per cell. **b-h.** UMAPs show (b) T cell clusters identified by CD3D, CD3E, and CD3G markers, (c) neutrophil clusters identified by ITGAX, S100A8, and S100A9 markers; (d) natural killer (NK) cell clusters identified by HCST, KLRD1, and NKG7 markers; (e) antigen-presenting cell clusters identified by CD74, HLA-DRA, and HLA-DRB1 markers; (f) microglia clusters identified by CD14, MRC1, and MARCKS markers; (g) macrophage clusters identified by CD68, CX3CR1, and TMEM119 markers; and (h) B-cell clusters identified by CD79A, CD79B, and MS4A1 markers. All violin plots show the specificity of color-coded given markers.

Table 8

Human Aggregated 0.1							
	p_val	avg_logFC	pct.1	pct.2	p_val_adj	cluster	gene
CD3D	7.23E-201	0.65027434	0.518	0.008	9.13E-197	0	CD3D
IL32	5.25E-158	0.62305934	0.524	0.045	6.63E-154	0	IL32
IL7R	2.85E-154	0.79112627	0.477	0.03	3.60E-150	0	IL7R
RPS27	1.16E-142	0.74339721	0.998	0.869	1.46E-138	0	RPS27
CCL5	1.71E-132	0.8015399	0.736	0.19	2.16E-128	0	CCL5
TRAC	5.92E-121	0.37117286	0.334	0.006	7.47E-117	0	TRAC
CD3G	8.28E-116	0.3578629	0.335	0.009	1.05E-111	0	CD3G
RPS3	2.49E-113	0.6306876	0.976	0.852	3.15E-109	0	RPS3
RPS27A	2.62E-110	0.58021687	0.998	0.883	3.31E-106	0	RPS27A
RPS15A	1.24E-102	0.55561914	0.992	0.884	1.56E-98	0	RPS15A
RPS12	6.31E-102	0.58839633	0.998	0.913	7.97E-98	0	RPS12
RPL41	1.50E-94	0.47945907	0.997	0.95	1.89E-90	0	RPL41
RPL30	7.21E-93	0.53919875	0.989	0.869	9.11E-89	0	RPL30
CD2	9.05E-93	0.44050457	0.413	0.064	1.14E-88	0	CD2
B2M	2.48E-88	0.45330905	1	0.973	3.13E-84	0	B2M
RPL23A	5.98E-87	0.53821345	0.968	0.76	7.55E-83	0	RPL23A
RPS29	8.74E-82	0.55014519	0.907	0.683	1.10E-77	0	RPS29
RPS19	1.25E-78	0.46198034	0.988	0.942	1.58E-74	0	RPS19
RPS25	6.85E-78	0.49288774	0.921	0.732	8.65E-74	0	RPS25
TRBC2	1.62E-77	0.3486681	0.332	0.045	2.04E-73	0	TRBC2
CD52	1.11E-71	0.51086941	0.578	0.219	1.41E-67	0	CD52
RPS18	1.99E-69	0.40989496	0.998	0.971	2.52E-65	0	RPS18
RPL10	1.46E-68	0.43244126	0.994	0.961	1.84E-64	0	RPL10
RPL3	8.35E-65	0.44844461	0.977	0.876	1.05E-60	0	RPL3
RPS14	9.33E-65	0.41671147	0.994	0.953	1.18E-60	0	RPS14
RPL14	9.15E-61	0.43097707	0.915	0.781	1.16E-56	0	RPL14
RPL13	1.92E-58	0.34957412	1	0.991	2.43E-54	0	RPL13
RPS21	1.05E-57	0.43741868	0.864	0.673	1.33E-53	0	RPS21
GZMA	1.26E-56	0.41755518	0.534	0.19	1.59E-52	0	GZMA
GZMH	2.05E-55	0.35656597	0.433	0.131	2.59E-51	0	GZMH
RPL34	6.38E-53	0.37585497	0.992	0.931	8.06E-49	0	RPL34
RPS7	6.59E-53	0.38821788	0.945	0.798	8.33E-49	0	RPS7
HLA-A	2.53E-49	0.40373725	0.915	0.735	3.20E-45	0	HLA-A
RPL35A	3.57E-47	0.35483006	0.942	0.761	4.51E-43	0	RPL35A

RPL19	2.34E-46	0.3419281	0.974	0.919	2.95E-42	0	RPL19
RPSA	6.05E-46	0.4514565	0.817	0.654	7.64E-42	0	RPSA
RORA	2.89E-45	0.25061652	0.279	0.062	3.66E-41	0	RORA
RPL21	5.62E-45	0.40079316	0.95	0.806	7.10E-41	0	RPL21
RPS15	7.85E-42	0.328754	0.96	0.877	9.92E-38	0	RPS15
RPL32	1.05E-41	0.34271517	0.991	0.921	1.33E-37	0	RPL32
RPS28	1.99E-41	0.36309297	0.934	0.833	2.51E-37	0	RPS28
RPL10A	6.71E-40	0.36745164	0.831	0.64	8.48E-36	0	RPL10A
RPL37	1.74E-37	0.30227831	0.957	0.903	2.20E-33	0	RPL37
CALM1	6.81E-36	0.33791636	0.681	0.426	8.60E-32	0	CALM1
MT-CYB	1.93E-35	0.29737386	0.998	0.987	2.44E-31	0	MT-CYB
RPL35	7.01E-35	0.31427341	0.899	0.787	8.85E-31	0	RPL35
RPS5	1.18E-33	0.33587389	0.797	0.624	1.48E-29	0	RPS5
RPL11	1.59E-32	0.30146557	0.959	0.886	2.01E-28	0	RPL11
RPS23	5.28E-32	0.26956843	0.98	0.935	6.67E-28	0	RPS23
RPLP2	7.80E-32	0.28632293	0.945	0.879	9.85E-28	0	RPLP2
HLA-B	4.76E-30	0.27016961	0.98	0.883	6.01E-26	0	HLA-B
CD69	1.68E-29	0.26045417	0.34	0.137	2.12E-25	0	CD69
RPL18	6.34E-29	0.27232671	0.928	0.871	8.00E-25	0	RPL18
RPL7A	9.42E-29	0.27391009	0.934	0.858	1.19E-24	0	RPL7A
RPL26	1.07E-28	0.27556402	0.953	0.857	1.35E-24	0	RPL26
RPL39	1.22E-28	0.25296076	0.986	0.953	1.55E-24	0	RPL39
RPL28	2.28E-28	0.26639399	0.982	0.955	2.88E-24	0	RPL28
RPS2	2.50E-28	0.25838704	0.991	0.964	3.16E-24	0	RPS2
HLA-C	2.36E-27	0.30480015	0.692	0.498	2.99E-23	0	HLA-C
MYL12A	5.51E-27	0.30504112	0.663	0.462	6.95E-23	0	MYL12A
RPL36	8.37E-27	0.29761543	0.846	0.739	1.06E-22	0	RPL36
ZFP36L2	5.82E-25	0.30761921	0.544	0.328	7.35E-21	0	ZFP36L2
HCST	1.31E-24	0.28461049	0.544	0.339	1.66E-20	0	HCST
RPS3A	1.03E-23	0.25015791	0.977	0.903	1.30E-19	0	RPS3A
RPS4X	5.58E-23	0.26703832	0.896	0.798	7.05E-19	0	RPS4X
RPL13A	5.74E-23	0.25836138	0.909	0.829	7.25E-19	0	RPL13A
EEF1D	3.64E-22	0.25369843	0.625	0.454	4.60E-18	0	EEF1D
TXNIP	5.04E-22	0.3032635	0.652	0.421	6.37E-18	0	TXNIP
RPL36AL	1.10E-21	0.26398333	0.578	0.398	1.39E-17	0	RPL36AL
TOMM7	1.32E-21	0.26679813	0.547	0.366	1.67E-17	0	TOMM7
GNLY	1.08E-20	0.30510405	0.532	0.282	1.37E-16	0	GNLY
PTPRC	5.36E-20	0.25414227	0.712	0.566	6.77E-16	0	PTPRC
RPL38	1.84E-19	0.26016834	0.706	0.552	2.33E-15	0	RPL38
JUN	6.12E-14	0.28035073	0.547	0.398	7.73E-10	0	JUN

C1QB	3.50E-198	0.99986991	0.545	0.022	4.42E-194	1	C1QB
RGS1	1.40E-197	1.15460635	0.674	0.086	1.76E-193	1	RGS1
APOE	2.30E-195	1.93909055	0.547	0.027	2.91E-191	1	APOE
CD74	1.94E-191	1.59838759	0.885	0.334	2.45E-187	1	CD74
C3	1.61E-189	0.87715926	0.491	0.01	2.04E-185	1	C3
C1QA	2.34E-182	0.87512968	0.54	0.032	2.95E-178	1	C1QA
C1QC	3.65E-181	0.67815448	0.477	0.011	4.61E-177	1	C1QC
APOC1	4.76E-171	1.27217559	0.451	0.011	6.01E-167	1	APOC1
SPP1	4.94E-170	2.14916712	0.595	0.077	6.25E-166	1	SPP1
HLA-DRA	4.64E-146	1.32437753	0.838	0.305	5.86E-142	1	HLA-DRA
NPC2	1.54E-142	0.7390196	0.667	0.148	1.95E-138	1	NPC2
TREM2	3.06E-142	0.43142997	0.371	0.005	3.86E-138	1	TREM2
HLA-DPA1	3.79E-124	1.09354969	0.687	0.203	4.79E-120	1	HLA-DPA1
SGK1	2.52E-123	0.64495477	0.468	0.056	3.18E-119	1	SGK1
PLXDC2	1.74E-122	0.50460983	0.498	0.069	2.20E-118	1	PLXDC2
A2M	2.70E-120	0.44067859	0.322	0.006	3.41E-116	1	A2M
HLA-DQB1	4.15E-118	0.72645562	0.5	0.076	5.25E-114	1	HLA-DQB1
SLC1A3	1.51E-115	0.43485331	0.32	0.008	1.91E-111	1	SLC1A3
FCGBP	3.26E-114	0.90949732	0.326	0.011	4.12E-110	1	FCGBP
HLA-DRB5	1.02E-112	0.76518225	0.628	0.161	1.29E-108	1	HLA-DRB5
GSN	1.38E-112	0.43311489	0.426	0.047	1.74E-108	1	GSN
HLA-DRB1	3.06E-107	0.61933422	0.446	0.063	3.86E-103	1	HLA-DRB1
MARCKS	4.83E-105	0.46682619	0.446	0.063	6.10E-101	1	MARCKS
CTSB	3.37E-102	0.67212362	0.64	0.199	4.26E-98	1	CTSB
HSPA1A	2.51E-100	1.26250803	0.613	0.174	3.17E-96	1	HSPA1A
RNASET2	8.59E-94	0.52513276	0.543	0.138	1.09E-89	1	RNASET2
CLEC5A	5.31E-93	0.38576587	0.342	0.031	6.71E-89	1	CLEC5A
HTRA1	7.51E-90	0.31607763	0.259	0.008	9.49E-86	1	HTRA1
CST3	3.96E-89	0.58441478	0.696	0.242	5.00E-85	1	CST3
HSPA1B	8.14E-85	0.67219507	0.477	0.103	1.03E-80	1	HSPA1B
OGFRL1	1.45E-83	0.39036497	0.423	0.079	1.83E-79	1	OGFRL1
YWHAH	6.36E-83	0.40253899	0.403	0.07	8.03E-79	1	YWHAH
VSIG4	1.33E-80	0.2839851	0.295	0.026	1.68E-76	1	VSIG4
HLA-DPB1	2.12E-79	0.88242508	0.592	0.209	2.68E-75	1	HLA-DPB1
MSR1	1.31E-78	0.27713055	0.261	0.017	1.65E-74	1	MSR1
MEF2A	2.06E-76	0.35922108	0.392	0.073	2.60E-72	1	MEF2A
SAT1	1.73E-74	0.68046494	0.914	0.539	2.19E-70	1	SAT1
MS4A7	3.33E-73	0.4042976	0.426	0.096	4.20E-69	1	MS4A7
HLA-DQA1	4.38E-72	0.45309795	0.354	0.06	5.53E-68	1	HLA-DQA1
HSPB1	9.41E-72	0.46943282	0.3	0.038	1.19E-67	1	HSPB1

GRN	2.62E-71	0.44273475	0.552	0.179	3.31E-67	1	GRN
XIST	1.24E-69	0.50162703	0.32	0.048	1.56E-65	1	XIST
LPCAT2	1.73E-69	0.25637108	0.279	0.031	2.18E-65	1	LPCAT2
FCGR2A	4.15E-67	0.35561166	0.417	0.1	5.24E-63	1	FCGR2A
OLR1	1.29E-66	0.29081708	0.295	0.039	1.63E-62	1	OLR1
KCTD12	4.69E-63	0.34756204	0.392	0.093	5.93E-59	1	KCTD12
LAPTM5	1.10E-62	0.47893421	0.719	0.363	1.38E-58	1	LAPTM5
MEF2C	4.84E-60	0.31165113	0.381	0.09	6.11E-56	1	MEF2C
HLA-DMA	5.17E-60	0.31439336	0.387	0.094	6.53E-56	1	HLA-DMA
HSPH1	2.64E-58	0.59506773	0.344	0.077	3.33E-54	1	HSPH1
CSF1R	8.01E-58	0.27363231	0.326	0.065	1.01E-53	1	CSF1R
TGFBI	1.43E-57	0.41108446	0.351	0.081	1.81E-53	1	TGFBI
HERPUD1	1.71E-53	0.45794072	0.487	0.179	2.17E-49	1	HERPUD1
CCDC88A	1.81E-53	0.30467257	0.442	0.139	2.29E-49	1	CCDC88A
CXCL16	3.29E-53	0.25355728	0.315	0.066	4.16E-49	1	CXCL16
MS4A6A	2.82E-52	0.35853525	0.446	0.146	3.56E-48	1	MS4A6A
GLUL	3.01E-52	0.51477661	0.543	0.224	3.80E-48	1	GLUL
S100A11	1.18E-51	0.45622482	0.752	0.428	1.48E-47	1	S100A11
HLA-DMB	2.81E-51	0.2679067	0.327	0.076	3.55E-47	1	HLA-DMB
FTL	2.19E-50	0.60810711	0.966	0.887	2.76E-46	1	FTL
PSAP	7.18E-49	0.42352409	0.615	0.277	9.07E-45	1	PSAP
CD81	8.43E-49	0.38153167	0.459	0.169	1.06E-44	1	CD81
STAB1	1.42E-47	0.26334299	0.284	0.06	1.80E-43	1	STAB1
TUBA1B	6.58E-47	0.51504442	0.45	0.174	8.31E-43	1	TUBA1B
CD163	9.22E-47	0.38612935	0.381	0.121	1.17E-42	1	CD163
CAPG	1.79E-46	0.26267295	0.336	0.09	2.26E-42	1	CAPG
LIMS1	2.57E-45	0.30087871	0.426	0.147	3.25E-41	1	LIMS1
ZFP36L1	3.36E-45	0.45409254	0.549	0.25	4.25E-41	1	ZFP36L1
RGS10	5.00E-44	0.26623393	0.369	0.115	6.32E-40	1	RGS10
HMOX1	8.18E-44	0.52742677	0.306	0.078	1.03E-39	1	HMOX1
IFNGR1	2.52E-43	0.28465822	0.367	0.115	3.18E-39	1	IFNGR1
WSB1	1.22E-42	0.36771719	0.477	0.196	1.55E-38	1	WSB1
CTSZ	6.27E-42	0.26346876	0.392	0.132	7.92E-38	1	CTSZ
AIF1	6.81E-39	0.30570215	0.549	0.24	8.60E-35	1	AIF1
NEAT1	4.71E-38	0.4697748	0.962	0.868	5.94E-34	1	NEAT1
ANXA5	7.82E-38	0.25464976	0.444	0.178	9.87E-34	1	ANXA5
GNAS	8.74E-38	0.34004266	0.574	0.297	1.10E-33	1	GNAS
COTL1	1.10E-37	0.32117947	0.626	0.311	1.39E-33	1	COTL1
ATP6V1B2	8.32E-37	0.25423382	0.284	0.08	1.05E-32	1	ATP6V1B2
ACTB	8.93E-35	0.51171532	0.935	0.87	1.13E-30	1	ACTB

ALOX5AP	2.69E-34	0.40387685	0.36	0.137	3.40E-30	1	ALOX5AP
DNAJB1	1.32E-33	0.43979851	0.345	0.127	1.67E-29	1	DNAJB1
CD14	2.82E-32	0.37697912	0.504	0.23	3.57E-28	1	CD14
HSP90AA1	4.35E-32	0.88479949	0.736	0.598	5.49E-28	1	HSP90AA1
TYROBP	6.86E-30	0.28003285	0.727	0.429	8.66E-26	1	TYROBP
RAC1	7.85E-30	0.25268309	0.489	0.247	9.92E-26	1	RAC1
SLC11A1	2.13E-29	0.29081981	0.466	0.212	2.69E-25	1	SLC11A1
GAPDH	5.00E-29	0.49033615	0.795	0.598	6.32E-25	1	GAPDH
TYMP	8.17E-28	0.26690798	0.475	0.237	1.03E-23	1	TYMP
HSPD1	9.17E-28	0.30732039	0.338	0.135	1.16E-23	1	HSPD1
FCER1G	1.83E-27	0.28161607	0.613	0.345	2.31E-23	1	FCER1G
CSTB	7.28E-26	0.32733315	0.363	0.163	9.19E-22	1	CSTB
CTSD	8.30E-25	0.34729531	0.433	0.228	1.05E-20	1	CTSD
NR4A1	6.44E-22	0.25246364	0.326	0.147	8.13E-18	1	NR4A1
CD63	5.52E-21	0.30512497	0.581	0.38	6.97E-17	1	CD63
MT-ND5	2.16E-20	0.34936411	0.901	0.839	2.72E-16	1	MT-ND5
HSP90AB1	3.74E-20	0.2666212	0.568	0.355	4.73E-16	1	HSP90AB1
MT-ND4	4.24E-20	0.27235933	0.993	0.999	5.36E-16	1	MT-ND4
LGALS1	5.16E-19	0.45018057	0.565	0.394	6.52E-15	1	LGALS1
VIM	4.80E-17	0.36245039	0.736	0.594	6.06E-13	1	VIM
ENO1	5.20E-17	0.25692508	0.437	0.268	6.57E-13	1	ENO1
MALAT1	2.76E-15	0.27319826	0.996	1	3.49E-11	1	MALAT1
MT-ND3	5.13E-08	0.27117315	0.964	0.997	0.00064739	1	MT-ND3
FCN1	0	1.07066636	0.873	0.052	0	2	FCN1
NAMPT	1.82E-292	1.41223135	0.934	0.145	2.30E-288	2	NAMPT
LYZ	4.99E-280	1.69676795	0.905	0.13	6.30E-276	2	LYZ
S100A8	1.09E-279	2.34810271	0.876	0.112	1.37E-275	2	S100A8
S100A9	1.39E-269	2.53199949	0.931	0.189	1.76E-265	2	S100A9
VCAN	4.10E-258	1.48567928	0.873	0.126	5.18E-254	2	VCAN
CTSS	1.08E-245	1.1237539	0.938	0.207	1.36E-241	2	CTSS
S100A12	1.07E-239	1.18825616	0.664	0.031	1.35E-235	2	S100A12
EREG	4.63E-189	1.09674026	0.608	0.052	5.85E-185	2	EREG
TIMP1	2.42E-186	1.41933062	0.747	0.13	3.06E-182	2	TIMP1
CD55	5.21E-185	0.81094696	0.708	0.106	6.58E-181	2	CD55
FTH1	4.70E-184	1.28650095	0.994	0.824	5.94E-180	2	FTH1
CD300E	9.54E-183	0.61139531	0.498	0.017	1.20E-178	2	CD300E
MNDA	4.32E-182	0.75890916	0.697	0.099	5.46E-178	2	MNDA
CFD	3.36E-173	0.51603814	0.552	0.04	4.24E-169	2	CFD
S100A6	2.20E-169	0.96530837	0.979	0.564	2.78E-165	2	S100A6
THBS1	3.63E-167	0.99062082	0.531	0.041	4.58E-163	2	THBS1

CEBPB	2.25E-162	0.84922885	0.847	0.245	2.84E-158	2	CEBPB
C5AR1	4.03E-162	0.54491309	0.548	0.047	5.10E-158	2	C5AR1
FTL1	9.84E-162	0.97318854	1	0.879	1.24E-157	2	FTL
CFP	1.82E-152	0.41708982	0.473	0.028	2.30E-148	2	CFP
NEAT11	5.27E-151	0.9603049	1	0.859	6.66E-147	2	NEAT1
TKT	7.84E-144	0.51841958	0.608	0.094	9.90E-140	2	TKT
CSTA	5.84E-143	0.43177058	0.521	0.053	7.37E-139	2	CSTA
FOS	1.37E-140	0.94734678	0.921	0.416	1.73E-136	2	FOS
SOCS3	1.94E-140	0.61794591	0.587	0.084	2.45E-136	2	SOCS3
PLBD1	2.85E-139	0.46321922	0.461	0.035	3.60E-135	2	PLBD1
SAT11	3.13E-137	0.91230251	0.986	0.526	3.96E-133	2	SAT1
DUSP1	2.67E-136	0.82611424	0.917	0.437	3.37E-132	2	DUSP1
PLAUR	3.26E-135	0.87790084	0.651	0.132	4.11E-131	2	PLAUR
FPR1	7.85E-135	0.44527841	0.51	0.057	9.91E-131	2	FPR1
MXD1	4.74E-130	0.48117004	0.506	0.059	5.99E-126	2	MXD1
SOD2	1.33E-128	0.55642887	0.562	0.085	1.69E-124	2	SOD2
MCL1	1.70E-125	0.70576081	0.807	0.279	2.15E-121	2	MCL1
CD141	2.95E-124	0.66928044	0.716	0.172	3.72E-120	2	CD14
SRGN	4.83E-124	0.96433499	0.952	0.652	6.11E-120	2	SRGN
SLC2A3	1.88E-123	0.80237337	0.755	0.241	2.37E-119	2	SLC2A3
AIF11	7.60E-123	0.6113731	0.739	0.19	9.59E-119	2	AIF1
ACSL1	8.97E-119	0.43114187	0.469	0.056	1.13E-114	2	ACSL1
COTL11	2.13E-115	0.59143292	0.811	0.263	2.69E-111	2	COTL1
GCA	8.09E-110	0.35099092	0.415	0.043	1.02E-105	2	GCA
CD36	1.64E-109	0.33584898	0.336	0.017	2.07E-105	2	CD36
SLC11A11	9.49E-108	0.52998597	0.654	0.161	1.20E-103	2	SLC11A1
NCF2	1.62E-106	0.3864783	0.471	0.068	2.04E-102	2	NCF2
MPEG1	3.84E-106	0.35565334	0.419	0.047	4.85E-102	2	MPEG1
CLEC12A	6.25E-106	0.33576871	0.375	0.032	7.89E-102	2	CLEC12A
KLF4	1.91E-102	0.34888622	0.413	0.048	2.42E-98	2	KLF4
FGL2	1.63E-101	0.47490467	0.527	0.101	2.06E-97	2	FGL2
VIM1	1.73E-101	0.69265388	0.932	0.538	2.19E-97	2	VIM
APLP2	2.60E-100	0.44610717	0.606	0.149	3.29E-96	2	APLP2
ATP2B1- AS1	1.49E-99	0.338058	0.402	0.047	1.88E-95	2	ATP2B1- AS1
APOBEC3A	2.50E-99	0.32662349	0.263	0.004	3.16E-95	2	APOBEC3A
CD44	4.42E-98	0.58394789	0.651	0.196	5.59E-94	2	CD44
VMP1	9.03E-98	0.58163099	0.676	0.208	1.14E-93	2	VMP1
TALDO1	2.47E-97	0.39947414	0.506	0.099	3.12E-93	2	TALDO1
TSPO	1.62E-96	0.54166649	0.701	0.239	2.04E-92	2	TSPO

ATP2B1	8.25E-95	0.58030792	0.537	0.126	1.04E-90	2	ATP2B1
PSAP1	4.84E-94	0.49265742	0.747	0.245	6.11E-90	2	PSAP
SERPINB1	4.18E-93	0.51995064	0.579	0.153	5.28E-89	2	SERPINB1
CST31	2.28E-92	0.47968706	0.761	0.233	2.87E-88	2	CST3
TNFAIP2	5.25E-92	0.30475047	0.355	0.036	6.63E-88	2	TNFAIP2
LST1	2.53E-88	0.4910249	0.498	0.109	3.19E-84	2	LST1
LILRB2	4.01E-88	0.31410615	0.336	0.034	5.07E-84	2	LILRB2
TYMP1	3.94E-86	0.4304885	0.647	0.19	4.98E-82	2	TYMP
TNFRSF1B	3.99E-86	0.42850007	0.577	0.156	5.03E-82	2	TNFRSF1B
IRAK3	9.46E-86	0.30757894	0.398	0.06	1.19E-81	2	IRAK3
MAFB	1.46E-85	0.47322955	0.51	0.116	1.84E-81	2	MAFB
THBD	1.12E-84	0.47708474	0.376	0.054	1.42E-80	2	THBD
AC020656.1	1.18E-84	0.25931736	0.276	0.017	1.50E-80	2	AC020656.1
SLC43A2	7.27E-84	0.34629557	0.4	0.063	9.18E-80	2	SLC43A2
BRI3	9.27E-84	0.40456727	0.579	0.161	1.17E-79	2	BRI3
SMIM25	2.11E-83	0.30080065	0.293	0.023	2.67E-79	2	SMIM25
CES1	2.88E-83	0.28622746	0.297	0.024	3.64E-79	2	CES1
MYD88	1.17E-81	0.27600752	0.359	0.048	1.48E-77	2	MYD88
BCL2A1	1.24E-81	0.35574087	0.431	0.079	1.57E-77	2	BCL2A1
OAZ1	3.13E-81	0.49645297	0.88	0.494	3.95E-77	2	OAZ1
IL1R2	3.60E-81	0.28249189	0.261	0.014	4.55E-77	2	IL1R2
ATP13A3	1.70E-80	0.42890508	0.463	0.099	2.15E-76	2	ATP13A3
GK	1.87E-80	0.37278131	0.411	0.071	2.36E-76	2	GK
ITGAX	2.13E-80	0.4302464	0.456	0.096	2.70E-76	2	ITGAX
PPIF	2.83E-79	0.42130769	0.359	0.052	3.58E-75	2	PPIF
S100A4	9.83E-79	0.55821594	0.958	0.665	1.24E-74	2	S100A4
PECAM1	1.44E-76	0.27759744	0.328	0.042	1.81E-72	2	PECAM1
TFRC	2.77E-76	0.43377136	0.33	0.044	3.50E-72	2	TFRC
BLVRB	3.93E-76	0.28023157	0.347	0.049	4.96E-72	2	BLVRB
IL1B	6.21E-76	0.60690064	0.427	0.084	7.85E-72	2	IL1B
HBEGF	2.07E-75	0.32289025	0.392	0.068	2.61E-71	2	HBEGF
CYBB	3.71E-74	0.34719826	0.498	0.124	4.68E-70	2	CYBB
EVI2B	1.82E-73	0.37187264	0.517	0.141	2.30E-69	2	EVI2B
CPVL	3.36E-71	0.28686096	0.353	0.057	4.24E-67	2	CPVL
ANPEP	3.51E-71	0.30380218	0.259	0.022	4.44E-67	2	ANPEP
S100A10	1.23E-70	0.49628626	0.795	0.371	1.55E-66	2	S100A10
CEBPD	1.01E-69	0.45347843	0.61	0.209	1.28E-65	2	CEBPD
NLRP3	9.93E-69	0.28651819	0.28	0.031	1.25E-64	2	NLRP3
LTA4H	2.56E-67	0.28876191	0.355	0.064	3.24E-63	2	LTA4H
CSF3R	1.87E-66	0.2731056	0.363	0.067	2.36E-62	2	CSF3R

CLEC7A	2.59E-66	0.32032387	0.458	0.116	3.27E-62	2	CLEC7A
RETN	4.18E-66	0.25973993	0.259	0.026	5.28E-62	2	RETN
GPCPD1	5.64E-66	0.31583261	0.398	0.086	7.12E-62	2	GPCPD1
LGALS11	7.21E-66	0.35716452	0.79	0.331	9.11E-62	2	LGALS1
CD93	1.53E-65	0.30224274	0.365	0.069	1.94E-61	2	CD93
METTL9	2.74E-65	0.29662318	0.403	0.09	3.46E-61	2	METTL9
ETS2	4.29E-64	0.2784504	0.39	0.083	5.42E-60	2	ETS2
AP1S2	1.76E-63	0.3076152	0.425	0.102	2.22E-59	2	AP1S2
H3F3A	5.96E-63	0.4332578	0.938	0.707	7.53E-59	2	H3F3A
RGS2	2.20E-62	0.48424936	0.479	0.143	2.77E-58	2	RGS2
DUSP6	1.09E-61	0.35101273	0.369	0.079	1.38E-57	2	DUSP6
GLIPR1	1.15E-61	0.3575445	0.523	0.172	1.45E-57	2	GLIPR1
RILPL2	1.81E-61	0.27515082	0.363	0.075	2.28E-57	2	RILPL2
SERPINA1	3.89E-61	0.26949852	0.347	0.068	4.92E-57	2	SERPINA1
PABPC1	1.17E-60	0.41118386	0.83	0.462	1.48E-56	2	PABPC1
TYROBP1	3.30E-60	0.42078985	0.819	0.408	4.17E-56	2	TYROBP
ANXA2	5.86E-60	0.34638381	0.548	0.186	7.40E-56	2	ANXA2
ANXA1	9.78E-59	0.45248092	0.674	0.311	1.23E-54	2	ANXA1
RNF130	2.54E-58	0.26169229	0.376	0.086	3.20E-54	2	RNF130
YBX3	3.71E-58	0.30508995	0.407	0.104	4.69E-54	2	YBX3
ASAH1	2.75E-57	0.31405152	0.506	0.161	3.48E-53	2	ASAH1
FCGRT	8.37E-57	0.30963157	0.463	0.138	1.06E-52	2	FCGRT
S100A11	1.17E-56	0.39570836	0.822	0.414	1.48E-52	2	S100A11
ARL4A	1.19E-56	0.2577974	0.29	0.049	1.50E-52	2	ARL4A
SPI1	2.02E-56	0.27049654	0.398	0.1	2.55E-52	2	SPI1
SAMSN1	6.01E-56	0.35273055	0.485	0.158	7.59E-52	2	SAMSN1
TLR2	1.38E-55	0.25453689	0.324	0.065	1.74E-51	2	TLR2
ZEB2	6.95E-55	0.42502015	0.653	0.289	8.78E-51	2	ZEB2
FGR	1.59E-53	0.26401124	0.365	0.089	2.01E-49	2	FGR
IVNS1ABP	4.11E-53	0.31823528	0.413	0.117	5.19E-49	2	IVNS1ABP
CXCL8	5.26E-53	0.52457489	0.29	0.051	6.65E-49	2	CXCL8
LGALS3	6.60E-53	0.26100651	0.392	0.102	8.34E-49	2	LGALS3
MAT2A	9.98E-53	0.370633	0.429	0.129	1.26E-48	2	MAT2A
FOSL2	1.50E-52	0.31401259	0.448	0.138	1.90E-48	2	FOSL2
ZFP36	2.01E-52	0.35984027	0.67	0.296	2.54E-48	2	ZFP36
KDM6B	3.48E-52	0.28201676	0.369	0.092	4.40E-48	2	KDM6B
GLUL1	7.61E-52	0.35530429	0.585	0.218	9.61E-48	2	GLUL
SDCBP	5.39E-51	0.31010609	0.469	0.156	6.81E-47	2	SDCBP
MAP3K8	1.97E-50	0.3274125	0.382	0.106	2.49E-46	2	MAP3K8
ACTB1	7.88E-50	0.32464683	0.99	0.855	9.95E-46	2	ACTB

HIF1A	1.17E-49	0.34376027	0.434	0.137	1.48E-45	2	HIF1A
PTPRE	4.43E-49	0.28037445	0.442	0.142	5.59E-45	2	PTPRE
RNF149	3.80E-48	0.2819063	0.45	0.149	4.80E-44	2	RNF149
MIDN	8.53E-48	0.30420587	0.475	0.166	1.08E-43	2	MIDN
CTNNB1	4.08E-47	0.26769064	0.351	0.093	5.15E-43	2	CTNNB1
CHD1	7.17E-47	0.28654185	0.425	0.138	9.06E-43	2	CHD1
MS4A6A1	9.02E-47	0.25243869	0.459	0.149	1.14E-42	2	MS4A6A
SLC25A37	1.80E-45	0.26157141	0.376	0.107	2.27E-41	2	SLC25A37
GRN1	4.50E-45	0.26817531	0.527	0.195	5.68E-41	2	GRN
VAPA	7.74E-45	0.28510901	0.442	0.155	9.77E-41	2	VAPA
MT-ND1	4.51E-44	0.3024284	0.994	0.987	5.70E-40	2	MT-ND1
IFITM3	2.58E-43	0.27422555	0.257	0.052	3.26E-39	2	IFITM3
JUNB	5.04E-43	0.37290592	0.707	0.364	6.37E-39	2	JUNB
SLC25A6	2.55E-42	0.2908818	0.5	0.206	3.22E-38	2	SLC25A6
FLNA	3.36E-41	0.27787998	0.492	0.195	4.24E-37	2	FLNA
GSTO1	3.71E-41	0.28058945	0.411	0.145	4.69E-37	2	GSTO1
SERP1	3.51E-40	0.26759909	0.539	0.234	4.44E-36	2	SERP1
FCER1G1	9.29E-40	0.31515472	0.68	0.331	1.17E-35	2	FCER1G
NABP1	2.65E-38	0.25953801	0.34	0.105	3.35E-34	2	NABP1
ZFAND5	2.81E-38	0.25843981	0.39	0.136	3.55E-34	2	ZFAND5
GSTP1	4.63E-38	0.27310792	0.554	0.249	5.85E-34	2	GSTP1
GAPDH1	1.45E-37	0.28961577	0.849	0.586	1.83E-33	2	GAPDH
VEGFA	2.55E-35	0.2698626	0.297	0.086	3.22E-31	2	VEGFA
NFKBIA	7.61E-35	0.37890001	0.625	0.329	9.61E-31	2	NFKBIA
CCNL1	1.23E-34	0.29518638	0.577	0.296	1.56E-30	2	CCNL1
GADD45B	5.70E-34	0.29875706	0.413	0.164	7.20E-30	2	GADD45B
FOSB	3.72E-33	0.31761445	0.519	0.246	4.70E-29	2	FOSB
AREG	3.20E-31	0.41817951	0.49	0.229	4.04E-27	2	AREG
RPL7	1.24E-30	0.28133029	0.869	0.619	1.57E-26	2	RPL7
EMP3	1.69E-30	0.26120498	0.593	0.319	2.13E-26	2	EMP3
ATP1B3	2.02E-30	0.30662969	0.373	0.151	2.55E-26	2	ATP1B3
ACTG1	8.45E-25	0.28785232	0.871	0.719	1.07E-20	2	ACTG1
NKG7	1.06E-198	1.19590292	0.944	0.261	1.34E-194	3	NKG7
GNLY1	5.25E-192	1.29070575	0.912	0.21	6.64E-188	3	GNLY
GZMB	4.06E-171	0.92530111	0.666	0.093	5.13E-167	3	GZMB
SPON2	4.71E-165	0.65885181	0.537	0.041	5.95E-161	3	SPON2
FGFBP2	1.18E-157	0.69931177	0.601	0.071	1.49E-153	3	FGFBP2
PRF1	2.10E-140	0.71878931	0.666	0.125	2.65E-136	3	PRF1
CD247	2.38E-129	0.61750828	0.599	0.102	3.00E-125	3	CD247
KLRF1	1.36E-121	0.44605019	0.392	0.025	1.72E-117	3	KLRF1

CST7	2.81E-120	0.67171302	0.651	0.148	3.55E-116	3	CST7
KLRD1	5.62E-120	0.659764	0.629	0.123	7.10E-116	3	KLRD1
PTGDS	6.71E-117	0.78154766	0.358	0.019	8.48E-113	3	PTGDS
KLRB1	7.04E-94	0.55174532	0.584	0.134	8.89E-90	3	KLRB1
CD7	3.75E-76	0.41633311	0.433	0.085	4.73E-72	3	CD7
CCL4	9.35E-73	1.48685636	0.595	0.208	1.18E-68	3	CCL4
GZMA1	8.50E-70	0.50460088	0.621	0.204	1.07E-65	3	GZMA
CLIC3	6.89E-69	0.360563	0.312	0.042	8.70E-65	3	CLIC3
CTSW	2.09E-65	0.33897988	0.351	0.062	2.65E-61	3	CTSW
ARL4C	7.23E-65	0.55596717	0.61	0.237	9.13E-61	3	ARL4C
B2M1	9.58E-64	0.44090655	1	0.976	1.21E-59	3	B2M
CMC1	1.70E-58	0.37023623	0.375	0.085	2.15E-54	3	CMC1
HOPX	5.22E-58	0.39065662	0.414	0.106	6.60E-54	3	HOPX
PLAC8	4.79E-51	0.38781167	0.453	0.148	6.05E-47	3	PLAC8
GZMM	3.41E-41	0.33432215	0.366	0.114	4.30E-37	3	GZMM
HLA-B1	2.23E-40	0.36141649	0.981	0.893	2.82E-36	3	HLA-B
HLA-A1	4.29E-39	0.34636514	0.914	0.755	5.42E-35	3	HLA-A
HLA-E	7.69E-39	0.42717828	0.741	0.501	9.71E-35	3	HLA-E
CCL3	2.39E-38	0.87551698	0.373	0.126	3.02E-34	3	CCL3
CCL51	3.92E-37	0.41185883	0.614	0.281	4.95E-33	3	CCL5
ABHD17A	4.53E-37	0.31369558	0.409	0.153	5.72E-33	3	ABHD17A
GZMH1	3.33E-31	0.29333917	0.418	0.167	4.20E-27	3	GZMH
IER2	2.01E-30	0.41391348	0.608	0.367	2.54E-26	3	IER2
CALM11	6.54E-29	0.40175048	0.666	0.457	8.27E-25	3	CALM1
HLA-C1	6.03E-28	0.41999928	0.69	0.519	7.62E-24	3	HLA-C
MYL12A1	8.93E-27	0.37404888	0.67	0.482	1.13E-22	3	MYL12A
UBB	6.39E-26	0.33466439	0.547	0.324	8.07E-22	3	UBB
HCST1	9.97E-22	0.29861896	0.575	0.353	1.26E-17	3	HCST
JAK1	4.37E-21	0.27184847	0.394	0.204	5.52E-17	3	JAK1
BTG1	6.24E-20	0.29842221	0.838	0.704	7.88E-16	3	BTG1
IRF1	4.34E-18	0.25371506	0.377	0.196	5.49E-14	3	IRF1
EFHD2	2.83E-14	0.27871619	0.405	0.258	3.57E-10	3	EFHD2
ID2	9.49E-14	0.25501452	0.511	0.34	1.20E-09	3	ID2
IFITM2	1.70E-13	0.25768245	0.397	0.248	2.15E-09	3	IFITM2
ARPC2	2.00E-11	0.25811266	0.56	0.46	2.53E-07	3	ARPC2
IGKC	5.72E-261	1.40415088	0.604	0.002	7.23E-257	4	IGKC
IGHM	5.96E-193	0.95605061	0.415	0	7.53E-189	4	IGHM
CD79A	1.02E-184	0.43551617	0.415	0.001	1.29E-180	4	CD79A
MS4A1	2.51E-183	0.64967975	0.528	0.005	3.17E-179	4	MS4A1
BANK1	5.47E-154	0.44400116	0.453	0.005	6.91E-150	4	BANK1

SPIB	4.28E-94	0.27592698	0.264	0.002	5.40E-90	4	SPIB
RALGPS2	5.63E-67	0.37463608	0.34	0.011	7.12E-63	4	RALGPS2
BCL11A	2.25E-55	0.33361519	0.321	0.013	2.85E-51	4	BCL11A
CD79B	4.59E-51	0.50386956	0.396	0.025	5.80E-47	4	CD79B
LTB	2.89E-30	0.55531211	0.547	0.084	3.65E-26	4	LTB
RPL18A	8.91E-20	0.85611211	0.962	0.903	1.13E-15	4	RPL18A
RPS271	2.59E-19	0.79086187	0.981	0.905	3.27E-15	4	RPS27
CD37	4.48E-19	0.75943176	0.66	0.216	5.66E-15	4	CD37
RPL211	2.27E-18	0.7416658	0.962	0.845	2.87E-14	4	RPL21
HLA-DRA1	1.25E-17	0.69298393	0.943	0.424	1.58E-13	4	HLA-DRA
RPS8	8.34E-17	0.68955362	0.981	0.902	1.05E-12	4	RPS8
RPS121	9.63E-17	0.66065732	0.962	0.937	1.22E-12	4	RPS12
RPS231	1.50E-16	0.61578485	0.943	0.948	1.89E-12	4	RPS23
RPL131	2.67E-15	0.57157263	0.981	0.994	3.38E-11	4	RPL13
RPS181	4.97E-15	0.63693083	0.981	0.979	6.27E-11	4	RPS18
CD521	8.54E-15	0.5596182	0.774	0.313	1.08E-10	4	CD52
RPL23A1	1.14E-14	0.63409375	0.943	0.818	1.44E-10	4	RPL23A
HLA-DPB11	5.90E-14	0.52174896	0.755	0.293	7.45E-10	4	HLA-DPB1
RPL111	7.97E-14	0.60784486	0.981	0.905	1.01E-09	4	RPL11
RPL191	1.14E-13	0.5918168	0.981	0.934	1.45E-09	4	RPL19
RPS20	4.31E-13	0.60626145	0.906	0.612	5.44E-09	4	RPS20
RPL411	5.72E-13	0.46406293	0.962	0.964	7.23E-09	4	RPL41
RPS51	5.75E-13	0.67386137	0.943	0.668	7.26E-09	4	RPS5
RPS11	1.35E-12	0.59071341	0.925	0.812	1.71E-08	4	RPS11
RPL371	2.34E-12	0.51577661	0.962	0.918	2.95E-08	4	RPL37
RPSA1	2.82E-12	0.5630805	0.943	0.696	3.56E-08	4	RPSA
RPS191	3.80E-12	0.53599444	0.962	0.955	4.80E-08	4	RPS19
RPL341	4.83E-12	0.46019346	0.962	0.948	6.10E-08	4	RPL34
RPS16	5.45E-12	0.56382803	0.943	0.865	6.88E-08	4	RPS16
CD741	5.67E-12	0.46763381	0.887	0.46	7.17E-08	4	CD74
RPS211	6.52E-12	0.57011188	0.925	0.724	8.24E-08	4	RPS21
EEF1B2	8.57E-12	0.57323314	0.906	0.574	1.08E-07	4	EEF1B2
RPS4X1	1.08E-11	0.47019669	0.962	0.824	1.37E-07	4	RPS4X
RPL321	2.92E-11	0.51260625	0.981	0.94	3.68E-07	4	RPL32
RPL9	3.22E-11	0.50601748	0.925	0.912	4.07E-07	4	RPL9
RPL33	3.46E-11	0.46871492	0.962	0.904	4.37E-07	4	RPL3
RPL35A1	3.48E-11	0.49833183	0.925	0.811	4.39E-07	4	RPL35A
RPS3A1	3.79E-11	0.52612203	0.962	0.924	4.79E-07	4	RPS3A
RPL7A1	3.88E-11	0.43608445	0.981	0.878	4.90E-07	4	RPL7A
EEF1A1	4.71E-11	0.43058635	1	0.989	5.95E-07	4	EEF1A1

RPL13A1	4.95E-11	0.58730153	0.962	0.85	6.25E-07	4	RPL13A
HLA-DQA11	5.05E-11	0.3637108	0.434	0.126	6.38E-07	4	HLA-DQA1
RPL12	1.10E-10	0.49076068	0.943	0.857	1.39E-06	4	RPL12
TCF4	1.16E-10	0.48365912	0.283	0.062	1.46E-06	4	TCF4
RPS281	1.72E-10	0.52332423	0.962	0.861	2.18E-06	4	RPS28
RPL351	2.10E-10	0.52205273	0.943	0.817	2.66E-06	4	RPL35
RPL8	2.74E-10	0.50372149	0.925	0.827	3.47E-06	4	RPL8
RPL301	3.55E-10	0.52211053	0.962	0.902	4.48E-06	4	RPL30
RPLP1	4.25E-10	0.43940152	0.981	0.988	5.37E-06	4	RPLP1
RPL5	5.01E-10	0.57605106	0.906	0.724	6.33E-06	4	RPL5
RPL181	5.55E-10	0.47390595	0.943	0.886	7.02E-06	4	RPL18
RPL391	6.77E-10	0.45919983	0.962	0.963	8.55E-06	4	RPL39
RPS6	8.13E-10	0.48848886	0.943	0.877	1.03E-05	4	RPS6
HLA-DQB11	1.03E-09	0.31968478	0.509	0.173	1.30E-05	4	HLA-DQB1
RPS27A1	1.09E-09	0.4639377	0.981	0.915	1.37E-05	4	RPS27A
RPS151	3.09E-09	0.39969814	0.962	0.9	3.90E-05	4	RPS15
RPS22	3.12E-09	0.41707334	0.981	0.971	3.94E-05	4	RPS2
RPS291	3.94E-09	0.52943894	0.925	0.744	4.98E-05	4	RPS29
RPS13	6.12E-09	0.43621629	0.962	0.843	7.73E-05	4	RPS13
RPLP21	1.62E-08	0.47580692	0.943	0.897	0.00020443	4	RPLP2
RPS71	1.63E-08	0.4144666	0.962	0.838	0.00020534	4	RPS7
RPS251	3.76E-08	0.40615279	0.925	0.784	0.00047524	4	RPS25
NOP53	4.41E-08	0.43036038	0.566	0.284	0.00055741	4	NOP53
RPS10	4.86E-08	0.51218262	0.717	0.439	0.00061365	4	RPS10
RPS9	5.17E-08	0.38587749	0.962	0.84	0.00065326	4	RPS9
RPL27	6.94E-08	0.37841154	0.906	0.65	0.00087655	4	RPL27
RPL29	8.76E-08	0.46881807	0.962	0.877	0.00110705	4	RPL29
RPL23	1.24E-07	0.4199305	0.887	0.614	0.00156955	4	RPL23
RPL10A1	1.80E-07	0.43942822	0.906	0.691	0.00227561	4	RPL10A
RPL37A	2.02E-07	0.42814967	0.925	0.862	0.00255264	4	RPL37A
PRDM2	2.13E-07	0.25828751	0.283	0.085	0.00268875	4	PRDM2
RPS15A1	2.30E-07	0.37474522	0.962	0.914	0.00290863	4	RPS15A
HLA-DPA11	2.32E-07	0.25045842	0.679	0.314	0.00293451	4	HLA-DPA1
RPL101	3.55E-07	0.37003566	1	0.97	0.004489	4	RPL10
RPLP0	4.01E-07	0.43347425	0.811	0.623	0.00506024	4	RPLP0
RPL15	6.06E-07	0.36672824	0.962	0.874	0.00765844	4	RPL15
RPS31	1.29E-06	0.35895276	0.962	0.886	0.01625313	4	RPS3
FAU	2.14E-06	0.35699112	0.962	0.89	0.02707248	4	FAU
RPL361	3.97E-06	0.43589777	0.887	0.768	0.05017614	4	RPL36
RPL6	6.29E-06	0.3252139	0.906	0.829	0.07939476	4	RPL6

RPL27A	1.84E-05	0.33871989	0.849	0.788	0.23288281	4	RPL27A
EEF1D1	2.16E-05	0.30470671	0.755	0.498	0.27310884	4	EEF1D
RPL281	6.55E-05	0.26069788	1	0.962	0.82695377	4	RPL28
RPS141	6.61E-05	0.2957851	0.962	0.965	0.83460765	4	RPS14
RPL22	9.03E-05	0.40137737	0.83	0.691	1	4	RPL22
KLF2	0.00015377	0.30968741	0.491	0.273	1	4	KLF2
RPL261	0.00019635	0.27057698	0.943	0.883	1	4	RPL26
RPL4	0.00021209	0.30328726	0.792	0.585	1	4	RPL4
RPL381	0.00031392	0.2561704	0.868	0.591	1	4	RPL38
TXNIP1	0.00173717	0.28740202	0.679	0.484	1	4	TXNIP
RPL31	0.00372821	0.25970862	0.566	0.423	1	4	RPL31

We next compared the immune infiltrate of our spontaneous and implanted QPP models to human high- and low- grade glioma (HGG and LGG, respectively). Our 15-sample human tumor cohort included nine histopathologically diagnosed HGG tumor samples and six LGG tumors samples (two grade II oligodendroglioma and four grade II diffuse astrocytoma; **Table 3**). When comparing the main immune constituents of LGG and HGG tumors, we observed a shift from a more microglial signature to a more macrophage like signature respectively. Similar to the mouse allograft tumors, higher grade human tumors were characterized by an increase in the number of lymphoid infiltrates as well as an increase in infiltrating neutrophils compared to the spontaneous mouse tumors or human LGG tumors, respectively (**Figure 16**). Even though these differences warrant further investigation, none of these differences impact the overall conclusion that the QPP mouse and allograft tumors represent improved preclinical models to study GBM.

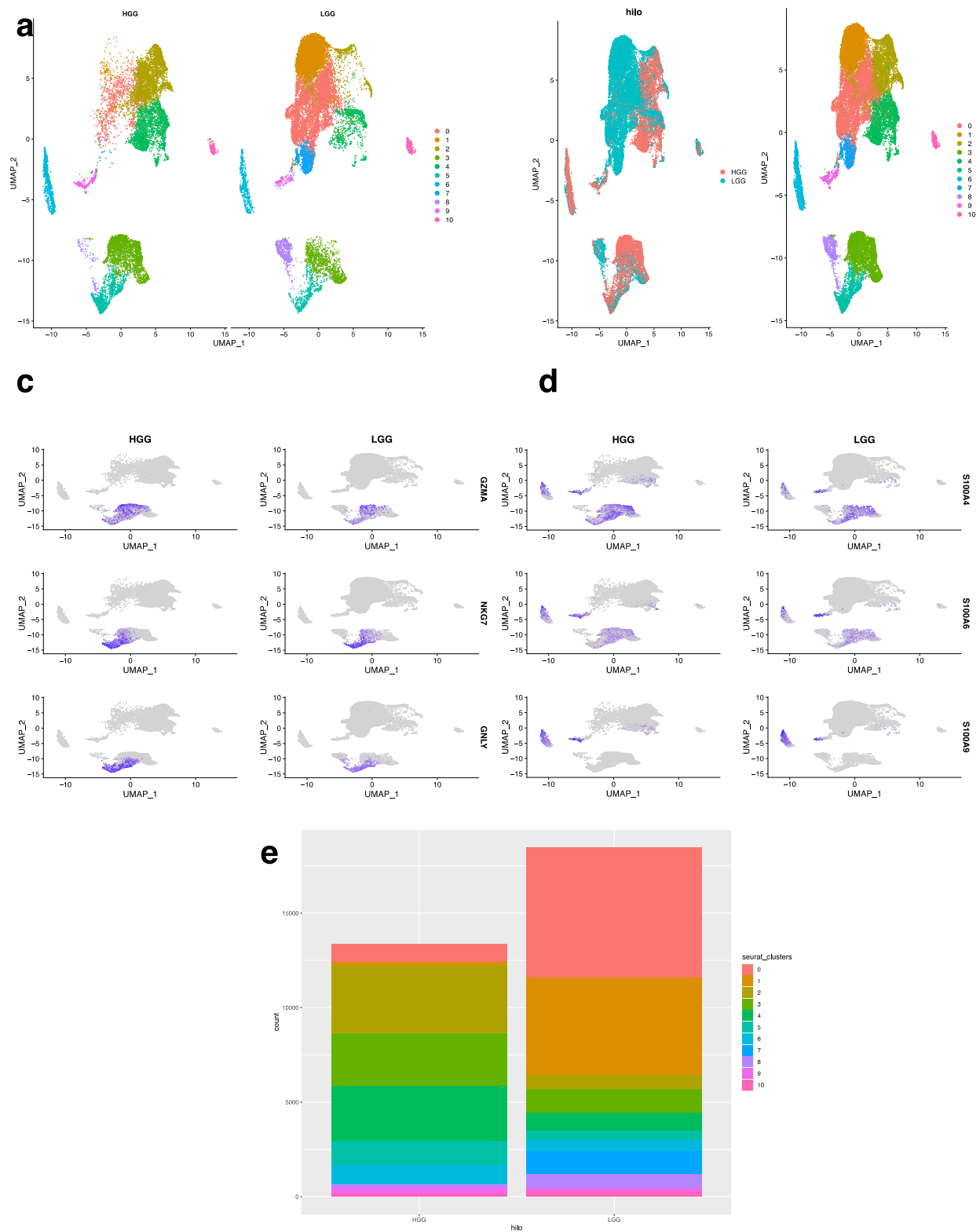


Figure 16: Comparison of human GBM and human low-grade glioma (LGG)

immune constituents. **a.** UMAPs show aggregate of CD45+ immune infiltrates from n=9 GBM patients at surgical resection compared to n=6 LGG patients at the same time point. **b.** UMAPs show the immune constituents GBM and LGG patients are overlaid to better display the similarities and differences between the groups. **c.** UMAPs identifying lymphoid clusters in samples from GBM (high-grade glioma; HGG) and LGG patients. **d.** UMAPs identifying myeloid clusters in samples from GBM (high-grade glioma; HGG) and LGG patients. **e.** Bar plot of the number of cells per cluster in samples from GBM (HGG) or LGG patients.

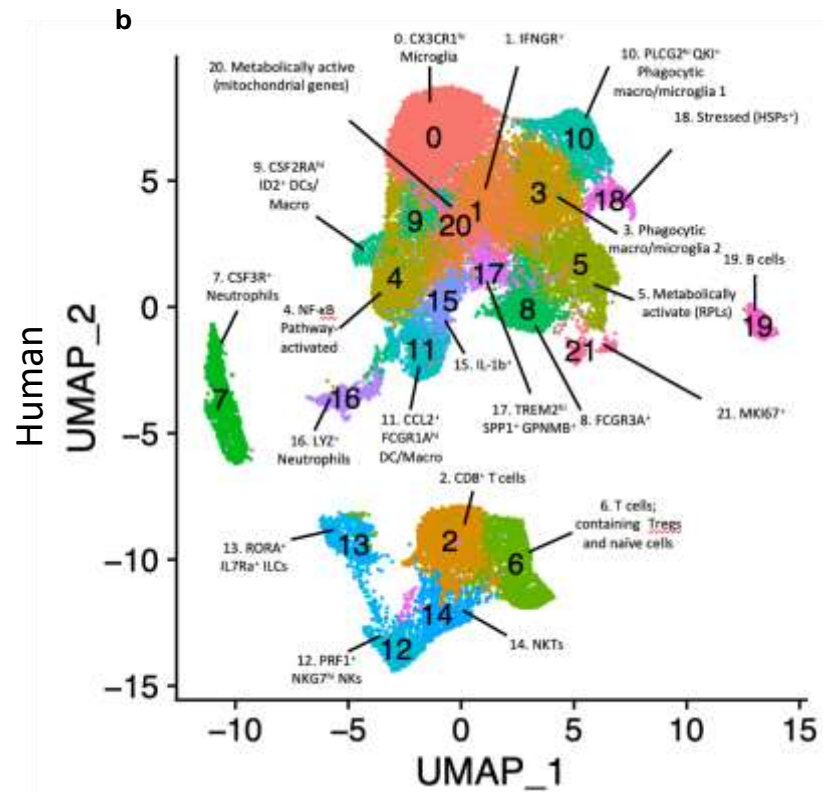
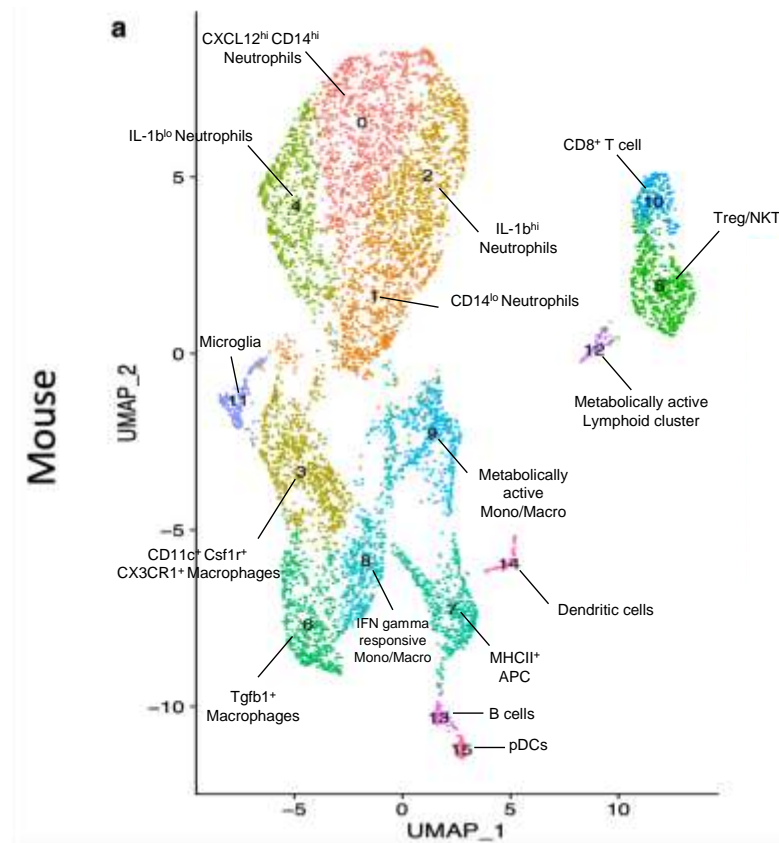


Figure 17: Clustering to reveal subtypes. Resolution (0.65;0.8) **a.** Combined mouse spontaneous and implanted QPP tumor dataset with 9 PC's determined by elbowplot. **b.** Aggregated human GBM dataset with 20 PC's determined by elbowplot.

We next performed subtype clustering to determine the minor immune constituents [resolution = 0.65] and to identify subpopulations among the major immune cell clusters (**Fig. 17a, b**) in mouse and human tumors. In our combined mouse tumor dataset, we found populations of Cxcl12^{hi}Cd14^{hi} neutrophils, Cd14^{lo} neutrophils, Il1-b^{hi} neutrophils, Cd11c⁺Csf1r⁺Cx3cr1⁺ macrophages, Il-1b^{lo} neutrophils, Treg/NKT, Tgfb1⁺ macrophages, MHCII⁺ APCs, Ifn gamma-responsive monocytes/macrophages, metabolically active monocytes/macrophages, Cd8⁺ T cells, microglia, metabolically active lymphoid, B cells, dendritic cells, and pDCs. In the human glioma samples, we found populations of CX3CR1^{hi} microglia, IFNGR⁺ microglia, CD8⁺ T cells, phagocytic microglia/macrophages, NF-kB pathway-activated myeloid cells, protein-producing myeloid cells, Tregs, naïve T cells, CSF3R⁺ neutrophils, FCGR3A⁺ myeloid cells, CSF2RA^{hi} ID2⁺ DCs/macrophages, PLCG2^{hi} QKI⁺ phagocytic microglia/macrophages, CCL2⁺ FCGR1A^{hi} DCs/macrophages, PRF1⁺ NKG7^{hi} NK-cells, RORA⁺ IL7Ra⁺ ILCs, NKTs, IL1b⁺ myeloid cells, LYZ⁺ neutrophils, TREM2^{hi} SPP1⁺ GPNMB⁺ myeloid cells, stressed (HSP⁺) B cells, metabolically active myeloid cells, and proliferating myeloid cells. The full lists of genes upregulated for each cluster is presented in **Table 9 (mice)** and **Table 10 (human)**.

Table 9

Mouse Aggregated 0.65 Resolution							
	p_val	avg_logFC	pct.1	pct.2	p_val_adj	cluster	gene
S100a9	0	1.66170392	0.987	0.377	0	0	S100a9
Cxcl2	0	1.56643525	0.769	0.152	0	0	Cxcl2
S100a8	0	1.55123637	0.989	0.411	0	0	S100a8
Srgn	0	1.27317391	0.993	0.647	0	0	Srgn
Clec4d	7.60E-256	0.73989149	0.763	0.228	1.03E-251	0	Clec4d
Cd14	1.18E-254	0.97243026	0.668	0.18	1.60E-250	0	Cd14
Cd9	1.31E-254	0.91030189	0.852	0.321	1.77E-250	0	Cd9
Ier3	2.25E-237	0.93822366	0.787	0.268	3.06E-233	0	Ier3
AC110211.1	1.31E-234	0.64092573	0.614	0.143	1.78E-230	0	AC110211.1
Eif1	5.17E-228	0.79966458	0.982	0.711	7.01E-224	0	Eif1
Grina	2.91E-218	0.71109384	0.829	0.315	3.95E-214	0	Grina
Mcl1	3.04E-218	0.78927509	0.941	0.509	4.13E-214	0	Mcl1
Cd44	1.54E-206	0.68415544	0.757	0.282	2.09E-202	0	Cd44
Cebpb	2.08E-199	0.82532794	0.901	0.485	2.82E-195	0	Cebpb
Hdc	4.73E-196	0.70291051	0.543	0.132	6.43E-192	0	Hdc
Gm5483	8.15E-191	1.21678104	0.398	0.07	1.11E-186	0	Gm5483
S100a11	3.47E-182	0.82295	0.86	0.482	4.72E-178	0	S100a11
Dusp1	5.86E-172	0.67499559	0.816	0.357	7.96E-168	0	Dusp1
Retnlg	2.23E-163	0.73706833	0.462	0.106	3.03E-159	0	Retnlg
Pnrc1	4.50E-159	0.57711937	0.746	0.316	6.10E-155	0	Pnrc1
Stfa2l1	6.07E-159	0.85347225	0.38	0.076	8.24E-155	0	Stfa2l1
Acod1	1.29E-155	0.53790747	0.382	0.077	1.75E-151	0	Acod1
Slc7a11	6.34E-155	0.60959318	0.459	0.116	8.61E-151	0	Slc7a11
Mxd1	1.56E-153	0.60149026	0.671	0.246	2.12E-149	0	Mxd1
Fth1	1.40E-147	0.79471787	0.986	0.953	1.90E-143	0	Fth1
Cxcr2	1.85E-147	0.54190838	0.639	0.212	2.52E-143	0	Cxcr2
Fxyd5	5.01E-146	0.58681797	0.93	0.663	6.80E-142	0	Fxyd5
Basp1	2.27E-141	0.69721201	0.699	0.308	3.08E-137	0	Basp1
Cd24a	1.00E-140	0.48970473	0.621	0.213	1.36E-136	0	Cd24a
Il1b	4.63E-139	0.8595725	0.715	0.306	6.28E-135	0	Il1b
Btg1	3.79E-138	0.62352721	0.914	0.615	5.14E-134	0	Btg1
S100a6	7.76E-137	0.83161381	0.887	0.631	1.05E-132	0	S100a6
Tyrobp	2.18E-134	0.56317059	0.98	0.775	2.95E-130	0	Tyrobp
Msr1	5.42E-134	0.5757664	0.863	0.458	7.35E-130	0	Msr1
Csf1	8.13E-133	0.47806218	0.445	0.123	1.10E-128	0	Csf1
Rnf149	4.98E-127	0.55937105	0.779	0.396	6.76E-123	0	Rnf149

Hcar2	1.37E-125	0.36616984	0.438	0.116	1.86E-121	0	Hcar2
Lyst	6.41E-124	0.47463486	0.634	0.247	8.70E-120	0	Lyst
Ccr1	3.53E-122	0.52230251	0.686	0.318	4.79E-118	0	Ccr1
Cd300lf	1.81E-119	0.46095266	0.622	0.252	2.45E-115	0	Cd300lf
Plk3	7.77E-114	0.42177922	0.446	0.14	1.06E-109	0	Plk3
Samsn1	2.31E-112	0.44917895	0.536	0.198	3.13E-108	0	Samsn1
Trib1	4.16E-112	0.41603395	0.502	0.175	5.65E-108	0	Trib1
Egr1	1.24E-110	0.47235225	0.592	0.235	1.69E-106	0	Egr1
Asprv1	1.77E-110	0.50554638	0.313	0.072	2.41E-106	0	Asprv1
Csf3r	2.93E-110	0.4467905	0.685	0.286	3.98E-106	0	Csf3r
lqsec1	1.45E-109	0.32967979	0.407	0.118	1.97E-105	0	lqsec1
Trem1	9.57E-109	0.3087171	0.314	0.072	1.30E-104	0	Trem1
Smox	2.92E-107	0.38606791	0.418	0.129	3.96E-103	0	Smox
Adam8	2.28E-106	0.37947286	0.459	0.151	3.10E-102	0	Adam8
G0s2	2.12E-105	0.62750846	0.253	0.049	2.88E-101	0	G0s2
Gabarap	3.85E-105	0.46179843	0.817	0.513	5.23E-101	0	Gabarap
Junb	4.85E-105	0.54912371	0.8	0.472	6.59E-101	0	Junb
Id1	2.62E-104	0.42840253	0.374	0.105	3.56E-100	0	Id1
Chd7	9.44E-103	0.48080708	0.589	0.257	1.28E-98	0	Chd7
Il1r2	3.85E-102	0.4927426	0.475	0.168	5.22E-98	0	Il1r2
Dmxl2	1.00E-98	0.32254044	0.385	0.114	1.36E-94	0	Dmxl2
Il1rn	2.58E-98	0.4758584	0.417	0.135	3.50E-94	0	Il1rn
Clec4e	7.21E-98	0.35600247	0.367	0.106	9.79E-94	0	Clec4e
Slpi	4.56E-96	0.56906204	0.422	0.14	6.20E-92	0	Slpi
Lcn2	2.56E-94	0.48459984	0.346	0.098	3.48E-90	0	Lcn2
Wfdc21	6.18E-93	0.31139886	0.283	0.066	8.40E-89	0	Wfdc21
Pkm	8.19E-92	0.49681373	0.809	0.532	1.11E-87	0	Pkm
Ptafr	4.70E-91	0.35516718	0.487	0.185	6.39E-87	0	Ptafr
Plek	1.09E-90	0.50606289	0.522	0.231	1.48E-86	0	Plek
Tnfrsf23	5.25E-90	0.26797287	0.324	0.089	7.12E-86	0	Tnfrsf23
Cstb	5.06E-88	0.46971601	0.7	0.371	6.87E-84	0	Cstb
Ifitm2	5.80E-88	0.56647274	0.753	0.448	7.87E-84	0	Ifitm2
Gapdh	5.01E-87	0.52095689	0.853	0.671	6.80E-83	0	Gapdh
C5ar1	3.80E-85	0.34486783	0.455	0.173	5.15E-81	0	C5ar1
Igf1r	1.21E-84	0.31356773	0.356	0.111	1.64E-80	0	Igf1r
Ftl1	2.20E-84	0.44506395	0.993	0.876	2.99E-80	0	Ftl1
Rab7	5.93E-84	0.45056668	0.567	0.282	8.05E-80	0	Rab7
Entpd1	1.11E-83	0.31857897	0.397	0.138	1.51E-79	0	Entpd1
Nudt4	2.26E-82	0.28445093	0.385	0.13	3.06E-78	0	Nudt4
Klhdc4	3.22E-81	0.26042485	0.323	0.096	4.37E-77	0	Klhdc4

E230032D23Rik	1.63E-80	0.29417915	0.356	0.113	2.21E-76	0	E230032D23Rik
Lcp1	1.20E-78	0.42711353	0.753	0.484	1.63E-74	0	Lcp1
Fcer1g	1.71E-78	0.42086012	0.957	0.737	2.33E-74	0	Fcer1g
Cxcr4	4.98E-77	0.35023844	0.522	0.229	6.76E-73	0	Cxcr4
Mcemp1	1.41E-74	0.29270564	0.369	0.129	1.91E-70	0	Mcemp1
Tpd52	2.49E-74	0.37903317	0.647	0.355	3.37E-70	0	Tpd52
Lmnb1	5.90E-72	0.30827813	0.346	0.12	8.01E-68	0	Lmnb1
Marcksl1	9.51E-71	0.48800414	0.38	0.146	1.29E-66	0	Marcksl1
Cyp4f18	4.34E-66	0.39822103	0.541	0.277	5.90E-62	0	Cyp4f18
Actg1	8.78E-66	0.55255644	0.866	0.738	1.19E-61	0	Actg1
Nfkbia	6.60E-64	0.51969966	0.615	0.35	8.96E-60	0	Nfkbia
Slc16a3	7.01E-64	0.27633198	0.369	0.144	9.51E-60	0	Slc16a3
Card19	1.83E-62	0.27424577	0.476	0.216	2.49E-58	0	Card19
Ccl3	8.03E-61	0.35220759	0.384	0.152	1.09E-56	0	Ccl3
H3f3b	9.08E-61	0.33211406	0.926	0.829	1.23E-56	0	H3f3b
Prdx5	8.32E-58	0.39357999	0.694	0.445	1.13E-53	0	Prdx5
Ninj1	1.70E-57	0.33656933	0.515	0.258	2.31E-53	0	Ninj1
Txnip	4.87E-56	0.33903611	0.584	0.326	6.61E-52	0	Txnip
Gadd45b	1.20E-54	0.3054554	0.41	0.18	1.63E-50	0	Gadd45b
H3f3a	1.59E-54	0.34329093	0.815	0.688	2.16E-50	0	H3f3a
Tlr2	2.02E-53	0.27792919	0.359	0.151	2.74E-49	0	Tlr2
Lasp1	2.71E-53	0.25180523	0.372	0.16	3.68E-49	0	Lasp1
Diaph1	6.45E-53	0.28591534	0.468	0.235	8.76E-49	0	Diaph1
Adipor1	4.01E-50	0.27236881	0.448	0.221	5.45E-46	0	Adipor1
Neat1	4.88E-50	0.32169719	0.664	0.415	6.63E-46	0	Neat1
Ubc	6.70E-50	0.32787497	0.722	0.501	9.10E-46	0	Ubc
Cd33	1.23E-49	0.2580069	0.392	0.179	1.67E-45	0	Cd33
Marcks	2.83E-49	0.34873057	0.663	0.427	3.85E-45	0	Marcks
Tnfaip2	4.19E-48	0.375413	0.446	0.226	5.69E-44	0	Tnfaip2
Btg2	3.25E-47	0.34693734	0.659	0.422	4.41E-43	0	Btg2
Spag9	5.11E-47	0.27915929	0.456	0.241	6.94E-43	0	Spag9
Emilin2	3.90E-46	0.25072631	0.443	0.221	5.30E-42	0	Emilin2
Eno1	6.65E-44	0.3220481	0.522	0.304	9.03E-40	0	Eno1
Vasp	6.66E-44	0.28012259	0.534	0.317	9.05E-40	0	Vasp
Snx20	9.83E-43	0.25075714	0.447	0.238	1.33E-38	0	Snx20
Ccrl2	1.76E-42	0.26975083	0.334	0.147	2.38E-38	0	Ccrl2
Csf2rb	5.51E-42	0.28995518	0.426	0.227	7.48E-38	0	Csf2rb
Lilr4b	1.47E-41	0.25580148	0.356	0.169	1.99E-37	0	Lilr4b
Zcchc6	1.07E-40	0.27019553	0.443	0.243	1.45E-36	0	Zcchc6
Gng5	1.75E-40	0.27495489	0.716	0.53	2.38E-36	0	Gng5

Itgam	2.71E-37	0.25593913	0.459	0.262	3.67E-33	0	Itgam	
Son	2.96E-37	0.26173103	0.697	0.492	4.02E-33	0	Son	
Jun	2.57E-35	0.30790333	0.661	0.462	3.49E-31	0	Jun	
Ccl4	3.84E-35	0.47895501	0.325	0.16	5.21E-31	0	Ccl4	
Myh9	4.01E-34	0.26321997	0.554	0.364	5.44E-30	0	Myh9	
Iqgap1	4.15E-33	0.26008016	0.615	0.431	5.63E-29	0	Iqgap1	
Ubb	4.20E-33	0.26400607	0.82	0.723	5.70E-29	0	Ubb	
Aldoa	3.00E-32	0.30070279	0.598	0.419	4.08E-28	0	Aldoa	
Cd53	9.98E-31	0.25746336	0.522	0.349	1.35E-26	0	Cd53	
Txn1	2.74E-29	0.30218337	0.574	0.416	3.72E-25	0	Txn1	
Pim1	8.15E-19	0.25246892	0.421	0.289	1.11E-14	0	Pim1	
Csf3r1	2.26E-116	0.56721908	0.673	0.291	3.07E-112	1	Csf3r	
Cxcr21	6.43E-83	0.40673716	0.554	0.227	8.74E-79	1	Cxcr2	
Rgs2	4.19E-80	0.49519546	0.656	0.372	5.69E-76	1	Rgs2	
Marcks1	1.46E-56	0.4303309	0.672	0.428	1.98E-52	1	Marcks	
Fxyd51	7.42E-48	0.34558936	0.838	0.678	1.01E-43	1	Fxyd5	
Eif11	4.26E-47	0.30120953	0.912	0.723	5.78E-43	1	Eif1	
Junb1	5.95E-47	0.3284538	0.71	0.487	8.08E-43	1	Junb	
Btg11	2.00E-43	0.30593989	0.85	0.626	2.71E-39	1	Btg1	
Cxcr41	9.80E-42	0.29258876	0.452	0.24	1.33E-37	1	Cxcr4	
Tyrobp1	8.33E-40	0.32798126	0.938	0.783	1.13E-35	1	Tyrobp	
Txnip1	2.16E-39	0.35840937	0.531	0.335	2.94E-35	1	Txnip	
Ubb1	3.15E-39	0.30849195	0.838	0.722	4.28E-35	1	Ubb	
Alox5ap	1.65E-38	0.36093251	0.615	0.438	2.24E-34	1	Alox5ap	
Neurl3	1.01E-37	0.32136652	0.514	0.315	1.37E-33	1	Neurl3	
Gng51	2.14E-33	0.3062973	0.67	0.538	2.90E-29	1	Gng5	
Ypel3	1.50E-32	0.26053646	0.438	0.262	2.03E-28	1	Ypel3	
Arpc1b	2.20E-30	0.28330939	0.719	0.604	2.98E-26	1	Arpc1b	
H3f3b1	2.55E-30	0.26363552	0.905	0.833	3.46E-26	1	H3f3b	
Rnf1491	1.30E-29	0.27444538	0.6	0.424	1.77E-25	1	Rnf149	
Cdk2ap2	1.75E-29	0.39462927	0.464	0.307	2.38E-25	1	Cdk2ap2	
Ubc1	7.44E-27	0.2795143	0.636	0.514	1.01E-22	1	Ubc	
Gngt2	1.14E-26	0.28540296	0.394	0.247	1.54E-22	1	Gngt2	
Lcp11	2.03E-25	0.26869434	0.634	0.503	2.76E-21	1	Lcp1	
Son1	4.92E-25	0.26546248	0.622	0.503	6.68E-21	1	Son	
Fcer1g1	4.01E-22	0.25296913	0.909	0.745	5.45E-18	1	Fcer1g	
Pfn1	8.38E-22	0.25523608	0.73	0.637	1.14E-17	1	Pfn1	
Selplg	2.48E-21	0.25505351	0.512	0.379	3.36E-17	1	Selplg	
	1-Jun	1.55E-20	0.2980708	0.588	0.473	2.11E-16	1	Jun
Fos	5.00E-19	0.27603889	0.543	0.412	6.79E-15	1	Fos	

Btg21	7.25E-19	0.2753589	0.555	0.438	9.85E-15	1	Btg2
Cd52	7.85E-18	0.26399475	0.899	0.83	1.07E-13	1	Cd52
Id2	3.05E-14	0.26819919	0.463	0.353	4.14E-10	1	Id2
S100a91	0	1.54243598	1	0.39	0	2	S100a9
Cxcr22	0	0.87992166	0.834	0.2	0	2	Cxcr2
S100a81	2.73E-294	1.38459298	1	0.423	3.71E-290	2	S100a8
Lrg1	1.28E-263	0.861296	0.512	0.076	1.73E-259	2	Lrg1
Csf3r2	7.43E-226	0.77149104	0.842	0.277	1.01E-221	2	Csf3r
Il1b1	2.28E-225	1.09794264	0.842	0.301	3.09E-221	2	Il1b
S100a111	2.68E-214	0.93407049	0.913	0.485	3.64E-210	2	S100a11
Retnlg1	9.79E-210	1.29435074	0.53	0.107	1.33E-205	2	Retnlg
Hdc1	3.93E-207	0.69689356	0.6	0.135	5.33E-203	2	Hdc
Srgn1	2.47E-175	0.84759613	0.99	0.656	3.35E-171	2	Srgn
Lcn21	4.29E-171	0.77390713	0.452	0.091	5.83E-167	2	Lcn2
Msr11	2.60E-150	0.70956881	0.893	0.464	3.54E-146	2	Msr11
Mmp9	5.40E-146	0.43051677	0.37	0.068	7.33E-142	2	Mmp9
Hp	3.46E-140	0.57075726	0.474	0.119	4.69E-136	2	Hp
Tyrobp2	1.57E-139	0.63943738	0.993	0.779	2.13E-135	2	Tyrobp
Wfdc211	1.29E-138	0.51424165	0.348	0.063	1.75E-134	2	Wfdc21
Alox5ap1	5.11E-138	0.64451309	0.807	0.418	6.93E-134	2	Alox5ap
Fxyd52	1.92E-133	0.62331414	0.939	0.669	2.61E-129	2	Fxyd5
S100a61	5.37E-133	0.91305055	0.913	0.634	7.30E-129	2	S100a6
Junb2	1.04E-132	0.69248829	0.837	0.476	1.42E-128	2	Junb
Slpi1	5.06E-131	0.66624248	0.492	0.139	6.87E-127	2	Slpi
Btg12	1.70E-129	0.58672077	0.95	0.618	2.30E-125	2	Btg1
Cebpd	9.29E-127	0.4396429	0.434	0.112	1.26E-122	2	Cebpd
Stfa2l11	1.35E-126	0.65543973	0.382	0.083	1.83E-122	2	Stfa2l1
Mcl11	1.80E-125	0.58746291	0.893	0.525	2.44E-121	2	Mcl1
Lcp12	7.49E-125	0.61069308	0.809	0.484	1.02E-120	2	Lcp1
Grina1	5.53E-124	0.57531731	0.752	0.337	7.51E-120	2	Grina
Dusp11	2.58E-120	0.62586146	0.787	0.371	3.51E-116	2	Dusp1
Ifitm21	4.78E-114	0.67432773	0.805	0.449	6.49E-110	2	Ifitm2
Btg22	1.70E-111	0.65958065	0.767	0.415	2.31E-107	2	Btg2
Eif12	6.31E-109	0.52348968	0.974	0.719	8.56E-105	2	Eif1
Sorl1	5.16E-108	0.46534498	0.56	0.208	7.00E-104	2	Sorl1
Trim30b	6.67E-107	0.33082843	0.352	0.084	9.05E-103	2	Trim30b
Il1r21	7.01E-106	0.5403801	0.511	0.171	9.52E-102	2	Il1r2
Cd521	1.61E-103	0.5465103	0.981	0.821	2.18E-99	2	Cd52
Tnfaip21	9.29E-100	0.51795504	0.564	0.218	1.26E-95	2	Tnfaip2
Selplg1	5.51E-99	0.54400863	0.694	0.36	7.48E-95	2	Selplg

Pygl	4.34E-98	0.35019611	0.414	0.122	5.89E-94	2	Pygl
Mxd11	6.79E-93	0.43379852	0.63	0.261	9.22E-89	2	Mxd1
Klf2	1.97E-86	0.45917849	0.432	0.146	2.68E-82	2	Klf2
Txnip2	6.64E-86	0.49525714	0.657	0.324	9.01E-82	2	Txnip
Nfam1	1.47E-84	0.38609928	0.464	0.171	2.00E-80	2	Nfam1
H2-Q10	2.26E-83	0.27504312	0.27	0.061	3.07E-79	2	H2-Q10
Ccr11	3.15E-81	0.42688615	0.67	0.329	4.28E-77	2	Ccr1
Gcnt2	6.25E-81	0.34721403	0.445	0.16	8.49E-77	2	Gcnt2
AC110211.11	5.44E-79	0.35089329	0.472	0.171	7.39E-75	2	AC110211.
Gsr	2.25E-78	0.42418974	0.511	0.214	3.06E-74	2	Gsr
Zfp36	7.39E-78	0.49346018	0.647	0.338	1.00E-73	2	Zfp36
Fos1	1.29E-77	0.58065147	0.701	0.395	1.75E-73	2	Fos
Cebpb1	2.04E-74	0.44772201	0.845	0.501	2.78E-70	2	Cebpb
Id11	3.98E-72	0.38541258	0.355	0.114	5.40E-68	2	Id1
Igf1r1	7.39E-72	0.29051653	0.361	0.116	1.00E-67	2	Igf1r
Cd331	1.20E-71	0.34770066	0.452	0.177	1.63E-67	2	Cd33
Fcer1g2	5.44E-71	0.45164932	0.949	0.743	7.38E-67	2	Fcer1g
Lyst1	7.94E-71	0.40585648	0.572	0.264	1.08E-66	2	Lyst
F630028O10Rik	2.02E-70	0.30045191	0.303	0.087	2.74E-66	2	F630028O1
Ifitm1	9.41E-69	0.44301186	0.488	0.202	1.28E-64	2	Ifitm1
Gm54831	3.71E-65	0.48029507	0.303	0.089	5.04E-61	2	Gm5483
Rgs21	1.34E-64	0.4384202	0.657	0.377	1.82E-60	2	Rgs2
Clec4d1	2.00E-64	0.30647727	0.584	0.262	2.71E-60	2	Clec4d
Rnf1492	5.94E-64	0.3997033	0.712	0.413	8.06E-60	2	Rnf149
Marcks2	1.97E-63	0.41932072	0.719	0.427	2.67E-59	2	Marcks
Stk17b	1.33E-60	0.36778589	0.508	0.245	1.81E-56	2	Stk17b
Ogfrl1	2.51E-59	0.30803591	0.416	0.172	3.40E-55	2	Ogfrl1
Gda	2.04E-57	0.32817289	0.359	0.137	2.78E-53	2	Gda
Ubb2	7.40E-56	0.37270352	0.864	0.72	1.00E-51	2	Ubb
Tpd521	6.24E-55	0.38463954	0.626	0.365	8.47E-51	2	Tpd52
Pglyrp1	6.80E-54	0.29362614	0.294	0.101	9.23E-50	2	Pglyrp1
Adipor11	1.66E-53	0.30032088	0.475	0.224	2.25E-49	2	Adipor1
Socs3	1.38E-52	0.33341677	0.391	0.166	1.87E-48	2	Socs3
Fbxl5	8.69E-52	0.27175039	0.31	0.113	1.18E-47	2	Fbxl5
Mcomp11	1.14E-51	0.25473045	0.353	0.137	1.55E-47	2	Mcomp1
Cdk2ap21	3.05E-50	0.44690321	0.537	0.301	4.14E-46	2	Cdk2ap2
Jund	3.07E-50	0.39411828	0.634	0.396	4.17E-46	2	Jund
Map1lc3b	7.04E-50	0.33566683	0.568	0.323	9.56E-46	2	Map1lc3b
Ssh2	2.29E-48	0.3157074	0.468	0.235	3.10E-44	2	Ssh2
Neurl31	2.02E-47	0.34973932	0.561	0.313	2.74E-43	2	Neurl3

Neat11	2.73E-47	0.35939954	0.676	0.42	3.70E-43	2	Neat1
H3f3b2	2.74E-47	0.34128613	0.936	0.83	3.73E-43	2	H3f3b
Ier2	3.83E-47	0.36490613	0.482	0.258	5.20E-43	2	Ier2
Cd300lf1	1.14E-46	0.28514352	0.526	0.272	1.55E-42	2	Cd300lf
Arpc1b1	4.22E-46	0.3420462	0.76	0.601	5.73E-42	2	Arpc1b
Ncf2	5.56E-45	0.33794779	0.539	0.304	7.55E-41	2	Ncf2
Gabarap1	6.16E-45	0.31891819	0.747	0.529	8.36E-41	2	Gabarap
Dmxl21	7.79E-45	0.2578527	0.321	0.128	1.06E-40	2	Dmxl2
Egr11	3.58E-44	0.35806931	0.492	0.255	4.86E-40	2	Egr1
Zyx	3.90E-44	0.29829912	0.406	0.196	5.29E-40	2	Zyx
Spi1	3.82E-43	0.32774168	0.639	0.413	5.18E-39	2	Spi1
Cxcr42	6.23E-40	0.30750706	0.463	0.243	8.46E-36	2	Cxcr4
Fgl2	8.46E-40	0.26778523	0.356	0.164	1.15E-35	2	Fgl2
Pfn11	1.39E-39	0.33729699	0.76	0.635	1.89E-35	2	Pfn1
Anxa2	2.46E-39	0.2957031	0.557	0.326	3.34E-35	2	Anxa2
Gnai2	5.12E-39	0.32050067	0.719	0.572	6.95E-35	2	Gnai2
Iqgap11	1.18E-37	0.30628368	0.637	0.433	1.60E-33	2	Iqgap1
Taldo1	1.20E-37	0.34440696	0.58	0.386	1.63E-33	2	Taldo1
Ypel31	2.18E-37	0.26150723	0.471	0.261	2.96E-33	2	Ypel3
Cd441	2.87E-37	0.27473797	0.553	0.317	3.90E-33	2	Cd44
Ier5	6.82E-37	0.27680742	0.553	0.339	9.25E-33	2	Ier5
Coro1a	9.80E-36	0.3346889	0.716	0.596	1.33E-31	2	Coro1a
Vasp1	2.58E-35	0.30244511	0.524	0.324	3.50E-31	2	Vasp
H3f3a1	2.93E-35	0.27214184	0.82	0.69	3.97E-31	2	H3f3a
Ppp1r18	2.16E-34	0.25365011	0.421	0.229	2.93E-30	2	Ppp1r18
Gmfg	4.78E-34	0.31902513	0.476	0.291	6.49E-30	2	Gmfg
Actg11	6.31E-33	0.29965617	0.86	0.742	8.57E-29	2	Actg1
Trib11	1.16E-31	0.25247743	0.378	0.197	1.58E-27	2	Trib1
Pkm1	7.53E-31	0.30711841	0.708	0.55	1.02E-26	2	Pkm
Rhog	2.62E-29	0.25989715	0.461	0.283	3.55E-25	2	Rhog
Gpsm3	4.31E-28	0.25162644	0.432	0.264	5.86E-24	2	Gpsm3
Pim11	4.57E-28	0.29374341	0.465	0.287	6.21E-24	2	Pim1
Son2	4.97E-28	0.25501091	0.672	0.5	6.75E-24	2	Son
Prdx51	9.01E-28	0.26331051	0.652	0.456	1.22E-23	2	Prdx5
Rac2	1.67E-24	0.25566084	0.524	0.356	2.27E-20	2	Rac2
Ccl6	4.43E-22	0.30386012	0.312	0.172	6.02E-18	2	Ccl6
Wfdc17	7.33E-05	0.41606892	0.28	0.229	0.99448246	2	Wfdc17
Apoe	0	2.4922607	0.987	0.345	0	3	Apoe
C1qb	0	1.74566865	0.89	0.107	0	3	C1qb
C1qa	0	1.68216127	0.864	0.089	0	3	C1qa

C1qc	0	1.50168247	0.858	0.086	0	3	C1qc
Lgmn	0	1.01680616	0.836	0.192	0	3	Lgmn
Ms4a7	0	1.01635238	0.689	0.077	0	3	Ms4a7
Selenop	0	0.77883626	0.564	0.077	0	3	Selenop
Trem2	0	0.55749246	0.553	0.066	0	3	Trem2
Ctsc	3.10E-284	0.95405539	0.749	0.178	4.21E-280	3	Ctsc
Ctss	4.86E-281	1.12400766	0.962	0.415	6.59E-277	3	Ctss
H2-Aa	1.10E-280	1.23413375	0.823	0.209	1.50E-276	3	H2-Aa
H2-Eb1	9.84E-280	1.18805745	0.807	0.194	1.34E-275	3	H2-Eb1
H2-Ab1	3.01E-276	1.21889005	0.842	0.22	4.09E-272	3	H2-Ab1
Cxcl16	8.55E-273	0.62625976	0.643	0.116	1.16E-268	3	Cxcl16
Vcam1	1.31E-256	0.48537347	0.289	0.015	1.78E-252	3	Vcam1
Itgb5	6.24E-244	0.52871507	0.607	0.114	8.46E-240	3	Itgb5
Cd74	4.93E-240	1.23136108	0.895	0.327	6.70E-236	3	Cd74
Aif1	1.12E-238	0.7044236	0.694	0.167	1.52E-234	3	Aif1
Pf4	2.13E-235	0.38436849	0.276	0.015	2.90E-231	3	Pf4
Acp5	3.12E-231	0.57045807	0.453	0.064	4.24E-227	3	Acp5
Olfml3	9.60E-228	0.37827659	0.383	0.04	1.30E-223	3	Olfml3
Cd81	4.54E-225	0.54679953	0.48	0.072	6.16E-221	3	Cd81
Fcrls	2.44E-224	0.59528207	0.348	0.033	3.32E-220	3	Fcrls
Axl	1.06E-223	0.39988541	0.463	0.067	1.44E-219	3	Axl
Tmem176b	2.73E-216	0.61018994	0.499	0.085	3.71E-212	3	Tmem176b
C3ar1	3.50E-214	0.38202152	0.431	0.059	4.75E-210	3	C3ar1
Csf1r	4.40E-201	0.6134836	0.728	0.216	5.98E-197	3	Csf1r
Cx3cr1	3.79E-200	0.50581193	0.506	0.094	5.15E-196	3	Cx3cr1
Hexb	9.89E-200	0.68551014	0.645	0.168	1.34E-195	3	Hexb
Lpl	3.58E-197	0.42166834	0.295	0.026	4.85E-193	3	Lpl
Mmp14	6.74E-195	0.43926631	0.463	0.079	9.14E-191	3	Mmp14
Lyz2	2.22E-193	0.82972927	0.915	0.377	3.01E-189	3	Lyz2
Gatm	1.44E-192	0.5259946	0.43	0.07	1.96E-188	3	Gatm
Tmem176a	2.10E-191	0.53452172	0.425	0.068	2.86E-187	3	Tmem176a
Cadm1	2.10E-182	0.27387895	0.251	0.019	2.85E-178	3	Cadm1
Blvrb	3.50E-181	0.35485553	0.355	0.048	4.76E-177	3	Blvrb
Ctsz	1.73E-175	0.74658835	0.841	0.37	2.34E-171	3	Ctsz
Cybb	1.64E-167	0.51582388	0.633	0.172	2.23E-163	3	Cybb
Ctsa	1.54E-166	0.53794402	0.686	0.224	2.09E-162	3	Ctsa
Mafb	2.85E-160	0.53723159	0.655	0.181	3.87E-156	3	Mafb
Calr	1.22E-159	0.69729634	0.756	0.312	1.66E-155	3	Calr
Adgre1	3.42E-159	0.2779008	0.294	0.035	4.64E-155	3	Adgre1
Cd68	3.22E-154	0.53567702	0.712	0.249	4.37E-150	3	Cd68

Hsp90b1	6.27E-153	0.62682334	0.69	0.253	8.52E-149	3	Hsp90b1
Lair1	3.16E-149	0.40718346	0.504	0.12	4.30E-145	3	Lair1
Ctsh	9.27E-148	0.54249623	0.722	0.268	1.26E-143	3	Ctsh
H2-DMa	2.17E-145	0.47008521	0.599	0.174	2.94E-141	3	H2-DMa
Pmepa1	6.63E-145	0.49625796	0.453	0.106	9.00E-141	3	Pmepa1
Tmem119	6.01E-143	0.27580964	0.284	0.036	8.16E-139	3	Tmem119
H2-DMb1	6.18E-142	0.49264565	0.52	0.136	8.40E-138	3	H2-DMb1
Trf	1.24E-140	0.44695449	0.411	0.088	1.69E-136	3	Trf
Psap	4.07E-139	0.68254113	0.968	0.603	5.52E-135	3	Psap
Grn	7.19E-139	0.61568254	0.738	0.306	9.76E-135	3	Grn
Hexa	1.52E-134	0.41313775	0.548	0.161	2.07E-130	3	Hexa
Ly86	4.44E-133	0.38397067	0.535	0.148	6.03E-129	3	Ly86
Ctsb	5.14E-132	0.78420309	0.89	0.502	6.98E-128	3	Ctsb
Hpgds	2.51E-130	0.28948341	0.308	0.049	3.41E-126	3	Hpgds
Npc2	4.08E-130	0.49999658	0.82	0.365	5.54E-126	3	Npc2
Stab1	3.60E-127	0.36749005	0.383	0.082	4.89E-123	3	Stab1
Ntpcr	1.19E-125	0.26069523	0.297	0.048	1.62E-121	3	Ntpcr
Ms4a6c	2.24E-125	0.45172535	0.637	0.21	3.04E-121	3	Ms4a6c
Tmem86a	2.53E-125	0.33946917	0.406	0.094	3.43E-121	3	Tmem86a
Mt1	3.52E-123	0.54642063	0.401	0.092	4.78E-119	3	Mt1
Lipa	3.61E-118	0.29998028	0.32	0.061	4.91E-114	3	Lipa
Mpeg1	5.33E-114	0.53341003	0.744	0.34	7.23E-110	3	Mpeg1
Ms4a6d	6.10E-114	0.32821867	0.5	0.139	8.28E-110	3	Ms4a6d
Pdia6	9.28E-113	0.39789527	0.461	0.132	1.26E-108	3	Pdia6
Gpr65	1.39E-110	0.2558174	0.301	0.057	1.89E-106	3	Gpr65
Ptgs1	6.46E-107	0.28686992	0.257	0.042	8.76E-103	3	Ptgs1
Prdx1	1.34E-106	0.50047661	0.58	0.225	1.82E-102	3	Prdx1
Cd72	5.34E-106	0.31331301	0.303	0.059	7.25E-102	3	Cd72
Pdia3	1.80E-104	0.42471536	0.542	0.196	2.45E-100	3	Pdia3
Lgals3bp	1.18E-102	0.33586061	0.401	0.105	1.61E-98	3	Lgals3bp
Unc93b1	1.30E-102	0.39981745	0.592	0.224	1.76E-98	3	Unc93b1
Snx5	2.41E-99	0.28914695	0.401	0.108	3.27E-95	3	Snx5
Dab2	3.46E-95	0.28979613	0.33	0.077	4.70E-91	3	Dab2
Bst2	1.39E-90	0.29350922	0.496	0.164	1.88E-86	3	Bst2
Abca1	4.61E-90	0.27400811	0.279	0.059	6.26E-86	3	Abca1
Fcgr2b	6.48E-90	0.38987525	0.449	0.146	8.79E-86	3	Fcgr2b
mt-Co3	1.13E-89	0.55231822	0.991	0.807	1.54E-85	3	mt-Co3
Lamp1	2.37E-88	0.39825499	0.605	0.258	3.22E-84	3	Lamp1
Itm2b	6.93E-86	0.49071572	0.833	0.54	9.41E-82	3	Itm2b
Gusb	1.77E-85	0.29268985	0.368	0.105	2.40E-81	3	Gusb

Sdf2l1	3.00E-85	0.2648171	0.281	0.063	4.07E-81	3	Sdf2l1
mt-Co2	1.51E-82	0.46141744	0.991	0.796	2.05E-78	3	mt-Co2
mt-Atp6	3.62E-80	0.50024165	0.993	0.797	4.92E-76	3	mt-Atp6
Ucp2	4.53E-74	0.4385731	0.686	0.376	6.15E-70	3	Ucp2
mt-Nd1	7.02E-74	0.45496189	0.864	0.564	9.53E-70	3	mt-Nd1
Creg1	1.56E-71	0.29439776	0.399	0.138	2.12E-67	3	Creg1
Lrp1	4.67E-71	0.26980016	0.421	0.145	6.34E-67	3	Lrp1
mt-Nd2	1.73E-70	0.41726285	0.868	0.566	2.34E-66	3	mt-Nd2
mt-Co1	5.06E-70	0.39990687	0.988	0.832	6.86E-66	3	mt-Co1
Hsp90ab1	2.90E-69	0.38497572	0.741	0.403	3.93E-65	3	Hsp90ab1
Akr1a1	3.22E-66	0.33362586	0.56	0.265	4.38E-62	3	Akr1a1
Rgs1	7.19E-64	0.46813637	0.504	0.218	9.76E-60	3	Rgs1
mt-Cytb	1.41E-63	0.44252172	0.914	0.721	1.91E-59	3	mt-Cytb
Hspa5	5.76E-63	0.49890645	0.665	0.388	7.82E-59	3	Hspa5
Rrbp1	2.57E-61	0.34361667	0.677	0.364	3.49E-57	3	Rrbp1
Itgax	2.11E-60	0.25160512	0.377	0.137	2.86E-56	3	Itgax
Erp29	3.42E-60	0.29890269	0.52	0.24	4.65E-56	3	Erp29
Sirpa	4.70E-58	0.26648684	0.458	0.194	6.39E-54	3	Sirpa
Pld4	4.89E-57	0.26462338	0.408	0.16	6.64E-53	3	Pld4
mt-Nd4	6.74E-56	0.37996358	0.901	0.668	9.15E-52	3	mt-Nd4
Ssr4	8.20E-53	0.2566805	0.51	0.242	1.11E-48	3	Ssr4
Hspa8	4.00E-52	0.35274293	0.763	0.473	5.44E-48	3	Hspa8
Tgfb1	6.83E-52	0.42839186	0.613	0.329	9.27E-48	3	Tgfb1
Ybx1	1.13E-51	0.3315291	0.639	0.376	1.53E-47	3	Ybx1
Tgfbr1	3.92E-51	0.26799338	0.446	0.198	5.32E-47	3	Tgfbr1
Pla2g7	4.39E-51	0.28260691	0.466	0.212	5.96E-47	3	Pla2g7
Man2b1	2.76E-50	0.33760044	0.516	0.262	3.75E-46	3	Man2b1
Fabp5	1.64E-49	0.58382975	0.297	0.107	2.23E-45	3	Fabp5
Ptma	3.64E-48	0.30896865	0.813	0.535	4.95E-44	3	Ptma
Atp5g1	1.85E-47	0.25792491	0.399	0.178	2.51E-43	3	Atp5g1
Zeb2	1.18E-46	0.30218944	0.563	0.292	1.60E-42	3	Zeb2
mt-Nd3	1.43E-46	0.30232099	0.642	0.363	1.94E-42	3	mt-Nd3
Tubb5	8.33E-43	0.25098661	0.387	0.173	1.13E-38	3	Tubb5
Rps2	3.85E-40	0.33902254	0.851	0.634	5.22E-36	3	Rps2
Rps17	4.30E-40	0.2719018	0.615	0.372	5.84E-36	3	Rps17
AY036118	1.38E-35	0.35310131	0.307	0.137	1.87E-31	3	AY036118
Rpl10a	1.10E-34	0.27348237	0.713	0.448	1.50E-30	3	Rpl10a
Cd63	1.35E-34	0.3806127	0.582	0.355	1.84E-30	3	Cd63
Rplp1	6.82E-30	0.26237272	0.934	0.837	9.25E-26	3	Rplp1
B2m	9.99E-30	0.31486047	0.836	0.676	1.36E-25	3	B2m

Ctsd	2.81E-29	0.49716801	0.692	0.52	3.82E-25	3	Ctsd
Lgals3	1.74E-18	0.31582721	0.561	0.4	2.36E-14	3	Lgals3
Gm42418	5.19E-18	0.35291062	0.994	0.973	7.04E-14	3	Gm42418
Hcar21	0	1.18605973	0.721	0.101	0	4	Hcar2
Cstb1	4.73E-265	1.39905577	0.898	0.365	6.41E-261	4	Cstb
Basp11	1.48E-262	1.19689841	0.884	0.306	2.01E-258	4	Basp1
Gadd45b1	4.33E-261	1.37617063	0.695	0.161	5.88E-257	4	Gadd45b
Hilpda	2.25E-247	1.04734608	0.505	0.073	3.06E-243	4	Hilpda
Ftl11	1.82E-209	1.12435473	0.998	0.88	2.47E-205	4	Ftl1
Ccl31	4.19E-209	1.03113235	0.615	0.138	5.68E-205	4	Ccl3
Ankrd33b	1.40E-190	0.47331491	0.377	0.049	1.91E-186	4	Ankrd33b
Syne1	9.55E-190	0.47282847	0.384	0.051	1.30E-185	4	Syne1
Ccrl21	5.32E-189	0.90515338	0.571	0.131	7.23E-185	4	Ccrl2
Cd24a1	2.76E-183	0.74480658	0.723	0.219	3.75E-179	4	Cd24a
Fnip2	4.97E-177	0.43427285	0.395	0.059	6.75E-173	4	Fnip2
Dedd2	3.56E-176	0.4697938	0.439	0.076	4.83E-172	4	Dedd2
Fth11	2.61E-174	1.25726779	0.995	0.953	3.54E-170	4	Fth1
E230032D23Rik1	3.09E-167	0.51402475	0.508	0.108	4.19E-163	4	E230032D23Rik1
Cd631	1.82E-152	0.87828407	0.815	0.335	2.48E-148	4	Cd63
lfrd1	2.46E-149	0.6730361	0.381	0.069	3.34E-145	4	lfrd1
Il1rn1	3.63E-146	0.80076685	0.523	0.136	4.93E-142	4	Il1rn
Pnrc11	1.49E-144	0.75229405	0.779	0.33	2.02E-140	4	Pnrc1
Ninj11	7.83E-143	0.69044447	0.69	0.25	1.06E-138	4	Ninj1
Eif13	3.16E-142	0.81342675	0.96	0.724	4.29E-138	4	Eif1
Tmem189	1.31E-137	0.52482767	0.547	0.156	1.78E-133	4	Tmem189
Maff	9.75E-136	0.28840681	0.263	0.032	1.32E-131	4	Maff
Msrb12	4.05E-135	0.75094827	0.892	0.471	5.49E-131	4	Msrb1
Ccl41	1.20E-134	0.8466748	0.544	0.145	1.63E-130	4	Ccl4
Rhov	2.73E-129	0.39961329	0.342	0.061	3.71E-125	4	Rhov
Gla	4.62E-128	0.34078539	0.345	0.062	6.27E-124	4	Gla
Bri3	3.91E-126	0.71528354	0.711	0.32	5.31E-122	4	Bri3
1700017B05Rik	2.52E-124	0.47523771	0.49	0.135	3.42E-120	4	1700017B05Rik
Ier31	7.75E-123	0.72290984	0.74	0.294	1.05E-118	4	Ier3
Cxcl21	1.49E-122	1.16824391	0.602	0.193	2.02E-118	4	Cxcl2
Cd91	1.07E-118	0.7383265	0.779	0.349	1.46E-114	4	Cd9
Atp6v1a	3.92E-117	0.41742098	0.408	0.097	5.33E-113	4	Atp6v1a
Gabarap2	2.46E-115	0.61217343	0.861	0.521	3.35E-111	4	Gabarap
Bnip3l	5.57E-115	0.72009507	0.555	0.197	7.56E-111	4	Bnip3l
Slc31a2	2.64E-113	0.34442712	0.306	0.056	3.59E-109	4	Slc31a2
Lrrfip2	5.57E-106	0.45609035	0.384	0.095	7.56E-102	4	Lrrfip2

Card191	9.97E-105	0.63077562	0.574	0.217	1.35E-100	4	Card19
Gm20406	1.31E-104	0.26232442	0.269	0.045	1.78E-100	4	Gm20406
Ero1l	2.52E-104	0.48489657	0.358	0.083	3.43E-100	4	Ero1l
Atf3	1.09E-102	0.53911809	0.395	0.102	1.48E-98	4	Atf3
Klhdc41	3.65E-91	0.33711922	0.376	0.1	4.96E-87	4	Klhdc4
Tiparp	4.84E-91	0.38972069	0.305	0.068	6.57E-87	4	Tiparp
Bnip3	9.42E-91	0.37294944	0.352	0.088	1.28E-86	4	Bnip3
Tpi1	2.26E-89	0.59943699	0.621	0.28	3.06E-85	4	Tpi1
Irak2	9.03E-89	0.29621104	0.323	0.076	1.23E-84	4	Irak2
Sh2d3c	4.10E-88	0.3514107	0.334	0.083	5.57E-84	4	Sh2d3c
Samsn11	1.32E-86	0.55740667	0.539	0.211	1.79E-82	4	Samsn1
Mcl12	5.52E-85	0.57367792	0.869	0.533	7.50E-81	4	Mcl1
Iqsec11	8.14E-84	0.3560367	0.416	0.129	1.11E-79	4	Iqsec1
Cebpb2	1.03E-83	0.61152072	0.845	0.507	1.40E-79	4	Cebpb
Ctsb1	2.86E-80	0.48267602	0.84	0.511	3.88E-76	4	Ctsb
Sqstm1	1.82E-79	0.31807739	0.361	0.104	2.47E-75	4	Sqstm1
Atp6v1c1	2.01E-79	0.29359963	0.295	0.071	2.73E-75	4	Atp6v1c1
Nceh1	2.22E-79	0.28546786	0.277	0.063	3.01E-75	4	Nceh1
Hmox1	6.07E-79	0.31165138	0.431	0.139	8.24E-75	4	Hmox1
Mxd12	1.90E-78	0.52790461	0.611	0.269	2.58E-74	4	Mxd1
Plgrkt	7.88E-77	0.35590021	0.368	0.112	1.07E-72	4	Plgrkt
Thbs1	8.25E-77	0.50516991	0.315	0.081	1.12E-72	4	Thbs1
Plin2	6.74E-76	0.56753499	0.59	0.274	9.16E-72	4	Plin2
Tnfrsf231	4.56E-75	0.29822279	0.344	0.096	6.19E-71	4	Tnfrsf23
Clec4d2	5.02E-75	0.51408224	0.602	0.266	6.81E-71	4	Clec4d
2-Jun	4.24E-74	0.60449346	0.763	0.46	5.76E-70	4	Jun
Bhlhe40	4.48E-74	0.37803353	0.458	0.167	6.09E-70	4	Bhlhe40
Jdp2	1.00E-73	0.33149377	0.358	0.107	1.36E-69	4	Jdp2
Sdcbp	6.37E-72	0.46958419	0.632	0.321	8.65E-68	4	Sdcbp
Lasp11	6.78E-72	0.34882124	0.444	0.162	9.21E-68	4	Lasp1
Dusp12	1.40E-71	0.52278131	0.732	0.384	1.90E-67	4	Dusp1
Ppp1r15a	1.79E-71	0.37781098	0.392	0.129	2.43E-67	4	Ppp1r15a
Gns	2.42E-70	0.38784274	0.448	0.17	3.28E-66	4	Gns
Mbnl2	3.96E-69	0.3871331	0.44	0.165	5.38E-65	4	Mbnl2
1810058l24Rik	1.28E-68	0.41614748	0.516	0.225	1.73E-64	4	1810058l24
Ubc2	9.06E-68	0.48459546	0.773	0.505	1.23E-63	4	Ubc
Eif5	7.09E-67	0.46809572	0.597	0.305	9.62E-63	4	Eif5
Ctsd1	1.46E-65	0.33091516	0.824	0.508	1.98E-61	4	Ctsd
Lyst2	1.59E-65	0.43243077	0.585	0.268	2.16E-61	4	Lyst
Osgin1	4.11E-65	0.27207141	0.321	0.095	5.58E-61	4	Osgin1

Bcl2l1	1.79E-64	0.26974877	0.337	0.105	2.43E-60	4	Bcl2l1
Mif	2.06E-63	0.57463582	0.579	0.302	2.80E-59	4	Mif
Smox1	6.54E-63	0.35355677	0.4	0.142	8.87E-59	4	Smox
Pgam1	1.11E-62	0.4706058	0.563	0.283	1.50E-58	4	Pgam1
H3f3b3	1.91E-62	0.51289265	0.945	0.831	2.59E-58	4	H3f3b
Npc1	1.88E-61	0.28582556	0.331	0.105	2.55E-57	4	Npc1
Ptafr1	8.66E-60	0.3524022	0.473	0.199	1.18E-55	4	Ptafr
Rab71	9.44E-58	0.36946609	0.582	0.291	1.28E-53	4	Rab7
Ldha	3.70E-57	0.65606045	0.605	0.377	5.03E-53	4	Ldha
Cyp4f181	1.13E-54	0.59008357	0.547	0.287	1.54E-50	4	Cyp4f18
Rnh1	3.69E-54	0.39704167	0.494	0.233	5.01E-50	4	Rnh1
Ankrd12	4.07E-54	0.46326955	0.473	0.22	5.53E-50	4	Ankrd12
Slc7a11	4.45E-54	0.41092114	0.373	0.138	6.04E-50	4	Slc7a11
Btg13	4.53E-54	0.44893547	0.863	0.632	6.15E-50	4	Btg1
Cpne2	2.16E-53	0.2675508	0.294	0.093	2.93E-49	4	Cpne2
Txn11	7.32E-53	0.87834499	0.627	0.417	9.93E-49	4	Txn1
Mirt1	1.13E-52	0.28095845	0.305	0.101	1.54E-48	4	Mirt1
Acod11	1.40E-52	0.38686877	0.3	0.097	1.90E-48	4	Acod1
AC110211.12	2.15E-52	0.33138781	0.44	0.179	2.92E-48	4	AC110211.
Aldoa1	4.61E-52	0.44855532	0.677	0.419	6.26E-48	4	Aldoa
Eea1	9.68E-52	0.3015235	0.3	0.1	1.31E-47	4	Eea1
Neat12	1.44E-51	0.46310358	0.702	0.421	1.96E-47	4	Neat1
Gpr137b	5.24E-51	0.26300881	0.276	0.087	7.11E-47	4	Gpr137b
Pnpla7	5.66E-51	0.26639339	0.308	0.105	7.69E-47	4	Pnpla7
Srgn2	6.94E-50	0.36005046	0.923	0.668	9.43E-46	4	Srgn
Pkm2	9.91E-50	0.42361234	0.777	0.546	1.34E-45	4	Pkm
Cited2	2.05E-49	0.39109287	0.355	0.139	2.78E-45	4	Cited2
Kpna4	2.17E-49	0.26759842	0.348	0.131	2.95E-45	4	Kpna4
Dgkz	1.48E-48	0.29829673	0.408	0.176	2.01E-44	4	Dgkz
Eno11	2.90E-48	0.41317745	0.561	0.309	3.94E-44	4	Eno1
Itpr2	1.09E-46	0.41418208	0.269	0.092	1.48E-42	4	Itpr2
Atp6v0b	1.19E-46	0.36431641	0.616	0.371	1.62E-42	4	Atp6v0b
Grina2	1.38E-46	0.31896537	0.653	0.353	1.88E-42	4	Grina
Ptp4a1	7.99E-46	0.27856155	0.34	0.134	1.08E-41	4	Ptp4a1
Rnf1493	1.03E-45	0.38377599	0.685	0.421	1.40E-41	4	Rnf149
Slc2a1	1.68E-45	0.25272319	0.318	0.118	2.28E-41	4	Slc2a1
Cd300lf2	3.41E-45	0.33198821	0.539	0.275	4.63E-41	4	Cd300lf
Ubb3	1.61E-44	0.41176187	0.829	0.726	2.19E-40	4	Ubb
Psap1	3.74E-44	0.67176513	0.789	0.625	5.08E-40	4	Psap
Litaf	6.42E-44	0.31868078	0.456	0.222	8.72E-40	4	Litaf

Gapdh1	2.72E-43	0.55574688	0.8	0.683	3.69E-39	4	Gapdh
H3f3a2	2.94E-40	0.40721613	0.813	0.693	4.00E-36	4	H3f3a
Tra2a	3.77E-40	0.41315614	0.453	0.237	5.12E-36	4	Tra2a
Soat1	1.71E-39	0.27511427	0.376	0.17	2.33E-35	4	Soat1
Zfp292	1.06E-37	0.29619	0.418	0.207	1.43E-33	4	Zfp292
Map1lc3b1	1.34E-37	0.33031995	0.558	0.328	1.82E-33	4	Map1lc3b
Tyrobp3	3.70E-37	0.32228789	0.945	0.787	5.02E-33	4	Tyrobp
Ier51	1.66E-36	0.30879556	0.577	0.34	2.25E-32	4	Ier5
Cd442	6.68E-36	0.28938356	0.563	0.32	9.07E-32	4	Cd44
Tax1bp1	1.01E-35	0.28614623	0.489	0.271	1.37E-31	4	Tax1bp1
Atp6v0e	1.31E-35	0.34207087	0.55	0.346	1.78E-31	4	Atp6v0e
Csf11	1.37E-35	0.30219377	0.339	0.146	1.86E-31	4	Csf1
Ostf1	1.63E-35	0.3770702	0.56	0.361	2.21E-31	4	Ostf1
Por	2.90E-35	0.25952831	0.315	0.135	3.94E-31	4	Por
Ccnl1	2.64E-34	0.32221706	0.484	0.273	3.58E-30	4	Ccnl1
Tnfrsf1b	4.74E-33	0.26579601	0.361	0.172	6.43E-29	4	Tnfrsf1b
Atp6v1e1	4.76E-32	0.25992543	0.376	0.189	6.46E-28	4	Atp6v1e1
Atp6v1g1	1.54E-31	0.29244426	0.566	0.36	2.09E-27	4	Atp6v1g1
Rsrc2	1.96E-31	0.30922994	0.389	0.204	2.66E-27	4	Rsrc2
Hk2	6.59E-31	0.52222041	0.323	0.159	8.95E-27	4	Hk2
Rbpj	1.47E-30	0.26170414	0.392	0.203	1.99E-26	4	Rbpj
Lgals31	4.03E-30	0.4379803	0.598	0.398	5.47E-26	4	Lgals3
Fxyd53	1.72E-27	0.26050383	0.823	0.685	2.34E-23	4	Fxyd5
Rps27	3.64E-27	0.26650506	0.929	0.87	4.95E-23	4	Rps27
Gna13	1.34E-26	0.25716749	0.329	0.167	1.82E-22	4	Gna13
Snx201	1.34E-26	0.26206304	0.431	0.248	1.82E-22	4	Snx20
Gng52	1.39E-26	0.27883724	0.689	0.541	1.89E-22	4	Gng5
Nisch	1.86E-26	0.30008722	0.415	0.241	2.52E-22	4	Nisch
Klf6	2.48E-26	0.28777037	0.473	0.283	3.37E-22	4	Klf6
AA467197	3.25E-26	0.32719142	0.358	0.185	4.41E-22	4	AA467197
Fcer1g3	8.28E-26	0.27517184	0.894	0.752	1.12E-21	4	Fcer1g
Efhd2	1.52E-25	0.26985635	0.521	0.34	2.06E-21	4	Efhd2
Egr12	1.06E-24	0.28586683	0.453	0.263	1.44E-20	4	Egr1
Prdx6	9.44E-22	0.2697511	0.402	0.238	1.28E-17	4	Prdx6
Pgk1	1.98E-19	0.27377841	0.4	0.251	2.69E-15	4	Pgk1
Zfp36l2	5.95E-18	0.29905441	0.553	0.411	8.07E-14	4	Zfp36l2
Plbd1	1.11E-13	0.26931357	0.342	0.224	1.51E-09	4	Plbd1
Hsp90aa1	6.73E-08	0.27008335	0.382	0.302	0.00091359	4	Hsp90aa1
AW112010	0	1.31070878	0.904	0.146	0	5	AW112010
Trbc2	0	1.27035035	0.848	0.044	0	5	Trbc2

Cd3g	0	1.09843038	0.832	0.045	0	5	Cd3g
Nkg7	0	1.05083312	0.717	0.043	0	5	Nkg7
Tnfrsf4	0	0.96616541	0.549	0.015	0	5	Tnfrsf4
Cd3d	0	0.9386687	0.799	0.045	0	5	Cd3d
Trac	0	0.91737036	0.717	0.042	0	5	Trac
Tnfrsf18	0	0.76187511	0.585	0.032	0	5	Tnfrsf18
Ptprcap	0	0.75757735	0.734	0.055	0	5	Ptprcap
Odc1	0	0.75538968	0.471	0.038	0	5	Odc1
H2-Q7	0	0.75199661	0.757	0.124	0	5	H2-Q7
Cd2	0	0.72089158	0.636	0.03	0	5	Cd2
Cd3e	0	0.68837717	0.694	0.038	0	5	Cd3e
Icos	0	0.68018685	0.464	0.016	0	5	Icos
Ctla2a	0	0.64919411	0.46	0.034	0	5	Ctla2a
Gimap4	0	0.62437578	0.591	0.031	0	5	Gimap4
Thy1	0	0.61559665	0.618	0.035	0	5	Thy1
Lck	0	0.60238277	0.65	0.037	0	5	Lck
Gimap3	0	0.56899473	0.574	0.026	0	5	Gimap3
Gimap1	0	0.54212188	0.572	0.035	0	5	Gimap1
Ets1	0	0.5372332	0.529	0.046	0	5	Ets1
Il2rb	0	0.53072901	0.52	0.035	0	5	Il2rb
Cd28	0	0.50929891	0.486	0.015	0	5	Cd28
Lat	0	0.45108756	0.466	0.025	0	5	Lat
Gimap6	0	0.42688525	0.433	0.026	0	5	Gimap6
Skap1	0	0.42237237	0.475	0.025	0	5	Skap1
Cd4	0	0.38453758	0.35	0.01	0	5	Cd4
Gimap5	0	0.37002845	0.413	0.022	0	5	Gimap5
Bcl11b	0	0.36972009	0.413	0.021	0	5	Bcl11b
Cd247	0	0.36580913	0.357	0.013	0	5	Cd247
Zap70	0	0.36362019	0.379	0.016	0	5	Zap70
Cd5	0	0.31788409	0.315	0.008	0	5	Cd5
Ctla4	7.87E-308	0.43948173	0.33	0.012	1.07E-303	5	Ctla4
1-Sep	3.44E-304	0.40483466	0.46	0.037	4.68E-300	5	
Pdcd1	5.84E-300	0.44963465	0.426	0.03	7.92E-296	5	Pdcd1
Ctsw	2.68E-299	0.46265894	0.444	0.034	3.64E-295	5	Ctsw
Ms4a4b	9.57E-297	0.67455676	0.578	0.067	1.30E-292	5	Ms4a4b
S100a10	3.72E-296	0.82522366	0.812	0.158	5.05E-292	5	S100a10
Il7r	1.61E-291	0.68049286	0.518	0.055	2.18E-287	5	Il7r
Ikzf2	4.21E-287	0.58512374	0.342	0.017	5.71E-283	5	Ikzf2
Inpp4b	3.68E-280	0.35729593	0.391	0.027	5.00E-276	5	Inpp4b
Trbc1	2.85E-276	0.70483291	0.389	0.027	3.87E-272	5	Trbc1

Rps15a	6.59E-273	1.2289765	0.995	0.643	8.95E-269	5	Rps15a
Ptpn22	1.11E-268	0.43289895	0.482	0.05	1.50E-264	5	Ptpn22
Rpl12	2.18E-265	1.10160406	0.982	0.468	2.96E-261	5	Rpl12
Sh2d1a	1.91E-264	0.32585911	0.303	0.013	2.59E-260	5	Sh2d1a
Sh2d2a	9.33E-251	0.33991685	0.366	0.026	1.27E-246	5	Sh2d2a
Tnfrsf9	5.87E-250	0.47975305	0.337	0.021	7.97E-246	5	Tnfrsf9
Ltb	2.57E-245	0.72045713	0.723	0.151	3.48E-241	5	Ltb
Cd6	1.86E-244	0.29066793	0.274	0.011	2.53E-240	5	Cd6
Gm8369	9.74E-244	0.38960288	0.386	0.033	1.32E-239	5	Gm8369
Rabgap1l	9.70E-239	0.33536034	0.388	0.034	1.32E-234	5	Rabgap1l
Rps24	2.11E-235	1.00702375	0.998	0.743	2.86E-231	5	Rps24
Dusp2	6.57E-233	0.53293069	0.516	0.072	8.92E-229	5	Dusp2
Sdf4	1.17E-229	1.01232219	0.654	0.148	1.58E-225	5	Sdf4
Il18r1	1.98E-229	0.30599235	0.297	0.017	2.69E-225	5	Il18r1
Rpl5	1.09E-224	0.88604178	0.946	0.427	1.48E-220	5	Rpl5
Ablim1	1.44E-224	0.32162191	0.351	0.029	1.96E-220	5	Ablim1
Rpl3	4.10E-223	0.86827777	0.966	0.444	5.56E-219	5	Rpl3
Cxcr6	7.28E-219	0.46994303	0.384	0.036	9.89E-215	5	Cxcr6
Rps18	8.51E-219	0.92212113	0.98	0.577	1.16E-214	5	Rps18
Gimap9	4.85E-215	0.26874122	0.29	0.018	6.58E-211	5	Gimap9
Cxcr3	7.02E-208	0.25738977	0.264	0.015	9.53E-204	5	Cxcr3
Rps4x	2.23E-205	0.87198162	0.984	0.529	3.02E-201	5	Rps4x
Rpl13	4.09E-205	0.85469653	0.998	0.756	5.56E-201	5	Rpl13
Rpsa	3.35E-204	0.87108154	0.996	0.65	4.55E-200	5	Rpsa
Rps23	3.62E-204	0.79008626	0.986	0.705	4.91E-200	5	Rps23
Rpl27a	4.65E-204	0.78994997	0.993	0.784	6.31E-200	5	Rpl27a
Cst7	1.73E-200	0.31467229	0.391	0.043	2.35E-196	5	Cst7
Rps3a1	1.36E-198	0.83189705	0.982	0.707	1.85E-194	5	Rps3a1
Tox	1.14E-195	0.25337268	0.261	0.016	1.54E-191	5	Tox
Rps14	9.05E-195	0.73343322	0.998	0.792	1.23E-190	5	Rps14
Cish	7.05E-194	0.30126107	0.317	0.027	9.57E-190	5	Cish
Rpl19	1.31E-193	0.73845949	0.995	0.756	1.78E-189	5	Rpl19
Ly6a	2.36E-193	0.69707076	0.638	0.135	3.21E-189	5	Ly6a
Tmsb10	4.27E-193	0.74533664	0.929	0.321	5.79E-189	5	Tmsb10
Rps7	5.17E-193	0.81096564	0.975	0.582	7.01E-189	5	Rps7
Shisa5	1.39E-192	0.64081927	0.826	0.272	1.89E-188	5	Shisa5
Rplp11	5.11E-192	0.77968451	0.995	0.834	6.94E-188	5	Rplp1
Rps13	7.37E-191	0.76066422	0.98	0.704	1.00E-186	5	Rps13
Tpt1	1.05E-188	0.74302073	0.998	0.945	1.43E-184	5	Tpt1
Eef1a1	1.09E-186	0.76008675	0.993	0.859	1.47E-182	5	Eef1a1

Pkp3	4.78E-185	0.27668211	0.303	0.026	6.49E-181	5	Pkp3
Msi2	7.33E-185	0.28220651	0.313	0.029	9.95E-181	5	Msi2
Rpl30	7.28E-184	0.7588994	0.978	0.715	9.88E-180	5	Rpl30
Rps10	8.12E-180	0.73849196	0.986	0.758	1.10E-175	5	Rps10
H2-K1	3.22E-179	0.82961713	0.969	0.555	4.37E-175	5	H2-K1
Rpl23	4.95E-177	0.69583696	0.995	0.845	6.72E-173	5	Rpl23
Rpl22	1.77E-176	0.68089544	0.946	0.467	2.40E-172	5	Rpl22
Rpl32	1.40E-175	0.80005602	0.991	0.666	1.90E-171	5	Rpl32
Rpl9	2.73E-175	0.6954583	0.978	0.706	3.71E-171	5	Rpl9
Rack1	1.59E-172	0.7120201	0.94	0.494	2.17E-168	5	Rack1
Rpl17	1.96E-172	0.6874616	0.993	0.782	2.67E-168	5	Rpl17
Rps20	3.89E-172	0.80916553	0.973	0.624	5.28E-168	5	Rps20
Rpl11	3.03E-170	0.67482572	0.976	0.642	4.11E-166	5	Rpl11
Rps3	1.17E-169	0.66628149	0.989	0.702	1.59E-165	5	Rps3
Rpl7	1.50E-169	0.67264083	0.957	0.527	2.04E-165	5	Rpl7
Rps5	1.72E-169	0.73514735	0.978	0.607	2.34E-165	5	Rps5
Rpl39	7.32E-165	0.7074698	0.989	0.725	9.94E-161	5	Rpl39
Rpl34	1.60E-163	0.66790536	0.989	0.754	2.17E-159	5	Rpl34
Rpl29	1.84E-163	0.655639	0.897	0.395	2.50E-159	5	Rpl29
Rpl23a	9.12E-163	0.64582039	0.92	0.439	1.24E-158	5	Rpl23a
Rps6	4.77E-162	0.68257331	0.942	0.492	6.47E-158	5	Rps6
Pdcd4	8.02E-162	0.34729758	0.377	0.054	1.09E-157	5	Pdcd4
Eef1b2	1.19E-161	0.65069777	0.866	0.36	1.62E-157	5	Eef1b2
Rps15	5.29E-160	0.64063115	0.949	0.524	7.19E-156	5	Rps15
Lgals1	2.51E-157	0.70900236	0.728	0.225	3.41E-153	5	Lgals1
Rpl22l1	4.45E-157	0.61179584	0.737	0.247	6.04E-153	5	Rpl22l1
Rac21	1.17E-155	0.59469164	0.848	0.332	1.59E-151	5	Rac2
Tbc1d10c	1.90E-154	0.26283068	0.319	0.038	2.58E-150	5	Tbc1d10c
Rplp0	6.65E-154	0.7173751	0.982	0.652	9.03E-150	5	Rplp0
Rinl	3.30E-153	0.36373512	0.471	0.091	4.48E-149	5	Rinl
Rps16	1.29E-151	0.6393008	0.995	0.846	1.75E-147	5	Rps16
Rpl10a1	3.94E-151	0.64321532	0.933	0.434	5.34E-147	5	Rpl10a
Rpl36a	3.85E-150	0.64402848	0.844	0.345	5.23E-146	5	Rpl36a
Rpl21	8.15E-150	0.62801053	0.973	0.729	1.11E-145	5	Rpl21
Rpl27	8.20E-150	0.57888337	0.841	0.351	1.11E-145	5	Rpl27
Tbc1d4	1.65E-148	0.31143726	0.272	0.027	2.24E-144	5	Tbc1d4
Eif3e	9.33E-148	0.38985275	0.554	0.131	1.27E-143	5	Eif3e
Rpl24	7.07E-147	0.61162254	0.946	0.583	9.60E-143	5	Rpl24
Rpl18a	5.04E-146	0.63156694	0.995	0.816	6.84E-142	5	Rpl18a
Rpl14	6.21E-146	0.61229381	0.928	0.477	8.44E-142	5	Rpl14

Rpl8	1.12E-145	0.60148367	0.978	0.682	1.52E-141	5	Rpl8
Pla2g16	1.38E-145	0.31523107	0.38	0.061	1.88E-141	5	Pla2g16
Rpl4	1.59E-144	0.58863526	0.866	0.364	2.15E-140	5	Rpl4
Ndfip1	3.94E-140	0.2870697	0.342	0.051	5.35E-136	5	Ndfip1
Naca	2.38E-139	0.56824541	0.879	0.405	3.23E-135	5	Naca
Rpl26	3.05E-139	0.58495591	0.98	0.696	4.15E-135	5	Rpl26
Bcl2	2.78E-138	0.3892916	0.339	0.05	3.78E-134	5	Bcl2
Rps12	3.91E-137	0.61181601	0.991	0.793	5.31E-133	5	Rps12
Anxa6	2.91E-136	0.32043575	0.404	0.074	3.95E-132	5	Anxa6
Rpl15	1.27E-135	0.61079331	0.937	0.518	1.73E-131	5	Rpl15
Npm1	1.28E-135	0.52339637	0.737	0.258	1.74E-131	5	Npm1
Rpl18	5.61E-135	0.5886987	0.976	0.681	7.62E-131	5	Rpl18
Rps11	1.30E-133	0.60849987	0.996	0.726	1.77E-129	5	Rps11
Rps19	7.19E-132	0.63778932	0.995	0.691	9.76E-128	5	Rps19
Eif3h	8.94E-132	0.45311829	0.685	0.229	1.21E-127	5	Eif3h
Fkbp3	1.17E-131	0.27692474	0.351	0.057	1.60E-127	5	Fkbp3
Ptpn18	2.13E-129	0.50390252	0.717	0.259	2.89E-125	5	Ptpn18
Rplp2	6.48E-128	0.52355226	0.989	0.786	8.80E-124	5	Rplp2
Ccl5	1.83E-126	1.20508096	0.431	0.09	2.49E-122	5	Ccl5
Spn	1.03E-124	0.26744879	0.319	0.049	1.40E-120	5	Spn
Cd82	2.37E-124	0.42463536	0.476	0.116	3.22E-120	5	Cd82
Serpina3g	5.16E-124	0.30519368	0.326	0.051	7.00E-120	5	Serpina3g
Rps8	7.49E-121	0.56749903	0.98	0.819	1.02E-116	5	Rps8
Rhoh	1.13E-119	0.32098371	0.442	0.099	1.54E-115	5	Rhoh
Il2rg	5.56E-119	0.28629192	0.389	0.078	7.55E-115	5	Il2rg
Ppia	2.17E-118	0.54796804	0.911	0.501	2.94E-114	5	Ppia
Hcst	8.08E-118	0.42045839	0.553	0.158	1.10E-113	5	Hcst
Eef1g	1.34E-116	0.433677	0.607	0.197	1.82E-112	5	Eef1g
Lag3	3.00E-116	0.26757742	0.303	0.047	4.08E-112	5	Lag3
Rpl36	1.27E-114	0.55011099	0.969	0.616	1.73E-110	5	Rpl36
H2afv	2.87E-114	0.28189492	0.37	0.073	3.90E-110	5	H2afv
Ccnd2	4.29E-114	0.42259717	0.514	0.14	5.82E-110	5	Ccnd2
Rps22	5.87E-114	0.56871364	0.949	0.63	7.96E-110	5	Rps2
Eef1d	8.84E-113	0.35551263	0.565	0.171	1.20E-108	5	Eef1d
Rpl6	2.98E-110	0.50433115	0.971	0.644	4.05E-106	5	Rpl6
Sumo2	3.19E-110	0.42170875	0.647	0.234	4.33E-106	5	Sumo2
Rpl7a	2.03E-107	0.48924303	0.889	0.44	2.76E-103	5	Rpl7a
Smc4	3.06E-105	0.27076794	0.315	0.057	4.16E-101	5	Smc4
Rps21	7.52E-105	0.52799806	0.967	0.738	1.02E-100	5	Rps21
Klrd1	2.32E-103	0.45675563	0.375	0.082	3.15E-99	5	Klrd1

Ifi27	8.13E-102	0.26242945	0.322	0.062	1.10E-97	5	Ifi27	
Fkbp1a	5.84E-100	0.28774435	0.393	0.093	7.93E-96	5	Fkbp1a	
S100a13	1.24E-99	0.31700037	0.426	0.11	1.69E-95	5	S100a13	
Snrpf	1.28E-99	0.29988953	0.455	0.122	1.74E-95	5	Snrpf	
Btf3	2.96E-99	0.41866327	0.813	0.381	4.02E-95	5	Btf3	
Limd2	1.86E-97	0.34177161	0.542	0.171	2.52E-93	5	Limd2	
Hsp90ab11	3.07E-97	0.48992975	0.841	0.401	4.17E-93	5	Hsp90ab11	
Hnrnpa1	5.75E-97	0.34969824	0.502	0.152	7.81E-93	5	Hnrnpa1	
Mbnl1	2.41E-96	0.41679345	0.652	0.245	3.27E-92	5	Mbnl1	
Cyb5a	1.14E-93	0.25150264	0.321	0.066	1.54E-89	5	Cyb5a	
Slc25a4	3.39E-93	0.25241084	0.348	0.077	4.60E-89	5	Slc25a4	
Rps27a	2.48E-92	0.46121857	0.975	0.806	3.36E-88	5	Rps27a	
Rbm3	3.20E-90	0.43824491	0.804	0.396	4.34E-86	5	Rbm3	
Rpl37a	1.51E-89	0.46165519	0.986	0.811	2.05E-85	5	Rpl37a	
Arl6ip1	4.27E-89	0.42922311	0.591	0.221	5.79E-85	5	Arl6ip1	
Uqcrh	2.85E-88	0.42689061	0.73	0.349	3.87E-84	5	Uqcrh	
Kmt2a	7.98E-88	0.25749537	0.361	0.087	1.08E-83	5	Kmt2a	
Aes	2.91E-86	0.30535079	0.471	0.146	3.95E-82	5	Aes	
Rps26	5.14E-86	0.4687765	0.922	0.598	6.98E-82	5	Rps26	
Ifi27l2a	4.56E-82	0.62988432	0.647	0.26	6.19E-78	5	Ifi27l2a	
Rpl13a	9.08E-82	0.34154223	0.496	0.168	1.23E-77	5	Rpl13a	
Eif3f	4.38E-81	0.36382953	0.69	0.298	5.94E-77	5	Eif3f	
Atp5g2	1.25E-80	0.34405252	0.621	0.251	1.69E-76	5	Atp5g2	
Maf	9.09E-80	0.49854129	0.38	0.108	1.23E-75	5	Maf	
Eif3m	8.27E-79	0.28168037	0.431	0.133	1.12E-74	5	Eif3m	
Nol7	1.84E-78	0.27806891	0.395	0.113	2.50E-74	5	Nol7	
Hif1a	2.28E-78	0.3919549	0.467	0.159	3.10E-74	5	Hif1a	
Serbp1	1.20E-77	0.35357167	0.641	0.274	1.63E-73	5	Serbp1	
Akap13	2.53E-77	0.3717877	0.6	0.249	3.44E-73	5	Akap13	
Ran	2.81E-76	0.28976023	0.458	0.149	3.81E-72	5	Ran	
Pfdn5	2.54E-75	0.38196985	0.788	0.414	3.44E-71	5	Pfdn5	
Psmb8	2.68E-75	0.36168741	0.707	0.32	3.64E-71	5	Psmb8	
Snrpe	4.21E-73	0.29118307	0.514	0.188	5.71E-69	5	Snrpe	
Eef2	3.03E-72	0.40506747	0.777	0.419	4.11E-68	5	Eef2	
Pebp1	1.51E-71	0.263107	0.402	0.125	2.05E-67	5	Pebp1	
Cox7a2l	1.71E-71	0.31458419	0.563	0.227	2.32E-67	5	Cox7a2l	
	7-Sep	1.46E-68	0.29516824	0.495	0.186	1.98E-64	5	
Eif3i	5.12E-67	0.25209391	0.386	0.121	6.95E-63	5	Eif3i	
Park7	3.30E-66	0.26369801	0.411	0.137	4.48E-62	5	Park7	
Psmb1	1.53E-65	0.27704935	0.513	0.2	2.08E-61	5	Psmb1	

Rpl35a	1.58E-64	0.37708744	0.967	0.818	2.14E-60	5	Rpl35a
Dad1	1.51E-63	0.28025621	0.518	0.208	2.05E-59	5	Dad1
Arhgdib	2.60E-62	0.34888885	0.687	0.348	3.52E-58	5	Arhgdib
Rps271	8.09E-62	0.38635182	0.986	0.865	1.10E-57	5	Rps27
Rps171	8.49E-62	0.35671071	0.708	0.369	1.15E-57	5	Rps17
Eea11	1.74E-61	0.31790875	0.33	0.099	2.36E-57	5	Eea1
Rpl38	4.47E-60	0.42268536	0.92	0.65	6.07E-56	5	Rpl38
Abrac1	6.85E-60	0.27039636	0.476	0.185	9.30E-56	5	Abrac1
Anp32b	1.58E-59	0.27658788	0.505	0.205	2.14E-55	5	Anp32b
Sub1	5.24E-58	0.31242975	0.612	0.283	7.12E-54	5	Sub1
Rps25	1.37E-55	0.32500182	0.895	0.621	1.86E-51	5	Rps25
Psmb9	1.68E-55	0.25174979	0.429	0.16	2.28E-51	5	Psmb9
Ndufa4	1.01E-53	0.26023223	0.476	0.197	1.36E-49	5	Ndufa4
Srsf3	2.81E-53	0.27591941	0.478	0.202	3.81E-49	5	Srsf3
Ogt	3.91E-53	0.26179934	0.466	0.189	5.31E-49	5	Ogt
Cox6c	5.85E-52	0.26747162	0.616	0.299	7.94E-48	5	Cox6c
Atp5h	1.14E-51	0.28339962	0.643	0.331	1.54E-47	5	Atp5h
Cox7c	1.60E-51	0.29119004	0.645	0.339	2.18E-47	5	Cox7c
Itgb1	1.41E-50	0.27677412	0.357	0.13	1.92E-46	5	Itgb1
H2-D1	1.50E-49	0.33943884	0.94	0.672	2.04E-45	5	H2-D1
Ptma1	2.01E-49	0.37138472	0.855	0.537	2.73E-45	5	Ptma
Hint1	4.38E-49	0.25366152	0.525	0.236	5.95E-45	5	Hint1
Ppib	1.07E-48	0.26050406	0.569	0.276	1.46E-44	5	Ppib
Tmsb4x	5.61E-48	0.34075592	1	0.956	7.62E-44	5	Tmsb4x
Slc25a3	2.31E-47	0.26642804	0.574	0.284	3.13E-43	5	Slc25a3
B2m1	1.41E-46	0.28605814	0.937	0.671	1.91E-42	5	B2m
Rpl28	3.34E-45	0.30789742	0.94	0.684	4.53E-41	5	Rpl28
S100a4	4.64E-45	0.38491281	0.538	0.241	6.31E-41	5	S100a4
Gnas	8.48E-43	0.26579246	0.627	0.346	1.15E-38	5	Gnas
Rpl31	2.13E-41	0.25043102	0.632	0.344	2.89E-37	5	Rpl31
Capg	1.48E-40	0.26316272	0.513	0.25	2.01E-36	5	Capg
Pabpc1	3.99E-39	0.27894176	0.625	0.364	5.42E-35	5	Pabpc1
H2afz	6.32E-39	0.31012954	0.601	0.323	8.58E-35	5	H2afz
Ifngr1	1.71E-36	0.31062243	0.455	0.231	2.33E-32	5	Ifngr1
Rpl37	1.34E-33	0.27306545	0.947	0.79	1.82E-29	5	Rpl37
Myl6	1.95E-30	0.25146303	0.792	0.538	2.65E-26	5	Myl6
Rpl35	1.67E-28	0.2564852	0.652	0.396	2.27E-24	5	Rpl35
Fn1	0	1.22821542	0.723	0.082	0	6	Fn1
S100a41	0	1.20821848	0.916	0.213	0	6	S100a4
F13a1	0	0.91447633	0.588	0.039	0	6	F13a1

Chil3	5.35E-293	1.9294092	0.658	0.101	7.26E-289	6	Chil3
Vcan	3.05E-273	0.46102304	0.326	0.015	4.14E-269	6	Vcan
Ccl9	3.29E-272	0.73242284	0.506	0.054	4.46E-268	6	Ccl9
Lyz21	5.22E-256	1.91913286	0.951	0.389	7.09E-252	6	Lyz2
Ms4a6c1	2.07E-234	0.74376197	0.836	0.206	2.82E-230	6	Ms4a6c
Emp3	8.60E-224	0.77986429	0.82	0.234	1.17E-219	6	Emp3
Ccr2	1.80E-209	0.75024009	0.723	0.165	2.44E-205	6	Ccr2
Ahnak	5.10E-203	0.64467799	0.66	0.14	6.93E-199	6	Ahnak
Crip1	2.57E-199	1.0127757	0.793	0.23	3.49E-195	6	Crip1
Clec4a3	5.97E-194	0.42901353	0.422	0.053	8.10E-190	6	Clec4a3
Mafb1	7.58E-189	0.84200134	0.73	0.188	1.03E-184	6	Mafb
Lgals32	2.17E-186	1.12157878	0.914	0.376	2.95E-182	6	Lgals3
Ifitm3	7.47E-183	1.01710427	0.859	0.311	1.01E-178	6	Ifitm3
Ifitm6	3.67E-177	0.62996998	0.449	0.07	4.98E-173	6	Ifitm6
Mcub	5.00E-168	0.26014332	0.291	0.026	6.79E-164	6	Mcub
Dbi	9.35E-168	0.52105021	0.611	0.145	1.27E-163	6	Dbi
Gpx1	1.44E-166	0.81852696	0.881	0.366	1.96E-162	6	Gpx1
Vim	1.73E-166	1.20651389	0.826	0.345	2.35E-162	6	Vim
S100a101	6.57E-165	0.7272643	0.672	0.173	8.93E-161	6	S100a10
Tgfb1	3.07E-160	1.03207093	0.844	0.318	4.16E-156	6	Tgfb1
Msr1	3.19E-155	0.43540776	0.439	0.075	4.33E-151	6	Msr1
Ms4a6d1	3.21E-152	0.58978564	0.59	0.141	4.35E-148	6	Ms4a6d
Ccl61	3.39E-147	0.81921393	0.598	0.154	4.60E-143	6	Ccl6
Clec4a1	5.29E-145	0.302947	0.328	0.042	7.18E-141	6	Clec4a1
Flna	1.18E-143	0.41905142	0.527	0.118	1.61E-139	6	Flna
Plac8	7.63E-142	0.661898	0.66	0.177	1.04E-137	6	Plac8
Tgfb1	7.23E-137	0.54270965	0.66	0.205	9.81E-133	6	Tgfb1
Lrp11	4.66E-136	0.46493447	0.568	0.141	6.33E-132	6	Lrp1
Smpdl3a	5.10E-136	0.44621354	0.449	0.092	6.92E-132	6	Smpdl3a
Mgst1	1.61E-133	0.34885362	0.33	0.047	2.19E-129	6	Mgst1
Anxa5	2.52E-132	0.44922769	0.529	0.13	3.42E-128	6	Anxa5
Tmsb101	6.70E-129	0.75564632	0.824	0.334	9.10E-125	6	Tmsb10
Sirpb1c	3.42E-126	0.39710954	0.494	0.116	4.64E-122	6	Sirpb1c
Napsa	2.15E-122	0.45669903	0.6	0.171	2.92E-118	6	Napsa
Ctsc1	2.82E-122	0.48142959	0.664	0.2	3.82E-118	6	Ctsc
Pid1	1.89E-113	0.40497537	0.477	0.114	2.56E-109	6	Pid1
Cybb1	5.25E-110	0.52032612	0.6	0.187	7.12E-106	6	Cybb
Anxa21	1.88E-109	0.62389676	0.752	0.318	2.56E-105	6	Anxa2
Wfdc171	1.66E-108	0.50586243	0.635	0.202	2.25E-104	6	Wfdc17
Atp1a1	7.61E-108	0.33869736	0.5	0.132	1.03E-103	6	Atp1a1

Aprt	4.29E-106	0.45631974	0.617	0.209	5.83E-102	6	Aprt
Ctss1	1.15E-105	0.40738477	0.965	0.43	1.55E-101	6	Ctss
Rpl36al	1.62E-102	0.40155337	0.686	0.252	2.20E-98	6	Rpl36al
Sec61g	6.26E-100	0.44476536	0.723	0.292	8.50E-96	6	Sec61g
Hp1	1.65E-99	0.59178429	0.471	0.131	2.24E-95	6	Hp
Clec4a2	4.27E-98	0.29895492	0.344	0.069	5.80E-94	6	Clec4a2
Metrn1	1.94E-97	0.33275865	0.395	0.092	2.64E-93	6	Metrn1
Cd681	4.05E-96	0.43826704	0.701	0.263	5.50E-92	6	Cd68
Rap1b	7.02E-92	0.45330109	0.65	0.26	9.53E-88	6	Rap1b
Emb	1.01E-89	0.34496414	0.48	0.141	1.37E-85	6	Emb
Sec61b	3.90E-89	0.42513012	0.719	0.316	5.29E-85	6	Sec61b
Npc21	2.25E-88	0.41235288	0.84	0.376	3.05E-84	6	Npc2
Tln1	5.45E-88	0.4108838	0.729	0.324	7.40E-84	6	Tln1
Lamp11	8.88E-87	0.36364091	0.68	0.262	1.21E-82	6	Lamp1
Slc25a5	1.26E-86	0.35981585	0.619	0.231	1.71E-82	6	Slc25a5
F10	1.43E-86	0.3612777	0.359	0.083	1.95E-82	6	F10
Fcgr2b1	5.60E-86	0.42063413	0.49	0.151	7.60E-82	6	Fcgr2b
Irf5	1.32E-83	0.27508687	0.4	0.105	1.79E-79	6	Irf5
Pitpna	1.38E-83	0.3995899	0.676	0.285	1.87E-79	6	Pitpna
Ecm1	1.23E-81	0.48652864	0.312	0.07	1.67E-77	6	Ecm1
Mrpl33	1.31E-79	0.37935184	0.559	0.205	1.78E-75	6	Mrpl33
Prdx11	2.17E-79	0.44243479	0.611	0.232	2.94E-75	6	Prdx1
Rpl10	4.73E-78	0.41632988	0.953	0.685	6.42E-74	6	Rpl10
Emilin21	7.61E-78	0.35396591	0.598	0.221	1.03E-73	6	Emilin2
Lgmn1	1.09E-77	0.57053403	0.596	0.228	1.47E-73	6	Lgmn
Esd	1.72E-77	0.35477001	0.49	0.163	2.33E-73	6	Esd
Lst1	3.68E-77	0.40807057	0.713	0.306	4.99E-73	6	Lst1
Thbs11	4.62E-75	0.7975466	0.334	0.084	6.28E-71	6	Thbs1
Akr1a11	1.28E-74	0.34250935	0.646	0.266	1.74E-70	6	Akr1a1
Sem1	2.29E-74	0.37820196	0.82	0.429	3.11E-70	6	Sem1
Fcgr1	3.67E-74	0.29511615	0.424	0.124	4.99E-70	6	Fcgr1
Pld41	5.05E-74	0.27571423	0.494	0.16	6.86E-70	6	Pld4
Atp5h1	5.46E-74	0.33709422	0.721	0.327	7.41E-70	6	Atp5h
Tkt	7.00E-73	0.33278296	0.482	0.168	9.50E-69	6	Tkt
Hspa81	2.65E-72	0.43719635	0.854	0.473	3.59E-68	6	Hspa8
Eif4a1	1.30E-71	0.37518182	0.711	0.337	1.77E-67	6	Eif4a1
Psma7	5.50E-71	0.32217108	0.604	0.245	7.47E-67	6	Psma7
Gda1	1.28E-70	0.31661954	0.438	0.138	1.74E-66	6	Gda
Rplp01	9.79E-70	0.4294687	0.934	0.658	1.33E-65	6	Rplp0
Ndufa41	2.35E-69	0.29819333	0.525	0.195	3.20E-65	6	Ndufa4

Tspo	2.93E-69	0.35748023	0.721	0.338	3.97E-65	6	Tspo
Tagln2	7.24E-67	0.40899792	0.494	0.183	9.82E-63	6	Tagln2
Rpl291	2.31E-66	0.3785054	0.807	0.405	3.13E-62	6	Rpl29
Lgals11	5.81E-66	0.55034835	0.578	0.24	7.89E-62	6	Lgals1
Csf1r1	3.48E-65	0.25837387	0.615	0.239	4.72E-61	6	Csf1r
Gm2a	6.35E-65	0.33379607	0.668	0.29	8.62E-61	6	Gm2a
Ppp1ca	2.56E-64	0.28967535	0.623	0.266	3.47E-60	6	Ppp1ca
Tmsb4x1	4.48E-63	0.40905737	0.996	0.956	6.09E-59	6	Tmsb4x
Hint11	5.62E-61	0.28248855	0.568	0.235	7.63E-57	6	Hint1
Adgre5	4.01E-60	0.2843804	0.428	0.148	5.44E-56	6	Adgre5
Rpl351	1.18E-59	0.34256942	0.76	0.389	1.60E-55	6	Rpl35
Calm1	1.25E-59	0.39655199	0.828	0.513	1.69E-55	6	Calm1
Ucp21	3.30E-59	0.33740627	0.758	0.379	4.48E-55	6	Ucp2
Pirb	8.52E-59	0.28823923	0.451	0.165	1.16E-54	6	Pirb
Atp5a1	9.50E-59	0.26131041	0.496	0.192	1.29E-54	6	Atp5a1
Capg1	2.29E-58	0.3435689	0.568	0.247	3.11E-54	6	Capg
Capzb	4.66E-58	0.30020912	0.689	0.336	6.32E-54	6	Capzb
Ctsa1	1.15E-57	0.26049237	0.588	0.245	1.56E-53	6	Ctsa
Psap2	4.95E-57	0.31895263	0.965	0.613	6.72E-53	6	Psap
Rpl7a1	7.17E-57	0.30909169	0.854	0.446	9.73E-53	6	Rpl7a
Manf	4.22E-56	0.27181347	0.404	0.142	5.72E-52	6	Manf
Dynll1	5.06E-56	0.3103401	0.617	0.288	6.86E-52	6	Dynll1
Itgb2	8.65E-56	0.29171618	0.57	0.249	1.17E-51	6	Itgb2
Atox1	2.02E-55	0.272443	0.768	0.373	2.74E-51	6	Atox1
Cox5b	2.71E-55	0.28186221	0.639	0.305	3.67E-51	6	Cox5b
Rnh11	3.74E-54	0.37794046	0.529	0.235	5.07E-50	6	Rnh1
Ybx11	5.37E-54	0.29715797	0.723	0.377	7.29E-50	6	Ybx1
Smdt1	8.26E-54	0.25165231	0.492	0.198	1.12E-49	6	Smdt1
Rps27a1	1.58E-53	0.36049335	0.945	0.809	2.14E-49	6	Rps27a
Rap1a	1.74E-53	0.26434385	0.504	0.206	2.37E-49	6	Rap1a
Gsr1	6.27E-53	0.27185107	0.531	0.223	8.52E-49	6	Gsr
Cox7c1	7.60E-53	0.27247464	0.686	0.338	1.03E-48	6	Cox7c
Capza2	2.71E-52	0.27100274	0.576	0.26	3.68E-48	6	Capza2
App	3.40E-52	0.25220896	0.414	0.152	4.62E-48	6	App
Ctsh1	1.54E-51	0.27611536	0.639	0.287	2.09E-47	6	Ctsh
Cox6c1	2.27E-51	0.26897456	0.627	0.3	3.09E-47	6	Cox6c
Cyba	2.59E-51	0.29748462	0.904	0.615	3.52E-47	6	Cyba
Cmtm7	4.14E-51	0.26665805	0.455	0.182	5.62E-47	6	Cmtm7
Tpt11	7.42E-51	0.32055532	0.994	0.945	1.01E-46	6	Tpt1
Atp5f1	1.13E-50	0.25820057	0.541	0.241	1.53E-46	6	Atp5f1

Rps28	1.25E-50	0.31917011	0.914	0.623	1.69E-46	6	Rps28
Prdx52	2.72E-50	0.3293149	0.811	0.45	3.69E-46	6	Prdx5
Rps4x1	2.73E-50	0.28656161	0.906	0.538	3.71E-46	6	Rps4x
Rps29	3.32E-50	0.3026027	0.988	0.862	4.51E-46	6	Rps29
Gnb2	6.24E-50	0.27450697	0.693	0.363	8.47E-46	6	Gnb2
Eif3f1	8.67E-50	0.32054312	0.615	0.306	1.18E-45	6	Eif3f
Atp5d	8.70E-50	0.25272003	0.543	0.239	1.18E-45	6	Atp5d
Alox5ap2	1.02E-49	0.27706044	0.812	0.431	1.39E-45	6	Alox5ap
Rpl281	2.13E-47	0.31308114	0.92	0.688	2.89E-43	6	Rpl28
Eif3k	6.18E-47	0.27135761	0.529	0.246	8.39E-43	6	Eif3k
Ptpn1	1.64E-46	0.29716991	0.613	0.309	2.23E-42	6	Ptpn1
Ifi2712a1	3.25E-46	0.30736038	0.58	0.268	4.41E-42	6	Ifi2712a
Rpl71	1.89E-45	0.28035937	0.877	0.537	2.57E-41	6	Rpl7
Rps191	3.58E-45	0.28104604	0.957	0.696	4.86E-41	6	Rps19
Pdia61	2.15E-44	0.26120355	0.381	0.148	2.92E-40	6	Pdia6
Arhgdib1	2.57E-44	0.28408898	0.658	0.352	3.48E-40	6	Arhgdib
Pycard	2.59E-44	0.262026	0.416	0.17	3.51E-40	6	Pycard
Mrpl52	2.10E-43	0.25590728	0.607	0.305	2.84E-39	6	Mrpl52
Cox4i1	2.47E-43	0.26292915	0.801	0.474	3.35E-39	6	Cox4i1
Tgm2	4.22E-43	0.47487754	0.418	0.181	5.73E-39	6	Tgm2
Lyn	5.43E-43	0.25933227	0.578	0.284	7.37E-39	6	Lyn
Ifngr11	3.35E-42	0.27221702	0.496	0.229	4.54E-38	6	Ifngr1
H2afz1	4.11E-42	0.26051185	0.625	0.323	5.58E-38	6	H2afz
Fyb	6.93E-42	0.27842617	0.697	0.385	9.41E-38	6	Fyb
Spi11	2.53E-41	0.27612723	0.727	0.413	3.43E-37	6	Spi1
Rpl35a1	4.01E-41	0.2744372	0.971	0.818	5.44E-37	6	Rpl35a
Rpl181	4.69E-40	0.28087256	0.926	0.687	6.37E-36	6	Rpl18
Rpl341	4.06E-39	0.2536784	0.953	0.759	5.52E-35	6	Rpl34
Rbm31	1.27E-37	0.25308178	0.703	0.407	1.72E-33	6	Rbm3
C5ar11	5.06E-37	0.27324724	0.426	0.191	6.87E-33	6	C5ar1
Actb	2.59E-36	0.26317385	0.998	0.983	3.52E-32	6	Actb
Fcgr3	3.80E-36	0.25103867	0.66	0.361	5.16E-32	6	Fcgr3
Pou2f2	8.16E-36	0.27688383	0.381	0.162	1.11E-31	6	Pou2f2
Calr1	1.03E-35	0.29520563	0.609	0.336	1.40E-31	6	Calr
Ctsl	1.69E-35	0.32909924	0.318	0.121	2.29E-31	6	Ctsl
Plin21	1.98E-35	0.33466483	0.545	0.283	2.69E-31	6	Plin2
Gngt21	7.81E-34	0.38627868	0.482	0.247	1.06E-29	6	Gngt2
Pgk11	6.47E-30	0.3371698	0.469	0.248	8.79E-26	6	Pgk1
Hmox11	9.89E-28	0.70571816	0.328	0.152	1.34E-23	6	Hmox1
Mt11	3.25E-22	0.41451322	0.252	0.113	4.42E-18	6	Mt1

Sat1	9.82E-21	0.3297721	0.666	0.448	1.33E-16	6	Sat1
Ctsb2	1.49E-16	0.29420743	0.752	0.524	2.02E-12	6	Ctsb
H2-Eb11	0	2.08002658	0.988	0.198	0	7	H2-Eb1
H2-Aa1	0	2.0325602	0.992	0.214	0	7	H2-Aa
H2-Ab11	0	2.01494423	0.996	0.227	0	7	H2-Ab1
Cd741	0	2.00662513	1	0.336	0	7	Cd74
H2-DMb11	0	0.86473163	0.843	0.123	0	7	H2-DMb1
H2-DMa1	0	0.85461169	0.883	0.165	0	7	H2-DMa
Ciita	0	0.73572353	0.774	0.079	0	7	Ciita
H2-Oa	0	0.71001573	0.595	0.019	0	7	H2-Oa
Cbfa2t3	0	0.63476266	0.669	0.044	0	7	Cbfa2t3
H2-DMb2	0	0.52230541	0.438	0.012	0	7	H2-DMb2
Olfm1	2.27E-286	0.38511976	0.395	0.025	3.08E-282	7	Olfm1
Syng2	3.31E-272	0.73885665	0.774	0.152	4.50E-268	7	Syng2
Ckb	1.99E-268	0.51858092	0.51	0.055	2.70E-264	7	Ckb
Wdfy4	3.46E-260	0.4761288	0.47	0.047	4.69E-256	7	Wdfy4
Napsa1	4.37E-256	0.77301438	0.76	0.159	5.94E-252	7	Napsa
Kmo	7.65E-253	0.28490616	0.306	0.014	1.04E-248	7	Kmo
Ifi205	5.07E-235	0.54655818	0.389	0.033	6.89E-231	7	Ifi205
Rnase6	4.98E-224	0.36733159	0.419	0.041	6.76E-220	7	Rnase6
H2afy	2.82E-196	0.60755082	0.742	0.194	3.83E-192	7	H2afy
Pak1	1.15E-194	0.3099696	0.333	0.029	1.56E-190	7	Pak1
Ccnd1	1.56E-191	0.45574772	0.401	0.047	2.12E-187	7	Ccnd1
Crip11	1.57E-183	0.85013512	0.8	0.231	2.13E-179	7	Crip1
Atox11	4.87E-180	0.74672461	0.899	0.364	6.61E-176	7	Atox1
Gm2a1	5.69E-175	0.73707236	0.812	0.279	7.72E-171	7	Gm2a
Plbd11	8.48E-169	0.57336797	0.718	0.198	1.15E-164	7	Plbd1
Fcgrt	2.17E-159	0.25798544	0.284	0.026	2.95E-155	7	Fcgrt
Plac81	6.88E-158	0.80952336	0.685	0.176	9.34E-154	7	Plac8
Rps111	5.01E-156	0.7289898	0.996	0.729	6.81E-152	7	Rps11
Slamf7	1.23E-154	0.34283053	0.411	0.062	1.67E-150	7	Slamf7
Tmsb102	1.43E-149	0.73128098	0.897	0.329	1.93E-145	7	Tmsb10
Cst3	2.64E-144	1.18967515	0.942	0.557	3.58E-140	7	Cst3
Klrk1	5.19E-140	0.33760754	0.401	0.064	7.04E-136	7	Klrk1
Lsp1	2.38E-135	0.58747781	0.782	0.285	3.24E-131	7	Lsp1
Rps4x2	2.73E-134	0.64064499	0.982	0.533	3.70E-130	7	Rps4x
Rpl141	1.08E-133	0.61911844	0.919	0.482	1.47E-129	7	Rpl14
Rps192	1.20E-133	0.618292	0.996	0.693	1.63E-129	7	Rps19
Naaa	2.41E-133	0.48063286	0.361	0.058	3.28E-129	7	Naaa
Ifitm31	8.56E-131	0.84990448	0.819	0.315	1.16E-126	7	Ifitm3

Rpsa1	7.70E-130	0.65103835	0.998	0.653	1.04E-125	7	Rpsa
Rpl10a2	2.43E-127	0.58335694	0.929	0.439	3.30E-123	7	Rpl10a
Psmb81	2.52E-127	0.56522143	0.812	0.315	3.42E-123	7	Psmb8
Plekho1	3.79E-126	0.37510451	0.552	0.137	5.15E-122	7	Plekho1
Eef1b21	3.89E-123	0.63850536	0.835	0.367	5.29E-119	7	Eef1b2
H2afz2	3.22E-122	0.65839565	0.772	0.312	4.37E-118	7	H2afz
Sub11	2.78E-121	0.51679803	0.748	0.276	3.77E-117	7	Sub1
Rpl42	9.87E-121	0.50944049	0.877	0.368	1.34E-116	7	Rpl4
Itgb7	2.74E-120	0.31078169	0.413	0.081	3.73E-116	7	Itgb7
Psme1	1.30E-117	0.54447276	0.722	0.272	1.77E-113	7	Psme1
Klrd11	6.72E-116	0.37546294	0.417	0.081	9.12E-112	7	Klrd1
Nsa2	1.28E-115	0.42635661	0.692	0.234	1.74E-111	7	Nsa2
Rpl352	2.88E-115	0.5596737	0.829	0.385	3.91E-111	7	Rpl35
Rpl131	4.10E-115	0.57272819	0.988	0.759	5.57E-111	7	Rpl13
Cd721	2.29E-114	0.36883717	0.353	0.062	3.12E-110	7	Cd72
Gpx11	8.17E-114	0.51902523	0.871	0.368	1.11E-109	7	Gpx1
Rps51	3.41E-112	0.5684602	0.96	0.612	4.63E-108	7	Rps5
Rps201	9.56E-112	0.56572161	0.968	0.628	1.30E-107	7	Rps20
Rpl33	9.40E-109	0.51773928	0.921	0.452	1.28E-104	7	Rpl3
Cfp	8.22E-107	0.33749984	0.365	0.071	1.12E-102	7	Cfp
Rpl7a2	2.63E-106	0.47346013	0.925	0.442	3.58E-102	7	Rpl7a
Rps61	5.05E-104	0.49866306	0.915	0.498	6.86E-100	7	Rps6
Rpl36a1	1.03E-103	0.52784297	0.802	0.353	1.40E-99	7	Rpl36a
Rpl282	1.27E-103	0.51523514	0.97	0.684	1.72E-99	7	Rpl28
Rplp02	2.78E-103	0.53565861	0.976	0.655	3.77E-99	7	Rplp0
Pkib	2.41E-102	0.27013282	0.294	0.048	3.27E-98	7	Pkib
Nap111	3.52E-102	0.32274087	0.496	0.132	4.78E-98	7	Nap111
Rps181	1.60E-101	0.50788338	0.962	0.582	2.17E-97	7	Rps18
Rpl321	2.41E-101	0.55648625	0.964	0.671	3.27E-97	7	Rpl32
Rpl151	1.06E-100	0.52189739	0.923	0.523	1.44E-96	7	Rpl15
Gpr171	2.10E-100	0.25283832	0.274	0.042	2.86E-96	7	Gpr171
Ifitm11	5.91E-100	1.36676733	0.575	0.206	8.02E-96	7	Ifitm1
Rack11	6.20E-99	0.47242201	0.933	0.499	8.42E-95	7	Rack1
Rpl18a1	3.95E-98	0.47078727	0.99	0.818	5.36E-94	7	Rpl18a
Rpl61	3.43E-95	0.49231434	0.972	0.647	4.65E-91	7	Rpl6
Eif3f2	4.69E-94	0.40095267	0.74	0.297	6.37E-90	7	Eif3f
Gdi2	9.76E-94	0.42749901	0.696	0.277	1.32E-89	7	Gdi2
Cox7a211	1.62E-92	0.38711043	0.627	0.225	2.20E-88	7	Cox7a21
Rps241	9.44E-92	0.469147	0.98	0.747	1.28E-87	7	Rps24
Rps71	2.56E-90	0.47330302	0.94	0.589	3.48E-86	7	Rps7

Ptma2	4.23E-88	0.45684329	0.935	0.533	5.74E-84	7	Ptma
Rpl121	4.98E-87	0.39087267	0.917	0.477	6.76E-83	7	Rpl12
Rpl261	8.87E-87	0.44022658	0.978	0.699	1.20E-82	7	Rpl26
Npm11	1.01E-86	0.38914888	0.685	0.266	1.37E-82	7	Npm1
Atpif1	3.29E-86	0.38495789	0.534	0.18	4.47E-82	7	Atpif1
Rpl191	6.57E-86	0.4425841	0.988	0.759	8.93E-82	7	Rpl19
Rpl182	2.32E-84	0.43445032	0.97	0.684	3.15E-80	7	Rpl18
Dbnl	8.30E-84	0.27742674	0.411	0.109	1.13E-79	7	Dbnl
Pgls	3.68E-83	0.29326495	0.472	0.14	5.00E-79	7	Pgls
Ptms	8.18E-83	0.40859505	0.571	0.205	1.11E-78	7	Ptms
Rps81	1.91E-82	0.44451572	0.992	0.82	2.60E-78	7	Rps8
Rpl221	3.01E-80	0.42701585	0.877	0.477	4.09E-76	7	Rpl22
Rps121	6.62E-80	0.4289245	0.976	0.796	8.99E-76	7	Rps12
Psmb91	2.13E-79	0.35578384	0.488	0.158	2.89E-75	7	Psmb9
Rpl391	5.22E-79	0.43535717	0.944	0.731	7.09E-75	7	Rpl39
Rps261	7.85E-78	0.4680936	0.917	0.601	1.07E-73	7	Rps26
Eef1g1	5.35E-77	0.31729808	0.569	0.204	7.26E-73	7	Eef1g
Rplp12	7.93E-77	0.42325205	0.996	0.836	1.08E-72	7	Rplp1
Ndufa6	2.22E-76	0.34653876	0.577	0.217	3.02E-72	7	Ndufa6
Rpl35a2	1.40E-74	0.39732764	0.988	0.817	1.90E-70	7	Rpl35a
Tmsb4x2	1.52E-74	0.60511853	1	0.956	2.06E-70	7	Tmsb4x
Id21	2.51E-74	0.57339545	0.706	0.34	3.41E-70	7	Id2
Smdt11	4.35E-73	0.329746	0.534	0.195	5.91E-69	7	Smdt1
Rpl23a1	2.46E-72	0.37652715	0.857	0.448	3.34E-68	7	Rpl23a
Rpl361	4.54E-72	0.41333753	0.944	0.621	6.16E-68	7	Rpl36
Rpl311	2.37E-71	0.33285295	0.742	0.338	3.22E-67	7	Rpl31
Rps231	4.33E-71	0.35698289	0.98	0.708	5.88E-67	7	Rps23
Ctsh2	1.12E-70	0.34229725	0.685	0.284	1.51E-66	7	Ctsh
Hsp90ab12	1.59E-70	0.38284633	0.823	0.406	2.16E-66	7	Hsp90ab1
Rpl51	1.66E-70	0.34792511	0.865	0.438	2.26E-66	7	Rpl5
Rps15a1	2.45E-70	0.27720986	0.95	0.65	3.33E-66	7	Rps15a
Rps161	4.60E-70	0.39275044	0.98	0.849	6.25E-66	7	Rps16
Rpl211	4.72E-69	0.3958752	0.97	0.732	6.41E-65	7	Rpl21
Rpl231	1.30E-68	0.37634716	0.986	0.847	1.76E-64	7	Rpl23
Dock10	5.62E-68	0.26483874	0.468	0.152	7.63E-64	7	Dock10
Rps9	9.85E-68	0.37682333	0.996	0.883	1.34E-63	7	Rps9
Eef21	2.27E-67	0.39141252	0.804	0.42	3.09E-63	7	Eef2
Rps27a2	5.30E-67	0.40389943	0.964	0.808	7.20E-63	7	Rps27a
Rpl81	7.02E-67	0.38485285	0.952	0.687	9.53E-63	7	Rpl8
Tspo1	1.91E-66	0.46562529	0.706	0.34	2.60E-62	7	Tspo

Rpl27a1	4.71E-66	0.36746039	0.98	0.787	6.39E-62	7	Rpl27a
Dek	9.56E-66	0.25568221	0.399	0.121	1.30E-61	7	Dek
Ifitm61	3.32E-65	0.27019374	0.323	0.081	4.50E-61	7	Ifitm6
Slfn5	1.57E-64	0.39275534	0.433	0.142	2.13E-60	7	Slfn5
Sla	6.31E-63	0.25711088	0.411	0.131	8.57E-59	7	Sla
Eif3k1	1.67E-62	0.29670952	0.581	0.242	2.27E-58	7	Eif3k
Pomp	1.89E-62	0.32308993	0.562	0.233	2.57E-58	7	Pomp
Rpl72	1.96E-62	0.3559758	0.901	0.536	2.66E-58	7	Rpl7
Cnn2	9.16E-62	0.27738241	0.462	0.163	1.24E-57	7	Cnn2
Eef1a11	1.29E-61	0.37681042	0.982	0.861	1.75E-57	7	Eef1a1
Mdh2	2.25E-61	0.4291055	0.45	0.17	3.06E-57	7	Mdh2
Rps210	9.96E-61	0.36754513	0.931	0.634	1.35E-56	7	Rps2
Rps31	1.29E-60	0.31811401	0.966	0.706	1.75E-56	7	Rps3
Rpl171	6.86E-60	0.34814266	0.968	0.786	9.32E-56	7	Rpl17
Hspe1	2.73E-59	0.26818965	0.468	0.17	3.70E-55	7	Hspe1
Rpl241	5.25E-59	0.34794981	0.913	0.589	7.13E-55	7	Rpl24
Atp5g21	6.42E-59	0.30660417	0.589	0.256	8.72E-55	7	Atp5g2
Rpl36a1	1.69E-58	0.29139509	0.603	0.259	2.29E-54	7	Rpl36a1
Rpl292	2.37E-58	0.43859839	0.728	0.412	3.22E-54	7	Rpl29
Rpl271	2.58E-58	0.32071961	0.734	0.364	3.50E-54	7	Rpl27
Hint12	8.12E-58	0.26953648	0.569	0.236	1.10E-53	7	Hint1
Tspan13	1.16E-57	0.25780185	0.377	0.12	1.57E-53	7	Tspan13
Rps281	1.93E-56	0.37754432	0.893	0.626	2.62E-52	7	Rps28
Naca1	2.86E-56	0.34058896	0.778	0.417	3.88E-52	7	Naca
Rpl111	5.76E-56	0.34522054	0.931	0.649	7.83E-52	7	Rpl11
Rps3a11	5.80E-56	0.32241566	0.95	0.712	7.87E-52	7	Rps3a1
Ap1s2	9.46E-56	0.29844717	0.312	0.092	1.28E-51	7	Ap1s2
Rps291	1.05E-55	0.35609643	0.988	0.863	1.43E-51	7	Rps29
Phf11b	2.37E-55	0.30210184	0.266	0.068	3.21E-51	7	Phf11b
Rps101	2.59E-55	0.32296352	0.964	0.762	3.51E-51	7	Rps10
Actb1	6.72E-54	0.37831377	1	0.983	9.13E-50	7	Actb
Erp291	1.27E-51	0.27911936	0.556	0.245	1.72E-47	7	Erp29
Tap1	2.27E-51	0.25000153	0.403	0.145	3.08E-47	7	Tap1
Ppib1	2.47E-51	0.26518345	0.605	0.276	3.35E-47	7	Ppib
Rps141	3.48E-51	0.29110542	0.982	0.795	4.73E-47	7	Rps14
Ly6a1	3.15E-50	0.70829555	0.405	0.158	4.27E-46	7	Ly6a
Tmem176a1	4.35E-50	0.28394336	0.3	0.089	5.91E-46	7	Tmem176a
S100a42	2.19E-49	0.59407246	0.546	0.243	2.97E-45	7	S100a4
Actr3	1.34E-48	0.30609193	0.671	0.352	1.81E-44	7	Actr3
Rpl301	6.66E-48	0.3136296	0.935	0.721	9.05E-44	7	Rpl30

Mrpl521	1.52E-47	0.26585518	0.625	0.304	2.07E-43	7	Mrpl52
Rps172	2.57E-47	0.27211595	0.722	0.371	3.49E-43	7	Rps17
Rps211	4.24E-47	0.30940377	0.942	0.742	5.76E-43	7	Rps21
Psme2	5.16E-47	0.292787	0.522	0.233	7.01E-43	7	Psme2
Tmem176b1	6.34E-47	0.31488593	0.333	0.11	8.61E-43	7	Tmem176b
Rpl101	7.80E-47	0.34040707	0.919	0.688	1.06E-42	7	Rpl10
Cycc	8.22E-47	0.26685567	0.363	0.131	1.12E-42	7	Cycc
Set	1.36E-45	0.25556877	0.504	0.223	1.84E-41	7	Set
Ywhah	1.45E-45	0.2719007	0.444	0.185	1.97E-41	7	Ywhah
Hspa82	1.28E-44	0.32733906	0.804	0.478	1.74E-40	7	Hspa8
Limd21	1.35E-44	0.25963046	0.44	0.182	1.83E-40	7	Limd2
Rpl91	1.83E-44	0.27871827	0.94	0.711	2.49E-40	7	Rpl9
Rps131	1.39E-43	0.27530426	0.929	0.711	1.89E-39	7	Rps13
Rps151	3.14E-43	0.29083688	0.867	0.534	4.26E-39	7	Rps15
Cxcl161	1.40E-42	0.2864545	0.393	0.151	1.90E-38	7	Cxcl16
Ms4a4c	3.54E-42	0.37674712	0.355	0.133	4.80E-38	7	Ms4a4c
Ifngr12	4.58E-42	0.26464186	0.5	0.23	6.21E-38	7	Ifngr1
Rpl41	1.97E-41	0.28410434	0.978	0.878	2.68E-37	7	Rpl41
Psma71	1.94E-40	0.25772247	0.522	0.252	2.63E-36	7	Psma7
Sec61b1	3.48E-39	0.2824309	0.605	0.326	4.72E-35	7	Sec61b
Ly6e	4.81E-39	0.27620424	0.78	0.453	6.54E-35	7	Ly6e
Rpl342	3.47E-38	0.2685966	0.956	0.759	4.71E-34	7	Rpl34
Rpl381	3.42E-37	0.25437259	0.909	0.653	4.64E-33	7	Rpl38
Rps251	5.92E-36	0.25145965	0.893	0.623	8.03E-32	7	Rps25
Rpl37a1	1.08E-34	0.26307539	0.974	0.813	1.47E-30	7	Rpl37a
Nfkb1	8.91E-34	0.25838888	0.363	0.158	1.21E-29	7	Nfkb1
Rpl371	1.67E-33	0.2580345	0.948	0.792	2.27E-29	7	Rpl37
Taldo11	1.37E-32	0.27591083	0.663	0.386	1.86E-28	7	Taldo1
Irf7	2.79E-25	0.31481206	0.312	0.14	3.79E-21	7	Irf7
Irf8	1.87E-24	0.53313528	0.359	0.197	2.54E-20	7	Irf8
Ppt1	1.04E-18	0.3576248	0.341	0.197	1.41E-14	7	Ppt1
Isg15	2.69E-16	0.31011397	0.3	0.159	3.65E-12	7	Isg15
Isg151	0	1.38909275	0.805	0.121	0	8	Isg15
Irf71	0	1.11941867	0.77	0.106	0	8	Irf7
Ms4a4c1	0	0.99111612	0.718	0.106	0	8	Ms4a4c
Ifi204	0	0.82651404	0.735	0.101	0	8	Ifi204
Ifit3	0	0.82444672	0.523	0.039	0	8	Ifit3
Slfn51	1.62E-300	0.82698792	0.739	0.119	2.19E-296	8	Slfn5
Oasl1	2.05E-296	0.47128163	0.391	0.022	2.78E-292	8	Oasl1
Oasl2	8.82E-293	0.66722754	0.687	0.1	1.20E-288	8	Oasl2

Cxcl10	6.34E-288	1.33908547	0.405	0.026	8.60E-284	8	Cxcl10
Ly6c2	5.76E-283	1.39167294	0.658	0.099	7.82E-279	8	Ly6c2
Ifi211	2.78E-263	0.53083544	0.481	0.048	3.78E-259	8	Ifi211
Zbp1	1.41E-258	0.61720323	0.615	0.09	1.91E-254	8	Zbp1
Ifit1	2.44E-251	0.71442536	0.426	0.037	3.31E-247	8	Ifit1
Plac82	2.06E-245	1.24962072	0.776	0.17	2.80E-241	8	Plac8
Ifit2	3.24E-235	0.49582178	0.381	0.03	4.39E-231	8	Ifit2
Gbp2	2.49E-226	0.66142689	0.447	0.049	3.38E-222	8	Gbp2
Fcgr11	1.96E-219	0.69967342	0.615	0.11	2.66E-215	8	Fcgr1
Chil31	9.20E-216	1.32783342	0.611	0.106	1.25E-211	8	Chil3
Ifitm32	5.56E-214	1.36489793	0.891	0.311	7.55E-210	8	Ifitm3
Oas3	8.39E-212	0.35514008	0.372	0.033	1.14E-207	8	Oas3
Rsad2	3.87E-199	0.81557438	0.34	0.03	5.25E-195	8	Rsad2
Parp14	3.54E-191	0.5651769	0.597	0.114	4.80E-187	8	Parp14
Rnf213	1.21E-189	0.44793567	0.512	0.081	1.64E-185	8	Rnf213
Ifi47	1.29E-189	0.53903067	0.496	0.077	1.75E-185	8	Ifi47
Rtp4	1.60E-182	0.47268617	0.471	0.071	2.18E-178	8	Rtp4
Ifi213	2.55E-180	0.34151538	0.352	0.036	3.46E-176	8	Ifi213
Ly6e1	2.99E-172	0.87598427	0.93	0.442	4.06E-168	8	Ly6e
Ifi209	3.48E-172	0.53436147	0.473	0.078	4.72E-168	8	Ifi209
Ifi207	1.56E-170	0.46949032	0.514	0.092	2.12E-166	8	Ifi207
Pnp	2.29E-164	0.66626213	0.619	0.153	3.11E-160	8	Pnp
Ms4a6d2	1.15E-162	0.67641404	0.603	0.142	1.56E-158	8	Ms4a6d
Usp18	1.52E-161	0.34917669	0.321	0.034	2.06E-157	8	Usp18
Ms4a6c2	7.38E-159	0.73428596	0.73	0.216	1.00E-154	8	Ms4a6c
Ifi27l2a2	4.06E-156	1.22445365	0.745	0.257	5.51E-152	8	Ifi27l2a
Tgfb2	1.02E-155	0.94323218	0.835	0.321	1.38E-151	8	Tgfb2
Mx1	1.31E-151	0.31752137	0.296	0.03	1.78E-147	8	Mx1
Slfn4	1.50E-142	0.68994452	0.451	0.085	2.03E-138	8	Slfn4
Ifi203	7.72E-141	0.62131822	0.551	0.131	1.05E-136	8	Ifi203
Xaf1	8.21E-141	0.32167531	0.399	0.064	1.11E-136	8	Xaf1
Ctss2	2.15E-139	0.81877515	0.909	0.436	2.92E-135	8	Ctss
Stat1	4.17E-138	0.60455568	0.634	0.181	5.66E-134	8	Stat1
Bst21	4.22E-137	0.57580021	0.619	0.165	5.73E-133	8	Bst2
Gbp3	9.09E-136	0.26352385	0.28	0.031	1.23E-131	8	Gbp3
Ccr21	2.31E-135	0.68505187	0.628	0.174	3.14E-131	8	Ccr2
Mndal	3.70E-135	0.55256223	0.56	0.14	5.02E-131	8	Mndal
Herc6	2.71E-131	0.31768101	0.344	0.051	3.67E-127	8	Herc6
Stat2	3.08E-131	0.35611029	0.393	0.067	4.18E-127	8	Stat2
Ifi206	3.46E-127	0.28182352	0.284	0.035	4.70E-123	8	Ifi206

Tor3a	2.13E-126	0.29605684	0.35	0.054	2.89E-122	8	Tor3a
Slfn1	2.54E-125	0.5034587	0.619	0.176	3.45E-121	8	Slfn1
Npc22	7.16E-123	0.79505759	0.802	0.381	9.72E-119	8	Npc2
Samhd1	5.33E-116	0.60196352	0.704	0.255	7.24E-112	8	Samhd1
Ddx58	5.57E-116	0.26940833	0.319	0.049	7.56E-112	8	Ddx58
Trafd1	1.51E-113	0.34407872	0.401	0.082	2.05E-109	8	Trafd1
Igtp	7.05E-112	0.2917386	0.344	0.059	9.57E-108	8	Igtp
Ccl2	1.84E-111	0.48168662	0.253	0.031	2.49E-107	8	Ccl2
Xist	3.16E-111	0.35555397	0.29	0.04	4.29E-107	8	Xist
Tspo2	3.68E-111	0.71777366	0.747	0.337	5.00E-107	8	Tspo
Ifih1	2.33E-110	0.26287226	0.282	0.04	3.16E-106	8	Ifih1
Ifi2051	2.39E-108	0.28040066	0.288	0.041	3.24E-104	8	Ifi205
Gm21188	2.98E-105	0.25272446	0.282	0.042	4.04E-101	8	Gm21188
Ms4a6b	2.72E-102	0.46399747	0.605	0.199	3.69E-98	8	Ms4a6b
Mafb2	8.67E-102	0.48990562	0.634	0.198	1.18E-97	8	Mafb
Znfx1	9.65E-102	0.27270051	0.321	0.057	1.31E-97	8	Znfx1
Trim30a	3.13E-100	0.40443809	0.539	0.159	4.25E-96	8	Trim30a
Ifi35	1.07E-97	0.30207757	0.379	0.082	1.45E-93	8	Ifi35
Prdx53	7.23E-97	0.69899197	0.846	0.449	9.82E-93	8	Prdx5
Sdc3	1.85E-96	0.28365385	0.317	0.058	2.51E-92	8	Sdc3
Lyz22	2.78E-94	0.9942384	0.8	0.403	3.78E-90	8	Lyz2
S100a43	1.55E-92	0.62864066	0.658	0.235	2.11E-88	8	S100a4
Daxx	8.47E-92	0.25081226	0.294	0.053	1.15E-87	8	Daxx
Lgals3bp1	1.14E-91	0.37713265	0.434	0.112	1.55E-87	8	Lgals3bp
Irgm1	1.91E-91	0.27240886	0.302	0.056	2.59E-87	8	Irgm1
Aif11	1.59E-90	0.50786074	0.574	0.192	2.16E-86	8	Aif1
Phf11b1	1.69E-90	0.31798073	0.323	0.064	2.29E-86	8	Phf11b
Psmb10	1.75E-90	0.37769049	0.498	0.151	2.38E-86	8	Psmb10
Isg20	2.70E-88	0.32172917	0.337	0.072	3.67E-84	8	Isg20
Trim30d	6.04E-88	0.26820895	0.329	0.068	8.20E-84	8	Trim30d
Sp100	2.05E-85	0.3578094	0.473	0.14	2.78E-81	8	Sp100
Klra2	8.39E-85	0.26184503	0.333	0.071	1.14E-80	8	Klra2
Ogfr	2.01E-84	0.25595124	0.362	0.084	2.74E-80	8	Ogfr
Fn11	5.31E-84	0.44080005	0.422	0.108	7.21E-80	8	Fn1
Lst11	5.40E-84	0.49363876	0.71	0.308	7.33E-80	8	Lst1
Cybb2	3.29E-83	0.45515431	0.564	0.191	4.47E-79	8	Cybb
Gbp7	4.86E-83	0.301005	0.329	0.072	6.60E-79	8	Gbp7
Ass1	5.95E-80	0.25337144	0.27	0.05	8.08E-76	8	Ass1
Tapbp	1.62E-78	0.37866909	0.545	0.197	2.19E-74	8	Tapbp
F101	4.49E-78	0.36174319	0.354	0.085	6.09E-74	8	F10

1600014C10Rik	6.30E-76	0.34950074	0.372	0.099	8.55E-72	8	1600014C1
Sppl2a	9.06E-76	0.29874616	0.418	0.12	1.23E-71	8	Sppl2a
Zufsp	2.60E-75	0.27825641	0.364	0.093	3.53E-71	8	Zufsp
Ctsc2	1.08E-74	0.34004427	0.584	0.208	1.46E-70	8	Ctsc
Nampt	1.47E-74	0.28848834	0.352	0.088	2.00E-70	8	Nampt
Epsti1	3.25E-74	0.32329361	0.407	0.117	4.41E-70	8	Epsti1
Pid11	5.32E-71	0.34422731	0.412	0.121	7.22E-67	8	Pid1
Msr11	9.60E-71	0.26296184	0.34	0.084	1.30E-66	8	Msr1
Tor1aip1	1.77E-70	0.30924705	0.453	0.147	2.40E-66	8	Tor1aip1
Lgals9	2.31E-70	0.28042222	0.344	0.09	3.14E-66	8	Lgals9
Slfn2	1.50E-68	0.44984605	0.761	0.382	2.04E-64	8	Slfn2
Wfdc172	1.05E-67	0.51246496	0.558	0.21	1.42E-63	8	Wfdc17
B2m2	1.16E-67	0.52172341	0.922	0.675	1.57E-63	8	B2m
C3	6.74E-67	0.29383041	0.344	0.091	9.15E-63	8	C3
Samd9l	1.21E-65	0.25972703	0.311	0.078	1.65E-61	8	Samd9l
9930111J21Rik2	1.72E-65	0.32912118	0.455	0.155	2.34E-61	8	9930111J2
Sp110	5.97E-65	0.25715381	0.337	0.091	8.10E-61	8	Sp110
Tgm21	2.09E-64	0.53003831	0.477	0.177	2.84E-60	8	Tgm2
Grn1	4.31E-64	0.46671673	0.675	0.324	5.85E-60	8	Grn
Zeb21	2.63E-62	0.43232586	0.652	0.294	3.57E-58	8	Zeb2
Fam46a	3.27E-62	0.26791265	0.372	0.11	4.44E-58	8	Fam46a
Fcgr2b2	2.18E-61	0.33934482	0.449	0.156	2.96E-57	8	Fcgr2b
H2-T23	2.39E-61	0.33512879	0.504	0.192	3.24E-57	8	H2-T23
Psme21	2.64E-61	0.30468668	0.566	0.231	3.59E-57	8	Psme2
AY0361181	6.40E-61	0.64774737	0.393	0.135	8.68E-57	8	AY036118
Actb2	3.97E-60	0.45140563	0.998	0.983	5.39E-56	8	Actb
Psmb82	1.03E-59	0.36202028	0.683	0.326	1.40E-55	8	Psmb8
Tmsb103	1.11E-58	0.4994202	0.7	0.345	1.50E-54	8	Tmsb10
Emp31	2.96E-58	0.37968213	0.576	0.254	4.02E-54	8	Emp3
Lgals33	6.06E-58	0.41334201	0.747	0.391	8.22E-54	8	Lgals3
Capza21	8.64E-58	0.3357519	0.584	0.261	1.17E-53	8	Capza2
Hck	7.48E-56	0.28038463	0.42	0.147	1.02E-51	8	Hck
Selenow	1.50E-55	0.31207673	0.414	0.149	2.04E-51	8	Selenow
Axl1	7.47E-54	0.27488043	0.311	0.091	1.01E-49	8	Axl
Csf1r2	1.02E-53	0.27528259	0.582	0.243	1.39E-49	8	Csf1r
Fcgr4	1.03E-53	0.2540199	0.321	0.094	1.40E-49	8	Fcgr4
Rrbp11	3.57E-50	0.34607988	0.714	0.371	4.84E-46	8	Rrbp1
Tap11	5.56E-49	0.28066581	0.397	0.146	7.55E-45	8	Tap1
Ccr5	2.41E-48	0.2588645	0.331	0.109	3.27E-44	8	Ccr5
Psme11	4.31E-48	0.2966112	0.599	0.282	5.86E-44	8	Psme1

Hspa83	1.47E-47	0.42908348	0.757	0.482	2.00E-43	8	Hspa8
Sod2	6.76E-47	0.2913433	0.265	0.077	9.18E-43	8	Sod2
Cd682	4.00E-45	0.33699864	0.576	0.274	5.43E-41	8	Cd68
Crip12	1.33E-44	0.3960007	0.545	0.251	1.81E-40	8	Crip1
Mpeg11	1.23E-43	0.30978344	0.679	0.358	1.67E-39	8	Mpeg1
Cxcl162	1.24E-43	0.30707576	0.393	0.151	1.69E-39	8	Cxcl16
Lgals12	2.18E-43	0.31586834	0.541	0.244	2.96E-39	8	Lgals1
Irf1	8.96E-43	0.27965496	0.35	0.128	1.22E-38	8	Irf1
Psap3	1.66E-39	0.31250304	0.895	0.62	2.25E-35	8	Psap
Ahnak1	5.19E-39	0.25610348	0.399	0.162	7.04E-35	8	Ahnak
Gpr141	3.31E-38	0.26212049	0.309	0.112	4.49E-34	8	Gpr141
Ctsz1	1.41E-37	0.25576035	0.706	0.395	1.91E-33	8	Ctsz
Vim1	2.14E-37	0.52044087	0.617	0.362	2.90E-33	8	Vim
Tgfb11	2.93E-37	0.28175221	0.471	0.221	3.98E-33	8	Tgfb1
S100a102	3.29E-37	0.3550645	0.438	0.193	4.47E-33	8	S100a10
Akr1a12	8.88E-36	0.28765364	0.529	0.276	1.20E-31	8	Akr1a1
Atox12	3.82E-35	0.26977805	0.665	0.383	5.19E-31	8	Atox1
Gm424181	7.98E-34	0.76315271	0.996	0.973	1.08E-29	8	Gm42418
Chmp4b	4.81E-33	0.25305184	0.492	0.254	6.54E-29	8	Chmp4b
H2-D11	2.86E-32	0.30018138	0.885	0.679	3.88E-28	8	H2-D1
Capg2	9.46E-32	0.26641643	0.496	0.254	1.28E-27	8	Capg
Sem11	2.03E-30	0.27921837	0.675	0.442	2.76E-26	8	Sem1
Gpx12	3.64E-30	0.28035161	0.65	0.386	4.94E-26	8	Gpx1
Tagln21	7.71E-28	0.27809342	0.393	0.192	1.05E-23	8	Tagln2
Esd1	1.12E-24	0.26106786	0.352	0.175	1.52E-20	8	Esd
Ly6a2	1.24E-24	0.32368254	0.348	0.162	1.68E-20	8	Ly6a
mt-Co21	4.47E-242	1.58313504	1	0.803	6.06E-238	9	mt-Co2
mt-Co11	1.70E-239	1.55373715	1	0.837	2.31E-235	9	mt-Co1
mt-Co31	1.14E-230	1.49823704	1	0.814	1.55E-226	9	mt-Co3
mt-Atp61	2.92E-230	1.4844315	1	0.804	3.97E-226	9	mt-Atp6
mt-Nd41	3.93E-220	1.38955585	0.998	0.67	5.33E-216	9	mt-Nd4
mt-Cytb1	3.59E-217	1.41994743	1	0.722	4.87E-213	9	mt-Cytb
mt-Nd21	7.79E-209	1.35650713	0.986	0.57	1.06E-204	9	mt-Nd2
mt-Nd11	4.35E-202	1.29488257	0.993	0.567	5.91E-198	9	mt-Nd1
mt-Nd31	6.02E-125	0.83875234	0.8	0.363	8.17E-121	9	mt-Nd3
Zeb22	1.37E-87	0.8522551	0.667	0.295	1.86E-83	9	Zeb2
Gm424182	1.18E-85	1.25287324	1	0.973	1.61E-81	9	Gm42418
Malat1	2.37E-81	0.60265262	0.993	0.981	3.22E-77	9	Malat1
mt-Nd5	1.51E-68	0.55113935	0.599	0.264	2.05E-64	9	mt-Nd5
Pid12	7.84E-56	0.4538297	0.383	0.125	1.06E-51	9	Pid1

Rrbp12	6.31E-54	0.51702681	0.672	0.377	8.57E-50	9	Rrbp1
Ciita1	2.26E-35	0.40693793	0.312	0.117	3.07E-31	9	Ciita
mt-Nd4l	1.19E-34	0.28602511	0.339	0.135	1.61E-30	9	mt-Nd4l
Mafb3	1.37E-27	0.39386022	0.429	0.215	1.86E-23	9	Mafb
Lrp12	2.13E-27	0.29185757	0.356	0.16	2.90E-23	9	Lrp1
Ccr22	8.81E-26	0.33492309	0.401	0.193	1.20E-21	9	Ccr2
Nktr	5.58E-23	0.30736137	0.424	0.246	7.58E-19	9	Nktr
Fn12	3.67E-22	0.30066408	0.282	0.119	4.99E-18	9	Fn1
Fyb1	5.60E-22	0.37912083	0.564	0.398	7.61E-18	9	Fyb
Pou2f21	1.61E-19	0.34389107	0.326	0.169	2.19E-15	9	Pou2f2
Parp141	7.49E-19	0.25957129	0.284	0.139	1.02E-14	9	Parp14
Son3	2.49E-18	0.2821775	0.651	0.509	3.38E-14	9	Son
Dock101	3.22E-18	0.25701847	0.317	0.165	4.37E-14	9	Dock10
Luc7l2	1.25E-16	0.28380512	0.443	0.294	1.70E-12	9	Luc7l2
Rsrp1	1.31E-14	0.28669449	0.514	0.376	1.77E-10	9	Rsrp1
Mycbp2	1.74E-14	0.26880114	0.346	0.215	2.36E-10	9	Mycbp2
Mbnl11	3.17E-14	0.25701992	0.408	0.269	4.30E-10	9	Mbnl1
Ankrd11	1.10E-13	0.26853189	0.475	0.34	1.50E-09	9	Ankrd11
Ptprc	1.96E-10	0.26411969	0.589	0.506	2.66E-06	9	Ptprc
Ccl51	0	2.3379578	0.883	0.09	0	10	Ccl5
Nkg71	0	1.94156065	0.996	0.065	0	10	Nkg7
Cd3g1	0	1.70750913	0.996	0.076	0	10	Cd3g
Ms4a4b1	0	1.41851364	0.946	0.078	0	10	Ms4a4b
Trbc21	0	1.38207015	0.958	0.077	0	10	Trbc2
Cd8a	0	1.36129715	0.9	0.024	0	10	Cd8a
Cd8b1	0	1.31110852	0.917	0.026	0	10	Cd8b1
Cd3d1	0	1.26130359	0.983	0.074	0	10	Cd3d
Klrd12	0	1.19105203	0.892	0.077	0	10	Klrd1
Cxcr61	0	1.14750385	0.867	0.035	0	10	Cxcr6
Trac1	0	0.92311369	0.892	0.067	0	10	Trac
Cd3e1	0	0.90765816	0.85	0.064	0	10	Cd3e
Ctla2a1	0	0.88946101	0.704	0.045	0	10	Ctla2a
Ptprcap1	0	0.83439764	0.888	0.081	0	10	Ptprcap
Thy11	0	0.7971329	0.825	0.055	0	10	Thy1
Il2rb1	0	0.78563449	0.783	0.049	0	10	Il2rb
Ctsw1	0	0.78125445	0.733	0.042	0	10	Ctsw
Sh2d2a1	0	0.60083914	0.617	0.033	0	10	Sh2d2a
Klrc1	0	0.54586812	0.546	0.016	0	10	Klrc1
Klre1	0	0.50470162	0.479	0.015	0	10	Klre1
Lck1	1.60E-299	0.65901752	0.746	0.063	2.17E-295	10	Lck

Pdcd11	3.07E-284	0.59355294	0.612	0.042	4.17E-280	10	Pdcd1
AW1120101	2.06E-279	1.91462904	1	0.178	2.79E-275	10	AW112010
Tcrg-C2	5.54E-272	0.28760724	0.279	0.005	7.52E-268	10	Tcrg-C2
Ifng	7.40E-263	0.5609075	0.425	0.019	1.00E-258	10	Ifng
Gm156	1.03E-259	0.593648	0.317	0.008	1.40E-255	10	Gm156
Trbc11	9.02E-255	1.004099	0.55	0.038	1.23E-250	10	Trbc1
Cd160	2.30E-251	0.28940473	0.258	0.004	3.12E-247	10	Cd160
Gimap41	2.35E-251	0.61770299	0.646	0.055	3.19E-247	10	Gimap4
Prf1	2.42E-247	0.40678835	0.346	0.012	3.29E-243	10	Prf1
Klrc2	5.77E-247	0.34596769	0.379	0.015	7.83E-243	10	Klrc2
Ikzf3	7.04E-247	0.39123479	0.433	0.022	9.55E-243	10	Ikzf3
Cd21	2.04E-244	0.58027527	0.654	0.058	2.77E-240	10	Cd2
Gimap11	2.14E-236	0.52762483	0.638	0.058	2.91E-232	10	Gimap1
Skap11	1.45E-235	0.48170764	0.558	0.043	1.97E-231	10	Skap1
Cish1	7.85E-225	0.4454651	0.496	0.035	1.07E-220	10	Cish
H2-Q71	7.97E-220	0.91153496	0.908	0.149	1.08E-215	10	H2-Q7
Cd226	1.12E-217	0.31151757	0.346	0.015	1.52E-213	10	Cd226
Gm83691	6.21E-215	0.45880761	0.538	0.044	8.43E-211	10	Gm8369
Sema6d	1.88E-211	0.31795035	0.312	0.012	2.55E-207	10	Sema6d
Serpina3g1	9.03E-205	0.57449147	0.575	0.055	1.23E-200	10	Serpina3g
Klrk11	7.93E-203	0.63999688	0.629	0.068	1.08E-198	10	Klrk1
Lat1	8.73E-197	0.46427036	0.512	0.044	1.19E-192	10	Lat
Themis	9.33E-188	0.30516459	0.354	0.02	1.27E-183	10	Themis
Lag31	1.21E-187	0.49836997	0.529	0.05	1.64E-183	10	Lag3
Cst71	1.44E-185	0.46505759	0.546	0.054	1.96E-181	10	Cst7
	11-Sep	4.91E-165	0.40725511	0.517	0.055	6.66E-161	10
Tox1	1.83E-162	0.32229905	0.354	0.024	2.48E-158	10	Tox
Gimap51	7.83E-159	0.34894992	0.438	0.04	1.06E-154	10	Gimap5
Inpp4b1	3.03E-157	0.37263069	0.446	0.042	4.12E-153	10	Inpp4b
Ltb1	2.28E-155	0.79160532	0.838	0.173	3.09E-151	10	Ltb
Ablim11	7.03E-155	0.37046827	0.438	0.041	9.55E-151	10	Ablim1
Bcl11b1	1.01E-153	0.35455218	0.425	0.039	1.37E-149	10	Bcl11b
Gimap31	7.19E-152	0.41392839	0.496	0.054	9.76E-148	10	Gimap3
Ptpn221	3.61E-150	0.44172368	0.546	0.068	4.90E-146	10	Ptpn22
Tnfrsf91	6.48E-150	0.44514974	0.396	0.034	8.80E-146	10	Tnfrsf9
Hcst1	2.38E-149	0.68153861	0.808	0.168	3.23E-145	10	Hcst
Gimap61	1.15E-148	0.37975872	0.446	0.044	1.56E-144	10	Gimap6
Bcl21	2.42E-146	0.53875065	0.496	0.058	3.28E-142	10	Bcl2
Gzmb	4.15E-146	0.51650466	0.283	0.016	5.64E-142	10	Gzmb
Ets11	1.08E-145	0.43968465	0.542	0.068	1.47E-141	10	Ets1

Rps15a2	3.14E-144	1.40156146	1	0.659	4.26E-140	10	Rps15a
Sh2d1a1	1.59E-143	0.28786409	0.342	0.026	2.16E-139	10	Sh2d1a
Dut	1.76E-138	0.32362433	0.362	0.031	2.39E-134	10	Dut
Itk	2.82E-137	0.27409049	0.321	0.024	3.83E-133	10	Itk
Tnfrsf181	1.79E-135	0.40615296	0.5	0.061	2.43E-131	10	Tnfrsf18
Gimap7	5.24E-135	0.28877796	0.321	0.024	7.11E-131	10	Gimap7
Rpl122	1.30E-132	1.07543737	1	0.491	1.77E-128	10	Rpl12
Cd27	1.47E-130	0.29417949	0.342	0.029	1.99E-126	10	Cd27
Grap2	4.75E-129	0.26054181	0.329	0.027	6.45E-125	10	Grap2
Zap701	4.33E-126	0.29828472	0.362	0.034	5.88E-122	10	Zap70
Rgs16	1.74E-124	0.3199342	0.279	0.02	2.37E-120	10	Rgs16
Rps182	5.37E-123	1.00039123	1	0.596	7.29E-119	10	Rps18
Rpl310	1.65E-118	0.89889447	0.992	0.468	2.24E-114	10	Rpl3
Pla2g161	2.63E-118	0.36952671	0.5	0.071	3.56E-114	10	Pla2g16
S100a103	3.14E-118	0.64520118	0.817	0.189	4.27E-114	10	S100a10
Eif3e1	2.37E-115	0.49941526	0.688	0.147	3.21E-111	10	Eif3e
Rpl22l11	1.21E-114	0.74829081	0.862	0.265	1.64E-110	10	Rpl22l1
Rps242	7.10E-114	0.9481297	1	0.755	9.64E-110	10	Rps24
Rps72	2.84E-113	0.89087821	1	0.6	3.86E-109	10	Rps7
Rps132	1.03E-112	0.83831953	1	0.717	1.40E-108	10	Rps13
Rpl52	1.13E-112	0.83782167	0.988	0.45	1.53E-108	10	Rpl5
Rpl322	1.53E-109	0.90610854	1	0.681	2.07E-105	10	Rpl32
Rps4x3	3.18E-108	0.88042123	0.996	0.55	4.32E-104	10	Rps4x
Rpl27a2	5.75E-107	0.79568893	1	0.793	7.81E-103	10	Rpl27a
Rack12	1.42E-106	0.79380838	0.992	0.514	1.93E-102	10	Rack1
Prkch	2.26E-106	0.3352782	0.442	0.062	3.07E-102	10	Prkch
Ifi271	3.10E-105	0.36738122	0.462	0.069	4.20E-101	10	Ifi27
Rpl132	5.62E-104	0.8413502	1	0.768	7.63E-100	10	Rpl13
Rps3a12	2.02E-102	0.7872509	1	0.72	2.75E-98	10	Rps3a1
Rpsa2	2.65E-102	0.87385629	1	0.666	3.60E-98	10	Rpsa
Eef1a12	5.68E-102	0.78744362	1	0.865	7.71E-98	10	Eef1a1
Lgals13	1.33E-100	0.74308076	0.838	0.244	1.81E-96	10	Lgals1
Eef1b22	3.93E-100	0.72433568	0.95	0.381	5.34E-96	10	Eef1b2
Rps102	3.50E-99	0.72464372	1	0.768	4.74E-95	10	Rps10
Rpl23a2	4.20E-99	0.72921885	0.967	0.46	5.71E-95	10	Rpl23a
Eif3m1	8.70E-99	0.42462916	0.638	0.139	1.18E-94	10	Eif3m
Rpl272	1.26E-98	0.66217449	0.933	0.371	1.71E-94	10	Rpl27
Rps232	6.73E-98	0.73687977	0.996	0.718	9.14E-94	10	Rps23
Npm12	3.43E-97	0.65571023	0.854	0.276	4.66E-93	10	Npm1
Fkbp31	5.75E-97	0.32239152	0.442	0.068	7.81E-93	10	Fkbp3

Rpl392	5.85E-96	0.74051499	0.996	0.737	7.94E-92	10	Rpl39
Rpl302	7.00E-96	0.72534348	1	0.727	9.50E-92	10	Rpl30
Rplp03	9.80E-96	0.78839696	1	0.666	1.33E-91	10	Rplp0
S100a44	1.29E-95	0.71051224	0.875	0.243	1.75E-91	10	S100a4
Rpl10a3	6.07E-95	0.73393335	0.983	0.456	8.24E-91	10	Rpl10a
Rps32	6.74E-95	0.69088716	1	0.715	9.15E-91	10	Rps3
Rpl43	8.70E-95	0.71655504	0.925	0.386	1.18E-90	10	Rpl4
Rps62	9.35E-95	0.72613941	0.988	0.511	1.27E-90	10	Rps6
Rpl73	3.61E-94	0.70555385	0.988	0.547	4.90E-90	10	Rpl7
Rps152	4.35E-94	0.69595586	0.975	0.543	5.90E-90	10	Rps15
Rpl36a2	1.55E-93	0.65983517	0.938	0.365	2.10E-89	10	Rpl36a
Cd48	1.71E-93	0.44397444	0.579	0.123	2.33E-89	10	Cd48
Tpt12	3.80E-93	0.66858096	1	0.947	5.15E-89	10	Tpt1
Shisa51	4.65E-93	0.65293755	0.858	0.297	6.31E-89	10	Shisa5
Rps52	8.01E-93	0.74320025	1	0.624	1.09E-88	10	Rps5
Rpl92	1.43E-92	0.68983479	1	0.718	1.94E-88	10	Rpl9
Naca2	2.50E-92	0.66192592	0.954	0.425	3.39E-88	10	Naca
Rpl192	4.37E-92	0.69442478	1	0.767	5.93E-88	10	Rpl19
Rpl152	9.51E-92	0.68937379	0.996	0.536	1.29E-87	10	Rpl15
Rpl293	1.87E-91	0.65583425	0.979	0.415	2.54E-87	10	Rpl29
Rps142	1.98E-91	0.69450543	0.996	0.802	2.69E-87	10	Rps14
Rpl232	1.00E-90	0.67796674	1	0.852	1.36E-86	10	Rpl23
Tbc1d10c1	1.43E-90	0.28296002	0.367	0.05	1.94E-86	10	Tbc1d10c
Rpl112	2.50E-90	0.68807877	0.992	0.657	3.40E-86	10	Rpl11
Eif3h1	3.73E-90	0.56413317	0.783	0.247	5.07E-86	10	Eif3h
H2-K11	8.04E-90	0.77758968	0.992	0.573	1.09E-85	10	H2-K1
Rplp13	1.45E-89	0.70553084	1	0.842	1.96E-85	10	Rplp1
Rac22	1.65E-89	0.61865063	0.925	0.353	2.24E-85	10	Rac2
Rps202	6.90E-89	0.74959905	0.992	0.64	9.37E-85	10	Rps20
2010111I01Rik	2.44E-87	0.33192581	0.404	0.063	3.32E-83	10	2010111I01
Gm9493	4.48E-87	0.28818123	0.371	0.053	6.08E-83	10	Gm9493
Dusp21	5.55E-87	0.47868435	0.492	0.094	7.53E-83	10	Dusp2
Rhoh1	1.34E-86	0.38837472	0.542	0.111	1.82E-82	10	Rhoh
Cblb	2.11E-86	0.26765755	0.338	0.044	2.86E-82	10	Cblb
Rps112	2.23E-85	0.69107685	1	0.739	3.03E-81	10	Rps11
Rpl242	2.35E-85	0.65404811	0.996	0.598	3.19E-81	10	Rpl24
Rpl172	7.11E-85	0.66619583	1	0.792	9.65E-81	10	Rpl17
Rpl18a2	2.02E-83	0.63623551	1	0.825	2.75E-79	10	Rpl18a
Jaml	7.31E-83	0.43051816	0.508	0.105	9.93E-79	10	Jaml
Rbm32	3.57E-82	0.69689121	0.892	0.412	4.84E-78	10	Rbm3

Atxn1	5.64E-82	0.27081167	0.321	0.042	7.65E-78	10	Atxn1
Sub12	1.90E-81	0.6251822	0.817	0.291	2.58E-77	10	Sub1
Rpl222	1.44E-80	0.62088179	0.983	0.488	1.95E-76	10	Rpl22
Rpl183	5.13E-80	0.6092564	1	0.694	6.96E-76	10	Rpl18
Rps122	6.73E-79	0.64581445	1	0.802	9.13E-75	10	Rps12
AC163354.1	9.19E-79	0.31139385	0.312	0.042	1.25E-74	10	AC163354.
Rpl262	1.03E-77	0.6223138	0.996	0.709	1.40E-73	10	Rpl26
H2-Q6	1.33E-77	0.3063755	0.379	0.061	1.80E-73	10	H2-Q6
Rps162	3.62E-77	0.55944741	1	0.853	4.92E-73	10	Rps16
Rpl7a3	1.63E-76	0.57509372	0.962	0.459	2.22E-72	10	Rpl7a
Rps212	1.81E-76	0.64539085	0.988	0.643	2.45E-72	10	Rps2
Rin1	1.87E-76	0.35532827	0.504	0.108	2.53E-72	10	Rin1
Uqcrh1	2.75E-76	0.54244478	0.879	0.361	3.74E-72	10	Uqcrh
Mettl23	2.94E-76	0.29868267	0.404	0.071	3.99E-72	10	Mettl23
Rpl142	2.01E-75	0.5820174	0.988	0.496	2.74E-71	10	Rpl14
Rpl212	2.83E-75	0.56181241	0.996	0.74	3.84E-71	10	Rpl21
Arl6ip11	4.51E-75	0.50174445	0.733	0.233	6.12E-71	10	Arl6ip1
Rpl82	2.44E-74	0.58297258	1	0.695	3.31E-70	10	Rpl8
Cdk6	1.20E-73	0.34297168	0.388	0.068	1.63E-69	10	Cdk6
Rps82	2.42E-73	0.59133337	1	0.826	3.29E-69	10	Rps8
Slc25a41	7.03E-73	0.30337241	0.442	0.087	9.54E-69	10	Slc25a4
Eef1d1	1.39E-71	0.41826114	0.642	0.186	1.89E-67	10	Eef1d
Rps262	7.58E-71	0.62384006	0.962	0.612	1.03E-66	10	Rps26
Ybx3	4.68E-70	0.30624993	0.392	0.072	6.36E-66	10	Ybx3
Snrpe1	1.00E-69	0.42936612	0.654	0.199	1.36E-65	10	Snrpe
Lsm5	3.01E-69	0.27274292	0.371	0.065	4.09E-65	10	Lsm5
Psmb83	9.15E-69	0.52367819	0.854	0.333	1.24E-64	10	Psmb8
H2-T22	2.55E-68	0.32961666	0.462	0.1	3.47E-64	10	H2-T22
Eef1g2	5.31E-68	0.4788323	0.671	0.214	7.21E-64	10	Eef1g
Gng2	6.27E-68	0.33654199	0.5	0.117	8.51E-64	10	Gng2
Sumo21	2.11E-67	0.44912061	0.729	0.25	2.87E-63	10	Sumo2
Ppia1	4.64E-66	0.56961202	0.971	0.518	6.30E-62	10	Ppia
Rpl343	5.90E-66	0.53988222	1	0.765	8.01E-62	10	Rpl34
Ms4a6b1	8.81E-65	0.48781484	0.671	0.211	1.20E-60	10	Ms4a6b
Mbnl12	8.14E-64	0.48969724	0.746	0.261	1.10E-59	10	Mbnl1
Eif3f3	1.20E-63	0.45485786	0.808	0.312	1.62E-59	10	Eif3f
Tmsb4x3	2.26E-63	0.60734849	1	0.958	3.07E-59	10	Tmsb4x
Atp5g22	3.53E-63	0.43798442	0.742	0.264	4.79E-59	10	Atp5g2
Cd69	3.18E-62	0.27767439	0.308	0.05	4.31E-58	10	Cd69
AU020206	4.09E-62	0.34870531	0.492	0.12	5.56E-58	10	AU020206

Cox6c2	5.54E-60	0.42274829	0.792	0.307	7.52E-56	10	Cox6c
Id22	1.93E-59	0.59151059	0.846	0.349	2.62E-55	10	Id2
Hnrnpa11	8.18E-59	0.43098332	0.554	0.167	1.11E-54	10	Hnrnpa1
Psmb92	4.05E-58	0.35765364	0.575	0.168	5.50E-54	10	Psmb9
H2afv1	2.53E-57	0.33923833	0.392	0.086	3.43E-53	10	H2afv
Snrpf1	8.70E-57	0.33566935	0.504	0.136	1.18E-52	10	Snrpf
Rplp21	1.01E-56	0.4420601	1	0.795	1.37E-52	10	Rplp2
Anxa61	1.58E-56	0.27064119	0.404	0.09	2.14E-52	10	Anxa6
Tmsb104	3.02E-56	0.45799067	0.904	0.351	4.11E-52	10	Tmsb10
Ly6a3	3.83E-56	0.47428717	0.567	0.161	5.20E-52	10	Ly6a
Rpl13a1	1.49E-54	0.37517179	0.575	0.181	2.02E-50	10	Rpl13a
Ptpn181	1.53E-54	0.4319956	0.738	0.28	2.08E-50	10	Ptpn18
Btf31	1.65E-54	0.45225328	0.854	0.4	2.25E-50	10	Btf3
Rps173	4.94E-54	0.4492454	0.85	0.38	6.71E-50	10	Rps17
Hspe11	5.53E-54	0.38835891	0.567	0.178	7.50E-50	10	Hspe1
Cox7a2l2	7.16E-54	0.40245759	0.667	0.239	9.72E-50	10	Cox7a2l
Il2rg1	1.46E-53	0.27228099	0.4	0.092	1.98E-49	10	Il2rg
Rps27rt	1.49E-53	0.29229045	0.429	0.106	2.02E-49	10	Rps27rt
Rps193	1.63E-53	0.50474368	0.996	0.705	2.22E-49	10	Rps19
Pfdn51	1.09E-49	0.44315932	0.871	0.429	1.47E-45	10	Pfdn5
Ifi27l2a3	1.14E-48	0.657431	0.708	0.276	1.54E-44	10	Ifi27l2a
Rpl62	4.88E-48	0.44512403	0.979	0.659	6.63E-44	10	Rpl6
S100a131	6.59E-47	0.29232169	0.446	0.124	8.95E-43	10	S100a13
Saraf	9.70E-47	0.25847694	0.412	0.107	1.32E-42	10	Saraf
Abrac11	9.86E-47	0.33383907	0.575	0.195	1.34E-42	10	Abrac1
Psmb11	3.32E-46	0.35597218	0.588	0.212	4.51E-42	10	Psmb1
B4galnt1	5.31E-46	0.29689145	0.433	0.12	7.21E-42	10	B4galnt1
Hsp90ab13	2.82E-45	0.482927	0.862	0.421	3.83E-41	10	Hsp90ab1
Ppib2	6.27E-45	0.36707397	0.696	0.285	8.52E-41	10	Ppib
Rps213	1.38E-43	0.41993306	0.992	0.748	1.87E-39	10	Rps21
Rps27a3	1.52E-43	0.39624652	0.996	0.813	2.06E-39	10	Rps27a
Atp5h2	2.53E-43	0.37215543	0.754	0.342	3.44E-39	10	Atp5h
Eif3i1	6.87E-43	0.27688722	0.446	0.131	9.33E-39	10	Eif3i
Rpl362	1.77E-42	0.40839419	0.983	0.632	2.40E-38	10	Rpl36
Atp5c1	2.69E-42	0.3321524	0.558	0.202	3.65E-38	10	Atp5c1
Hint13	1.50E-41	0.37429655	0.621	0.247	2.04E-37	10	Hint1
Uba52	2.06E-41	0.26117054	0.388	0.106	2.79E-37	10	Uba52
Apobec3	2.42E-40	0.27957774	0.492	0.159	3.29E-36	10	Apobec3
Ndufa42	4.67E-40	0.32931533	0.558	0.207	6.33E-36	10	Ndufa4
Eef22	1.42E-39	0.39579945	0.825	0.434	1.93E-35	10	Eef2

Rpl312	1.47E-39	0.32684255	0.775	0.352	1.99E-35	10	Rpl31
B2m3	1.93E-39	0.36887229	0.979	0.682	2.62E-35	10	B2m
Ran1	4.70E-39	0.33915521	0.475	0.162	6.38E-35	10	Ran
Srsf31	6.13E-39	0.30768689	0.567	0.212	8.32E-35	10	Srsf3
Cox5a	8.34E-37	0.32142559	0.621	0.26	1.13E-32	10	Cox5a
Rtraf	1.65E-36	0.27518273	0.425	0.137	2.24E-32	10	Rtraf
Mndal1	3.73E-36	0.29865418	0.471	0.158	5.07E-32	10	Mndal
Dad11	8.35E-36	0.28069342	0.571	0.221	1.13E-31	10	Dad1
Ccl42	1.73E-35	1.1814702	0.479	0.17	2.35E-31	10	Ccl4
Rpl35a3	3.01E-35	0.33896093	1	0.823	4.09E-31	10	Rpl35a
Psmb3	5.33E-35	0.30215489	0.542	0.214	7.24E-31	10	Psmb3
H2-T231	7.91E-35	0.3011561	0.538	0.203	1.07E-30	10	H2-T23
Ndufa13	3.76E-34	0.31910223	0.654	0.297	5.11E-30	10	Ndufa13
Atp5d1	3.35E-33	0.30492413	0.588	0.25	4.55E-29	10	Atp5d
Spcs2	9.78E-33	0.25517677	0.533	0.204	1.33E-28	10	Spcs2
Krtcap2	2.08E-32	0.26966128	0.462	0.167	2.83E-28	10	Krtcap2
Arhgdib2	7.72E-32	0.32204326	0.729	0.362	1.05E-27	10	Arhgdib
Cox7b	1.29E-31	0.27266581	0.512	0.202	1.75E-27	10	Cox7b
Limd22	3.09E-31	0.26925542	0.496	0.19	4.19E-27	10	Limd2
Ifi2031	3.68E-31	0.25008514	0.442	0.151	5.00E-27	10	Ifi203
Psma2	1.78E-30	0.25966745	0.483	0.186	2.41E-26	10	Psma2
Rpl37a2	1.78E-29	0.31147832	0.996	0.818	2.41E-25	10	Rpl37a
Rps252	3.01E-29	0.32749373	0.95	0.631	4.08E-25	10	Rps25
Stk17b1	5.48E-29	0.27301612	0.6	0.261	7.44E-25	10	Stk17b
Serbp11	3.20E-28	0.29054965	0.625	0.292	4.34E-24	10	Serbp1
Eif3k2	6.08E-28	0.26186483	0.575	0.256	8.26E-24	10	Eif3k
Sp1001	1.71E-27	0.27105559	0.412	0.154	2.33E-23	10	Sp100
Ubl5	1.76E-27	0.28512643	0.654	0.32	2.39E-23	10	Ubl5
Cox4i11	3.07E-27	0.30092051	0.833	0.487	4.17E-23	10	Cox4i1
Pabpc11	7.44E-27	0.30156814	0.704	0.373	1.01E-22	10	Pabpc1
Atp5f11	3.08E-26	0.26378513	0.558	0.253	4.19E-22	10	Atp5f1
Slc25a51	1.13E-25	0.29075567	0.546	0.249	1.54E-21	10	Slc25a5
Rpl283	1.01E-24	0.29553559	0.938	0.696	1.38E-20	10	Rpl28
Cox8a	2.19E-24	0.27035697	0.846	0.517	2.97E-20	10	Cox8a
H2-D12	1.18E-23	0.29008905	0.954	0.684	1.61E-19	10	H2-D1
Ptma3	8.34E-23	0.33535097	0.862	0.552	1.13E-18	10	Ptma
Atp5j	2.11E-22	0.25855868	0.546	0.273	2.86E-18	10	Atp5j
Anp32b1	3.37E-22	0.25087106	0.483	0.22	4.58E-18	10	Anp32b
Rpl372	4.17E-22	0.25393578	0.971	0.797	5.66E-18	10	Rpl37
Slc25a31	2.40E-21	0.25505262	0.575	0.297	3.26E-17	10	Slc25a3

Ppp1ca1	3.77E-21	0.25111633	0.558	0.283	5.12E-17	10	Ppp1ca
Capg3	1.60E-19	0.25863546	0.525	0.262	2.17E-15	10	Capg
Hmgb1	1.81E-17	0.26553091	0.571	0.316	2.45E-13	10	Hmgb1
Hmgb2	1.21E-11	0.36923194	0.429	0.237	1.64E-07	10	Hmgb2
Ccl32	0.00037962	0.70751281	0.258	0.178	1	10	Ccl3
Sparc	0	1.78610888	0.917	0.008	0	11	Sparc
Olfml31	0	1.4163955	0.897	0.055	0	11	Olfml3
Fcrls1	0	1.40948035	0.84	0.046	0	11	Fcrls
Syngr1	0	0.81999506	0.744	0.037	0	11	Syngr1
Gpr34	0	0.70360379	0.59	0.015	0	11	Gpr34
Serpine2	0	0.65730643	0.615	0.008	0	11	Serpine2
Plxdc2	0	0.65376565	0.603	0.019	0	11	Plxdc2
Cd34	0	0.43285486	0.397	0.006	0	11	Cd34
Crybb1	0	0.41523413	0.295	0.002	0	11	Crybb1
Pmp22	0	0.34807359	0.346	0.004	0	11	Pmp22
Cd811	4.28E-304	1.93974019	0.974	0.093	5.82E-300	11	Cd81
Slco2b1	3.89E-280	0.33853897	0.378	0.008	5.27E-276	11	Slco2b1
Trem21	1.69E-279	1.58723443	0.949	0.095	2.29E-275	11	Trem2
Ldhb	1.07E-274	0.63641806	0.59	0.028	1.45E-270	11	Ldhb
Ctsf	1.84E-265	0.29755042	0.295	0.004	2.49E-261	11	Ctsf
Siglech	1.33E-261	0.72054925	0.551	0.025	1.81E-257	11	Siglech
Cfh	1.48E-249	0.48235075	0.462	0.017	2.00E-245	11	Cfh
Tmem1191	1.16E-238	0.88404868	0.673	0.047	1.57E-234	11	Tmem119
P2ry12	3.52E-236	0.69926895	0.551	0.029	4.77E-232	11	P2ry12
C1qc1	1.04E-226	2.24317982	0.994	0.143	1.42E-222	11	C1qc
C1qa1	2.50E-226	2.57868625	1	0.147	3.39E-222	11	C1qa
Ctsl1	1.65E-224	1.57318138	0.936	0.117	2.24E-220	11	Ctsl
Abhd12	2.61E-215	0.84189947	0.769	0.074	3.54E-211	11	Abhd12
C1qb1	1.95E-203	2.30772578	1	0.166	2.65E-199	11	C1qb
Ccl12	6.27E-194	1.15278189	0.481	0.027	8.51E-190	11	Ccl12
Hexb1	1.82E-186	2.16952456	1	0.198	2.47E-182	11	Hexb
Ltc4s	2.79E-173	0.61968133	0.571	0.046	3.79E-169	11	Ltc4s
Scoc	3.05E-171	0.43825874	0.468	0.03	4.14E-167	11	Scoc
Cx3cr11	8.43E-162	1.20051106	0.814	0.119	1.14E-157	11	Cx3cr1
Ly861	3.43E-155	1.32367035	0.917	0.17	4.66E-151	11	Ly86
Ptgs11	1.98E-153	0.58317815	0.571	0.052	2.68E-149	11	Ptgs1
Trf1	6.61E-148	0.78444443	0.769	0.105	8.97E-144	11	Trf
Timp2	9.28E-146	0.87802026	0.808	0.124	1.26E-141	11	Timp2
Selenop1	6.33E-143	0.94996687	0.769	0.111	8.59E-139	11	Selenop
Cst72	2.39E-142	0.92356214	0.571	0.059	3.24E-138	11	Cst7

Tanc2	1.19E-129	0.26707493	0.314	0.017	1.62E-125	11	Tanc2
Anxa3	2.13E-128	0.63177297	0.686	0.094	2.89E-124	11	Anxa3
Rnase4	1.87E-127	0.49479668	0.532	0.055	2.54E-123	11	Rnase4
Bin1	5.54E-127	0.57835621	0.603	0.073	7.52E-123	11	Bin1
Golm1	1.61E-126	0.43794474	0.429	0.035	2.18E-122	11	Golm1
Lgmn2	5.69E-126	1.36444751	0.974	0.239	7.72E-122	11	Lgmn
Hpgds1	1.42E-122	0.52572136	0.564	0.064	1.92E-118	11	Hpgds
Ckb1	1.75E-118	0.5251062	0.603	0.075	2.38E-114	11	Ckb
Gas6	4.89E-118	0.32272743	0.301	0.017	6.64E-114	11	Gas6
Csf1r3	8.81E-115	1.20800722	0.91	0.252	1.20E-110	11	Csf1r
Lgals3bp2	4.55E-111	0.79487889	0.712	0.121	6.17E-107	11	Lgals3bp
Itgb51	9.15E-107	0.75807018	0.782	0.148	1.24E-102	11	Itgb5
Ctsd2	1.88E-103	2.0545842	1	0.526	2.56E-99	11	Ctsd
Lpl1	7.12E-103	0.73185805	0.429	0.044	9.67E-99	11	Lpl
Lpcat2	2.21E-102	0.62287925	0.686	0.117	3.00E-98	11	Lpcat2
Camk1	7.24E-101	0.47531881	0.519	0.067	9.84E-97	11	Camk1
Lag32	7.27E-101	0.489196	0.487	0.057	9.87E-97	11	Lag3
Grn2	2.63E-99	1.19586416	0.974	0.334	3.57E-95	11	Grn
Ctsz2	5.52E-95	1.38041971	0.968	0.404	7.50E-91	11	Ctsz
Gpr84	2.30E-94	0.34916873	0.308	0.024	3.13E-90	11	Gpr84
Cst31	3.90E-94	2.14190616	0.994	0.575	5.30E-90	11	Cst3
Comt	1.39E-93	0.37201465	0.468	0.057	1.89E-89	11	Comt
Glul	2.38E-93	0.47041472	0.442	0.052	3.23E-89	11	Glul
Mertk	3.28E-92	0.30158061	0.321	0.026	4.45E-88	11	Mertk
Mef2c	4.19E-92	0.61711295	0.59	0.096	5.69E-88	11	Mef2c
Ctss3	1.42E-91	1.39353289	1	0.457	1.93E-87	11	Ctss
Pde3b	3.23E-88	0.25470843	0.314	0.026	4.39E-84	11	Pde3b
Arsb	5.38E-88	0.28588786	0.301	0.024	7.31E-84	11	Arsb
Itm2b1	2.01E-87	1.3127326	0.994	0.559	2.73E-83	11	Itm2b
Gusb1	2.06E-86	0.57363853	0.641	0.12	2.80E-82	11	Gusb
Rgs10	3.65E-84	0.75807018	0.731	0.171	4.96E-80	11	Rgs10
Hexa1	5.34E-83	0.75291378	0.756	0.187	7.25E-79	11	Hexa
Tbxas1	4.52E-76	0.29229694	0.372	0.043	6.13E-72	11	Tbxas1
Creg11	5.27E-75	0.68527433	0.667	0.153	7.16E-71	11	Creg1
Itm2c	1.43E-74	0.61034383	0.673	0.156	1.94E-70	11	Itm2c
Ctsa2	5.19E-74	0.83745531	0.84	0.257	7.05E-70	11	Ctsa
Gatm1	4.05E-73	0.52245605	0.545	0.096	5.49E-69	11	Gatm
Tcn2	2.46E-72	0.50252139	0.519	0.092	3.34E-68	11	Tcn2
Hebp1	3.13E-71	0.26201309	0.276	0.025	4.26E-67	11	Hebp1
Slamf9	3.90E-69	0.29925523	0.372	0.047	5.30E-65	11	Slamf9

Cd180	1.16E-68	0.33835568	0.391	0.053	1.57E-64	11	Cd180
Daglb	1.25E-68	0.29869536	0.365	0.046	1.70E-64	11	Daglb
Aif12	4.64E-68	0.69621533	0.763	0.207	6.30E-64	11	Aif1
Lrpap1	7.24E-67	0.40553384	0.429	0.067	9.83E-63	11	Lrpap1
Pld42	1.46E-65	0.56724617	0.692	0.173	1.99E-61	11	Pld4
Ergic3	1.85E-63	0.34319716	0.404	0.062	2.51E-59	11	Ergic3
Dst	2.36E-63	0.27190105	0.308	0.036	3.21E-59	11	Dst
Oxct1	1.43E-61	0.27984106	0.321	0.04	1.94E-57	11	Oxct1
Pla2g15	2.08E-60	0.30490976	0.333	0.044	2.82E-56	11	Pla2g15
Lair11	4.51E-60	0.51078844	0.628	0.148	6.13E-56	11	Lair1
Ctsb3	1.22E-59	0.99772031	0.974	0.53	1.65E-55	11	Ctsb
Tmem176a2	7.95E-59	0.38147157	0.5	0.095	1.08E-54	11	Tmem176a
Cd683	4.56E-58	0.69318172	0.827	0.283	6.19E-54	11	Cd68
Lap3	1.86E-57	0.25296585	0.295	0.036	2.52E-53	11	Lap3
Tmem176b2	2.33E-56	0.42212542	0.551	0.117	3.16E-52	11	Tmem176b
Arhgap5	1.58E-55	0.34296702	0.41	0.071	2.15E-51	11	Arhgap5
Npc23	1.32E-54	0.70146096	0.917	0.399	1.80E-50	11	Npc2
Pld3	1.34E-54	0.36907409	0.417	0.075	1.81E-50	11	Pld3
Lamp12	3.39E-51	0.66353191	0.776	0.282	4.60E-47	11	Lamp1
Sirpa1	1.13E-50	0.55793498	0.679	0.21	1.53E-46	11	Sirpa
Ppfia4	1.16E-50	0.36102549	0.417	0.079	1.58E-46	11	Ppfia4
Bst22	1.34E-50	0.5278923	0.66	0.186	1.82E-46	11	Bst2
P2ry13	2.65E-50	0.27315397	0.308	0.045	3.60E-46	11	P2ry13
Tmed3	8.11E-50	0.35160664	0.429	0.085	1.10E-45	11	Tmed3
Sdf2l11	8.76E-49	0.31528499	0.41	0.077	1.19E-44	11	Sdf2l1
Unc93b11	1.69E-48	0.55247518	0.724	0.25	2.29E-44	11	Unc93b1
Pmepa11	4.46E-48	0.37384761	0.545	0.131	6.06E-44	11	Pmepa1
Ssr41	1.50E-46	0.52305171	0.718	0.259	2.03E-42	11	Ssr4
Atraid	1.81E-46	0.25697742	0.314	0.05	2.46E-42	11	Atraid
Plxnb2	1.49E-45	0.31460863	0.417	0.085	2.02E-41	11	Plxnb2
Adgre11	1.69E-45	0.28901743	0.327	0.055	2.29E-41	11	Adgre1
Bsg	3.06E-45	0.55294273	0.679	0.23	4.16E-41	11	Bsg
Scamp2	3.15E-45	0.39628666	0.494	0.122	4.27E-41	11	Scamp2
Pycard1	1.18E-44	0.45393713	0.603	0.179	1.60E-40	11	Pycard
Erp292	1.24E-44	0.55024684	0.712	0.257	1.69E-40	11	Erp29
Atp8a1	6.77E-44	0.27537373	0.346	0.062	9.19E-40	11	Atp8a1
Apoe1	1.84E-43	1.26719682	0.808	0.4	2.50E-39	11	Apoe
Asah1	3.68E-43	0.3577478	0.462	0.108	4.99E-39	11	Asah1
Ctsh3	6.84E-43	0.57251286	0.788	0.302	9.28E-39	11	Ctsh
mt-Nd22	1.24E-42	0.92895326	0.955	0.588	1.68E-38	11	mt-Nd2

Pon2	2.09E-42	0.26875985	0.321	0.056	2.84E-38	11	Pon2
mt-Nd32	1.06E-41	0.74630837	0.846	0.381	1.44E-37	11	mt-Nd3
Tuba1b	1.30E-41	0.51695209	0.5	0.133	1.76E-37	11	Tuba1b
Tgfr2	1.35E-41	0.29812074	0.378	0.077	1.83E-37	11	Tgfr2
Cd63	2.45E-41	0.65275844	0.878	0.366	3.32E-37	11	Cd63
Ntpcr1	5.50E-41	0.29175407	0.346	0.067	7.47E-37	11	Ntpcr
Tmcc3	1.03E-40	0.27750312	0.314	0.055	1.40E-36	11	Tmcc3
mt-Cytb2	1.69E-40	0.88107447	0.981	0.734	2.30E-36	11	mt-Cytb
Cd92	1.75E-40	0.57887148	0.917	0.376	2.38E-36	11	Cd9
Frmd4a	6.28E-40	0.28206272	0.308	0.054	8.53E-36	11	Frmd4a
Tpp1	6.42E-40	0.32450076	0.423	0.098	8.71E-36	11	Tpp1
Fcgr31	6.87E-40	0.57851747	0.827	0.373	9.33E-36	11	Fcgr3
Serinc3	3.62E-39	0.5844663	0.705	0.289	4.91E-35	11	Serinc3
mt-Nd12	5.94E-39	0.81634103	0.929	0.586	8.06E-35	11	mt-Nd1
Cyfp1	1.79E-38	0.35379466	0.481	0.128	2.42E-34	11	Cyfp1
Abca11	6.04E-38	0.29175107	0.359	0.075	8.20E-34	11	Abca1
Irf81	2.49E-37	0.35674069	0.622	0.199	3.38E-33	11	Irf8
B2m4	3.77E-37	0.70080689	0.981	0.686	5.12E-33	11	B2m
Sft2d1	4.05E-37	0.28028408	0.365	0.08	5.50E-33	11	Sft2d1
Cd722	4.88E-37	0.38667248	0.359	0.077	6.63E-33	11	Cd72
Ppp1r14b	5.47E-37	0.31232323	0.41	0.099	7.42E-33	11	Ppp1r14b
Hsp90b11	2.76E-36	0.50310971	0.744	0.286	3.74E-32	11	Hsp90b1
mt-Nd42	2.08E-35	0.76349043	0.968	0.684	2.83E-31	11	mt-Nd4
Glmp	2.35E-35	0.33769249	0.417	0.106	3.19E-31	11	Glmp
Fcgr12	4.67E-35	0.36359796	0.494	0.138	6.34E-31	11	Fcgr1
Selenof	1.19E-34	0.32306224	0.506	0.15	1.62E-30	11	Selenof
Hmgn1	3.31E-33	0.25224729	0.282	0.054	4.49E-29	11	Hmgn1
Kctd12	2.04E-32	0.38739103	0.481	0.144	2.78E-28	11	Kctd12
mt-Co32	2.75E-32	0.72764608	1	0.822	3.74E-28	11	mt-Co3
Laptm4a	5.96E-31	0.3117751	0.449	0.132	8.09E-27	11	Laptm4a
Pdia31	9.87E-31	0.41666416	0.596	0.222	1.34E-26	11	Pdia3
Os9	1.82E-30	0.2790035	0.397	0.107	2.47E-26	11	Os9
Fkbp2	5.31E-30	0.28531577	0.359	0.092	7.21E-26	11	Fkbp2
Tmem86a1	3.52E-29	0.29006444	0.417	0.118	4.78E-25	11	Tmem86a
Qk	3.65E-29	0.36648495	0.526	0.18	4.95E-25	11	Qk
Tubb51	3.92E-29	0.41432838	0.532	0.187	5.32E-25	11	Tubb5
Man2b11	4.62E-29	0.44272576	0.66	0.279	6.27E-25	11	Man2b1
Lat2	1.00E-28	0.27049327	0.321	0.077	1.36E-24	11	Lat2
Epb41l2	3.55E-28	0.34873819	0.455	0.145	4.82E-24	11	Epb41l2
Lrp13	3.79E-28	0.32055621	0.506	0.165	5.14E-24	11	Lrp1

Axl2	1.00E-27	0.28240787	0.372	0.1	1.36E-23	11	Axl
mt-Atp62	1.43E-27	0.62677513	0.994	0.812	1.95E-23	11	mt-Atp6
Ctsc3	1.79E-27	0.37149076	0.615	0.226	2.42E-23	11	Ctsc
Calr2	2.28E-27	0.5431763	0.712	0.348	3.09E-23	11	Calr
Mafb4	2.48E-27	0.42356654	0.609	0.22	3.37E-23	11	Mafb
Ndufc2	2.54E-27	0.25269188	0.417	0.122	3.45E-23	11	Ndufc2
Spp1	9.99E-27	1.07842806	0.417	0.126	1.36E-22	11	Spp1
mt-Nd4l1	1.25E-26	0.32379305	0.442	0.141	1.70E-22	11	mt-Nd4l
mt-Co22	2.68E-26	0.61495139	0.994	0.811	3.64E-22	11	mt-Co2
Gnas1	3.04E-26	0.56485996	0.705	0.361	4.12E-22	11	Gnas
Fcgr41	3.38E-26	0.27588213	0.372	0.104	4.58E-22	11	Fcgr4
Rpn2	3.66E-26	0.26254642	0.378	0.109	4.97E-22	11	Rpn2
Cd300c2	2.28E-25	0.37247727	0.654	0.284	3.10E-21	11	Cd300c2
Slc11a1	4.45E-25	0.26385638	0.417	0.128	6.04E-21	11	Slc11a1
mt-Nd51	1.40E-24	0.43763987	0.628	0.278	1.90E-20	11	mt-Nd5
Rrbp13	4.78E-24	0.4260395	0.763	0.387	6.49E-20	11	Rrbp1
Mpeg12	8.82E-24	0.42307056	0.763	0.372	1.20E-19	11	Mpeg1
Rplp14	6.39E-23	0.48907986	0.936	0.845	8.68E-19	11	Rplp1
Rhob	9.22E-23	0.2539799	0.321	0.089	1.25E-18	11	Rhob
Clta	1.32E-22	0.38315487	0.744	0.402	1.79E-18	11	Clta
Arl6ip12	2.67E-22	0.32200765	0.577	0.243	3.62E-18	11	Arl6ip1
Ppib3	1.05E-21	0.33529147	0.628	0.292	1.42E-17	11	Ppib
mt-Co12	1.73E-20	0.42914484	0.994	0.844	2.36E-16	11	mt-Co1
Rpl10a4	2.46E-20	0.40422633	0.821	0.466	3.34E-16	11	Rpl10a
Pdia62	5.41E-18	0.25885553	0.417	0.159	7.35E-14	11	Pdia6
Ptms1	1.34E-17	0.33171831	0.5	0.225	1.82E-13	11	Ptms
Tgfbr11	3.68E-17	0.30194588	0.494	0.216	4.99E-13	11	Tgfbr1
Lamp2	7.59E-17	0.27392228	0.494	0.218	1.03E-12	11	Lamp2
Itgam1	1.65E-16	0.32192919	0.577	0.28	2.24E-12	11	Itgam
Cd37	1.68E-16	0.25359049	0.455	0.189	2.28E-12	11	Cd37
Tmem59	4.02E-16	0.27526218	0.429	0.185	5.45E-12	11	Tmem59
Hspe12	1.57E-15	0.25778488	0.436	0.185	2.13E-11	11	Hspe1
Atp5g23	1.81E-15	0.28610047	0.551	0.274	2.46E-11	11	Atp5g2
Ly6e2	8.86E-14	0.30394546	0.769	0.47	1.20E-09	11	Ly6e
Tmsb4x4	9.32E-14	0.40253506	0.994	0.958	1.26E-09	11	Tmsb4x
Laptm5	1.50E-13	0.29784658	0.891	0.643	2.03E-09	11	Laptm5
Cd84	1.54E-13	0.25557526	0.442	0.203	2.10E-09	11	Cd84
Selplg2	3.28E-13	0.30898323	0.654	0.389	4.45E-09	11	Selplg
Rps123	3.49E-12	0.34071925	0.878	0.808	4.73E-08	11	Rps12
Ppia2	4.57E-11	0.26280683	0.801	0.527	6.21E-07	11	Ppia

Ccl62	9.76E-11	0.28432948	0.391	0.182	1.33E-06	11	Ccl6
Rpl353	6.91E-10	0.29698844	0.622	0.412	9.38E-06	11	Rpl35
Cyba1	1.30E-08	0.26627293	0.84	0.632	0.00017631	11	Cyba
Rps292	3.36E-08	0.29808246	0.91	0.871	0.00045676	11	Rps29
H2-K12	4.09E-08	0.31101157	0.769	0.584	0.00055505	11	H2-K1
Rps214	4.20E-08	0.28447662	0.84	0.651	0.00056989	11	Rps2
Eef1a13	4.73E-07	0.25996628	0.929	0.868	0.00641764	11	Eef1a1
Lck2	1.31E-52	0.62687561	0.566	0.081	1.78E-48	12	Lck
Ikzf21	1.78E-42	0.77484764	0.355	0.04	2.41E-38	12	Ikzf2
mt-Atp63	1.63E-39	1.34932103	1	0.814	2.21E-35	12	mt-Atp6
Gimap8	4.70E-38	0.36222729	0.263	0.025	6.38E-34	12	Gimap8
mt-Nd43	2.19E-37	1.1827713	1	0.687	2.98E-33	12	mt-Nd4
mt-Cytb3	2.89E-37	1.34452452	1	0.737	3.92E-33	12	mt-Cytb
mt-Co13	5.43E-35	1.19752243	0.987	0.846	7.37E-31	12	mt-Co1
mt-Co33	9.18E-35	1.22498691	0.987	0.824	1.25E-30	12	mt-Co3
mt-Nd13	2.80E-34	1.10716374	0.987	0.589	3.80E-30	12	mt-Nd1
mt-Co23	4.96E-33	1.11200345	1	0.813	6.73E-29	12	mt-Co2
mt-Nd23	1.69E-32	1.12290226	0.987	0.592	2.29E-28	12	mt-Nd2
Ccdc88c	1.39E-30	0.33286324	0.342	0.05	1.89E-26	12	Ccdc88c
Cd3e2	1.21E-29	0.50197896	0.461	0.087	1.64E-25	12	Cd3e
Ets12	5.56E-29	0.43025083	0.434	0.081	7.55E-25	12	Ets1
Trac2	1.56E-26	0.48938363	0.461	0.092	2.11E-22	12	Trac
Bcl11b2	1.33E-25	0.33202886	0.316	0.049	1.81E-21	12	Bcl11b
mt-Nd33	4.69E-23	0.78869676	0.803	0.387	6.37E-19	12	mt-Nd3
Icos1	5.62E-23	0.2685698	0.303	0.049	7.63E-19	12	Icos
Il2rb2	8.29E-23	0.37331657	0.368	0.071	1.13E-18	12	Il2rb
Cblb1	2.62E-22	0.29371704	0.303	0.051	3.55E-18	12	Cblb
mt-Nd52	5.13E-22	0.68461345	0.697	0.281	6.96E-18	12	mt-Nd5
Rabgap1l1	5.52E-21	0.37150726	0.316	0.059	7.50E-17	12	Rabgap1l
Bcl22	1.13E-20	0.50089647	0.342	0.071	1.54E-16	12	Bcl2
H2-Q61	2.86E-20	0.30840139	0.342	0.07	3.88E-16	12	H2-Q6
Ablim12	4.28E-18	0.29080785	0.276	0.052	5.81E-14	12	Ablim1
Atrx	4.46E-18	0.50335191	0.579	0.209	6.06E-14	12	Atrx
Spn1	9.62E-18	0.29160546	0.316	0.068	1.31E-13	12	Spn
Rhoh2	9.30E-17	0.36152712	0.434	0.123	1.26E-12	12	Rhoh
Prkch1	1.41E-16	0.3196009	0.316	0.073	1.92E-12	12	Prkch
Acap1	1.86E-16	0.27336148	0.276	0.056	2.53E-12	12	Acap1
Mbnl13	2.62E-16	0.55429441	0.632	0.274	3.56E-12	12	Mbnl1
Rpsa3	2.70E-16	0.91522199	0.934	0.675	3.67E-12	12	Rpsa
Ptpn222	2.91E-16	0.29979561	0.342	0.082	3.96E-12	12	Ptpn22

Gm26917	2.33E-15	0.47218243	0.382	0.108	3.16E-11	12	Gm26917
Cd3g2	1.74E-14	0.39358464	0.395	0.105	2.37E-10	12	Cd3g
Gimap32	3.75E-14	0.26284449	0.289	0.067	5.09E-10	12	Gimap3
Lag33	5.92E-14	0.30339088	0.276	0.065	8.04E-10	12	Lag3
H2-Q72	6.26E-14	0.43716924	0.487	0.172	8.50E-10	12	H2-Q7
Trbc22	2.01E-13	0.34066207	0.382	0.105	2.73E-09	12	Trbc2
Nkg72	6.02E-13	0.25924373	0.355	0.095	8.17E-09	12	Nkg7
Kmt2a1	6.50E-13	0.367136	0.355	0.106	8.82E-09	12	Kmt2a
Tnfrsf182	1.08E-12	0.2795501	0.289	0.074	1.46E-08	12	Tnfrsf18
Akap131	2.13E-12	0.53324071	0.579	0.273	2.90E-08	12	Akap13
H2-K13	3.37E-12	0.67853244	0.868	0.585	4.57E-08	12	H2-K1
Uhrf2	5.32E-12	0.28132815	0.289	0.08	7.22E-08	12	Uhrf2
AC149090.1	7.26E-12	0.4340896	0.434	0.162	9.86E-08	12	AC149090.
Rapgef6	1.21E-11	0.26317175	0.342	0.104	1.64E-07	12	Rapgef6
AU0202061	1.30E-11	0.38302843	0.382	0.131	1.77E-07	12	AU020206
Macf1	1.41E-11	0.44589786	0.408	0.153	1.92E-07	12	Macf1
Ptprc1	2.66E-11	0.557817	0.75	0.508	3.61E-07	12	Ptprc
Ankrd111	2.78E-11	0.4890289	0.618	0.346	3.78E-07	12	Ankrd11
Pnn	2.47E-10	0.34578935	0.395	0.15	3.36E-06	12	Pnn
Tia1	1.06E-09	0.25677573	0.263	0.078	1.44E-05	12	Tia1
Arglu1	2.36E-09	0.34635478	0.461	0.208	3.20E-05	12	Arglu1
Malat11	3.57E-09	0.26076303	1	0.981	4.84E-05	12	Malat1
Ahnak2	4.42E-09	0.36094477	0.421	0.176	6.00E-05	12	Ahnak
Rinl2	4.60E-09	0.29803781	0.329	0.119	6.24E-05	12	Rinl
Ccnd21	4.60E-09	0.35732435	0.408	0.167	6.25E-05	12	Ccnd2
Ptprcap2	7.61E-09	0.31692473	0.316	0.107	0.00010335	12	Ptprcap
Fubp1	7.63E-09	0.30487787	0.355	0.139	0.00010364	12	Fubp1
Prrc2c	8.12E-09	0.39177906	0.513	0.262	0.00011022	12	Prrc2c
Cd3d2	8.20E-09	0.27560405	0.316	0.103	0.00011126	12	Cd3d
Ms4a4b2	4.49E-08	0.32809882	0.303	0.106	0.00060961	12	Ms4a4b
Nktr1	5.08E-08	0.30864598	0.5	0.255	0.00068974	12	Nktr
Ankrd121	1.21E-07	0.43002847	0.461	0.24	0.00163995	12	Ankrd12
Il7r1	1.56E-07	0.3480023	0.263	0.09	0.0021229	12	Il7r
Maf1	2.13E-07	0.40282943	0.316	0.128	0.00289185	12	Maf
Prpf38b	5.28E-07	0.31224762	0.408	0.2	0.00716506	12	Prpf38b
Ttc14	5.32E-07	0.32279308	0.382	0.182	0.00722524	12	Ttc14
Luc7l21	4.89E-06	0.40245399	0.487	0.301	0.06632683	12	Luc7l2
Kcnq1ot1	1.31E-05	0.27490134	0.263	0.11	0.17738072	12	Kcnq1ot1
Peli1	1.63E-05	0.25002658	0.382	0.192	0.22156429	12	Peli1
Srrm2	2.63E-05	0.31327893	0.579	0.391	0.35637839	12	Srrm2

Wnk1	5.40E-05	0.28771007	0.447	0.269	0.73340007	12	Wnk1
Pnlsr	0.00012041	0.25770561	0.434	0.261	1	12	Pnlsr
H2-D13	0.00036118	0.42485693	0.816	0.692	1	12	H2-D1
Rpl363	0.00057798	0.35345987	0.803	0.642	1	12	Rpl36
Gm424183	0.00291708	0.39362144	0.987	0.975	1	12	Gm42418
Igkc	0	4.85433083	0.708	0.01	0	13	Igkc
Iglc2	0	1.2883057	0.625	0.002	0	13	Iglc2
Cd79b	0	1.09591377	0.653	0.007	0	13	Cd79b
Cd79a	0	1.07977328	0.722	0	0	13	Cd79a
Ly6d	0	1.07071262	0.694	0.011	0	13	Ly6d
Mzb1	0	1.00917544	0.514	0.005	0	13	Mzb1
Iglc3	0	0.91419319	0.597	0.008	0	13	Iglc3
Ebf1	0	0.81576298	0.556	0	0	13	Ebf1
Ms4a1	0	0.54302808	0.431	0.001	0	13	Ms4a1
Ighd	0	0.54288129	0.347	0.001	0	13	Ighd
Fcmr	0	0.49387163	0.403	0	0	13	Fcmr
Gm30211	0	0.46694491	0.306	0.001	0	13	Gm30211
Bank1	3.93E-293	0.62348082	0.417	0.005	5.34E-289	13	Bank1
Iglc1	2.70E-286	3.15081468	0.319	0.002	3.67E-282	13	Iglc1
Ighm	8.48E-106	2.10975211	0.764	0.08	1.15E-101	13	Ighm
Ralgps2	2.61E-85	0.31725733	0.278	0.011	3.54E-81	13	Ralgps2
Bcl11a	2.08E-77	0.57721989	0.444	0.032	2.83E-73	13	Bcl11a
Btla	2.46E-61	0.25858392	0.292	0.017	3.34E-57	13	Btla
H2-DMb21	5.21E-51	0.34753992	0.403	0.039	7.07E-47	13	H2-DMb2
H2-Ob	1.08E-50	0.30069231	0.264	0.017	1.46E-46	13	H2-Ob
Gimap62	1.10E-45	0.44214616	0.444	0.054	1.49E-41	13	Gimap6
Siglecg	5.49E-45	0.28535858	0.264	0.02	7.45E-41	13	Siglecg
Mef2c1	5.98E-44	0.57979451	0.597	0.102	8.12E-40	13	Mef2c
Man1a	1.60E-40	0.3019661	0.333	0.034	2.17E-36	13	Man1a
Tcf4	3.69E-38	0.71964612	0.514	0.086	5.01E-34	13	Tcf4
Dnajc7	2.86E-37	0.52396621	0.542	0.097	3.89E-33	13	Dnajc7
Fchsd2	6.74E-35	0.35379732	0.361	0.047	9.15E-31	13	Fchsd2
Ptprcap3	2.41E-32	0.41172905	0.556	0.105	3.28E-28	13	Ptprcap
Gm83692	2.74E-32	0.45375069	0.389	0.057	3.72E-28	13	Gm8369
Chchd10	1.36E-31	0.27422356	0.264	0.028	1.85E-27	13	Chchd10
Pkig	2.24E-31	0.37604846	0.375	0.056	3.05E-27	13	Pkig
Abhd17b	1.31E-30	0.25502493	0.278	0.032	1.78E-26	13	Abhd17b
Rps203	1.39E-30	1.07555753	0.972	0.649	1.88E-26	13	Rps20
Rps4x4	6.17E-30	0.93030594	0.958	0.561	8.38E-26	13	Rps4x
Rpl123	1.62E-29	1.06157058	0.917	0.505	2.19E-25	13	Rpl12

Rnase61	2.75E-29	0.3434294	0.403	0.065	3.74E-25	13	Rnase6
Gimap12	4.91E-29	0.34596189	0.431	0.074	6.67E-25	13	Gimap1
Rps243	5.70E-28	1.1187088	0.986	0.761	7.74E-24	13	Rps24
Sell	4.54E-27	0.36884985	0.431	0.079	6.16E-23	13	Sell
Rpl133	9.47E-25	0.86658737	0.958	0.774	1.29E-20	13	Rpl13
Rps194	1.09E-24	0.94372649	0.917	0.713	1.48E-20	13	Rps19
Rps183	1.18E-24	0.83002796	0.944	0.606	1.60E-20	13	Rps18
Apobec31	2.13E-24	0.48935182	0.597	0.166	2.89E-20	13	Apobec3
Foxp1	2.58E-24	0.55564947	0.472	0.11	3.51E-20	13	Foxp1
Zbtb20	8.51E-24	0.44279465	0.361	0.067	1.16E-19	13	Zbtb20
Serp1	9.89E-24	0.48441426	0.667	0.205	1.34E-19	13	Serp1
Rpl83	2.68E-23	0.71971887	0.944	0.704	3.64E-19	13	Rpl8
Rpl10a5	1.26E-22	0.72528634	0.917	0.47	1.72E-18	13	Rpl10a
Rps53	1.53E-22	0.76183555	0.931	0.634	2.07E-18	13	Rps5
Swap70	1.79E-22	0.26635238	0.347	0.062	2.43E-18	13	Swap70
Rpl53	2.45E-22	0.69342154	0.889	0.464	3.33E-18	13	Rpl5
Rps103	4.38E-22	0.7767498	0.944	0.775	5.95E-18	13	Rps10
Rps3a13	4.92E-22	0.72885516	0.944	0.727	6.68E-18	13	Rps3a1
Rpl18a3	5.72E-22	0.7688827	0.944	0.829	7.76E-18	13	Rpl18a
Rpl233	5.80E-22	0.69542573	0.958	0.856	7.88E-18	13	Rpl23
Rpl213	6.24E-22	0.75516061	0.917	0.747	8.47E-18	13	Rpl21
Rpl36a3	1.16E-21	0.58143715	0.889	0.38	1.57E-17	13	Rpl36a
Rps163	1.22E-21	0.71430511	0.931	0.857	1.66E-17	13	Rps16
Rps73	1.34E-21	0.77593454	0.903	0.611	1.82E-17	13	Rps7
Rpl323	1.42E-21	0.76710285	0.944	0.689	1.93E-17	13	Rpl32
Cnp	3.35E-21	0.25693092	0.319	0.057	4.55E-17	13	Cnp
Rps113	4.78E-21	0.74785324	0.889	0.746	6.49E-17	13	Rps11
H2-DMa2	5.25E-21	0.45750044	0.681	0.212	7.13E-17	13	H2-DMa
Rpl74	6.09E-21	0.64412474	0.931	0.558	8.27E-17	13	Rpl7
Cd742	6.86E-21	0.59832151	0.917	0.378	9.31E-17	13	Cd74
Rpl193	7.51E-21	0.72923553	0.944	0.774	1.02E-16	13	Rpl19
Rpl313	1.53E-20	0.65422195	0.889	0.482	2.08E-16	13	Rpl3
Cd371	1.54E-20	0.52324474	0.583	0.191	2.08E-16	13	Cd37
Rpl303	5.22E-20	0.73870602	0.917	0.734	7.08E-16	13	Rpl30
Rpl27a3	6.21E-20	0.77108516	0.917	0.799	8.43E-16	13	Rpl27a
Rack13	1.04E-19	0.60478661	0.917	0.526	1.41E-15	13	Rack1
Rpl263	1.23E-19	0.66350852	0.944	0.717	1.68E-15	13	Rpl26
Ly6a4	1.47E-19	0.77053134	0.583	0.171	1.99E-15	13	Ly6a
Rps15a3	1.74E-19	0.70885785	0.944	0.668	2.36E-15	13	Rps15a
Hmgn11	2.15E-19	0.28609351	0.306	0.057	2.92E-15	13	Hmgn1

Rps133	2.47E-19	0.74166489	0.903	0.725	3.35E-15	13	Rps13
Rpl393	3.29E-19	0.70357208	0.931	0.744	4.47E-15	13	Rpl39
Ly862	6.57E-19	0.33355732	0.597	0.182	8.92E-15	13	Ly86
H2-Aa2	1.47E-18	0.3907419	0.778	0.265	2.00E-14	13	H2-Aa
Rpsa4	2.21E-18	0.71674029	0.903	0.675	3.01E-14	13	Rpsa
Rps33	3.83E-18	0.61923875	0.931	0.723	5.20E-14	13	Rps3
H2-Oa1	3.97E-18	0.26767881	0.306	0.058	5.39E-14	13	H2-Oa
Rplp04	1.60E-17	0.56774736	0.931	0.675	2.17E-13	13	Rplp0
Rpl93	2.53E-17	0.59244931	0.917	0.726	3.43E-13	13	Rpl9
Rpl113	5.27E-17	0.53207282	0.944	0.666	7.16E-13	13	Rpl11
Rpl184	6.45E-17	0.6044294	0.917	0.702	8.75E-13	13	Rpl18
Rpl344	7.41E-17	0.61907254	0.917	0.772	1.01E-12	13	Rpl34
Rps272	9.66E-17	0.74038634	0.944	0.874	1.31E-12	13	Rps27
Rpl63	1.63E-16	0.51790112	0.944	0.668	2.21E-12	13	Rpl6
Rpl143	1.83E-16	0.55479282	0.875	0.51	2.49E-12	13	Rpl14
Rhoh3	2.02E-16	0.31457266	0.444	0.123	2.74E-12	13	Rhoh
Ppdpf	2.10E-16	0.26898738	0.333	0.076	2.85E-12	13	Ppdpf
Rps63	2.39E-16	0.53420225	0.889	0.524	3.25E-12	13	Rps6
H2-Eb12	2.59E-16	0.2977468	0.722	0.25	3.51E-12	13	H2-Eb1
Rpl173	2.67E-16	0.60890407	0.917	0.798	3.62E-12	13	Rpl17
Rps143	2.98E-16	0.57545119	0.903	0.807	4.04E-12	13	Rps14
Rps91	4.85E-16	0.52715966	0.931	0.891	6.59E-12	13	Rps9
Rpl284	5.43E-16	0.4893585	0.917	0.703	7.37E-12	13	Rpl28
Rps83	5.51E-16	0.54104059	0.958	0.831	7.49E-12	13	Rps8
Plac83	7.92E-16	0.63902674	0.611	0.208	1.08E-11	13	Plac8
Cd691	1.47E-15	0.30219003	0.278	0.057	1.99E-11	13	Cd69
Rps253	2.49E-15	0.51620249	0.903	0.64	3.38E-11	13	Rps25
Rpl223	3.86E-15	0.59170047	0.847	0.502	5.24E-11	13	Rpl22
Rplp15	8.66E-15	0.60486108	0.931	0.846	1.18E-10	13	Rplp1
Rpl354	1.08E-14	0.48492985	0.819	0.413	1.46E-10	13	Rpl35
Rps215	1.08E-14	0.60089483	0.903	0.755	1.47E-10	13	Rps21
Rabgap1l2	1.38E-14	0.25818031	0.278	0.06	1.87E-10	13	Rabgap1l
Rpl243	2.21E-14	0.49165462	0.931	0.609	2.99E-10	13	Rpl24
Ets13	2.55E-14	0.26803416	0.333	0.082	3.47E-10	13	Ets1
Rps153	4.00E-14	0.53395306	0.889	0.555	5.43E-10	13	Rps15
Rpl44	4.28E-14	0.43924364	0.847	0.4	5.81E-10	13	Rpl4
Rpl153	9.73E-14	0.52323412	0.861	0.548	1.32E-09	13	Rpl15
Rps233	1.03E-13	0.53227768	0.931	0.726	1.39E-09	13	Rps23
4930523C07Rik	2.18E-13	0.33099373	0.361	0.101	2.96E-09	13	4930523C0
Rps124	2.21E-13	0.53025488	0.917	0.808	3.00E-09	13	Rps12

Rps216	2.65E-13	0.51011854	0.889	0.653	3.59E-09	13	Rps2
Ifi2032	5.47E-13	0.38333256	0.472	0.158	7.43E-09	13	Ifi203
Rps263	5.66E-13	0.51897755	0.875	0.621	7.68E-09	13	Rps26
Npm13	7.89E-13	0.40034282	0.667	0.292	1.07E-08	13	Npm1
Rpl37a3	8.48E-13	0.48604195	0.958	0.823	1.15E-08	13	Rpl37a
Herpud1	1.03E-12	0.27252143	0.319	0.084	1.40E-08	13	Herpud1
Mndal2	1.03E-12	0.28252501	0.486	0.166	1.40E-08	13	Mndal
Naca3	1.14E-12	0.43529178	0.806	0.439	1.55E-08	13	Naca
Rpl35a4	1.14E-12	0.46587298	0.944	0.828	1.55E-08	13	Rpl35a
Rpl364	1.49E-12	0.46836323	0.903	0.641	2.02E-08	13	Rpl36
Ly6e3	1.57E-12	0.4432088	0.861	0.472	2.13E-08	13	Ly6e
Rpl273	1.81E-12	0.36950298	0.778	0.386	2.46E-08	13	Rpl27
Rps174	2.31E-12	0.40769621	0.75	0.392	3.13E-08	13	Rps17
Rplp22	2.89E-12	0.48210519	0.917	0.801	3.92E-08	13	Rplp2
Rpl22l12	3.37E-12	0.36658147	0.639	0.282	4.58E-08	13	Rpl22l1
Rps27rt1	3.56E-12	0.26781554	0.375	0.114	4.84E-08	13	Rps27rt
Rpl314	6.73E-12	0.44398264	0.694	0.364	9.13E-08	13	Rpl31
mt-Co34	7.15E-12	0.32006423	1	0.824	9.71E-08	13	mt-Co3
Fau	8.57E-12	0.38872234	1	0.964	1.16E-07	13	Fau
mt-Nd53	9.02E-12	0.35173333	0.639	0.282	1.22E-07	13	mt-Nd5
Eef1a14	9.94E-12	0.43767227	0.944	0.869	1.35E-07	13	Eef1a1
Rps282	1.52E-11	0.48000653	0.875	0.642	2.07E-07	13	Rps28
Eef1b23	2.08E-11	0.39222811	0.75	0.397	2.82E-07	13	Eef1b2
Ptma4	2.44E-11	0.46495935	0.847	0.559	3.32E-07	13	Ptma
mt-Atp64	2.56E-11	0.34425769	1	0.814	3.48E-07	13	mt-Atp6
Rpl294	2.57E-11	0.51142895	0.75	0.432	3.49E-07	13	Rpl29
Eif3f4	2.61E-11	0.37250521	0.681	0.326	3.55E-07	13	Eif3f
Rps27a4	2.66E-11	0.43062389	0.931	0.818	3.61E-07	13	Rps27a
Rpl23a3	4.42E-11	0.42228695	0.792	0.474	6.00E-07	13	Rpl23a
Eif3e2	6.75E-11	0.27399745	0.444	0.162	9.16E-07	13	Eif3e
Sub13	1.79E-10	0.34499257	0.639	0.306	2.42E-06	13	Sub1
Tpt13	3.44E-10	0.37512049	0.986	0.949	4.66E-06	13	Tpt1
Napsa2	5.96E-10	0.33433463	0.486	0.2	8.09E-06	13	Napsa
Pou2f22	1.11E-09	0.26891458	0.458	0.176	1.51E-05	13	Pou2f2
Sec11c	1.31E-09	0.36526206	0.403	0.154	1.78E-05	13	Sec11c
Ltb2	5.03E-09	0.35659403	0.458	0.194	6.83E-05	13	Ltb
Crlf3	7.33E-09	0.25080136	0.333	0.118	9.95E-05	13	Crlf3
Irf82	1.31E-08	0.26667436	0.486	0.205	0.00017747	13	Irf8
Cd47	1.32E-08	0.31189976	0.597	0.303	0.00017986	13	Cd47
Eef1g3	1.60E-08	0.28276639	0.5	0.227	0.00021776	13	Eef1g

Eef23	1.91E-08	0.35786001	0.736	0.445	0.00025891	13	Eef2
Rpl13a2	3.28E-08	0.33336309	0.431	0.192	0.00044562	13	Rpl13a
Bst23	3.33E-08	0.51426641	0.431	0.195	0.00045275	13	Bst2
Rpl7a4	5.36E-08	0.3299133	0.764	0.473	0.00072725	13	Rpl7a
Pold4	5.55E-08	0.28045512	0.417	0.182	0.00075306	13	Pold4
Uqcrh2	6.76E-08	0.25834766	0.694	0.376	0.0009172	13	Uqcrh
Rpl382	9.04E-08	0.37931028	0.861	0.67	0.00122762	13	Rpl38
Rps293	1.00E-07	0.33465834	0.931	0.871	0.00135798	13	Rps29
Tsc22d3	1.31E-07	0.30197071	0.417	0.185	0.00178304	13	Tsc22d3
Atp5c11	5.02E-07	0.26436391	0.444	0.212	0.00681444	13	Atp5c1
Eif4a2	5.37E-07	0.25809993	0.347	0.146	0.00728485	13	Eif4a2
Arhgdib3	1.47E-06	0.27412892	0.639	0.372	0.01993012	13	Arhgdib
Rpl102	2.10E-06	0.30959689	0.875	0.703	0.02853085	13	Rpl10
Rpl373	2.61E-06	0.30679292	0.903	0.802	0.0354876	13	Rpl37
Hsp90ab14	2.67E-06	0.30770441	0.708	0.434	0.03624913	13	Hsp90ab1
Btf32	3.30E-06	0.25149133	0.667	0.413	0.04476643	13	Btf3
Shisa52	9.43E-06	0.26159019	0.556	0.314	0.12801166	13	Shisa5
H2-K14	5.18E-05	0.27666222	0.792	0.586	0.70279405	13	H2-K1
Ppia3	7.71E-05	0.30069231	0.708	0.532	1	13	Ppia
Ssr42	0.00012301	0.25708562	0.458	0.267	1	13	Ssr4
Syng21	0.00074909	0.28257177	0.347	0.196	1	13	Syng2
Ccr7	0	1.8985952	0.956	0.012	0	14	Ccr7
Fscn1	0	1.78095487	0.809	0.008	0	14	Fscn1
Cacnb3	0	1.00389293	0.838	0.002	0	14	Cacnb3
Ramp3	0	0.97294871	0.603	0.011	0	14	Ramp3
Il4i1	0	0.93128387	0.662	0.008	0	14	Il4i1
Ccl22	0	0.84587949	0.426	0.002	0	14	Ccl22
Il12b	0	0.76336519	0.309	0	0	14	Il12b
Bcl2l14	0	0.58143529	0.368	0.003	0	14	Bcl2l14
Nudt17	0	0.51669074	0.412	0	0	14	Nudt17
Strip2	0	0.38448877	0.353	0.001	0	14	Strip2
Adcy6	0	0.28015518	0.265	0	0	14	Adcy6
Tmem150c	0	0.28000841	0.279	0	0	14	Tmem150c
Socs2	9.29E-308	0.98337703	0.794	0.022	1.26E-303	14	Socs2
Slc27a3	1.62E-281	0.36413945	0.279	0.001	2.21E-277	14	Slc27a3
Tbc1d41	7.94E-257	1.43262405	0.897	0.038	1.08E-252	14	Tbc1d4
Grasp	6.84E-250	0.37966173	0.397	0.005	9.29E-246	14	Grasp
Gnb4	5.17E-241	0.60771379	0.471	0.009	7.02E-237	14	Gnb4
Serpinb9	4.40E-220	0.84688232	0.588	0.017	5.97E-216	14	Serpinb9
Cmc2	7.25E-183	0.54287473	0.515	0.016	9.84E-179	14	Cmc2

Serpinb6b	2.36E-179	0.98001508	0.574	0.021	3.21E-175	14	Serpinb6b
Stat4	3.45E-173	0.87445926	0.735	0.038	4.68E-169	14	Stat4
Relb	1.89E-171	1.02327621	0.868	0.058	2.57E-167	14	Relb
Etv3	8.76E-162	0.92799322	0.809	0.052	1.19E-157	14	Etv3
Slc4a8	3.33E-159	0.30898982	0.265	0.004	4.52E-155	14	Slc4a8
Cd200	8.66E-156	0.56673881	0.544	0.022	1.18E-151	14	Cd200
Nostrin	1.54E-152	0.29598832	0.309	0.006	2.08E-148	14	Nostrin
Cd83	5.54E-151	0.97639871	0.721	0.043	7.53E-147	14	Cd83
Snn	8.56E-148	0.31734866	0.309	0.006	1.16E-143	14	Snn
Nr4a3	9.20E-147	0.5755026	0.426	0.014	1.25E-142	14	Nr4a3
Rogdi	2.72E-146	0.82037618	0.765	0.05	3.69E-142	14	Rogdi
Net1	8.77E-142	0.66931478	0.441	0.016	1.19E-137	14	Net1
Traf1	4.42E-138	1.27866119	0.926	0.087	6.00E-134	14	Traf1
Tmem123	3.53E-135	1.32937552	0.779	0.06	4.79E-131	14	Tmem123
Birc2	4.89E-131	0.8744472	0.824	0.067	6.64E-127	14	Birc2
Lactb	3.83E-126	0.72156377	0.647	0.041	5.20E-122	14	Lactb
Tbc1d8	2.74E-124	0.4741058	0.574	0.031	3.72E-120	14	Tbc1d8
Pcgf5	9.80E-123	0.94269715	0.838	0.076	1.33E-118	14	Pcgf5
Tuba1a	5.71E-121	0.86567107	0.706	0.053	7.75E-117	14	Tuba1a
Hmgn3	5.58E-117	0.31472666	0.309	0.009	7.57E-113	14	Hmgn3
Myo1g	2.10E-114	0.89050393	0.779	0.07	2.85E-110	14	Myo1g
Sema7a	2.28E-113	0.25139069	0.265	0.006	3.09E-109	14	Sema7a
Mreg	1.11E-107	0.31022705	0.338	0.012	1.51E-103	14	Mreg
Il15ra	1.16E-104	0.41045461	0.353	0.014	1.58E-100	14	Il15ra
Zmynd15	4.95E-104	0.83508954	0.5	0.029	6.72E-100	14	Zmynd15
Tspan3	8.08E-101	0.42071502	0.426	0.021	1.10E-96	14	Tspan3
Fam60a	5.11E-99	0.38627289	0.397	0.018	6.94E-95	14	Fam60a
Avpi1	1.14E-98	0.45049015	0.412	0.02	1.55E-94	14	Avpi1
Swap70	4.01E-94	0.69875332	0.662	0.059	5.45E-90	14	Swap70
Ncoa7	8.96E-93	0.6990032	0.515	0.035	1.22E-88	14	Ncoa7
Tnip3	8.35E-92	0.4528915	0.412	0.022	1.13E-87	14	Tnip3
Ly75	1.03E-90	0.36089421	0.338	0.015	1.40E-86	14	Ly75
Map3k14	3.47E-87	0.56222575	0.632	0.057	4.71E-83	14	Map3k14
Arhgef40	4.75E-87	0.26891664	0.279	0.01	6.45E-83	14	Arhgef40
Lima1	4.83E-86	0.37858307	0.338	0.015	6.56E-82	14	Lima1
Arl5c	2.39E-83	0.69185943	0.574	0.049	3.25E-79	14	Arl5c
Poglut1	5.34E-81	0.26761125	0.294	0.012	7.24E-77	14	Poglut1
Clic4	2.89E-80	0.7343716	0.662	0.07	3.93E-76	14	Clic4
Tmcc31	3.37E-76	0.60395153	0.588	0.055	4.57E-72	14	Tmcc31
Aebp2	7.49E-76	0.62752261	0.676	0.075	1.02E-71	14	Aebp2

Tpm1	9.00E-76	0.46094269	0.412	0.027	1.22E-71	14	Tpm1
Spint2	1.33E-75	0.43155855	0.485	0.038	1.81E-71	14	Spint2
Csrp1	2.73E-69	0.49463497	0.412	0.03	3.70E-65	14	Csrp1
Ktn1	3.57E-68	0.69091831	0.574	0.061	4.85E-64	14	Ktn1
Map4k4	1.27E-67	1.09451032	0.809	0.136	1.73E-63	14	Map4k4
Ccl52	2.65E-67	2.052469	0.779	0.111	3.59E-63	14	Ccl5
Rel	1.20E-65	0.82070289	0.794	0.127	1.63E-61	14	Rel
Flt3	1.05E-64	0.326694	0.368	0.025	1.42E-60	14	Flt3
Itga4	1.31E-64	0.85811421	0.809	0.135	1.77E-60	14	Itga4
P2ry10	7.68E-64	0.32740762	0.368	0.025	1.04E-59	14	P2ry10
Grk3	2.69E-63	0.5727613	0.544	0.057	3.65E-59	14	Grk3
Ccdc88a	6.52E-62	0.6318014	0.618	0.077	8.85E-58	14	Ccdc88a
Syngr22	8.28E-62	1.16802199	0.882	0.19	1.12E-57	14	Syngr2
Gpr132	1.49E-61	0.36631215	0.441	0.038	2.02E-57	14	Gpr132
Cbfa2t31	8.50E-61	0.63979103	0.647	0.083	1.15E-56	14	Cbfa2t3
Plxnc1	8.88E-60	0.41755664	0.5	0.05	1.21E-55	14	Plxnc1
Lrrk1	1.07E-59	0.47938898	0.574	0.067	1.45E-55	14	Lrrk1
Specc1	8.30E-58	0.51382921	0.515	0.056	1.13E-53	14	Specc1
Polb	4.61E-57	0.39816567	0.456	0.044	6.25E-53	14	Polb
Fam49a	5.40E-57	0.35592026	0.471	0.046	7.33E-53	14	Fam49a
Fabp51	8.61E-57	1.59762834	0.721	0.12	1.17E-52	14	Fabp5
H2-Q62	9.64E-57	0.54852879	0.559	0.068	1.31E-52	14	H2-Q6
Tmem131l	9.82E-55	0.4532722	0.515	0.059	1.33E-50	14	Tmem131l
Nfkb2	1.74E-53	0.43185331	0.5	0.056	2.36E-49	14	Nfkb2
Bcl2a1d	7.67E-53	0.6054517	0.529	0.066	1.04E-48	14	Bcl2a1d
Lpp	2.92E-51	0.37254816	0.456	0.048	3.96E-47	14	Lpp
Rap2b	2.81E-50	0.63783799	0.603	0.091	3.82E-46	14	Rap2b
Pik3r1	6.54E-50	0.55243468	0.559	0.076	8.88E-46	14	Pik3r1
Uap1	6.67E-50	0.42910125	0.309	0.023	9.06E-46	14	Uap1
Gyg	1.22E-49	0.58059788	0.412	0.042	1.66E-45	14	Gyg
Cxcl163	5.04E-47	0.82501902	0.779	0.162	6.84E-43	14	Cxcl16
Anxa31	1.40E-46	0.75730166	0.618	0.102	1.90E-42	14	Anxa3
Cnn21	1.05E-44	0.76838249	0.779	0.179	1.43E-40	14	Cnn2
H2-Q73	1.26E-44	0.75998786	0.794	0.169	1.71E-40	14	H2-Q7
St8sia4	1.88E-44	0.5539451	0.529	0.076	2.55E-40	14	St8sia4
Pcyt1a	2.57E-44	0.39782813	0.471	0.059	3.48E-40	14	Pcyt1a
Crip13	4.03E-44	1.63558764	0.882	0.266	5.48E-40	14	Crip1
Lsp11	1.79E-43	1.29226898	0.897	0.315	2.43E-39	14	Lsp1
Cblb2	2.94E-43	0.41547316	0.426	0.05	3.99E-39	14	Cblb
Arl5a	2.06E-42	0.33569861	0.397	0.044	2.80E-38	14	Arl5a

Tubb2a	4.01E-42	0.31319731	0.324	0.03	5.45E-38	14	Tubb2a
Spr	4.23E-42	0.28788616	0.353	0.035	5.74E-38	14	Spr
Tagln22	2.96E-41	1.23094277	0.779	0.201	4.02E-37	14	Tagln2
Psme22	3.69E-41	1.16963743	0.809	0.249	5.01E-37	14	Psme2
Samsn12	4.92E-41	1.00808882	0.838	0.234	6.68E-37	14	Samsn1
Cytip	7.34E-40	0.88858799	0.765	0.197	9.96E-36	14	Cytip
Tmem131	1.15E-39	0.43117338	0.471	0.066	1.56E-35	14	Tmem131
Nfkbib	1.96E-38	0.37836318	0.426	0.056	2.66E-34	14	Nfkbib
Marcksl11	2.57E-38	0.86721884	0.735	0.17	3.48E-34	14	Marcksl1
Tmem176a3	3.49E-38	0.62962209	0.574	0.099	4.73E-34	14	Tmem176a
Tmem176b3	6.46E-38	0.67939496	0.632	0.121	8.77E-34	14	Tmem176b
Klrk12	9.17E-38	0.45115424	0.529	0.084	1.24E-33	14	Klrk1
Mthfd2	7.42E-37	0.41191211	0.338	0.038	1.01E-32	14	Mthfd2
Rftn1	1.60E-36	0.31661513	0.338	0.037	2.17E-32	14	Rftn1
Cd40	3.10E-36	0.30993142	0.294	0.029	4.21E-32	14	Cd40
Cst32	4.64E-36	1.70975626	0.985	0.58	6.29E-32	14	Cst3
Bcl2a1a	5.13E-36	0.48459447	0.412	0.056	6.96E-32	14	Bcl2a1a
4930523C07Rik1	7.68E-36	0.42435688	0.559	0.1	1.04E-31	14	4930523C0
Anxa4	1.02E-35	0.28818286	0.368	0.044	1.38E-31	14	Anxa4
Tapbpl	6.29E-35	0.32886528	0.368	0.046	8.54E-31	14	Tapbpl
Trim35	2.86E-33	0.320078	0.382	0.051	3.88E-29	14	Trim35
Rps27l	3.19E-33	1.21036024	0.706	0.217	4.33E-29	14	Rps27l
Nudt9	1.18E-32	0.27704925	0.309	0.035	1.60E-28	14	Nudt9
Arhgap31	1.55E-32	0.45036271	0.441	0.07	2.11E-28	14	Arhgap31
Gfpt1	4.45E-32	0.30314691	0.353	0.045	6.04E-28	14	Gfpt1
Psmb84	6.23E-32	0.87574462	0.882	0.346	8.46E-28	14	Psmb8
Vwa5a	1.32E-31	0.30441787	0.324	0.039	1.79E-27	14	Vwa5a
Arap2	2.36E-31	0.28944522	0.324	0.039	3.20E-27	14	Arap2
Map3k1	8.68E-31	0.43131057	0.412	0.065	1.18E-26	14	Map3k1
Fchsd21	1.68E-30	0.25992122	0.353	0.047	2.28E-26	14	Fchsd2
Bcl2a1b	6.27E-30	1.12995765	0.691	0.211	8.51E-26	14	Bcl2a1b
Nuak2	6.29E-30	0.28491649	0.309	0.038	8.55E-26	14	Nuak2
Calm11	8.29E-30	1.42829591	0.926	0.532	1.13E-25	14	Calm1
Nrip1	9.90E-30	0.54830686	0.5	0.097	1.34E-25	14	Nrip1
Iscu	1.29E-29	0.6431484	0.691	0.193	1.75E-25	14	Iscu
Il7r2	6.31E-29	0.49215789	0.485	0.088	8.56E-25	14	Il7r
Glpr2	1.57E-28	0.62887836	0.412	0.072	2.13E-24	14	Glpr2
Ctnna1	2.20E-28	0.35788879	0.397	0.064	2.99E-24	14	Ctnna1
Apobec32	2.45E-28	0.56132686	0.632	0.166	3.33E-24	14	Apobec3
Epsti11	1.17E-27	0.71486112	0.559	0.134	1.59E-23	14	Epsti1

Ikbkb	1.39E-27	0.46468083	0.588	0.142	1.89E-23	14	Ikbkb
Rab8b	2.07E-27	0.48931671	0.529	0.116	2.81E-23	14	Rab8b
Psmg4	7.44E-27	0.32680101	0.368	0.058	1.01E-22	14	Psmg4
Rnaset2a	2.18E-26	0.39321476	0.368	0.06	2.97E-22	14	Rnaset2a
Etv6	1.72E-25	0.29592666	0.353	0.056	2.34E-21	14	Etv6
Got1	2.92E-25	0.34634741	0.309	0.045	3.97E-21	14	Got1
Stk4	3.03E-25	0.41506058	0.515	0.115	4.12E-21	14	Stk4
Smarce1	6.66E-25	0.4049336	0.426	0.084	9.04E-21	14	Smarce1
Nfe2l1	1.38E-24	0.26943622	0.368	0.061	1.87E-20	14	Nfe2l1
N4bp2l1	1.70E-24	0.3338138	0.382	0.068	2.30E-20	14	N4bp2l1
Frmd4a	1.81E-24	0.28944522	0.353	0.057	2.45E-20	14	Frmd4a
Psme12	1.89E-24	0.76722625	0.75	0.3	2.57E-20	14	Psme1
Sub14	3.03E-24	0.72556974	0.779	0.305	4.12E-20	14	Sub1
Mif4gd	4.03E-24	0.40129992	0.426	0.085	5.47E-20	14	Mif4gd
Dennd4a	6.78E-24	0.42391432	0.588	0.149	9.20E-20	14	Dennd4a
Actn1	1.98E-23	0.39373003	0.529	0.125	2.69E-19	14	Actn1
Malat12	2.16E-23	0.81138171	0.985	0.982	2.93E-19	14	Malat1
Zfp36l1	2.82E-23	0.54360309	0.721	0.231	3.82E-19	14	Zfp36l1
Filip1l	2.88E-23	0.33472699	0.397	0.075	3.91E-19	14	Filip1l
Tubb52	5.03E-23	0.51583478	0.647	0.19	6.83E-19	14	Tubb5
Ptms2	2.00E-22	0.60696565	0.676	0.227	2.72E-18	14	Ptms
Zmiz2	4.44E-22	0.27973309	0.382	0.072	6.03E-18	14	Zmiz2
Pgap2	5.55E-22	0.25853021	0.324	0.054	7.53E-18	14	Pgap2
Ccdc50	1.07E-21	0.28226021	0.397	0.078	1.45E-17	14	Ccdc50
Wnk11	1.17E-21	0.71082579	0.706	0.267	1.59E-17	14	Wnk1
Sdhaf1	1.26E-21	0.26816782	0.279	0.042	1.71E-17	14	Sdhaf1
Zfand6	1.32E-21	0.38244614	0.412	0.087	1.79E-17	14	Zfand6
Rnf115	1.58E-21	0.31810278	0.382	0.075	2.14E-17	14	Rnf115
Rassf2	2.43E-21	0.32070766	0.5	0.119	3.31E-17	14	Rassf2
H2-Q4	2.97E-21	0.2547841	0.324	0.055	4.03E-17	14	H2-Q4
Bmp2k	9.47E-21	0.3971027	0.441	0.102	1.29E-16	14	Bmp2k
Jak2	1.56E-20	0.43292445	0.515	0.135	2.12E-16	14	Jak2
Phf11b2	2.42E-20	0.40946761	0.382	0.08	3.29E-16	14	Phf11b
Cd274	4.28E-20	0.26674941	0.353	0.067	5.81E-16	14	Cd274
Clec2d	6.95E-20	0.40991782	0.529	0.144	9.44E-16	14	Clec2d
Sri	8.28E-20	0.43893664	0.588	0.184	1.12E-15	14	Sri
Zfc3h1	1.22E-19	0.31525397	0.368	0.075	1.66E-15	14	Zfc3h1
Ube2l6	1.62E-19	0.25735691	0.265	0.042	2.20E-15	14	Ube2l6
Rabgap1l3	2.02E-19	0.27455661	0.324	0.059	2.74E-15	14	Rabgap1l
Psmb93	2.03E-19	0.44385235	0.588	0.178	2.76E-15	14	Psmb9

Gadd45b2	4.36E-19	0.42225438	0.647	0.205	5.92E-15	14	Gadd45b
Dennd5a	4.87E-19	0.28340291	0.397	0.087	6.61E-15	14	Dennd5a
Nabp1	5.49E-19	0.37989496	0.338	0.067	7.45E-15	14	Nabp1
Irf83	2.24E-18	0.73933075	0.588	0.205	3.04E-14	14	Irf8
Actb3	5.07E-18	0.86656649	1	0.984	6.89E-14	14	Actb
Nfat5	5.10E-18	0.31036085	0.441	0.109	6.92E-14	14	Nfat5
H2-K15	8.37E-18	0.63722036	0.912	0.585	1.14E-13	14	H2-K1
Irf11	1.62E-17	0.35893083	0.5	0.14	2.20E-13	14	Irf1
Cdc42ep3	2.11E-17	0.26710025	0.309	0.06	2.87E-13	14	Cdc42ep3
H2afz3	2.35E-17	0.95722582	0.735	0.341	3.20E-13	14	H2afz
Chp1	2.97E-17	0.28532999	0.324	0.067	4.03E-13	14	Chp1
Uvrag	3.17E-17	0.3506876	0.485	0.137	4.30E-13	14	Uvrag
Tbc1d1	4.12E-17	0.25971611	0.338	0.072	5.59E-13	14	Tbc1d1
Ttyh3	4.86E-17	0.25712109	0.397	0.094	6.60E-13	14	Ttyh3
Icam1	8.47E-17	0.34425346	0.368	0.085	1.15E-12	14	Icam1
Actg12	9.81E-17	0.79436241	0.897	0.753	1.33E-12	14	Actg1
Ass11	1.07E-16	0.31742376	0.309	0.063	1.45E-12	14	Ass1
Rps195	1.41E-16	0.65207893	0.971	0.713	1.91E-12	14	Rps19
Synj1	1.73E-16	0.26621206	0.368	0.085	2.35E-12	14	Synj1
Ctsh4	8.04E-16	0.45579857	0.765	0.309	1.09E-11	14	Ctsh
Foxp11	9.12E-16	0.37218004	0.412	0.111	1.24E-11	14	Foxp1
Atpif11	1.45E-15	0.46601863	0.559	0.202	1.96E-11	14	Atpif1
Arf4	3.65E-15	0.41509915	0.529	0.18	4.95E-11	14	Arf4
Sp140	3.71E-15	0.37511778	0.426	0.12	5.03E-11	14	Sp140
Etnk1	4.10E-15	0.29420903	0.368	0.091	5.56E-11	14	Etnk1
Nup98	5.86E-15	0.25326193	0.279	0.057	7.96E-11	14	Nup98
Rgs11	6.66E-15	0.55617456	0.632	0.242	9.05E-11	14	Rgs1
Tmsb4x5	9.63E-15	1.11796786	0.985	0.959	1.31E-10	14	Tmsb4x
Pdpf1	1.01E-14	0.31674519	0.324	0.076	1.37E-10	14	Pdpf
Mrpl14	1.19E-14	0.26674941	0.353	0.088	1.61E-10	14	Mrpl14
Rab21	2.55E-14	0.28055284	0.441	0.128	3.47E-10	14	Rab21
Atox13	2.95E-14	0.61279464	0.735	0.399	4.00E-10	14	Atox1
Tes	4.63E-14	0.26996621	0.412	0.116	6.29E-10	14	Tes
Tpm4	5.32E-14	0.37746551	0.485	0.164	7.22E-10	14	Tpm4
Ppp4r2	6.98E-14	0.27697429	0.412	0.118	9.48E-10	14	Ppp4r2
Stat3	2.68E-13	0.40374596	0.544	0.212	3.64E-09	14	Stat3
Pde4b	3.48E-13	0.27864465	0.294	0.069	4.73E-09	14	Pde4b
Tap12	1.13E-12	0.26860471	0.485	0.161	1.54E-08	14	Tap1
Wdr1	1.71E-12	0.28072148	0.456	0.152	2.33E-08	14	Wdr1
Stat11	2.21E-12	0.34620553	0.559	0.21	3.01E-08	14	Stat1

Smchd1	2.65E-12	0.43652419	0.426	0.147	3.60E-08	14	Smchd1
Txndc17	2.88E-12	0.69707828	0.397	0.137	3.91E-08	14	Txndc17
Basp12	3.82E-12	0.36367028	0.779	0.353	5.19E-08	14	Basp1
Klf61	5.37E-12	0.53019854	0.647	0.296	7.29E-08	14	Klf6
Pfkfb3	8.51E-12	0.2767062	0.382	0.117	1.15E-07	14	Pfkfb3
H2-Aa3	1.01E-11	0.47148821	0.676	0.266	1.37E-07	14	H2-Aa
Vcp	1.20E-11	0.33470181	0.456	0.164	1.62E-07	14	Vcp
Herpud11	1.28E-11	0.29051246	0.309	0.084	1.74E-07	14	Herpud1
Marcks3	1.31E-11	0.46896551	0.853	0.453	1.78E-07	14	Marcks
Ogfrl11	2.30E-11	0.27182362	0.529	0.195	3.13E-07	14	Ogfrl1
Rcsd1	2.63E-11	0.29880932	0.353	0.105	3.58E-07	14	Rcsd1
Rpsa5	4.10E-11	0.42238528	0.985	0.674	5.57E-07	14	Rpsa
Ddx6	5.40E-11	0.31361913	0.5	0.191	7.33E-07	14	Ddx6
Krit1	2.41E-10	0.25602309	0.397	0.134	3.27E-06	14	Krit1
H2-D14	2.95E-10	0.38120452	0.941	0.691	4.01E-06	14	H2-D1
H2-Eb13	2.96E-10	0.55111549	0.618	0.251	4.01E-06	14	H2-Eb1
AY0361182	5.73E-10	0.46368762	0.412	0.151	7.78E-06	14	AY036118
Cd743	1.41E-09	0.27292263	0.765	0.38	1.92E-05	14	Cd74
Tctex1d2	1.52E-09	0.28007747	0.338	0.112	2.06E-05	14	Tctex1d2
Tnfaip8	1.85E-09	0.28456419	0.441	0.172	2.51E-05	14	Tnfaip8
B2m5	2.20E-09	0.48726693	0.897	0.69	2.98E-05	14	B2m
Tuba1b1	3.14E-09	0.28125456	0.382	0.139	4.26E-05	14	Tuba1b
Cd471	3.93E-09	0.3180085	0.618	0.303	5.34E-05	14	Cd47
Gpr183	5.43E-09	0.29926223	0.279	0.086	7.37E-05	14	Gpr183
Hsp90ab15	8.41E-09	0.39265246	0.735	0.433	0.00011411	14	Hsp90ab1
Tapbp1	1.47E-08	0.2762	0.5	0.219	0.00019997	14	Tapbp
Slc6a6	1.97E-08	0.26859959	0.544	0.246	0.00026776	14	Slc6a6
Myl61	2.94E-08	0.46504289	0.765	0.557	0.00039929	14	Myl6
Ppia4	3.76E-08	0.43147826	0.75	0.531	0.00051083	14	Ppia
Cfl1	3.93E-08	0.4009226	0.794	0.607	0.00053341	14	Cfl1
Anxa51	4.09E-08	0.25677714	0.397	0.158	0.0005555	14	Anxa5
Arhgdia	5.70E-08	0.27302169	0.603	0.308	0.00077427	14	Arhgdia
Slc25a32	6.69E-08	0.28416817	0.588	0.304	0.0009083	14	Slc25a3
Slc38a2	9.71E-08	0.27071464	0.529	0.25	0.00131891	14	Slc38a2
AW1120102	1.04E-07	0.46974118	0.471	0.204	0.00141599	14	AW112010
Sumo22	1.48E-07	0.38863356	0.5	0.265	0.00200419	14	Sumo2
S100a45	1.53E-07	0.46561033	0.559	0.262	0.00207862	14	S100a4
Tpm3	1.53E-07	0.26265405	0.706	0.393	0.00208314	14	Tpm3
Arhgap30	1.63E-07	0.35707348	0.544	0.289	0.00221633	14	Arhgap30
Mpc1	2.37E-07	0.26926559	0.353	0.143	0.00321423	14	Mpc1

Nfkb11	2.69E-07	0.27378861	0.397	0.171	0.00365326	14	Nfkb1
Hspa84	4.18E-07	0.32485653	0.765	0.499	0.00567511	14	Hspa8
Tspo3	4.32E-07	0.45875681	0.618	0.364	0.00586533	14	Tspo
Id23	5.77E-07	0.26920207	0.691	0.363	0.00783219	14	Id2
Anxa22	6.54E-07	0.48465826	0.603	0.348	0.00887583	14	Anxa2
Chchd2	9.39E-07	0.32191475	0.676	0.448	0.01275359	14	Chchd2
Nfkb1a	1.14E-06	0.25435919	0.676	0.381	0.01546223	14	Nfkb1a
Selplg3	1.37E-06	0.26746632	0.676	0.392	0.01862507	14	Selplg
Akap132	1.63E-06	0.26450147	0.529	0.274	0.02214746	14	Akap13
Myl12a	2.24E-06	0.26382212	0.603	0.344	0.03042948	14	Myl12a
Rgs101	2.28E-06	0.40329898	0.382	0.181	0.03101469	14	Rgs10
Ccnd22	2.60E-06	0.28326553	0.382	0.168	0.0353645	14	Ccnd2
Samhd11	7.26E-06	0.27728071	0.529	0.284	0.09858823	14	Samhd1
Gpx4	1.24E-05	0.26807317	0.559	0.325	0.16896894	14	Gpx4
Isg152	4.93E-05	0.3262523	0.353	0.167	0.66973806	14	Isg15
mt-Co14	0.00017026	0.26805256	0.985	0.846	1	14	mt-Co1
Atrx1	0.00068417	0.28910045	0.368	0.212	1	14	Atrx
Ostf11	0.00072733	0.2535032	0.574	0.377	1	14	Ostf1
Npc24	0.00209792	0.39966531	0.559	0.409	1	14	Npc2
Ly6d1	0	2.52331731	0.985	0.009	0	15	Ly6d
Siglech1	0	2.14766729	1	0.027	0	15	Siglech
Cox6a2	0	1.49614741	0.846	0.007	0	15	Cox6a2
Ccr9	0	1.45875422	0.923	0.006	0	15	Ccr9
Iglc31	0	1.050626	0.769	0.007	0	15	Iglc3
Atp1b1	0	1.03484213	0.831	0.004	0	15	Atp1b1
Klk1	0	0.88732774	0.369	0.001	0	15	Klk1
Fcrla	0	0.7660435	0.646	0.007	0	15	Fcrla
Smim5	0	0.76315499	0.662	0.004	0	15	Smim5
Gm21762	0	0.737241	0.692	0.001	0	15	Gm21762
Dntt	0	0.62110985	0.492	0	0	15	Dntt
Mzb11	0	0.50676531	0.508	0.006	0	15	Mzb1
Cd300c	0	0.43824186	0.462	0.002	0	15	Cd300c
Upb1	0	0.40926046	0.4	0.001	0	15	Upb1
Sh3bgr	0	0.34681454	0.292	0.001	0	15	Sh3bgr
Bcl11a1	2.81E-295	1.12302752	0.877	0.029	3.81E-291	15	Bcl11a
Spib	3.56E-295	0.40633392	0.4	0.004	4.83E-291	15	Spib
Lefty1	3.53E-270	0.37378326	0.415	0.005	4.79E-266	15	Lefty1
Cd209d	3.22E-238	0.52914482	0.323	0.003	4.37E-234	15	Cd209d
AC140186.1	1.74E-220	0.36305526	0.369	0.005	2.36E-216	15	AC140186.
Rnase62	2.03E-204	1.44339562	0.969	0.06	2.75E-200	15	Rnase6

Cd7	1.28E-187	0.88623279	0.662	0.026	1.74E-183	15	Cd7
Pacsin1	6.06E-181	0.42949799	0.431	0.01	8.22E-177	15	Pacsin1
Gm5547	7.22E-166	0.54949145	0.554	0.02	9.80E-162	15	Gm5547
Ighm1	5.19E-158	1.00838179	0.985	0.079	7.04E-154	15	Ighm
Spns3	4.28E-155	0.30825098	0.308	0.006	5.81E-151	15	Spns3
Rpgrip1	2.19E-153	0.63043351	0.554	0.022	2.98E-149	15	Rpgrip1
Tcf41	7.77E-152	1.5685299	0.954	0.083	1.05E-147	15	Tcf4
Dirc2	1.86E-136	0.46627576	0.508	0.021	2.53E-132	15	Dirc2
Dnajc71	6.63E-136	1.29206568	0.954	0.093	9.00E-132	15	Dnajc7
Tsc22d1	5.27E-133	0.54176402	0.462	0.018	7.16E-129	15	Tsc22d1
Cxxc5	2.13E-131	0.32451177	0.369	0.011	2.89E-127	15	Cxxc5
Tubgcp5	2.72E-129	0.55885598	0.631	0.036	3.69E-125	15	Tubgcp5
Nucb2	1.74E-126	0.75246046	0.738	0.052	2.36E-122	15	Nucb2
Clec10a	3.32E-125	0.47294402	0.446	0.017	4.51E-121	15	Clec10a
P2ry14	2.52E-120	0.53607609	0.569	0.031	3.42E-116	15	P2ry14
Paqr5	6.05E-120	0.25028557	0.262	0.005	8.21E-116	15	Paqr5
Cd8b11	9.28E-100	1.07994323	0.662	0.051	1.26E-95	15	Cd8b1
Mctp2	1.38E-99	0.32132705	0.354	0.014	1.87E-95	15	Mctp2
Runx2	1.25E-98	0.71104902	0.723	0.065	1.70E-94	15	Runx2
Ly6c21	8.98E-94	1.65617026	0.954	0.131	1.22E-89	15	Ly6c2
Cnp1	8.08E-92	0.5555141	0.646	0.054	1.10E-87	15	Cnp
Dap	2.24E-90	0.73858096	0.769	0.082	3.04E-86	15	Dap
Kmo1	3.67E-90	0.44255582	0.492	0.031	4.98E-86	15	Kmo
Ctsl2	9.99E-89	1.25004605	0.923	0.129	1.36E-84	15	Ctsl
Bst24	4.10E-88	1.9413683	1	0.19	5.56E-84	15	Bst2
Pltp	1.73E-86	0.62852762	0.569	0.044	2.35E-82	15	Pltp
Irf84	3.35E-84	1.87979815	1	0.201	4.55E-80	15	Irf8
St8sia41	2.76E-82	0.79831475	0.708	0.075	3.75E-78	15	St8sia4
Rell1	2.02E-81	0.56049386	0.615	0.055	2.75E-77	15	Rell1
Khk	1.17E-79	0.39095299	0.446	0.029	1.59E-75	15	Khk
Sell1	4.31E-78	0.72687267	0.708	0.077	5.84E-74	15	Sell
Pafah1b3	1.51E-76	0.46733878	0.508	0.039	2.05E-72	15	Pafah1b3
Plac84	3.50E-69	1.54662585	1	0.205	4.75E-65	15	Plac8
Pgls1	6.20E-68	0.84383607	0.892	0.157	8.42E-64	15	Pgls
Cdh1	9.66E-66	0.26568239	0.277	0.013	1.31E-61	15	Cdh1
Mef2c2	1.04E-65	0.64785337	0.754	0.101	1.41E-61	15	Mef2c
Blnk	1.52E-65	0.29018299	0.354	0.022	2.07E-61	15	Blnk
Lair12	2.73E-64	0.91016912	0.877	0.152	3.70E-60	15	Lair1
Snx51	3.25E-64	0.68384971	0.831	0.131	4.41E-60	15	Snx5
Tnfrsf13b	3.63E-63	0.4239773	0.492	0.045	4.93E-59	15	Tnfrsf13b

Ccnd11	5.00E-63	0.67401474	0.6	0.068	6.79E-59	15	Ccnd1
Pld43	1.61E-61	0.82055001	0.923	0.178	2.18E-57	15	Pld4
Ptprcap4	1.98E-60	0.60546913	0.754	0.103	2.69E-56	15	Ptprcap
Tmem229b	2.01E-60	0.2600567	0.323	0.02	2.72E-56	15	Tmem229b
Spint21	2.35E-60	0.37948221	0.446	0.038	3.19E-56	15	Spint2
Fyn	2.66E-59	0.58205503	0.631	0.079	3.61E-55	15	Fyn
Mvb12a	2.92E-59	0.58825702	0.631	0.081	3.97E-55	15	Mvb12a
Tmed31	6.56E-59	0.55988435	0.662	0.088	8.91E-55	15	Tmed3
Jaml1	6.29E-57	0.64936552	0.738	0.113	8.54E-53	15	Jaml
Rpl315	7.27E-56	1.35355943	1	0.361	9.87E-52	15	Rpl31
Tspan131	2.51E-55	0.74021953	0.769	0.133	3.40E-51	15	Tspan13
Mgat1	1.35E-54	0.40826617	0.538	0.061	1.83E-50	15	Mgat1
Lpgat1	3.23E-53	0.43409686	0.492	0.053	4.38E-49	15	Lpgat1
Slc44a2	5.39E-53	0.58931187	0.692	0.106	7.32E-49	15	Slc44a2
Syngr23	1.38E-51	0.87956328	0.862	0.191	1.87E-47	15	Syngr2
Ly6a5	3.01E-51	1.40001633	0.815	0.169	4.08E-47	15	Ly6a
Ptp4a3	3.19E-50	0.27488057	0.338	0.026	4.32E-46	15	Ptp4a3
Serp11	1.46E-48	0.75950158	0.877	0.204	1.99E-44	15	Serp1
Ptp4a3	4.13E-48	0.38798489	0.415	0.042	5.61E-44	15	Ptp4a3
Rabgap1l4	5.93E-48	0.4488975	0.492	0.058	8.05E-44	15	Rabgap1l
Ppfia41	7.10E-48	0.49361099	0.585	0.082	9.63E-44	15	Ppfia4
Cybb3	2.22E-46	0.7412005	0.938	0.211	3.01E-42	15	Cybb
Abhd17a	3.84E-46	0.44549746	0.569	0.081	5.21E-42	15	Abhd17a
Ppp1r14b1	3.84E-45	0.49663552	0.631	0.101	5.21E-41	15	Ppp1r14b
Ech1	3.88E-43	0.448474	0.569	0.086	5.27E-39	15	Ech1
Abhd17b1	2.62E-42	0.30413219	0.338	0.031	3.56E-38	15	Abhd17b
Il7r3	1.10E-41	0.44792689	0.585	0.088	1.49E-37	15	Il7r
Tcf12	2.01E-41	0.37402403	0.446	0.055	2.73E-37	15	Tcf12
Ctsh5	2.82E-41	0.93104795	0.938	0.307	3.82E-37	15	Ctsh
Fdps	2.97E-41	0.26716829	0.277	0.021	4.03E-37	15	Fdps
Cd472	4.32E-41	0.83514295	0.954	0.3	5.86E-37	15	Cd47
Tagln23	4.49E-40	0.63041428	0.846	0.2	6.09E-36	15	Tagln2
Card11	5.68E-40	0.25146312	0.308	0.027	7.72E-36	15	Card11
Rps6ka1	1.43E-37	0.44766938	0.585	0.102	1.94E-33	15	Rps6ka1
Apobec33	3.81E-37	0.56359912	0.738	0.165	5.18E-33	15	Apobec3
Svbp	4.82E-37	0.4396933	0.523	0.083	6.54E-33	15	Svbp
Sec61b2	6.85E-37	0.75988154	0.969	0.34	9.30E-33	15	Sec61b
Prkca	7.32E-37	0.26288134	0.292	0.027	9.93E-33	15	Prkca
H2-T232	2.73E-34	0.70044939	0.769	0.209	3.71E-30	15	H2-T23
Sema4b	6.52E-34	0.25974922	0.292	0.029	8.85E-30	15	Sema4b

Ramp1	1.53E-33	0.35249128	0.446	0.066	2.08E-29	15	Ramp1
Uvrage1	1.50E-32	0.42306136	0.646	0.135	2.04E-28	15	Uvrage1
Rps204	3.42E-32	0.89163965	1	0.649	4.64E-28	15	Rps204
Plekha3	4.55E-32	0.33955236	0.4	0.056	6.17E-28	15	Plekha3
Bmyc	1.14E-31	0.30006791	0.385	0.052	1.55E-27	15	Bmyc
Mbnl14	1.68E-31	0.71766435	0.846	0.272	2.28E-27	15	Mbnl14
Gnas2	2.42E-30	0.73794998	0.892	0.364	3.28E-26	15	Gnas2
Cd164	2.71E-30	0.41955284	0.569	0.115	3.68E-26	15	Cd164
Eif3f5	8.35E-30	0.62873983	0.908	0.324	1.13E-25	15	Eif3f5
Fam174a	9.63E-30	0.32066484	0.431	0.068	1.31E-25	15	Fam174a
Pqlc3	1.32E-29	0.25041129	0.323	0.04	1.80E-25	15	Pqlc3
Fgfr1op2	1.49E-29	0.47798173	0.646	0.153	2.03E-25	15	Fgfr1op2
Slamf9	1.92E-29	0.32162224	0.369	0.052	2.61E-25	15	Slamf9
Hsp90b12	8.52E-29	0.58651411	0.892	0.291	1.16E-24	15	Hsp90b12
Tbc1d81	1.24E-28	0.28882944	0.292	0.034	1.68E-24	15	Tbc1d81
Ly6e4	1.32E-28	0.76768741	1	0.471	1.79E-24	15	Ly6e4
Ly863	4.00E-28	0.43686385	0.723	0.181	5.43E-24	15	Ly863
Sec61g1	4.72E-28	0.57322238	0.892	0.318	6.40E-24	15	Sec61g1
Gna15	3.45E-27	0.270327	0.323	0.043	4.68E-23	15	Gna15
Scimp	3.66E-27	0.30677661	0.4	0.064	4.98E-23	15	Scimp
Rps114	5.24E-27	0.7245801	1	0.745	7.12E-23	15	Rps114
Rps244	5.28E-27	0.76959444	1	0.761	7.17E-23	15	Rps244
Rap1a1	6.06E-27	0.5529547	0.754	0.223	8.23E-23	15	Rap1a1
Lgals14	8.29E-27	0.62849611	0.831	0.26	1.12E-22	15	Lgals14
Reep5	1.58E-26	0.53014166	0.754	0.234	2.14E-22	15	Reep5
Rexo2	5.15E-26	0.34162716	0.431	0.077	7.00E-22	15	Rexo2
Hnrnpa12	6.17E-26	0.4319021	0.677	0.176	8.37E-22	15	Hnrnpa12
Arhgef6	1.13E-25	0.2874588	0.369	0.058	1.53E-21	15	Arhgef6
Xbp1	1.76E-25	0.48907373	0.692	0.199	2.39E-21	15	Xbp1
Bloc1s2	2.83E-25	0.30400222	0.385	0.064	3.84E-21	15	Bloc1s2
Gltf	6.94E-25	0.42796802	0.554	0.129	9.42E-21	15	Gltf
Rpl103	8.31E-25	0.65800416	1	0.702	1.13E-20	15	Rpl103
Rps4x5	1.03E-24	0.69880781	1	0.561	1.39E-20	15	Rps4x5
Serinc31	1.98E-24	0.46686722	0.862	0.293	2.68E-20	15	Serinc31
Pkig1	2.52E-24	0.27791267	0.354	0.056	3.42E-20	15	Pkig1
Ppm1m	3.77E-24	0.2969007	0.323	0.048	5.12E-20	15	Ppm1m
Krtcap21	4.59E-24	0.46684735	0.631	0.173	6.24E-20	15	Krtcap21
Ppia5	7.01E-24	0.65375805	0.985	0.529	9.52E-20	15	Ppia5
Herpud12	8.62E-24	0.34615701	0.431	0.083	1.17E-19	15	Herpud12
Rgs102	1.01E-23	0.49572789	0.646	0.179	1.38E-19	15	Rgs102

Rpl36a2	2.50E-23	0.50721664	0.8	0.279	3.40E-19	15	Rpl36a2
12-Sep	2.58E-23	0.31329883	0.385	0.068	3.50E-19	15	
Grn3	2.76E-23	0.55873891	0.908	0.343	3.74E-19	15	Grn
Rac23	6.11E-23	0.51978864	0.938	0.368	8.30E-19	15	Rac2
Smim14	8.18E-23	0.44502262	0.554	0.14	1.11E-18	15	Smim14
Sub15	6.09E-22	0.60494167	0.785	0.305	8.27E-18	15	Sub1
Rpl13a3	1.27E-21	0.39491655	0.662	0.19	1.73E-17	15	Rpl13a
Stx7	2.11E-21	0.35333158	0.508	0.122	2.86E-17	15	Stx7
Mtdh	3.56E-21	0.4219614	0.738	0.237	4.84E-17	15	Mtdh
Rpl194	4.56E-21	0.54144395	1	0.773	6.20E-17	15	Rpl19
Klrd13	1.02E-20	0.27673705	0.477	0.102	1.38E-16	15	Klrd1
Lag34	1.81E-20	0.29443663	0.354	0.064	2.45E-16	15	Lag3
Atp5g24	2.13E-20	0.47012144	0.769	0.276	2.90E-16	15	Atp5g2
Csf2rb2	3.18E-20	0.30703211	0.323	0.056	4.32E-16	15	Csf2rb2
Dctn6	4.38E-20	0.25580277	0.292	0.047	5.95E-16	15	Dctn6
Hmgb11	5.28E-20	0.46140711	0.8	0.32	7.17E-16	15	Hmgb1
Rpl316	5.34E-20	0.56634767	0.969	0.482	7.25E-16	15	Rpl3
Rnf187	1.69E-19	0.50065374	0.415	0.095	2.29E-15	15	Rnf187
Ablim13	1.73E-19	0.26396088	0.308	0.052	2.35E-15	15	Ablim1
Hvcn1	1.95E-19	0.25328634	0.292	0.048	2.65E-15	15	Hvcn1
Pkib1	2.26E-19	0.33514202	0.338	0.063	3.06E-15	15	Pkib
Lsp12	2.71E-19	0.43924193	0.831	0.316	3.67E-15	15	Lsp1
Unc93b12	2.91E-19	0.48866634	0.723	0.257	3.95E-15	15	Unc93b1
Rps3a14	2.99E-19	0.51742568	0.985	0.727	4.06E-15	15	Rps3a1
Clec12a	3.15E-19	0.31058439	0.354	0.07	4.27E-15	15	Clec12a
Manf1	4.49E-19	0.39382905	0.554	0.157	6.09E-15	15	Manf
Cct5	4.87E-19	0.31571609	0.508	0.13	6.61E-15	15	Cct5
Rpl304	5.69E-19	0.50994201	1	0.734	7.72E-15	15	Rpl30
Spcs21	6.36E-19	0.4154699	0.646	0.212	8.63E-15	15	Spcs2
Sec11c1	1.15E-18	0.38179812	0.538	0.153	1.56E-14	15	Sec11c
Sdc4	3.86E-18	0.28195793	0.308	0.056	5.24E-14	15	Sdc4
Hspe13	4.01E-18	0.45475944	0.6	0.187	5.44E-14	15	Hspe1
Rpl75	4.75E-18	0.48282062	1	0.558	6.45E-14	15	Rpl7
Rpl45	9.72E-18	0.4494049	0.923	0.4	1.32E-13	15	Rpl4
Ifnar2	1.20E-17	0.32353356	0.508	0.138	1.64E-13	15	Ifnar2
H2-Q74	1.82E-17	0.49306097	0.569	0.171	2.47E-13	15	H2-Q7
Rps184	2.11E-17	0.47778183	1	0.606	2.87E-13	15	Rps18
Ptms3	2.13E-17	0.39627679	0.677	0.227	2.90E-13	15	Ptms
Napsa3	2.84E-17	0.452789	0.631	0.199	3.86E-13	15	Napsa
Rpl295	4.03E-17	0.52051706	0.908	0.431	5.47E-13	15	Rpl29

Prr13	4.70E-17	0.37418148	0.615	0.198	6.38E-13	15	Prr13
Rps144	9.15E-17	0.43528139	1	0.807	1.24E-12	15	Rps14
Npm14	1.01E-16	0.35151402	0.8	0.291	1.37E-12	15	Npm1
Ssr43	1.16E-16	0.36039215	0.723	0.265	1.58E-12	15	Ssr4
Eef24	2.94E-16	0.48335966	0.923	0.444	3.99E-12	15	Eef2
Ptma5	3.02E-16	0.49815122	0.954	0.559	4.10E-12	15	Ptma
Rps54	3.47E-16	0.45339357	1	0.633	4.71E-12	15	Rps5
2410015M20Rik	4.45E-16	0.31653679	0.492	0.141	6.05E-12	15	2410015M2
Rps175	5.46E-16	0.44469302	0.831	0.392	7.42E-12	15	Rps17
Rpl124	5.71E-16	0.4080801	0.969	0.505	7.76E-12	15	Rpl12
Psme13	7.18E-16	0.39536276	0.769	0.3	9.74E-12	15	Psme1
mt-Co15	8.93E-16	0.40472225	1	0.846	1.21E-11	15	mt-Co1
Rps164	1.00E-15	0.42800793	1	0.857	1.36E-11	15	Rps16
Rpl36a4	1.07E-15	0.4555456	0.862	0.381	1.45E-11	15	Rpl36a
Rpl154	1.22E-15	0.46157195	0.969	0.548	1.65E-11	15	Rpl15
Atp6v1d	1.80E-15	0.30894333	0.462	0.13	2.44E-11	15	Atp6v1d
Rpl285	1.84E-15	0.44802425	1	0.702	2.50E-11	15	Rpl28
Evi2a	1.97E-15	0.28445368	0.462	0.128	2.67E-11	15	Evi2a
Rpl264	2.48E-15	0.42605284	1	0.716	3.36E-11	15	Rpl26
Rpl10a6	2.71E-15	0.41916175	0.985	0.469	3.68E-11	15	Rpl10a
Rpl114	3.00E-15	0.41653556	0.985	0.666	4.07E-11	15	Rpl11
Stat21	3.23E-15	0.26423689	0.369	0.088	4.39E-11	15	Stat2
H2afy1	3.74E-15	0.31514747	0.662	0.229	5.07E-11	15	H2afy
Psmb85	4.43E-15	0.36899947	0.831	0.346	6.01E-11	15	Psmb8
Eif3h2	6.43E-15	0.36759475	0.677	0.261	8.73E-11	15	Eif3h
Cd8a1	6.79E-15	0.31098311	0.277	0.052	9.22E-11	15	Cd8a
Rpl22l13	8.73E-15	0.35626743	0.738	0.282	1.19E-10	15	Rpl22l1
Rpl35a5	1.10E-14	0.39741717	1	0.828	1.49E-10	15	Rpl35a
Rpl54	1.43E-14	0.46408443	0.908	0.464	1.94E-10	15	Rpl5
Rpl394	1.45E-14	0.42779551	1	0.744	1.97E-10	15	Rpl39
Npc25	1.54E-14	0.37940355	0.892	0.406	2.09E-10	15	Npc2
Rplp05	1.55E-14	0.42858924	1	0.675	2.11E-10	15	Rplp0
Foxp12	2.16E-14	0.26152318	0.415	0.111	2.93E-10	15	Foxp1
Rps15a4	2.39E-14	0.31661575	0.985	0.668	3.24E-10	15	Rps15a
Rack14	2.62E-14	0.42275171	0.954	0.526	3.55E-10	15	Rack1
Psmb12	2.84E-14	0.31496993	0.615	0.221	3.85E-10	15	Psmb1
Rpl94	3.32E-14	0.39488703	1	0.725	4.50E-10	15	Rpl9
Rps64	3.93E-14	0.40385947	0.985	0.524	5.34E-10	15	Rps6
mt-Atp65	4.80E-14	0.39798696	1	0.815	6.52E-10	15	mt-Atp6
Psap4	6.94E-14	0.46459394	0.969	0.636	9.43E-10	15	Psap

Tmem591	7.44E-14	0.30227644	0.554	0.187	1.01E-09	15	Tmem59
mt-Co35	1.00E-13	0.37557939	1	0.824	1.36E-09	15	mt-Co3
Rbm33	1.43E-13	0.40519002	0.862	0.425	1.94E-09	15	Rbm3
mt-Nd34	1.83E-13	0.36827355	0.846	0.387	2.48E-09	15	mt-Nd3
Malat13	2.27E-13	0.36862892	1	0.982	3.09E-09	15	Malat1
Ndufb11	2.29E-13	0.28031974	0.508	0.164	3.11E-09	15	Ndufb11
Selenos	2.47E-13	0.28634279	0.446	0.135	3.36E-09	15	Selenos
Dbnl1	2.49E-13	0.27905008	0.431	0.128	3.39E-09	15	Dbnl
Rpl18a4	2.93E-13	0.35656193	1	0.829	3.98E-09	15	Rpl18a
Eif3k3	3.91E-13	0.3243071	0.662	0.263	5.30E-09	15	Eif3k
Rpl234	4.22E-13	0.37279552	1	0.855	5.73E-09	15	Rpl23
Rplp16	4.63E-13	0.36468608	1	0.846	6.29E-09	15	Rplp1
Rps74	4.77E-13	0.37111341	0.985	0.61	6.47E-09	15	Rps7
Jpt1	5.69E-13	0.27879642	0.585	0.207	7.72E-09	15	Jpt1
Rpl144	6.51E-13	0.3918897	0.938	0.509	8.84E-09	15	Rpl14
Rps254	6.98E-13	0.38141218	0.985	0.639	9.48E-09	15	Rps25
Snrpd2	7.25E-13	0.29127057	0.477	0.156	9.84E-09	15	Snrpd2
Eef1g4	7.33E-13	0.30085883	0.615	0.226	9.95E-09	15	Eef1g
Cd372	8.50E-13	0.28633338	0.554	0.192	1.15E-08	15	Cd37
H13	1.04E-12	0.26113611	0.492	0.16	1.41E-08	15	H13
Rps92	1.09E-12	0.36514038	1	0.89	1.48E-08	15	Rps9
Atp5c12	1.10E-12	0.31432049	0.569	0.211	1.49E-08	15	Atp5c1
Eef1b24	1.19E-12	0.34993161	0.846	0.396	1.61E-08	15	Eef1b2
mt-Co24	1.40E-12	0.26719584	1	0.813	1.91E-08	15	mt-Co2
Mpeg13	1.43E-12	0.3966281	0.8	0.377	1.94E-08	15	Mpeg1
Tnfaip81	1.52E-12	0.33937915	0.492	0.172	2.06E-08	15	Tnfaip8
mt-Nd54	1.57E-12	0.33982961	0.692	0.282	2.13E-08	15	mt-Nd5
Rpl324	1.75E-12	0.38709904	1	0.689	2.38E-08	15	Rpl32
Rps264	1.86E-12	0.41404297	0.954	0.621	2.52E-08	15	Rps26
Swi5	2.08E-12	0.28672386	0.446	0.143	2.83E-08	15	Swi5
Rpl7a5	2.24E-12	0.39493485	0.877	0.473	3.05E-08	15	Rpl7a
Rps84	2.36E-12	0.35572912	1	0.83	3.21E-08	15	Rps8
Cd692	2.77E-12	0.28250193	0.262	0.057	3.76E-08	15	Cd69
Tmem258	2.85E-12	0.29168612	0.477	0.161	3.87E-08	15	Tmem258
Rpl185	5.50E-12	0.34608865	1	0.702	7.46E-08	15	Rpl18
Tmed9	6.31E-12	0.27703659	0.538	0.196	8.56E-08	15	Tmed9
Emp32	6.78E-12	0.28505749	0.692	0.273	9.21E-08	15	Emp3
Cox7a2l3	7.45E-12	0.32586024	0.615	0.251	1.01E-07	15	Cox7a2l
Uqcrh3	7.64E-12	0.34031554	0.785	0.376	1.04E-07	15	Uqcrh
Rpl84	1.04E-11	0.34799139	1	0.703	1.41E-07	15	Rpl8

Dad12	1.75E-11	0.29198099	0.585	0.23	2.38E-07	15	Dad1
Ywhae	1.77E-11	0.29473685	0.569	0.222	2.40E-07	15	Ywhae
Rps134	2.36E-11	0.33525662	0.985	0.724	3.20E-07	15	Rps13
Rpl134	2.83E-11	0.34926916	1	0.774	3.84E-07	15	Rpl13
Hsp90ab16	2.86E-11	0.33672283	0.862	0.432	3.88E-07	15	Hsp90ab1
Arpc5l	3.34E-11	0.25857606	0.338	0.097	4.53E-07	15	Arpc5l
Spcs1	4.82E-11	0.26815054	0.4	0.13	6.54E-07	15	Spcs1
Nsa21	4.94E-11	0.30879779	0.631	0.263	6.71E-07	15	Nsa2
Minos1	5.80E-11	0.26448537	0.462	0.162	7.87E-07	15	Minos1
Ptpn6	6.42E-11	0.27057075	0.692	0.291	8.72E-07	15	Ptpn6
Irf2bp2	7.07E-11	0.27153639	0.646	0.263	9.59E-07	15	Irf2bp2
Sumo23	7.60E-11	0.28796884	0.631	0.263	1.03E-06	15	Sumo2
Cib1	1.06E-10	0.26595635	0.338	0.1	1.43E-06	15	Cib1
Eef1a15	1.94E-10	0.33225334	1	0.869	2.63E-06	15	Eef1a1
Rpl27a4	2.44E-10	0.30229729	1	0.799	3.31E-06	15	Rpl27a
Rpl365	2.53E-10	0.35693351	0.969	0.641	3.44E-06	15	Rpl36
Tmed2	2.73E-10	0.28693105	0.569	0.235	3.70E-06	15	Tmed2
Cd821	4.10E-10	0.26225128	0.415	0.142	5.57E-06	15	Cd82
Cox4i12	4.77E-10	0.36294829	0.862	0.495	6.48E-06	15	Cox4i1
Eif5a	6.88E-10	0.27688333	0.754	0.355	9.33E-06	15	Eif5a
Rpl214	7.18E-10	0.31725103	1	0.746	9.75E-06	15	Rpl21
Naca4	8.94E-10	0.32509741	0.831	0.439	1.21E-05	15	Naca
Cope	1.01E-09	0.25841536	0.446	0.167	1.37E-05	15	Cope
Rpl244	1.20E-09	0.32176073	0.985	0.608	1.63E-05	15	Rpl24
Rpl355	1.48E-09	0.34021868	0.785	0.413	2.00E-05	15	Rpl35
Smdt12	1.56E-09	0.29380586	0.523	0.217	2.11E-05	15	Smdt1
Tmed10	2.47E-09	0.25052866	0.569	0.242	3.35E-05	15	Tmed10
Rpl64	4.65E-09	0.33018999	0.954	0.668	6.31E-05	15	Rpl6
Rpl224	5.01E-09	0.2714854	0.923	0.502	6.80E-05	15	Rpl22
Rps34	1.17E-08	0.27679035	0.969	0.723	0.00015908	15	Rps3
Rps283	2.52E-08	0.3766887	0.938	0.642	0.00034255	15	Rps28
Rps234	3.89E-08	0.25604762	0.985	0.725	0.00052802	15	Rps23
Pfdn52	7.28E-08	0.26231415	0.785	0.441	0.00098802	15	Pfdn5
Rps273	7.53E-08	0.25079612	1	0.874	0.00102251	15	Rps27
Oaz1	1.43E-07	0.28035996	0.862	0.519	0.00194787	15	Oaz1
Tpt14	1.50E-07	0.27088755	1	0.948	0.00203975	15	Tpt1
Rps125	1.79E-07	0.26163829	0.985	0.808	0.00242953	15	Rps12
Ndufa61	4.06E-07	0.25555623	0.508	0.241	0.00550508	15	Ndufa6
Rpl274	5.49E-07	0.2660066	0.677	0.388	0.00745337	15	Rpl27
Rpl374	9.14E-07	0.30441636	0.954	0.801	0.01240869	15	Rpl37

Rpl345	9.28E-07	0.25624908	1	0.771	0.01259784	15	Rpl34
H2-K16	2.71E-06	0.25539469	0.892	0.585	0.03678966	15	H2-K1

Table 10

Human Aggregated 0.65 Resolution							
	p_val	avg_logFC	pct.1	pct.2	p_val_adj	cluster	gene
IL7R	0	0.79703308	0.598	0.112	0	0	IL7R
TXNIP	7.81E-271	0.70387446	0.885	0.5	1.27E-266	0	TXNIP
RPS27	0	0.63443096	0.997	0.923	0	0	RPS27
RPS12	4.63E-295	0.581001	0.999	0.965	7.52E-291	0	RPS12
RPS3	6.81E-284	0.56062751	0.99	0.915	1.11E-279	0	RPS3
RPS25	1.08E-266	0.53816619	0.976	0.842	1.76E-262	0	RPS25
LTB	0	0.53667081	0.461	0.09	0	0	LTB
RPS15A	1.33E-286	0.53174129	0.995	0.929	2.17E-282	0	RPS15A
RPL30	1.23E-261	0.52810151	0.987	0.929	2.00E-257	0	RPL30
RPL28	3.47E-276	0.52338767	0.995	0.948	5.63E-272	0	RPL28
RPL41	4.81E-304	0.52177298	0.997	0.973	7.81E-300	0	RPL41
RPSA	6.54E-213	0.51790081	0.916	0.709	1.06E-208	0	RPSA
RPL10	9.36E-244	0.51621871	0.997	0.977	1.52E-239	0	RPL10
BTG1	1.85E-199	0.51122871	0.924	0.656	3.01E-195	0	BTG1
CD52	4.36E-230	0.50502628	0.666	0.259	7.08E-226	0	CD52
RPL13	2.05E-286	0.50386735	0.999	0.989	3.33E-282	0	RPL13
IL32	2.29E-272	0.50021949	0.569	0.166	3.72E-268	0	IL32
RPS18	7.65E-241	0.47269121	0.999	0.98	1.24E-236	0	RPS18
RPS29	3.71E-184	0.46947275	0.892	0.671	6.03E-180	0	RPS29
CD3D	5.48E-307	0.46616882	0.6	0.164	8.90E-303	0	CD3D
RPS27A	4.58E-225	0.45563136	0.995	0.946	7.45E-221	0	RPS27A
EEF1A1	4.90E-223	0.45044607	0.998	0.991	7.96E-219	0	EEF1A1
RPL32	3.70E-196	0.45028129	0.991	0.953	6.02E-192	0	RPL32
RPL23A	1.76E-211	0.44961771	0.982	0.88	2.87E-207	0	RPL23A
RPL14	5.78E-196	0.44333427	0.962	0.843	9.39E-192	0	RPL14
RPS28	4.50E-185	0.44222057	0.962	0.845	7.30E-181	0	RPS28
RPS4X	4.66E-162	0.43942491	0.948	0.856	7.58E-158	0	RPS4X
RPL19	6.59E-203	0.43755233	0.994	0.952	1.07E-198	0	RPL19

RPLP1	3.07E-177	0.43149043	0.999	0.987	4.99E-173	0	RPLP1
RPL11	2.86E-193	0.42855161	0.987	0.945	4.65E-189	0	RPL11
CD2	1.26E-243	0.42727923	0.561	0.173	2.04E-239	0	CD2
RPL35A	6.34E-177	0.42615093	0.95	0.823	1.03E-172	0	RPL35A
RPS15	2.31E-198	0.41408459	0.982	0.917	3.76E-194	0	RPS15
RPS19	9.05E-154	0.40929089	0.993	0.965	1.47E-149	0	RPS19
TRAC	3.62E-251	0.39857492	0.475	0.123	5.88E-247	0	TRAC
B2M	1.13E-188	0.39766774	0.999	0.99	1.83E-184	0	B2M
RPLP2	9.13E-167	0.39693383	0.976	0.896	1.48E-162	0	RPLP2
RPL10A	5.58E-136	0.38761877	0.915	0.774	9.07E-132	0	RPL10A
RPL36	1.15E-133	0.38666502	0.892	0.737	1.87E-129	0	RPL36
RPS26	1.52E-97	0.38632201	0.656	0.436	2.48E-93	0	RPS26
TRBC2	2.17E-202	0.38438303	0.425	0.12	3.52E-198	0	TRBC2
RPL9	2.66E-155	0.3843725	0.983	0.929	4.33E-151	0	RPL9
RPS14	5.30E-167	0.38426766	0.995	0.97	8.61E-163	0	RPS14
RPL18A	1.49E-156	0.38176389	0.986	0.925	2.42E-152	0	RPL18A
RPL3	1.12E-142	0.37861371	0.977	0.925	1.81E-138	0	RPL3
RPS21	1.00E-123	0.37775783	0.861	0.685	1.63E-119	0	RPS21
TPT1	6.72E-153	0.37144806	0.998	0.993	1.09E-148	0	TPT1
RPL34	1.92E-121	0.3664228	0.973	0.925	3.12E-117	0	RPL34
RPS2	2.34E-149	0.35627388	0.997	0.977	3.81E-145	0	RPS2
RPS10	2.00E-105	0.35527032	0.786	0.571	3.26E-101	0	RPS10
RPL21	6.35E-114	0.34762747	0.974	0.901	1.03E-109	0	RPL21
KLRB1	3.04E-84	0.34349558	0.312	0.125	4.94E-80	0	KLRB1
RPL37	8.04E-121	0.3408937	0.972	0.894	1.31E-116	0	RPL37
HLA-A	1.50E-108	0.34065183	0.942	0.781	2.44E-104	0	HLA-A
RPS16	1.43E-119	0.33943543	0.966	0.903	2.33E-115	0	RPS16
RPL39	1.12E-121	0.33622092	0.983	0.93	1.83E-117	0	RPL39
RPL18	4.42E-126	0.33405034	0.974	0.903	7.18E-122	0	RPL18
RPS5	4.52E-97	0.33299319	0.864	0.714	7.34E-93	0	RPS5
RPS3A	1.22E-102	0.33116516	0.979	0.944	1.98E-98	0	RPS3A
RPL24	5.41E-103	0.33080763	0.905	0.775	8.78E-99	0	RPL24
RPL7A	2.44E-124	0.32919788	0.967	0.916	3.97E-120	0	RPL7A
FAU	1.37E-126	0.32913264	0.976	0.909	2.22E-122	0	FAU
RPS8	3.05E-100	0.3209374	0.979	0.928	4.96E-96	0	RPS8
RPL13A	3.82E-106	0.32058745	0.966	0.898	6.20E-102	0	RPL13A
RPS6	2.15E-96	0.31838212	0.969	0.913	3.50E-92	0	RPS6
HLA-C	3.15E-83	0.31609136	0.853	0.662	5.12E-79	0	HLA-C
RPS23	6.06E-116	0.31469711	0.991	0.959	9.84E-112	0	RPS23
EEF1D	6.37E-83	0.3110394	0.708	0.5	1.04E-78	0	EEF1D

RPL8	1.83E-92	0.30921734	0.918	0.84	2.98E-88	0	RPL8
RPL12	1.27E-98	0.30779205	0.96	0.895	2.06E-94	0	RPL12
TRBC1	3.88E-91	0.30670825	0.302	0.112	6.30E-87	0	TRBC1
RPL26	8.60E-109	0.30520477	0.98	0.93	1.40E-104	0	RPL26
RPL29	5.39E-92	0.30233831	0.958	0.898	8.75E-88	0	RPL29
RPS7	7.50E-96	0.30190475	0.958	0.874	1.22E-91	0	RPS7
RPL36AL	2.03E-70	0.28363553	0.664	0.466	3.29E-66	0	RPL36AL
RPL6	8.81E-79	0.28210427	0.917	0.857	1.43E-74	0	RPL6
MYL12A	4.43E-77	0.28180189	0.668	0.437	7.20E-73	0	MYL12A
S100A4	4.55E-64	0.28092392	0.755	0.524	7.39E-60	0	S100A4
CD3G	8.88E-166	0.27490208	0.374	0.107	1.44E-161	0	CD3G
RPL5	5.85E-67	0.27419628	0.887	0.779	9.51E-63	0	RPL5
CD48	7.95E-104	0.2683469	0.476	0.219	1.29E-99	0	CD48
RPS13	5.83E-68	0.26476183	0.944	0.887	9.47E-64	0	RPS13
RPS9	2.61E-74	0.26214881	0.941	0.878	4.23E-70	0	RPS9
RARRES3	2.51E-106	0.26161401	0.413	0.172	4.07E-102	0	RARRES3
GIMAP7	7.37E-90	0.25677112	0.402	0.181	1.20E-85	0	GIMAP7
RPL27	1.07E-61	0.25657394	0.8	0.674	1.73E-57	0	RPL27
HINT1	3.33E-59	0.25635667	0.506	0.322	5.42E-55	0	HINT1
GZMK	1.47E-82	0.25596789	0.321	0.125	2.39E-78	0	GZMK
TOMM7	7.29E-63	0.2532617	0.626	0.425	1.18E-58	0	TOMM7
ISG20	1.97E-88	0.25006168	0.343	0.141	3.20E-84	0	ISG20
APOE	0	1.74243208	0.992	0.367	0	1	APOE
APOC1	0	1.59322372	0.94	0.23	0	1	APOC1
SPP1	0	1.54743361	0.85	0.249	0	1	SPP1
HLA-DRA	0	1.0681564	0.973	0.445	0	1	HLA-DRA
CD74	0	0.99404764	0.991	0.541	0	1	CD74
FTL	0	0.99275117	0.997	0.907	0	1	FTL
HLA-DPA1	0	0.94181736	0.934	0.387	0	1	HLA-DPA1
C1QB	0	0.87920058	0.945	0.291	0	1	C1QB
FCGBP	0	0.84874739	0.622	0.109	0	1	FCGBP
C1QA	0	0.84769699	0.923	0.275	0	1	C1QA
HLA-DPB1	0	0.82138643	0.887	0.332	0	1	HLA-DPB1
C3	0	0.7322824	0.804	0.206	0	1	C3
SAT1	5.02E-290	0.71945467	0.981	0.641	8.15E-286	1	SAT1
CTSB	0	0.69591259	0.842	0.304	0	1	CTSB
NPC2	0	0.66099402	0.843	0.293	0	1	NPC2
RGS1	0	0.62280156	0.776	0.273	0	1	RGS1
CD81	0	0.6188377	0.855	0.384	0	1	CD81
C1QC	0	0.61499789	0.841	0.242	0	1	C1QC

A2M	0	0.60916567	0.738	0.186	0	1	A2M
HLA-DRB1	0	0.59190107	0.813	0.248	0	1	HLA-DRB1
MS4A7	0	0.59017317	0.749	0.227	0	1	MS4A7
CD163	0	0.58630181	0.644	0.146	0	1	CD163
FCGR3A	0	0.57429556	0.669	0.169	0	1	FCGR3A
TYROBP	1.77E-278	0.56823967	0.891	0.424	2.87E-274	1	TYROBP
FTH1	1.29E-239	0.56253339	0.99	0.912	2.09E-235	1	FTH1
ZFP36L1	6.83E-179	0.53109286	0.67	0.312	1.11E-174	1	ZFP36L1
PSAP	2.09E-266	0.52707182	0.776	0.319	3.39E-262	1	PSAP
CST3	1.38E-228	0.52650218	0.797	0.356	2.24E-224	1	CST3
AIF1	2.71E-256	0.52233733	0.821	0.347	4.41E-252	1	AIF1
RNASET2	5.53E-277	0.51872986	0.802	0.318	8.98E-273	1	RNASET2
DUSP1	1.03E-190	0.51409796	0.819	0.441	1.68E-186	1	DUSP1
TREM2	0	0.50109567	0.615	0.14	0	1	TREM2
S100A11	1.86E-196	0.48914705	0.847	0.498	3.01E-192	1	S100A11
MARCKS	3.68E-299	0.48490597	0.691	0.217	5.99E-295	1	MARCKS
SGK1	2.69E-216	0.47994562	0.628	0.226	4.38E-212	1	SGK1
FOS	3.04E-155	0.46970585	0.861	0.52	4.94E-151	1	FOS
MT2A	2.91E-125	0.4672544	0.458	0.187	4.73E-121	1	MT2A
MAFB	1.83E-252	0.43716261	0.548	0.157	2.98E-248	1	MAFB
CPM	0	0.43423705	0.44	0.081	0	1	CPM
CEBPD	9.33E-175	0.42977101	0.712	0.322	1.52E-170	1	CEBPD
HLA-DMA	1.51E-266	0.42607704	0.593	0.18	2.45E-262	1	HLA-DMA
FCER1G	2.49E-187	0.41958233	0.76	0.351	4.05E-183	1	FCER1G
SLC11A1	7.17E-227	0.41383347	0.654	0.23	1.16E-222	1	SLC11A1
GLDN	0	0.41336861	0.344	0.019	0	1	GLDN
EPB41L2	5.71E-302	0.39338106	0.522	0.123	9.29E-298	1	EPB41L2
SRGN	1.81E-106	0.38863846	0.888	0.716	2.94E-102	1	SRGN
RNASE1	2.67E-136	0.38531786	0.278	0.07	4.34E-132	1	RNASE1
RHOB	6.02E-202	0.3833012	0.493	0.153	9.78E-198	1	RHOB
CD14	3.40E-124	0.37790648	0.621	0.293	5.52E-120	1	CD14
MS4A6A	4.41E-194	0.37143812	0.621	0.233	7.16E-190	1	MS4A6A
HLA-DQB1	2.03E-190	0.36547458	0.573	0.198	3.30E-186	1	HLA-DQB1
SLC1A3	2.41E-215	0.35971219	0.545	0.167	3.92E-211	1	SLC1A3
ALOX5AP	2.13E-131	0.35650154	0.554	0.254	3.46E-127	1	ALOX5AP
LAPTM5	8.69E-125	0.35084664	0.752	0.437	1.41E-120	1	LAPTM5
SLCO2B1	2.39E-265	0.34805289	0.482	0.115	3.89E-261	1	SLCO2B1
HLA-DMB	9.18E-220	0.3470881	0.513	0.154	1.49E-215	1	HLA-DMB
MSR1	0	0.34653802	0.416	0.07	0	1	MSR1
PLXDC2	7.97E-194	0.34032913	0.513	0.169	1.29E-189	1	PLXDC2

CD63	1.45E-105	0.33649068	0.697	0.408	2.36E-101	1	CD63
ZFP36	1.10E-107	0.33400399	0.577	0.288	1.79E-103	1	ZFP36
RAC1	1.07E-125	0.33353751	0.638	0.326	1.74E-121	1	RAC1
VSIG4	4.03E-196	0.33262257	0.532	0.168	6.54E-192	1	VSIG4
GSN	8.93E-192	0.33140532	0.51	0.166	1.45E-187	1	GSN
FCGRT	2.83E-159	0.32190599	0.568	0.224	4.59E-155	1	FCGRT
NEAT1	7.14E-128	0.31275593	0.972	0.817	1.16E-123	1	NEAT1
GLUL	3.84E-129	0.30887939	0.58	0.257	6.24E-125	1	GLUL
TMIGD3	1.50E-208	0.30799531	0.336	0.07	2.44E-204	1	TMIGD3
TMEM176B	5.37E-259	0.30770091	0.378	0.072	8.72E-255	1	TMEM176B
FCGR2A	3.46E-189	0.30743941	0.459	0.139	5.62E-185	1	FCGR2A
CCL3	3.66E-94	0.30408145	0.5	0.221	5.95E-90	1	CCL3
CSF1R	5.73E-170	0.2991945	0.501	0.17	9.30E-166	1	CSF1R
CPVL	1.14E-173	0.29875164	0.445	0.14	1.85E-169	1	CPVL
PLTP	1.63E-263	0.29507253	0.292	0.04	2.64E-259	1	PLTP
KCTD12	3.92E-148	0.28923243	0.468	0.168	6.36E-144	1	KCTD12
YWHAH	5.85E-146	0.28864445	0.479	0.176	9.50E-142	1	YWHAH
C1orf162	1.31E-136	0.28257856	0.473	0.182	2.13E-132	1	C1orf162
QKI	1.82E-146	0.2821552	0.479	0.176	2.95E-142	1	QKI
CD9	1.16E-207	0.2814633	0.301	0.056	1.88E-203	1	CD9
CXCL16	3.77E-193	0.27777724	0.41	0.11	6.13E-189	1	CXCL16
HMOX1	1.68E-171	0.2766824	0.379	0.104	2.74E-167	1	HMOX1
HERPUD1	3.08E-73	0.2762519	0.535	0.302	5.00E-69	1	HERPUD1
CTSD	6.95E-93	0.2754683	0.471	0.223	1.13E-88	1	CTSD
ASAH1	1.08E-104	0.27274038	0.481	0.217	1.76E-100	1	ASAH1
MTRNR2L8	7.01E-279	0.27253767	0.309	0.042	1.14E-274	1	MTRNR2L8
IL18	5.01E-177	0.26628476	0.387	0.106	8.14E-173	1	IL18
HCLS1	4.29E-100	0.26465372	0.509	0.245	6.97E-96	1	HCLS1
DOCK4	2.63E-215	0.26404619	0.357	0.076	4.28E-211	1	DOCK4
HLA-DRB5	9.32E-106	0.26194478	0.532	0.233	1.51E-101	1	HLA-DRB5
SCIN	4.83E-231	0.26169029	0.308	0.052	7.85E-227	1	SCIN
MS4A4A	2.46E-137	0.25477692	0.401	0.132	4.00E-133	1	MS4A4A
SIGLEC10	2.61E-180	0.25228611	0.319	0.072	4.24E-176	1	SIGLEC10
TUBA1B	6.85E-93	0.2513223	0.609	0.32	1.11E-88	1	TUBA1B
MT-ND3	2.46E-62	0.25024083	0.991	0.985	4.00E-58	1	MT-ND3
CCL5	0	1.13571516	0.899	0.237	0	2	CCL5
GZMK1	0	0.91945206	0.675	0.088	0	2	GZMK
GZMA	0	0.88675629	0.825	0.193	0	2	GZMA
CD521	0	0.68494317	0.768	0.256	0	2	CD52
CD3D1	0	0.64527341	0.718	0.16	0	2	CD3D

HLA-C1	6.91E-259	0.62897548	0.944	0.656	1.12E-254	2	HLA-C
CD21	0	0.59445624	0.686	0.168	0	2	CD2
IL321	0	0.56851566	0.644	0.166	0	2	IL32
GZMH	0	0.55037573	0.556	0.13	0	2	GZMH
TRAC1	0	0.52399428	0.562	0.121	0	2	TRAC
RPL281	7.76E-247	0.52129036	0.991	0.949	1.26E-242	2	RPL28
RPS15A1	2.17E-257	0.5208304	0.997	0.93	3.53E-253	2	RPS15A
RPS261	9.14E-178	0.51790202	0.778	0.427	1.49E-173	2	RPS26
RPS251	8.88E-227	0.515894	0.978	0.845	1.44E-222	2	RPS25
RPS271	3.61E-224	0.50095625	0.999	0.924	5.87E-220	2	RPS27
RPS31	1.84E-211	0.48141314	0.993	0.917	3.00E-207	2	RPS3
HLA-A1	5.04E-177	0.47629733	0.963	0.782	8.19E-173	2	HLA-A
RPL411	9.00E-234	0.46596105	1	0.973	1.46E-229	2	RPL41
B2M1	1.10E-246	0.46515049	1	0.99	1.79E-242	2	B2M
CD8A	0	0.45772134	0.41	0.053	0	2	CD8A
SH3BGRL3	1.13E-130	0.4575486	0.838	0.576	1.84E-126	2	SH3BGRL3
BTG11	7.83E-141	0.43853433	0.921	0.663	1.27E-136	2	BTG1
TRBC21	1.37E-243	0.43255544	0.483	0.12	2.23E-239	2	TRBC2
TRBC11	1.21E-156	0.42509165	0.377	0.108	1.97E-152	2	TRBC1
TXNIP1	1.42E-119	0.41328335	0.821	0.516	2.31E-115	2	TXNIP
RPL23A1	6.68E-160	0.40540077	0.986	0.882	1.09E-155	2	RPL23A
MYL12A1	6.89E-120	0.39719764	0.731	0.435	1.12E-115	2	MYL12A
HCST	2.47E-123	0.39626569	0.662	0.355	4.01E-119	2	HCST
RPL101	4.46E-157	0.3948005	0.999	0.977	7.25E-153	2	RPL10
RARRES31	3.88E-197	0.38760786	0.517	0.165	6.30E-193	2	RARRES3
RPS121	1.04E-166	0.37905837	0.998	0.965	1.69E-162	2	RPS12
TMSB4X	1.79E-162	0.37388845	1	0.993	2.91E-158	2	TMSB4X
CD8B	0	0.35101707	0.327	0.037	0	2	CD8B
CD3G1	6.79E-230	0.34880619	0.444	0.105	1.10E-225	2	CD3G
RPL141	1.16E-115	0.34792193	0.948	0.848	1.88E-111	2	RPL14
RPL301	1.02E-136	0.34784717	0.993	0.93	1.65E-132	2	RPL30
RPSA1	3.79E-99	0.34551001	0.886	0.717	6.16E-95	2	RPSA
GIMAP71	3.25E-152	0.33889408	0.49	0.176	5.27E-148	2	GIMAP7
RPL131	1.36E-145	0.33199334	0.998	0.989	2.20E-141	2	RPL13
RPS291	6.02E-86	0.3230175	0.859	0.68	9.78E-82	2	RPS29
FAU1	1.14E-110	0.318962	0.975	0.91	1.84E-106	2	FAU
RPL36AL1	1.40E-74	0.316291	0.693	0.467	2.28E-70	2	RPL36AL
RPS151	3.76E-109	0.3158479	0.981	0.919	6.11E-105	2	RPS15
RPL10A1	1.55E-90	0.30845038	0.918	0.777	2.51E-86	2	RPL10A
RPL35A1	2.49E-90	0.30411541	0.934	0.828	4.04E-86	2	RPL35A

CST7	1.18E-151	0.30257861	0.451	0.144	1.92E-147	2	CST7
RPLP21	3.26E-91	0.29814739	0.96	0.9	5.30E-87	2	RPLP2
MYL12B	4.03E-78	0.29759827	0.604	0.358	6.55E-74	2	MYL12B
RPS27A1	1.32E-100	0.29548009	0.996	0.947	2.15E-96	2	RPS27A
CXCR6	4.81E-267	0.29187099	0.306	0.041	7.82E-263	2	CXCR6
ACTG1	3.24E-61	0.29133652	0.847	0.727	5.26E-57	2	ACTG1
RPS4X1	4.98E-78	0.28884716	0.939	0.859	8.09E-74	2	RPS4X
S100A41	2.34E-55	0.28835214	0.762	0.529	3.80E-51	2	S100A4
RPS191	1.28E-75	0.28388575	0.994	0.966	2.08E-71	2	RPS19
RPL7A1	1.17E-83	0.27948603	0.972	0.917	1.89E-79	2	RPL7A
RPS211	2.26E-68	0.27546657	0.842	0.692	3.67E-64	2	RPS21
PFN1	2.96E-50	0.27106442	0.615	0.43	4.82E-46	2	PFN1
CORO1A	5.27E-59	0.27047497	0.57	0.359	8.56E-55	2	CORO1A
APOBEC3G	3.78E-135	0.27043848	0.361	0.109	6.15E-131	2	APOBEC3G
EEF1D1	4.03E-56	0.26795658	0.702	0.506	6.54E-52	2	EEF1D
CD27	6.08E-252	0.26467276	0.292	0.039	9.89E-248	2	CD27
RPS141	6.68E-85	0.25906587	0.997	0.97	1.09E-80	2	RPS14
RPS71	1.64E-74	0.25852608	0.951	0.877	2.67E-70	2	RPS7
PPDPF	1.10E-98	0.25819632	0.398	0.158	1.78E-94	2	PPDPF
EVL	6.61E-80	0.25606654	0.463	0.223	1.07E-75	2	EVL
ACAP1	4.02E-124	0.25564536	0.39	0.13	6.53E-120	2	ACAP1
RPS281	2.83E-69	0.25477381	0.931	0.852	4.59E-65	2	RPS28
CD481	4.70E-83	0.25361647	0.475	0.225	7.64E-79	2	CD48
SOCS1	8.11E-153	0.25173219	0.33	0.083	1.32E-148	2	SOCS1
NKG7	2.23E-132	0.25162847	0.547	0.196	3.63E-128	2	NKG7
CCL4L2	0	1.85324246	0.914	0.1	0	3	CCL4L2
CCL31	0	1.84344995	0.976	0.176	0	3	CCL3
CCL3L1	0	1.48218375	0.82	0.069	0	3	CCL3L1
CCL4	0	1.32847918	0.905	0.292	0	3	CCL4
ITM2B	0	1.14010569	0.989	0.625	0	3	ITM2B
PDK4	0	1.1253048	0.869	0.082	0	3	PDK4
CH25H	0	1.12140697	0.734	0.03	0	3	CH25H
FOS1	0	1.07145627	0.984	0.514	0	3	FOS
IER2	0	1.05710964	0.881	0.341	0	3	IER2
IER3	0	1.02570424	0.75	0.142	0	3	IER3
MRC1	0	0.88992543	0.684	0.021	0	3	MRC1
JUN	0	0.88007266	0.912	0.463	0	3	JUN
OTUD1	0	0.82570106	0.672	0.076	0	3	OTUD1
A2M1	0	0.82462064	0.824	0.189	0	3	A2M
FOLR2	0	0.82364402	0.72	0.045	0	3	FOLR2

GPR34	0	0.80704488	0.784	0.13	0	3	GPR34
VSIG41	0	0.78174883	0.757	0.152	0	3	VSIG4
MS4A71	0	0.7813691	0.847	0.228	0	3	MS4A7
C1QB1	0	0.7464717	0.942	0.306	0	3	C1QB
C1QA1	0	0.73121852	0.902	0.292	0	3	C1QA
IFNGR1	0	0.68728479	0.744	0.184	0	3	IFNGR1
SMAP2	0	0.68270783	0.784	0.261	0	3	SMAP2
RNASET21	0	0.68158206	0.841	0.324	0	3	RNASET2
BIN1	0	0.67646574	0.69	0.145	0	3	BIN1
MIS18BP1	0	0.65431421	0.652	0.137	0	3	MIS18BP1
SLC1A31	0	0.650983	0.736	0.155	0	3	SLC1A3
FTL1	3.33E-245	0.63897884	0.999	0.909	5.41E-241	3	FTL
LTC4S	0	0.60708449	0.635	0.1	0	3	LTC4S
BHLHE41	0	0.58596761	0.604	0.091	0	3	BHLHE41
C1QC1	0	0.57881691	0.825	0.257	0	3	C1QC
EGR1	0	0.57686631	0.612	0.122	0	3	EGR1
LYVE1	0	0.56611727	0.494	0.01	0	3	LYVE1
FCGRT1	9.52E-304	0.56176704	0.694	0.218	1.55E-299	3	FCGRT
APOE1	9.73E-290	0.55210656	0.99	0.381	1.58E-285	3	APOE
CEBPD1	1.32E-207	0.53485734	0.761	0.326	2.15E-203	3	CEBPD
P2RY13	0	0.53467315	0.579	0.092	0	3	P2RY13
MS4A4A1	0	0.52014486	0.572	0.12	0	3	MS4A4A
CSF1R1	0	0.51426129	0.625	0.164	0	3	CSF1R
RGS10	2.48E-255	0.51094658	0.689	0.244	4.03E-251	3	RGS10
BTG2	4.05E-187	0.50091105	0.594	0.223	6.58E-183	3	BTG2
SGK11	1.51E-202	0.48805945	0.652	0.232	2.46E-198	3	SGK1
HTRA1	0	0.48155934	0.548	0.11	0	3	HTRA1
RHOB1	1.04E-235	0.46583612	0.548	0.154	1.69E-231	3	RHOB
MARCKS1	7.96E-236	0.4646083	0.683	0.229	1.29E-231	3	MARCKS
WASF2	1.96E-233	0.46257198	0.626	0.213	3.18E-229	3	WASF2
DAB2	0	0.45327859	0.512	0.082	0	3	DAB2
FCGR1A	0	0.4352492	0.495	0.099	0	3	FCGR1A
OGFRL1	3.55E-260	0.42646266	0.603	0.172	5.77E-256	3	OGFRL1
EGR3	0	0.42405921	0.409	0.049	0	3	EGR3
FRMD4A	0	0.4219756	0.484	0.086	0	3	FRMD4A
MAF	2.55E-292	0.42013343	0.511	0.111	4.14E-288	3	MAF
SLCO2B11	3.87E-263	0.41429684	0.511	0.12	6.29E-259	3	SLCO2B1
AIF11	3.11E-147	0.41083387	0.758	0.364	5.05E-143	3	AIF1
CEBPB	1.14E-145	0.40848875	0.715	0.334	1.85E-141	3	CEBPB
FCER1G1	4.83E-132	0.40746074	0.726	0.364	7.86E-128	3	FCER1G

CREG1	2.55E-276	0.40439999	0.449	0.091	4.14E-272	3	CREG1
SLC2A5	2.72E-302	0.40270708	0.467	0.088	4.43E-298	3	SLC2A5
SRGAP2	1.64E-285	0.39953197	0.5	0.107	2.66E-281	3	SRGAP2
CX3CR1	2.01E-300	0.39948617	0.453	0.083	3.26E-296	3	CX3CR1
HAVCR2	1.03E-188	0.39687531	0.477	0.143	1.68E-184	3	HAVCR2
SEC14L1	7.77E-280	0.39218548	0.473	0.099	1.26E-275	3	SEC14L1
CYBB	8.55E-166	0.38150309	0.548	0.196	1.39E-161	3	CYBB
TUBA1B1	1.43E-158	0.37155876	0.708	0.316	2.32E-154	3	TUBA1B
GYPC	2.18E-190	0.36963474	0.505	0.156	3.54E-186	3	GYPC
CD631	2.61E-109	0.36930816	0.724	0.411	4.24E-105	3	CD63
RAC11	1.80E-133	0.36461031	0.679	0.328	2.93E-129	3	RAC1
TNF	0	0.36298334	0.34	0.037	0	3	TNF
MTSS1	0	0.35952793	0.398	0.056	0	3	MTSS1
EPB41L21	2.34E-196	0.35297705	0.486	0.136	3.80E-192	3	EPB41L2
NINJ1	4.15E-229	0.35235984	0.433	0.099	6.75E-225	3	NINJ1
IRS2	2.49E-207	0.34995843	0.386	0.086	4.04E-203	3	IRS2
EGR2	0	0.34875495	0.345	0.036	0	3	EGR2
TMSB4X1	7.27E-121	0.34874444	1	0.993	1.18E-116	3	TMSB4X
ADGRG1	3.28E-249	0.3424328	0.446	0.095	5.33E-245	3	ADGRG1
SHTN1	1.76E-264	0.34236742	0.403	0.074	2.86E-260	3	SHTN1
MERTK	1.03E-267	0.34051982	0.396	0.069	1.68E-263	3	MERTK
CD811	3.38E-113	0.33904323	0.753	0.405	5.49E-109	3	CD81
GPN3	0	0.33773893	0.357	0.039	0	3	GPN3
C31	2.28E-153	0.33734552	0.637	0.237	3.71E-149	3	C3
NFKBIA	1.11E-118	0.33684594	0.631	0.297	1.80E-114	3	NFKBIA
IL6ST	1.23E-220	0.33547745	0.404	0.088	2.01E-216	3	IL6ST
SRGAP2B	5.38E-306	0.3354513	0.395	0.06	8.74E-302	3	SRGAP2B
NAA20	6.02E-261	0.33208151	0.398	0.073	9.78E-257	3	NAA20
LGMN	6.64E-271	0.32858727	0.361	0.056	1.08E-266	3	LGMN
C12orf75	2.64E-206	0.32701776	0.398	0.091	4.29E-202	3	C12orf75
AP005530.1	0	0.32675435	0.326	0.012	0	3	AP005530.1
DUSP6	4.44E-111	0.32364033	0.349	0.115	7.22E-107	3	DUSP6
IGSF6	5.04E-158	0.32283422	0.45	0.142	8.19E-154	3	IGSF6
CYFIP1	2.48E-198	0.31727945	0.415	0.102	4.03E-194	3	CYFIP1
SRGAP2C	8.88E-233	0.31383664	0.372	0.071	1.44E-228	3	SRGAP2C
ASAH11	3.12E-109	0.31252707	0.509	0.22	5.08E-105	3	ASAH1
CD99	2.56E-119	0.30747629	0.514	0.213	4.17E-115	3	CD99
CD84	3.77E-133	0.30383314	0.424	0.143	6.12E-129	3	CD84
CD141	4.39E-110	0.30134578	0.653	0.296	7.13E-106	3	CD14
ZFHX3	4.01E-212	0.30132885	0.371	0.077	6.51E-208	3	ZFHX3

TRA2B	1.80E-98	0.3011409	0.45	0.192	2.93E-94	3	TRA2B
MEF2C	1.31E-146	0.30074263	0.44	0.142	2.12E-142	3	MEF2C
APLP2	1.12E-103	0.29804726	0.49	0.21	1.82E-99	3	APLP2
MEF2A	3.47E-144	0.29750419	0.468	0.158	5.64E-140	3	MEF2A
TYROBP1	3.29E-88	0.2957934	0.778	0.447	5.35E-84	3	TYROBP
GNAS	4.02E-81	0.29531667	0.652	0.384	6.52E-77	3	GNAS
KLF6	1.94E-58	0.29467224	0.623	0.394	3.15E-54	3	KLF6
P2RY12	0	0.29456252	0.292	0.014	0	3	P2RY12
SRSF5	1.62E-82	0.29441989	0.598	0.329	2.64E-78	3	SRSF5
BRI3	1.16E-112	0.29281505	0.539	0.236	1.88E-108	3	BRI3
TPT11	3.37E-88	0.29166894	0.998	0.994	5.48E-84	3	TPT1
VSIR	1.37E-121	0.28641574	0.435	0.158	2.23E-117	3	VSIR
SOCS6	9.17E-283	0.2859495	0.303	0.035	1.49E-278	3	SOCS6
KLF2	9.03E-92	0.28253062	0.506	0.227	1.47E-87	3	KLF2
TREM2	5.41E-141	0.28180644	0.489	0.165	8.80E-137	3	TREM2
HERPUD11	1.23E-78	0.28084755	0.574	0.303	2.00E-74	3	HERPUD1
CSF2RA	1.19E-169	0.28041359	0.343	0.081	1.93E-165	3	CSF2RA
PICALM	3.37E-147	0.28006897	0.402	0.121	5.47E-143	3	PICALM
ATP6V0B	2.33E-92	0.27696557	0.537	0.259	3.79E-88	3	ATP6V0B
ADAP2	4.37E-134	0.26697345	0.363	0.106	7.10E-130	3	ADAP2
KCTD121	6.70E-102	0.26643395	0.444	0.177	1.09E-97	3	KCTD12
EIF1	5.07E-65	0.26641297	0.947	0.856	8.24E-61	3	EIF1
FKBP5	2.81E-73	0.26449673	0.564	0.304	4.57E-69	3	FKBP5
LILRB4	5.47E-134	0.26244108	0.378	0.114	8.90E-130	3	LILRB4
FCGR1B	3.61E-261	0.26173724	0.299	0.038	5.87E-257	3	FCGR1B
PLXDC21	1.10E-101	0.26046714	0.455	0.182	1.79E-97	3	PLXDC2
CYTL1	8.51E-289	0.25913412	0.282	0.029	1.38E-284	3	CYTL1
ITPR2	1.02E-134	0.25793972	0.36	0.104	1.66E-130	3	ITPR2
APBB1IP	3.53E-79	0.25765088	0.478	0.231	5.73E-75	3	APBB1IP
C3AR1	1.96E-118	0.25274907	0.359	0.114	3.19E-114	3	C3AR1
SPTLC2	6.06E-133	0.25004596	0.329	0.09	9.85E-129	3	SPTLC2
HLA-DRB11	0	1.40889277	0.875	0.261	0	4	HLA-DRB1
CD741	0	1.31658024	0.994	0.556	0	4	CD74
HLA-DRA1	0	1.06330318	0.984	0.461	0	4	HLA-DRA
HLA-DPA11	0	1.04952056	0.953	0.402	0	4	HLA-DPA1
C1QB2	0	1.03359147	0.921	0.314	0	4	C1QB
C1QC2	0	0.86021498	0.844	0.261	0	4	C1QC
FCGBP1	1.12E-299	0.86004768	0.577	0.13	1.82E-295	4	FCGBP
APOE2	5.83E-304	0.85980446	0.971	0.39	9.47E-300	4	APOE
C1QA2	0	0.85588036	0.887	0.3	0	4	C1QA

HLA-DRB51	0	0.83010598	0.784	0.218	0	4	HLA-DRB5
C32	0	0.80114247	0.768	0.229	0	4	C3
HLA-DQB11	0	0.74758589	0.749	0.193	0	4	HLA-DQB1
MS4A6A1	6.67E-267	0.62179387	0.705	0.237	1.08E-262	4	MS4A6A
SGK12	2.60E-229	0.61933161	0.681	0.234	4.23E-225	4	SGK1
HLA-DPB11	8.28E-216	0.61264214	0.822	0.356	1.35E-211	4	HLA-DPB1
CD142	3.16E-154	0.59937024	0.676	0.298	5.13E-150	4	CD14
CST31	3.42E-179	0.59800476	0.785	0.371	5.56E-175	4	CST3
APOC11	2.06E-226	0.57169954	0.772	0.269	3.36E-222	4	APOC1
XIST	4.01E-303	0.56686032	0.544	0.116	6.52E-299	4	XIST
CD812	5.34E-157	0.56018141	0.769	0.407	8.68E-153	4	CD81
NPC21	8.29E-193	0.55683104	0.74	0.321	1.35E-188	4	NPC2
HSPA1A	1.92E-94	0.54870117	0.396	0.154	3.12E-90	4	HSPA1A
SAT11	1.14E-135	0.53915985	0.956	0.654	1.85E-131	4	SAT1
RNASET22	1.07E-177	0.53791631	0.749	0.339	1.74E-173	4	RNASET2
HLA-DQA1	5.67E-269	0.52981371	0.551	0.133	9.21E-265	4	HLA-DQA1
CEBPD2	3.97E-118	0.51241861	0.674	0.339	6.44E-114	4	CEBPD
FCER1G2	2.41E-140	0.49249663	0.728	0.367	3.91E-136	4	FCER1G
SPP11	5.37E-186	0.49231444	0.739	0.279	8.72E-182	4	SPP1
ITM2B1	8.19E-139	0.48633447	0.901	0.637	1.33E-134	4	ITM2B
MAFB1	2.30E-96	0.47680977	0.438	0.18	3.73E-92	4	MAFB
SLC11A11	5.68E-129	0.46330918	0.586	0.251	9.23E-125	4	SLC11A1
FCGR3A1	2.03E-198	0.45056525	0.596	0.192	3.30E-194	4	FCGR3A
HLA-DMB1	2.44E-216	0.44243134	0.555	0.161	3.97E-212	4	HLA-DMB
MARCKS2	3.99E-160	0.43709883	0.621	0.24	6.48E-156	4	MARCKS
RGS11	3.05E-110	0.43550191	0.631	0.303	4.95E-106	4	RGS1
HLA-DMA1	8.12E-167	0.41132965	0.559	0.197	1.32E-162	4	HLA-DMA
CTSB1	3.39E-126	0.40312522	0.698	0.336	5.51E-122	4	CTSB
PSAP1	6.50E-104	0.40189617	0.657	0.345	1.06E-99	4	PSAP
ARHGAP24	8.12E-276	0.39574373	0.413	0.071	1.32E-271	4	ARHGAP24
SLC1A32	3.54E-154	0.38373528	0.531	0.181	5.75E-150	4	SLC1A3
TREM22	2.13E-141	0.37533043	0.489	0.168	3.45E-137	4	TREM2
ZFP36L11	3.90E-68	0.36940324	0.579	0.333	6.34E-64	4	ZFP36L1
CYBB1	6.23E-126	0.36685989	0.52	0.203	1.01E-121	4	CYBB
TUBA1B2	1.69E-84	0.36467664	0.608	0.329	2.75E-80	4	TUBA1B
HERPUD12	3.95E-84	0.35793299	0.58	0.305	6.42E-80	4	HERPUD1
A2M2	1.82E-132	0.34829362	0.587	0.218	2.95E-128	4	A2M
USP53	7.02E-141	0.33414748	0.397	0.116	1.14E-136	4	USP53
AIF12	5.27E-79	0.33386433	0.671	0.376	8.57E-75	4	AIF1
1-Jun	8.51E-26	0.33061809	0.639	0.494	1.38E-21	4	JUN

ALOX5AP1	4.30E-79	0.32971419	0.527	0.266	6.99E-75	4	ALOX5AP
MEF2A1	2.12E-111	0.3143978	0.441	0.164	3.45E-107	4	MEF2A
PLXDC22	5.77E-99	0.30956535	0.457	0.185	9.38E-95	4	PLXDC2
TYROBP2	2.53E-72	0.30700377	0.754	0.452	4.11E-68	4	TYROBP
YWHAH1	2.14E-97	0.3019927	0.459	0.188	3.48E-93	4	YWHAH
CSF1R2	7.06E-99	0.30182171	0.459	0.185	1.15E-94	4	CSF1R
APBB1IP1	3.34E-84	0.30124188	0.489	0.233	5.43E-80	4	APBB1IP
P2RY131	4.98E-109	0.29836796	0.366	0.118	8.09E-105	4	P2RY13
TMEM176B1	2.22E-123	0.29812933	0.321	0.087	3.61E-119	4	TMEM176B
DENND3	2.37E-122	0.29291884	0.356	0.106	3.85E-118	4	DENND3
SRGAP21	1.27E-116	0.29114467	0.382	0.123	2.06E-112	4	SRGAP2
LILRB41	4.79E-118	0.29064768	0.373	0.117	7.78E-114	4	LILRB4
HSPA1B	1.17E-84	0.28443327	0.285	0.089	1.90E-80	4	HSPA1B
FRMD4A1	1.45E-118	0.2788889	0.35	0.103	2.35E-114	4	FRMD4A
SLC25A37	1.64E-88	0.27748656	0.389	0.149	2.67E-84	4	SLC25A37
KCNMB1	1.51E-221	0.26886988	0.27	0.035	2.45E-217	4	KCNMB1
GPR341	9.97E-110	0.26859808	0.466	0.167	1.62E-105	4	GPR34
RAC12	6.84E-59	0.26740537	0.58	0.342	1.11E-54	4	RAC1
OLFML3	1.89E-151	0.26566051	0.284	0.058	3.08E-147	4	OLFML3
GRN	4.22E-61	0.25838686	0.452	0.231	6.86E-57	4	GRN
CYBA	2.86E-48	0.25791055	0.868	0.745	4.65E-44	4	CYBA
SRGAP1	9.85E-141	0.25637814	0.302	0.069	1.60E-136	4	SRGAP1
LPAR6	1.36E-97	0.2552488	0.323	0.103	2.20E-93	4	LPAR6
GSN1	1.80E-82	0.25387762	0.44	0.184	2.93E-78	4	GSN
LPCAT2	4.99E-109	0.25230161	0.356	0.112	8.10E-105	4	LPCAT2
EPB41L22	1.40E-85	0.25146476	0.388	0.149	2.28E-81	4	EPB41L2
S100A9	0	3.07249105	0.992	0.111	0	5	S100A9
S100A8	0	2.73051485	0.983	0.078	0	5	S100A8
LYZ	0	1.96559151	0.987	0.123	0	5	LYZ
VCAN	0	1.73430498	0.964	0.071	0	5	VCAN
TIMP1	0	1.5664738	0.719	0.112	0	5	TIMP1
NAMPT	0	1.49791455	0.929	0.122	0	5	NAMPT
S100A12	0	1.32246943	0.771	0.013	0	5	S100A12
EREG	0	1.18766158	0.638	0.029	0	5	EREG
S100A6	0	1.15047913	0.983	0.416	0	5	S100A6
FCN1	0	1.14270185	0.875	0.035	0	5	FCN1
NEAT11	0	1.12762637	0.999	0.82	0	5	NEAT1
CTSS	0	1.07406728	0.926	0.28	0	5	CTSS
THBS1	0	1.0398565	0.589	0.043	0	5	THBS1
PLAUR	0	1.02961818	0.675	0.087	0	5	PLAUR

SLC2A3	0	1.01711021	0.815	0.168	0	5	SLC2A3
FTH11	4.91E-295	0.94946744	0.997	0.914	7.98E-291	5	FTH1
SRGN1	8.13E-269	0.88237181	0.968	0.716	1.32E-264	5	SRGN
VIM	0	0.87232176	0.96	0.469	0	5	VIM
CD55	0	0.86452567	0.707	0.082	0	5	CD55
AREG	0	0.83614756	0.581	0.105	0	5	AREG
SOCS3	0	0.7944142	0.675	0.061	0	5	SOCS3
MNDA	0	0.79411705	0.759	0.139	0	5	MNDA
DUSP11	4.62E-275	0.7916861	0.923	0.447	7.51E-271	5	DUSP1
IL1B	0	0.76529553	0.435	0.053	0	5	IL1B
CEBPB1	4.56E-290	0.74566582	0.848	0.329	7.41E-286	5	CEBPB
S100A42	8.29E-260	0.72657871	0.951	0.518	1.35E-255	5	S100A4
MCL1	0	0.72501072	0.862	0.326	0	5	MCL1
CXCL8	2.24E-162	0.70579156	0.323	0.066	3.64E-158	5	CXCL8
CD44	0	0.65769604	0.675	0.154	0	5	CD44
VMP1	0	0.65682905	0.694	0.183	0	5	VMP1
SAT12	5.83E-183	0.64560694	0.98	0.654	9.47E-179	5	SAT1
FOS2	4.09E-183	0.64322864	0.936	0.527	6.64E-179	5	FOS
RGS2	3.67E-282	0.63892803	0.542	0.122	5.96E-278	5	RGS2
S100A10	1.60E-264	0.62754349	0.812	0.3	2.60E-260	5	S100A10
ANXA1	4.11E-266	0.61951066	0.715	0.235	6.69E-262	5	ANXA1
ATP2B1	1.31E-286	0.6036407	0.508	0.106	2.12E-282	5	ATP2B1
CD300E	0	0.59698358	0.493	0.016	0	5	CD300E
SOD2	0	0.5707768	0.537	0.072	0	5	SOD2
SERPINB1	1.97E-264	0.54956849	0.626	0.176	3.19E-260	5	SERPINB1
MXD1	0	0.54500404	0.518	0.037	0	5	MXD1
C5AR1	0	0.54477916	0.557	0.079	0	5	C5AR1
TKT	0	0.54189824	0.653	0.125	0	5	TKT
THBD	0	0.5282795	0.393	0.034	0	5	THBD
PLBD1	0	0.52142855	0.511	0.035	0	5	PLBD1
ZEB2	7.12E-214	0.51983165	0.655	0.221	1.16E-209	5	ZEB2
CD143	3.14E-190	0.51739871	0.757	0.294	5.10E-186	5	CD14
COTL1	9.69E-208	0.51200731	0.773	0.314	1.57E-203	5	COTL1
IL1R2	0	0.49181753	0.354	0.016	0	5	IL1R2
LGALS1	1.31E-224	0.49052294	0.792	0.284	2.12E-220	5	LGALS1
TSPO	1.12E-176	0.48827441	0.727	0.316	1.81E-172	5	TSPO
H3F3A	1.14E-156	0.48006287	0.945	0.718	1.85E-152	5	H3F3A
ATP13A3	0	0.4724248	0.453	0.07	0	5	ATP13A3
ITGAX	2.22E-300	0.47003669	0.455	0.076	3.61E-296	5	ITGAX
SLC11A12	3.56E-189	0.4628279	0.686	0.244	5.78E-185	5	SLC11A1

PABPC1	1.52E-159	0.4605953	0.844	0.459	2.47E-155	5	PABPC1
TYMP	2.09E-223	0.45944906	0.678	0.214	3.40E-219	5	TYMP
OAZ1	4.25E-152	0.44868641	0.899	0.563	6.91E-148	5	OAZ1
NCF2	0	0.44522862	0.504	0.057	0	5	NCF2
FOSL2	0	0.44328624	0.477	0.064	0	5	FOSL2
NFKBIA1	2.57E-89	0.44246058	0.602	0.306	4.17E-85	5	NFKBIA
PPIF	0	0.44028251	0.368	0.043	0	5	PPIF
CSTA	0	0.43963646	0.52	0.051	0	5	CSTA
CFD	0	0.4363509	0.506	0.075	0	5	CFD
FGL2	4.39E-236	0.43258142	0.539	0.134	7.13E-232	5	FGL2
ZFP361	3.18E-138	0.42753678	0.671	0.292	5.17E-134	5	ZFP36
ACTB	4.33E-126	0.42681511	0.975	0.848	7.03E-122	5	ACTB
MAT2A	1.93E-166	0.41964664	0.447	0.126	3.13E-162	5	MAT2A
CFP	0	0.41636732	0.452	0.018	0	5	CFP
APLP21	4.56E-205	0.41621074	0.635	0.202	7.42E-201	5	APLP2
TNFRSF1B	7.41E-198	0.41245706	0.54	0.156	1.20E-193	5	TNFRSF1B
FLNA	6.32E-265	0.40202384	0.515	0.108	1.03E-260	5	FLNA
EMP3	4.58E-181	0.40185748	0.608	0.206	7.44E-177	5	EMP3
EVI2B	5.56E-195	0.40064379	0.543	0.161	9.03E-191	5	EVI2B
JUNB	3.72E-105	0.39968176	0.708	0.366	6.05E-101	5	JUNB
GADD45B	3.09E-169	0.39898557	0.456	0.125	5.02E-165	5	GADD45B
GK	0	0.39620134	0.394	0.048	0	5	GK
ACSL1	2.97E-265	0.3957397	0.462	0.088	4.83E-261	5	ACSL1
BCL2A1	0	0.39188889	0.431	0.057	0	5	BCL2A1
ANXA2	3.76E-199	0.39081251	0.575	0.17	6.11E-195	5	ANXA2
FTL2	2.46E-132	0.39022919	1	0.91	4.00E-128	5	FTL
TALDO1	1.85E-213	0.39009765	0.526	0.141	3.00E-209	5	TALDO1
IVNS1ABP	1.23E-283	0.38944617	0.441	0.074	1.99E-279	5	IVNS1ABP
MIDN	3.26E-241	0.38624416	0.468	0.099	5.29E-237	5	MIDN
FPR1	2.00E-239	0.3840954	0.516	0.119	3.24E-235	5	FPR1
TFRC	1.10E-167	0.3836307	0.297	0.056	1.79E-163	5	TFRC
LCP1	1.18E-154	0.37615653	0.658	0.26	1.92E-150	5	LCP1
VEGFA	1.64E-220	0.37047778	0.327	0.05	2.66E-216	5	VEGFA
SAMSN1	1.22E-145	0.3691411	0.5	0.168	1.99E-141	5	SAMSN1
MPEG1	0	0.36771108	0.408	0.034	0	5	MPEG1
GLUL1	2.01E-83	0.36207427	0.561	0.271	3.26E-79	5	GLUL
CD93	3.73E-261	0.35414427	0.395	0.063	6.06E-257	5	CD93
PLEK	2.61E-151	0.35377742	0.437	0.126	4.25E-147	5	PLEK
KDM6B	0	0.3520708	0.383	0.048	0	5	KDM6B
HIF1A	5.53E-134	0.35195822	0.433	0.135	8.99E-130	5	HIF1A

APOBEC3A	0	0.34957152	0.289	0.006	0	5	APOBEC3A
GCA	4.60E-244	0.34633764	0.418	0.077	7.47E-240	5	GCA
KLF4	1.10E-285	0.34555908	0.395	0.057	1.79E-281	5	KLF4
PTPRE	5.50E-206	0.34241102	0.472	0.113	8.94E-202	5	PTPRE
HBEGF	2.15E-257	0.34056742	0.363	0.053	3.49E-253	5	HBEGF
MAP3K8	5.16E-144	0.34038299	0.376	0.099	8.39E-140	5	MAP3K8
CD36	0	0.33741032	0.345	0.02	0	5	CD36
FOSB	1.17E-75	0.33724791	0.534	0.264	1.91E-71	5	FOSB
GPCPD1	2.11E-246	0.33280161	0.408	0.072	3.43E-242	5	GPCPD1
GLIPR1	9.58E-141	0.33272709	0.52	0.182	1.56E-136	5	GLIPR1
YBX3	2.88E-165	0.32852322	0.409	0.104	4.69E-161	5	YBX3
TPM4	5.84E-143	0.32831795	0.421	0.123	9.49E-139	5	TPM4
DUSP61	8.64E-121	0.32751411	0.383	0.116	1.40E-116	5	DUSP6
ANPEP	0	0.3240007	0.269	0.016	0	5	ANPEP
CCNL1	5.84E-95	0.32203746	0.584	0.275	9.49E-91	5	CCNL1
BRI31	9.62E-116	0.32194718	0.576	0.238	1.56E-111	5	BRI3
SDCBP	9.18E-129	0.3214146	0.502	0.179	1.49E-124	5	SDCBP
TYROBP3	4.96E-93	0.32125438	0.833	0.448	8.06E-89	5	TYROBP
PSAP2	1.69E-105	0.31865336	0.715	0.342	2.75E-101	5	PSAP
GAPDH	4.14E-88	0.31745283	0.905	0.668	6.73E-84	5	GAPDH
CLEC12A	0	0.31654576	0.361	0.028	0	5	CLEC12A
METRNL	1.41E-141	0.31247721	0.431	0.126	2.29E-137	5	METRNL
PCBP1	1.98E-134	0.31062029	0.52	0.185	3.22E-130	5	PCBP1
AP1S2	9.15E-190	0.30981793	0.409	0.091	1.49E-185	5	AP1S2
ATP2B1-AS1	9.79E-191	0.30688779	0.4	0.087	1.59E-186	5	ATP2B1-AS1
S100A111	5.98E-76	0.30685364	0.829	0.513	9.72E-72	5	S100A11
MAFB2	3.40E-96	0.30554077	0.466	0.18	5.53E-92	5	MAFB
CES1	0	0.30437626	0.306	0.01	0	5	CES1
CHD1	3.54E-145	0.30264761	0.424	0.121	5.76E-141	5	CHD1
RNF149	7.72E-142	0.30170303	0.457	0.141	1.26E-137	5	RNF149
SLC43A2	3.62E-202	0.30071431	0.367	0.07	5.88E-198	5	SLC43A2
METTL9	1.63E-168	0.29513646	0.427	0.109	2.65E-164	5	METTL9
GRN1	9.29E-106	0.29473582	0.545	0.225	1.51E-101	5	GRN
ACTG11	4.25E-61	0.29314408	0.906	0.725	6.91E-57	5	ACTG1
RPL7	4.13E-72	0.2906147	0.874	0.647	6.72E-68	5	RPL7
AHNAK	5.75E-134	0.28920996	0.446	0.138	9.35E-130	5	AHNAK
TNFAIP2	2.61E-251	0.28350296	0.339	0.047	4.24E-247	5	TNFAIP2
MT-ND1	1.36E-90	0.28329611	0.999	0.986	2.20E-86	5	MT-ND1
NLRP3	1.23E-189	0.28267073	0.314	0.053	2.00E-185	5	NLRP3
RETN	0	0.28009688	0.266	0.014	0	5	RETN

UPP1	1.10E-137	0.28003737	0.361	0.094	1.79E-133	5	UPP1
LGALS3	2.63E-158	0.27990757	0.393	0.097	4.28E-154	5	LGALS3
SH3BGRL31	1.11E-69	0.27988382	0.857	0.582	1.81E-65	5	SH3BGRL3
LTA4H	3.86E-217	0.27896448	0.338	0.055	6.26E-213	5	LTA4H
VASP	8.96E-143	0.27840041	0.415	0.118	1.46E-138	5	VASP
SH3BP5	1.75E-170	0.2747658	0.353	0.075	2.84E-166	5	SH3BP5
IRAK3	8.29E-183	0.27436087	0.379	0.081	1.35E-178	5	IRAK3
ATP1B3	2.11E-54	0.27405245	0.357	0.164	3.44E-50	5	ATP1B3
AC020656.1	0	0.27240472	0.292	0.01	0	5	AC020656.1
GSTP1	7.48E-77	0.26946394	0.545	0.268	1.21E-72	5	GSTP1
CSF3R	4.58E-148	0.26457587	0.381	0.097	7.45E-144	5	CSF3R
BLVRB	7.91E-174	0.26417255	0.363	0.078	1.28E-169	5	BLVRB
AGFG1	1.10E-165	0.26407578	0.337	0.07	1.79E-161	5	AGFG1
ZFAND5	8.75E-107	0.26267351	0.374	0.119	1.42E-102	5	ZFAND5
FGR	1.86E-197	0.26265725	0.332	0.058	3.03E-193	5	FGR
SLC25A371	2.89E-86	0.26205624	0.4	0.15	4.70E-82	5	SLC25A37
TMEM167A	2.77E-138	0.26110288	0.355	0.09	4.50E-134	5	TMEM167A
NR4A1	5.15E-131	0.26103416	0.349	0.089	8.37E-127	5	NR4A1
SELL	2.57E-218	0.26084331	0.301	0.042	4.17E-214	5	SELL
TREM1	1.76E-276	0.26074895	0.297	0.03	2.86E-272	5	TREM1
NABP1	1.73E-101	0.25688511	0.341	0.105	2.81E-97	5	NABP1
JAML	3.75E-222	0.25674411	0.334	0.051	6.09E-218	5	JAML
CLEC4E	5.75E-229	0.25341748	0.271	0.031	9.34E-225	5	CLEC4E
ITGAM	1.17E-163	0.25094699	0.328	0.067	1.91E-159	5	ITGAM
ATP5MPL	2.16E-81	0.25092906	0.466	0.203	3.50E-77	5	ATP5MPL
MT-CO1	2.78E-67	0.25035963	1	0.994	4.52E-63	5	MT-CO1
GNLY	0	0.99012272	0.77	0.124	0	6	GNLY
NKG71	0	0.81971367	0.804	0.183	0	6	NKG7
CCL51	1.33E-188	0.53250984	0.753	0.268	2.17E-184	6	CCL5
RPS272	1.13E-124	0.44951356	0.995	0.927	1.83E-120	6	RPS27
HLA-B	2.59E-122	0.4492993	0.975	0.841	4.21E-118	6	HLA-B
KLRD1	1.51E-173	0.40417364	0.409	0.096	2.45E-169	6	KLRD1
CST71	2.17E-146	0.3939815	0.481	0.15	3.53E-142	6	CST7
RPS27A2	4.86E-109	0.38207365	0.999	0.948	7.90E-105	6	RPS27A
KLRB11	2.35E-107	0.37324134	0.393	0.127	3.82E-103	6	KLRB1
GZMH1	1.54E-121	0.36184468	0.454	0.15	2.51E-117	6	GZMH
RPS292	7.27E-69	0.34967592	0.848	0.686	1.18E-64	6	RPS29
PRF1	1.34E-149	0.3470058	0.397	0.103	2.17E-145	6	PRF1
RPS32	2.41E-85	0.33937198	0.994	0.919	3.91E-81	6	RPS3
ARL4C	2.07E-81	0.33839333	0.486	0.22	3.36E-77	6	ARL4C

RPL31	8.62E-83	0.33412415	0.987	0.926	1.40E-78	6	RPL3
GZMB	1.83E-156	0.33033977	0.361	0.081	2.97E-152	6	GZMB
PTPRC	1.40E-54	0.3291822	0.714	0.526	2.28E-50	6	PTPRC
FGFBP2	8.30E-187	0.32835667	0.312	0.052	1.35E-182	6	FGFBP2
RPS15A2	7.11E-77	0.31473201	0.997	0.932	1.15E-72	6	RPS15A
CALM1	4.26E-52	0.30718756	0.661	0.459	6.92E-48	6	CALM1
RPS142	5.97E-64	0.28709829	0.997	0.971	9.70E-60	6	RPS14
IL7R1	7.61E-43	0.28231243	0.337	0.159	1.24E-38	6	IL7R
RPL341	8.58E-61	0.28093648	0.985	0.927	1.39E-56	6	RPL34
MYL12A2	3.21E-40	0.27873392	0.627	0.452	5.21E-36	6	MYL12A
MT-CO11	9.55E-66	0.27151792	0.999	0.994	1.55E-61	6	MT-CO1
RPL102	1.69E-63	0.27056655	0.996	0.978	2.75E-59	6	RPL10
MT-ATP6	1.61E-67	0.25844218	1	0.996	2.62E-63	6	MT-ATP6
RPL23A2	5.16E-53	0.2580761	0.966	0.887	8.39E-49	6	RPL23A
PPP2R5C	1.83E-56	0.25041277	0.372	0.17	2.98E-52	6	PPP2R5C
GNLY1	0	1.90226783	0.977	0.125	0	7	GNLY
NKG72	0	1.47528761	0.98	0.185	0	7	NKG7
CCL41	1.28E-87	1.06246983	0.671	0.331	2.08E-83	7	CCL4
GZMB1	0	1.05031402	0.766	0.061	0	7	GZMB
FGFBP21	0	0.81780412	0.662	0.035	0	7	FGFBP2
PRF11	0	0.80916105	0.722	0.088	0	7	PRF1
KLRD11	0	0.77857681	0.695	0.085	0	7	KLRD1
PTGDS	0	0.72709072	0.328	0.014	0	7	PTGDS
CST72	0	0.71277092	0.708	0.142	0	7	CST7
SPON2	0	0.68134009	0.567	0.035	0	7	SPON2
CD247	0	0.63158658	0.61	0.101	0	7	CD247
HLA-B1	5.97E-153	0.58439449	0.987	0.843	9.69E-149	7	HLA-B
ARL4C1	2.70E-148	0.55644904	0.617	0.217	4.39E-144	7	ARL4C
CCL52	1.97E-111	0.52928638	0.695	0.282	3.21E-107	7	CCL5
GZMA1	9.32E-139	0.48593511	0.677	0.233	1.51E-134	7	GZMA
KLRB12	8.36E-208	0.48531994	0.558	0.122	1.36E-203	7	KLRB1
KLRF1	0	0.47218913	0.423	0.017	0	7	KLRF1
CALM11	3.75E-78	0.47077911	0.741	0.458	6.09E-74	7	CALM1
HOPX	3.12E-262	0.47072407	0.481	0.078	5.07E-258	7	HOPX
MYL12A3	3.48E-75	0.45057976	0.732	0.449	5.65E-71	7	MYL12A
CD7	2.76E-184	0.44445365	0.46	0.099	4.48E-180	7	CD7
GZMH2	3.13E-136	0.41861059	0.523	0.152	5.09E-132	7	GZMH
CLIC3	4.31E-292	0.40235821	0.353	0.035	7.00E-288	7	CLIC3
CTSW	3.82E-229	0.38333531	0.413	0.064	6.21E-225	7	CTSW
AREG1	5.14E-78	0.3617966	0.39	0.128	8.35E-74	7	AREG

CMC1	1.73E-147	0.36157202	0.366	0.077	2.81E-143	7	CMC1
GZMM	5.73E-143	0.3606099	0.437	0.109	9.31E-139	7	GZMM
ABHD17A	1.60E-132	0.35965522	0.453	0.125	2.61E-128	7	ABHD17A
PLAC8	1.05E-120	0.35801598	0.432	0.122	1.70E-116	7	PLAC8
B2M2	1.23E-87	0.35381713	1	0.99	2.00E-83	7	B2M
HLA-A2	4.38E-65	0.34123206	0.942	0.792	7.11E-61	7	HLA-A
EFHD2	2.25E-76	0.31632591	0.425	0.161	3.65E-72	7	EFHD2
UBB	5.49E-43	0.31589137	0.578	0.354	8.92E-39	7	UBB
CCL32	1.41E-19	0.31254443	0.412	0.244	2.30E-15	7	CCL3
HCST1	8.16E-41	0.30642086	0.601	0.374	1.33E-36	7	HCST
IFITM2	8.14E-63	0.30013327	0.459	0.202	1.32E-58	7	IFITM2
HLA-E	6.87E-36	0.29764185	0.774	0.616	1.12E-31	7	HLA-E
IRF1	1.20E-65	0.28203526	0.375	0.139	1.95E-61	7	IRF1
PTPRC1	2.74E-37	0.28169182	0.725	0.53	4.46E-33	7	PTPRC
PTMA	5.02E-37	0.27952833	0.937	0.891	8.16E-33	7	PTMA
JUND	6.03E-31	0.27206882	0.521	0.333	9.80E-27	7	JUND
JAK1	1.97E-50	0.27049275	0.42	0.195	3.20E-46	7	JAK1
RAP1B	2.08E-41	0.26881379	0.426	0.221	3.39E-37	7	RAP1B
ID2	1.34E-30	0.2678292	0.55	0.344	2.17E-26	7	ID2
ARPC2	5.06E-25	0.2598036	0.605	0.452	8.22E-21	7	ARPC2
7-Sep	1.29E-37	0.25552578	0.503	0.291	2.09E-33	7	7-Sep
METRNL1	8.22E-57	0.25513998	0.356	0.138	1.33E-52	7	METRNL
HLA-DRA2	1.64E-220	1.18533566	0.982	0.482	2.66E-216	8	HLA-DRA
HLA-DPB12	2.15E-213	1.15017679	0.87	0.371	3.49E-209	8	HLA-DPB1
AREG2	7.71E-165	1.12820054	0.503	0.124	1.25E-160	8	AREG
HLA-DPA12	4.17E-189	1.01271736	0.917	0.425	6.77E-185	8	HLA-DPA1
HLA-DRB52	2.49E-219	0.81485895	0.777	0.24	4.05E-215	8	HLA-DRB5
FTH12	1.33E-153	0.79645543	0.997	0.917	2.17E-149	8	FTH1
CST32	2.62E-184	0.73162373	0.905	0.38	4.26E-180	8	CST3
LYZ1	6.69E-229	0.72583568	0.718	0.165	1.09E-224	8	LYZ
HLA-DQB12	7.65E-160	0.71709746	0.666	0.219	1.24E-155	8	HLA-DQB1
CD742	1.97E-121	0.70923362	0.945	0.575	3.20E-117	8	CD74
FN1	6.67E-163	0.68250492	0.312	0.045	1.08E-158	8	FN1
SAT13	6.34E-108	0.67192312	0.952	0.666	1.03E-103	8	SAT1
TIMP11	5.67E-107	0.61262289	0.475	0.144	9.21E-103	8	TIMP1
HLA-DQA11	3.57E-176	0.56498739	0.578	0.147	5.80E-172	8	HLA-DQA1
S100A61	1.84E-84	0.53103076	0.801	0.443	2.99E-80	8	S100A6
VIM1	1.89E-94	0.52595949	0.88	0.489	3.08E-90	8	VIM
CTSS1	2.52E-104	0.51783743	0.709	0.312	4.09E-100	8	CTSS
COTL11	1.34E-88	0.46611007	0.696	0.333	2.17E-84	8	COTL1

S100A112	1.13E-81	0.45979024	0.865	0.521	1.83E-77	8	S100A11
NAMPT1	2.01E-116	0.45115928	0.551	0.168	3.26E-112	8	NAMPT
LST1	9.17E-82	0.43641381	0.513	0.203	1.49E-77	8	LST1
AIF13	1.62E-81	0.42293473	0.784	0.382	2.63E-77	8	AIF1
TYMP1	3.28E-110	0.41377619	0.623	0.231	5.32E-106	8	TYMP
TYROBP4	1.74E-83	0.40758721	0.864	0.458	2.83E-79	8	TYROBP
S100A101	2.47E-59	0.40419019	0.631	0.325	4.02E-55	8	S100A10
THBS11	5.16E-80	0.38858308	0.301	0.075	8.39E-76	8	THBS1
FCN11	8.47E-98	0.3839735	0.362	0.089	1.38E-93	8	FCN1
IFITM3	1.96E-107	0.36811055	0.357	0.087	3.18E-103	8	IFITM3
HLA-DRB12	1.12E-48	0.36135695	0.606	0.299	1.82E-44	8	HLA-DRB1
C1orf1621	3.07E-91	0.34212166	0.54	0.198	4.99E-87	8	C1orf162
FGL21	1.38E-85	0.33344318	0.453	0.151	2.25E-81	8	FGL2
PSAP3	3.65E-50	0.32981827	0.654	0.357	5.93E-46	8	PSAP
NPC22	1.88E-60	0.32783227	0.674	0.341	3.06E-56	8	NPC2
CPVL1	2.53E-98	0.32612943	0.488	0.159	4.11E-94	8	CPVL
RGS21	5.40E-75	0.32427394	0.417	0.141	8.77E-71	8	RGS2
FTL3	7.08E-51	0.3213019	0.992	0.914	1.15E-46	8	FTL
SRGN2	8.28E-32	0.32010409	0.88	0.728	1.35E-27	8	SRGN
S100A43	1.16E-35	0.31978331	0.797	0.54	1.89E-31	8	S100A4
LGALS11	8.99E-48	0.31438954	0.593	0.31	1.46E-43	8	LGALS1
SAP30	6.71E-68	0.31019035	0.395	0.14	1.09E-63	8	SAP30
CD1631	9.92E-56	0.31015426	0.457	0.191	1.61E-51	8	CD163
HLA-DMA2	2.04E-76	0.30896643	0.538	0.212	3.32E-72	8	HLA-DMA
NEAT12	5.84E-37	0.3076252	0.957	0.828	9.48E-33	8	NEAT1
DUSP12	1.86E-35	0.30081277	0.718	0.473	3.03E-31	8	DUSP1
FCGR3A2	2.30E-40	0.29126836	0.447	0.216	3.74E-36	8	FCGR3A
HLA-DQA2	4.94E-130	0.28567388	0.292	0.05	8.03E-126	8	HLA-DQA2
H3F3A1	6.80E-39	0.2853035	0.9	0.727	1.11E-34	8	H3F3A
CEBPD3	1.62E-44	0.28498109	0.65	0.353	2.64E-40	8	CEBPD
CTSH	1.06E-79	0.27798533	0.414	0.136	1.73E-75	8	CTSH
GPR183	8.44E-50	0.27408273	0.306	0.11	1.37E-45	8	GPR183
SERPINA1	4.20E-90	0.26764156	0.38	0.107	6.83E-86	8	SERPINA1
CFD1	7.99E-69	0.26556918	0.324	0.098	1.30E-64	8	CFD
ANXA21	2.27E-47	0.26211262	0.429	0.191	3.68E-43	8	ANXA2
CLEC7A	1.97E-68	0.25714805	0.453	0.169	3.20E-64	8	CLEC7A
AP1S21	5.91E-74	0.25514129	0.346	0.105	9.60E-70	8	AP1S2
NAP1L1	1.87E-25	0.25432625	0.43	0.259	3.05E-21	8	NAP1L1
RGS12	1.24E-14	0.2509235	0.467	0.325	2.02E-10	8	RGS1
MT-ATP61	6.43E-185	0.7491008	1	0.997	1.05E-180	9	MT-ATP6

SYNE2	9.10E-152	0.74356836	0.558	0.138	1.48E-147	9	SYNE2
MT-CYB	1.41E-146	0.70747523	1	0.991	2.29E-142	9	MT-CYB
MT-ND31	3.45E-132	0.68922111	1	0.986	5.61E-128	9	MT-ND3
MT-CO2	7.24E-151	0.63941212	1	0.993	1.18E-146	9	MT-CO2
MALAT1	4.72E-179	0.63501704	1	0.991	7.67E-175	9	MALAT1
IL7R2	1.74E-71	0.62596237	0.477	0.161	2.83E-67	9	IL7R
PTPRC2	3.75E-51	0.61534481	0.692	0.536	6.09E-47	9	PTPRC
MT-CO3	2.62E-138	0.60825209	1	0.996	4.25E-134	9	MT-CO3
MT-CO12	7.80E-121	0.60470951	1	0.994	1.27E-116	9	MT-CO1
RNF213	2.14E-47	0.575415	0.492	0.259	3.47E-43	9	RNF213
ZFP36L2	1.09E-33	0.56570899	0.623	0.493	1.77E-29	9	ZFP36L2
ETS1	5.17E-102	0.56395	0.453	0.124	8.41E-98	9	ETS1
TXNIP2	3.21E-40	0.54795276	0.757	0.541	5.21E-36	9	TXNIP
MT-ND5	5.27E-62	0.53844881	0.983	0.812	8.57E-58	9	MT-ND5
KIAA1551	1.08E-49	0.53281834	0.439	0.199	1.75E-45	9	KIAA1551
MT-ND11	4.40E-87	0.52549705	1	0.987	7.15E-83	9	MT-ND1
IKZF1	5.43E-61	0.52319478	0.492	0.218	8.82E-57	9	IKZF1
NKTR	9.65E-49	0.51762113	0.444	0.206	1.57E-44	9	NKTR
SMCHD1	1.44E-54	0.50087631	0.401	0.154	2.34E-50	9	SMCHD1
DDX17	9.56E-32	0.49509494	0.506	0.345	1.55E-27	9	DDX17
EML4	7.49E-70	0.45721017	0.344	0.096	1.22E-65	9	EML4
MACF1	1.85E-31	0.44664634	0.368	0.187	3.01E-27	9	MACF1
MT-ND4	2.76E-66	0.41195753	1	0.991	4.48E-62	9	MT-ND4
SYTL3	9.17E-36	0.38283052	0.315	0.127	1.49E-31	9	SYTL3
FYN	4.97E-40	0.37772444	0.317	0.121	8.08E-36	9	FYN
PIK3R1	2.54E-21	0.37745967	0.351	0.206	4.12E-17	9	PIK3R1
CEMIP2	1.72E-41	0.37034877	0.279	0.093	2.80E-37	9	CEMIP2
CNOT6L	8.52E-42	0.36984282	0.286	0.098	1.38E-37	9	CNOT6L
UTRN	1.36E-31	0.36887459	0.322	0.145	2.21E-27	9	UTRN
STK4	3.06E-19	0.36213136	0.403	0.277	4.97E-15	9	STK4
PRDM1	3.70E-33	0.36007284	0.303	0.126	6.01E-29	9	PRDM1
AKAP9	3.08E-20	0.35776154	0.329	0.191	5.00E-16	9	AKAP9
MT-ND2	5.36E-37	0.35512444	0.998	0.925	8.71E-33	9	MT-ND2
AHNAK1	2.25E-24	0.34460971	0.313	0.158	3.66E-20	9	AHNAK
ARAP2	1.50E-48	0.33962306	0.251	0.07	2.44E-44	9	ARAP2
PRRC2C	2.76E-16	0.33571947	0.403	0.298	4.48E-12	9	PRRC2C
PARP8	7.82E-42	0.33329141	0.286	0.097	1.27E-37	9	PARP8
AKNA	4.77E-27	0.33239736	0.301	0.139	7.75E-23	9	AKNA
PCSK7	5.09E-21	0.32412247	0.313	0.171	8.28E-17	9	PCSK7
N4BP2L2	3.82E-16	0.32290565	0.418	0.307	6.21E-12	9	N4BP2L2

ARGLU1	7.18E-19	0.32088505	0.389	0.257	1.17E-14	9	ARGLU1
RORA	2.37E-34	0.30505714	0.253	0.087	3.85E-30	9	RORA
AAK1	3.23E-23	0.30404947	0.286	0.137	5.24E-19	9	AAK1
TSC22D3	1.15E-08	0.30069428	0.43	0.383	0.00018617	9	TSC22D3
PPP2R5C1	9.64E-19	0.29257433	0.322	0.181	1.57E-14	9	PPP2R5C
CELF2	3.92E-07	0.28896646	0.356	0.312	0.00636269	9	CELF2
SLFN5	7.75E-24	0.28189431	0.258	0.112	1.26E-19	9	SLFN5
ATM	9.51E-11	0.281471	0.303	0.215	1.54E-06	9	ATM
TNRC6B	5.18E-12	0.2687975	0.258	0.157	8.42E-08	9	TNRC6B
MBNL1	7.28E-12	0.26798957	0.317	0.223	1.18E-07	9	MBNL1
ANKRD12	2.50E-07	0.26768992	0.315	0.256	0.00406669	9	ANKRD12
PRMT2	2.98E-08	0.26642654	0.284	0.211	0.00048405	9	PRMT2
MYH9	1.25E-10	0.26509031	0.282	0.19	2.02E-06	9	MYH9
CXCR4	8.93E-08	0.26037546	0.372	0.307	0.00145102	9	CXCR4
ACAP11	3.92E-14	0.25969341	0.27	0.153	6.37E-10	9	ACAP1
LUC7L3	5.59E-09	0.25756562	0.327	0.25	9.09E-05	9	LUC7L3
SF1	6.30E-08	0.25043393	0.294	0.226	0.0010241	9	SF1
SPP12	7.33E-236	1.7097027	0.934	0.297	1.19E-231	10	SPP1
FN11	0	1.48787867	0.596	0.04	0	10	FN1
VIM2	1.35E-153	1.13644797	0.917	0.494	2.20E-149	10	VIM
FTL4	1.81E-74	1.10064383	0.99	0.915	2.94E-70	10	FTL
PLIN2	6.37E-238	1.07617998	0.591	0.096	1.04E-233	10	PLIN2
RNASE11	1.55E-298	1.07392732	0.601	0.076	2.53E-294	10	RNASE1
LGALS12	9.22E-158	1.06442432	0.808	0.307	1.50E-153	10	LGALS1
FTH13	1.12E-73	1.0201996	0.99	0.918	1.82E-69	10	FTH1
NEAT13	1.97E-66	0.91202803	0.961	0.83	3.20E-62	10	NEAT1
GAPDH1	4.96E-108	0.87337682	0.927	0.678	8.06E-104	10	GAPDH
TGFBI	0	0.8720827	0.655	0.089	0	10	TGFBI
HMOX11	5.00E-105	0.86007325	0.474	0.124	8.13E-101	10	HMOX1
VCAN1	7.13E-213	0.82552734	0.689	0.123	1.16E-208	10	VCAN
MT2A1	5.83E-22	0.77844919	0.394	0.212	9.47E-18	10	MT2A
S100A102	6.67E-116	0.77501297	0.776	0.325	1.08E-111	10	S100A10
GLUL2	6.09E-107	0.72573563	0.723	0.279	9.90E-103	10	GLUL
ENO1	4.19E-122	0.66540956	0.71	0.263	6.80E-118	10	ENO1
CTSB2	2.39E-83	0.64298685	0.759	0.353	3.88E-79	10	CTSB
SAT14	1.10E-65	0.63429015	0.951	0.671	1.78E-61	10	SAT1
LDHA	6.47E-99	0.59074874	0.698	0.28	1.05E-94	10	LDHA
CTSD1	2.48E-74	0.57891904	0.596	0.24	4.03E-70	10	CTSD
SLC11A13	2.20E-86	0.57503509	0.679	0.266	3.58E-82	10	SLC11A1
RGS13	8.59E-74	0.57443532	0.72	0.318	1.40E-69	10	RGS1

CD1632	2.54E-106	0.56679921	0.611	0.19	4.13E-102	10	CD163
CSTB	2.87E-52	0.54399127	0.499	0.216	4.66E-48	10	CSTB
SLC2A31	1.32E-60	0.53431268	0.543	0.209	2.14E-56	10	SLC2A3
VEGFA1	1.92E-219	0.52131598	0.467	0.058	3.12E-215	10	VEGFA
SLC16A10	0	0.52067502	0.433	0.026	0	10	SLC16A10
ANXA22	1.69E-98	0.51694577	0.579	0.189	2.74E-94	10	ANXA2
PKM	1.17E-120	0.49742422	0.608	0.178	1.89E-116	10	PKM
GNPMB	1.50E-270	0.49544255	0.399	0.033	2.44E-266	10	GNPMB
ACTB1	8.82E-27	0.48839014	0.856	0.858	1.43E-22	10	ACTB
FCGBP2	9.02E-46	0.48280421	0.426	0.16	1.47E-41	10	FCGBP
PGK1	3.36E-76	0.4668784	0.572	0.22	5.45E-72	10	PGK1
AREG3	4.69E-28	0.46659914	0.326	0.137	7.61E-24	10	AREG
TPI1	3.00E-87	0.4595455	0.628	0.236	4.87E-83	10	TPI1
S100A113	1.42E-49	0.45699776	0.8	0.529	2.30E-45	10	S100A11
ZFP36L12	5.92E-45	0.45298683	0.652	0.343	9.61E-41	10	ZFP36L1
CTSL	2.91E-78	0.44121238	0.367	0.092	4.73E-74	10	CTSL
CLEC5A	1.45E-167	0.43930165	0.457	0.072	2.35E-163	10	CLEC5A
ALOX5AP2	6.90E-30	0.40301822	0.509	0.281	1.12E-25	10	ALOX5AP
LAPTM51	9.35E-44	0.39535588	0.754	0.464	1.52E-39	10	LAPTM5
TYMP2	1.23E-61	0.38695059	0.586	0.239	2.00E-57	10	TYMP
ADM	1.01E-211	0.38173577	0.277	0.019	1.64E-207	10	ADM
BNIP3L	4.71E-80	0.37472886	0.421	0.116	7.65E-76	10	BNIP3L
FABP5	3.06E-84	0.36934917	0.348	0.077	4.97E-80	10	FABP5
THBS12	6.58E-34	0.35414019	0.253	0.081	1.07E-29	10	THBS1
SLC25A372	9.38E-33	0.34945695	0.375	0.163	1.52E-28	10	SLC25A37
YBX1	2.61E-32	0.3432843	0.667	0.42	4.25E-28	10	YBX1
ASPH	4.10E-123	0.34327024	0.338	0.053	6.66E-119	10	ASPH
WSB1	2.47E-30	0.33988044	0.457	0.233	4.02E-26	10	WSB1
STAB1	6.42E-58	0.3396198	0.37	0.115	1.04E-53	10	STAB1
C5AR2	4.83E-178	0.3393707	0.258	0.02	7.85E-174	10	C5AR2
CD144	2.23E-29	0.33896077	0.601	0.321	3.62E-25	10	CD14
HK2	4.37E-123	0.33142877	0.265	0.033	7.11E-119	10	HK2
ZEB21	6.03E-37	0.32433538	0.516	0.247	9.81E-33	10	ZEB2
METRNL2	4.40E-67	0.31775551	0.448	0.14	7.15E-63	10	METRNL
ANKH	2.78E-128	0.31586851	0.328	0.048	4.51E-124	10	ANKH
BCAT1	3.70E-203	0.31207228	0.355	0.035	6.01E-199	10	BCAT1
LMNA	4.38E-176	0.31117082	0.268	0.022	7.11E-172	10	LMNA
DDIT4	7.30E-16	0.30947203	0.509	0.341	1.19E-11	10	DDIT4
LIMS1	3.28E-38	0.30781973	0.484	0.223	5.34E-34	10	LIMS1
ABCA1	1.29E-93	0.3052376	0.304	0.055	2.10E-89	10	ABCA1

S100A62	4.81E-26	0.30467143	0.698	0.453	7.81E-22	10	S100A6
NDRG1	4.84E-77	0.29746444	0.28	0.055	7.86E-73	10	NDRG1
FNDC3B	5.44E-102	0.295503	0.314	0.054	8.84E-98	10	FNDC3B
HIF1A1	6.11E-37	0.2934551	0.377	0.151	9.93E-33	10	HIF1A
ANXA5	5.53E-42	0.29198095	0.516	0.237	8.98E-38	10	ANXA5
GRB2	2.02E-47	0.28930654	0.489	0.204	3.28E-43	10	GRB2
GRN2	1.11E-36	0.28466468	0.509	0.241	1.81E-32	10	GRN
RPLP0	8.01E-23	0.28432068	0.754	0.612	1.30E-18	10	RPLP0
GSTO1	5.60E-48	0.28111037	0.477	0.191	9.11E-44	10	GSTO1
GPR1831	1.99E-44	0.28029956	0.336	0.113	3.23E-40	10	GPR183
SLC16A3	1.07E-63	0.27875765	0.394	0.117	1.74E-59	10	SLC16A3
ADAM8	1.29E-96	0.27799919	0.253	0.038	2.10E-92	10	ADAM8
GSN2	1.22E-33	0.27622882	0.436	0.198	1.98E-29	10	GSN
BNIP3	5.72E-196	0.2758417	0.268	0.02	9.29E-192	10	BNIP3
ERO1A	5.33E-100	0.27477978	0.302	0.051	8.66E-96	10	ERO1A
MT-ND51	1.02E-10	0.27454414	0.847	0.818	1.66E-06	10	MT-ND5
THBD1	5.14E-81	0.27048094	0.29	0.055	8.35E-77	10	THBD
PLAUR1	1.23E-46	0.26383248	0.375	0.126	2.00E-42	10	PLAUR
ZFP362	7.29E-20	0.26221207	0.513	0.315	1.18E-15	10	ZFP36
MSR11	1.82E-56	0.26062193	0.35	0.102	2.95E-52	10	MSR1
LGALS31	3.41E-28	0.25876359	0.29	0.115	5.55E-24	10	LGALS3
ELL2	1.92E-68	0.25443549	0.285	0.062	3.12E-64	10	ELL2
P4HB	1.09E-43	0.25389429	0.389	0.145	1.78E-39	10	P4HB
CCDC88A	1.47E-32	0.25329425	0.389	0.17	2.38E-28	10	CCDC88A
FCGR2B	2.38E-140	0.25144149	0.255	0.026	3.87E-136	10	FCGR2B
SDCBP1	1.04E-35	0.25112209	0.443	0.196	1.69E-31	10	SDCBP
IGKC	0	1.61735356	0.564	0.007	0	11	IGKC
IGHM	0	0.98154153	0.538	0.001	0	11	IGHM
RPS273	7.88E-87	0.84904204	1	0.931	1.28E-82	11	RPS27
RPS181	1.81E-73	0.70324964	1	0.982	2.94E-69	11	RPS18
RPS81	1.68E-79	0.69843901	1	0.933	2.72E-75	11	RPS8
RPL13A1	5.81E-70	0.6930171	1	0.905	9.44E-66	11	RPL13A
RPL18A1	4.59E-69	0.69094203	0.996	0.931	7.45E-65	11	RPL18A
CD37	4.03E-80	0.67977641	0.742	0.253	6.55E-76	11	CD37
MS4A1	0	0.67245466	0.542	0.005	0	11	MS4A1
RPS51	4.09E-59	0.66000401	0.942	0.729	6.65E-55	11	RPS5
RPS231	2.61E-75	0.64016164	0.996	0.963	4.24E-71	11	RPS23
RPL211	1.22E-65	0.6195189	0.996	0.909	1.98E-61	11	RPL21
LTB1	3.10E-94	0.61007436	0.591	0.128	5.04E-90	11	LTB
RPL342	4.55E-63	0.60307841	1	0.93	7.40E-59	11	RPL34

RPL302	5.38E-59	0.59929039	0.987	0.936	8.75E-55	11	RPL30
RPS212	2.20E-55	0.5925992	0.938	0.703	3.57E-51	11	RPS21
RPS122	1.84E-57	0.59185645	1	0.968	2.99E-53	11	RPS12
RPL111	3.28E-60	0.58504504	0.996	0.95	5.33E-56	11	RPL11
RPL391	1.38E-53	0.58156205	0.987	0.935	2.24E-49	11	RPL39
RPL321	7.33E-60	0.57507877	1	0.957	1.19E-55	11	RPL32
RPL371	3.32E-54	0.5638394	0.987	0.902	5.39E-50	11	RPL37
RPS11	5.37E-51	0.56104946	0.956	0.816	8.73E-47	11	RPS11
RPS293	5.48E-39	0.55540534	0.889	0.695	8.90E-35	11	RPS29
RPS101	2.83E-37	0.54590677	0.853	0.593	4.59E-33	11	RPS10
RPLP22	1.46E-50	0.53897702	0.987	0.905	2.38E-46	11	RPLP2
RPL33	2.94E-53	0.53489805	1	0.93	4.77E-49	11	RPL3
RPL181	1.09E-51	0.53317067	0.982	0.911	1.77E-47	11	RPL18
RPSA2	1.46E-41	0.52710003	0.933	0.731	2.37E-37	11	RPSA
RPS27A3	3.67E-52	0.52456365	1	0.952	5.96E-48	11	RPS27A
RPL132	1.03E-60	0.52383159	1	0.99	1.68E-56	11	RPL13
RPS3A1	3.08E-55	0.51522298	0.996	0.948	5.01E-51	11	RPS3A
RPL23A3	3.58E-46	0.51373171	0.996	0.891	5.83E-42	11	RPL23A
TXNIP3	8.96E-27	0.51307399	0.818	0.543	1.46E-22	11	TXNIP
RPL191	4.51E-50	0.50935516	0.996	0.957	7.33E-46	11	RPL19
RPL412	2.59E-52	0.50528686	1	0.975	4.22E-48	11	RPL41
RPS282	2.76E-39	0.5027996	0.987	0.858	4.49E-35	11	RPS28
RPS61	1.18E-45	0.4988879	0.996	0.919	1.91E-41	11	RPS6
RPL10A2	1.66E-38	0.49540398	0.942	0.788	2.69E-34	11	RPL10A
EEF1B2	1.17E-37	0.49414704	0.898	0.668	1.90E-33	11	EEF1B2
RPL361	2.25E-32	0.48911106	0.902	0.753	3.65E-28	11	RPL36
RPL121	3.14E-43	0.47968246	0.996	0.902	5.10E-39	11	RPL12
RPS161	2.58E-46	0.47686204	0.987	0.91	4.19E-42	11	RPS16
RPS72	5.25E-38	0.47564412	0.978	0.883	8.52E-34	11	RPS7
RPL35A2	1.38E-39	0.47315609	0.96	0.837	2.24E-35	11	RPL35A
RPS131	4.29E-40	0.46697145	0.969	0.893	6.98E-36	11	RPS13
RPL91	1.91E-41	0.46632951	0.978	0.935	3.10E-37	11	RPL9
RPL103	4.72E-43	0.46441274	1	0.979	7.67E-39	11	RPL10
RPS20	4.40E-35	0.46151511	0.871	0.636	7.16E-31	11	RPS20
RPS192	9.31E-38	0.46105578	0.996	0.968	1.51E-33	11	RPS19
CD522	1.96E-37	0.4599784	0.689	0.303	3.19E-33	11	CD52
RPL81	7.48E-31	0.45844988	0.929	0.848	1.22E-26	11	RPL8
CD79A	0	0.45822377	0.458	0.001	0	11	CD79A
CD79B	5.01E-262	0.44520287	0.382	0.018	8.14E-258	11	CD79B
RPS152	2.21E-40	0.43934972	0.987	0.924	3.59E-36	11	RPS15

RPL51	3.54E-31	0.43918954	0.924	0.79	5.76E-27	11	RPL5
RALGPS2	2.29E-291	0.43856882	0.364	0.014	3.73E-287	11	RALGPS2
RPL27A	2.88E-27	0.41730725	0.929	0.791	4.67E-23	11	RPL27A
RPL35	1.83E-26	0.41454402	0.902	0.827	2.98E-22	11	RPL35
RPS22	5.38E-38	0.41280365	0.996	0.979	8.74E-34	11	RPS2
RPS143	1.77E-36	0.4111592	1	0.972	2.88E-32	11	RPS14
BANK1	0	0.41050765	0.396	0.002	0	11	BANK1
RPL291	1.06E-29	0.40784568	0.978	0.904	1.72E-25	11	RPL29
RPL22	9.37E-24	0.40690075	0.853	0.701	1.52E-19	11	RPL22
EEF1A11	4.78E-40	0.40383275	1	0.991	7.77E-36	11	EEF1A1
RPS252	2.61E-33	0.40031142	0.964	0.857	4.23E-29	11	RPS25
RPL37A	1.28E-27	0.39586768	0.929	0.846	2.08E-23	11	RPL37A
RPL7A2	6.28E-36	0.39350155	0.982	0.921	1.02E-31	11	RPL7A
RPL261	6.89E-32	0.38688491	0.982	0.936	1.12E-27	11	RPL26
RPS15A3	6.14E-30	0.38584666	0.996	0.936	9.97E-26	11	RPS15A
RPS33	6.82E-30	0.38358183	0.982	0.924	1.11E-25	11	RPS3
FAU2	4.60E-29	0.3757063	0.987	0.916	7.48E-25	11	FAU
RPS4X2	5.18E-30	0.37239541	0.978	0.866	8.42E-26	11	RPS4X
TNFRSF13C	1.53E-291	0.36553672	0.32	0.01	2.49E-287	11	TNFRSF13C
RPLP11	2.62E-27	0.35221416	1	0.988	4.26E-23	11	RPLP1
RPLP01	8.29E-20	0.34953108	0.809	0.613	1.35E-15	11	RPLP0
NOP53	8.69E-25	0.3452136	0.564	0.286	1.41E-20	11	NOP53
RPS91	1.75E-24	0.33615536	0.973	0.884	2.84E-20	11	RPS9
RPL142	3.51E-24	0.33475427	0.956	0.856	5.71E-20	11	RPL14
RPL15	2.65E-20	0.32870611	0.96	0.909	4.31E-16	11	RPL15
PTMA1	2.31E-20	0.32026676	0.964	0.893	3.76E-16	11	PTMA
RPL271	3.45E-20	0.31998519	0.871	0.686	5.61E-16	11	RPL27
HLA-DRA3	8.22E-38	0.30850079	0.973	0.498	1.33E-33	11	HLA-DRA
BTG12	2.61E-14	0.30565296	0.858	0.687	4.23E-10	11	BTG1
RPL311	5.45E-16	0.29350817	0.64	0.426	8.85E-12	11	RPL31
RPL38	6.09E-15	0.28539163	0.773	0.565	9.89E-11	11	RPL38
RPL4	1.81E-12	0.28183064	0.724	0.57	2.94E-08	11	RPL4
RPL61	5.79E-17	0.28149485	0.942	0.863	9.41E-13	11	RPL6
ISG201	2.27E-21	0.28077297	0.396	0.162	3.69E-17	11	ISG20
PFDN5	5.64E-13	0.27527504	0.76	0.585	9.17E-09	11	PFDN5
JUND1	1.42E-09	0.27382421	0.498	0.341	2.31E-05	11	JUND
RACK1	1.24E-13	0.27036121	0.836	0.7	2.01E-09	11	RACK1
HLA-DPB13	1.01E-24	0.26531785	0.764	0.39	1.64E-20	11	HLA-DPB1
RPL241	1.07E-15	0.26370804	0.884	0.789	1.75E-11	11	RPL24
NACA	3.50E-13	0.25707442	0.929	0.841	5.69E-09	11	NACA

TOMM71	4.80E-10	0.25246745	0.622	0.447	7.80E-06	11	TOMM7
CCL42	2.36E-163	1.88328547	1	0.339	3.83E-159	12	CCL4
CCL4L21	1.22E-81	1.26562377	0.649	0.17	1.98E-77	12	CCL4L2
IFNG	0	0.96808128	0.401	0.016	0	12	IFNG
CCL53	6.31E-89	0.85774277	0.892	0.295	1.03E-84	12	CCL5
CD69	3.09E-88	0.78265281	0.698	0.202	5.02E-84	12	CD69
GZMA2	7.04E-75	0.7200059	0.766	0.25	1.14E-70	12	GZMA
GZMK2	2.65E-90	0.63043347	0.626	0.14	4.30E-86	12	GZMK
XCL2	5.64E-71	0.55585265	0.288	0.04	9.17E-67	12	XCL2
CD3D2	1.93E-68	0.55264344	0.685	0.21	3.14E-64	12	CD3D
HLA-C2	7.41E-45	0.53874203	0.941	0.681	1.20E-40	12	HLA-C
TNF1	3.24E-45	0.53867642	0.293	0.062	5.27E-41	12	TNF
CD22	1.76E-58	0.49642969	0.658	0.214	2.86E-54	12	CD2
CD523	1.69E-37	0.46839769	0.685	0.303	2.75E-33	12	CD52
DUSP2	1.20E-46	0.44637607	0.41	0.11	1.95E-42	12	DUSP2
GZMH3	1.92E-40	0.41471441	0.509	0.168	3.11E-36	12	GZMH
IL322	3.37E-34	0.39226258	0.55	0.21	5.48E-30	12	IL32
RPL282	3.04E-33	0.3911254	0.995	0.953	4.94E-29	12	RPL28
TRAC2	1.58E-47	0.38817408	0.527	0.16	2.57E-43	12	TRAC
CCL33	6.70E-14	0.37079012	0.477	0.25	1.09E-09	12	CCL3
HLA-A3	1.38E-18	0.33940713	0.941	0.799	2.24E-14	12	HLA-A
RPS253	8.78E-22	0.33362314	0.968	0.857	1.43E-17	12	RPS25
RPS262	1.35E-19	0.33242929	0.721	0.459	2.20E-15	12	RPS26
RPS34	1.23E-25	0.33238773	0.995	0.923	2.00E-21	12	RPS3
CD8A1	7.57E-54	0.32895226	0.387	0.085	1.23E-49	12	CD8A
RPS15A4	2.43E-23	0.32793264	0.995	0.936	3.95E-19	12	RPS15A
CD8B1	2.43E-47	0.32639751	0.306	0.063	3.94E-43	12	CD8B
RPL413	2.72E-26	0.32407868	0.995	0.975	4.42E-22	12	RPL41
B2M3	7.95E-28	0.32265381	1	0.991	1.29E-23	12	B2M
RPS274	1.29E-21	0.31568807	0.995	0.931	2.10E-17	12	RPS27
MYL12A4	3.06E-15	0.31303207	0.689	0.462	4.97E-11	12	MYL12A
TRBC22	4.09E-29	0.31275567	0.428	0.153	6.64E-25	12	TRBC2
BTG13	3.80E-17	0.31262023	0.883	0.686	6.18E-13	12	BTG1
CST73	1.55E-27	0.29677049	0.455	0.171	2.51E-23	12	CST7
ID21	3.90E-13	0.29006359	0.568	0.353	6.34E-09	12	ID2
CXCR41	2.69E-15	0.2876243	0.536	0.305	4.36E-11	12	CXCR4
RARRES32	2.02E-18	0.28097978	0.428	0.198	3.28E-14	12	RARRES3
CXCR61	1.17E-39	0.27964871	0.288	0.064	1.91E-35	12	CXCR6
RPL23A4	5.94E-17	0.27570457	0.973	0.892	9.65E-13	12	RPL23A
RPS123	1.71E-18	0.27216267	0.995	0.968	2.78E-14	12	RPS12

GIMAP72	1.75E-17	0.26928264	0.432	0.204	2.84E-13	12	GIMAP7
TMSB4X2	8.24E-17	0.26515662	1	0.993	1.34E-12	12	TMSB4X
SH3BGRL32	1.38E-11	0.26348716	0.748	0.601	2.25E-07	12	SH3BGRL3
CALM12	3.82E-13	0.25871161	0.685	0.471	6.21E-09	12	CALM1
HSPA1A1	3.41E-293	2.44055612	1	0.161	5.54E-289	13	HSPA1A
HSP90AA1	7.14E-135	2.1141961	0.995	0.558	1.16E-130	13	HSP90AA1
S100A91	3.24E-123	1.7177535	0.778	0.171	5.26E-119	13	S100A9
HSPH1	0	1.50170948	0.865	0.061	0	13	HSPH1
S100A81	2.05E-110	1.47308074	0.681	0.141	3.34E-106	13	S100A8
HSPA1B1	0	1.43642328	0.918	0.092	0	13	HSPA1B
DNAJB1	0	1.33561073	0.874	0.089	0	13	DNAJB1
HSPA6	0	1.30174897	0.614	0.028	0	13	HSPA6
LYZ2	5.79E-89	1.10585065	0.705	0.184	9.40E-85	13	LYZ
NEAT14	2.21E-70	1.01148575	0.995	0.832	3.59E-66	13	NEAT1
HSPD1	4.13E-106	0.93968533	0.647	0.141	6.71E-102	13	HSPD1
VCAN2	9.57E-120	0.91459515	0.71	0.133	1.56E-115	13	VCAN
TIMP12	7.20E-47	0.8224024	0.512	0.155	1.17E-42	13	TIMP1
S100A121	1.17E-116	0.75783113	0.488	0.067	1.91E-112	13	S100A12
S100A63	7.57E-53	0.74747406	0.855	0.455	1.23E-48	13	S100A6
UBC	6.00E-31	0.73535122	0.874	0.688	9.75E-27	13	UBC
HSPE1	2.12E-79	0.72275875	0.614	0.16	3.44E-75	13	HSPE1
FCN12	2.17E-132	0.71560235	0.618	0.094	3.53E-128	13	FCN1
HSP90AB1	1.97E-48	0.69980788	0.787	0.378	3.20E-44	13	HSP90AB1
HSPB1	8.52E-78	0.66698963	0.444	0.083	1.38E-73	13	HSPB1
CTSS2	2.52E-42	0.65915232	0.696	0.326	4.09E-38	13	CTSS
VIM3	7.26E-46	0.65696285	0.865	0.502	1.18E-41	13	VIM
SLC2A32	2.23E-58	0.64118388	0.652	0.213	3.62E-54	13	SLC2A3
BAG3	0	0.62947529	0.42	0.011	0	13	BAG3
NAMPT2	9.37E-81	0.60955369	0.705	0.178	1.52E-76	13	NAMPT
PLAUR2	3.68E-85	0.59507485	0.589	0.127	5.98E-81	13	PLAUR
IER5	8.79E-56	0.59349818	0.531	0.152	1.43E-51	13	IER5
NR4A11	6.20E-108	0.57658821	0.575	0.101	1.01E-103	13	NR4A1
LGALS13	4.34E-51	0.56946958	0.792	0.316	7.04E-47	13	LGALS1
COTL12	3.33E-54	0.54158376	0.812	0.343	5.41E-50	13	COTL1
SOCS31	1.55E-83	0.53290234	0.527	0.103	2.53E-79	13	SOCS3
FTH14	5.48E-25	0.51791686	0.995	0.92	8.90E-21	13	FTH1
SOD21	2.19E-64	0.49744202	0.464	0.103	3.56E-60	13	SOD2
CD441	8.59E-44	0.4833548	0.56	0.189	1.40E-39	13	CD44
S100A103	2.34E-40	0.47334057	0.754	0.334	3.80E-36	13	S100A10
ATP13A31	5.77E-64	0.46504171	0.444	0.095	9.38E-60	13	ATP13A3

ACTB2	5.80E-27	0.46283162	0.976	0.856	9.42E-23	13	ACTB
HMOX12	5.55E-37	0.45072243	0.425	0.131	9.02E-33	13	HMOX1
VMP11	2.06E-32	0.44716504	0.541	0.219	3.35E-28	13	VMP1
DNAJA1	2.89E-52	0.44593403	0.536	0.158	4.70E-48	13	DNAJA1
S100A44	5.56E-24	0.44109557	0.831	0.548	9.03E-20	13	S100A4
GADD45B1	5.22E-43	0.42975194	0.478	0.146	8.48E-39	13	GADD45B
EREG1	2.72E-40	0.42081748	0.329	0.074	4.42E-36	13	EREG
ANXA11	2.52E-24	0.41653476	0.565	0.269	4.10E-20	13	ANXA1
RGS22	2.76E-28	0.40782942	0.42	0.151	4.48E-24	13	RGS2
HSPA5	3.57E-18	0.4058734	0.415	0.192	5.81E-14	13	HSPA5
IL1B1	6.26E-50	0.40224446	0.372	0.079	1.02E-45	13	IL1B
BCL2A11	1.77E-69	0.40064132	0.425	0.081	2.88E-65	13	BCL2A1
ATP2B11	1.42E-32	0.39803121	0.411	0.133	2.31E-28	13	ATP2B1
MNDA1	4.09E-32	0.3936263	0.493	0.183	6.65E-28	13	MNDA
NCF21	7.68E-80	0.39330089	0.469	0.087	1.25E-75	13	NCF2
ZNF331	2.53E-28	0.39096173	0.338	0.105	4.11E-24	13	ZNF331
CXCL81	1.18E-21	0.38882434	0.271	0.084	1.92E-17	13	CXCL8
PABPC11	8.98E-25	0.38461642	0.792	0.484	1.46E-20	13	PABPC1
GAPDH2	4.15E-18	0.3816161	0.87	0.684	6.74E-14	13	GAPDH
TKT1	9.29E-38	0.36820992	0.488	0.162	1.51E-33	13	TKT
CD551	1.22E-34	0.36760439	0.415	0.127	1.98E-30	13	CD55
FTL5	1.03E-23	0.36690776	0.995	0.916	1.68E-19	13	FTL
SRGN3	1.27E-11	0.34136375	0.85	0.734	2.07E-07	13	SRGN
PLBD11	1.49E-58	0.32738213	0.362	0.069	2.42E-54	13	PLBD1
THBD2	1.57E-45	0.32474037	0.3	0.059	2.54E-41	13	THBD
MCL11	2.79E-14	0.31593718	0.599	0.365	4.53E-10	13	MCL1
ANXA23	2.04E-29	0.31178987	0.512	0.197	3.31E-25	13	ANXA2
ENO11	1.29E-18	0.30958636	0.531	0.274	2.09E-14	13	ENO1
FCGR2A1	1.56E-26	0.30552075	0.449	0.172	2.54E-22	13	FCGR2A
ZEB22	8.71E-20	0.3048902	0.522	0.252	1.42E-15	13	ZEB2
CSTA1	6.98E-51	0.30161565	0.382	0.084	1.13E-46	13	CSTA
PLEK1	3.17E-20	0.30082253	0.377	0.147	5.14E-16	13	PLEK
TYMP3	8.17E-24	0.29636693	0.556	0.246	1.33E-19	13	TYMP
AP1S22	2.70E-38	0.28921253	0.401	0.112	4.39E-34	13	AP1S2
TPI11	1.69E-15	0.28329203	0.469	0.246	2.75E-11	13	TPI1
FGD4	1.28E-27	0.28105618	0.324	0.098	2.09E-23	13	FGD4
FOSL21	4.21E-40	0.28022863	0.367	0.093	6.85E-36	13	FOSL2
LCP11	3.87E-19	0.28000749	0.57	0.288	6.28E-15	13	LCP1
GK1	1.74E-36	0.27965552	0.304	0.072	2.82E-32	13	GK
HSPA8	1.09E-15	0.2788985	0.512	0.279	1.77E-11	13	HSPA8

FLNA1	3.30E-28	0.27842135	0.401	0.136	5.36E-24	13	FLNA
IFI30	3.59E-38	0.278086	0.275	0.059	5.83E-34	13	IFI30
TSPO1	3.88E-19	0.27724744	0.633	0.344	6.31E-15	13	TSPO
GLUL3	1.43E-09	0.2731327	0.469	0.292	2.32E-05	13	GLUL
EVI2B1	1.07E-19	0.2731073	0.425	0.188	1.73E-15	13	EVI2B
MAP3K2	2.78E-27	0.27105799	0.377	0.126	4.52E-23	13	MAP3K2
PPIF1	5.39E-34	0.27011016	0.28	0.066	8.76E-30	13	PPIF
ZFAND2A	7.96E-80	0.26932496	0.261	0.028	1.29E-75	13	ZFAND2A
JMJD1C	2.95E-22	0.26813038	0.401	0.158	4.79E-18	13	JMJD1C
LDHA1	6.35E-08	0.26790078	0.435	0.292	0.00103137	13	LDHA
CFP1	8.46E-73	0.26690823	0.333	0.048	1.38E-68	13	CFP
PHACTR1	1.64E-44	0.26605481	0.29	0.057	2.66E-40	13	PHACTR1
SERPINB11	4.39E-21	0.26346641	0.478	0.208	7.13E-17	13	SERPINB1
MXD11	1.82E-29	0.26087605	0.28	0.072	2.95E-25	13	MXD1
VEGFA2	1.64E-28	0.25704714	0.271	0.069	2.67E-24	13	VEGFA
RPS111	6.04E-11	0.25468737	0.899	0.817	9.82E-07	13	RPS11
SDCBP2	7.53E-22	0.25408507	0.469	0.2	1.22E-17	13	SDCBP
HIF1A2	3.48E-17	0.25342311	0.367	0.155	5.66E-13	13	HIF1A
DSE	1.97E-24	0.25272158	0.338	0.111	3.20E-20	13	DSE
TGFBI1	7.04E-32	0.25266201	0.362	0.104	1.14E-27	13	TGFBI
HSP90AA11	2.91E-78	1.50764549	0.903	0.56	4.73E-74	14	HSP90AA1
HSPA1A2	3.12E-227	1.50372773	0.947	0.162	5.07E-223	14	HSPA1A
HSPA1B2	1.35E-181	1.0148449	0.696	0.096	2.19E-177	14	HSPA1B
DNAJB11	7.31E-192	0.9963993	0.696	0.093	1.19E-187	14	DNAJB1
GNLY2	5.04E-60	0.84699861	0.604	0.168	8.19E-56	14	GNLY
HSPA61	1.59E-137	0.71754199	0.367	0.033	2.58E-133	14	HSPA6
NKG73	3.18E-56	0.71731058	0.676	0.225	5.16E-52	14	NKG7
HSPE11	4.08E-52	0.58375538	0.527	0.162	6.63E-48	14	HSPE1
HSP90AB11	1.42E-20	0.553473	0.604	0.381	2.30E-16	14	HSP90AB1
HSPD11	3.28E-25	0.52810915	0.382	0.146	5.32E-21	14	HSPD1
HSPH11	7.28E-61	0.45875293	0.372	0.07	1.18E-56	14	HSPH1
CCL54	1.06E-25	0.45145939	0.643	0.3	1.72E-21	14	CCL5
UBC1	6.44E-15	0.42046422	0.812	0.689	1.05E-10	14	UBC
IL7R3	2.52E-15	0.41306384	0.372	0.169	4.10E-11	14	IL7R
KLRB13	1.20E-33	0.40412544	0.449	0.143	1.96E-29	14	KLRB1
RPS275	3.36E-25	0.39247611	0.995	0.931	5.45E-21	14	RPS27
HLA-B2	9.15E-22	0.36215594	0.966	0.85	1.49E-17	14	HLA-B
RPL343	1.55E-18	0.33921393	0.995	0.93	2.51E-14	14	RPL34
RPS27A4	3.34E-22	0.3345041	0.995	0.952	5.43E-18	14	RPS27A
CALM13	5.91E-14	0.31649809	0.681	0.471	9.60E-10	14	CALM1

RPS35	4.70E-17	0.29674621	0.971	0.924	7.63E-13	14	RPS3
RPL310	1.10E-16	0.29168928	0.981	0.93	1.79E-12	14	RPL3
RPL23A5	1.49E-13	0.29011893	0.961	0.892	2.41E-09	14	RPL23A
RPS294	1.02E-10	0.28167431	0.792	0.697	1.65E-06	14	RPS29
MYL12A5	3.14E-12	0.28151334	0.662	0.462	5.10E-08	14	MYL12A
RPS124	6.58E-13	0.2795715	0.99	0.968	1.07E-08	14	RPS12
RPS15A5	3.42E-15	0.26970983	0.986	0.937	5.56E-11	14	RPS15A
RPS182	2.95E-16	0.26838014	1	0.982	4.79E-12	14	RPS18
KLRD12	3.63E-15	0.25227149	0.3	0.118	5.89E-11	14	KLRD1
FTL6	1.39E-70	0.86013845	1	0.916	2.26E-66	15	FTL
AIF14	4.53E-48	0.79721964	0.747	0.396	7.36E-44	15	AIF1
TUBA1B3	3.80E-27	0.63892018	0.619	0.349	6.17E-23	15	TUBA1B
TMSB4X3	4.29E-61	0.63608916	1	0.993	6.97E-57	15	TMSB4X
APOC12	1.43E-38	0.56647255	0.727	0.306	2.32E-34	15	APOC1
C1QB3	1.08E-36	0.54397602	0.825	0.36	1.75E-32	15	C1QB
C1QA3	4.75E-31	0.50802642	0.742	0.344	7.72E-27	15	C1QA
TPT12	2.09E-47	0.50608518	1	0.994	3.39E-43	15	TPT1
ITM2B2	1.47E-26	0.48478396	0.918	0.656	2.39E-22	15	ITM2B
APOE3	2.78E-43	0.48011478	0.979	0.431	4.51E-39	15	APOE
EEF1B21	4.52E-21	0.44747963	0.871	0.669	7.35E-17	15	EEF1B2
BIN11	1.81E-23	0.44525071	0.443	0.194	2.94E-19	15	BIN1
S100A114	2.75E-18	0.42502382	0.737	0.535	4.47E-14	15	S100A11
RNASSET23	3.05E-14	0.4014027	0.577	0.371	4.95E-10	15	RNASSET2
RPL52	4.41E-22	0.39947145	0.959	0.79	7.16E-18	15	RPL5
RPS3A2	7.43E-23	0.39462074	0.995	0.948	1.21E-18	15	RPS3A
RPS232	9.43E-26	0.38473486	0.995	0.963	1.53E-21	15	RPS23
RPS62	3.33E-21	0.38271725	0.995	0.919	5.41E-17	15	RPS6
NACA1	5.65E-19	0.37812575	0.964	0.84	9.18E-15	15	NACA
RPS24	2.19E-21	0.37711847	1	0.962	3.56E-17	15	RPS24
FTH15	4.46E-30	0.3731208	0.995	0.92	7.24E-26	15	FTH1
RPS112	1.09E-17	0.37189997	0.954	0.816	1.77E-13	15	RPS11
RPL272	1.62E-14	0.36753412	0.84	0.687	2.63E-10	15	RPL27
RPS102	1.45E-13	0.36266472	0.753	0.596	2.35E-09	15	RPS10
RPL13A2	5.03E-20	0.34948769	0.99	0.905	8.17E-16	15	RPL13A
RPL212	7.21E-21	0.34924132	0.995	0.909	1.17E-16	15	RPL21
RPL292	1.51E-21	0.34841579	0.99	0.904	2.46E-17	15	RPL29
OAZ11	5.09E-12	0.34525832	0.716	0.588	8.27E-08	15	OAZ1
NPC23	8.99E-10	0.34514774	0.51	0.355	1.46E-05	15	NPC2
CST33	5.29E-10	0.33728164	0.567	0.405	8.60E-06	15	CST3
RPS132	7.72E-17	0.33645859	0.99	0.893	1.26E-12	15	RPS13

RPL37A1	3.89E-17	0.33553728	0.969	0.846	6.32E-13	15	RPL37A
RPS52	1.05E-16	0.33500125	0.912	0.73	1.70E-12	15	RPS5
ARPC1B	4.99E-08	0.33116025	0.433	0.319	0.0008111	15	ARPC1B
RACK11	1.29E-11	0.32788636	0.835	0.701	2.09E-07	15	RACK1
RAC13	3.22E-09	0.32087666	0.495	0.36	5.23E-05	15	RAC1
RGS101	3.23E-12	0.32001794	0.469	0.284	5.25E-08	15	RGS10
UBA52	7.35E-13	0.31353507	0.938	0.828	1.19E-08	15	UBA52
RPS263	1.03E-07	0.31284789	0.572	0.462	0.00167973	15	RPS26
RPL262	1.72E-16	0.31261438	1	0.936	2.79E-12	15	RPL26
RPLP12	8.40E-19	0.30997002	1	0.988	1.36E-14	15	RPLP1
RPL62	2.26E-13	0.30332411	0.99	0.862	3.68E-09	15	RPL6
RPS201	1.66E-09	0.30196547	0.747	0.639	2.70E-05	15	RPS20
RPL242	3.10E-10	0.30132528	0.907	0.789	5.04E-06	15	RPL24
RPS82	5.73E-15	0.29933508	1	0.934	9.30E-11	15	RPS8
RPL10A3	2.26E-11	0.29668887	0.948	0.789	3.68E-07	15	RPL10A
RPL71	1.31E-09	0.29549161	0.778	0.663	2.13E-05	15	RPL7
RPL221	8.99E-10	0.295459	0.814	0.702	1.46E-05	15	RPL22
FCER1G3	3.23E-05	0.29530207	0.485	0.397	0.52443803	15	FCER1G
YBX11	6.59E-05	0.29443734	0.464	0.428	1	15	YBX1
RPS4X3	4.37E-12	0.29409523	0.99	0.866	7.10E-08	15	RPS4X
RPS210	1.22E-15	0.29146028	1	0.979	1.98E-11	15	RPS2
RPS162	2.01E-14	0.28897198	0.985	0.91	3.26E-10	15	RPS16
SERF2	5.94E-10	0.28838408	0.784	0.648	9.65E-06	15	SERF2
RPL27A1	4.82E-11	0.28705607	0.912	0.791	7.82E-07	15	RPL27A
C1QC3	4.77E-12	0.28699934	0.536	0.308	7.76E-08	15	C1QC
FOLR21	2.60E-12	0.2864278	0.258	0.108	4.23E-08	15	FOLR2
RPL312	5.83E-14	0.28462213	0.995	0.93	9.47E-10	15	RPL3
A2M3	6.89E-08	0.2834533	0.397	0.248	0.00112023	15	A2M
RPL351	2.45E-12	0.28292762	0.979	0.826	3.97E-08	15	RPL35
RPL112	1.42E-15	0.28016602	1	0.95	2.31E-11	15	RPL11
ATP5F1E	2.88E-10	0.27901576	0.722	0.614	4.68E-06	15	ATP5F1E
RPLP02	1.15E-08	0.27892115	0.732	0.615	0.00018713	15	RPLP0
RPL151	1.15E-11	0.27866049	0.985	0.908	1.86E-07	15	RPL15
RPL23	9.23E-07	0.27814529	0.649	0.591	0.0150016	15	RPL23
RPS92	4.83E-13	0.27412909	0.985	0.884	7.85E-09	15	RPS9
RPL122	5.29E-10	0.26849142	0.985	0.902	8.59E-06	15	RPL12
RPL381	1.42E-05	0.26651356	0.603	0.568	0.23021925	15	RPL38
RPL7A3	1.01E-11	0.26531373	0.99	0.922	1.65E-07	15	RPL7A
GPR342	1.28E-10	0.26506287	0.361	0.19	2.08E-06	15	GPR34
CALM2	1.23E-06	0.26042884	0.438	0.34	0.02005238	15	CALM2

FCGRT2	2.12E-06	0.25912579	0.376	0.262	0.03437225	15	FCGRT
C12orf751	2.36E-10	0.2563221	0.253	0.118	3.84E-06	15	C12orf75
NINJ11	1.22E-11	0.25327438	0.278	0.129	1.98E-07	15	NINJ1
ARPC3	0.00022627	0.25265686	0.546	0.541	1	15	ARPC3
TUBA1B4	3.22E-133	1.63009052	0.961	0.344	5.24E-129	16	TUBA1B
STMN1	0	1.15619552	0.856	0.077	0	16	STMN1
HIST1H4C	9.64E-82	1.09615283	0.53	0.109	1.57E-77	16	HIST1H4C
TUBB	7.47E-189	1.09179198	0.851	0.141	1.21E-184	16	TUBB
HMGB2	4.70E-102	1.01643671	0.768	0.198	7.63E-98	16	HMGB2
CENPF	0	0.99325111	0.691	0.012	0	16	CENPF
H2AFZ	3.28E-111	0.96088691	0.79	0.201	5.33E-107	16	H2AFZ
HMGB1	1.57E-89	0.92190142	0.961	0.519	2.55E-85	16	HMGB1
HMG2	8.75E-118	0.9102583	0.823	0.209	1.42E-113	16	HMG2
TOP2A	0	0.85354907	0.63	0.004	0	16	TOP2A
MKI67	0	0.79927802	0.58	0.005	0	16	MKI67
ASPM	0	0.70384718	0.536	0.003	0	16	ASPM
PTTG1	0	0.62359601	0.547	0.028	0	16	PTTG1
GAPDH3	2.11E-29	0.58629812	0.89	0.684	3.43E-25	16	GAPDH
TUBB4B	3.53E-100	0.58387816	0.514	0.081	5.73E-96	16	TUBB4B
NUSAP1	0	0.57047192	0.508	0.008	0	16	NUSAP1
H2AFV	1.32E-87	0.56770537	0.663	0.152	2.15E-83	16	H2AFV
NUCKS1	1.86E-54	0.56336703	0.674	0.231	3.02E-50	16	NUCKS1
CALM2	2.87E-36	0.54512989	0.724	0.335	4.67E-32	16	CALM2
LGALS14	3.82E-13	0.54366285	0.519	0.322	6.22E-09	16	LGALS1
C1QB4	1.26E-31	0.52376508	0.812	0.361	2.05E-27	16	C1QB
TUBA1C	1.27E-146	0.52071004	0.486	0.049	2.07E-142	16	TUBA1C
ARL6IP1	5.45E-64	0.51731804	0.53	0.124	8.86E-60	16	ARL6IP1
UBE2C	0	0.50399106	0.414	0.001	0	16	UBE2C
CKS1B	8.86E-252	0.50344963	0.459	0.024	1.44E-247	16	CKS1B
PTMA2	3.09E-25	0.49710837	0.967	0.893	5.01E-21	16	PTMA
SMC4	5.56E-139	0.48965302	0.481	0.051	9.03E-135	16	SMC4
ACTB3	3.87E-22	0.48289478	0.978	0.856	6.29E-18	16	ACTB
RAN	3.23E-49	0.48218507	0.635	0.211	5.24E-45	16	RAN
NPC24	3.99E-30	0.4798154	0.735	0.352	6.48E-26	16	NPC2
AIF15	1.45E-18	0.45622935	0.685	0.398	2.35E-14	16	AIF1
HLA-DRB13	1.65E-22	0.45615361	0.641	0.309	2.69E-18	16	HLA-DRB1
PPIA	4.84E-28	0.43599392	0.746	0.428	7.86E-24	16	PPIA
HMMR	0	0.43012765	0.37	0.003	0	16	HMMR
JPT1	9.50E-41	0.42944128	0.486	0.146	1.54E-36	16	JPT1
BIRC5	0	0.42823469	0.425	0.004	0	16	BIRC5

TYMS	0	0.4212971	0.348	0.006	0	16	TYMS
CDK1	0	0.41819773	0.403	0.003	0	16	CDK1
KPNA2	1.47E-125	0.41642158	0.354	0.03	2.39E-121	16	KPNA2
CD743	1.21E-19	0.41241955	0.873	0.59	1.97E-15	16	CD74
PCLAF	0	0.40993316	0.392	0.007	0	16	PCLAF
DEK	3.27E-28	0.40194854	0.525	0.215	5.31E-24	16	DEK
CKS2	5.23E-166	0.39599256	0.37	0.024	8.50E-162	16	CKS2
MZT2B	2.09E-31	0.38447686	0.608	0.253	3.39E-27	16	MZT2B
CCNB1	0	0.37847346	0.309	0.003	0	16	CCNB1
VIM4	1.40E-13	0.37757051	0.74	0.505	2.28E-09	16	VIM
MARCKS3	2.82E-21	0.37695636	0.575	0.268	4.59E-17	16	MARCKS
PCNA	1.08E-75	0.37145282	0.32	0.04	1.75E-71	16	PCNA
H2AFX	3.31E-171	0.37139749	0.376	0.024	5.38E-167	16	H2AFX
ANP32B	1.87E-31	0.36656038	0.53	0.201	3.03E-27	16	ANP32B
CALM3	3.76E-39	0.36287362	0.47	0.138	6.10E-35	16	CALM3
TPX2	0	0.36248935	0.326	0.003	0	16	TPX2
TMPO	1.20E-43	0.36045584	0.414	0.102	1.95E-39	16	TMPO
GTSE1	0	0.35247851	0.337	0.002	0	16	GTSE1
SGO2	2.28E-249	0.33705587	0.304	0.009	3.70E-245	16	SGO2
CDKN3	0	0.33699785	0.304	0.006	0	16	CDKN3
SMC2	1.93E-90	0.33590667	0.365	0.043	3.14E-86	16	SMC2
NUF2	0	0.33573352	0.337	0.003	0	16	NUF2
ALOX5AP3	1.88E-16	0.33335556	0.547	0.285	3.05E-12	16	ALOX5AP
DUT	4.32E-31	0.3292148	0.381	0.114	7.01E-27	16	DUT
H3F3A2	2.23E-15	0.3231535	0.917	0.733	3.63E-11	16	H3F3A
CFL1	1.10E-15	0.32120489	0.829	0.629	1.79E-11	16	CFL1
UBE2S	5.37E-61	0.31987237	0.309	0.045	8.72E-57	16	UBE2S
PFN11	6.71E-12	0.31677404	0.646	0.446	1.09E-07	16	PFN1
C1QC4	2.20E-20	0.31632806	0.669	0.307	3.58E-16	16	C1QC
CAPG	4.23E-28	0.31368293	0.459	0.16	6.88E-24	16	CAPG
TPI12	5.15E-19	0.30854255	0.519	0.246	8.37E-15	16	TPI1
RHOA	1.30E-14	0.30797597	0.541	0.303	2.12E-10	16	RHOA
ZWINT	0	0.30486512	0.315	0.006	0	16	ZWINT
RRM2	0	0.30381687	0.282	0.003	0	16	RRM2
COX8A	2.55E-20	0.30272648	0.547	0.259	4.14E-16	16	COX8A
TK1	0	0.30003615	0.309	0.006	0	16	TK1
CCNB2	0	0.29965746	0.298	0.003	0	16	CCNB2
KNL1	0	0.29862503	0.282	0.004	0	16	KNL1
YBX12	2.92E-13	0.29579131	0.641	0.426	4.75E-09	16	YBX1
CKAP2	1.76E-78	0.29441959	0.287	0.031	2.86E-74	16	CKAP2

FAM111A	3.88E-34	0.29260504	0.309	0.072	6.30E-30	16	FAM111A
KIF20B	1.95E-69	0.29219163	0.326	0.044	3.16E-65	16	KIF20B
CEP55	0	0.29189119	0.304	0.003	0	16	CEP55
SPP13	1.50E-20	0.2866808	0.663	0.314	2.44E-16	16	SPP1
LDHA2	8.97E-16	0.28565288	0.552	0.29	1.46E-11	16	LDHA
HP1BP3	5.45E-15	0.28346608	0.381	0.173	8.86E-11	16	HP1BP3
CENPE	1.26E-212	0.28115829	0.26	0.008	2.05E-208	16	CENPE
ENO12	3.78E-13	0.2809611	0.497	0.275	6.15E-09	16	ENO1
SLC25A5	3.67E-14	0.28086566	0.442	0.223	5.97E-10	16	SLC25A5
HIST1H1D	1.01E-25	0.27837887	0.32	0.092	1.64E-21	16	HIST1H1D
AP2S1	2.32E-22	0.27720347	0.453	0.179	3.77E-18	16	AP2S1
CALR	9.25E-17	0.27670706	0.514	0.258	1.50E-12	16	CALR
HNRNPA2B1	5.74E-12	0.27628126	0.762	0.547	9.32E-08	16	HNRNPA2B1
HSP90B1	1.69E-14	0.27510153	0.503	0.264	2.75E-10	16	HSP90B1
FCGBP3	2.59E-11	0.27494567	0.359	0.166	4.22E-07	16	FCGBP
APOC13	1.28E-14	0.27214337	0.602	0.308	2.08E-10	16	APOC1
COTL13	7.41E-16	0.26790753	0.635	0.347	1.20E-11	16	COTL1
ANP32E	5.72E-38	0.26537543	0.348	0.081	9.30E-34	16	ANP32E
KIF11	0	0.26499709	0.276	0.004	0	16	KIF11
HNRNPA1	9.61E-12	0.26115704	0.613	0.392	1.56E-07	16	HNRNPA1
CDKN2C	5.18E-90	0.26106197	0.271	0.024	8.41E-86	16	CDKN2C
PKM1	3.04E-20	0.26060875	0.459	0.189	4.94E-16	16	PKM
C33	9.93E-14	0.26014599	0.541	0.272	1.61E-09	16	C3
APOE4	2.12E-11	0.25977294	0.707	0.436	3.44E-07	16	APOE
UBB1	1.44E-09	0.25648213	0.547	0.364	2.34E-05	16	UBB
RAD21	1.84E-26	0.25634536	0.37	0.115	3.00E-22	16	RAD21
CST34	8.08E-11	0.25491579	0.663	0.403	1.31E-06	16	CST3
DTYMK	7.01E-76	0.2542133	0.265	0.027	1.14E-71	16	DTYMK
ANAPC11	7.18E-24	0.25383909	0.398	0.139	1.17E-19	16	ANAPC11
IDH2	2.78E-33	0.25380844	0.376	0.101	4.51E-29	16	IDH2
RGS14	2.38E-06	0.25356702	0.486	0.33	0.03870318	16	RGS1
HLA-DRB14	5.39E-96	1.09676926	0.981	0.305	8.75E-92	17	HLA-DRB1
CD744	6.92E-47	0.7428604	1	0.588	1.12E-42	17	CD74
HLA-DPA13	5.86E-44	0.62937645	0.961	0.444	9.52E-40	17	HLA-DPA1
XIST1	4.03E-94	0.58620479	0.753	0.146	6.55E-90	17	XIST
HLA-DRA4	2.49E-38	0.55887709	0.987	0.501	4.05E-34	17	HLA-DRA
HLA-DQB13	3.07E-51	0.48292864	0.773	0.235	4.99E-47	17	HLA-DQB1
HLA-C3	3.94E-32	0.48246792	0.981	0.682	6.40E-28	17	HLA-C
C1QB5	1.08E-29	0.45668175	0.87	0.361	1.75E-25	17	C1QB
HLA-DQA12	6.98E-54	0.44358204	0.636	0.163	1.13E-49	17	HLA-DQA1

HLA-DRB53	4.75E-48	0.44207953	0.812	0.26	7.72E-44	17	HLA-DRB5
HLA-DPB14	1.04E-23	0.36760966	0.818	0.391	1.68E-19	17	HLA-DPB1
TRAC3	7.00E-37	0.33623017	0.558	0.162	1.14E-32	17	TRAC
B2M4	4.45E-23	0.3337207	1	0.991	7.23E-19	17	B2M
C34	6.75E-25	0.32476574	0.682	0.27	1.10E-20	17	C3
C1QC5	1.86E-22	0.32454052	0.721	0.307	3.03E-18	17	C1QC
CD23	2.48E-30	0.32345716	0.63	0.217	4.03E-26	17	CD2
IL323	5.10E-27	0.32316185	0.597	0.212	8.29E-23	17	IL32
MS4A6A2	2.16E-18	0.31227562	0.591	0.274	3.50E-14	17	MS4A6A
FCGBP4	5.19E-31	0.31159992	0.539	0.164	8.43E-27	17	FCGBP
GZMK3	6.02E-19	0.27458096	0.416	0.146	9.78E-15	17	GZMK
RPL104	4.23E-16	0.26566888	1	0.979	6.87E-12	17	RPL10
RPS264	1.50E-15	0.26178482	0.818	0.459	2.44E-11	17	RPS26
MALAT11	1.73E-20	0.26168156	1	0.991	2.81E-16	17	MALAT1
LTB2	1.56E-25	0.25809928	0.435	0.133	2.54E-21	17	LTB
C1QA4	1.47E-17	0.256592	0.766	0.345	2.39E-13	17	C1QA
RPS4X4	6.51E-13	0.25457234	0.968	0.866	1.06E-08	17	RPS4X
PLP1	0	4.02187449	1	0.002	0	18	PLP1
CRYAB	0	2.62118455	1	0.004	0	18	CRYAB
SELENOP	2.14E-296	2.45634161	0.983	0.038	3.48E-292	18	SELENOP
MBP	1.32E-97	2.34949444	0.983	0.143	2.14E-93	18	MBP
S100B	3.36E-298	2.33626242	0.983	0.038	5.46E-294	18	S100B
TUBA1A	3.20E-108	2.18273264	1	0.131	5.20E-104	18	TUBA1A
GPM6B	0	2.11522874	1	0.017	0	18	GPM6B
PTGDS1	0	2.040238	1	0.028	0	18	PTGDS
STMN11	6.76E-148	1.79816912	0.983	0.085	1.10E-143	18	STMN1
MARCKSL1	0	1.74844262	0.948	0.032	0	18	MARCKSL1
CLDND1	1.00E-193	1.67498164	1	0.065	1.63E-189	18	CLDND1
TF	0	1.64615474	0.983	0.001	0	18	TF
PPP1R14A	0	1.62363157	0.948	0.002	0	18	PPP1R14A
CNP	0	1.61181928	0.983	0.021	0	18	CNP
ERMN	0	1.53846218	0.983	0.006	0	18	ERMN
FEZ1	0	1.52879365	0.948	0.008	0	18	FEZ1
APLP1	0	1.47996649	0.983	0.001	0	18	APLP1
NKX6-2	0	1.39436559	0.948	0	0	18	NKX6-2
ANLN	0	1.3381416	0.948	0.004	0	18	ANLN
APOD	0	1.3374634	0.948	0	0	18	APOD
PEBP1	1.32E-72	1.33562416	0.966	0.19	2.14E-68	18	PEBP1
TMEM144	0	1.30293064	0.983	0.016	0	18	TMEM144
RTN4	4.04E-62	1.28037684	0.983	0.239	6.56E-58	18	RTN4

QKI1	3.55E-63	1.26067553	0.948	0.208	5.76E-59	18	QKI
DYNLL1	6.32E-52	1.24812197	0.931	0.239	1.03E-47	18	DYNLL1
SLC44A1	5.79E-290	1.23908364	0.914	0.033	9.40E-286	18	SLC44A1
CALM22	1.94E-43	1.22378213	0.966	0.338	3.16E-39	18	CALM2
MAG	0	1.22258985	0.931	0	0	18	MAG
EDIL3	0	1.20715886	0.879	0	0	18	EDIL3
CAMK2N1	0	1.18288457	0.879	0.013	0	18	CAMK2N1
ATP1B1	1.54E-262	1.14589578	0.931	0.038	2.50E-258	18	ATP1B1
HSPA2	0	1.14228288	0.948	0.001	0	18	HSPA2
RAPGEF5	0	1.12065725	0.862	0.001	0	18	RAPGEF5
MT3	0	1.11359549	0.879	0.005	0	18	MT3
PLA2G16	3.04E-118	1.10833714	0.948	0.094	4.95E-114	18	PLA2G16
TUBB2B	0	1.10543779	0.724	0.003	0	18	TUBB2B
TSC22D4	3.91E-128	1.10395788	0.914	0.08	6.35E-124	18	TSC22D4
FGFR2	0	1.10391585	0.879	0	0	18	FGFR2
ENPP2	0	1.08474722	0.914	0.002	0	18	ENPP2
Sep-71	5.51E-48	1.08315017	0.983	0.3	8.95E-44	18	7-Sep
SERPINI1	0	1.07849017	0.828	0.003	0	18	SERPINI1
PCDH9	0	1.07185847	0.897	0.003	0	18	PCDH9
SLAIN1	0	1.06939238	0.897	0.005	0	18	SLAIN1
AMER2	0	1.06826025	0.845	0.001	0	18	AMER2
PMP22	0	1.05782915	0.931	0.02	0	18	PMP22
ARHGAP21	3.15E-148	1.05756449	0.966	0.076	5.11E-144	18	ARHGAP21
QDPR	0	1.0556614	0.845	0.025	0	18	QDPR
SELENOW	1.75E-67	1.03830667	0.897	0.158	2.85E-63	18	SELENOW
MYLK	0	1.0380573	0.862	0.001	0	18	MYLK
MOG	0	1.03296549	0.897	0	0	18	MOG
TTLL7	0	1.00735108	0.845	0.001	0	18	TTLL7
KCNMB4	0	1.00556041	0.879	0.003	0	18	KCNMB4
CD91	3.68E-128	0.99551852	0.931	0.08	5.97E-124	18	CD9
SCD	0	0.98623899	0.81	0.021	0	18	SCD
DST	3.81E-129	0.98579442	0.862	0.069	6.19E-125	18	DST
MAP7	0	0.9848098	0.828	0.005	0	18	MAP7
MOBP	0	0.96318122	0.776	0	0	18	MOBP
UGT8	0	0.9623274	0.828	0.001	0	18	UGT8
CDKN1C	2.28E-302	0.95704771	0.879	0.028	3.71E-298	18	CDKN1C
CLDN11	0	0.93565915	0.793	0.001	0	18	CLDN11
MAP1B	0	0.9259819	0.81	0.004	0	18	MAP1B
STMN4	0	0.90877238	0.845	0.001	0	18	STMN4
SPOCK3	0	0.90231618	0.828	0	0	18	SPOCK3

UBB2	1.84E-30	0.9011952	0.914	0.364	2.99E-26	18	UBB
HAPLN2	0	0.89512776	0.776	0	0	18	HAPLN2
CNDP1	0	0.89504234	0.741	0	0	18	CNDP1
CNTN2	0	0.87368922	0.81	0	0	18	CNTN2
SEC11C	3.66E-86	0.87210647	0.845	0.1	5.94E-82	18	SEC11C
FAM107B	3.70E-85	0.86708347	0.879	0.109	6.01E-81	18	FAM107B
8-Sep	0	0.86121187	0.828	0.012	0	18	8-Sep
TUBB4A	0	0.85919621	0.81	0	0	18	TUBB4A
PRDX1	2.01E-45	0.85655681	0.914	0.229	3.26E-41	18	PRDX1
RGCC	3.60E-99	0.85631232	0.793	0.074	5.84E-95	18	RGCC
GSN3	8.83E-47	0.84793418	0.879	0.203	1.43E-42	18	GSN
SIRT2	3.98E-172	0.84457788	0.845	0.048	6.46E-168	18	SIRT2
FIS1	2.07E-61	0.84372609	0.81	0.129	3.36E-57	18	FIS1
TMEM59	3.63E-42	0.84350078	0.862	0.22	5.89E-38	18	TMEM59
KLK6	0	0.83739679	0.845	0	0	18	KLK6
TTYH1	0	0.83364444	0.741	0.003	0	18	TTYH1
PLEKHB1	0	0.82965174	0.69	0.007	0	18	PLEKHB1
TBCB	2.63E-77	0.82532448	0.793	0.096	4.28E-73	18	TBCB
SHTN11	1.31E-81	0.82256214	0.845	0.102	2.12E-77	18	SHTN1
RTN3	1.03E-87	0.81984716	0.828	0.092	1.67E-83	18	RTN3
C1orf122	3.19E-108	0.81204706	0.793	0.068	5.19E-104	18	C1orf122
VAPA	3.07E-39	0.80964412	0.81	0.199	4.99E-35	18	VAPA
SCD5	0	0.8082818	0.828	0.005	0	18	SCD5
SCRG1	0	0.80819112	0.793	0.012	0	18	SCRG1
CALM14	2.06E-28	0.80209943	1	0.472	3.35E-24	18	CALM1
LAMP2	1.95E-86	0.79221321	0.862	0.1	3.17E-82	18	LAMP2
CA2	0	0.7878349	0.69	0.004	0	18	CA2
APP	7.63E-188	0.7836444	0.793	0.038	1.24E-183	18	APP
SORT1	7.53E-135	0.77626169	0.776	0.052	1.22E-130	18	SORT1
SPARC	0	0.7642035	0.621	0.004	0	18	SPARC
CKB	7.62E-201	0.76164172	0.724	0.029	1.24E-196	18	CKB
OSBPL1A	1.22E-144	0.76007967	0.69	0.037	1.98E-140	18	OSBPL1A
RDX	4.27E-89	0.74847104	0.776	0.078	6.95E-85	18	RDX
ABCA2	0	0.74735697	0.759	0.012	0	18	ABCA2
DPYSL2	1.07E-110	0.74695833	0.793	0.066	1.74E-106	18	DPYSL2
GLTP	2.87E-170	0.74207487	0.776	0.04	4.67E-166	18	GLTP
4-Sep	0	0.72687787	0.724	0	0	18	4-Sep
OLIG1	0	0.72599293	0.672	0.004	0	18	OLIG1
MAL	0	0.72278157	0.793	0.011	0	18	MAL
PIP4K2A	1.92E-61	0.71303487	0.759	0.109	3.11E-57	18	PIP4K2A

SCARB2	1.63E-71	0.71235443	0.776	0.095	2.65E-67	18	SCARB2
FBXO32	6.88E-257	0.70834236	0.655	0.018	1.12E-252	18	FBXO32
PPA1	1.24E-44	0.6918957	0.672	0.114	2.02E-40	18	PPA1
C4orf48	3.74E-83	0.6868763	0.862	0.103	6.07E-79	18	C4orf48
SCCPDH	1.36E-228	0.68343397	0.741	0.026	2.20E-224	18	SCCPDH
GABARAPL2	1.41E-39	0.68016631	0.759	0.161	2.28E-35	18	GABARAPL2
CFL2	0	0.67670753	0.707	0.016	0	18	CFL2
MTUS1	1.24E-123	0.67616136	0.724	0.048	2.02E-119	18	MTUS1
NECAB1	0	0.67549915	0.741	0	0	18	NECAB1
PGRMC1	6.90E-139	0.66865436	0.707	0.04	1.12E-134	18	PGRMC1
PEX5L	0	0.66677394	0.655	0	0	18	PEX5L
CARNS1	0	0.66447009	0.655	0.002	0	18	CARNS1
FMNL2	5.89E-108	0.6634226	0.655	0.045	9.57E-104	18	FMNL2
EFHD1	0	0.65754335	0.741	0.001	0	18	EFHD1
EVI2A	6.62E-47	0.6574156	0.707	0.12	1.07E-42	18	EVI2A
TRIM2	0	0.65515508	0.638	0.003	0	18	TRIM2
KCNQ1OT1	2.60E-134	0.64959481	0.672	0.037	4.22E-130	18	KCNQ1OT1
SPP14	1.92E-30	0.64821747	0.983	0.316	3.12E-26	18	SPP1
ZFYVE16	4.61E-75	0.6443543	0.707	0.074	7.50E-71	18	ZFYVE16
SYT11	4.40E-241	0.63963821	0.759	0.026	7.15E-237	18	SYT11
NENF	8.05E-80	0.6391374	0.741	0.078	1.31E-75	18	NENF
LANCL1	0	0.63618379	0.655	0.013	0	18	LANCL1
CBR1	2.12E-129	0.63564456	0.672	0.039	3.45E-125	18	CBR1
ST18	0	0.63381954	0.638	0.006	0	18	ST18
NDRG11	9.45E-88	0.62995087	0.69	0.06	1.53E-83	18	NDRG1
CHADL	0	0.62911222	0.655	0.002	0	18	CHADL
PPDPF1	1.03E-37	0.62852884	0.793	0.18	1.67E-33	18	PPDPF
ZNF652	7.36E-62	0.62495478	0.672	0.082	1.20E-57	18	ZNF652
CMTM5	0	0.62143193	0.638	0	0	18	CMTM5
RNF13	1.04E-44	0.61949786	0.759	0.142	1.68E-40	18	RNF13
PAQR8	4.65E-220	0.61898573	0.655	0.021	7.56E-216	18	PAQR8
SLC12A2	0	0.61817017	0.638	0.012	0	18	SLC12A2
PACS2	9.72E-227	0.61672943	0.69	0.022	1.58E-222	18	PACS2
GLUL4	8.44E-25	0.61567131	0.862	0.292	1.37E-20	18	GLUL
SBDS	3.06E-66	0.61439349	0.672	0.076	4.98E-62	18	SBDS
SLC24A2	0	0.61230039	0.655	0	0	18	SLC24A2
GPRC5B	0	0.61204412	0.603	0	0	18	GPRC5B
PLEKHH1	0	0.61127571	0.672	0.001	0	18	PLEKHH1
SLC31A2	8.91E-75	0.60234344	0.776	0.088	1.45E-70	18	SLC31A2
NTM	0	0.60214204	0.655	0.001	0	18	NTM

ADIPOR2	1.48E-119	0.60198063	0.621	0.036	2.40E-115	18	ADIPOR2
MAPK8IP1	0	0.60180063	0.621	0.001	0	18	MAPK8IP1
FRYL	6.58E-76	0.59010021	0.655	0.063	1.07E-71	18	FRYL
SECISBP2L	5.24E-136	0.58604456	0.724	0.043	8.51E-132	18	SECISBP2L
CNTNAP4	0	0.58394789	0.569	0	0	18	CNTNAP4
DPYSL5	0	0.58386245	0.638	0	0	18	DPYSL5
ZBTB20	9.02E-49	0.57849457	0.69	0.104	1.47E-44	18	ZBTB20
BBX	3.13E-47	0.578102	0.69	0.11	5.09E-43	18	BBX
AL359091.1	0	0.57351731	0.552	0	0	18	AL359091.1
ANKS1B	0	0.57351731	0.621	0.001	0	18	ANKS1B
NCAM1	0	0.57239492	0.586	0.01	0	18	NCAM1
ELOVL1	1.12E-78	0.57201962	0.586	0.049	1.81E-74	18	ELOVL1
BACE1	1.19E-222	0.56868559	0.569	0.015	1.94E-218	18	BACE1
PHLDA3	0	0.55950145	0.603	0.005	0	18	PHLDA3
DSTN	1.68E-49	0.55921003	0.655	0.095	2.73E-45	18	DSTN
FNTA	1.94E-62	0.5587598	0.672	0.079	3.15E-58	18	FNTA
BEX3	1.52E-201	0.55507659	0.586	0.018	2.47E-197	18	BEX3
KCNK1	0	0.55467751	0.569	0	0	18	KCNK1
MGST3	2.31E-32	0.55437139	0.724	0.168	3.76E-28	18	MGST3
LIMCH1	0	0.55356739	0.552	0.001	0	18	LIMCH1
SLC22A17	0	0.55288486	0.638	0.002	0	18	SLC22A17
PRUNE2	0	0.55058473	0.569	0.004	0	18	PRUNE2
CLTA	3.54E-24	0.54729509	0.69	0.196	5.75E-20	18	CLTA
LARP6	0	0.54438547	0.603	0	0	18	LARP6
PTPRD	0	0.54430006	0.569	0	0	18	PTPRD
TJP1	0	0.54046423	0.603	0.004	0	18	TJP1
REEP3	1.24E-96	0.53892421	0.621	0.044	2.02E-92	18	REEP3
PXK	1.96E-114	0.53581808	0.621	0.037	3.19E-110	18	PXK
SYPL1	1.06E-53	0.52707956	0.569	0.066	1.73E-49	18	SYPL1
DYNC1I2	5.50E-66	0.52542765	0.672	0.075	8.93E-62	18	DYNC1I2
CCDC88A1	1.01E-21	0.51552285	0.621	0.175	1.65E-17	18	CCDC88A
SVIP	1.69E-91	0.51551182	0.621	0.046	2.75E-87	18	SVIP
GPR37	0	0.5140971	0.552	0	0	18	GPR37
AKIRIN1	2.64E-59	0.51326434	0.655	0.078	4.28E-55	18	AKIRIN1
SKP1	3.53E-21	0.51305531	0.759	0.268	5.74E-17	18	SKP1
SPART	2.67E-98	0.5128444	0.603	0.041	4.35E-94	18	SPART
ATOX1	1.82E-51	0.50627103	0.638	0.084	2.95E-47	18	ATOX1
PRKACB	6.25E-67	0.50465535	0.638	0.066	1.02E-62	18	PRKACB
MYRF	0	0.50330727	0.534	0.001	0	18	MYRF
EID1	2.10E-19	0.4990976	0.638	0.211	3.41E-15	18	EID1

TMEM63A	1.45E-149	0.49721787	0.603	0.026	2.35E-145	18	TMEM63A
CSRP1	1.32E-113	0.49638682	0.534	0.028	2.15E-109	18	CSRP1
KIF1B	3.33E-102	0.49579795	0.586	0.037	5.41E-98	18	KIF1B
ATP8A1	7.78E-118	0.49522451	0.534	0.026	1.26E-113	18	ATP8A1
ACTG12	2.52E-14	0.49324328	0.983	0.739	4.10E-10	18	ACTG1
MPC1	1.77E-40	0.49245718	0.552	0.081	2.88E-36	18	MPC1
MAP1A	0	0.49181182	0.517	0.001	0	18	MAP1A
RETREG1	2.66E-228	0.49024295	0.534	0.013	4.32E-224	18	RETREG1
MBNL2	1.19E-101	0.49009332	0.552	0.033	1.93E-97	18	MBNL2
CDK18	0	0.48959641	0.5	0.004	0	18	CDK18
VAMP2	1.40E-31	0.48548273	0.655	0.136	2.28E-27	18	VAMP2
TMEM125	0	0.48285177	0.466	0	0	18	TMEM125
KIF1A	0	0.48259548	0.5	0	0	18	KIF1A
FAR1	4.39E-55	0.48189358	0.552	0.06	7.13E-51	18	FAR1
PLLP	0	0.48182701	0.483	0.001	0	18	PLLP
ENDOD1	8.43E-213	0.48053048	0.5	0.012	1.37E-208	18	ENDOD1
RHOU	8.02E-202	0.48019315	0.5	0.013	1.30E-197	18	RHOU
TMEM165	2.52E-32	0.479234	0.586	0.11	4.10E-28	18	TMEM165
TTYH2	3.08E-178	0.47842406	0.5	0.015	5.00E-174	18	TTYH2
KTN1	7.43E-20	0.47831921	0.69	0.218	1.21E-15	18	KTN1
SOD1	1.98E-23	0.47580365	0.707	0.197	3.21E-19	18	SOD1
SLC48A1	0	0.47553072	0.517	0.007	0	18	SLC48A1
ROGDI	6.01E-110	0.47510319	0.534	0.029	9.76E-106	18	ROGDI
POLR2I	2.07E-66	0.4739316	0.603	0.06	3.36E-62	18	POLR2I
ZCCHC24	0	0.47265107	0.569	0.01	0	18	ZCCHC24
TMEM151A	0	0.47207105	0.466	0	0	18	TMEM151A
PLPP2	0	0.47190019	0.466	0	0	18	PLPP2
CD47	1.57E-40	0.47171717	0.672	0.114	2.55E-36	18	CD47
MYO6	2.46E-232	0.47129881	0.5	0.011	3.99E-228	18	MYO6
BOK	0	0.47053442	0.517	0.002	0	18	BOK
GNG7	6.71E-75	0.47022492	0.534	0.042	1.09E-70	18	GNG7
DIXDC1	0	0.46900016	0.517	0.003	0	18	DIXDC1
PCSK1N	0	0.46857439	0.448	0.003	0	18	PCSK1N
SCOC	2.10E-96	0.46856641	0.552	0.035	3.42E-92	18	SCOC
ZNF708	6.60E-100	0.46650667	0.569	0.036	1.07E-95	18	ZNF708
UBL3	3.18E-31	0.46563336	0.586	0.112	5.17E-27	18	UBL3
RAB40B	0	0.46280188	0.569	0.009	0	18	RAB40B
SYNJ2	1.85E-212	0.46170209	0.448	0.009	3.00E-208	18	SYNJ2
GJB1	0	0.46134557	0.466	0	0	18	GJB1
S100A1	0	0.46108928	0.431	0	0	18	S100A1

MXI1	8.10E-75	0.45842506	0.466	0.032	1.32E-70	18	MXI1
METR1	3.42E-85	0.45735312	0.517	0.034	5.55E-81	18	METR1
AMD1	9.82E-30	0.45730334	0.517	0.094	1.60E-25	18	AMD1
MOB3B	0	0.45521267	0.517	0.006	0	18	MOB3B
NDUFS7	9.86E-37	0.45521267	0.621	0.108	1.60E-32	18	NDUFS7
SASH1	0	0.45487305	0.483	0.006	0	18	SASH1
YWHAQ	9.36E-32	0.45414094	0.569	0.105	1.52E-27	18	YWHAQ
PTMA3	4.91E-13	0.4533129	1	0.893	7.98E-09	18	PTMA3
SERINC1	1.50E-35	0.45286409	0.638	0.116	2.44E-31	18	SERINC1
TBC1D12	2.26E-74	0.45266657	0.517	0.039	3.68E-70	18	TBC1D12
PEA15	9.50E-58	0.45220612	0.517	0.05	1.54E-53	18	PEA15
NCOA7	5.61E-49	0.45135414	0.517	0.058	9.11E-45	18	NCOA7
LGALS15	5.12E-10	0.44968363	0.69	0.323	8.31E-06	18	LGALS1
COX5B	2.17E-16	0.44800728	0.707	0.275	3.53E-12	18	COX5B
DNM3	0	0.44785655	0.466	0.002	0	18	DNM3
PHGDH	0	0.447175	0.466	0.003	0	18	PHGDH
AATK	0	0.44513314	0.534	0.005	0	18	AATK
KIF5C	0	0.44496318	0.466	0.005	0	18	KIF5C
BEX4	5.62E-44	0.44453753	0.603	0.086	9.14E-40	18	BEX4
GNAI1	4.06E-306	0.44326509	0.483	0.007	6.60E-302	18	GNAI1
TECR	6.50E-38	0.44225017	0.603	0.098	1.06E-33	18	TECR
ABHD17A1	3.45E-29	0.44196065	0.655	0.142	5.60E-25	18	ABHD17A
HSP90AA12	4.34E-17	0.44118887	0.948	0.564	7.05E-13	18	HSP90AA1
CTNNA1	1.05E-38	0.44050182	0.517	0.073	1.71E-34	18	CTNNA1
FOLH1	0	0.43928122	0.534	0	0	18	FOLH1
FA2H	0	0.43928122	0.466	0	0	18	FA2H
DHCR24	0	0.43868337	0.483	0.001	0	18	DHCR24
PHACTR3	0	0.43868337	0.379	0.001	0	18	PHACTR3
GOLGA4	7.86E-24	0.43852038	0.69	0.184	1.28E-19	18	GOLGA4
ELAVL3	0	0.43825654	0.517	0.001	0	18	ELAVL3
ERBB3	0	0.43808587	0.431	0.001	0	18	ERBB3
UCHL1	0	0.43791522	0.431	0.001	0	18	UCHL1
NT5DC1	5.99E-125	0.43728667	0.517	0.023	9.73E-121	18	NT5DC1
PLIN3	5.43E-55	0.43687848	0.534	0.056	8.82E-51	18	PLIN3
TCEAL4	2.38E-42	0.43685767	0.552	0.075	3.87E-38	18	TCEAL4
MAPT	0	0.43655108	0.466	0.003	0	18	MAPT
SGCB	0	0.43255464	0.5	0.007	0	18	SGCB
MAN2A1	3.12E-47	0.43252785	0.5	0.056	5.07E-43	18	MAN2A1
PAQR4	0	0.43153683	0.5	0.008	0	18	PAQR4
VWA1	8.61E-233	0.43085887	0.431	0.008	1.40E-228	18	VWA1

ANK3	1.92E-132	0.42936487	0.483	0.019	3.12E-128	18	ANK3
GPD1	0	0.42810792	0.466	0	0	18	GPD1
DLG1	1.04E-53	0.42501139	0.466	0.044	1.69E-49	18	DLG1
WSB1	2.16E-15	0.42470004	0.655	0.239	3.51E-11	18	WSB1
JAM3	0	0.42418568	0.466	0.004	0	18	JAM3
DDR1	0	0.42172084	0.466	0.006	0	18	DDR1
NUCKS11	5.47E-15	0.41980001	0.655	0.235	8.88E-11	18	NUCKS1
KIDINS220	2.10E-33	0.41814772	0.517	0.082	3.41E-29	18	KIDINS220
CLASP2	3.89E-82	0.41813393	0.483	0.031	6.32E-78	18	CLASP2
ABHD5	2.54E-60	0.41812045	0.466	0.039	4.12E-56	18	ABHD5
CCNQ	2.19E-74	0.4179685	0.466	0.032	3.57E-70	18	CCNQ
ARPP19	2.98E-48	0.41697295	0.586	0.075	4.84E-44	18	ARPP19
FAM131C	0	0.41680837	0.397	0	0	18	FAM131C
TMEM98	0	0.41638129	0.448	0.001	0	18	TMEM98
EMC2	1.39E-75	0.41623303	0.483	0.034	2.27E-71	18	EMC2
SCG5	0	0.41621051	0.448	0.001	0	18	SCG5
ARFGEF3	0	0.4159544	0.448	0.001	0	18	ARFGEF3
MGLL	6.00E-134	0.41377289	0.414	0.014	9.74E-130	18	MGLL
CCDC90B	9.25E-46	0.41237657	0.5	0.058	1.50E-41	18	CCDC90B
POLR2F	6.22E-30	0.41154897	0.448	0.07	1.01E-25	18	POLR2F
CEP170	2.27E-32	0.40725127	0.569	0.1	3.69E-28	18	CEP170
CRYBG3	1.36E-114	0.40722539	0.466	0.021	2.21E-110	18	CRYBG3
APBB1	2.13E-193	0.40584772	0.448	0.011	3.45E-189	18	APBB1
SLCO1A2	0	0.40546511	0.431	0	0	18	SLCO1A2
ABCA8	0	0.40546511	0.466	0	0	18	ABCA8
TMEM178A	0	0.40529424	0.414	0	0	18	TMEM178A
KCNJ10	0	0.40495259	0.431	0.001	0	18	KCNJ10
ENPP6	0	0.40461106	0.431	0.001	0	18	ENPP6
AK5	0	0.40426965	0.466	0.001	0	18	AK5
RBP7	5.69E-63	0.40320348	0.431	0.032	9.24E-59	18	RBP7
PARP1	1.16E-24	0.40068402	0.552	0.119	1.89E-20	18	PARP1
RNH1	8.32E-18	0.40009934	0.5	0.131	1.35E-13	18	RNH1
ACYP2	1.71E-77	0.39914235	0.448	0.028	2.77E-73	18	ACYP2
PDGFA	1.56E-254	0.39873796	0.414	0.006	2.54E-250	18	PDGFA
GAMT	2.86E-82	0.39632452	0.483	0.031	4.65E-78	18	GAMT
EPN2	4.05E-110	0.39626057	0.448	0.02	6.58E-106	18	EPN2
PAPSS1	1.16E-69	0.3959108	0.448	0.032	1.89E-65	18	PAPSS1
RAB10	1.22E-29	0.39497512	0.534	0.096	1.98E-25	18	RAB10
GPIHBP1	0	0.39381885	0.397	0	0	18	GPIHBP1
OCIAD1	5.88E-18	0.39347458	0.517	0.138	9.55E-14	18	OCIAD1

ABCA6	0	0.39339177	0.414	0	0	18	ABCA6
PTPN11	2.13E-48	0.39311854	0.448	0.045	3.45E-44	18	PTPN11
HEPN1	0	0.39296488	0.466	0.001	0	18	HEPN1
CHURC1	1.06E-31	0.39206366	0.586	0.106	1.72E-27	18	CHURC1
LHPP	2.49E-151	0.39121309	0.448	0.014	4.04E-147	18	LHPP
FDFT1	6.16E-49	0.38898579	0.414	0.038	1.00E-44	18	FDFT1
DNAJB2	1.47E-71	0.38759385	0.431	0.028	2.39E-67	18	DNAJB2
MTCH1	2.27E-21	0.38726201	0.5	0.113	3.69E-17	18	MTCH1
CLCN3	6.45E-63	0.38685202	0.483	0.04	1.05E-58	18	CLCN3
SESTD1	3.24E-111	0.38575295	0.448	0.02	5.27E-107	18	SESTD1
FTH16	2.74E-11	0.38425598	1	0.921	4.46E-07	18	FTH1
TRAPPC2L	2.37E-31	0.38377713	0.483	0.076	3.85E-27	18	TRAPPC2L
DYNC1H1	2.87E-18	0.38226089	0.534	0.143	4.66E-14	18	DYNC1H1
PRR18	0	0.38220825	0.397	0	0	18	PRR18
SRCIN1	0	0.38203738	0.414	0	0	18	SRCIN1
FAIM2	0	0.38143957	0.431	0.001	0	18	FAIM2
YWHAE	1.54E-19	0.38097101	0.5	0.118	2.50E-15	18	YWHAE
BCAS1	0	0.38015976	0.362	0.001	0	18	BCAS1
MRFAP1	1.18E-22	0.37998925	0.534	0.12	1.92E-18	18	MRFAP1
NDUFC2	9.17E-17	0.37957525	0.638	0.206	1.49E-12	18	NDUFC2
ZBTB16	7.80E-27	0.37857248	0.448	0.075	1.27E-22	18	ZBTB16
GCSH	3.75E-58	0.37793273	0.448	0.038	6.09E-54	18	GCSH
NPC1	5.69E-46	0.37735767	0.397	0.037	9.25E-42	18	NPC1
B3GAT1	9.67E-270	0.37734994	0.379	0.005	1.57E-265	18	B3GAT1
SLC6A8	3.63E-296	0.37658499	0.379	0.004	5.89E-292	18	SLC6A8
SPAG9	1.64E-24	0.3762958	0.5	0.099	2.67E-20	18	SPAG9
PTGES3	3.44E-13	0.37433123	0.603	0.219	5.59E-09	18	PTGES3
RUFY3	1.62E-61	0.37424163	0.483	0.041	2.64E-57	18	RUFY3
TMEM206	1.94E-96	0.37235082	0.431	0.021	3.16E-92	18	TMEM206
SLC25A4	4.69E-87	0.37168209	0.414	0.021	7.62E-83	18	SLC25A4
NINJ2	2.08E-64	0.37126436	0.362	0.022	3.38E-60	18	NINJ2
SNX6	1.08E-17	0.371099	0.569	0.16	1.75E-13	18	SNX6
CYP27A1	9.81E-169	0.37082421	0.414	0.01	1.59E-164	18	CYP27A1
AC018647.1	0	0.37037379	0.414	0	0	18	AC018647.1
SH3GL3	0	0.37037379	0.414	0	0	18	SH3GL3
TMEM87A	3.96E-36	0.37021431	0.483	0.067	6.44E-32	18	TMEM87A
AIF1L	0	0.37020292	0.414	0	0	18	AIF1L
RAD21	6.37E-20	0.37004647	0.5	0.117	1.03E-15	18	RAD21
FAM13C	0	0.36977588	0.362	0.001	0	18	FAM13C
AKAP11	2.59E-48	0.36974871	0.448	0.045	4.20E-44	18	AKAP11

ALCAM	4.10E-38	0.36937971	0.448	0.055	6.67E-34	18	ALCAM
RAB14	1.40E-26	0.36598461	0.534	0.103	2.28E-22	18	RAB14
ZDHHC9	5.09E-252	0.36551548	0.362	0.005	8.28E-248	18	ZDHHC9
PMP2	0	0.36441074	0.397	0.004	0	18	PMP2
NFIX	1.23E-259	0.36381639	0.414	0.006	2.01E-255	18	NFIX
TALDO11	1.34E-18	0.36360251	0.603	0.17	2.17E-14	18	TALDO1
CERS2	9.40E-40	0.36252084	0.448	0.053	1.53E-35	18	CERS2
LAMP1	1.62E-18	0.3622977	0.5	0.124	2.63E-14	18	LAMP1
MAP4K4	2.90E-17	0.36126211	0.414	0.095	4.71E-13	18	MAP4K4
RDH11	8.90E-34	0.35975886	0.466	0.066	1.45E-29	18	RDH11
DIP2B	1.13E-63	0.35930806	0.448	0.034	1.84E-59	18	DIP2B
GALNT7	7.49E-91	0.35923426	0.431	0.022	1.22E-86	18	GALNT7
AGPAT4	7.52E-162	0.35907423	0.414	0.011	1.22E-157	18	AGPAT4
ATP6V0B1	9.02E-11	0.35898086	0.638	0.285	1.47E-06	18	ATP6V0B
EPB41L3	2.29E-28	0.35864066	0.466	0.077	3.72E-24	18	EPB41L3
TOB2	2.05E-54	0.35840058	0.414	0.034	3.33E-50	18	TOB2
ADAMTS8	0	0.3583976	0.31	0	0	18	ADAMTS8
GRM3	0	0.35831216	0.397	0	0	18	GRM3
TCEAL7	0	0.35805589	0.362	0	0	18	TCEAL7
FAM171A1	0	0.35737283	0.397	0.001	0	18	FAM171A1
PSMB5	1.12E-30	0.35679202	0.414	0.058	1.83E-26	18	PSMB5
PJA2	6.58E-19	0.3565986	0.5	0.122	1.07E-14	18	PJA2
LGALS3BP	3.15E-46	0.35535418	0.397	0.037	5.12E-42	18	LGALS3BP
MAP7D1	1.39E-39	0.35433416	0.431	0.05	2.26E-35	18	MAP7D1
CLU	1.24E-294	0.35421973	0.31	0.003	2.02E-290	18	CLU
GTF2I	3.08E-19	0.35379082	0.534	0.134	5.00E-15	18	GTF2I
SRPK2	5.50E-28	0.35339599	0.448	0.073	8.94E-24	18	SRPK2
ARL2	2.33E-41	0.35293752	0.5	0.063	3.79E-37	18	ARL2
PTN	0	0.35268938	0.379	0.003	0	18	PTN
TPD52	2.56E-55	0.35264493	0.448	0.039	4.16E-51	18	TPD52
TERF2IP	6.01E-20	0.3519295	0.569	0.145	9.77E-16	18	TERF2IP
ANXA51	1.47E-12	0.35167673	0.638	0.245	2.38E-08	18	ANXA5
NDUFAF3	1.35E-25	0.35156898	0.534	0.107	2.20E-21	18	NDUFAF3
PADI2	5.71E-43	0.35004075	0.448	0.049	9.28E-39	18	PADI2
DNAJA11	1.45E-20	0.34997971	0.621	0.163	2.36E-16	18	DNAJA1
C21orf91	1.76E-102	0.34974055	0.431	0.02	2.85E-98	18	C21orf91
RABAC1	1.83E-16	0.3494971	0.586	0.177	2.97E-12	18	RABAC1
GPX4	1.88E-10	0.34888134	0.621	0.271	3.05E-06	18	GPX4
SRP14	1.82E-10	0.34667769	0.776	0.41	2.96E-06	18	SRP14
RBX1	9.07E-16	0.34659043	0.586	0.181	1.47E-11	18	RBX1

VXN	0	0.34601995	0.397	0	0	18	VXN
DNAJC6	0	0.34593453	0.379	0	0	18	DNAJC6
S100A13	3.17E-93	0.3456629	0.328	0.012	5.15E-89	18	S100A13
KAZN	0	0.34542219	0.345	0.001	0	18	KAZN
PROX1	0	0.34473948	0.397	0.002	0	18	PROX1
CXADR	4.18E-134	0.34473537	0.414	0.013	6.79E-130	18	CXADR
ARPC5	5.07E-10	0.34371178	0.638	0.299	8.23E-06	18	ARPC5
BLOC1S1	3.24E-17	0.34369219	0.621	0.187	5.26E-13	18	BLOC1S1
SEC62	2.28E-11	0.34342944	0.534	0.201	3.70E-07	18	SEC62
CALD1	0	0.34320509	0.345	0.003	0	18	CALD1
WRB	1.84E-103	0.34288289	0.379	0.015	2.98E-99	18	WRB
HTRA11	1.00E-15	0.34270446	0.534	0.15	1.63E-11	18	HTRA1
MVB12B	2.84E-82	0.34204199	0.345	0.016	4.61E-78	18	MVB12B
2-Sep	5.29E-18	0.34177936	0.569	0.156	8.60E-14	18	2-Sep
RASSF2	3.59E-23	0.34168249	0.466	0.09	5.83E-19	18	RASSF2
LAMTOR5	2.78E-14	0.34167841	0.5	0.148	4.51E-10	18	LAMTOR5
KLF13	3.88E-21	0.34087043	0.534	0.122	6.30E-17	18	KLF13
DDX24	1.51E-12	0.34081021	0.638	0.241	2.46E-08	18	DDX24
BNIP31	2.51E-64	0.34041026	0.397	0.026	4.07E-60	18	BNIP3
TMEM141	3.07E-43	0.34009792	0.466	0.053	4.98E-39	18	TMEM141
PLCL1	6.73E-178	0.33963396	0.345	0.007	1.09E-173	18	PLCL1
SPTLC21	4.32E-15	0.33962104	0.431	0.112	7.02E-11	18	SPTLC2
RAB2A	8.81E-20	0.33418431	0.569	0.144	1.43E-15	18	RAB2A
RNASE12	5.95E-26	0.33406621	0.517	0.092	9.66E-22	18	RNASE1
ATP1A1	1.42E-18	0.33380965	0.448	0.102	2.30E-14	18	ATP1A1
TMED10	1.67E-11	0.33377741	0.431	0.136	2.71E-07	18	TMED10
GJC2	0	0.33357903	0.345	0	0	18	GJC2
NCAM2	0	0.33357903	0.379	0	0	18	NCAM2
PCSK6	0	0.33340824	0.328	0.001	0	18	PCSK6
FAXDC2	0	0.33246939	0.379	0.002	0	18	FAXDC2
ZKSCAN1	3.04E-29	0.33193708	0.448	0.069	4.93E-25	18	ZKSCAN1
PRNP	1.65E-25	0.33190497	0.483	0.088	2.68E-21	18	PRNP
MFSD6	8.82E-115	0.33076153	0.397	0.015	1.43E-110	18	MFSD6
FAM229B	1.08E-290	0.32999846	0.362	0.004	1.75E-286	18	FAM229B
RNF141	4.61E-45	0.32862263	0.414	0.041	7.49E-41	18	RNF141
ZDHHC20	4.42E-38	0.32856382	0.431	0.051	7.18E-34	18	ZDHHC20
GAS7	4.61E-57	0.32777094	0.397	0.03	7.49E-53	18	GAS7
R3HCC1	2.00E-60	0.32694265	0.414	0.031	3.25E-56	18	R3HCC1
CCT3	4.88E-18	0.32683778	0.466	0.111	7.94E-14	18	CCT3
MIGA1	1.25E-60	0.3256188	0.414	0.031	2.03E-56	18	MIGA1

SPCS2	2.54E-12	0.32432148	0.586	0.212	4.13E-08	18	SPCS2
ARHGEF2	6.04E-47	0.32388096	0.448	0.045	9.82E-43	18	ARHGEF2
GPSM2	4.77E-150	0.32236872	0.397	0.011	7.75E-146	18	GPSM2
THY1	0	0.32047351	0.31	0.001	0	18	THY1
ZDHHC14	6.16E-68	0.32005103	0.397	0.025	1.00E-63	18	ZDHHC14
RAB9A	5.29E-36	0.31973006	0.414	0.05	8.60E-32	18	RAB9A
ENPP4	1.37E-66	0.31955178	0.397	0.026	2.22E-62	18	ENPP4
DLG2	0	0.31936463	0.345	0.002	0	18	DLG2
PAQR6	0	0.3191089	0.362	0.002	0	18	PAQR6
DYNC1LI2	1.06E-23	0.31902764	0.414	0.071	1.72E-19	18	DYNC1LI2
LDHB	3.60E-13	0.31829955	0.534	0.172	5.85E-09	18	LDHB
SPECC1	7.61E-28	0.31705047	0.414	0.062	1.24E-23	18	SPECC1
NIPAL3	8.77E-40	0.31697428	0.379	0.039	1.43E-35	18	NIPAL3
MTDH	4.40E-10	0.31648951	0.621	0.266	7.15E-06	18	MTDH
EPB41L23	3.72E-16	0.31639394	0.586	0.168	6.04E-12	18	EPB41L23
TACC1	1.01E-15	0.31636679	0.5	0.137	1.64E-11	18	TACC1
C9orf3	9.95E-199	0.31570551	0.345	0.006	1.62E-194	18	C9orf3
SGK3	3.28E-26	0.31521098	0.414	0.066	5.32E-22	18	SGK3
HES6	8.76E-63	0.31471294	0.31	0.017	1.42E-58	18	HES6
HSBP1	7.28E-19	0.31368141	0.483	0.113	1.18E-14	18	HSBP1
COPS9	2.28E-11	0.31316501	0.5	0.175	3.71E-07	18	COPS9
SERINC5	1.66E-46	0.31272069	0.414	0.039	2.70E-42	18	SERINC5
CXXC5	1.27E-44	0.31267092	0.362	0.032	2.07E-40	18	CXXC5
DOCK5	1.30E-33	0.31157858	0.379	0.045	2.12E-29	18	DOCK5
TIMP2	6.12E-13	0.31135351	0.466	0.14	9.95E-09	18	TIMP2
HSPE12	5.75E-13	0.31024183	0.517	0.166	9.34E-09	18	HSPE1
COBL	0	0.30883397	0.328	0	0	18	COBL
SLC6A1	0	0.30857773	0.293	0	0	18	SLC6A1
ARHGAP23	0	0.30857773	0.345	0	0	18	ARHGAP23
NFASC	0	0.30832155	0.328	0.001	0	18	NFASC
LIFR	0	0.30823617	0.362	0.001	0	18	LIFR
PTP4A2	2.72E-09	0.308208	0.534	0.218	4.42E-05	18	PTP4A2
ETFRF1	3.52E-61	0.30811391	0.379	0.026	5.73E-57	18	ETFRF1
ATP6V1E1	4.96E-23	0.30804535	0.414	0.073	8.06E-19	18	ATP6V1E1
LIPE	0	0.3068711	0.328	0.002	0	18	LIPE
DAAM2	0	0.30678584	0.328	0.002	0	18	DAAM2
DLC1	0	0.30678584	0.293	0.002	0	18	DLC1
HACD3	1.92E-47	0.3067401	0.414	0.038	3.12E-43	18	HACD3
RTKN	0	0.30627446	0.345	0.003	0	18	RTKN
RHOBTB3	3.73E-34	0.30608328	0.345	0.037	6.05E-30	18	RHOBTB3

DSEL	1.40E-224	0.30550789	0.293	0.003	2.27E-220	18	DSEL
MAPRE2	2.69E-42	0.30509887	0.397	0.039	4.37E-38	18	MAPRE2
GATM	1.07E-29	0.30442931	0.379	0.05	1.74E-25	18	GATM
SAR1B	2.67E-26	0.30393601	0.414	0.065	4.34E-22	18	SAR1B
PCMT1	7.60E-15	0.3018929	0.379	0.091	1.24E-10	18	PCMT1
RTL8C	1.90E-36	0.30172358	0.328	0.032	3.08E-32	18	RTL8C
PRKAR1A	2.10E-19	0.30067721	0.466	0.102	3.40E-15	18	PRKAR1A
REXO2	2.16E-33	0.3001097	0.379	0.045	3.51E-29	18	REXO2
LMBRD1	2.09E-30	0.29990625	0.414	0.058	3.40E-26	18	LMBRD1
STXBP3	7.80E-23	0.29962807	0.397	0.068	1.27E-18	18	STXBP3
CMC2	1.44E-27	0.29902018	0.397	0.058	2.34E-23	18	CMC2
SERINC3	5.76E-19	0.29862518	0.431	0.092	9.36E-15	18	SERINC3
CTTNBP2	1.18E-24	0.29851422	0.397	0.063	1.92E-20	18	CTTNBP2
KIAA1109	3.48E-23	0.29803723	0.397	0.067	5.66E-19	18	KIAA1109
RNF130	1.57E-10	0.29761173	0.466	0.163	2.55E-06	18	RNF130
MTMR10	5.48E-60	0.29744132	0.362	0.024	8.91E-56	18	MTMR10
RAB7A	8.80E-18	0.29721388	0.483	0.117	1.43E-13	18	RAB7A
CPOX	3.74E-122	0.29719853	0.362	0.011	6.07E-118	18	CPOX
10-Sep	2.35E-106	0.29669203	0.345	0.012	3.82E-102	18	10-Sep
HIGD1A	2.79E-34	0.29636075	0.345	0.037	4.54E-30	18	HIGD1A
COL4A5	0	0.29626582	0.328	0	0	18	COL4A5
TPPP	0	0.29618038	0.31	0	0	18	TPPP
CRYL1	4.57E-41	0.29611393	0.379	0.037	7.42E-37	18	CRYL1
ZNF488	0	0.29609495	0.328	0	0	18	ZNF488
MPDZ	0	0.29600953	0.31	0	0	18	MPDZ
STXBP6	0	0.29600953	0.345	0	0	18	STXBP6
BMP7	0	0.29592411	0.31	0	0	18	BMP7
RUFY2	5.13E-57	0.29577465	0.362	0.025	8.34E-53	18	RUFY2
NSL1	3.66E-25	0.29549714	0.431	0.072	5.95E-21	18	NSL1
CLIC4	1.55E-94	0.2954269	0.345	0.013	2.53E-90	18	CLIC4
NORAD	5.84E-20	0.29505845	0.448	0.094	9.48E-16	18	NORAD
RAB4A	3.42E-24	0.29473947	0.345	0.05	5.56E-20	18	RAB4A
CADM4	0	0.29455846	0.345	0.002	0	18	CADM4
TYRO3	0	0.29447317	0.328	0.002	0	18	TYRO3
ARL8A	4.58E-29	0.29441492	0.379	0.051	7.45E-25	18	ARL8A
TUBB2A	1.13E-82	0.29424756	0.328	0.014	1.83E-78	18	TUBB2A
USP54	0	0.29421733	0.345	0.002	0	18	USP54
COLGALT2	0	0.29345023	0.328	0.003	0	18	COLGALT2
SOX8	0	0.29345023	0.31	0.002	0	18	SOX8
ABHD17B	6.91E-77	0.29323779	0.328	0.015	1.12E-72	18	ABHD17B

PIGT	9.24E-21	0.29307973	0.362	0.063	1.50E-16	18	PIGT
SEMA6A	4.84E-290	0.29259859	0.345	0.003	7.87E-286	18	SEMA6A
PAK2	2.22E-07	0.29245855	0.414	0.173	0.00360204	18	PAK2
SNX1	7.03E-34	0.29238891	0.414	0.052	1.14E-29	18	SNX1
STRN	2.50E-49	0.29211773	0.362	0.029	4.06E-45	18	STRN
ITGAV	1.66E-22	0.29164008	0.379	0.063	2.69E-18	18	ITGAV
EGLN3	7.76E-213	0.29132248	0.31	0.004	1.26E-208	18	EGLN3
SESN1	2.00E-24	0.29132044	0.397	0.064	3.25E-20	18	SESN1
MFGE8	4.57E-67	0.29130526	0.328	0.017	7.43E-63	18	MFGE8
FUT8	2.00E-84	0.29122133	0.362	0.017	3.25E-80	18	FUT8
AGAP1	2.22E-184	0.29089748	0.31	0.005	3.61E-180	18	AGAP1
USP31	1.57E-166	0.2905576	0.31	0.006	2.55E-162	18	USP31
FRMD4B	1.06E-16	0.29019964	0.362	0.075	1.73E-12	18	FRMD4B
AHSA1	2.90E-25	0.28900608	0.414	0.067	4.71E-21	18	AHSA1
SFT2D1	4.07E-19	0.28850105	0.466	0.103	6.62E-15	18	SFT2D1
SCRN1	3.81E-64	0.2884553	0.345	0.02	6.19E-60	18	SCRN1
PON2	2.10E-45	0.28839148	0.362	0.031	3.41E-41	18	PON2
TSPAN15	9.84E-59	0.28820423	0.328	0.02	1.60E-54	18	TSPAN15
MAN2A2	9.39E-58	0.28795321	0.328	0.02	1.53E-53	18	MAN2A2
NIPA1	2.31E-104	0.28623428	0.31	0.01	3.75E-100	18	NIPA1
MTURN	5.08E-38	0.28599746	0.345	0.033	8.25E-34	18	MTURN
SLIRP	6.27E-18	0.28595034	0.397	0.083	1.02E-13	18	SLIRP
JOSD2	1.62E-28	0.28580203	0.362	0.048	2.63E-24	18	JOSD2
FAM234A	6.39E-103	0.283953	0.345	0.012	1.04E-98	18	FAM234A
ZNF536	0	0.28336241	0.328	0	0	18	ZNF536
CHRM5	0	0.28327697	0.276	0	0	18	CHRM5
NEMF	4.19E-15	0.28313558	0.448	0.116	6.81E-11	18	NEMF
DDRKG1	2.07E-22	0.28280771	0.414	0.074	3.36E-18	18	DDRKG1
TARSL2	1.73E-46	0.28211402	0.328	0.025	2.81E-42	18	TARSL2
MOSPD2	1.10E-53	0.28194769	0.362	0.026	1.78E-49	18	MOSPD2
SH3GLB1	2.46E-16	0.28183359	0.448	0.109	3.99E-12	18	SH3GLB1
MAP4K5	1.14E-37	0.28163693	0.362	0.037	1.85E-33	18	MAP4K5
MAP1LC3B	1.78E-10	0.28124477	0.448	0.151	2.90E-06	18	MAP1LC3B
TCF4	1.02E-18	0.28112034	0.431	0.091	1.65E-14	18	TCF4
VDAC2	1.39E-10	0.28022738	0.414	0.134	2.26E-06	18	VDAC2
PHYHIPL	0	0.28012092	0.31	0.002	0	18	PHYHIPL
NDUFB2	6.62E-07	0.27942281	0.517	0.252	0.01076207	18	NDUFB2
DMAC1	1.37E-27	0.27930956	0.379	0.053	2.23E-23	18	DMAC1
SPTBN1	3.05E-41	0.27812962	0.328	0.028	4.95E-37	18	SPTBN1
CADM2	0	0.2776542	0.31	0.002	0	18	CADM2

NPDC1	6.67E-154	0.27731444	0.293	0.005	1.08E-149	18	NPDC1
HIP1	1.23E-55	0.27655366	0.31	0.019	2.00E-51	18	HIP1
PCBP4	2.16E-106	0.27553258	0.276	0.007	3.51E-102	18	PCBP4
CNPY2	1.06E-15	0.27540543	0.397	0.092	1.72E-11	18	CNPY2
PLEKHB2	5.63E-20	0.27523132	0.414	0.081	9.15E-16	18	PLEKHB2
STX12	4.79E-20	0.27483829	0.414	0.081	7.79E-16	18	STX12
NASP	6.10E-13	0.27447882	0.431	0.121	9.91E-09	18	NASP
HOMER3	6.62E-22	0.27394961	0.31	0.045	1.08E-17	18	HOMER3
MCRIP1	1.09E-17	0.2738602	0.362	0.071	1.77E-13	18	MCRIP1
RALGAPA1	3.95E-24	0.27342173	0.362	0.055	6.42E-20	18	RALGAPA1
AFMID	3.80E-95	0.27341546	0.293	0.01	6.17E-91	18	AFMID
COL18A1	4.70E-118	0.27333087	0.328	0.009	7.63E-114	18	COL18A1
TULP4	4.29E-31	0.27325378	0.31	0.033	6.97E-27	18	TULP4
KLF9	6.28E-14	0.27311076	0.345	0.079	1.02E-09	18	KLF9
NAPEPLD	1.28E-98	0.27197838	0.31	0.01	2.07E-94	18	NAPEPLD
KIF21A	1.46E-46	0.27195672	0.31	0.022	2.37E-42	18	KIF21A
CRBN	7.12E-12	0.27185626	0.328	0.082	1.16E-07	18	CRBN
PSD3	2.31E-85	0.27180945	0.293	0.011	3.76E-81	18	PSD3
SRP9	1.05E-11	0.27148525	0.431	0.131	1.70E-07	18	SRP9
KIF13B	1.06E-28	0.27144174	0.31	0.036	1.72E-24	18	KIF13B
PRKCSH	1.37E-22	0.27134608	0.328	0.049	2.23E-18	18	PRKCSH
MORF4L1	3.11E-10	0.27131615	0.552	0.211	5.05E-06	18	MORF4L1
STAMBP	2.05E-34	0.27127717	0.345	0.037	3.32E-30	18	STAMBP
INF2	4.04E-84	0.27079645	0.31	0.012	6.57E-80	18	INF2
PTK2	1.37E-83	0.27079645	0.31	0.012	2.22E-79	18	PTK2
PAFAH1B2	1.08E-19	0.27069626	0.31	0.05	1.76E-15	18	PAFAH1B2
PDE1C	0	0.27029033	0.276	0	0	18	PDE1C
NACAD	0	0.27011946	0.276	0	0	18	NACAD
SOX10	0	0.27003404	0.31	0	0	18	SOX10
RPS6KA5	1.02E-30	0.26922235	0.328	0.037	1.66E-26	18	RPS6KA5
PRRG1	0	0.26918021	0.276	0.001	0	18	PRRG1
PHPT1	1.11E-10	0.26864964	0.414	0.131	1.80E-06	18	PHPT1
KIAA1324L	0	0.26849768	0.31	0.002	0	18	KIAA1324L
NRBP2	1.45E-66	0.26843676	0.293	0.014	2.35E-62	18	NRBP2
CDK19	6.69E-43	0.26837741	0.328	0.027	1.09E-38	18	CDK19
C1orf198	0	0.26832712	0.31	0.002	0	18	C1orf198
SLC11A2	7.53E-19	0.26818216	0.31	0.051	1.22E-14	18	SLC11A2
CACYBP	2.76E-15	0.26794603	0.379	0.086	4.48E-11	18	CACYBP
TMC6	2.32E-15	0.26786798	0.379	0.085	3.77E-11	18	TMC6
ANK2	1.24E-208	0.26738955	0.259	0.003	2.01E-204	18	ANK2

PEPD	4.55E-17	0.26633869	0.379	0.079	7.40E-13	18	PEPD
CERCAM	2.07E-188	0.26628265	0.276	0.004	3.37E-184	18	CERCAM
FERMT2	8.70E-190	0.26594231	0.293	0.004	1.41E-185	18	FERMT2
EIF5	4.01E-06	0.26546639	0.431	0.206	0.06508075	18	EIF5
TMEM106B	2.87E-29	0.26545247	0.345	0.042	4.66E-25	18	TMEM106B
GRIA2	0	0.26543202	0.293	0.002	0	18	GRIA2
PPP2R2B	2.10E-67	0.26541104	0.328	0.017	3.42E-63	18	PPP2R2B
NOVA1	1.30E-227	0.26483701	0.259	0.002	2.12E-223	18	NOVA1
RALGDS	6.57E-42	0.26381782	0.345	0.03	1.07E-37	18	RALGDS
ACER3	7.43E-25	0.26381782	0.328	0.044	1.21E-20	18	ACER3
FKBP2	4.13E-09	0.26321785	0.379	0.127	6.71E-05	18	FKBP2
TLE4	2.83E-16	0.26296315	0.397	0.088	4.60E-12	18	TLE4
TSPAN5	3.26E-54	0.26272917	0.31	0.019	5.31E-50	18	TSPAN5
DOCK9	9.78E-124	0.2624605	0.293	0.007	1.59E-119	18	DOCK9
NBPF1	4.50E-99	0.26093572	0.293	0.009	7.32E-95	18	NBPF1
ENOPH1	8.65E-37	0.2605972	0.345	0.034	1.41E-32	18	ENOPH1
BCAP29	3.80E-19	0.25979366	0.345	0.061	6.17E-15	18	BCAP29
PFDN2	5.26E-14	0.25927407	0.448	0.121	8.55E-10	18	PFDN2
ZCRB1	3.13E-15	0.25816897	0.379	0.086	5.08E-11	18	ZCRB1
CCP110	1.75E-42	0.25755344	0.31	0.025	2.85E-38	18	CCP110
HSPA81	1.14E-05	0.25744916	0.517	0.282	0.18538646	18	HSPA8
ZCCHC17	1.30E-16	0.25738692	0.328	0.063	2.12E-12	18	ZCCHC17
GAL3ST1	0	0.2570451	0.293	0	0	18	GAL3ST1
LGI3	0	0.25695967	0.293	0	0	18	LGI3
VBP1	4.00E-25	0.25600845	0.362	0.053	6.50E-21	18	VBP1
DNER	0	0.25542304	0.293	0.001	0	18	DNER
VAMP3	1.14E-22	0.25536042	0.345	0.053	1.85E-18	18	VAMP3
RAP1GDS1	2.46E-25	0.25533446	0.31	0.04	4.00E-21	18	RAP1GDS1
SLCO3A1	2.08E-39	0.25530784	0.31	0.026	3.38E-35	18	SLCO3A1
COL9A3	1.14E-286	0.25465562	0.293	0.002	1.86E-282	18	COL9A3
CUEDC2	3.37E-20	0.25463188	0.328	0.053	5.48E-16	18	CUEDC2
CPEB2	1.34E-68	0.25460739	0.31	0.015	2.18E-64	18	CPEB2
RYBP	1.43E-27	0.25418692	0.328	0.04	2.33E-23	18	RYBP
B3GAT3	7.51E-18	0.2540656	0.31	0.054	1.22E-13	18	B3GAT3
ETFB	3.03E-12	0.25391751	0.379	0.102	4.92E-08	18	ETFB
UBL5	1.11E-06	0.25373974	0.552	0.275	0.01801687	18	UBL5
TXNL4A	5.84E-11	0.25368664	0.362	0.103	9.49E-07	18	TXNL4A
SQLE	1.61E-58	0.25368259	0.293	0.016	2.61E-54	18	SQLE
C12orf76	1.19E-35	0.25348181	0.31	0.029	1.93E-31	18	C12orf76
ITGB8	4.15E-206	0.25346301	0.276	0.003	6.74E-202	18	ITGB8

PHLDB1	9.42E-123	0.25159178	0.259	0.005	1.53E-118	18	PHLDB1
APBA2	2.47E-59	0.25124858	0.31	0.018	4.02E-55	18	APBA2
IDH21	7.46E-12	0.25084366	0.379	0.104	1.21E-07	18	IDH2
BCAN	0	1.88292218	0.861	0.001	0	19	BCAN
SRI	7.01E-46	1.41136773	0.861	0.132	1.14E-41	19	SRI
PTPRZ1	0	1.37196706	0.806	0	0	19	PTPRZ1
OLIG11	0	1.26162735	0.75	0.005	0	19	OLIG1
C1orf61	0	1.24070969	0.75	0.004	0	19	C1orf61
TSC22D1	1.32E-304	1.22144476	0.806	0.014	2.14E-300	19	TSC22D1
ZBTB201	1.38E-52	1.20921371	0.833	0.104	2.24E-48	19	ZBTB20
GPM6B1	5.10E-246	1.16082908	0.833	0.02	8.29E-242	19	GPM6B
MARCKSL11	3.68E-148	1.14695653	0.833	0.034	5.99E-144	19	MARCKSL1
SOX4	7.68E-129	1.14058623	0.75	0.032	1.25E-124	19	SOX4
CKB1	6.02E-170	1.06103622	0.833	0.03	9.78E-166	19	CKB
CADM21	0	1.00964138	0.667	0.002	0	19	CADM2
TCF12	6.55E-58	1.00603302	0.639	0.053	1.06E-53	19	TCF12
NOVA11	0	0.98940275	0.694	0.002	0	19	NOVA1
MARCKS4	5.33E-22	0.98485635	0.861	0.271	8.67E-18	19	MARCKS
GPM6A	0	0.97018741	0.75	0	0	19	GPM6A
MAP2	0	0.9589234	0.694	0.001	0	19	MAP2
DBI	1.62E-18	0.95300638	0.806	0.264	2.64E-14	19	DBI
TUBA1A1	8.95E-46	0.93725754	0.889	0.133	1.45E-41	19	TUBA1A
SOX2	0	0.93588463	0.778	0.002	0	19	SOX2
TSC22D41	6.02E-43	0.92856082	0.694	0.083	9.79E-39	19	TSC22D4
GRIA21	0	0.89185834	0.528	0.002	0	19	GRIA2
PTN1	0	0.89041246	0.694	0.003	0	19	PTN
PMP21	0	0.80659034	0.694	0.004	0	19	PMP2
RPLP03	1.04E-13	0.80479056	0.889	0.616	1.69E-09	19	RPLP0
SCG3	0	0.79842242	0.694	0	0	19	SCG3
QKI2	7.51E-23	0.79708068	0.806	0.21	1.22E-18	19	QKI
MT-CO21	2.95E-12	0.79381267	0.972	0.993	4.80E-08	19	MT-CO2
HES61	1.07E-204	0.79351495	0.694	0.016	1.74E-200	19	HES6
OLIG2	0	0.78516168	0.722	0.001	0	19	OLIG2
SCD51	0	0.77692979	0.667	0.007	0	19	SCD5
SCRG11	2.40E-252	0.76918434	0.722	0.014	3.89E-248	19	SCRG1
C11orf96	0	0.75960447	0.611	0.001	0	19	C11orf96
TUBB2B1	0	0.73602026	0.639	0.005	0	19	TUBB2B
PIK3R11	1.26E-19	0.71440128	0.75	0.209	2.05E-15	19	PIK3R1
TTC3	1.32E-38	0.70715779	0.833	0.13	2.15E-34	19	TTC3
PHYHIPL1	0	0.70523634	0.639	0.002	0	19	PHYHIPL

METR1	2.85E-100	0.69811944	0.694	0.035	4.64E-96	19	METR1
EGFR	0	0.67890513	0.528	0	0	19	EGFR
DLL3	0	0.67873463	0.472	0	0	19	DLL3
KCNQ1OT1	2.73E-36	0.67544202	0.444	0.039	4.43E-32	19	KCNQ1OT1
NCAM1	1.75E-281	0.66670262	0.694	0.011	2.85E-277	19	NCAM1
NRXN1	0	0.66480576	0.694	0	0	19	NRXN1
NRCAM	0	0.66472049	0.528	0	0	19	NRCAM
LDHB1	2.27E-21	0.66271892	0.722	0.172	3.69E-17	19	LDHB
FXD6	0	0.66123098	0.639	0.003	0	19	FXD6
CAMK2N1	3.78E-140	0.64246176	0.556	0.015	6.15E-136	19	CAMK2N1
SOX8	0	0.63419948	0.556	0.002	0	19	SOX8
PCSK1N	0	0.63215849	0.667	0.003	0	19	PCSK1N
PTMS	1.65E-32	0.61082436	0.639	0.089	2.68E-28	19	PTMS
SHD	0	0.60562425	0.556	0.001	0	19	SHD
PRDX2	4.52E-32	0.59682413	0.694	0.106	7.34E-28	19	PRDX2
MT-ND4	1.47E-09	0.59681504	0.944	0.991	2.38E-05	19	MT-ND4
POLR2F	4.58E-35	0.5936438	0.583	0.07	7.43E-31	19	POLR2F
TCF4	9.57E-37	0.59293378	0.694	0.091	1.56E-32	19	TCF4
TNR	0	0.59061252	0.417	0	0	19	TNR
LSAMP	0	0.5744265	0.556	0.001	0	19	LSAMP
CPE	0	0.57400059	0.472	0.001	0	19	CPE
ZKSCAN1	9.01E-39	0.56283152	0.611	0.069	1.46E-34	19	ZKSCAN1
SMOC1	0	0.55944524	0.5	0	0	19	SMOC1
BEX1	0	0.55876335	0.556	0.001	0	19	BEX1
NFIB	0	0.55867814	0.583	0.001	0	19	NFIB
DPYSL3	0	0.55765626	0.556	0.002	0	19	DPYSL3
EEF2	8.18E-09	0.55172144	0.694	0.359	0.00013289	19	EEF2
RHOBTB3	1.68E-48	0.55115901	0.5	0.037	2.73E-44	19	RHOBTB3
MT3	5.37E-112	0.544046	0.361	0.008	8.73E-108	19	MT3
RCN2	2.66E-50	0.54229576	0.667	0.062	4.33E-46	19	RCN2
BEX3	2.71E-101	0.53893733	0.528	0.019	4.41E-97	19	BEX3
TTYH1	0	0.53563103	0.556	0.005	0	19	TTYH1
GNAS	1.09E-11	0.530092	0.833	0.409	1.77E-07	19	GNAS
STMN1	1.65E-31	0.5273598	0.639	0.087	2.68E-27	19	STMN1
FERMT1	0	0.52726965	0.556	0	0	19	FERMT1
SOX6	0	0.52692861	0.583	0	0	19	SOX6
RPS5	2.16E-06	0.52585376	0.917	0.732	0.03510189	19	RPS5
VCAN	3.01E-17	0.521194	0.667	0.141	4.89E-13	19	VCAN
HSP90AB1	5.10E-10	0.51738999	0.833	0.384	8.28E-06	19	HSP90AB1
LINC00461	0	0.51022884	0.444	0.001	0	19	LINC00461

HIPK2	2.93E-40	0.50777085	0.611	0.065	4.76E-36	19	HIPK2
MT-CO31	5.13E-07	0.50239184	1	0.996	0.00833085	19	MT-CO3
RAB2A1	2.62E-15	0.50195879	0.583	0.145	4.26E-11	19	RAB2A
YWHAE1	1.42E-15	0.49792868	0.528	0.119	2.30E-11	19	YWHAE
C1QL1	0	0.49384796	0.444	0	0	19	C1QL1
GRIA4	0	0.49316606	0.472	0.001	0	19	GRIA4
FAM181B	0	0.49282529	0.444	0.001	0	19	FAM181B
ETV1	0	0.49078308	0.444	0.003	0	19	ETV1
NFIX1	1.97E-237	0.48721923	0.5	0.007	3.20E-233	19	NFIX
MT-ATP62	5.42E-08	0.48597064	0.972	0.997	0.0008809	19	MT-ATP6
AKAP91	1.76E-09	0.48533318	0.556	0.195	2.86E-05	19	AKAP9
MAP1B1	2.20E-287	0.48442794	0.528	0.006	3.58E-283	19	MAP1B
EEF1A12	2.31E-06	0.47660517	1	0.992	0.03759231	19	EEF1A1
AC009041.2	0	0.47487943	0.389	0.002	0	19	AC009041.2
MAPT1	0	0.47326371	0.528	0.003	0	19	MAPT
LIMA1	2.19E-76	0.46394484	0.556	0.029	3.57E-72	19	LIMA1
RAB3IP	6.27E-160	0.46362386	0.528	0.012	1.02E-155	19	RAB3IP
RPL313	2.26E-06	0.4604146	0.972	0.931	0.03676484	19	RPL3
DST1	4.82E-26	0.4594223	0.528	0.072	7.83E-22	19	DST
GALNT13	0	0.45867989	0.472	0.001	0	19	GALNT13
CTTNBP21	6.06E-27	0.45554608	0.5	0.064	9.85E-23	19	CTTNBP2
NDUFA4	3.07E-06	0.45415128	0.639	0.337	0.04992587	19	NDUFA4
PPP1R12A	1.27E-12	0.44944013	0.583	0.161	2.07E-08	19	PPP1R12A
ATP6V0E2	3.15E-46	0.44107434	0.472	0.034	5.11E-42	19	ATP6V0E2
RPS265	6.35E-06	0.43516172	0.75	0.463	0.10310781	19	RPS26
RPL53	9.45E-06	0.432352	0.889	0.792	0.15347939	19	RPL5
ID1	4.66E-87	0.43148227	0.333	0.009	7.57E-83	19	ID1
DSTN1	5.07E-17	0.42644743	0.5	0.096	8.24E-13	19	DSTN
AL078639.1	0	0.42253586	0.417	0.001	0	19	AL078639.1
PEBP11	1.57E-13	0.42151307	0.667	0.192	2.56E-09	19	PEBP1
THRA	2.03E-79	0.4207367	0.472	0.02	3.30E-75	19	THRA
FYN1	5.57E-12	0.41955796	0.5	0.127	9.05E-08	19	FYN
GABPB1-AS1	2.77E-12	0.41805801	0.556	0.152	4.50E-08	19	GABPB1-AS1
NDRG2	2.00E-44	0.41358134	0.417	0.028	3.25E-40	19	NDRG2
RDX1	1.03E-20	0.40865013	0.5	0.08	1.67E-16	19	RDX
FIS11	1.06E-14	0.40585032	0.556	0.131	1.72E-10	19	FIS1
NDUFA5	1.46E-16	0.40482065	0.472	0.087	2.37E-12	19	NDUFA5
MEG3	0	0.40452746	0.361	0	0	19	MEG3
PHLDA1	7.90E-25	0.4036819	0.333	0.031	1.28E-20	19	PHLDA1

CCND2	7.35E-16	0.40302819	0.444	0.082	1.19E-11	19	CCND2
CCNI	7.18E-07	0.40274206	0.639	0.329	0.0116599	19	CCNI
GADD45G	6.05E-28	0.39772069	0.306	0.024	9.84E-24	19	GADD45G
KHDRBS3	8.27E-50	0.3964026	0.528	0.039	1.34E-45	19	KHDRBS3
POLR2J	6.04E-15	0.39158441	0.528	0.116	9.82E-11	19	POLR2J
PSIP1	8.81E-17	0.390647	0.5	0.096	1.43E-12	19	PSIP1
ASCL1	0	0.3866877	0.361	0	0	19	ASCL1
ASIC4	0	0.38660243	0.417	0	0	19	ASIC4
SIRT21	2.06E-12	0.38594488	0.306	0.051	3.34E-08	19	SIRT2
PCDH17	0	0.38557976	0.444	0.001	0	19	PCDH17
MAPK10	0	0.38319759	0.444	0.004	0	19	MAPK10
RTN1	4.16E-58	0.38128431	0.444	0.024	6.76E-54	19	RTN1
MYL6B	3.04E-70	0.37970394	0.5	0.025	4.95E-66	19	MYL6B
TCAF1	4.27E-49	0.37962083	0.417	0.025	6.94E-45	19	TCAF1
PLP11	1.22E-134	0.37927483	0.361	0.006	1.98E-130	19	PLP1
RAMP1	2.21E-42	0.37804309	0.389	0.025	3.59E-38	19	RAMP1
SKP11	1.03E-08	0.37676137	0.667	0.269	0.00016771	19	SKP1
HNRNPA11	3.32E-06	0.37021892	0.694	0.395	0.05389261	19	HNRNPA1
MKLN1	5.50E-26	0.36857174	0.444	0.052	8.94E-22	19	MKLN1
TMEM100	0	0.36755423	0.333	0	0	19	TMEM100
ANGPTL2	0	0.36695755	0.389	0.001	0	19	ANGPTL2
DNER1	0	0.36602062	0.389	0.002	0	19	DNER
MFF	1.51E-19	0.36432543	0.472	0.075	2.45E-15	19	MFF
RPL72	7.78E-05	0.36274827	0.833	0.665	1	19	RPL7
YBX13	4.22E-05	0.35799013	0.694	0.428	0.6854533	19	YBX1
ZNF428	1.46E-15	0.3578962	0.389	0.065	2.38E-11	19	ZNF428
SUMO2	1.29E-05	0.35232294	0.639	0.33	0.2099895	19	SUMO2
MT-CO13	2.90E-06	0.35088523	0.972	0.994	0.04712799	19	MT-CO1
POLR2J3.1	1.38E-09	0.35069596	0.472	0.131	2.25E-05	19	POLR2J3.1
ARPC1A	4.53E-21	0.34812667	0.417	0.056	7.36E-17	19	ARPC1A
PPP1R14B	7.47E-11	0.34759089	0.472	0.122	1.21E-06	19	PPP1R14B
RFTN2	0	0.34736905	0.389	0.001	0	19	RFTN2
RPL231	1.96E-05	0.34713782	0.917	0.591	0.3187813	19	RPL23
GCSH1	1.20E-23	0.34681781	0.361	0.039	1.95E-19	19	GCSH
PFN2	0	0.34575154	0.417	0.002	0	19	PFN2
NDUFC21	1.74E-08	0.34465848	0.583	0.207	0.00028246	19	NDUFC2
OPHN1	1.51E-216	0.34464634	0.361	0.004	2.46E-212	19	OPHN1
SNRPN	6.42E-19	0.34394211	0.472	0.076	1.04E-14	19	SNRPN
SBDS1	1.47E-18	0.34213287	0.472	0.078	2.39E-14	19	SBDS
PGRMC11	9.12E-18	0.34175037	0.333	0.043	1.48E-13	19	PGRMC1

EIF1AX	1.12E-07	0.34069661	0.444	0.147	0.00181249	19	EIF1AX
NDUFS5	0.00018005	0.34030276	0.472	0.241	1	19	NDUFS5
PCDH91	1.69E-162	0.33660669	0.389	0.006	2.75E-158	19	PCDH9
GTF2I1	7.23E-11	0.33641342	0.5	0.134	1.17E-06	19	GTF2I
FAM110B	9.83E-54	0.33542734	0.306	0.012	1.60E-49	19	FAM110B
UQCRH	6.27E-06	0.33351478	0.611	0.299	0.10187162	19	UQCRH
RTN41	1.08E-07	0.33331719	0.611	0.242	0.00175806	19	RTN4
HSPE13	2.20E-06	0.33310862	0.444	0.167	0.03569864	19	HSPE1
SRP141	0.00090423	0.33240218	0.667	0.411	1	19	SRP14
RIC3	2.92E-59	0.33172986	0.361	0.016	4.74E-55	19	RIC3
SEC621	1.71E-06	0.3315513	0.5	0.202	0.02786472	19	SEC62
SEM1	1.42E-05	0.33150761	0.444	0.175	0.23121854	19	SEM1
SRPK21	2.41E-13	0.32977461	0.389	0.074	3.91E-09	19	SRPK2
RPAIN	7.35E-13	0.32858935	0.389	0.075	1.20E-08	19	RPAIN
CADPS	0	0.32850407	0.278	0	0	19	CADPS
FGF12	0	0.32833352	0.361	0	0	19	FGF12
KIF1B1	5.16E-27	0.32686867	0.389	0.039	8.38E-23	19	KIF1B
S100B1	7.44E-18	0.32460428	0.333	0.042	1.21E-13	19	S100B
CALD11	1.13E-160	0.32458884	0.306	0.004	1.84E-156	19	CALD1
ENHO	1.88E-224	0.32450389	0.361	0.003	3.05E-220	19	ENHO
RGCC1	2.03E-14	0.32444984	0.417	0.076	3.30E-10	19	RGCC
CAMLG	1.05E-17	0.32331229	0.472	0.08	1.70E-13	19	CAMLG
RTN31	2.46E-11	0.32229018	0.417	0.095	3.99E-07	19	RTN3
SELENOW1	1.21E-10	0.32228496	0.556	0.16	1.97E-06	19	SELENOW
NPDC11	4.63E-146	0.32204366	0.361	0.006	7.52E-142	19	NPDC1
RPS4Y1	9.30E-08	0.32032444	0.611	0.231	0.00151175	19	RPS4Y1
ELOB	6.47E-07	0.31889401	0.611	0.26	0.010518	19	ELOB
CASD1	5.58E-37	0.31823303	0.389	0.029	9.07E-33	19	CASD1
SCOC1	3.45E-33	0.31114139	0.417	0.036	5.60E-29	19	SCOC
TNK2	4.91E-25	0.31097706	0.361	0.036	7.97E-21	19	TNK2
MTPN	1.54E-07	0.31088074	0.472	0.159	0.00250632	19	MTPN
ZNHIT1	1.83E-10	0.30942925	0.444	0.112	2.97E-06	19	ZNHIT1
TOMM20	1.29E-06	0.3090328	0.528	0.21	0.02099936	19	TOMM20
ARPP21	0	0.30821608	0.306	0	0	19	ARPP21
KIF3A	2.54E-42	0.30598952	0.361	0.022	4.12E-38	19	KIF3A
TSPAN3	8.67E-19	0.30420481	0.417	0.061	1.41E-14	19	TSPAN3
DSEL1	6.60E-181	0.30413132	0.333	0.004	1.07E-176	19	DSEL
AP1S1	6.73E-25	0.30199517	0.306	0.026	1.09E-20	19	AP1S1
DDR11	3.24E-85	0.30031695	0.306	0.008	5.26E-81	19	DDR1
AMER21	1.30E-138	0.29879526	0.306	0.004	2.11E-134	19	AMER2

GOLIM4	7.67E-21	0.29735031	0.389	0.049	1.25E-16	19	GOLIM4
CCDC88A2	3.47E-07	0.29703718	0.5	0.177	0.00564395	19	CCDC88A
NFIA	1.21E-28	0.29595086	0.361	0.032	1.97E-24	19	NFIA
NDUFB6	8.19E-14	0.29583656	0.389	0.07	1.33E-09	19	NDUFB6
RPL182	0.00131308	0.29447125	0.889	0.912	1	19	RPL18
HIST1H4C1	5.11E-10	0.29386572	0.444	0.114	8.30E-06	19	HIST1H4C
PHF14	2.32E-15	0.29244012	0.472	0.089	3.77E-11	19	PHF14
C12orf57	5.36E-07	0.2918489	0.472	0.167	0.00871311	19	C12orf57
AURKAIP1	4.16E-07	0.28969672	0.417	0.132	0.00675274	19	AURKAIP1
SRP91	3.07E-05	0.28932391	0.361	0.132	0.49908918	19	SRP9
ZFAS1	1.54E-06	0.28893977	0.639	0.282	0.02507952	19	ZFAS1
TERF2IP1	1.92E-10	0.28880353	0.528	0.146	3.12E-06	19	TERF2IP
CLNS1A	7.72E-14	0.28833557	0.472	0.097	1.25E-09	19	CLNS1A
ALCAM1	2.92E-15	0.28831435	0.361	0.056	4.75E-11	19	ALCAM
NR2F1	0	0.28751153	0.306	0	0	19	NR2F1
DLGAP1	0	0.28725576	0.306	0	0	19	DLGAP1
DLL1	0	0.28648886	0.306	0.001	0	19	DLL1
GLCCI1	1.23E-13	0.2860937	0.278	0.039	2.00E-09	19	GLCCI1
CNN3	8.12E-253	0.28597791	0.278	0.002	1.32E-248	19	CNN3
CLCN31	5.89E-25	0.28584852	0.389	0.041	9.56E-21	19	CLCN3
PNISR	0.00019782	0.28550403	0.667	0.369	1	19	PNISR
MAP1A1	3.20E-153	0.28393675	0.278	0.003	5.19E-149	19	MAP1A
NAP1L11	1.69E-05	0.28281164	0.583	0.267	0.27428663	19	NAP1L1
ZEB1	4.07E-28	0.28270643	0.306	0.023	6.61E-24	19	ZEB1
RAP2A	6.89E-14	0.28177087	0.306	0.046	1.12E-09	19	RAP2A
APC	1.08E-16	0.28168949	0.333	0.045	1.75E-12	19	APC
NACA2	0.00091694	0.28106813	0.861	0.842	1	19	NACA
ZNF431	1.24E-13	0.27998196	0.306	0.046	2.01E-09	19	ZNF431
HNRNPR	6.35E-11	0.27901492	0.528	0.14	1.03E-06	19	HNRNPR
PDAP1	1.20E-10	0.27899506	0.389	0.087	1.95E-06	19	PDAP1
MAGED1	7.77E-70	0.2777537	0.306	0.009	1.26E-65	19	MAGED1
NDUFB21	0.00017137	0.27770194	0.5	0.253	1	19	NDUFB2
ZCCHC241	7.46E-47	0.27547646	0.278	0.012	1.21E-42	19	ZCCHC24
KLRC2	9.11E-55	0.27522376	0.278	0.01	1.48E-50	19	KLRC2
CLASP21	4.85E-20	0.27442824	0.306	0.032	7.88E-16	19	CLASP2
C1orf1221	1.31E-11	0.27396118	0.361	0.071	2.13E-07	19	C1orf122
GABARAPL21	3.43E-06	0.2733365	0.444	0.163	0.05574116	19	GABARAPL2
LUC7L31	2.91E-07	0.27332049	0.639	0.252	0.00472765	19	LUC7L3
BEX2	5.64E-47	0.2732044	0.306	0.014	9.16E-43	19	BEX2
RPSA3	0.0003311	0.27261619	0.944	0.734	1	19	RPSA

MAP9	2.52E-48	0.27253219	0.306	0.014	4.10E-44	19	MAP9
EID11	1.94E-08	0.27220622	0.611	0.211	0.00031591	19	EID1
NME1	1.86E-13	0.27189065	0.333	0.054	3.03E-09	19	NME1
CSNK1E	1.48E-21	0.27113605	0.333	0.035	2.41E-17	19	CSNK1E
SLC25A3	0.00319079	0.2700992	0.472	0.286	1	19	SLC25A3
ZNF7081	5.24E-14	0.26891994	0.278	0.037	8.51E-10	19	ZNF708
MT-ND52	0.00456119	0.26891637	0.889	0.818	1	19	MT-ND5
TCEA1	4.36E-08	0.26740281	0.444	0.134	0.00070852	19	TCEA1
FKBP3	7.13E-09	0.26733289	0.333	0.078	0.00011579	19	FKBP3
KIZ	5.22E-28	0.2671707	0.278	0.02	8.49E-24	19	KIZ
NLGN1	0	0.26654339	0.278	0	0	19	NLGN1
NKAIN4	0	0.26620235	0.306	0	0	19	NKAIN4
SOD11	8.61E-07	0.26617149	0.528	0.198	0.01399829	19	SOD1
DPP6	0	0.26594665	0.278	0.001	0	19	DPP6
ZNF462	0	0.26586143	0.306	0.001	0	19	ZNF462
TRIM9	0	0.26586143	0.278	0.001	0	19	TRIM9
RND2	2.19E-272	0.2652651	0.278	0.001	3.55E-268	19	RND2
ENAH	7.96E-253	0.26509479	0.278	0.002	1.29E-248	19	ENAH
APP1	5.50E-13	0.26466566	0.278	0.041	8.93E-09	19	APP
GRID2	3.08E-285	0.26449892	0.306	0.002	5.01E-281	19	GRID2
ZBTB161	5.94E-09	0.26419194	0.333	0.076	9.65E-05	19	ZBTB16
SLC44A11	9.47E-18	0.26401276	0.306	0.036	1.54E-13	19	SLC44A1
ATP6V1G1	0.00024495	0.26345133	0.472	0.238	1	19	ATP6V1G1
TXN	1.54E-05	0.26344182	0.444	0.172	0.25003401	19	TXN
FHL1	9.69E-164	0.26296831	0.306	0.003	1.57E-159	19	FHL1
POLD2	1.93E-27	0.26283555	0.306	0.024	3.14E-23	19	POLD2
CD24	5.31E-119	0.26160973	0.278	0.004	8.64E-115	19	CD24
GOLM1	2.11E-119	0.26144003	0.306	0.005	3.42E-115	19	GOLM1
BPTF	1.51E-07	0.26031727	0.556	0.196	0.00244919	19	BPTF
PDLIM5	2.82E-25	0.25578947	0.333	0.03	4.58E-21	19	PDLIM5
SPCS21	3.18E-08	0.25552176	0.611	0.213	0.00051608	19	SPCS2
SETD5	1.32E-13	0.25542608	0.389	0.07	2.15E-09	19	SETD5
CCSER2	6.69E-12	0.2547129	0.361	0.069	1.09E-07	19	CCSER2
FMC1	2.69E-23	0.25446869	0.333	0.033	4.37E-19	19	FMC1
CCT31	1.13E-07	0.25417683	0.389	0.112	0.00183912	19	CCT3
QDPR1	4.01E-19	0.25380895	0.278	0.028	6.52E-15	19	QDPR
HSBP11	1.80E-06	0.25227547	0.361	0.114	0.02923302	19	HSBP1
CASK	3.19E-19	0.25191462	0.306	0.033	5.19E-15	19	CASK

We identified consistency among all three datasets (mouse implanted, mouse spontaneous, and human samples) within the lymphoid compartment, which include T cells that are marked by Cd3d, e, g, in the mouse (CD3D, E, G; in the human), NK cells that are marked by Klrd1, Nkg7, Nktr (KLRD1, NKG7, NKTR in human), and B-cells that are marked by Cd79a, Cd79b, Ms4a7 (CD79A, CD79B, MS4A7 in human) (**Figure 18a, b**). With regard to myeloid cells, we used the following markers to indicate: Cd14 in mouse (CD14 in human) for monocytes, Grn (GRN in human) for microglia, C1qa (C1QA in human) for complement-expressing microglia, Itgam (ITGAM in human) for macrophages, Pirb (LILRB1 in human) for M0-like macrophages, Il1b (IL1B in human) for M1-like macrophages, Mrc1 (MRC1 in human) for M2-like macrophages, Itgax (ITGAX in human) for dendritic cells, and S100a8 (S100A8 in human) for myeloid-derived suppressor cells. Similar with lymphoid subpopulations, each of these myeloid subtypes was detected in both QPP spontaneous and allograft mouse datasets as well as in the human dataset. Further, given the spectrum nature of myeloid cell polarization, many of these markers were predictably identified across multiple myeloid subtypes (**Fig. 19a, b**). The number of cells that passed QC for each sample is available in **Table 11**. Taken together, single-cell analysis of the immune infiltrates of murine and human GBM tissues was consistent with our histopathological analysis. Our findings support the hypothesis that tumors derived from both spontaneous and allograft QPP tumors models faithfully recapitulate the immune constituents of human GBM.

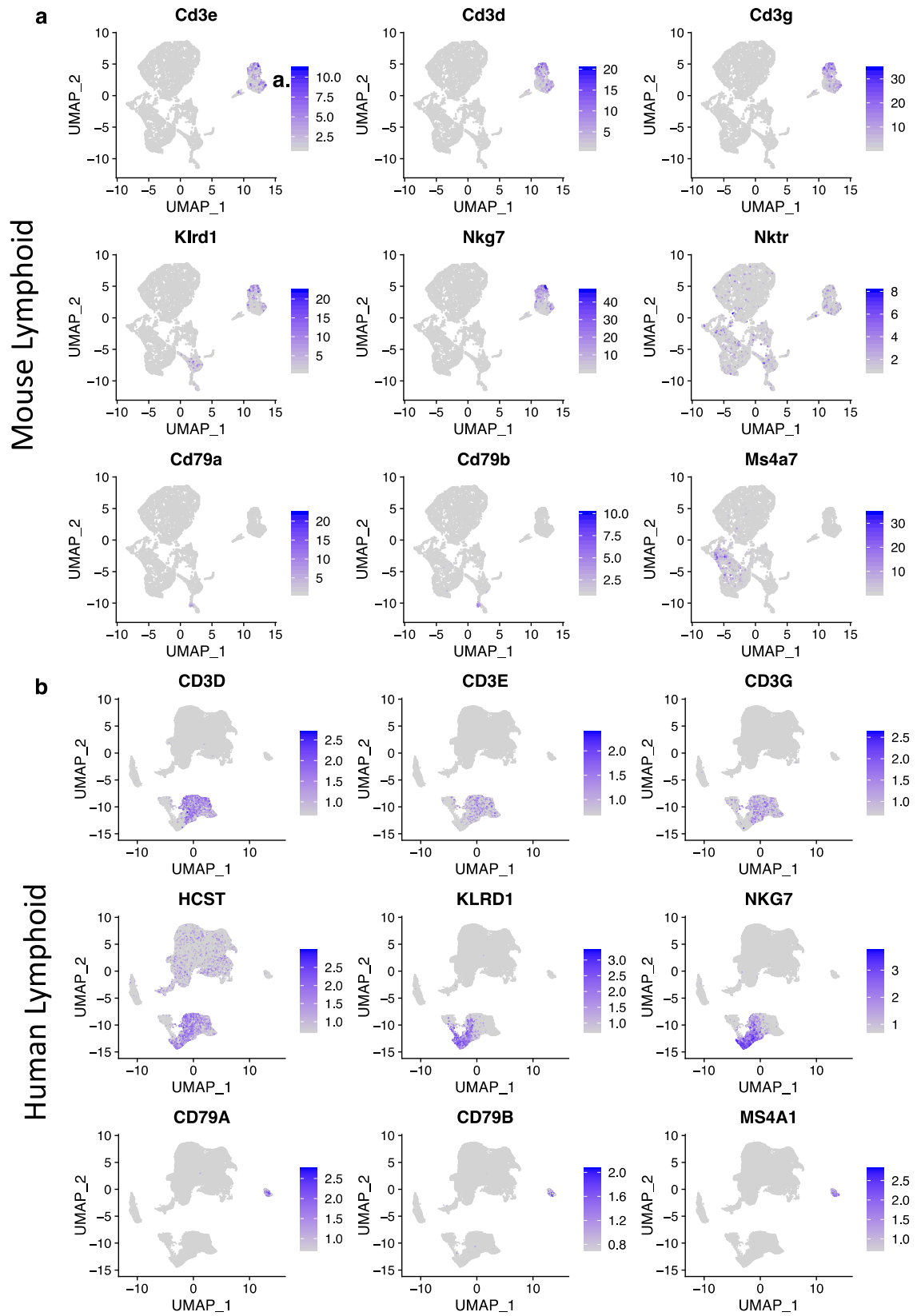


Figure 18: Lymphoid cell subtypes of human GBM are identified in the QPP model.

Resolution (0.65) clustering to reveal lymphoid subtypes in the QPP mouse model tumor or human GBM. **a, b.** UMAPs of immune constituents from (a) QPP-derived tumor (n=6) and (b) patient glioma (n=15) samples show clusters of lymphoid subtypes. Representative markers for the following populations: Cd3d, e, g (CD3D, E, G) – T cells; Klrd1, Nkg7, Nktr (KLRD1, NKG7, NKTR) – NK cells; Cd79a, Cd79b, Ms4a7 (CD79A, CD79B, MS4A7) – B cells.

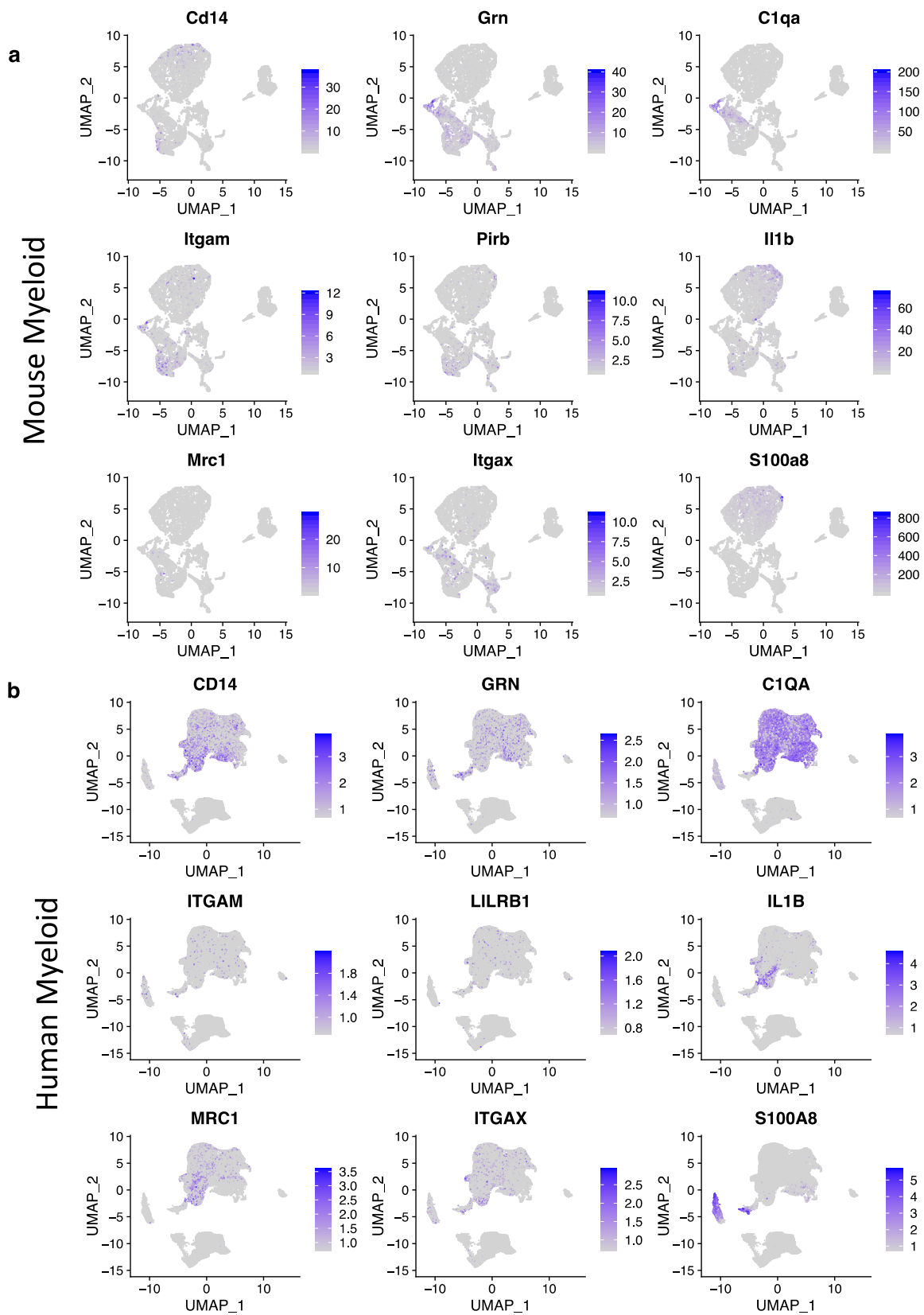


Figure 19: Myeloid cell subtypes of human GBM are identified in the QPP model.

Resolution (0.65) clustering to reveal myeloid subtypes in the QPP mouse model tumor or human glioma. **a, b.** UMAPs of immune constituents from (a) QPP-derived tumor (n=6) and (b) patient glioma (n=15) samples show clusters of myeloid subtypes. Representative markers for the following populations Cd14 (CD14) – monocyte, Grn (GRN) – microglia, - C1qa (C1QA) – complement-expressing microglia, Itgam (ITGAM) – macrophages, Pirb (LILRB1) – M0-like macrophages, Il1b (IL1B) – M1-like macrophages, Mrc1 (MRC1) – M2-like macrophages, Itgax (ITGAX) – dendritic cells, S100a8 (S100A8) – myeloid-derived suppressor cells. Given the spectral nature of myeloid differentiation and polarization many of these markers will be present in multiple subsets.

Table 11

Dataset	Cells Passed QC	Unique Genes Observed	Mouse 1 / Patient 1	Mouse 2 / Patient 2	Mouse 3 / Patient 3	Patient 4	Patient 5	Patient 6	Patient 7	Patient 8	Patient 9	Patient 10
Spontaneous	1387	11355	559	782	46							
Implanted	5493	13153	2721	1175	1597							
Human	11762	16249	7	2955	179	20	223	157	1604	1827	1415	3375

Table 12

Sample Name	RNA Shannon Heterogeneity Index	SCT Shannon Heterogeneity Index		
Implanted	8.415306	8.540268		
Spontaneous	7.0425	7.160237		
Combined	8.638796	8.764518		
Human	10.2189	10.2189		
Chi-Squared Test of Heterogeneity				
	Neutrophil	Micro/Macro	APC	
Implanted	2843	1039		686
Spontaneous	200	816		289
Summary Statistics	X-squared = 1151.3	df = 4	p-value < 2.2e-16	

Comparison of the diversity of immune species in QPP and human disease

To quantify the diversity of immune species in our cohorts, we calculated the Shannon Diversity Index (SDI) for each dataset (**Table 12**). The greatest diversity in immune cell populations was identified in the GBM cohort (SDI = 10.2779). The immune compartment was less diverse in QPP7 allograft tumors (SDI = 8.54) and in spontaneous QPP tumors (SDI = 7.16). When combined, the diversity of the combined QPP7 allograft and spontaneous QPP dataset was similar to that of the QPP7 allograft tumors alone (SDI = 8.76). Chi-squared analysis determined that the heterogeneity was statistically significantly different among the three datasets (**Table 12**).

To identify high-level signaling pathways that are conserved between our combined murine models and human GBM, we performed Gene Ontology (GO) analysis on the upregulated genes from each subtype cluster (Chen, 2020) (**Table 13**). GO analysis identified that canonical immune function pathways, including immune response (cluster 0 mouse, cluster 8 human), innate immune response (cluster 0 mouse, cluster 8 human), and response to external stimulus (cluster 3 mouse, cluster 9 human) were consistently upregulated in myeloid cells. Lastly, we also observed novel GO pathways, such as peptide signaling, in both myeloid and lymphoid arms in both species. Overall, our findings show that the immune compartments of tumors derived from spontaneous and QPP7 tumors are similar to those found human GBM.

Table 13

Mouse Cluster Upregulated Gene Ontologies

Cluster	Biological Process	Cellular Component	Molecular Function
Cxcl12hi Cd14hi Neutrophils	<p>Significantly Enriched Pathways</p> <ul style="list-style-type: none"> immune system process response to external stimulus defense response immune response regulation of response to stress response to external biotic stimulus response to other organism response to cytokine response to biotic stimulus regulation of response to external stimulus inflammatory response innate immune response regulation of defense response ion homeostasis regulation of inflammatory response cellular metal ion homeostasis cellular cation homeostasis metal ion homeostasis cellular ion homeostasis myeloid leukocyte migration 	<p>Significantly Enriched Pathways</p> <ul style="list-style-type: none"> extracellular region extracellular region part 	
Cd14lo Neutrophils			
Il1-bhi Neutrophils	<p>Significantly Enriched Pathways</p> <ul style="list-style-type: none"> immune system process response to external stimulus response to external biotic stimulus response to other organism inflammatory response leukocyte migration leukocyte chemotaxis myeloid leukocyte migration cell chemotaxis regulation of inflammatory response osteoclast differentiation neutrophil chemotaxis fat cell differentiation neutrophil migration granulocyte chemotaxis positive regulation of inflammatory response regulation of epithelial cell differentiation acute inflammatory response 	<p>Significantly Enriched Pathways</p> <ul style="list-style-type: none"> extracellular region extracellular region part 	

Cd11c+ Csf1r+ Cx3cr1+ Macrophages	<p>Significantly Enriched Pathways</p> <p>immune system process regulation of multicellular organismal process defense response response to external stimulus regulation of immune system process immune response innate immune response organonitrogen compound catabolic process regulation of response to external stimulus inflammatory response regulation of cell migration positive regulation of response to external stimulus antigen processing and presentation lymphocyte mediated immunity regulation of inflammatory response antigen processing and presentation of peptide antigen macrophage activation immunoglobulin mediated immune response B cell mediated immunity antigen processing and presentation of exogenous antigen</p>	<p>Significantly Enriched Pathways</p> <p>extracellular region extracellular space extracellular region part vesicle lysic vacuole lysosome vacuole cytoplasmic vesicle intracellular vesicle integral component of membrane intrinsic component of membrane plasma membrane part endosome cell surface late endosome external side of plasma membrane plasma membrane protein complex extracellular matrix collagen-containing extracellular matrix lysosomal membrane</p>	peptidase acti
IL-1blo Neutrophils	<p>Significantly Enriched Pathways</p> <p>cell death coenzyme metabolic process ADP metabolic process purine nucleoside diphosphate metabolic process purine ribonucleoside diphosphate metabolic process pyruvate metabolic process ribonucleoside diphosphate metabolic process nucleoside diphosphate metabolic process nucleotide catabolic process monocarboxylic acid biosynthetic process nucleoside phosphate catabolic process apoptotic mitochondrial changes regeneration organic acid transport carbohydrate catabolic process carboxylic acid transport glycolytic process ATP generation from ADP pyruvate biosynthetic process regulation of anion transport</p>		cytokine recept cytokin
Treg/NKT	<p>Significantly Enriched Pathways</p> <p>organonitrogen compound biosynthetic process translation peptide biosynthetic process amide biosynthetic process peptide metabolic process cellular amide metabolic process ribonucleoprotein complex biogenesis ribosome biogenesis ribonucleoprotein complex assembly ribonucleoprotein complex subunit organization ribosome assembly cytoplasmic translation ribosomal small subunit biogenesis</p>	<p>Significantly Enriched Pathways</p> <p>cytosolic ribosome ribosomal subunit cytosolic part ribosome ribonucleoprotein complex synapse cytosolic small ribosomal subunit small ribosomal subunit cytosolic large ribosomal subunit large ribosomal subunit extracellular region nucleolus cell surface external side of plasma membrane postsynaptic density asymmetric synapse neuron to neuron synapse postsynaptic specialization polysome polysomal ribosome</p>	structural const structural

Tgfb1+ Macrophages	<p>Significantly Enriched Pathway</p> <p>defense response response to external stimulus cell proliferation immune response inflammatory response negative regulation of multicellular organismal process negative regulation of developmental process tube morphogenesis tube development anatomical structure formation involved in morphogenesis blood vessel morphogenesis blood vessel development vasculature development cardiovascular system development response to wounding wound healing response to inorganic substance angiogenesis mononuclear cell migration extracellular matrix organization</p> <p>GeneRatio</p>	<p>Significantly Enriched Pathways</p> <p>extracellular region extracellular region part extracellular space vesicle cytoplasmic vesicle intracellular vesicle collagen-containing extracellular matrix extracellular matrix secretory vesicle extracellular exosome extracellular vesicle</p> <p>GeneRatio</p>	calcium ion bind
MhcII+ APC	<p>Significantly Enriched Pathway</p> <p>cellular amide metabolic process peptide metabolic process translation peptide biosynthetic process amide biosynthetic process antigen processing and presentation ribosome biogenesis antigen processing and presentation of exogenous antigen response to interferon-gamma antigen processing and presentation of peptide antigen ribosomal large subunit biogenesis ribosome assembly</p> <p>GeneRatio</p>	<p>Significantly Enriched Pathways</p> <p>cytosolic ribosome ribosomal subunit cytosolic part ribosome ribonucleoprotein complex lytic vacuole lysosome vacuole cytosolic large ribosomal subunit large ribosomal subunit cytosolic small ribosomal subunit small ribosomal subunit</p> <p>GeneRatio</p>	structural const structural
IFN gamma responsive Mono/Macro	<p>Significantly Enriched Pathways</p> <p>defense response immune system process response to external stimulus immune response response to external biotic stimulus response to other organism response to biotic stimulus multi-organism process response to cytokine innate immune response cellular response to cytokine stimulus defense response to other organism immune effector process regulation of defense response response to bacterium response to virus response to interferon-beta defense response to virus positive regulation of defense response regulation of innate immune response</p> <p>GeneRatio</p>		
Metabolically active Mono/Macro			

Cd8+ T cell	<p>Significantly Enriched Pathways</p> <p>organonitrogen compound biosynthetic process translation peptide biosynthetic process amide biosynthetic process peptide metabolic process cellular amide metabolic process immune response ribosome biogenesis ribosome ribonucleoprotein complex biogenesis ribonucleoprotein complex assembly ribonucleoprotein complex subunit organization ribosome assembly ribosomal large subunit biogenesis cytoplasmic translation ribosomal small subunit biogenesis</p>	<p>Significantly Enriched Pathways</p> <p>cytosolic ribosome ribosomal subunit cytosolic part ribosome ribonucleoprotein complex synapse cytosolic small ribosomal subunit small ribosomal subunit cytosolic large ribosomal subunit large ribosomal subunit cell surface external side of plasma membrane side of membrane postsynaptic density asymmetric synapse neuron to neuron synapse postsynaptic specialization polysome polysomal ribosome</p>	structural const structural
Microglia	<p>Significantly Enriched Pathways</p> <p>organonitrogen compound catabolic process protein catabolic process inflammatory response regulation of response to external stimulus behavior regulation of inflammatory response positive regulation of response to external stimulus locomotory behavior macrophage activation</p>	<p>Significantly Enriched Pathways</p> <p>extracellular region extracellular space extracellular region part vesicle lytic vacuole lysosome vacuole cytoplasmic vesicle intracellular vesicle cell surface endosome extracellular matrix collagen-containing extracellular matrix late endosome neuronal cell body apical part of cell receptor complex plasma membrane receptor complex</p>	peptidase activ
Metabolically active lymphoid cluster			
B cells	<p>Significantly Enriched Pathways</p> <p>translation peptide biosynthetic process amide biosynthetic process peptide metabolic process cellular amide metabolic process organonitrogen compound biosynthetic process ribosome biogenesis ribonucleoprotein complex biogenesis cytoplasmic translation ribosomal small subunit biogenesis ribosome assembly rRNA processing rRNA metabolic process ncRNA processing ncRNA metabolic process ribonucleoprotein complex assembly ribonucleoprotein complex subunit organization ribosomal large subunit biogenesis</p>	<p>Significantly Enriched Pathways</p> <p>cytosolic ribosome ribosomal subunit cytosolic part ribosome ribonucleoprotein complex synapse cytosolic large ribosomal subunit large ribosomal subunit cytosolic small ribosomal subunit small ribosomal subunit neuron part synapse part postsynaptic density asymmetric synapse neuron to neuron synapse postsynaptic specialization postsynapse nucleolus polysome polysomal ribosome</p>	structural const structural nu

Dendritic cells			
pDCs			

Human Cluster Upregulated Gene Ontologies

Cluster	Biological Process	Cellular Component	Molecular Function
---------	--------------------	--------------------	--------------------

CX3CR1 ^{hi} Microglia			<p>transmembrane signal</p> <p>signal</p> <p>molecular</p> <p>histone</p> <p>metal ion transmembrane</p>
IFNGR+			<p>signaling</p> <p>molecular</p> <p>transmembrane signaling</p>
CD8+ T Cells			<p>structural molecule</p> <p>structural constituent of</p> <p>antigen</p>
Phagocytic macro/microglia			
NF-κB Pathway Activated			<p>luciferase-type RNA polym</p> <p>RNA po</p>

PLCG2 ^{hi} QKI ⁺ Phagocytic macro/microglia			
CCL2+ FCGR1A ^{hi} DC/Macro	<p>Significantly Enriched Pathways</p> <p>defense response inflammatory response leukocyte adhesion leukocyte chemotaxis cellular response to interferon-gamma cell chemotaxis response to interferon-gamma myeloid leukocyte adhesion regulation of ERK1 and ERK2 cascade ERK1 and ERK2 cascade mononuclear cell migration neutrophil chemotaxis neutrophil migration granulocyte chemotaxis granulocyte migration</p>		<p>receptor activator activity</p> <p>receptor ligand activity</p> <p>receptor regulator activity</p> <p>cytokine receptor binding</p>
PRF1+ NKG7 ^{hi} NKs			
RORA+ IL7Ra+ ILCs			
NKTs	<p>Significantly Enriched Pathways</p> <p>antigen binding</p>		<p>site of me</p> <p>cytosolic small ribosomal</p> <p>small ribosomal</p>

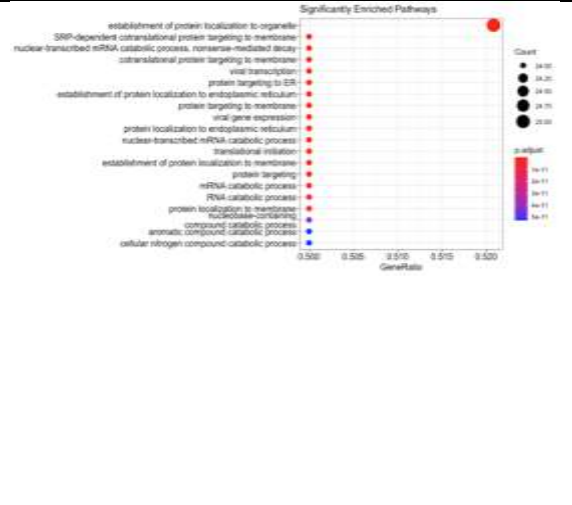
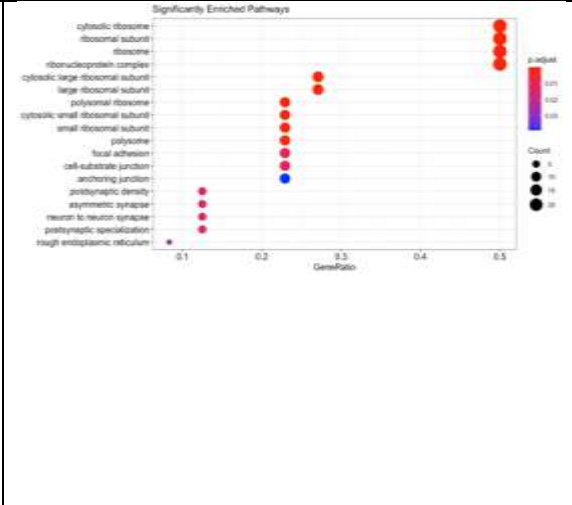
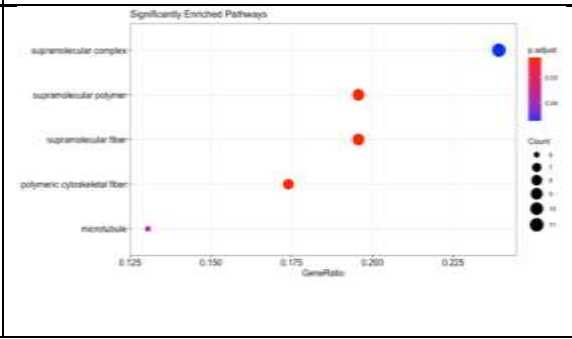
B cells			structural constituent of r structural molecu RNA RNA
Metabolically active (Mitochondrial)			
MKI67+			structural constituent of

Table 13: Conserved Gene Ontology (GO) pathways from immune isolates of QPP-derived tumors and human GBM. We took the full list of positively differentially expressed genes for each cluster at the subtype resolution [0.65 for mice 0.8 for humans] we performed GO pathway analysis on this full list for each cluster and catalogued the top gene ontologies for each cluster in biological processes, molecular function, and cellular component.

Discussion

In this study, we characterized the immune compartment of spontaneous and allograft QPP tumors alongside human GBM samples to determine whether QPP tumors represent an improved pre-clinical tool to model and study the immunogenic diversity of human GBM. The limited availability of animal models that faithfully recapitulate the pathogenesis, histopathology, and development of GBM likely contribute to the poor clinical success rate of candidate drugs against this deadly disease. To address this resource gap, we previously developed the QPP GEMM, which spontaneously develops heterogeneous tumors with features similar to human GBM (Shingu et al 2017). We encourage others to characterize other available models, as there is a paucity of models in general for gliomas, and, furthermore, for studies that require an intact immune system.

First, we created the QPP7 cell line model, which we derived from a spontaneous tumor from a QPP GEMM. We used QPP7 to derive secondary tumors by implanting cells into the striatum of C57Bl6/j mice. Immunohistochemistry and scSEQ analyses of both spontaneous QPP and allograft QPP7 tumors showed that, for both models, the immune compartment closely approximated that found in human GBM. Specifically, both mouse tumor models and human GBM tissue were characterized by an immune compartment

dominated by immunosuppressive myeloid cells, with relatively smaller populations of NK, B and T cells. This finding is consistent with other recent studies of human GBM (Friebel et al., 2020; Klemm et al., 2020). Subtype analysis of the myeloid compartment demonstrated similar complexity and proportions of myeloid cell subtypes between the mouse and human glioma cohorts.

Interestingly, although the immune cell populations were similar between mouse and human tumors, they appear to be driven by different transcriptomic programs (i.e. CSFR3+ neutrophils in humans compared to Cxcl12^{hi}Cd14^{hi} neutrophils in mouse). We observed an enrichment of neutrophils, T cells, and NK cells in QPP7 allograft tumors compared to spontaneous QPP tumors. In human tumor tissue, we observed increased lymphoid and neutrophil infiltration in HGG tumors compared to LGG tumors, as well as a shift in the myeloid population from one of a more microglial-dominant signature to a more macrophage-dominant signature (Venteicher et al., 2017). This may indicate that the QPP7 allograft model, which has been cultured *ex vivo*, has increased aggressiveness compared to the spontaneous QPP model.

Slight variations were observed among the three tumor types. Higher neutrophil infiltration was detected in QPP-derived tumors compared to human tumors. This discrepancy might reveal a *bona fide* over-representation of intratumoral neutrophils in the QPP model, and/or it could indicate a methodological artifact. For example, it could result from the high overlap of MDSC and neutrophil transcriptomic profiles. Differences in the immune constituents between spontaneous and allograft QPP tumors might also result from the microenvironmental response to the mechanical implantation procedure or from the different tumor progression trajectories of these tumors. The spontaneous model presumably initiates from a few cells transformed by cre-lox recombination and then progresses into an aggressive tumor, whereas the implanted tumor starts with a bolus of

50,000 cells that have survived the selective pressure of serial passaging *in vitro*. Of note, implanted QPP tumors were enriched for neutrophils, T cells, and NK cells compared to spontaneous QPP tumors. This increase in lymphoid and neutrophil infiltration, as well as a shift from a microglial-dominant to a more macrophage-dominant myeloid population, was also observed when we compared HGG tumors to LGG tumors. Overall, these findings and the survival curve shortening suggests that implanted QPP7 cells result in a more aggressive disease compared to the spontaneous QPP model, and, thus, QPP7 allograft tumors may be more suitable for studying aggressive GBM.

GO analysis of QPP-derived and patient GBM samples showed enrichment in gene cluster with canonical immune functions, such as immune response, defense response, and regulation of immune system processes, in all three cohorts. Surprisingly, our GO analysis also found upregulation of peptide synthesis in the T cell compartment as well as peptide binding in the myeloid compartment in all three cohorts, suggesting a signaling mechanism is active that warrants further investigation.

Tumors derived from our spontaneous and QPP7 allograft models better recapitulate human disease compared to available GBM models. Currently, the most prevalent GBM model is the GL261 mouse glioma system. The GL261 cell line was generated by injecting methylcholanthrene into the brain of C57BL/6J mice to induce tumors, and divergent clones subsequently derived from the resulting tumor have been used by various groups (Szatmári et al., 2006). GL261 tumors harbor activating *Kras* mutations (expressed in ~1% of patients) and have a high TMB (GL261 – 4978/MB, GBM – 2.7/MB). They express high MHC-1 protein levels, but GL261 tumors have relatively limited expression of other immune antigens, including MHC II, B7-1, and B7-2, resulting in a limited, immunogenic phenotype. These characteristics of GL261 tumors, which vary in important ways from most GBM tumors, could explain why GL261 mouse models respond to immunotherapeutics that have

been shown to be ineffective for patients with GBM. As previously described, our QPP GEMM animals develop heterogeneous tumors, with features like all four human GBM subtypes recapitulated in different mice. It is thus reasonable to speculate that further characterization of our QPP model, as well as of human GBM tumors, may further support that the QPP model offers an opportunity to model immunogenically diverse populations like the human disease, as shown by our IHC and scSEQ findings for the cohorts in this study (Shingu et al., 2017).

Other spontaneous models of GBM include the sleeping beauty transposase-mediated model (Ohlfest et al., 2005) and virally induced systems, such as AAV or RCAS (Miyai et al., 2017). The latter systems typically rely on strong mutagenic drivers that are not common in human GBM, such as mutant *Kras*. By contrast, our spontaneously arising QPP model is induced by deletion of three key tumor-suppressor genes that are frequently mutated/deleted in human GBM patients (Gao et al., 2013; Verhaak et al., 2010). Further, our QPP-derived tumors harbor a TMB more similar to human disease compared to GL261 tumors, and our findings here show that the intratumoral immune constituents of QPP-derived tumors are similar to those found in human GBM.

Recent back-to-back publications (Friebel et al., 2020; Klemm et al., 2020) showed that patients with GBM have a highly variable immune infiltrate composed of myeloid, neutrophil, and T cell components, with smaller proportions of other immune populations present. Friebel et al performed CyTOF analysis to produce a protein-level view of the immune cell populations in primary and metastatic lesions and in IDH wild type versus IDH mutant tumors, while Klemm et al investigated the transcriptomic changes that occur with different tumor origin and IDH status the QPP models are IDH-wt. These observations are in line with what is observed in our dataset.

This study validates the QPP model as an important preclinical tool to study the immune microenvironment of GBM. Like human GBM tumors, QPP tumors are characterized by a predominantly myeloid infiltrating population with smaller T, B and NK cell populations. On the basis of their similarity to human tumors, spontaneous QPP and QPP7 allograft models could improve the accuracy of preclinical studies to predict clinical outcomes for therapeutics, and particularly for immunotherapeutic strategies for patients with GBM.

Chapter 3 – Arginase as a target in GBM

Results

Investigate the Cellular Role of Arg1 on Immune Cell Function in Normal Brain and GBM

Arg1 is a canonical marker used to define the TAM population. While its role in pathogen response is well defined, its role in cancer remains relatively unstudied. (**Figure 20**) Our preliminary immunohistochemistry (IHC) and scSEQ analyses of naive brains from C57Bl6/j (B6) mice confirmed that the majority of immune cells in this non-pathogenic context are resting microglia with low Arg1 expression. (**Figure 21**) In pathogen response, Arg1 upregulation transforms macrophages from their classically activated (pathogen response) phenotype to their alternatively activated (wound healing) phenotype through poorly understood mechanisms. To understand its role in T cell activation and phagocytosis (Pudlo, M. Céline Demougeot, 2016), we will elucidate the role of Arg1 in basic myeloid cell biology in both immortalized cell lines and primary cultures of myeloid cells. We previously used our QPP inducible GEMM of spontaneous GBM, as well as our QPP-derived cell lines implanted in the striatum of immunocompetent B6 mice, to further investigate the immune constituents in GBM tumors via IHC analyses which are summarized in **Figure 4**.

L-Arginine Metabolism in Myeloid Cells

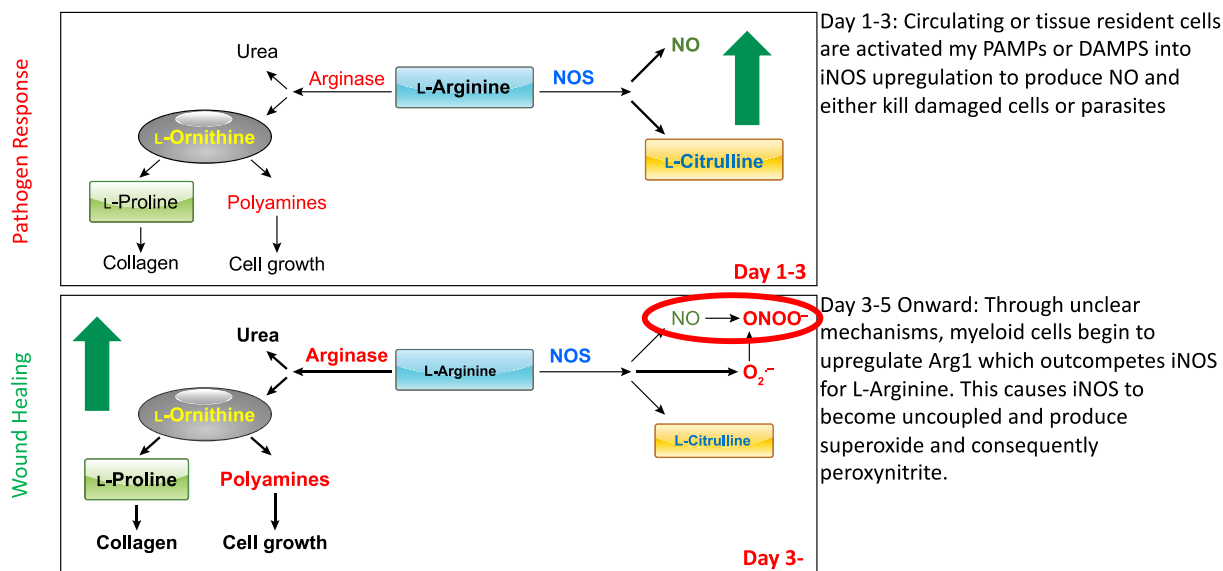


Figure 20 Arginine Metabolism in Myeloid Cells. Adapted from Caldwell, R.W., Rodriguez, P.C., Toque, H.A., Narayanan, S.P., Caldwell, R.B., 2018. Arginase: A Multifaceted Enzyme Important in Health and Disease. *Physiol. Rev.* 98, 641–665. <https://doi.org/10.1152/physrev.00037.2016> to show the cancer specific relevance of this pathway

Naïve Mouse Brain – Negative Controls

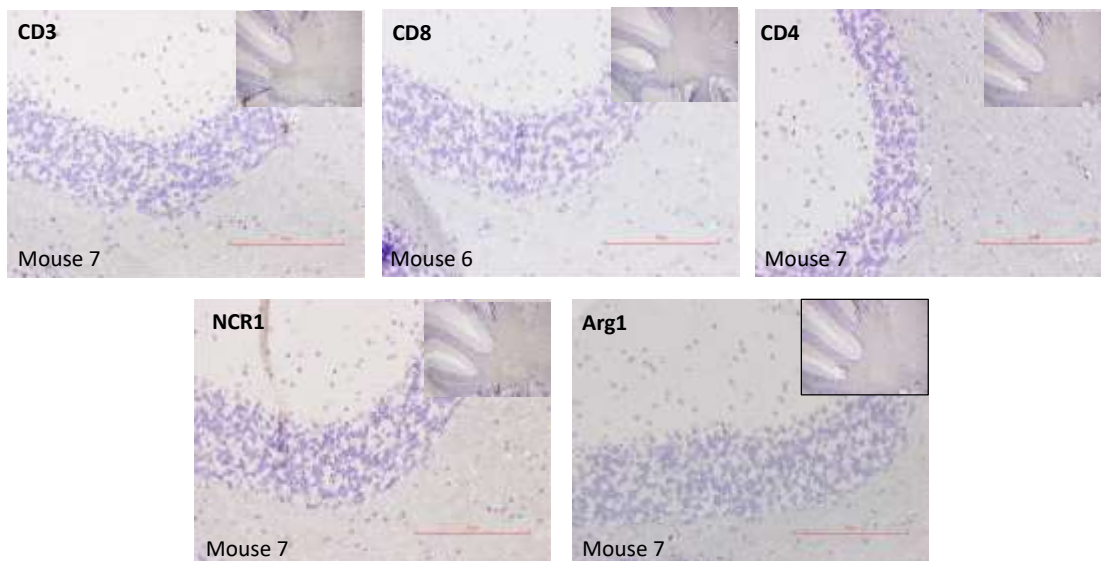


Figure 21 IHC for Immune Markers in the Naïve Mouse Brain. Representative stains of n=5 C57Bl6/j mice showing expression of Cd3, Cd8, Cd4, Ncr1, and Arg1 in the naïve brain. The negative stains confirm arginase is expressed in the pathogenic condition alone

We hypothesize removal of Arg1 in myeloid cells infiltrating GBM will increase survival and tumor-specific immune response. To determine the role of Arg1 in tumor progression *in vivo*, we have acquired Arg1^{flox} mice and crossed them with our CX3CR1-Cre^{ERT2} lines, to create mice homozygous for both genes. These crosses have created mice in which Arg1 KO can be selectively induced in myeloid cells with a tamoxifen injection. (**Figure 22**)

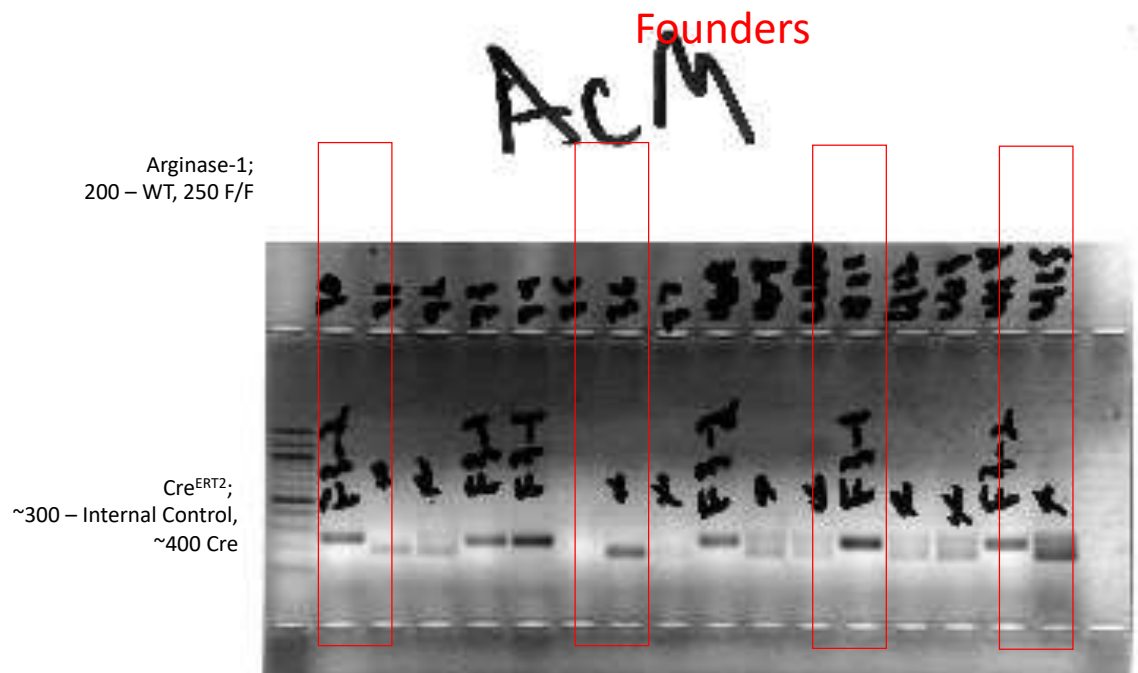


Figure 22 Genotyping of Founders of Inducible Arg1 Knock-out Colony. Top half of the Gel shows genotyping against the Arg1 locus with the inserted flox allele showing up at 250bp while the wild type allele shows up at 200bp. The bottom half of the gel shows

genotyping against the Cre locus, and internal control is included to ensure a successful PCR reaction occurred, the internal control shows up ~300bp while the Cre shows up ~400bp.

Determine the Impact of Arginine Metabolism in Glioma Progression

To test our the importance of Arginine metabolism at a systems biology level a cohort of (n=7) of B6 mice were implanted with 50,000 QPP#7 cells into their striatum. One group received water with L-arginine *ad-libitum* while the other group received water with a control salt (potassium hydrochloride). Animals were monitored for survival until they need to be euthanized and Kaplan-Meier survival curves were be generated. (**Figure 23**)

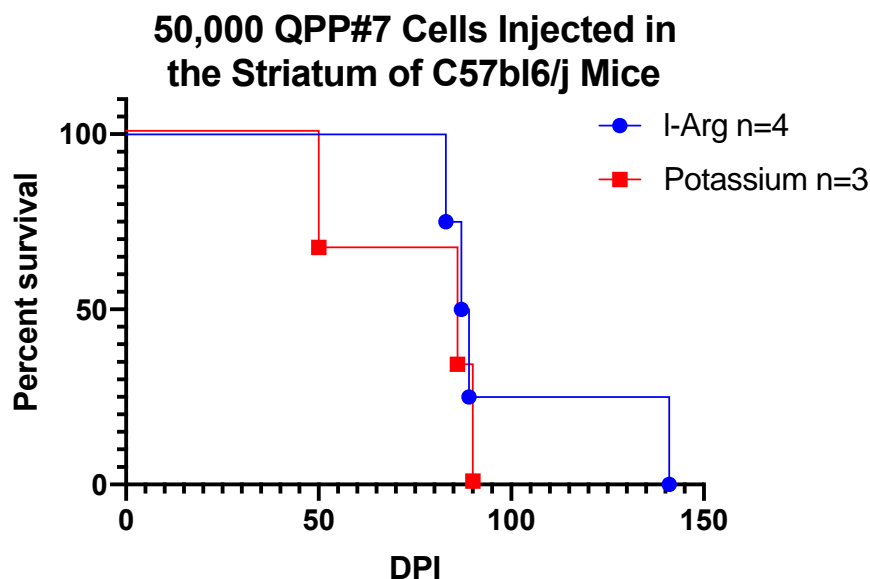


Figure 23 Dietary L-Arginine Hydrochloride Survival Curve Kaplan-meier survival curve showing the survival comparison of mice provided L-Arginine hydrochloride or a control salt in drinking water *ad-libitum*.

In order to determine the appropriate time point for tamozifen administration we confirmed the expression of our cassette using the mTmG allele by checking for expression

of GFP in myeloid cells in various organs at various time points. We were still able to see myeloid cells expressing GFP after 3 weeks in circulation which led us to select our 2 week injection time point for the next set of experiments (**Figure 24**)

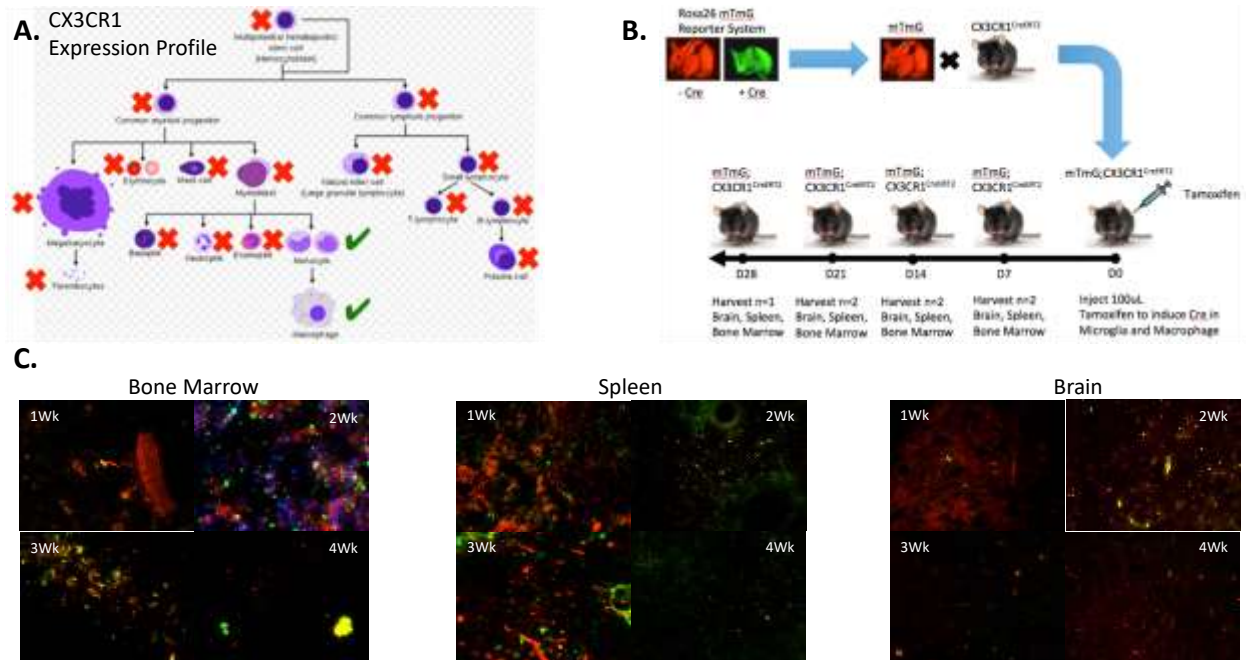


Figure 24 mTmG Tracer experiments with Cx3Cr1-Cre^{ERT2} mice. a. Expression profile of Cx3cr1 in the myeloid and lymphoid arms of the immune system. b. mTmG schematic as well as breeding schema and experimental flow chart. c. Bone Marrow, Spleen, and Brain collected at 1, 2, 3, and 4 week post tamoxifen injection.

We assessed the impact of Arg1 ablation in macrophages and microglia on tumor progression in AC mice. To this end, I implanted 200,000 QPP#7 cells into the striatum of a cohort of AC mice (n=8), which were be evenly divided into two groups. Cohorts were randomized to receive a tamoxifen or vehicle injection at one-week post tumor implantation, and then every two weeks until euthanasia. This two-week injection regimen was based on our preliminary results in **Figure 25** (50% animals with QPP#7-derived tumors moribund ~40 days post injection).

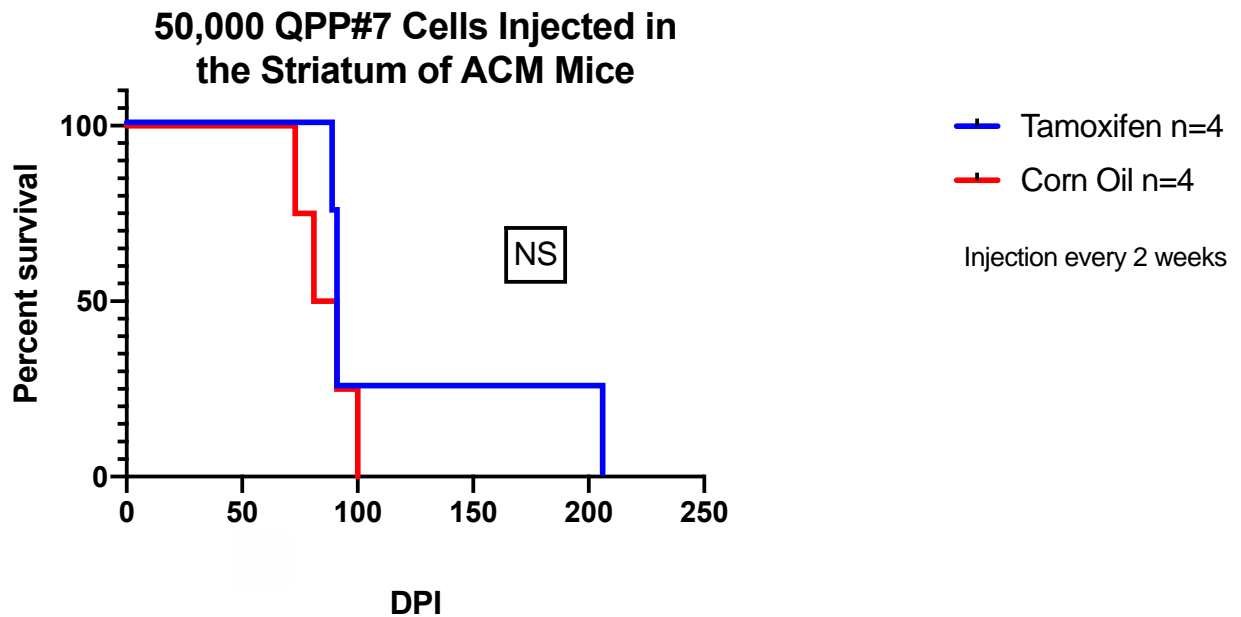


Figure 25 Survival of QPP7 cells injected into ACM Mice with Tamoxifen Injection every 2 weeks Kaplan-meier survival curve showing the survival comparison of mice injected with either tamoxifen or corn oil once every two weeks.

These results were unfortunately less than promising and so I implanted 200,000 QPP#7 cells into the striatum of a cohort of AC mice (n=23), which were divided into two groups weighted toward tamoxifen treatment. Cohorts were randomized to receive a tamoxifen or vehicle injection at one week post tumor implantation, and then every week until euthanasia. The results of these experiments are summarized in **Figure 26**.

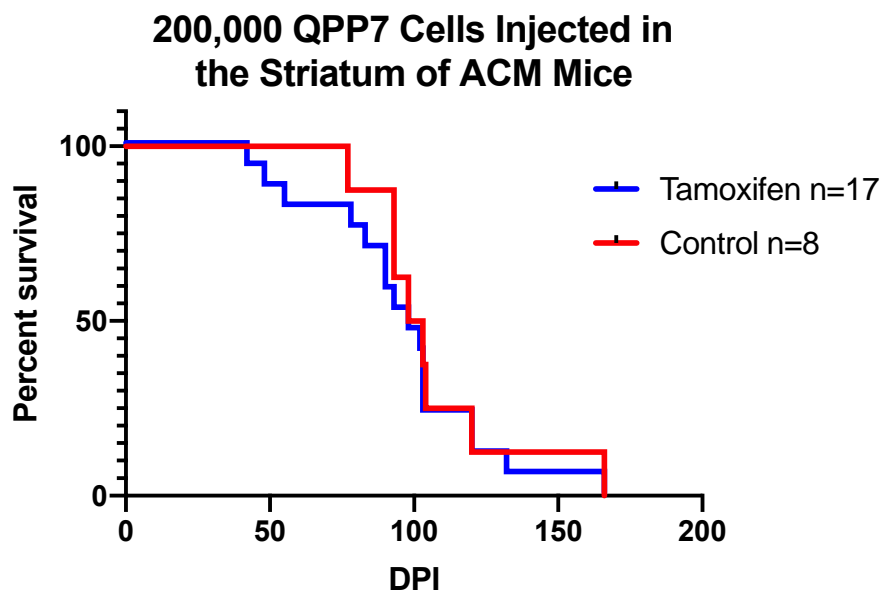


Figure 26 Survival of QPP7 cells injected into ACM Mice with Tamoxifen Injection every week Kaplan-meier survival curve showing the survival comparison of mice injected with either tamoxifen or corn oil once every week. Survival curve shows the overall survival of ACM Mice when implanted with 200,000 QPP7 cells in the striatum

These results were unfortunately also less than promising. When we profiled immune infiltrates under Arg1-expressing and -deficient conditions by IHC, we found that the knockout of Arg1 was incomplete as shown in **Figure 27**.

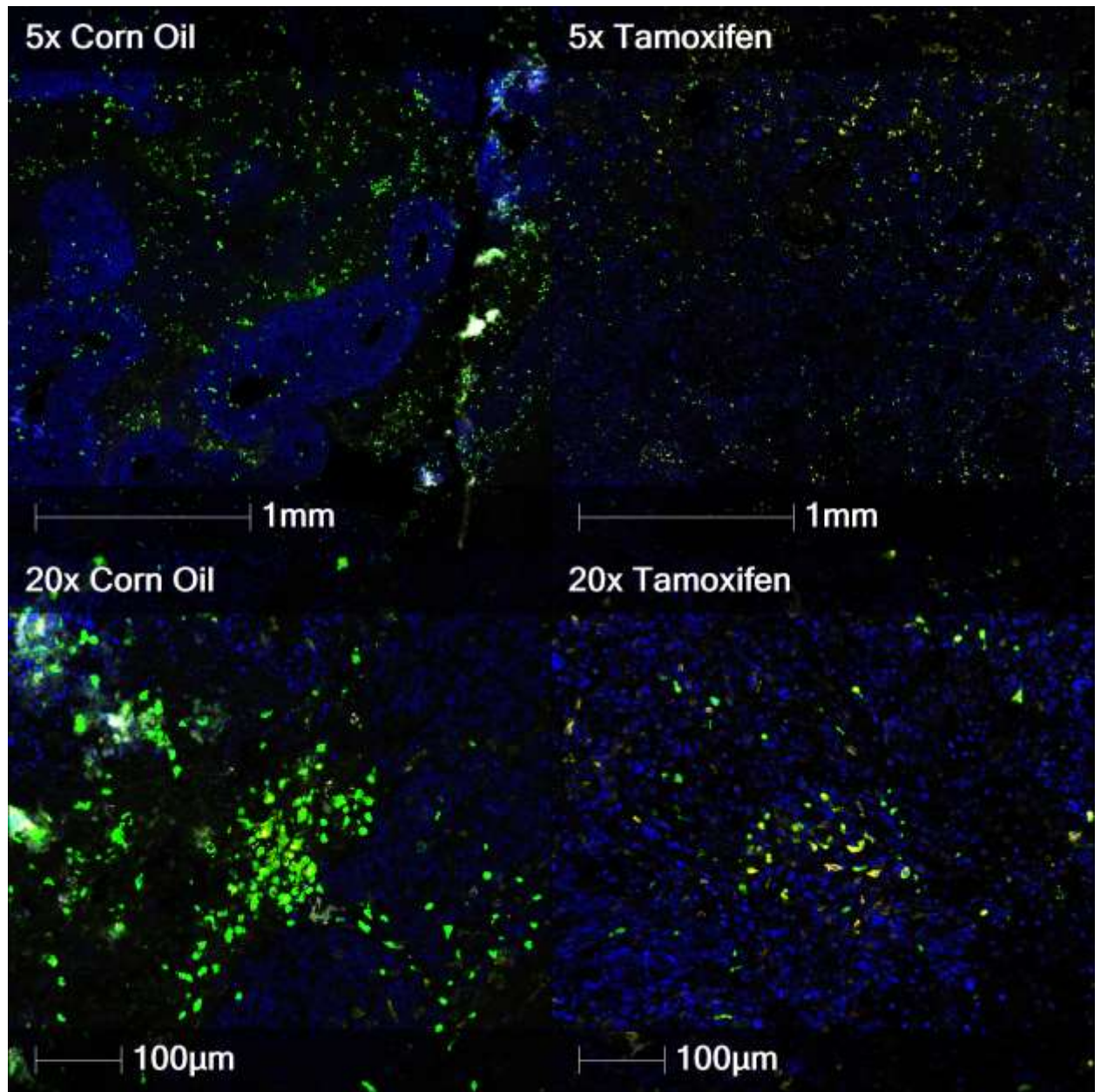


Figure 27 Arginase Expression in Control and Tamoxifen Injected Mice. Top Panels show representative images with Arg1 shown in Green at lower magnification while the bottom panels show Arg1 expression at higher magnification

Although we were able to potentially show a dysregulation of the Arg1 axis through iNos staining (**Figure 28**), our removal of Arg1 from the tumor microenvironment was clearly

insufficient. Due to these observations, we decided to switch to a continual release pellet, the experiments which test this are currently underway. **Figure 29**

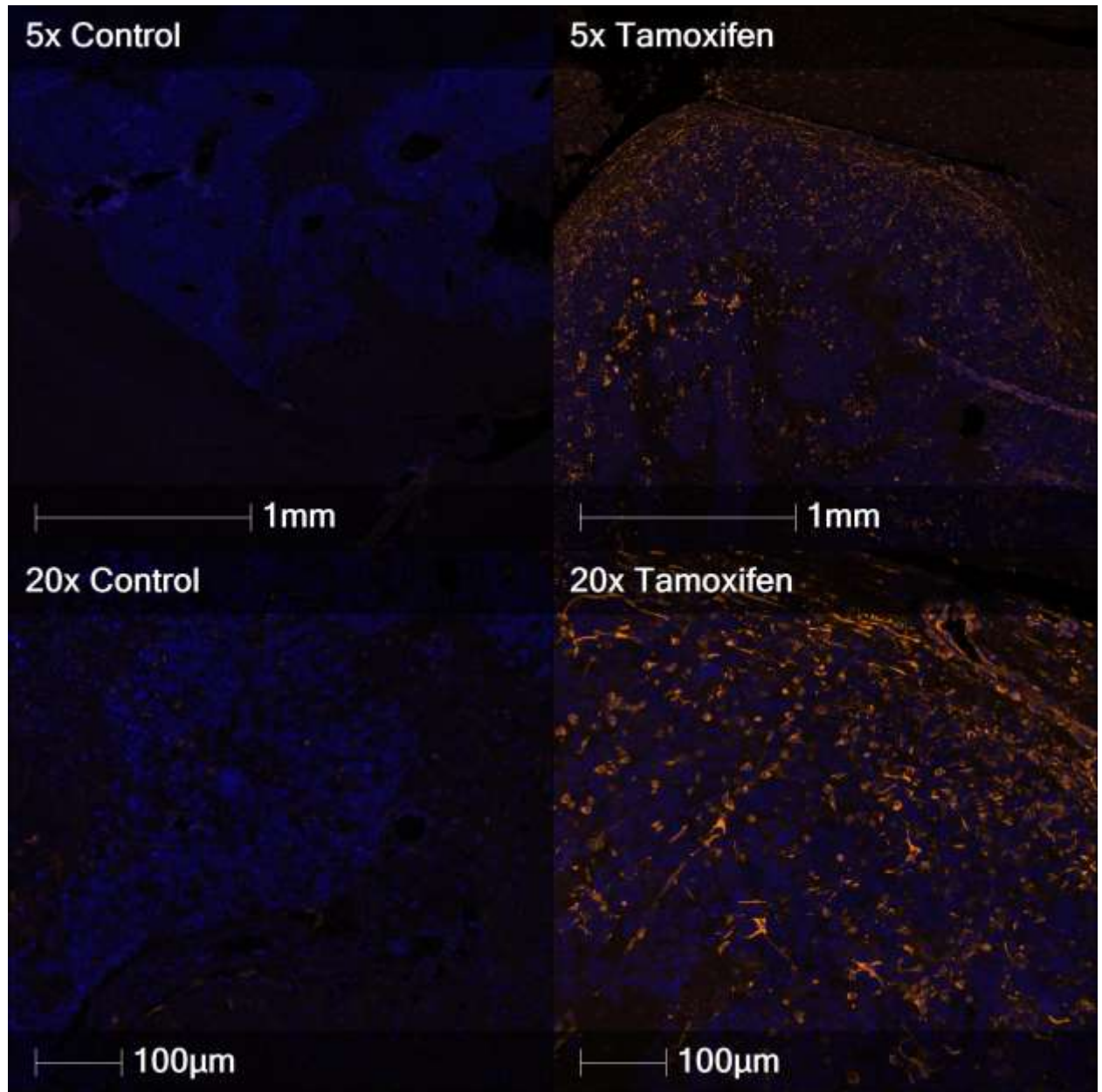


Figure 28 Inducible Nitric Oxide Synthase Expression in Control and Tamoxifen Injected Mice. Top Panels show representative images with iNos shown in Green at lower magnification while the bottom panels show iNos expression at higher magnification.

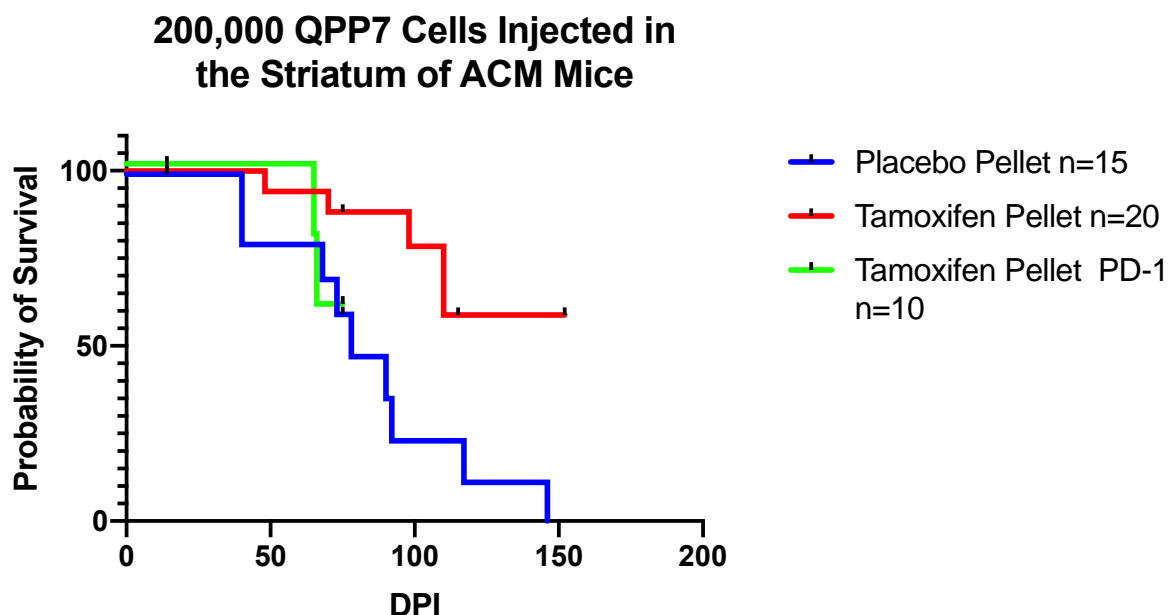


Figure 29 Survival of QPP7 cells injected into ACM Mice with Tamoxifen Slow Release Pellets. Kaplan-meier survival curve showing the survival comparison of mice injected with either tamoxifen or control slow release pellets.

Many commercially available inhibitors of Arg1 exist from both natural and synthetic sources.(Pudlo, M. Céline Demougeot, 2016) There are two inhibitor classes, reversible and irreversible, whose main side-effects are accumulation of toxic protein through inhibition of arginase in the liver, which can be ameliorated by drugs such as sodium benzoate. While most of these inhibitors have only been tested in the context of pathogen infection, they appear to be relatively well tolerated over long periods of administration, although with limited efficacy. Screens were carried out on molecules from each class with the highest reported K_i as single agents through our partners at IACS.

IACS has generated a library of compounds with cell-free inhibition of Arg1 and selected one compound IACS-009102 which was confirmed at ~5x selectivity compared to Arg2. **(Figure 30)** I then utilized Arg1 inhibitors provided by IACS and evaluate them for enzyme inhibition activity in vitro as determined by Rapidfire Mass Spectrometry. **(Figure 31)**

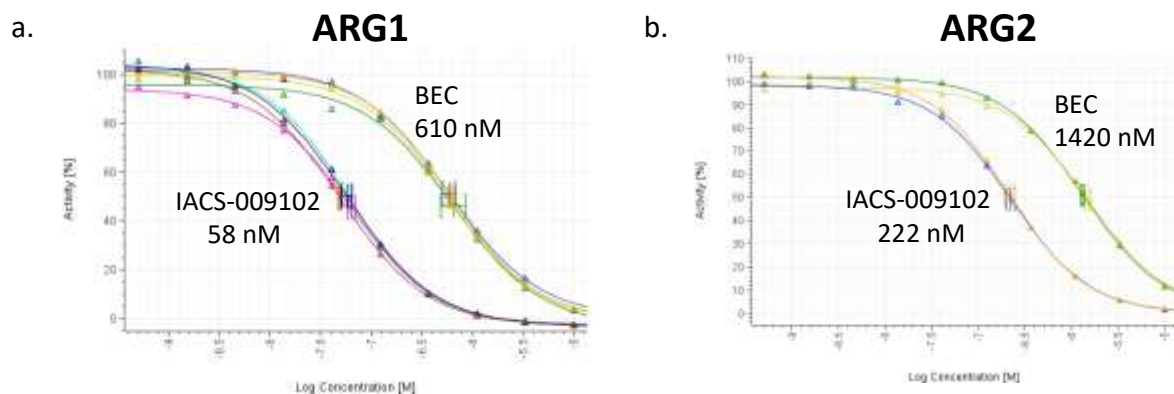


Figure 30 IACS-009102 is a Reversible, Selective, Potent Inhibitor of Arg1 in a Cell-free Setting a. Shows the inhibition of Arg1 by IACS-009102 compared to an irreversible inhibitor BEC, IC_{50} are reported. b. Shows the inhibition of Arg2 by IACS-009102 compared to an irreversible inhibitor BEC, IC_{50} are reported.

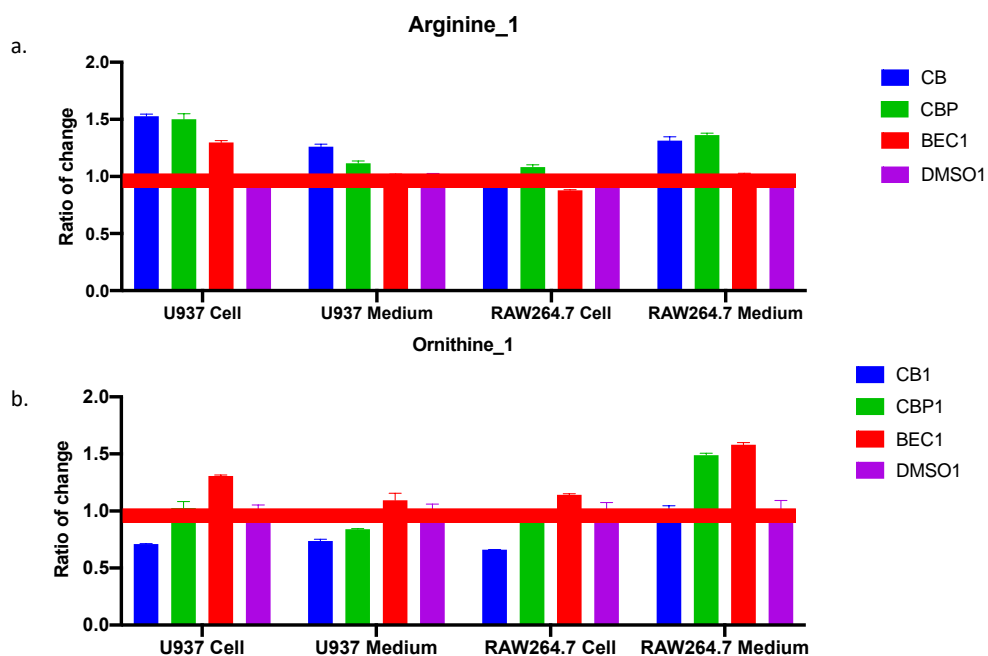


Figure 31 IACS-009102 is a Reversible, Selective, Potent Inhibitor of Arg1 in-vitro. a. Shows increased arginine accumulation with treatment of all 3 Arg1 inhibitors

indicating an inhibition of Arginase-1. b. Shows decreased ornithine accumulation with treatment of all 3 Arg1 inhibitors indicating an inhibition of Arginase-1

Based on *in vitro* results, I plan to test Arg1 inhibitors in an established GBM model. Two cohorts of n=10 B6 mice will be implanted with 200,000 QPP#7 cells into their striatum. One group will receive an Arg1 inhibitor in a dosing schedule determined from the literature or, if necessary, in collaboration with IACS scientists. The other group will receive vehicle. Mice will be monitored as mentioned above.

Furthermore, we have carried out two sets of in-vivo pilot experiments to confirm that our compound is able to cross the BBB and to enter the tumor microenvironment. In the first set of experiments mice were given 100mg/kg of the Arg1 inhibitor IACS-070400 orally and we found excellent concentration and distribution of the drug in the periphery, (Peak 100uM, detection 24h later) but more importantly we also observed brain penetrance of the compound at a concentration of greater than 1uM for at least 8h. (**Figure 32**) This is above the concentration at which we observed an effect in-vitro as demonstrated in **Figure 31**.

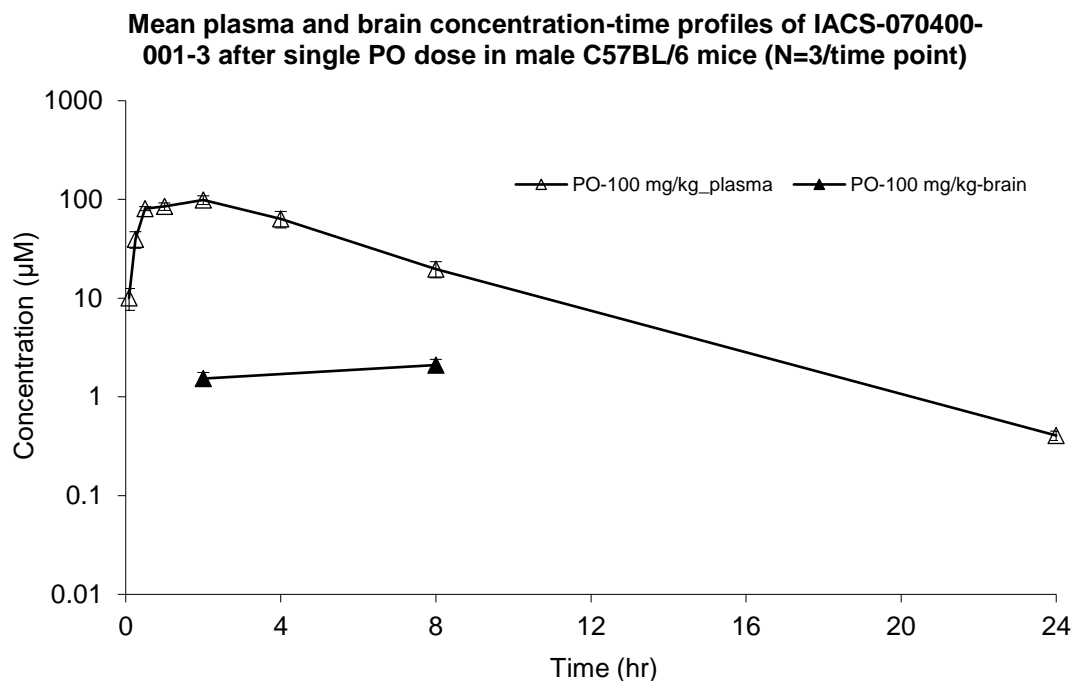


Figure 32 Distribution of IACS-070400 in Naïve Mice Graph showing the concentration in μM of IACS-070400 in both peripheral plasma and brain homogenate at the indicated time points.

Since we know the compound can enter into the naïve brain, we next aimed to determine if our compound could enter into the TME in a spontaneous GBM setting. To test this, we administered 100mg/kg IACS-070400 to sQPP tumor bearing mice and at 6h post administration collected tumor, brain, and spleen to determine drug perfusion. This set of experiments not only confirmed our initial observations that our drug was able to enter the brain, but showed that we were able to enter the tumor microenvironment as well. (**Figure 33**)

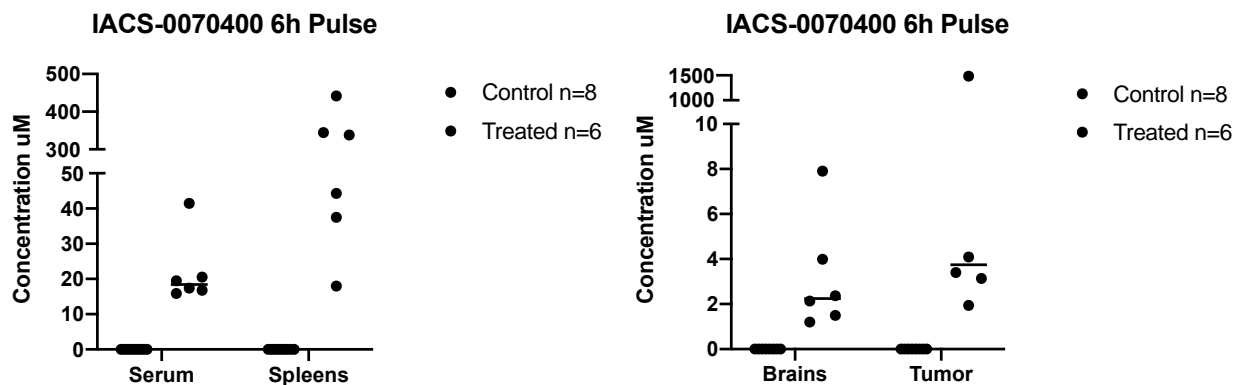


Figure 33 Distribution of IACS-070400 in sQPP Bearing Mice Graph showing the concentration in uM of IACS-070400 in both peripheral serum as well as spleen and brain or tumor homogenate at 6 hours post administration.

Discussion

In this set of experiments, we aimed to determine whether or not modulation of arginine metabolism in a mouse mode of glioblastoma would translate into increased anti-tumor immune response as well as survival. Immunotherapies have been successful in other cancers that were previously treated as a death sentence but in their current iteration they are not effective in GBM. One of the reasons that may explain this failure is that GBM is a

disease defined by myeloid cell infiltration and current therapies are targeted predominantly at activation of the lymphoid arm of the immune cells.

First, we created the Arg1^{flox/flox} Cx3cr1-Cre^{ERT2} mouse (ACM) in order to genetically target a potential therapeutic target specifically in the myeloid cells in an inducible fashion. Once the founders of the colony had been established (**Figure 22**) we performed a series of experiments to confirm expression of the cassette and deletion of Arg1 in a short-term setting. We found the founders of the colony to be both homozygous for the Arg1^{fl} allele and to be expressing Cre^{ERT2}. We furthermore confirmed induction of the cassette in macrophages with the mTmG allele. (**Figure 24**)

In parallel we performed an experiment where QPP7 cells were implanted orthotopically into the striatum of C57Bl6/j mice and then given L-Arginine hydrochloride ad libitum in their water. This was compared to a control group of mice that received potassium hydrochloride. Although our numbers were small in this experiment, we were able to see one long term survivor that gave us an indication these experiments might hold therapeutic value. (**Figure 23**)

Given these observations we implanted the same QPP7 cell line orthotopically into the striatum of our ACM mice as shown in **Figure 25**. In the first round of implantations we injected tamoxifen every two weeks starting one week after implantation. We waited one week before starting treatment in order to allow the tumor to engraft before starting treatment and then the injection of tamoxifen every two weeks was based off our observations in **Figure 24c**. Unfortunately, the results were not statistically significant, and so we decided to increase the injections to once a week which is summarized in **Figure 26**. This also did not show a statistically significant increase in survival, at which point we realized that there is a continual release of circulating myeloid cells from the bone marrow. Furthermore, That tamoxifen has a circulating half-life of approximately six hours which

explains the Arg1 expressing cells observed in **Figure 27**. This observation led us to plan an experiment with slow release tamoxifen pellets that would continually allow for the deletion of arginase which is summarized in **Figure 29**.

While the initial round of experiments for this project have not had the projected increase on survival that we had hoped for, we remain optimistic that with careful consideration of the systems biology level implications of tamoxifen administration we will be able to see an increased survival. We have shown that roughly 7.5:1 of TAM's are from the periphery compared with tissue resident microglia and we have preliminary evidence to show that, with sustained deletion of Arg1 in the circulating myeloid cells, we are able to have a benefit in survival. Furthermore, we have combined this with a lymphoid based therapy in the hopes of synergy although as of yet this doesn't appear to be of benefit.

If we do see an increase in survival with the sustained removal of Arg1, this opens the door for the clearly pharmacologically active compound that we have demonstrated in a cell free setting, (**Figure 30**) in-vitro, (**Figure 31**) in naïve mice, (**Figure 32**) and in a spontaneously generated model of GBM (**Figure 33**) is able to enter the brain and effectively inhibit Arg1. We need to first, however, determine whether or not there is a beneficial impact of the complete removal of Arg1 from the TME in **Figure 29**.

Chapter 4 – Modeling Brain Metastasis

Results

Implantation of Cell Line Library

We implanted two NSCLC lines (344p, 393p), three melanoma lines (BP, YUMM3.1, YUMM5.2), two MDST lines (LPA3-T13, LPA2-T22), and two RCC lines (13881, 13882) heterotopically into the striatum of the brain in order to model metastasis after the metastatic niche has formed from the four primary human indications to the brain. Summary features of each of the cell line can be found in **Table 14**

Table 14

Model Name	Primary Tumor	Mouse Derived From	Original Manuscript or Contributing Lab
13881	RCC	Cas9 Transgenic/ B6	Genovese Lab
13882	RCC	Cas9 Transgenic/ B6	Genovese Lab
344P	NSCLC	129Sv	Gibbons, D. L. et al. (2009) 'Contextual extracellular cues promote tumor cell EMT and metastasis by regulating miR-200 family expression', Genes and Development, 23(18), pp. 2140–2151. doi: 10.1101/gad.1820209.
393P	NSCLC	129Sv	Gibbons, D. L. et al. (2009) 'Contextual extracellular cues promote tumor cell EMT and metastasis by regulating miR-200 family expression', Genes and Development, 23(18), pp. 2140–2151. doi: 10.1101/gad.1820209.
BP	Melanoma	C57Bl6/j	Cooper, Z. A. et al. (2014) 'Response to BRAF inhibition in Melanoma is enhanced when combined with immune checkpoint blockade', Cancer Immunology Research, 2(7), pp. 643–

			654. doi: 10.1158/2326-6066.CIR-13-0215.
LPA2-T22	MDST	FVB	Federico, L. et al. (2017) 'A murine preclinical syngeneic transplantation model for breast cancer precision medicine', Science Advances, 3(4), pp. 1–12. doi: 10.1126/sciadv.1600957.
LPA3-T13	MDST	FVB	Federico, L. et al. (2017) 'A murine preclinical syngeneic transplantation model for breast cancer precision medicine', Science Advances, 3(4), pp. 1–12. doi: 10.1126/sciadv.1600957.
YUMM3.1	Melanoma	C57Bl6/j	Meeth, K. et al. (2016) 'The YUMM lines: a series of congenic mouse melanoma cell lines with defined genetic alterations', Pigment Cell and Melanoma Research, 29(5), pp. 590–597. doi: 10.1111/pcmr.12498.
YUMM5.2	Melanoma	C57Bl6/j	Meeth, K. et al. (2016) 'The YUMM lines: a series of congenic mouse melanoma cell lines with defined genetic alterations', Pigment Cell and

			Melanoma Research, 29(5), pp. 590–597. doi: 10.1111/pcmr.12498.
--	--	--	---

We implanted each of the lines above and varied the cell number which we then monitored for penetrance and survival, the results of which are summarized in **Table 15**

Table 15

Model	Disease	Tag	Cell # Injected	Take-Rate (Appx.)	Median Survival (Appx.)
344P	murine lung	Luciferase	3x10 ³	80%	28 days
			1x10 ⁴	100%	30 days
			1x10 ⁵	80%	30 days
			3x10 ⁵	100%	28 days
393P	murine lung	Luciferase	3x10 ³	90%	74 days
			1x10 ⁴	90%	47 days
			1x10 ⁵	90%	47 days
			3x10 ⁵	100%	55 days
YUMM5.2	murine melanoma	Luciferase	3x10 ³	80%	70 days
			1x10 ⁴	100%	43 days
			3x10 ⁴	100%	43 days
			1x10 ⁵	80%	49 days
			3x10 ⁵	100%	34 days
YUMM3.1	murine melanoma	Luciferase	3x10 ³	100%	35 days
			1x10 ⁴	80%	35 days
			1x10 ⁵	100%	28 days
			3x10 ⁵	100%	13 days
BP	murine melanoma	Luciferase	3x10 ³	60%	48 days
			1x10 ⁴	60%	34 days
			1x10 ⁵	80%	28 days
			3x10 ⁵	80%	28 days
LPA2-T22	MDST	no tag	1x 10 ⁴	20%	NA
			1x 10 ⁵	60%	69 Days
LPA3-T13	MDST	No tag	3 x 10 ³	60%	84 days
			3 x 10 ⁴	100%	60 days
			3x10 ⁵	100%	42 Days

We observed issues with engraftment in the RCC models which precluded our study of them. We are currently working on optimization of the implantation in order to have a viable tumor to study. **(Figure 34)** A second complication we came across was extracranial growth in both of the NSCLC lines as well as one of the melanoma lines (YUMM5.2) which was not ameliorated by a variety of methods. **(Figure 35)**

Our MDST models grew in a fashion consistent with that observed in patients, namely that it was contained in the CNS and engrafted, as well as two of the melanoma models. (BP, YUMM3.1) **(Figure 36)** It is also important to note that both of these models grow in a syngeneic setting which is essential to test immunomodulatory therapies.

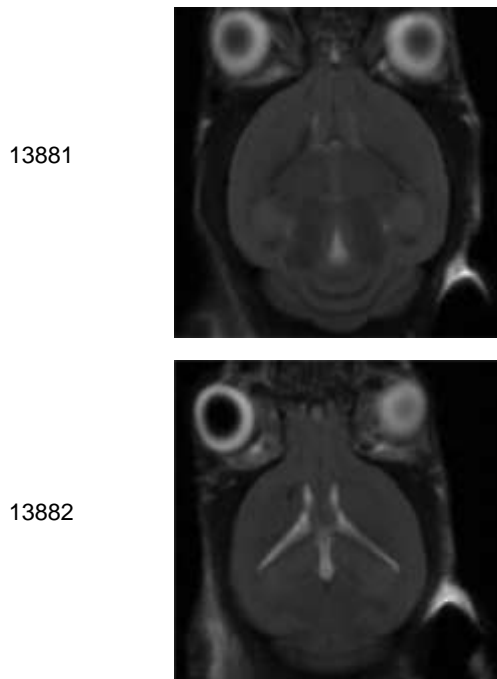
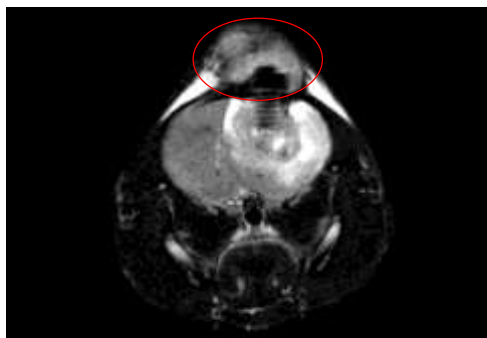


Figure 34 MRI of Kidney Cancer Models MRI of 13881 and 13882 RCC Models Implanted heterotopically into the striatum of C57Bl6/j Mice at 52DPI.

344P



393P

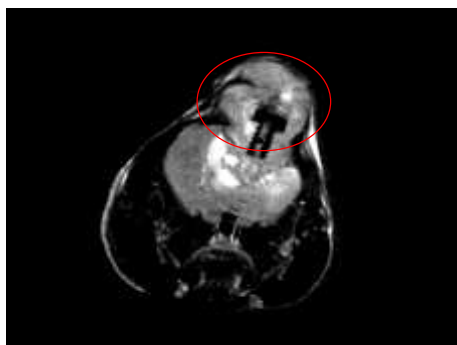


Figure 35 MRI of Lung Cancer Models MRI of 344p and 393p NSCLC Models Implanted heterotopically into the striatum of C57Bl6/j Mice at endpoint.

BP



YUMM3.1



Figure 36 Post-mortem Photographs of Skin Cancer Models YUMM3.1 and BP

Melanoma Models Implanted heterotopically into the striatum of C57Bl6/j Mice post-mortem.

Radiotherapy

Given these observations we implanted 100,000 cells of either the BP or YUMM3.1 heterotopically into the striatum, waited 7 days to detect the tumors by BLI and then subjected a cohort of n=5 mice to either 20gY spatially-fractionated radiation or control in a single dose. We observed a 100% response rate in the BP model compared to 0% survival in the control setting. This is in contrast to what we observed in the YUMM3.1 model which was 0% survival which is the same observed in the control group. (Figure 37)

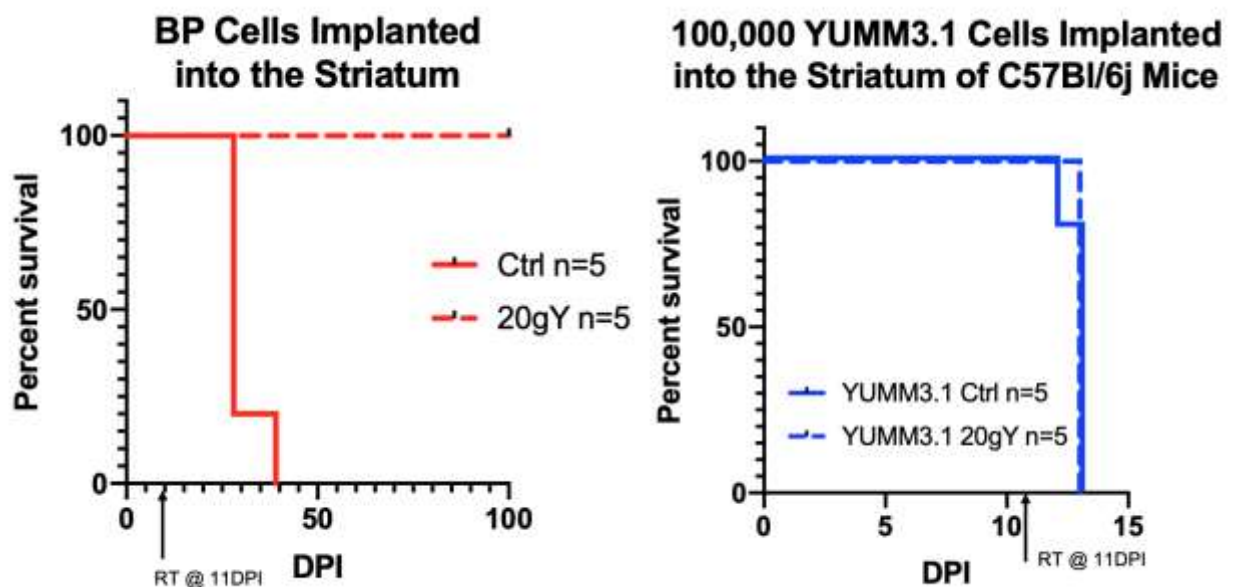


Figure 37 Response of BP and YUMM3.1 Models to 20gY Spatially Fractionated

Radiotherapy. Kaplan-meier survival curves showing the progression of melanoma growth in the striatum of the brain. Left pane shows BP models while the right panel shows the YUMM3.1 model. Arrow indicates the timepoint of 20gY spatially fractionated radiotherapy.

Immune Modulation

We next performed a set of immunomodulatory experiments in which we tested a small molecule inhibitor against Csf1r as well as checkpoint blockade in the forms of anti-Pd1 and anti-Lag3 monoclonal antibodies. When looking at Csf1ri we did not observe any benefit in survival, in fact there is a trend toward worse survival when treating with this compound alone and when used in combination with checkpoint blockade in the form of anti-Pd-1. (**Figure 38**)

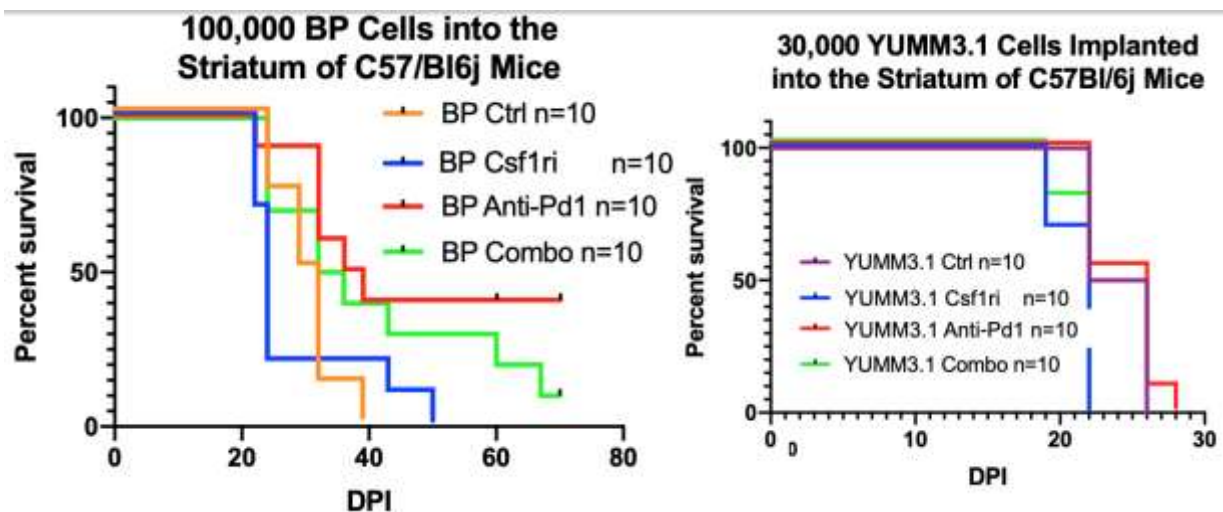


Figure 38 Response of BP and YUMM3.1 Models to Various Immunomodulatory

Therapies. Kaplan-meier survival curves showing the progression of melanoma growth in the striatum of the brain. Left pane shows BP models while the right panel shows the YUMM3.1 model. Groups include control, Csf1r inhibition with BLZ945, anti-PD-1 monoclonal antibody, and combination therapy of these two agents.

We used phenotypic analyses to determine if these immunomodulatory experiments were indeed having the purported effect of the drug administered. In the case of Csf1ri we were able to demonstrate that upon administration of the drug macrophages in the tumor do go down, but that there still is no increased benefit of survival which leads us to believe this

is not an actionable target. This reduction in macrophage infiltration was seen in both the BP (Figure 39) and the YUMM3.1 (Figure 40) Model.

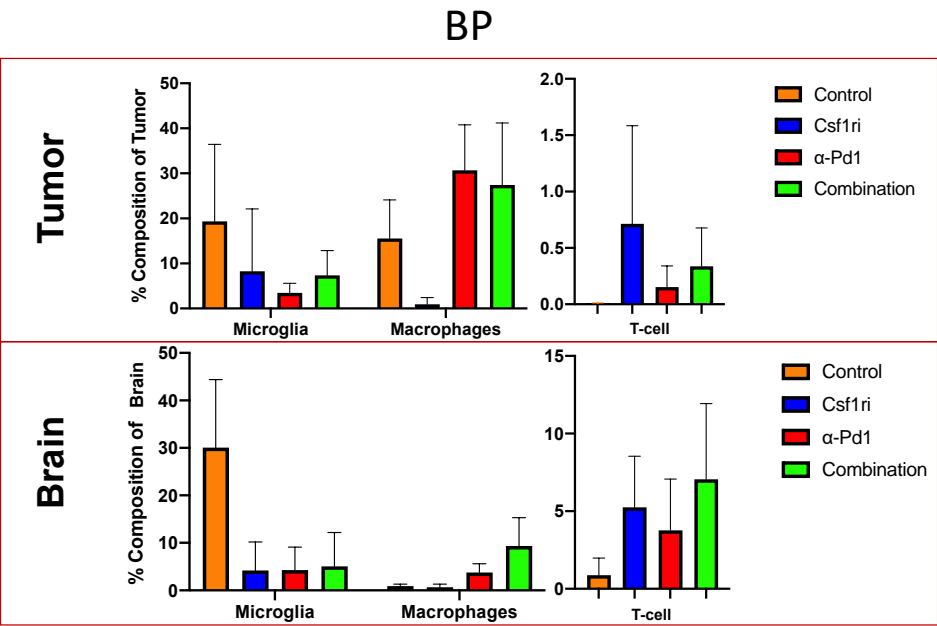


Figure 39 Quantification of Immune Infiltrates of BP Model. Quantification of multiplexed immunofluorescent images and immune populations from the BP model under control, Csf1ri, anti-Pd-1, and the combination of the two.

YUMM3.1

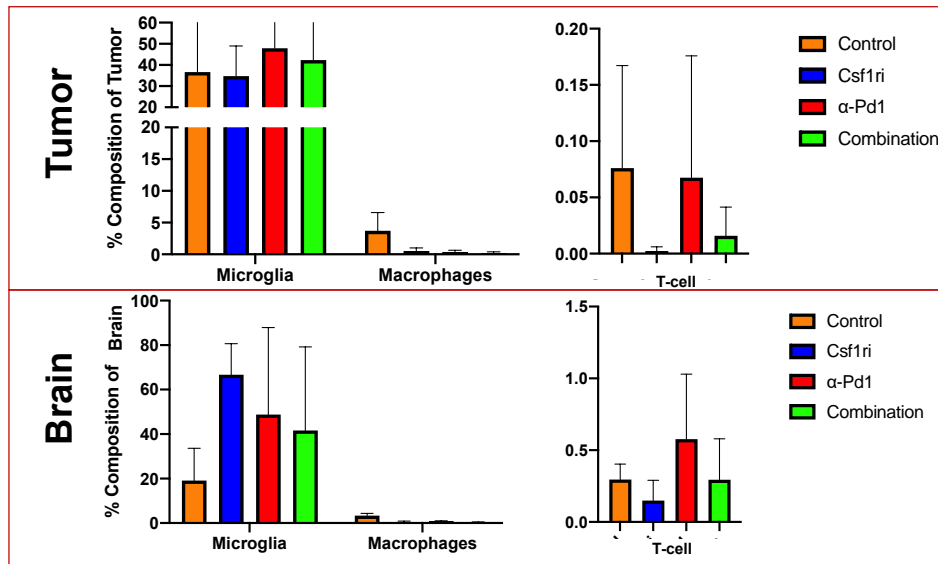


Figure 40 Quantification of Immune Infiltrates of YUMM3.1 Model. Quantification of multiplexed immunofluorescent images and immune populations from the YUMM3.1 model under control, Csfr1ri, anti-Pd-1, and the combination of the two.

In the checkpoint blockade experiments we observed similar results with the two models as were observed in the radiotherapy experiments. Namely, we observed a response to both anti-Pd1 and anti-Lag3 treatment in the BP model while no increase in survival was observed in the YUMM3.1. It is worth noting that the extension in survival observed with anti-Lag3 treatment in the BP model only trended toward significance and was not statistically significant. (**Figure 41**)

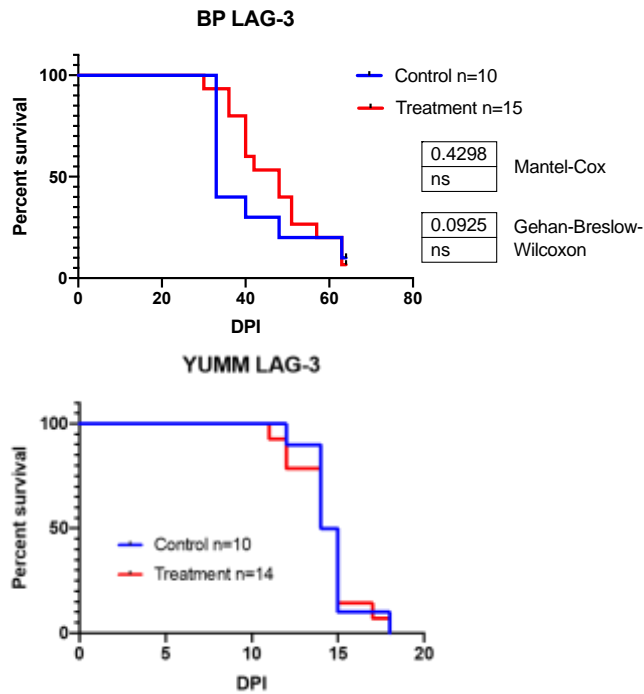


Figure 41 Response of BP and YUMM3.1 Models to anti-Lag-3 Monoclonal Antibody.

Kaplan-meier survival curves showing the progression of melanoma growth in the striatum of the brain. Top pane shows BP models while the bottom panel shows the YUMM3.1 model.

Discussion

It is a truism in cancer that 90% of deaths are caused by metastasis. While unfortunately difficult to find data on there is one small dataset from Norway that indicates while primary cancer deaths remained stagnant over the period of 2005-2016 metastatic cancer deaths nearly tripled.(Dillekås et al., 2019) Brain cancer metastasis are a large patient population with a poor prognosis. While there have been some advances unfortunately more failures exist. In these experiments we aimed to first establish a landscape of potential models for CNS metastasis, expose them to various therapeutic

modalities with real world clinical implications, and then determine how they performed in these studies and potentially in further ones.

We found through several rounds of implantation that there was in general not a large difference between survival length and the amount of cells implanted. In general, the lines tended to engraft or not, and the starting cell number has a minimal impact on the overall survival curve. These experiments lead to several technical difficulties. For example, the RCC lines studied did not form tumors when implanted heterotopically into the brain as seen in **Figure 31**. The NSCLC lines exhibited massive extracranial outgrowths that are not clinically relevant and create artificially long survival curves due to lack of pressure building in the cranium as seen in **Figure 32**. Our melanoma and MDST lines both grew in a fashion where the engrafted and were nicely contained within the CNS and thus we decided to move forward with one of them for the battery of therapeutics. It is important to note we are also pursuing other models of RCC and NSCLC to continue our studies.

We chose to expose the melanoma models to radiotherapy first. With a spatially fractionated dose of 20gY we were able to observe a complete eradication of the tumors in the BP model. In contrast with the YUMM3.1 we were not able to extend survival at all. This response in the BP model, although initially exciting, does not mimic what happens in patients, and what we observed in the YUMM3.1 is more in line with clinical observations.

We next began the immunomodulatory round of experiments. We first aimed to evaluate Csf1ri which prevent macrophages from entering the tumor microenvironment which are purportedly helping the tumor to grow. Although we were able to show a complete ablation of macrophages with Csf1ri in both the BP and the YUMM3.1 models (**Figures 40, 41**) this did not translate into an increase in survival and, in fact, when combined with the anti-PD-1 it was not synergistic. These results led us to believe that although the drug is

acting in the reported fashion, it is not effective at increasing anti-tumor immune response and should not be pursued in this setting further.

Anti-Pd-1 therapy is effective in a subset of patients, and when we exposed both of our melanoma models we found that one of our models had a response and one did not. The BP model showed a response, and while we were not able to show a large increase in T-cells trafficked to the tumor, we were able to show an increase in T cells trafficked to the brain. The YUMM3.1 model did not show this trend and also did not show an increase in survival. Although preliminary, these findings would suggest that there are some cell intrinsic factors that inform whether or not the immune system can recognize and reject tumor cells under checkpoint blockade. These two responses furthermore suggest that we can model a range of responses to lymphoid therapy. Since we were able to show some mild effect here we sought to further synergize on this lymphoid based therapy by investigating another form of checkpoint blockade.

Based on clinical observations, we thought anti-Lag-3 therapy might be synergistic with anti-PD-1 therapy.(Lipson et al., 2021) First, we determined the single agent efficacy of this monoclonal antibody in our two models however. While we had a trend toward significance in the BP model, anti-Lag-3 treatment did not lead to a statistically significant increase in survival. (**Figure 42**)

We next aim to take these single agent therapies and use them in informed combinations. We have partnered with the Brain Metastasis Clinic to further translate these combinations into a clinical trial.

Discussion

Throughout the works contained in this thesis significant contributions have been made to the knowledge surrounding CNS cancers. With regard to the tumor cells themselves, a larger body of knowledge is available regarding the mutational profile of craniopharyngiomas, the similarity of a mouse model of GBM has been confirmed and expounded upon as well as several models of cancer metastasizing to the brain have been characterized. The immune compartment in all of these experimental settings has had a particular focus. In craniopharyngioma, mutations were found that suggest immunotherapeutics particularly in combination with other treatments, may hold promise for this disease. The immune infiltrates of the QPP models were compared to the immune infiltrates of human glioma by IHC as well as scSeq and the similarities and differences were summarized. Arg1 is an enzyme expressed by the immune arm that we targeted as a therapeutic foothold. Finally, in the metastasis to the brain experiments we tested many immunomodulatory therapeutics as well as thoroughly assayed how immune infiltrates in the CNS were changed upon treatment.

We began the craniopharyngioma experiments by providing the demographics of our six patients including the median age of 54.5 (range 33-78), sex with an even distribution, that four patients were primary with the other two being recurrent and unspecified respectively, half of our sample being papillary with one adamantinomatous and two undefined, and various locations of origin. We found the population to generally be genomically stable with low TMB and stable MSI but positive for PD-L1. We discovered BRAF, CTNNB1, NF2, MITF, SETD2, and PIK3CA pathway mutations that may have therapeutic significance or mechanistic

implications on etiology and progression. Finally, we observed an amplification of EGFR which has many therapeutically viable options specifically designed for the CNS.

For our analysis of the QPP models we first established the implanted QPP models from various spontaneous QPP tumor bearing mice and characterized their penetrance and latency for the QPP7 which was found to be roughly 100% with a median survival of 55 days. We calculated the TMB of five of the spontaneous QPP mice and found them to have an average of 22.225 (range 4.875-386.9) while the QPP7 model we implanted had a TMB of 2.775 which are both in line with what is observed in patients. We next compared IHC against Arg1, Cd3, Cd4, Cd8, Cd11b, and Nk1.1 in the implanted QPP, spontaneous QPP and a cohort of human glioma patients. In all three datasets we found the myeloid cells to be the predominant infiltrating population, with all others being present although in small proportion. Due to the relatively limited information that can be obtained with single color IHC we next chose to investigate the infiltrates by scSeq. In sum, we found that all three populations were dominated by a suppressive myeloid population with components of T, B and NK cells. Finally, we were able to observe a similar increase in neutrophil and lymphoid immune infiltrates when comparing our spontaneous QPP model and the implanted QPP7 that we see in comparing our LGG patient samples to our HGG ones.

In testing whether Arg1 is a viable target in GBM we first made an inducible KO mouse model whereby Arg1f/f is deleted upon tamoxifen exposure under a Cx3cr1-Cre^{ERT2} promoter. We completed an experiment with supplementary dietary arginine administered ad-libitum. We completed several rounds of pulsed Arg1 KO experiments in a mouse model to show that Arg1 reduction did not occur and thus did not have an impact on survival. We are currently carrying out experiments with sustained KO of Arg1 to determine if this has a more beneficial impact, particularly if combined with lymphoid therapies. If we see a benefit with this latest round of experiments we have performed the necessary background

to show that we have a drug to inhibit Arg1 that works in a cell free and in-vitro setting. Furthermore we have shown that this compound has the ability to enter the naïve as well as spontaneous tumor bearing brain.

Finally, in modeling of tumors that metastasize to the brain, we found that in general altering the number of cells implanted has little effect on penetrance of latency with some exception near extreme ends of the spectrum (you need a sufficient number of cells to escape initial immune recognition from the surgery and many orders of magnitude more cells may shorten survival curves slightly). When looking into model derived from mice with RCC we found that they did not engraft, which provides obvious problems for studying tumors. When investigating the NSCLC lines we found they exhibited an extreme extracranial growth that is not representative of what happens in patients which is also problematic. When looking at the MDST and melanoma models they behaved in the fashion that you would expect from metastasis to the brain, namely that they stayed contained within the CNS, engrafted, all in a syngeneic setting. We then decided to test our two melanoma models in a therapeutic setting. We first looked at RT where we found one model to be completely responsive and one model to be completely resistant. In general, all patients are resistant but that does not mean this treatment modality won't be useful for combination therapies. We next began a battery of immunomodulatory experiments whereby we tested Csf1r inhibition which was shown to have no effect despite the fact that it was able to reduce infiltrating macrophages in the tumor. We were further able to show that our models recapitulated what is seen in various settings of checkpoint blockade. One of our models was responsive to anti-PD-1 treatment with a trend towards significance in Lag-3 similar to what is observed in patients, while another of our models was completely recalcitrant to all therapies.

In summary, these works have contributed to various areas of CNS Cancer Research in novel ways. While none of these works have lead to cures, I hope that they may act as some small stepping stone along the way toward making CNS Cancers treatable.

References

- Ahmet, A., Blaser, S., Stephens, D., Guger, S., Rutka, J.T., Hamilton, J., 2006. Weight gain in craniopharyngioma - A model for hypothalamic obesity. *J. Pediatr. Endocrinol. Metab.* 19, 121–127.
<https://doi.org/10.1515/JPEM.2006.19.2.121/MACHINEREADABLECITATION/RIS>
- Alonso, M.M., Jiang, H., Yokoyama, T., Xu, J., Bekele, N.B., Lang, F.F., Kondo, S., Gomez-Manzano, C., Fueyo, J., 2008. Delta-24-RGD in combination with RAD001 induces enhanced anti-glioma effect via autophagic cell death. *Mol. Ther.* 16, 487–493.
<https://doi.org/10.1038/SJ.MT.6300400>
- Apps, J.R., Carreno, G., Gonzalez-Meljem, J.M., Haston, S., Guiho, R., Cooper, J.E., Manshaei, S., Jani, N., Hölsken, A., Pettorini, B., Beynon, R.J., Simpson, D.M., Fraser, H.C., Hong, Y., Hallang, S., Stone, T.J., Virasami, A., Donson, A.M., Jones, D., Aquilina, K., Spoudeas, H., Joshi, A.R., Grundy, R., Storer, L.C.D., Korbonits, M., Hilton, D.A., Tossell, K., Thavaraj, S., Ungless, M.A., Gil, J., Buslei, R., Hankinson, T., Hargrave, D., Goding, C., Andoniadou, C.L., Brogan, P., Jacques, T.S., Williams, H.J., Martinez-Barbera, J.P., 2018. Tumour compartment transcriptomics demonstrates the activation of inflammatory and odontogenic programmes in human adamantinomatous craniopharyngioma and identifies the MAPK/ERK pathway as a novel therapeutic target. *Acta Neuropathol.* 135, 757–777. <https://doi.org/10.1007/S00401-018-1830-2>

- Auwerda, G.A., Carneiro, M.O., Hartl, C., Poplin, R., del Angel, G., Levy-Moonshine, A., Jordan, T., Shakir, K., Roazen, D., Thibault, J., Banks, E., Garimella, K. V., Altshuler, D., Gabriel, S., DePristo, M.A., 2013. From FastQ Data to High-Confidence Variant Calls: The Genome Analysis Toolkit Best Practices Pipeline. *Curr. Protoc. Bioinforma.* 43. <https://doi.org/10.1002/0471250953.bi1110s43>
- Aylwin, S.J.B., Bodi, I., Beaney, R., 2016. Pronounced response of papillary craniopharyngioma to treatment with vemurafenib, a BRAF inhibitor. *Pituitary* 19, 544–546. <https://doi.org/10.1007/S11102-015-0663-4>
- Ballester, L.Y., Fuller, G.N., Powell, S.Z., Sulman, E.P., Patel, K.P., Luthra, R., Routbort, M.J., 2017. Retrospective analysis of molecular and immunohistochemical characterization of 381 primary brain tumors. *J. Neuropathol. Exp. Neurol.* 76, 179–188. <https://doi.org/10.1093/jnen/nlw119>
- Bandopadhyay, P., Ramkissoon, L.A., Jain, P., Bergthold, G., Wala, J., Zeid, R., Schumacher, S.E., Urbanski, L., O'Rourke, R., Gibson, W.J., Pelton, K., Ramkissoon, S.H., Han, H.J., Zhu, Y., Choudhari, N., Silva, A., Boucher, K., Henn, R.E., Kang, Y.J., Knoff, D., Paoletta, B.R., Gladden-Young, A., Varlet, P., Pages, M., Horowitz, P.M., Federation, A., Malkin, H., Tracy, A.A., Seepo, S., Ducar, M., Van Hummelen, P., Santi, M., Buccoliero, A.M., Scagnet, M., Bowers, D.C., Giannini, C., Puget, S., Hawkins, C., Tabori, U., Klekner, A., Bogner, L., Burger, P.C., Eberhart, C., Rodriguez, F.J., Hill, D.A., Mueller, S., Haas-Kogan, D.A., Phillips, J.J., Santagata, S., Stiles, C.D., Bradner, J.E., Jabado, N., Goren, A., Grill, J., Ligon, A.H., Goumnerova, L., Waanders, A.J., Storm, P.B., Kieran, M.W., Ligon, K.L., Beroukhi, R., Resnick, A.C., 2016. MYB-QKI rearrangements in angiocentric glioma drive tumorigenicity through a tripartite mechanism. *Nat. Genet.* 48, 273–282. <https://doi.org/10.1038/ng.3500>

Bertolotto, C., Lesueur, F., Giuliano, S., Strub, T., De Lichy, M., Bille, K., Dessen, P., D'Hayer, B., Mohamdi, H., Remenieras, A., Maubec, E., De La Fouchardière, A., Molinié, V., Vabres, P., Dalle, S., Poulalhon, N., Martin-Denavit, T., Thomas, L., Andry-Benzaquen, P., Dupin, N., Boitier, F., Rossi, A., Perrot, J.L., Labeille, B., Robert, C., Escudier, B., Caron, O., Brugières, L., Saule, S., Gardie, B., Gad, S., Richard, S., Couturier, J., Teh, B.T., Ghiorzo, P., Pastorino, L., Puig, S., Badenas, C., Olsson, H., Ingvar, C., Rouleau, E., Lidereau, R., Bahadoran, P., Vielh, P., Corda, E., Blanché, H., Zelenika, D., Galan, P., Aubin, F., Bachollet, B., Becuwe, C., Berthet, P., Jean Bignon, Y., Bonadona, V., Bonafe, J.L., Bonnet-Dupeyron, M.N., Cambazard, F., Chevrant-Breton, J., Coupier, I., Dalac, S., Demange, L., D'Incan, M., Dugast, C., Faivre, L., Vincent-Fétita, L., Gauthier-Villars, M., Gilbert, B., Grange, F., Grob, J.J., Humbert, P., Janin, N., Joly, P., Kerob, D., Lasset, C., Leroux, D., Levang, J., Limacher, J.M., Livideanu, C., Longy, M., Lortholary, A., Stoppa-Lyonnet, D., Mansard, S., Mansuy, L., Marrou, K., Matéus, C., Maugard, C., Meyer, N., Nogues, C., Souteyrand, P., Venat-Bouvet, L., Zattara, H., Chaudru, V., Lenoir, G.M., Lathrop, M., Davidson, I., Avril, M.F., Demenais, F., Ballotti, R., Bressac-De Paillerets, B., 2011. A SUMOylation-defective MITF germline mutation predisposes to melanoma and renal carcinoma. *Nat.* 2011 4807375 480, 94–98. <https://doi.org/10.1038/nature10539>

Brastianos, P.K., Santagata, S., 2016. ENDOCRINE TUMORS: BRAF V600E mutations in papillary craniopharyngioma. *Eur. J. Endocrinol.* 174, R139–R144. <https://doi.org/10.1530/EJE-15-0957>

Brastianos, P.K., Taylor-Weiner, A., Manley, P.E., Jones, R.T., Dias-Santagata, D., Thorner, A.R., Lawrence, M.S., Rodriguez, F.J., Bernardo, L.A., Schubert, L., Sunkavalli, A., Shillingford, N., Calicchio, M.L., Lidov, H.G.W., Taha, H., Martinez-Lage, M., Santi, M., Storm, P.B., Lee, J.Y.K., Palmer, J.N., Adappa, N.D., Scott, R.M., Dunn, I.F., Laws,

E.R., Stewart, C., Ligon, K.L., Hoang, M.P., Van Hummelen, P., Hahn, W.C., Louis, D.N., Resnick, A.C., Kieran, M.W., Getz, G., Santagata, S., 2014. Exome sequencing identifies BRAF mutations in papillary craniopharyngiomas. *Nat. Genet.* 46, 161–165. <https://doi.org/10.1038/ng.2868>

Brennan, C.W., Verhaak, R.G.W., McKenna, A., Campos, B., Noushmehr, H., Salama, S.R., Zheng, S., Chakravarty, D., Sanborn, J.Z., Berman, S.H., Beroukhi, R., Bernard, B., Wu, C.J., Genovese, G., Shmulevich, I., Barnholtz-Sloan, J., Zou, L., Vegesna, R., Shukla, S.A., Ciriello, G., Yung, W.K., Zhang, W., Sougnez, C., Mikkelsen, T., Aldape, K., Bigner, D.D., Van Meir, E.G., Prados, M., Sloan, A., Black, K.L., Eschbacher, J., Finocchiaro, G., Friedman, W., Andrews, D.W., Guha, A., Iacocca, M., O'Neill, B.P., Foltz, G., Myers, J., Weisenberger, D.J., Penny, R., Kucherlapati, R., Perou, C.M., Hayes, D.N., Gibbs, R., Marra, M., Mills, G.B., Lander, E.S., Spellman, P., Wilson, R., Sander, C., Weinstein, J., Meyerson, M., Gabriel, S., Laird, P.W., Haussler, D., Getz, G., Chin, L., Benz, C., Barrett, W., Ostrom, Q., Wolinsky, Y., Bose, B., Boulous, P.T., Boulous, M., Brown, J., Czerinski, C., Eppley, M., Kempista, T., Kitko, T., Koyfman, Y., Rabeno, B., Rastogi, P., Sugarman, M., Swanson, P., Yalamanchii, K., Otey, I.P., Liu, Y.S., Xiao, Y., Auman, J.T., Chen, P.C., Hadjipanayis, A., Lee, E., Lee, S., Park, P.J., Seidman, J., Yang, Lixing, Kalkanis, S., Poisson, L.M., Raghunathan, A., Scarpace, L., Bressler, R., Eakin, A., Iype, L., Kreisberg, R.B., Leinonen, K., Reynolds, S., Rovira, H., Thorsson, V., Annala, M.J., Paulauskis, J., Curley, E., Hatfield, M., Mallery, D., Morris, S., Shelton, T., Shelton, C., Sherman, M., Yena, P., Cuppini, L., DiMeco, F., Eoli, M., Maderna, E., Pollo, B., Saini, M., Balu, S., Hoadley, K.A., Li, L., Miller, C.R., Shi, Y., Topal, M.D., Wu, J., Dunn, G., Giannini, C., Aksoy, B.A., Antipin, Y., Borsu, L., Cerami, E., Gao, J., Gross, B., Jacobsen, A., Ladanyi, M., Lash, A., Liang, Y., Reva, B., Schultz, N., Shen, R., Socci, N.D., Viale, A., Ferguson, M.L., Chen, Q.R., Demchok,

J.A., Dillon, L.A.L., Mills Shaw, K.R., Sheth, M., Tarnuzzer, R., Wang, Z., Yang, Liming, Davidsen, T., Guyer, M.S., Ozenberger, B.A., Sofia, H.J., Bergsten, J., Eckman, J., Harr, J., Smith, C., Tucker, K., Winemiller, C., Zach, L.A., Ljubimova, J.Y., Eley, G., Ayala, B., Jensen, M.A., Kahn, A., Pihl, T.D., Pot, D.A., Wan, Y., Hansen, N., Hothi, P., Lin, B., Shah, N., Yoon, J.G., Lau, C., Berens, M., Ardlie, K., Carter, S.L., Cherniack, A.D., Noble, M., Cho, J., Cibulskis, K., DiCara, D., Frazer, S., Gabriel, S.B., Gehlenborg, N., Gentry, J., Heiman, D., Kim, J., Jing, R., Lawrence, M., Lin, P., Mallard, W., Onofrio, R.C., Saksena, G., Schumacher, S., Stojanov, P., Tabak, B., Voet, D., Zhang, H., Dees, N.N., Ding, L., Fulton, L.L., Fulton, R.S., Kanchi, K.L., Mardis, E.R., Wilson, R.K., Baylin, S.B., Harshyne, L., Cohen, M.L., Devine, K., Sloan, A.E., Van Den Berg, S.R., Berger, M.S., Carlin, D., Craft, B., Ellrott, K., Goldman, M., Goldstein, T., Grifford, M., Ma, S., Ng, S., Stuart, J., Swatloski, T., Waltman, P., Zhu, J., Foss, R., Frentzen, B., McTiernan, R., Yachnis, A., Mao, Y., Akbani, R., Bogler, O., Fuller, G.N., Liu, W., Liu, Y., Lu, Y., Protopopov, A., Ren, X., Sun, Y., Yung, W.K.A., Zhang, J., Chen, K., Weinstein, J.N., Bootwalla, M.S., Lai, P.H., Triche, T.J., Van Den Berg, D.J., Gutmann, D.H., Lehman, N.L., Brat, D., Olson, J.J., Mastrogiannis, G.M., Devi, N.S., Zhang, Z., Lipp, E., McLendon, R., 2013. The somatic genomic landscape of glioblastoma. *Cell* 155, 462. <https://doi.org/10.1016/j.cell.2013.09.034>

Buslei, R., Nolde, M., Hofmann, B., Meissner, S., Eyupoglu, I.Y., Siebzehnriibl, F., Hahnen, E., Kreutzer, J., Fahlbusch, R., 2005. Common mutations of β -catenin in adamantinomatous craniopharyngiomas but not in other tumours originating from the sellar region. *Acta Neuropathol.* 109, 589–597. <https://doi.org/10.1007/s00401-005-1004-x>

Butler, A., Hoffman, P., Smibert, P., Papalexi, E., Satija, R., 2018. Integrating single-cell transcriptomic data across different conditions, technologies, and species. *Nat.*

Biotechnol. 36, 411–420. <https://doi.org/10.1038/nbt.4096>

Caldwell, R.W., Rodriguez, P.C., Toque, H.A., Narayanan, S.P., Caldwell, R.B., 2018.

Arginase: A Multifaceted Enzyme Important in Health and Disease. *Physiol. Rev.* 98, 641–665. <https://doi.org/10.1152/physrev.00037.2016>

Castro-Vega, L.J., Kiando, S.R., Burnichon, N., Buffet, A., Amar, L., Simian, C., Berdelou, A., Galan, P., Schlumberger, M., Bouatia-Naji, N., Favier, J., Bressac-De Paillerets, B., Gimenez-Roqueplo, A.P., 2016. The MITF, p.E318K Variant, as a Risk Factor for Pheochromocytoma and Paraganglioma. *J. Clin. Endocrinol. Metab.* 101, 4764–4768. <https://doi.org/10.1210/JC.2016-2103>

Cerami, E., Gao, J., Dogrusoz, U., Gross, B.E., Sumer, S.O., Aksoy, B.A., Jacobsen, A., Byrne, C.J., Heuer, M.L., Larsson, E., Antipin, Y., Reva, B., Goldberg, A.P., Sander, C., Schultz, N., 2012a. The cBio cancer genomics portal: an open platform for exploring multidimensional cancer genomics data. *Cancer Discov.* 2, 401–4. <https://doi.org/10.1158/2159-8290.CD-12-0095>

Cerami, E., Gao, J., Dogrusoz, U., Gross, B.E., Sumer, S.O., Aksoy, B.A., Jacobsen, A., Byrne, C.J., Heuer, M.L., Larsson, E., Antipin, Y., Reva, B., Goldberg, A.P., Sander, C., Schultz, N., 2012b. The cBio Cancer Genomics Portal: An open platform for exploring multidimensional cancer genomics data. *Cancer Discov.* 2, 401–404. <https://doi.org/10.1158/2159-8290.CD-12-0095>

Chalmers, Z.R., Connelly, C.F., Fabrizio, D., Gay, L., Ali, S.M., Ennis, R., Schrock, A., Campbell, B., Shlien, A., Chmielecki, J., Huang, F., He, Y., Sun, J., Tabori, U., Kennedy, M., Lieber, D.S., Roels, S., White, J., Otto, G.A., Ross, J.S., Garraway, L., Miller, V.A., Stephens, P.J., Frampton, G.M., 2017. Analysis of 100,000 human cancer genomes reveals the landscape of tumor mutational burden. *Genome Med.* 9, 1–14.

<https://doi.org/10.1186/s13073-017-0424-2>

Chen, A.J., Paik, J.H., Zhang, H., Shukla, S.A., Mortensen, R., Hu, J., Ying, H., Hu, B., Hurt, J., Farny, N., Dong, C., Xiao, Y., Wang, Y.A., Silver, P.A., Chin, L., Vasudevan, S., Depinho, R.A., 2012. STAR RNA-binding protein Quaking suppresses cancer via stabilization of specific miRNA. *Genes Dev.* 26, 1459–1472.

<https://doi.org/10.1101/gad.189001.112>

Chen, K., Liu, J., Liu, S., Xia, M., Zhang, X., Han, D., Jiang, Y., Wang, C., Cao, X., 2017. Methyltransferase SETD2-Mediated Methylation of STAT1 Is Critical for Interferon Antiviral Activity. *Cell* 170, 492-506.e14. <https://doi.org/10.1016/J.CELL.2017.06.042>

Chen, S., 2020. Gene Ontologies of scSeq Data.

Chen, Z., Hambardzumyan, D., 2018. Immune Microenvironment in Glioblastoma Subtypes. *Front. Immunol.* 9, 1004. <https://doi.org/10.3389/fimmu.2018.01004>

Choi, Y.J., Oh, H.R., Choi, M.R., Gwak, M., An, C.H., Chung, Y.J., Yoo, N.J., Lee, S.H., 2014. Frameshift mutation of a histone methylation-related gene SETD1B and its regional heterogeneity in gastric and colorectal cancers with high microsatellite instability. *Hum. Pathol.* 45, 1674–1681.
<https://doi.org/10.1016/J.HUMPATH.2014.04.013>

Chongsathidkiet, P., Jackson, C., Koyama, S., Loebel, F., Cui, X., Farber, S.H., Woroniecka, K., Elsamadicy, A.A., Dechant, C.A., Kemeny, H.R., Sanchez-Perez, L., Cheema, T.A., Souders, N.C., Herndon, J.E., Coumans, J.V., Everitt, J.I., Nahed, B. V., Sampson, J.H., Gunn, M.D., Martuza, R.L., Dranoff, G., Curry, W.T., Fecci, P.E., 2018. Sequestration of T cells in bone marrow in the setting of glioblastoma and other intracranial tumors. *Nat. Med.* 24, 1459–1468. <https://doi.org/10.1038/s41591-018-0135-2>

- Cibulskis, K., Lawrence, M.S., Carter, S.L., Sivachenko, A., Jaffe, D., Sougnez, C., Gabriel, S., Meyerson, M., Lander, E.S., Getz, G., 2013. Sensitive detection of somatic point mutations in impure and heterogeneous cancer samples. *Nat. Biotechnol.* 31, 213–219. <https://doi.org/10.1038/nbt.2514>
- Cooper, Z.A., Juneja, V.R., Sage, P.T., Frederick, D.T., Piris, A., Mitra, D., Lo, J.A., Hodi, F.S., Freeman, G.J., Bosenberg, M.W., McMahon, M., Flaherty, K.T., Fisher, D.E., Sharpe, A.H., Wargo, J.A., 2014. Response to BRAF inhibition in melanoma is enhanced when combined with immune checkpoint blockade. *Cancer Immunol. Res.* 2, 643. <https://doi.org/10.1158/2326-6066.CIR-13-0215>
- Coy, S., Rashid, R., Lin, J.R., Du, Z., Donson, A.M., Hankinson, T.C., Foreman, N.K., Manley, P.E., Kieran, M.W., Reardon, D.A., Sorger, P.K., Santagata, S., 2018. Multiplexed immunofluorescence reveals potential PD-1/PD-L1 pathway vulnerabilities in craniopharyngioma. *Neuro. Oncol.* 20, 1101–1112. <https://doi.org/10.1093/neuonc/noy035>
- Dan, H.C., Sun, M., Yang, L., Feldman, R.I., Sui, X.-M., Chen Ou, C., Nellist, M., Yeung, R.S., J Halley, D.J., Nicosia, S. V, Pledger, W.J., Cheng, J.Q., 2002. Phosphatidylinositol 3-kinase/Akt pathway regulates tuberous sclerosis tumor suppressor complex by phosphorylation of tuberin. *ADDITIONS AND CORRECTIONS. J. Biol. Chem.* 277, 22848. <https://doi.org/10.1074/jbc.A116.205838>
- Davies, M.A., Saiag, P., Robert, C., Grob, J.J., Flaherty, K.T., Arance, A., Chiarion-Sileni, V., Thomas, L., Lesimple, T., Mortier, L., Moschos, S.J., Hogg, D., Márquez-Rodas, I., Del Vecchio, M., Lebbé, C., Meyer, N., Zhang, Y., Huang, Y., Mookerjee, B., Long, G. V., 2017. Dabrafenib plus trametinib in patients with BRAF V600-mutant melanoma brain metastases (COMBI-MB): a multicentre, multicohort, open-label, phase 2 trial. *Lancet*.

Oncol. 18, 863–873. [https://doi.org/10.1016/S1470-2045\(17\)30429-1](https://doi.org/10.1016/S1470-2045(17)30429-1)

De Groot, J.F., Penas-Prado, M., Mandel, J.J., O'Brien, B.J., Weathers, S.-P.S., Zhou, S., Hunter, K., Alfaro-Munoz, K., Fuller, G.N., Huse, J., Rao, G., Weinberg, J.S., Prabhu, S.S., Ferguson, S.D., Yuan, Y., Vence, L.M., Allison, J.P., Sharma, P., Heimberger, A.B., 2018. Window-of-opportunity clinical trial of a PD-1 inhibitor in patients with recurrent glioblastoma. *J. Clin. Oncol.* 36, 2008.

https://doi.org/10.1200/JCO.2018.36.15_suppl.2008

DePristo, M.A., Banks, E., Poplin, R., Garimella, K. V, Maguire, J.R., Hartl, C., Philippakis, A.A., del Angel, G., Rivas, M.A., Hanna, M., McKenna, A., Fennell, T.J., Kernytzsky, A.M., Sivachenko, A.Y., Cibulskis, K., Gabriel, S.B., Altshuler, D., Daly, M.J., 2011. A framework for variation discovery and genotyping using next-generation DNA sequencing data. *Nat. Genet.* 43, 491–498. <https://doi.org/10.1038/ng.806>

Ebersole, T.A., Chen, Q., Justice, M.J., Artzt, K., 1996. in *Embryogenesis and Myelination Signal Transduction Proteins* 12.

Federico, L., Chong, Z., Zhang, D., McGrail, D.J., Zhao, W., Jeong, K.J., Vellano, C.P., Ju, Z., Gagea, M., Liu, S., Mitra, S., Dennison, J.B., Lorenzi, P.L., Cardnell, R., Diao, L., Wang, J., Lu, Y., Byers, L.A., Perou, C.M., Lin, S.Y., Mills, G.B., 2017. A murine preclinical syngeneic transplantation model for breast cancer precision medicine. *Sci. Adv.* 3, 1–12. <https://doi.org/10.1126/sciadv.1600957>

Fjalldal, S., Holmer, H., Rylander, L., Elfving, M., Ekman, B., Österberg, K., Erfurth, E.M., 2013. Hypothalamic involvement predicts cognitive performance and psychosocial health in long-term survivors of childhood craniopharyngioma. *J. Clin. Endocrinol. Metab.* 98, 3253–3262. <https://doi.org/10.1210/JC.2013-2000>

Flaherty, K.T., Infante, J.R., Daud, A., Gonzalez, R., Kefford, R.F., Sosman, J., Hamid, O.,

Schuchter, L., Cebon, J., Ibrahim, N., Kudchadkar, R., Burris, H.A., Falchook, G., Algazi, A., Lewis, K., Long, G. V., Puzanov, I., Lebowitz, P., Singh, A., Little, S., Sun, P., Allred, A., Ouellet, D., Kim, K.B., Patel, K., Weber, J., 2012. Combined BRAF and MEK Inhibition in Melanoma with BRAF V600 Mutations. *N. Engl. J. Med.* 367, 1694–1703.

https://doi.org/10.1056/NEJMOA1210093/SUPPL_FILE/NEJMOA1210093_DISCLOSURES.PDF

Friebel, E., Kapolou, K., Unger, S., Núñez, N.G., Utz, S., Rushing, E.J., Regli, L., Weller, M., Greter, M., Tugues, S., Neidert, M.C., Becher, B., 2020. Single-Cell Mapping of Human Brain Cancer Reveals Tumor-Specific Instruction of Tissue-Invasive Leukocytes. *Cell* 181, 1626-1642.e20. <https://doi.org/10.1016/j.cell.2020.04.055>

G. Wu, S.M.J.M., 2004. Metabolic and Therapeutic Aspects of Amino Acids in Clinical Nutrition. CRC Press Second Edi, 153–167.

G, C., H, Y., JL, W., JP, C., JM, D., JL, C., 1984. [Craniopharyngioma in the same family]. *Neurochirurgie.* 30, 347–349.

Gao, J., Aksoy, B.A., Dogrusoz, U., Dresdner, G., Gross, B., Sumer, S.O., Sun, Y., Jacobsen, A., Sinha, R., Larsson, E., Cerami, E., Sander, C., Schultz, N., 2013. Integrative analysis of complex cancer genomics and clinical profiles using the {cBioPortal}. *Sci Signal* 6, pl1. <https://doi.org/10.1126/scisignal.2004088>

Garrè, M.L., Cama, A., 2007. Craniopharyngioma: Modern concepts in pathogenesis and treatment. *Curr. Opin. Pediatr.* 19, 471–479. <https://doi.org/10.1097/MOP.0b013e3282495a22>

Genoud, V., Marinari, E., Nikolaev, S.I., Castle, J.C., Bukur, V., Dietrich, P.Y., Okada, H., Walker, P.R., 2018. Responsiveness to anti-PD-1 and anti-CTLA-4 immune checkpoint

blockade in SB28 and GL261 mouse glioma models. *Oncoimmunology* 7, 1–10.

<https://doi.org/10.1080/2162402X.2018.1501137>

Geraldo, L.H.M., Garcia, C., da Fonseca, A.C.C., Dubois, L.G.F., de Sampaio e Spohr, T.C.L., Matias, D., de Camargo Magalhães, E.S., do Amaral, R.F., da Rosa, B.G., Grimaldi, I., Leser, F.S., Janeiro, J.M., Macharia, L., Wanjiru, C., Pereira, C.M., Moura-Neto, V., Freitas, C., Lima, F.R.S., 2019. Glioblastoma Therapy in the Age of Molecular Medicine. *Trends in Cancer* 5, 46–65. <https://doi.org/10.1016/j.trecan.2018.11.002>

Gibbons, D.L., Lin, W., Creighton, C.J., Rizvi, Z.H., Gregory, P.A., Goodall, G.J., Thilaganathan, N., Du, L., Zhang, Y., Pertsemlidis, A., Kurie, J.M., 2009. Contextual extracellular cues promote tumor cell EMT and metastasis by regulating miR-200 family expression. *Genes Dev.* 23, 2140–2151. <https://doi.org/10.1101/gad.1820209>

Goschzik, T., Gessi, M., Dreschmann, V., Gebhardt, U., Wang, L., Yamaguchi, S., Wheeler, D.A., Lauriola, L., Lau, C.C., Müller, H.L., Pietsch, T., 2017. Genomic alterations of adamantinomatous and papillary craniopharyngioma. *J. Neuropathol. Exp. Neurol.* 76, 126–134. <https://doi.org/10.1093/jnen/nlw116>

Green, A.L., Yeh, J.S., Dias, P.S., 2002. Craniopharyngioma in a mother and daughter. *Acta Neurochir. (Wien)*. 144, 403–404. <https://doi.org/10.1007/S007010200058>

Gubin, M.M., Esaulova, E., Ward, J.P., Malkova, O.N., Runci, D., Wong, P., Noguchi, T., Arthur, C.D., Meng, W., Alspach, E., Medrano, R.F.V., Fronick, C., Fehlings, M., Newell, E.W., Fulton, R.S., Sheehan, K.C.F., Oh, S.T., Schreiber, R.D., Artyomov, M.N., 2018. High-Dimensional Analysis Delineates Myeloid and Lymphoid Compartment Remodeling during Successful Immune-Checkpoint Cancer Therapy. *Cell* 175, 1014-1030.e19. <https://doi.org/10.1016/j.cell.2018.09.030>

Gutin, P.H., Klemme, W.M., Lagger, R.L., MacKay, A.R., Pitts, L.H., Hosobuchi, Y., 1980.

Management of the unresectable cystic craniopharyngioma by aspiration through an Ommaya reservoir drainage system. *J. Neurosurg.* 52, 36–40.

<https://doi.org/10.3171/JNS.1980.52.1.0036>

Hafemeister, C., Satija, R., 2019. Normalization and variance stabilization of single-cell RNA-seq data using regularized negative binomial regression. *bioRxiv* 576827.

<https://doi.org/10.1101/576827>

Hara, T., Akutsu, H., Takano, S., Kino, H., Ishikawa, E., Tanaka, S., Miyamoto, H., Sakamoto, N., Hattori, K., Sakata-Yanagimoto, M., Chiba, S., Hiyama, T., Masumoto, T., Matsumura, A., 2019. Clinical and biological significance of adamantinomatous craniopharyngioma with CTNNB1 mutation. *J. Neurosurg.* 131, 217–226.

<https://doi.org/10.3171/2018.3.JNS172528>

Hölsken, A., Buchfelder, M., Fahlbusch, R., Blümcke, I., Buslei, R., 2010. Tumour cell migration in adamantinomatous craniopharyngiomas is promoted by activated Wnt-signalling. *Acta Neuropathol.* 119, 631–639. <https://doi.org/10.1007/S00401-010-0642-9/FIGURES/5>

Hölsken, A., Gebhardt, M., Buchfelder, M., Fahlbusch, R., Blümcke, I., Buslei, R., 2011. EGFR signaling regulates tumor cell migration in craniopharyngiomas. *Clin. Cancer Res.* 17, 4367–4377. <https://doi.org/10.1158/1078-0432.CCR-10-2811>

Hussain, S.F., Yang, D., Suki, D., Aldape, K., Grimm, E., Heimberger, A.B., 2006. The role of human glioma-infiltrating microglia/macrophages in mediating antitumor immune responses¹. *Neuro. Oncol.* 8, 261–279. <https://doi.org/10.1215/15228517-2006-008>

Internò, V., De Santis, P., Stucci, L.S., Rudà, R., Tucci, M., Soffietti, R., Porta, C., 2021. Prognostic Factors and Current Treatment Strategies for Renal Cell Carcinoma Metastatic to the Brain: An Overview. *Cancers (Basel)*. 13.

<https://doi.org/10.3390/CANCERS13092114>

Jane, J.A., Laws, E.R., 2006. Craniopharyngioma. *Pituitary* 9, 323–326.

<https://doi.org/10.1007/s11102-006-0413-8>

Janku, F., Tsimberidou, A.M., Garrido-Laguna, I., Wang, X., Luthra, R., Hong, D.S., Naing, A., Falchook, G.S., Moroney, J.W., Piha-Paul, S.A., Wheler, J.J., Moulder, S.L., Fu, S., Kurzrock, R., 2011. PIK3CA Mutations in Patients with Advanced Cancers Treated with PI3K/AKT/mTOR Axis Inhibitors. *Mol Cancer Ther* 10, 558–565.

<https://doi.org/10.1158/1535-7163.MCT-10-0994>

Johanns, T.M., Ward, J.P., Miller, C.A., Wilson, C., Kobayashi, D.K., Bender, D., Alexandrov, A., Mardis, E.R., Artyomov, M.N., Schreiber, R.D., Dunn, G.P., 2016. Endogenous Neoantigen-specific CD8 T Cells Identified in Two Glioblastoma Models Using a Cancer Immunogenics Approach. *Cancer Immunol. Res.* 176, 139–148.

<https://doi.org/10.1016/j.physbeh.2017.03.040>

Juric, D., Rodon, J., Tabernero, J., Janku, F., Burris, H.A., Schellens, J.H.M., Middleton, M.R., Berlin, J., Schuler, M., Marta, G.M., Rugo, H.S., Ruth, S.B., Huang, A., Bootle, D., Demanse, D., Blumenstein, L., Coughlin, C., Quadts, C., Baselga, J., 2018.

Phosphatidylinositol 3-Kinase α -Selective Inhibition With Alpelisib (BYL719) in PIK3CA-Altered Solid Tumors: Results From the First-in-Human Study. *J. Clin. Oncol.* 36, 1291–1299. <https://doi.org/10.1200/JCO.2017.72.7107>

Klemm, F., Maas, R.R., Bowman, R.L., Kornete, M., Soukup, K., Nassiri, S., Brouland, J.P., Iacobuzio-Donahue, C.A., Brennan, C., Tabar, V., Gutin, P.H., Daniel, R.T., Hegi, M.E., Joyce, J.A., 2020. Interrogation of the Microenvironmental Landscape in Brain Tumors Reveals Disease-Specific Alterations of Immune Cells. *Cell* 181, 1643-1660.e17.

<https://doi.org/10.1016/j.cell.2020.05.007>

- Larkin, S.J., Preda, V., Karavitaki, N., Grossman, A., Ansorge, O., 2014. BRAF V600E mutations are characteristic for papillary craniopharyngioma and may coexist with CTNNB1-mutated adamantinomatous craniopharyngioma. *Acta Neuropathol.* 127, 927–929. <https://doi.org/10.1007/s00401-014-1270-6>
- Lo, A.C., Howard, A.F., Nichol, A., Sidhu, K., Abdulsatar, F., Hasan, H., Goddard, K., 2014. Long-term outcomes and complications in patients with craniopharyngioma: The British Columbia cancer agency experience. *Int. J. Radiat. Oncol. Biol. Phys.* 88, 1011–1018. <https://doi.org/10.1016/j.ijrobp.2014.01.019>
- MACCARTY, W.C., RUSSELL, D.G., 1958. Tuberous Sclerosis1. <https://doi.org/10.1148/71.6.833> 71, 833–839. <https://doi.org/10.1148/71.6.833>
- Markham, A., 2017. Copanlisib: First Global Approval. *Drugs* 2017 7718 77, 2057–2062. <https://doi.org/10.1007/S40265-017-0838-6>
- Marucci, G., de Biase, D., Zoli, M., Faustini-Fustini, M., Bacci, A., Pasquini, E., Visani, M., Mazzatenta, D., Frank, G., Tallini, G., 2015. Targeted BRAF and CTNNB1 next-generation sequencing allows proper classification of nonadenomatous lesions of the sellar region in samples with limiting amounts of lesional cells. *Pituitary* 18, 905–911. <https://doi.org/10.1007/s11102-015-0669-y>
- McKenna, A., Hanna, M., Banks, E., Sivachenko, A., Cibulskis, K., Kernytsky, A., Garimella, K., Altshuler, D., Gabriel, S., Daly, M., DePristo, M.A., 2010. The Genome Analysis Toolkit: A MapReduce framework for analyzing next-generation DNA sequencing data. *Genome Res.* 20, 1297–1303. <https://doi.org/10.1101/gr.107524.110>
- Meeth, K., Wang, J.X., Micevic, G., Damsky, W., Bosenberg, M.W., 2016. The YUMM lines: a series of congenic mouse melanoma cell lines with defined genetic alterations. *Pigment Cell Melanoma Res.* 29, 590–597. <https://doi.org/10.1111/pcmr.12498>

- Mestas, J., Hughes, C.C.W., 2004. Of Mice and Not Men: Differences between Mouse and Human Immunology. *J. Immunol.* 172, 2731–2738.
<https://doi.org/10.4049/jimmunol.172.5.2731>
- Miska, J., Rashidi, A., Lee-Chang, C., Gao, P., Lopez-Rosas, A., Zhang, P., Burga, R., Castro, B., Xiao, T., Han, Y., Hou, D., Sampat, S., Cordero, A., Stoolman, J.S., Horbinski, C.M., Burns, M., Reshetnyak, Y.K., Chandel, N.S., Lesniak, M.S., 2021. Polyamines drive myeloid cell survival by buffering intracellular pH to promote immunosuppression in glioblastoma. *Sci. Adv.* 7, 8929–8946.
https://doi.org/10.1126/SCIADV.ABC8929/SUPPL_FILE/ABC8929_TABLE_S1.XLSX
- Miyai, M., Tomita, H., Soeda, A., Yano, H., Iwama, T., Hara, A., 2017. Current trends in mouse models of glioblastoma. *J. Neurooncol.* 135, 423–432.
<https://doi.org/10.1007/s11060-017-2626-2>
- Miyazawa, H., Yamaguchi, Y., Sugiura, Y., Honda, K., Kondo, K., Matsuda, F., Yamamoto, T., Suematsu, M., Miura, M., 2017. Rewiring of embryonic glucose metabolism via suppression of PFK-1 and aldolase during mouse chorioallantoic branching. *J. Cell Sci.* 130, e1.1–e1.1. <https://doi.org/10.1242/jcs.201335>
- Ohlfest, J.R., Demorest, Z.L., Motooka, Y., Vengco, I., Oh, S., Chen, E., Scappaticci, F.A., Saplis, R.J., Ekker, S.C., Low, W.C., Freese, A.B., Largaespada, D.A., 2005. Combinatorial antiangiogenic gene therapy by nonviral gene transfer using the Sleeping Beauty transposon causes tumor regression and improves survival in mice bearing intracranial human glioblastoma. *Mol. Ther.* 12, 778–788.
<https://doi.org/10.1016/j.ymthe.2005.07.689>
- Olsson, D.S., Andersson, E., Bryngelsson, I.L., Nilsson, A.G., Johannsson, G., 2015. Excess mortality and morbidity in patients with craniopharyngioma, especially in

patients with childhood onset: a population-based study in Sweden. *J. Clin. Endocrinol. Metab.* 100, 467–474. <https://doi.org/10.1210/JC.2014-3525>

Pilanc, P., Wojnicki, K., Roura, A.J., Cyranowski, S., Ellert-Miklaszewska, A., Ochocka, N., Gielniewski, B., Grzybowski, M.M., Błaszczyk, R., Stańczak, P.S., Dobrzański, P., Kaminska, B., 2021. A Novel Oral Arginase 1/2 Inhibitor Enhances the Antitumor Effect of PD-1 Inhibition in Murine Experimental Gliomas by Altering the Immunosuppressive Environment. *Front. Oncol.* 11. <https://doi.org/10.3389/FONC.2021.703465>

Pudlo, M. Céline Demougeot, and C.G.-T., 2016. Arginase Inhibitors: A Rational Approach Over One Century. *Med. Res. Rev.* 36, 705–748. <https://doi.org/10.1002/med>

Qaddoumi, I., Orisme, W., Wen, J., Santiago, T., Gupta, K., Dalton, J.D., Tang, B., Hauptfear, K., Punchihewa, C., Easton, J., Mulder, H., Boggs, K., Shao, Y., Rusch, M., Becksfort, J., Gupta, P., Wang, S., Lee, R.P., Brat, D., Peter Collins, V., Dahiya, S., George, D., Konomos, W., Kurian, K.M., McFadden, K., Serafini, L.N., Nickols, H., Perry, A., Shurtleff, S., Gajjar, A., Boop, F.A., Klimo, P.D., Mardis, E.R., Wilson, R.K., Baker, S.J., Zhang, J., Wu, G., Downing, J.R., Tatevossian, R.G., Ellison, D.W., 2016. Genetic alterations in uncommon low-grade neuroepithelial tumors: BRAF, FGFR1, and MYB mutations occur at high frequency and align with morphology. *Acta Neuropathol.* 131, 833–845. <https://doi.org/10.1007/s00401-016-1539-z>

Reilly, K.M., Loisel, D.A., Bronson, R.T., McLaughlin, M.E., Jacks, T., 2000. Nf1;Trp53 mutant mice develop glioblastoma with evidence of strain-specific effects. *Nat. Genet.* 26, 109–113. <https://doi.org/10.1038/79075>

Ren, J., Dai, C., Zhou, X., Barnes, J.A., Chen, X., Wang, Y., Yuan, L., Shingu, T., Heimberger, A.B., Chen, Y., Hu, J., 2021. Qki is an essential regulator of microglial phagocytosis in demyelination. *J. Exp. Med.* 218. <https://doi.org/10.1084/jem.20190348>

- Shay, T., Jojic, V., Zuk, O., Rothamel, K., Puyraimond-Zemmour, D., Feng, T., Wakamatsu, E., Benoist, C., Koller, D., Regev, A., 2013. Conservation and divergence in the transcriptional programs of the human and mouse immune systems. *Proc. Natl. Acad. Sci. U. S. A.* 110, 2946–2951. <https://doi.org/10.1073/pnas.1222738110>
- Shen, E., Van Swearingen, A.E.D., Price, M.J., Bulsara, K., Verhaak, R.G.W., Baëta, C., Painter, B.D., Reitman, Z.J., Salama, A.K.S., Clarke, J.M., Anders, C.K., Fecci, P.E., Goodwin, C.R., Walsh, K.M., 2022. A Need for More Molecular Profiling in Brain Metastases. *Front. Oncol.* 11, 5810. <https://doi.org/10.3389/FONC.2021.785064/BIBTEX>
- Shin, S., Zhou, H., He, C., Wei, Y., Wang, Y., Shingu, T., Zeng, A., Wang, S., Zhou, X., Li, H., Zhang, Q., Mo, Q., Long, J., Lan, F., Chen, Y., Hu, J., 2021. Qki activates Srebp2-mediated cholesterol biosynthesis for maintenance of eye lens transparency. *Nat. Commun.* 12, 1–18. <https://doi.org/10.1038/s41467-021-22782-0>
- Shingu, T., Ho, A.L., Yuan, L., Zhou, X., Dai, C., Zheng, S., Wang, Q., Zhong, Y., Chang, Q., Horner, J.W., Liebelt, B.D., Yao, Y., Hu, B., Chen, Y., Fuller, G.N., Verhaak, R.G.W., Heimberger, A.B., Hu, J., 2017. Qki deficiency maintains stemness of glioma stem cells in suboptimal environment by downregulating endolysosomal degradation. *Nat. Genet.* 49, 75–86. <https://doi.org/10.1038/ng.3711>
- Slattery, W.H., 2015. Neurofibromatosis type 2. *Otolaryngol. Clin. North Am.* 48, 443–460. <https://doi.org/10.1016/J.OTC.2015.02.005>
- Stache, C., Bils, C., Fahlbusch, R., Flitsch, J., Buchfelder, M., Stefanits, H., Czech, T., Gaip, U., Frey, B., Buslei, R., Hölsken, A., 2016. Drug priming enhances radiosensitivity of adamantinomatous craniopharyngioma via downregulation of survivin. *Neurosurg. Focus* 41. <https://doi.org/10.3171/2016.9.FOCUS16316>

- Stuart, T., Butler, A., Hoffman, P., Hafemeister, C., Papalexi, E., Mauck, W.M., Hao, Y., Stoeckius, M., Smibert, P., Satija, R., 2019. Comprehensive Integration of Single-Cell Data. *Cell* 177, 1888-1902.e21. <https://doi.org/10.1016/j.cell.2019.05.031>
- Szatmári, T., Lumniczky, K., Désaknai, S., Trajcevski, S., Hídvégi, E.J., Hamada, H., Sáfrány, G., 2006. Detailed characterization of the mouse glioma 261 tumor model for experimental glioblastoma therapy. *Cancer Sci.* 97, 546–553. <https://doi.org/10.1111/j.1349-7006.2006.00208.x>
- Venteicher, A.S., Tirosh, I., Hebert, C., Yizhak, K., Neftel, C., Filbin, M.G., Hovestadt, V., Escalante, L.E., Shaw, M.L., Rodman, C., Gillespie, S.M., Dionne, D., Luo, C.C., Ravichandran, H., Mylvaganam, R., Mount, C., Onozato, M.L., Nahed, B. V., Wakimoto, H., Curry, W.T., Iafrate, A.J., Rivera, M.N., Frosch, M.P., Golub, T.R., Brastianos, P.K., Getz, G., Patel, A.P., Monje, M., Cahill, D.P., Rozenblatt-Rosen, O., Louis, D.N., Bernstein, B.E., Regev, A., Suvà, M.L., 2017. Decoupling genetics, lineages, and microenvironment in IDH-mutant gliomas by single-cell RNA-seq. *Science* (80-.). 355. <https://doi.org/10.1126/science.aai8478>
- Verhaak, R.G.W., Hoadley, K.A., Purdom, E., Wang, V., Qi, Y., Wilkerson, M.D., Miller, C.R., Ding, L., Golub, T., Mesirov, J.P., Alexe, G., Lawrence, M., O’Kelly, M., Tamayo, P., Weir, B.A., Gabriel, S., Winckler, W., Gupta, S., Jakkula, L., Feiler, H.S., Hodgson, J.G., James, C.D., Sarkaria, J.N., Brennan, C., Kahn, A., Spellman, P.T., Wilson, R.K., Speed, T.P., Gray, J.W., Meyerson, M., Getz, G., Perou, C.M., Hayes, D.N., 2010. Integrated Genomic Analysis Identifies Clinically Relevant Subtypes of Glioblastoma Characterized by Abnormalities in PDGFRA, IDH1, EGFR, and NF1. *Cancer Cell* 17, 98–110. <https://doi.org/10.1016/j.ccr.2009.12.020>
- Woroniecka, K., Chongsathidkiet, P., Rhodin, K., Kemeny, H., Dechant, C., Harrison Farber,

S., Elsamadicy, A.A., Cui, X., Koyama, S., Jackson, C., Hansen, L.J., Johanns, T.M., Sanchez-Perez, L., Chandramohan, V., Yu, Y.R.A., Bigner, D.D., Giles, A., Healy, P., Dranoff, G., Weinhold, K.J., Dunn, G.P., Fecci, P.E., 2018. T-cell exhaustion signatures vary with tumor type and are severe in glioblastoma. *Clin. Cancer Res.* 24, 4175–4186. <https://doi.org/10.1158/1078-0432.CCR-17-1846>

Yue, F., Cheng, Y., Breschi, A., Vierstra, J., Wu, W., Ryba, T., Sandstrom, R., Ma, Z., Davis, C., Pope, B.D., Shen, Y., Pervouchine, D.D., Djebali, S., Thurman, R.E., Kaul, R., Rynes, E., Kirilusha, A., Marinov, G.K., Williams, B.A., Trout, D., Amrhein, H., Fisher-Aylor, K., Antoshechkin, I., DeSalvo, G., See, L.H., Fastuca, M., Drenkow, J., Zaleski, C., Dobin, A., Prieto, P., Lagarde, J., Bussotti, G., Tanzer, A., Denas, O., Li, K., Bender, M.A., Zhang, M., Byron, R., Groudine, M.T., McCleary, D., Pham, L., Ye, Z., Kuan, S., Edsall, L., Wu, Y.C., Rasmussen, M.D., Bansal, M.S., Kellis, M., Keller, C.A., Morrissey, C.S., Mishra, T., Jain, D., Dogan, N., Harris, R.S., Cayting, P., Kawli, T., Boyle, A.P., Euskirchen, G., Kundaje, A., Lin, S., Lin, Y., Jansen, C., Malladi, V.S., Cline, M.S., Erickson, D.T., Kirkup, V.M., Learned, K., Sloan, C.A., Rosenbloom, K.R., De Sousa, B.L., Beal, K., Pignatelli, M., Flicek, P., Lian, J., Kahveci, T., Lee, D., Kent, W.J., Santos, M.R., Herrero, J., Notredame, C., Johnson, A., Vong, S., Lee, K., Bates, D., Neri, F., Diegel, M., Canfield, T., Sabo, P.J., Wilken, M.S., Reh, T.A., Giste, E., Shafer, A., Kuttyavin, T., Haugen, E., Dunn, D., Reynolds, A.P., Neph, S., Humbert, R., Hansen, R.S., De Bruijn, M., Selleri, L., Rudensky, A., Josefowicz, S., Samstein, R., Eichler, E.E., Orkin, S.H., Levasseur, D., Papayannopoulou, T., Chang, K.H., Skoultschi, A., Gosh, S., Disteché, C., Treuting, P., Wang, Y., Weiss, M.J., Blobel, G.A., Cao, X., Zhong, S., Wang, T., Good, P.J., Lowdon, R.F., Adams, L.B., Zhou, X.Q., Pazin, M.J., Feingold, E.A., Wold, B., Taylor, J., Mortazavi, A., Weissman, S.M., Stamatoyannopoulos, J.A., Snyder, M.P., Guigo, R., Gingeras, T.R., Gilbert, D.M.,

Hardison, R.C., Beer, M.A., Ren, B., 2014. A comparative encyclopedia of DNA elements in the mouse genome. *Nature* 515, 355–364.

<https://doi.org/10.1038/nature13992>

Zanotelli, V., Bodenmiller, B., 2017. A flexible image segmentation pipeline for heterogeneous multiplexed tissue images based on pixel classification 1–11.

Zheng, W., Ibáñez, G., Wu, H., Blum, G., Zeng, H., Dong, A., Li, F., Hajian, T., Allali-Hassani, A., Amaya, M.F., Siarheyeva, A., Yu, W., Brown, P.J., Schapira, M., Vedadi, M., Min, J., Luo, M., 2012. Sinefungin Derivatives as Inhibitors and Structure Probes of Protein Lysine Methyltransferase SETD2. *J. Am. Chem. Soc.* 134, 18004.

<https://doi.org/10.1021/JA307060P>

Zhou, M., Veenstra Editors, T., n.d. Proteomics for Biomarker Discovery Methods in Molecular Biology 1002.

Zhou, X., He, C., Ren, J., Dai, C., Stevens, S.R., Wang, Q., Zamler, D., Shingu, T., Yuan, L., Chandregowda, C.R., Wang, Y., Ravikumar, V., Rao, A.U.K., Zhou, F., Zheng, H., Rasband, M.N., Chen, Y., Lan, F., Heimberger, A.B., Segal, B.M., Hu, J., 2020. Mature myelin maintenance requires Qki to coactivate PPAR β -RXR α -mediated lipid metabolism. *J. Clin. Invest.* <https://doi.org/10.1172/jci131800>

Zhou, X., Shin, S., He, C., Zhang, Q., Rasband, M.N., Ren, J., Dai, C., Zorrilla-Veloz, R.I., Shingu, T., Yuan, L., Wang, Y., Chen, Y., Lan, F., Hu, J., 2021. Qki regulates myelinogenesis through srebp2-dependent cholesterol biosynthesis. *Elife* 10, 1–34. <https://doi.org/10.7554/eLife.60467>

Material and Methods

Study population

Multiplatform analysis covering the tumor mutational burden (TMB), microsatellite instability (MSI), high-throughput sequencing, *in situ* hybridization, and immunohistochemical study was performed on six craniopharyngioma tumors in adults and identified in the Caris Life Sciences database. The purpose of the database is to provide a genetic profiling record, but annotation of clinical data is limited. As such, the history, treatment, and survivorship outcomes of patients are not included. The histologic diagnosis is based on WHO guidelines (ICD10-2016). This study involved collection of existing data and publicly available diagnostic specimens, and the information gathering process precludes direct and indirect identification of subjects, which therefore exempts it from requiring institutional review board approval under HHS regulations at 45 CFR 46.101(b).

Mouse Models

The QPP spontaneous glioma model exists on a mixed background and is maintained in the Hu laboratory at MD Anderson Cancer Center in the Department of Cancer Biology. Frozen Sperm have also been deposited in the MD Anderson Mouse Transgenics Core

Cell Lines

Cell Lines - Cell line was generated in 2017 at MDACC in the Hu laboratory, as the cells are primary, they have not been banked, tested, or authenticated, however the cells are available for sharing with the community upon request.

Patient Data

Patient information with sex, genomic information as well as site of resection etc. are available in **Table 3**.

Genetic analysis

Genomic DNA was extracted from formalin-fixed paraffin-embedded (FFPE) tumor blocks using the QIAamp DNA FFPE DNA Extraction Kit (Qiagen Sciences, Germantown, MD

20874). Genes of interest were amplified using the Illumina TruSEQ amplicon cancer hotspot (47 genes; n=1)(Illumina, San Diego, CA) or the Agilent customized pan-cancer panel (592 genes; n=4)(Agilent Technologies, Santa Clara, CA) and sequenced with the Illumina MiSEQ and Illumina NextSEQ platforms, respectively, out of a total of 1.4 megabases of DNA. The analysis focused on the TMB, MSI, and specific gene mutations and their transcriptional effect. TMB was measured by counting all non-synonymous missense mutations found per tumor that had not been previously described as germline alterations, the threshold used for TMB was 17 mutations/megabase based on concordance data with MSI in colorectal cancer. MSI was examined using over 7,000 target microsatellite loci and compared to the reference genome hg19 from the University of California, Santa Cruz (UCSC) Genome Browser database. The threshold to determine MSI by NGS was 46 or more loci with insertions or deletions to generate a sensitivity of > 95% and specificity of > 99%. Variants were detected with a >99% confidence interval based on the frequency of identified mutations and amplicon coverage, with an average coverage of > 500 and an analytic sensitivity of 5%.

Gene amplification and expression

Both fluorescent and chromogenic *in situ* hybridization were used to detect amplifications in *cMET*, *Her2* and *cMET* amplifications, respectively, as well as gene fusion of *ALK*. Analysis by immunohistochemistry (IHC) was performed on full FFPE sections to assess the expression of EGFR, Her2/Neu, cMET, PD-L1 and ALK. Slides were stained using automated techniques, per the manufacturer's instructions, and were optimized and validated per Clinical Laboratory Improvement Amendments CLIA/CAO and international Organization for Standardization (ISO) requirements. Staining was scored for intensity (0 = no staining; 1+ = weak staining; 2+ = moderate staining; 3+ = strong staining) and staining percentage (0-100%). Results were categorized as positive or negative by defined thresholds specific to each marker based on published clinical literature that associates biomarker status with

patient responses to therapeutic agents. For PD-L1, the primary antibody used was SP142 (Spring Biosciences). The staining was regarded as positive if its intensity on the membrane of the tumor cells was $\geq 2+$ and the percentage of positively stained cells was $>5\%$. A board-certified pathologist evaluated all IHC results independently. For gene fusion detection, anchored multiplex PCR was performed for targeted RNA sequencing using the ArcherDx fusion assay (Archer FusionPlex Solid Tumor panel). The formalin-fixed paraffin-embedded tumor samples were microdissected to enrich the sample to $\geq 20\%$ tumor nuclei, and mRNA was isolated and reverse transcribed into complementary DNA (cDNA). Unidirectional gene-specific primers were used to enrich for target regions, followed by Next-Generation sequencing (Illumina MiSeq platform). Targets included 52 genes, and the full list can be found at <http://archerdx.com/fusionplex-assays/solid-tumor>.

Materials Availability

- Cell Lines – QPP7 cell line was generated in 2017 at MDACC in the Hu laboratory, as the cells are primary, they have not been banked, tested, or authenticated, however the cells are available for sharing with the community upon request.
- Reagents – This study did not generate any unique reagents
- Mouse lines – ACM Mice are available by request from Giulio Draetta

Data and Code Availability

- The authors affirm that all data necessary for confirming the conclusions of this article are present within the article, figures, tables, and the database available through Caris Life Sciences.
- Dataset – The single cell sequencing dataset has been deposited in the GEO database under the accession number GSE147275 with access token opejqqwmtvwxhwb
- Code – Code used to generate figures and analyze data is available at https://github.com/zamlerd/Single_Cell_Sequencing

KEY RESOURCES TABLE

REAGENT or RESOURCE	SOURCE	IDENTIFIER
Antibodies – Supplemental Table 1		
Biological Samples		
Patient Tissue	MD Anderson Cancer Center	
Critical Commercial Assays		
10x 3' Single Cell Sequencing v3 Chemistry		
NovaRed Impact IHC Staining		
Deposited Data		
Single Cell Sequencing dataset	This Manuscript	GSE147275
Experimental Models: Cell Lines		
QPP7	Hu Laboratory	
Experimental Models: Organisms/Strains		
QPP Model	Hu Laboratory	
ACM Model	Draetta Laboratory	
C57Bl6/j	Jackson Labs	IMSR_JAX:000664
Software and Algorithms		
Rstudio	www.rstudio.com	SCR_000432

Cell Ranger	https://support.10xgenomics.com/single-cell-gene-expression/software/pipelines/latest/installation	SCR_017344
Seurat	Satijalab.org	SCR_007322
Custom Pipeline	https://github.com/zamlerd/Single_Cell_Sequencing	

Cell lines. The QPP7 cell line was cultured in the commercially available NeuroCult Basal Medium (Mouse & Rat; Cat # 05700; Stemcell Technologies Inc., Cambridge, MA) with the NeuroCult Proliferation Supplement (Mouse & Rat; Stemcell Technologies, Inc.) added. Cells were cultured as spheres and subcultured every 2-3 days at a 1:10 ratio with Accutase (Innovative Cell Technologies, Inc.; San Diego, CA) as the dissociation solution. The 344p, 393p, and BP models were cultured as an adherent monolayer in RPMI supplemented with 10% FBS and 1x Pen/Strep and subcultured 1:5 every 4-7 days. The 13881 and 13882 models were cultured as an adherent monolayer in DMEM supplemented with 10% FBS and 1x Pen/Strep and subcultured every 2-5 days. The YUMM3.1 and YUMM5.2 models were cultured as an adherent monolayer in DMEM/F12 supplemented with 1x MEM Non-essential Amino Acids, 10% FBS and 1x Pen/Strep.

Murine glioma models. All manipulations were performed with Institutional Animal Care and Use Committee approval at The University of Texas MD Anderson Cancer (MD Anderson).

To trigger the spontaneous QPP gliomas, tamoxifen was dissolved in corn oil at the concentration of 10 mg/ml and injected subcutaneously in a total volume of 20 μ L in P7 and P8 mice to induce glioma development in the Nes-CreERT2; Qk^{L/L}; Pten^{L/L}; Trp53^{L/L} background. The mice were monitored for neurological symptoms or other signs of ill health every other day and were euthanized and necropsied when moribund. To implant QPP gliomas, cells were cultured as described above until the time of surgical implantation. The QPP cells were dissociated with Accutase (Innovative Cell Technologies, Inc.) for 5-10 minutes at room temperature, the Accutase was neutralized by dilution with medium, and the cells were pelleted by centrifugation. Automated cell counting was performed and the cells were resuspended at a concentration of 2.5×10^4 cells per μ L. Mice were anesthetized with a combination of ketamine and xylazine and 5×10^4 QPP cells were implanted at the stereotactic coordinates of +0.5 mm forward and +2 mm lateral right from the bregma at a depth of 3mm. After the anesthesia was reversed with atipamezole, the mice were monitored until signs of tumor burden appeared, at which point they were euthanized by transcardial perfusion with Tyrode's solution (Sigma-Aldrich, Inc., St. Louis, MO. Tyrode's solution is a salt formulation designed to keep the heart beating while flushing blood from the mouse's circulatory system during transcardial perfusion). Their brains were removed and fixed in paraformaldehyde.

Immunohistochemistry. Tissues were embedded in paraffin, serially sectioned on a microtome at 5 μ M, and stained with hematoxylin and eosin. Specifically, sections on microscope slides were stained with freshly filtered hematoxylin for 30 seconds and then with eosin for 15 seconds before dehydration in two 1-minute washes of 95% ethanol followed by three 1-minute washes in 100% ethanol, and finally, three quick rinses in xylene before application of cover slips to slides. For antibody staining, tissue sections were baked

for 1 hour at 60 °C before being washed three times in xylene for 5 minutes, followed by washes in 100%, 95%, 70%, and 50% ethanol and then tap water. Antigen retrieval was performed using a Biogenix easy-retrieval microwave set at 95°C for 10 minutes in sodium citrate buffer at pH 6.0. Slides were then washed in PBS for 5 minutes before being blocked with 3% BSA at room temperature for 1 hour. Slides were then incubated overnight at 4°C at the dilutions listed in **Table 4**. The next morning, slides were washed three times in PBS with 0.1% Tween for 5 minutes before incubation with the appropriate HRP-conjugated secondary antibody for 1 hour at room temperature. Slides were then washed three times in PBS for 5 minutes before being developed using the NovaRED chromagen incorporation kit. Cover slips were then applied to the slides in aqueous mounting medium. For our immunohistochemistry analysis, we quantified the number of cells by hand in the area of 396mm² (20x field). Antibody catalog numbers and dilutions and RRIDs (RRID is a number used by the Resource Identification Portal) are found in **Table 4**.

Single-cell sequencing. Mice with implanted QPP tumors were perfused with Tyrode's solution before the tumors were reduced to a single-cell suspension and frozen in Bambanker cell-freezing medium (Wako Chemicals USA, Inc., Richmond, VA) at -80 °C. Gliomas were mechanically dissociated with scissors while suspended in Accutase solution (Innovative Cell Technologies, Inc.) at room temperature and then serially drawn through 25-, 10- and 5-mL pipettes before being drawn through an 181/2-gauge syringe. After 10 minutes of dissociation, cells were spun down at 420 x g for 5 minutes at 4 °C and then resuspended in 10 mL of a 0.9N sucrose solution and spun down again at 800 x g for 8 minutes at 4 °C with the brake off. Once sufficient samples were accumulated to be run in the 10x pipeline (10x Genomics; 6230 Stoneridge Mall Road, Pleasanton, CA 94588), cells were then thawed and resuspended in 1 mL of PBS containing 1% BSA, for manual counting. Cells were then stained with the CD45 antibody (BD Biosciences, San Jose, CA,

cat #: 555482) at 1:5 for human or (Tonbo Biosciences, San Diego, CA, cat #: 50-0454-U100) at 1:10 for mice for 20 minutes on ice. Samples had Sytox blue added just before sorting so that only live CD45+ cells would be collected. Cells were then sorted in a solution of 50% FBS and 0.5% BSA in PBS, spun down, and resuspended at a concentration of 700-1200 cells/uL for microfluidics on the 10x platform (10x Genomics). The 10x protocol, which is publicly available, was followed to generate the cDNA libraries that were sequenced. (https://assets.ctfassets.net/an68im79xiti/2NaoOhmA0jot0ggwcyEKaC/fc58451fd97d9cbe012c0abbb097cc38/CG000204_ChromiumNextGEMSingleCell3_v3.1_Rev_C.pdf)

The libraries were sequenced on an Illumina next-seq 500, and up to 4 indexed samples were multiplexed into one output flow cell using the Illumina high-output sequencing kit (V2.5) in paired-end sequencing (R1, 26nt; R2, 98nt, and i7 index 8nt) as instructed in the 10x Genomics 3' Single-cell RNA sequencing kit.

The data were then analyzed using the cellranger pipeline (10x Genomics) to generate gene count matrices. The mkfastq argument (10x Genomics) was used to separate individual samples with simple csv sample sheets to indicate the well that was used on the i7 index plate to label each sample. The count argument (10x Genomics) was then used with the expected number of cells for each mouse or patient. For the mice, the expected cell numbers were 10,000, whereas for patients, the numbers varied between 2,000 and 8,000. Mice were aligned with the mm10 genome, and humans were aligned with GRCh38. The aggr argument (10x Genomics) was then used to aggregate samples from each condition (spontaneous QPP, implanted QPP, and patient) for further analysis. Once gene-count matrices were generated, they were read into an adapted version of the Seurat pipeline (Butler et al., 2018; Stuart et al., 2019) for filtering, normalization, and plotting. Genes that were expressed in less than three cells were ignored, and cells that expressed less than 200 genes or more than 2500 genes were excluded, to remove potentially poor-

and high-PCR artifact cells, respectively. Finally, to generate a percentage of mitochondrial DNA variability and to exclude any cells with more than 25% mitochondrial DNA (as these may be doublets or low-quality dying cells), cells were normalized using regression to remove the percent mitochondrial DNA variable via the `scTransform` (Hafemeister and Satija, 2019) command. Next, the cell clusters were identified and visualized using SNN and UMAP, respectively, before generating a list of differentially-expressed genes for each cluster. A list of differentially-expressed genes was generated to label our clusters at low resolution (0.1). These clusters' labels were based on at least three differentially-expressed genes, and violin plots were generated to show the relative specificity to the cluster.

Identification of the clusters was as follows: Neutrophils: CD24a, S100a8, and S100a9; antigen-presenting cells: CD74 (MHCII), H2-Eb1, and H2-Aa; T cells: Cd3d, Cd3e, and Cd3g; and microglia and macrophages: Cd68, Cx3cr1, and Tmem119. For analyses performed on the combination of implanted and spontaneous QPP models, we joined the datasets (using the `FindIntegrationAnchors` command to determine genes that can be used to integrate two datasets—after the determination of the Anchors used the `IntegrateData` command) with the aforementioned anchors to combine our two datasets. Data were then normalized using the `scTransform` command, which uses regression analysis to remove the percentage of mitochondrial DNA from each cell. Datasets were then processed for principal component analysis (PCA) with the `RunPCA` command, and elbow plots were printed with the `ElbowPlot` command in order to determine the optimal number of PCs for clustering. Datasets then were submitted to cluster analysis with `RunUMAP` and `FindNeighbors` commands before `FindClusters` was run with either 0.1 or 0.65 resolution for low- and high-resolution clustering, respectively. Differentially-expressed genes were identified using cutoffs for `min.pct` = 0.25 and `logfc.threshold` = 0.25. Plots were generated with either the `DimPlot`, `FeaturePlot` or `VlnPlot` commands. For consistency, the same markers (or

homologs) were used to designate these populations regardless of the species, except that CD24a and ITGAX were used interchangeably to label neutrophil clusters, and Nktr and HCST were used to label NK clusters in mice and humans, respectively.

Gene Ontology Analysis. Gene ontology analyses were performed as previously published and publicly available code adapted to our dataset. (Chen, 2020)

Phenoptics We began by staining mice at moribund timepoints with a panel containing Tmem119, F4/80 and Cd3 in order to identify Microglia, Macrophages, and T-cells. We then performed whole slide scans and analyzed the images using the HALO software suite. The process of converting the images to data points is roughly as follows, regions are first defined and then a machine learning algorithm is trained to define these regions. Next, cells are identified by DAPI nuclear staining, which becomes the nucleus, and then we extend computationally a small region to create an artificial cytoplasm. Microglia are defined as Tmem119+ F4/80-, Macrophages were defined as F4/80+ Tmem119+/-, T-cells were defined as Cd3+.

Vita

Daniel Bernard Zamler is the son of Sherwin and Monica Zamler. After completing his work at Wylie E. Groves in Beverly Hills Michigan in 2009, he entered the University of Michigan in Ann Arbor, Michigan. He received the degree of Bachelor of Science with a major in Neuroscience from University of Michigan in May, 2013. For the next three years, he worked as a research technician in the Department of Neurosurgery at University of Michigan. In August of 2017 he entered The University of Texas MD Anderson Cancer Center UTHHealth Graduate School of Biomedical Sciences.

Permanent address:

32331 Mayfair

Beverly Hills, Michigan 48025